

CAA PAPER 2000/5

**DGPS GUIDANCE FOR HELICOPTER
APPROACHES TO OFFSHORE
PLATFORMS**

Volume 1: Experimental Procedures

Volume 2: DGPS Equipment Performance

Volume 3: DGPS Approach Guidance

Prepared by JRA Stevens, Senior Project Engineer

Approved by DJ Dyer, Business Manager

REPORT PREPARED BY CONTROL SYSTEMS GROUP
CRANFIELD AEROSPACE LTD, CRANFIELD, BEDFORD
AND PUBLISHED BY
CIVIL AVIATION AUTHORITY, LONDON, NOVEMBER 2000

CAA PAPER 2000/5

**DGPS GUIDANCE FOR HELICOPTER
APPROACHES TO OFFSHORE
PLATFORMS**

Volume 1: Experimental Procedures

Volume 2: DGPS Equipment Performance

Volume 3: DGPS Approach Guidance

Prepared by JRA Stevens, Senior Project Engineer
Approved by DJ Dyer, Business Manager

REPORT PREPARED BY CONTROL SYSTEMS GROUP
CRANFIELD AEROSPACE LTD, CRANFIELD, BEDFORD
AND PUBLISHED BY
CIVIL AVIATION AUTHORITY, LONDON, NOVEMBER 2000

© Civil Aviation Authority 2000

ISBN 0 86039 791 2

Printed and distributed by
Westward documedia Limited, 37 Windsor Street, Cheltenham, England

General Foreword

The research reported in this paper was funded by the Safety Regulation Group of the UK Civil Aviation Authority, and was performed by Cranfield University. The work was instigated primarily in response to the findings of the Helicopter Human Factors Working Group reported in CAA Paper 87007 (Recommendations 4.1.1 and 4.2.1). The Helicopter Human Factors Working Group was formed in response to Recommendation 1 of the Report of the Helicopter Airworthiness Review Panel (HARP Report - CAP 491). Additional impetus was provided by Recommendation 4.4 in AAIB Aircraft Accident Report 5/88 (Report on the incident to Sikorsky S76A helicopter G-BHYB near Fulmar A Oil Platform in the North Sea on 09 December 1987). Trials subsequently performed to evaluate a visual glideslope indicator in response to this recommendation demonstrated the unsuitability of that technology for the application (CAA Paper 95011 refers); it was considered that an instrument-based approach aid would be capable of fulfilling the need identified.

This paper comprises an overview of the research performed, followed by three parts containing unabridged versions of the three volumes of the Cranfield University final project report (ref. CA/CSG/7052 Issue 1, dated 01 November 1999). The first volume, 'Experimental Procedures', describes the three measurement systems utilised, the data recorded and the experimental procedures employed for the trials. The second, 'DGPS Equipment Performance', covers the extraction of the helicopter 'truth' position reference using post-processed GPS measurements, compares the real time Differential GPS (DGPS) position data with the 'truth', and discusses the various factors which were found to affect the availability and accuracy of the real time DGPS data. Volume 3, 'DGPS Approach Guidance', reports on how the approach guidance information was generated and presented to the pilots, and discusses the flyability aspects assessed.

The CAA fully supports the conclusions drawn from the trials, and considers the results encouraging in terms of the potential of DGPS as an instrument aid for conducting offshore approaches. It is recognised, however, that considerable further work is required before the technology could be introduced into service. In particular, a hazard analysis needs to be performed to establish the overall system performance required, and appropriate airworthiness and operational requirements need to be developed. Work on further analysis of the trials data to establish the effects of satellite failures is currently in progress, and an investigation of the effects of rotors on GPS reception is planned for start in FY 2000/01. These activities will contribute to a clearer picture of suitable system configurations and operating procedures. An in-service trials programme can then be instigated in co-operation with the Industry. Apart from helping to gain confidence and experience with the system, this will allow the issues of increasing the GPS data and pilot sample size and expanding the range of helicopter types and operating conditions to be addressed.

All of the trials described in this paper were undertaken prior to the US Government's decision, announced in May 2000, to discontinue the intentional degradation known as Selective Availability (SA) of the civilian GPS positioning service. It is the opinion of the author of this paper that all of the conclusions remain valid, and this view is supported by the CAA. It is now intended, however, to undertake additional investigations to quantify both the stand-alone and the DGPS performance when operating in a non-SA environment, and to estimate the likely impact upon the flight trial results.

Safety Regulation Group
November 2000

Overview

Introduction

Few navigational aids are available to assist the pilots of helicopters operating to oil and gas installations in the North Sea. Many of the platforms are beyond the coverage of both land-based navigational beacons and of ATC surveillance radar, and the platforms themselves lack the approach aid equipment (such as ILS) which is commonplace at onshore aerodromes. The helicopter operators' preferred solution for the en-route navigational task has been to employ area navigation (RNAV) equipment which requires input from a position sensor. Historically, long range terrestrial systems such as Decca Navigator have been used as the position sensor. More recently, however, the satellite-based technology of the Global Positioning System (GPS) is taking over as Decca is phased out. Operational procedures based on the use of this equipment ensure safe separation from any conflicting traffic in the absence of radar coverage.

Following the arrival of the helicopter in the vicinity of the destination platform at the end of the en-route phase of the flight, the weather conditions frequently prevent the pilot from directly commencing a safe visual approach to the helideck. To assist in this situation, many platforms are equipped with a non-directional beacon (NDB), which is essentially a low power medium-frequency radio transmitter. The platform NDB and the associated direction finding equipment carried on the aircraft provide only a relative bearing indication, and do not allow the helicopter's range from the platform to be determined. The only available source of range information is the helicopter's airborne weather radar display, upon which the destination platform will appear as one of several targets without any positive identification. The helicopter operators have devised approach procedures which rely on the use of the weather radar to maintain safe separation from the platform (and any other obstacles) until visual contact can be established. The fact that the weather radar is neither designed nor certificated as a navigational aid means that this is far from being an ideal solution, and this is reflected in the imposition of relatively conservative approach minima, i.e. if visual contact with the platform cannot be established at a range of 0.75nm then the approach attempt must be abandoned.

A need therefore exists for an accurate and reliable instrument approach aid for use at offshore platforms, and Differential GPS (DGPS) was identified as offering the potential to fulfil this need at relatively low cost. Differential GPS is a technique which aims to improve upon the accuracy of unaugmented or 'raw' GPS, by determining the errors in the individual satellite signals using measurements made at a fixed location. These errors, known as differential corrections, are then transmitted via a separate data link to the mobile user receiver where they may be used to correct the raw measurements.

In view of the need identified and the emergence of DGPS technology, in 1994 the UK Civil Aviation Authority (CAA) launched a research project to investigate the use of DGPS for helicopter instrument approaches to offshore platforms. The primary aims of the project were:

- to demonstrate the suitability of the technology for the task, and
- to provide the knowledge and experience required to support its introduction.

Other objectives of the flight trials programme were:

- to quantify the performance of representative DGPS equipment installed in a helicopter when operating in the vicinity of offshore structures, and
- to investigate flyability and piloting issues such as approach trajectories, and cockpit displays and indications.

At present, the only airworthiness and operational requirements that exist in relation to offshore approaches are those written specifically for operations using airborne weather radar. These requirements are unsuitable for application to any other potential form of offshore approach guidance. Hence, a longer term objective of the research project was to use the information gathered from the flight trials programme to develop generic requirements for offshore approach guidance, together with the airworthiness requirements specific to the various elements of a DGPS system.

Being aware of the considerable amount of work completed or under way elsewhere to address the wide ranging technical issues associated with the use of GPS technology, the CAA first commissioned a literature search and review. The purpose of this exercise was to identify, obtain and examine all existing literature that could be relevant to the use of DGPS for offshore helicopter approaches in order to establish the extent and quality of work already undertaken, and thus avoid unnecessary duplication of effort. In the event, it was discovered that very little had been reported on the application of DGPS to helicopter operations, and nothing was identified that addressed the conditions that prevail at offshore platforms; in particular, the large number of reflectors which could give rise to additional errors caused by 'multipath' reception. The findings of the literature survey enabled a flight trials project specification for a proof of concept trial to be produced which would fulfil the CAA's objectives. The specification addressed the general configurations of the ground and airborne systems, the nature of the flight testing to be performed, and the data collection and analysis required.

The invitation to tender for the work, based on the specification, was issued in 1995 and the contract was awarded to the College of Aeronautics, Cranfield University. The flight trials were conducted during 1996 using a helicopter chartered from Bond Helicopters Limited, which was equipped with a DGPS trials installation designed by Cranfield Aerospace Ltd (the commercial arm of the College of Aeronautics). A total of seven test flights were conducted during which data was collected at four offshore platforms, nominally representing low, medium and high multipath environments. The current weather radar approach pattern was flown using DGPS guidance, and alternative 'DGPS approach' trajectories were also investigated.

Trials Aircraft and Equipment

The flight trials were performed using a Sikorsky S76C helicopter, registration G-SSSC, which was based at Aberdeen airport. Typical of the smaller North Sea support helicopters, the S76C seats up to twelve passengers in addition to the two flight crew. In order to obtain as much benefit as possible from the trials, the aircraft was fitted with a comprehensive instrumentation system which was mounted on a removable pallet to enable the aircraft to be rapidly converted from its normal revenue-earning role to the trials configuration.

The trials installation allowed DGPS correction signals from two alternative sources to be received and processed concurrently on the helicopter, permitting a direct comparison of their performance to be made. A medium frequency (MF) receiver allowed differential

corrections to be received from any of a number of marine radio beacon transmitters, known as 'reference stations', located in the British Isles and mainland Europe. These stations provide a broadcast service to participating users around the coast. A subscription service operated in the UK at the time of the trials, but has now been superseded by an open system. The second source of differential corrections was provided in the form of a 'private' local reference station, which was temporarily located on the subject offshore platform for each individual trial. The platform base station was housed in a self-contained aluminium enclosure, designed to satisfy the stringent safety requirements of the oil companies, and transmitted corrections to the aircraft using a UHF datalink. Differential corrections from these two sources were fed to two separate, but otherwise identical DGPS receiver units manufactured by Navstar Systems Ltd.

On some of the flights a third receiver, produced by Trimble Navigation Ltd, was used in an attempt to investigate the extent of correlation between the performance of different manufacturers' DGPS equipment. Data from a fourth airborne GPS unit, which was not supplied with differential corrections, was recorded and used during post-flight analysis to reconstruct a 'truth' position history for the aircraft.

Interfaces were provided between the aircraft instrumentation pallet and a number of the existing aircraft systems so that parameters such as airspeed and altitude could be accessed, and to allow DGPS-derived data to be displayed in the cockpit. The aircraft instrumentation incorporated a high speed real-time data processing unit together with two IBM-compatible PC computers. One PC was dedicated to data recording, and the second was located in the aircraft cabin to allow parameters to be monitored and changed in flight. GPS receivers and data recording equipment were also sited at two fixed locations in order to provide logged data for post-trial processing. The first of these locations was on the 'target' offshore platform, packaged with the platform reference correction station. The second was a surveyed onshore site in Aberdeen.

DGPS Approach Procedures

Prior to commencing the trials, it was realised that neither the normal onshore ILS approach profile nor the current airborne weather radar procedure represented the most suitable form of approach for use with DGPS guidance at an offshore platform. A completely new approach profile was therefore designed for the trials.

In the horizontal plane, the new offshore approach involved a straight approach track which was offset laterally by a fixed distance to remain clear of the platform. In the vertical plane, the approach comprised an initial fixed angle glide-path segment to provide a descent from (typically) 800ft to 200ft above sea level, followed by a level segment leading up to the Missed Approach Point (MAP). It also included a missed approach procedure in the form of a fixed climb-out angle overshoot, which returned the aircraft to a safe altitude in the event that a landing was not possible.

The approach profile was programmed into the trials instrumentation system which was configured to provide guidance information to the pilot in the form of deviations from the pre-programmed flight path. The data presentation was designed to replicate, as far as was possible, the familiar onshore ILS indications of localiser deviation, derived from the DGPS horizontal position, and glideslope deviation, derived by combining the aircraft radio altimeter output with the current DGPS horizontal position solution. The localiser and glideslope indications were displayed throughout the approach, with a seamless transition implemented between the different segments. Range information (in the form of distance to

the platform and/or to the MAP) was also provided, together with associated mode indications.

Flight Trials

A series of seven test flights was undertaken at approximately monthly intervals between April and October 1996. Five comprised full offshore approach trials, and the remaining two were devoted to equipment proving and to two exercises at onshore locations. The aircraft crew composition was the same for each trial. The aircraft was commanded by a Bond Helicopters Senior Training Captain with the flying being shared with the CAA's Senior Helicopter Test Pilot. Cranfield University and CAA provided the Flight Test Engineer and Flight Test Observer respectively.

The offshore test flights were performed at four different platforms close to Aberdeen. The platforms were selected to provide a representative cross-section of the different forms of platform construction and layout encountered in the North Sea, in order to permit the investigation of any significant differences in their GPS multipath characteristics. Consequently, to enable GPS performance data to be collected over a broadly consistent spatial pattern relative to each platform, a nominally identical series of manoeuvres was performed at each offshore location. These comprised a number of orbits around the platform at ranges of between 0.1nm and 2nm, together with a series of weather radar approaches which each incorporated an over-flight of the platform followed by outbound (to 4nm range) and inbound legs. The tracks for the inbound legs were arranged to cover all four compass quadrants, forming a four-leaved clover pattern in plan view.

In addition, a series of DGPS approaches was performed at each location to enable the pilots to evaluate the effects of changes to a number of the parameters which defined the approach profile and/or the instrument sensitivities.

DGPS Performance

A commercial post-processing software package was used to derive a 'truth' position history for the aircraft using recorded data from the aircraft reference GPS receiver, together with data from the two fixed recording systems (onshore and platform). The post-processing technique made use of the so-called carrier phase observable associated with each of the satellite signals in order to obtain a greater level of accuracy, and to provide increased immunity to multipath effects. Many GPS receivers are capable of taking carrier phase measurements. However, at the time of the trials, carrier phase ambiguity resolution was considered an immature technique owing to the substantial period of time necessary for the solution to converge. During the trials programme the use of carrier phase techniques was therefore limited to the post processing truth system. The real-time corrections relied upon code phase only.

The position solutions recorded by each of the real-time differentially corrected receivers were compared with the 'truth' solution to determine the errors associated with each receiver. Only the horizontal component of the GPS solution errors was considered during this analysis. These data were analysed to examine the variation in performance with correction source (onshore and platform), range from the platforms, platform design, manoeuvre type and receiver design.

A summary of the results obtained is shown in the table below.

	Onshore differential corrections	Platform-based differential corrections
Number of samples	33684	29444
Mean error	3.5m	7.0m
95% error	7.0m	16.7m
Maximum error	21.0m	123.1m

Summary of DGPS Receiver Performance (horizontal error)

For the receiver supplied with differential corrections from the onshore source, the results were consistent with those which might be expected when using similar equipment at a 'clean' location (a 95% confidence limit of 7.0m, and a maximum error of 21.0m in over 30,000 samples).

The corresponding results using the platform-based correction source exhibited significantly greater errors, with a maximum value of 123.1m being observed. This was attributed to the differential correction station having been subjected to signal disturbances from the platform structure, and suggests that considerable care must be taken in the positioning of any such reference station to avoid multipath effects.

No evidence was observed for the aircraft GPS receiver itself having been affected by multipath effects whilst manoeuvring in the vicinity of the platform, although additional trials to provide a larger data set are needed to provide additional confidence that this will always be the case. The error contribution due to multipath generated by the airframe and rotors was estimated from ground testing to be no more than 2m.

No significant differences between the performance of the two dissimilar GPS receivers, designed by different manufacturers, were found.

Pilot Evaluation of DGPS Approaches

A total of 61 approaches were performed during the course of the trials programme, 46 of which took place at offshore platforms. Initial reactions to the DGPS approach profile and guidance presentation were very favourable. The approach guidance was generally found to be easy to fly and provided smooth and consistent indications. A number of modifications were evaluated over the course of the test flights, partly in order to investigate the effect of varying some of the approach parameters, and also as a result of observations and feedback from the pilots during and after each flight.

Aspects of the approach profile evaluated included approach and overshoot angles, transition to level segment, removal of level segment, alternative go-around techniques, curved approach segments, and crosswind and reduced speed approaches. Man-machine interface issues investigated included lateral and vertical guidance sensitivities, presentation of range information, annunciation of mode changes, and input of approach data.

Valuable information was generated on the suitability of the new approach profile and the corresponding guidance presentations, which will be of considerable benefit in the

formulation of airworthiness and operational requirements and associated advisory material in the future.

Safety Regulation Group
November 2000

Volume I
Experimental Procedures

Contents

	<i>Page</i>
1 INTRODUCTION	1
2 REFERENCES	3
3 ABBREVIATIONS	4
4 TRIALS AIRFRAME AND AIRBORNE EQUIPMENT	6
4.1 GPS Antenna	10
4.2 RF Preamplifier and Signal Splitter	10
4.3 GPS 1, 2 and 3 (Navstar XR5-M12)	11
4.4 GPS 4 (Trimble TNL-2100)	13
4.5 RF Circulator and DC Block	15
4.6 MF Datalink Receiver and Antenna	15
4.7 UHF Datalink Receiver, Relay and Antennas	16
4.8 Electronic Computer Unit (ECU)	17
4.9 Data Recorder	18
4.10 Vertical Gyro	18
4.11 Aircraft Interface Box	18
4.12 Laptop PC	18
4.13 Radio Altimeter	19
4.14 Air Data Computer	19
4.15 Racal RNAV-2	19
4.16 DME Indicator	19
4.17 HSI/ADI/Autopilot	20
4.18 LED Indicators	20
5 PLATFORM SYSTEM	21
5.1 GPS Antenna	22
5.2 RF Signal Splitter	22
5.3 GPS 1 and 2 (Navstar XR5-M12)	22
5.4 UHF Datalink Transmitter and Antenna	22
5.5 Electronic Computer Unit (ECU)	23
5.6 Data Recorder	23
6 ONSHORE SYSTEM	24
6.1 GPS Antenna	24
6.2 GPS Receiver (Navstar XR5-M12)	25
6.3 Electronic Computer Unit (ECU)	25
6.4 Data Recorder	25

	<i>Page</i>	
7	DATA RECORDING	26
7.1	Data Message Structure	26
7.2	GPS Truth Message Format	28
7.3	GPS Ephemeris Message Format	29
7.4	GPS Navigation Message Format	31
7.5	RTCM Correction Message Format	32
7.6	Aircraft Data Message Format	33
7.7	Time Synchronisation	33
8	TRIALS PROCEDURES	39
8.1	Flight Trials	39
8.2	DGPS Equipment Configuration	40
8.3	Pre-Flight Preparation	43
8.4	Flight Trial Procedure	45
8.5	Constraints on Flight Trial Manoeuvres	47
8.6	Post-Flight Activities	48
8.7	Post-Flight Processing	48

LIST OF ILLUSTRATIONS

Figure 1	Aircraft Trials Equipment Installation	9
Figure 2	Microstrip Implementation of 4-Output Wilkinson Divider	11
Figure 3	Platform System Equipment	21
Figure 4	Onshore System Equipment	24
Figure 5	Temporal Relationship Between GPS Receiver 1PPS and RS232 Outputs	34
Figure 6	ECU Algorithm to Determine Absolute Time to 1ms Resolution	35
Figure 7	Trials Airframe, Sikorsky S76C G-SSSC	51
Figure 8	G-SSSC Cockpit Layout	51
Figure 9	DGPS Trials Pallet Installation	52
Figure 10	GPS Antenna Installation	52
Figure 11	MF and Tail UHF Antenna Installation	53
Figure 12	Nose UHF Antenna Installation	53
Figure 13	Cockpit LED Indicators	54
Figure 14	Platform Reference System	54
Figure 15	Onshore System Antenna	55
Figure 16	Aberdeen and Longside	56
Figure 17	Northern North Sea	57

LIST OF TABLES.

Table 1	S76C G-SSSC Technical Specifications	6
Table 2	S76C G-SSSC Principal Avionic Equipment	7
Table 3	Manufacturer's Declared Performance for Navstar XR5-M12	12
Table 4	Manufacturer's Declared Performance for Trimble TNL-2100	14
Table 5	Messages Recorded by Airborne Data System	27
Table 6	Messages Recorded by Platform Data System	27

	<i>Page</i>	
Table 7	Messages Recorded by Onshore Data System	27
Table 8	GPS Truth Message Format	29
Table 9	GPS Ephemeris Message Format	30
Table 10	GPS Navigation Message Format	31
Table 11	RTCM Correction Message Format	32
Table 12	Aircraft Data Message Format	33
Table 13	DGPS Flight Trials	39
Table 14	Airborne Equipment Configuration on each Flight	41
Table 15	Airborne Equipment Part, Serial and Version Numbers	42
Table 16	Platform System Part, Serial and Version Numbers	43
Table 17	Onshore System Part, Serial and Version Numbers	43

1 INTRODUCTION

During 1996 a series of flight trials was undertaken in the North Sea to examine the use of Differential Global Positioning System (DGPS) equipment as an approach aid for offshore installations. The flight trials had three basic objectives:

- (1) To acquire knowledge and experience to support the development of both generic, and DGPS-specific, airworthiness and operational requirements and associated advisory material, for the conduct of offshore approaches.
- (2) To quantify by scientific means the accuracy which may be achieved in a DGPS system operating to/from offshore platforms.
- (3) To assess the flyability of the system in the applicable environment.

The flight trials programme was undertaken by the Flight Systems and Measurement Laboratories (now incorporated into Cranfield Aerospace Ltd) of the College of Aeronautics, Cranfield University in the role of prime contractor on behalf of the UK Civil Aviation Authority.

Flight trials were performed using a Sikorsky S76C helicopter chartered by Cranfield from Bond Helicopters Ltd. The aircraft was fitted with a special purpose experimental DGPS installation which was complemented by additional recording equipment sited at fixed locations.

In the course of seven test flights totalling 36 hours, over 70 predefined manoeuvres were performed at a set of four offshore production platforms with differing topside layouts. At each platform, approach trajectories and guidance presentations based upon the use of DGPS data were evaluated by the trials team which comprised representatives from CAA, Bond and Cranfield.

Post-flight processing of the data recorded during each trial enabled an assessment to be made of the performance of the real-time airborne DGPS equipment, and an understanding to be gained of some of the issues likely to affect GPS performance in the offshore environment. The trials installation allowed a comparison to be made between two alternative sources of differential corrections and between receivers produced by two different manufacturers.

The Final Report on the trials programme consists of three volumes, of which this document ('Experimental Procedures') represents Volume 1. The three volumes are structured as follows:

Volume 1 (this document) contains a description of the three measurement systems employed and of the data recorded by each system, and includes details of the experimental procedures employed on each of the flight trials.

Volume 2 ('DGPS Equipment Performance') presents and discusses the results of a comparison between the real-time DGPS data and a 'truth' reference which was derived, using techniques described in the report, from post-processed GPS measurements. A discussion is included of various factors which were found to affect the availability and precision of the real-time DGPS data, and these results are summarised in the form of a series of conclusions and suggestions for future work.

Volume 3 ('DGPS Approach Guidance') describes how the approach guidance information was generated and presented to the aircraft pilots over the course of the trials programme. Details are presented of the offshore approaches which were undertaken using the experimental installation, together with a comprehensive discussion of the flyability results which includes a series of conclusions and suggestions for future work.

2 REFERENCES

- 1 ICD-GPS-200, 'NAVSTAR GPS Space Segment and Navigation User Interfaces', Arinc Research Corporation, 1997.
- 2 'RTCM Recommended Standards for Differential Navstar GPS Service', Radio Technical Commission for Maritime Services, 1998.
- 3 Helszajn J, 'Microwave Planar Passive Circuits and Filters', Wiley, 1994.
- 4 Williams DA, CoA-FS-96-416, 'Report on Initial Ground Trials', FSML, 1996.
- 5 Williams DA, CoA-FS-96-418, 'Report on Test Flight 1', FSML, 1996.
- 6 Williams DA, CoA-FS-96-422, 'Report on Test Flight 2', FSML, 1996.
- 7 Dodson K, Mortimer ND, Talbot N, FTR 9793E, 'Flight Test Report (Beatrice Field)', CAA, 1996.
- 8 Williams DA, CoA-FS-95-423, 'Note on Antenna Reception Properties', FSML, 1996.
- 9 Dodson KM, Stevens JRA, Talbot N, FTR 10215E, 'Flight Test Report (Longside)', CAA, 1997.
- 10 Williams DA, CoA-FS-96-426, 'Report on Test Flight 4', FSML, 1996.
- 11 Dodson KM, Stevens JRA, Talbot N, FTR 10216E, 'Flight Test Report (Piper Bravo)', CAA, 1997.
- 12 Williams DA, CoA-FS-96-427, 'Report on Test Flight 5', FSML, 1996.
- 13 Dodson KM, Stevens JRA, Talbot N, FTR 10217E, 'Flight Test Report (Tartan)', CAA, 1997.
- 14 Stevens JRA, CA/CSG/7047, 'Report on Test Flight 6', CAe, 1997.
- 15 Dodson KM, Stevens JRA, Talbot N, FTR 10218E, 'Flight Test Report (Buchan A)', CAA, 1997.
- 16 Stevens JRA, CA/CSG/7048, 'Report on Test Flight 7', CAe, 1997.

3 ABBREVIATIONS

ADI	Attitude Director Indicator
ARINC	Aeronautical Radio, Inc
baud	Information units per second
Bond	Bond Helicopters Ltd
C/A	Coarse/Acquisition
CAA	Civil Aviation Authority
CAe	Cranfield Aerospace Ltd
CDU	Control Display Unit
CEP	Circular Error Probable
Cranfield	Cranfield University, Cranfield Aerospace Ltd
CSI	Communication Systems International
dB	Decibel
DC	Direct Current
deg	Degree
DGPS	Differential Global Positioning System
DiffTech	Differential Technology Ltd
DME	Distance Measuring Equipment
DoD	Department of Defense
ECU	Electronic Computer Unit
EPA	Identifier for airborne GPS Ephemeris data
EPP	Identifier for platform GPS Ephemeris data
EPROM	Erasable Programmable Read-Only Memory
EPS	Identifier for onshore GPS Ephemeris data
FAA	Federal Aviation Administration
FP	Floating Point
fsd	Full Scale Deflection
FSML	Flight Systems and Measurement Laboratories
ft	Feet
FTE	Flight Test Engineer
g	Acceleration due to gravity
GD1	Identifier for MF-corrected Navstar GPS Navigation data
GD2	Identifier for UHF-corrected Navstar GPS Navigation data
GD3	Identifier for MF-corrected Trimble GPS Navigation data
GPS	Global Positioning System
H-field	Magnetic field
HSI	Horizontal Situation Indicator
Hz	Hertz
IF	Intermediate Frequency
IFR	Instrument Flight Rules
ILS	Instrument Landing System
kg	Kilogram
kt	Knot
lb	Pound
L-band	Region of electromagnetic spectrum around 1.5GHz
LED	Light Emitting Diode
L1	GPS Link 1 Frequency (1575.42 MHz)
m	Metre
Mbit	Megabit
Mbyte	Megabyte
MF	Medium Frequency
MSK	Minimum Shift Keying

msl	Mean Sea Level
NAV	Navigation
Navstar	Navstar Systems Ltd
nm	Nautical Mile
NV1	Identifier for Aircraft data
OS	Ordnance Survey
PC	Personal Computer
PCMCIA	Personal Computer Memory Card Industry Association
PDOP	Position Dilution of Precision
ppm	Parts Per Million
PRN	Pseudo-Random Noise (GPS Satellite Identifier)
rad	Radian
Radalt	Radio altimeter
ref	Reference
RF	Radio Frequency
RMS	Root Mean Square
RNAV-2	Racal Avionics Area Navigation System 2
RS232	Electronics Industry Association Recommended Standard 232
R/T	Radio Telephony
RTCM	Radio Technical Commission for Maritime Services
RTCM-SC104	RTCM Special Committee Number 104
RTM	Identifier for MF RTCM Correction data
RTU	Identifier for UHF RTCM Correction data
s	Second
SA	Selective Availability
TRA	Identifier for airborne Truth GPS receiver data
Trimble	Trimble Navigation Ltd
TRP	Identifier for platform Truth GPS receiver data
TRS	Identifier for onshore Truth GPS receiver data
TSIP	Trimble Standard Interface Protocol
TSO	Technical Standard Order
UHF	Ultra High Frequency
UK	United Kingdom
US	United States
UTC	Universal Time Co-ordinated
V	Volt
VHF	Very High Frequency
VOR	VHF Omni Range
W	Watt
WGS84	World Geodetic System 1984
λ	Wavelength
Ω	Ohm
1PPS	One Pulse-Per-Second
2-D	Two dimensional
3-D	Three dimensional

4 TRIALS AIRFRAME AND AIRBORNE EQUIPMENT.

A Sikorsky S76C helicopter, registration G-SSSC (Figure 7, page 51), was employed as the trials airframe for the offshore DGPS test flights.

This aircraft, which is fully equipped for UK offshore support operations, is operated by Bond Helicopters Ltd from their base at Aberdeen (Dyce) airport. The airborne equipment installation, described in detail in this section, was designed to facilitate rapid installation onto and removal from the aircraft. This permitted the DGPS test flights to be undertaken at intervals over a period of several months during spring, summer and autumn of 1996, with the aircraft resuming its normal intensive schedule of offshore flights during the intervening periods.

Table 1 presents a summary of the aircraft technical specifications.

Fuselage dimensions	13.2 × 2.1 × 4.0 m
Main rotor	Four bladed, 13.4m dia
Tail rotor	Four bladed, 2.4m dia
Engine type	2 off Turbomeca Arriel 1s1
Maximum take-off weight	11,700lb
Empty weight, offshore equipped (without DGPS equipment)	7,400lb
Crew (offshore operations)	2
Passenger capacity	12
Fuel capacity	2,200lb
Maximum range	460nm plus IFR reserves
Best range speed	140kt

Table 1 S76C G-SSSC Technical Specifications (source: Bond Helicopters Ltd)

The S76C is considered to be representative of the small- to medium-size helicopters currently in use for North Sea offshore support operations. The aircraft incorporated the latest technology avionics and cockpit instrumentation which was of considerable benefit to the execution of the trials programme.

The principal items of cockpit avionics and instrumentation fitted to the aircraft, and their respective locations, are shown in Table 2 and on Figure 8 (page 51).

Number	Description	Type
2	VHF Navigation receiver (VOR/ILS)	Collins VIR 32
2	VHF Communication receiver	Collins VHF 22
1	DME	Collins DME 32
1	Transponder	Collins TDR 90
1	Decca Navigator	Racal-Decca Mk32
1	Area Navigation System	Racal RNAV-2
1	Radio Altimeter	Collins ALT 50
1	Autopilot (4-axis)	Honeywell SPZ 7600
1	Weather Radar	Bendix RDR 1400
2	Attitude Director Indicator (ADI)	Honeywell AD 650
2	Horizontal Situation Indicator (HSI)	Astronautics

Table 2 S76C G-SSSC Principal Avionic Equipment (source: Bond Helicopters Ltd)

In order to support the programme of DGPS test flights, a series of aircraft modifications was undertaken to support the installation of a DGPS Trials Pallet in the rear baggage bay (Figure 9, page 52). These modifications included the provision of power supply wiring, signal interconnections with existing avionic equipment, and the installation of additional antennas and associated RF cabling.

Aircraft modifications were performed by engineering staff from Bond whereas the DGPS Trials Pallet was designed, constructed and tested at Cranfield prior to being released, fully assembled and tested, to Bond for installation on the aircraft.

The locations of the additional antennas (depicted in Figure 7, page 51) were determined by Bond, in consultation with Cranfield. The experimental nature of the installations was such that standard design schemes, or details of approved antenna positions, were not generally available from the aircraft manufacturer to assist with this design process.

Carriage of the trials equipment involved an additional weight penalty of some 35kg (75lb). The trials pallet, and some of the antennas, were removed from the aircraft during the intervening periods between test flights allowing it to resume normal revenue-earning service.

All of the aircraft modifications were performed under CAA design approvals held by Cranfield and Bond, and were approved by the CAA on the basis that the additional equipment was to be used only for experimental test flights and not for normal transport operations. The test flights were performed under the aircraft's normal Transport (Passenger) Category Certificate of Airworthiness.

The modifications undertaken for the trials programme provided the aircraft, once the DGPS pallet had been installed and configured, with the following capabilities:

- (1) Three GPS receivers capable of determining real-time differentially corrected navigation solutions. The configuration of each receiver was different, allowing comparisons to be made between the use of two alternative sources of differential corrections, and between GPS equipment from two different manufacturers.
- (2) An independent GPS receiver configured to provide raw satellite code and carrier phase measurements for later processing into a 'truth' position solution against which the performance of the real-time GPS equipment could be compared.
- (3) An L-band antenna system capable of supporting all of the on-board GPS receivers.
- (4) Two radio receivers and associated antenna installations configured to receive differential GPS corrections transmitted by two different methods.
- (5) A data processing and recording system configured to record information output by each of the on-board GPS receivers, together with selected parameters derived from other aircraft systems.
- (6) A data processor capable of generating the data required to drive the aircraft cockpit displays, using the real-time DGPS solution data. The approach trajectory profile was defined by parameters entered into the system in flight.

Figure 1 shows, in block diagrammatic form, the additional items of equipment carried on the test flights together with the related RF, data and signal interconnections. Power supplies to the trials pallet have been omitted from the diagram to improve clarity: these were derived from the aircraft non-essential 28VDC bus via dedicated cockpit circuit breakers, and enabled the equipment to remain powered without interruption throughout the engine start and shutdown sequences.

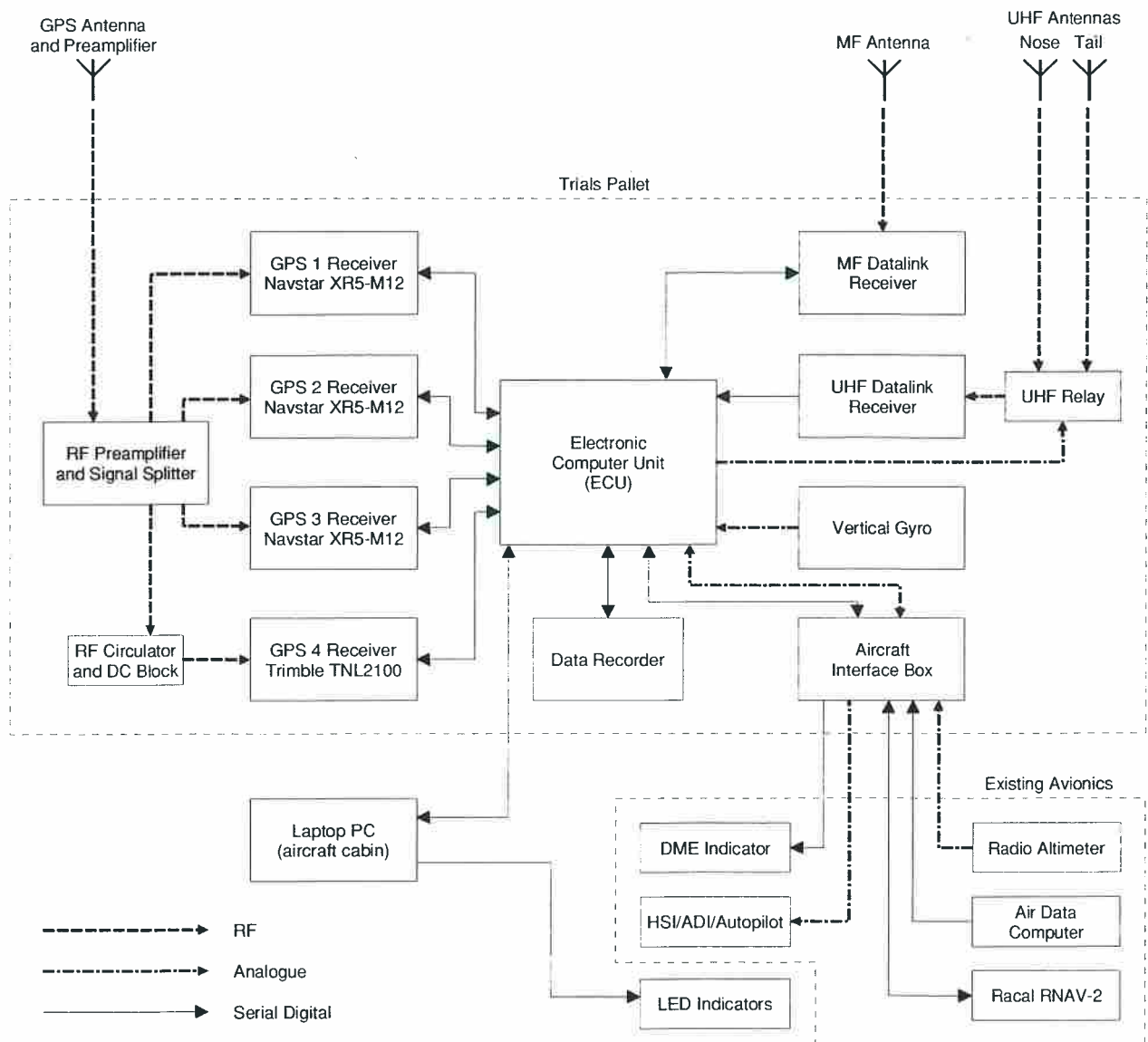


Figure 1 Aircraft Trials Equipment Installation

4.1 GPS Antenna

GPS satellite signals were received via an Aeroantenna Technology model AT575-12 antenna mounted on the top of the aircraft tail fin. This is a standard right-hand circularly polarised GPS antenna, incorporating an RF preamplifier powered from a 12V DC supply fed via the antenna cable. The amplifier possessed a nominal gain of 26.5dB at the GPS L1 centre frequency of 1575.42MHz.

In this location (Figure 10, page 52) the GPS antenna was above the level of the main rotor disc but was immediately adjacent to the tail rotor, and to an anticollision light and a VHF transmit/receive antenna. The antenna base and its mounting fairing were electrically bonded to the top of the tail fin.

Although no specific requirements are defined by the manufacturer, the AT575-12 antenna is normally used with a ground plane of at least 20cm diameter which is considerably greater than the available width at the top of the tail fin. A number of alternative mounting locations were considered, some of which would have offered the opportunity to employ a larger ground plane, but were rejected due to inaccessibility during installation and/or proximity to the main rotor.

Approximately six metres of low-loss RF cabling (type RG400) connected the antenna to the trials pallet.

4.2 RF Preamplifier and Signal Splitter

Signals received from the GPS antenna were provided with additional amplification by means of a 20dB low-noise amplifier supplied by Navstar Systems Ltd. This amplifier was not installed until midway through the trials programme for the reasons outlined in section 4.4.

In order to divide the received (and amplified) RF signal equally between the four GPS receivers a passive signal splitter, also supplied by Navstar Systems Ltd, with one input and four output ports was installed immediately following the preamplifier.

The signal splitter employed a series of Wilkinson dividers (ref 3), each of which consists of two quarter-wavelength transmission lines with characteristic impedance $\sqrt{2}$ times the input/output impedance (50Ω in this application) whose 'far' ends are interconnected by a pure resistance with value twice the input/output impedance.

The circuit has the property that the three ports are matched and that the power at the input port is divided equally between the output ports with identical phase lag.

The Navstar splitter contained three such Wilkinson circuits, with the second and third connected to the two outputs of the first so as to provide four output ports. The splitter was constructed using microstrip transmission lines on a PCB substrate, using the arrangement shown in Figure 2. Surface mounted 100Ω resistors were employed to interconnect the output of each transmission line pair.

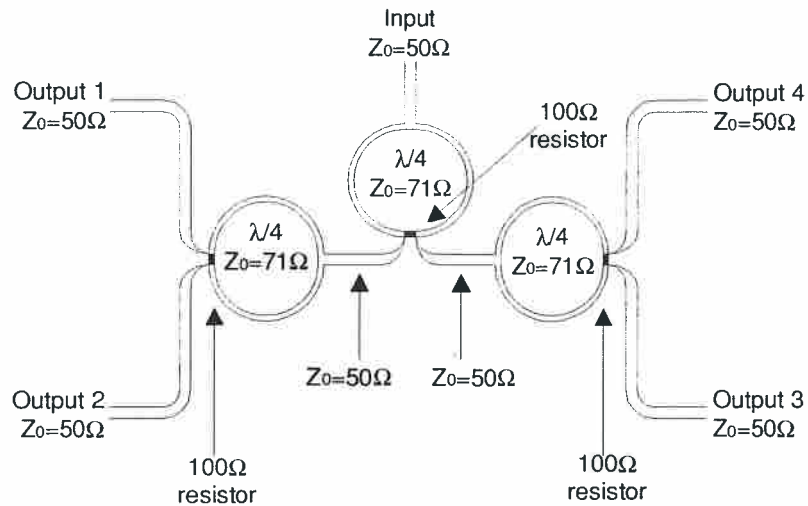


Figure 2 Microstrip Implementation of 4-Output Wilkinson Divider (DC blocking components omitted)

Additional components, not shown on the diagram, were included to provide DC blocking between each of the network terminals. These were necessary in order to prevent unwanted interactions between the antenna preamplifier supply voltages which were present on the input of each GPS receiver. With DC blocking in place there was no adverse effect upon the operation of the individual receivers.

4.3 GPS 1, 2 and 3 (Navstar XR5-M12)

Three out of the four GPS receivers used for the airborne installation employed identical hardware, but with each receiver configured for a different function. This configuration was accomplished partly through a software-based setup held in internal non-volatile memory, and partly by means of slightly differing data connections appropriate to the function of each receiver.

The receiver used was the XR5-M12 produced by Navstar Systems Ltd. The XR5-M12 is a ruggedised GPS 'engine' constructed to US DoD standards and intended for use in a wide variety of civil and military applications. The receiver contains no built-in display or control facilities but provides for communications with a host computer via a number of serial data ports.

The XR5-M12 uses only the GPS L1 C/A code signal and is capable of independently tracking up to twelve satellites simultaneously (thereby typically allowing all visible satellites to be tracked concurrently).

The XR5-M12 is capable of accepting differential corrections in RTCM SC-104 format (ref 2) and of providing a differentially-corrected position solution. In addition, it is capable of performing and outputting measurements on the satellite carrier phase (integer and fractional portions of carrier cycles received) in addition to the C/A pseudorange-based measurements.

Position solutions output by the XR5-M12 are computed using data from up to five satellites at any given time, the receiver automatically selecting its preferred set of satellites on a continuous basis. In the event that only three satellites are usable, the

receiver will attempt to compute a two-dimensional position solution by retaining its last known altitude estimate.

The manufacturer's performance specifications for the XR5-M12 are listed in Table 3.

Receiver	Twelve channel C/A code, L1 frequency
Satellites	Up to 12 satellites tracked
Accuracy	Positional: 15m RMS (PDOP<3) * Differential mode: 1-3m CEP (PDOP≤3) * Velocity: 0.3m/s (PDOP<3) *
Update rate	Status message output 4 times a second
Velocity	Maximum speed Mach 2
Acceleration	Maximum acceleration 6g, jerk 4g/s
1 PPS	±50ns *
Time to first fix	30s (with current ephemeris)

* subject to the US DoD policy on Selective Availability

Table 3 Manufacturer's Declared Performance for Navstar XR5-M12

Whilst not intended specifically for civil aviation applications, XR5-M12 receivers had previously been successfully employed on a variety of fixed and rotary-wing aircraft (both civil and military), and the unit was felt to be representative of a typical low to medium cost C/A receiver. In addition, a considerable amount of advice and information on the internal operation of the receiver was provided by the manufacturer throughout the course of the trials programme.

Of the three Navstar GPS receivers used in the airborne installation, the first was configured to operate in stand-alone navigation mode (i.e. no differential corrections were applied to the receiver) and to output at a 1Hz rate its position/velocity/time solution and status together with code and carrier phase measurements for all satellites in view. Data recorded from GPS receiver 1 was used, in combination with similar data logged on the target platform and at an onshore location, to determine a 'truth' position history of the aircraft using carrier-phase post flight analysis software. As a result, this unit is referred to as the 'truth' aircraft receiver.

The second Navstar GPS receiver was provided (via an RS232 datalink operating at 4800 baud) with RTCM format differential corrections supplied by the aircraft MF datalink receiver (section 4.6) and was configured to output its position/velocity/time solution and status information at a 1Hz rate.

The third Navstar GPS was also provided with 4800 baud RS232 differential corrections in RTCM format, but supplied by the aircraft UHF datalink receiver

(section 4.7). It was configured to output position/velocity/time and status information in an identical manner to the MF-corrected GPS receiver 2. This receiver was included to enable a direct comparison to be made between operations using two different sources of RTCM corrections.

Each receiver communicated with the Electronic Computer Unit (ECU, section 4.8) via RS232 serial datalinks operating at 9600 baud, using Navstar's proprietary Data Monitor format.

4.4 **GPS 4 (Trimble TNL-2100)**

The fourth GPS receiver used on the airborne installation was a TNL-2100 unit produced by Trimble Navigation Ltd. The receiver was included in order to provide a comparison between the performance of receivers from two different manufacturers in an otherwise identical environment.

The TNL-2100 is intended specifically for civil aviation applications and provides a series of navigation, waypoint entry and flight planning facilities via a two-line LED display and front-panel controls.

For the DGPS flight trials programme, the front panel facilities were ignored and communication occurred directly with the receiver's internal navigation processor. This was connected to the ECU via an RS232 serial datalink operating at 9600 baud, using Trimble's proprietary TSIP protocol, and was configured to output the receiver's position/velocity/time solution and status information at a 1Hz rate.

Trimble produce a version of the TNL-2100 receiver, known as the TNL-2100T, which is compliant with the FAA specification TSO-C129 but which is not, however, capable of operating in a differentially-corrected mode. In order to allow the performance of the TNL-2100 to be compared directly against that of the Navstar receiver when operating in differential mode, the trials used a specially modified version of the receiver which is otherwise identical to the TNL-2100T but which possesses the capability of accepting differential corrections in RTCM-SC104 format.

The TNL-2100 was provided with RTCM format corrections from the aircraft MF receiver (section 4.6) via an RS232 datalink operating at 4800 baud.

The TNL-2100 tracks only the GPS L1 C/A code signal and contains six independent tracking channels: if more than six satellites are visible, the receiver appears to attempt to track more than six by employing a multiplexing technique on certain of the channels.

Position solutions output by the TNL-2100 are computed using data from up to four satellites at any given time, the receiver automatically selecting its preferred set of satellites on a continuous basis. In the event that only three satellites are usable, the receiver will attempt to compute a two-dimensional position solution by retaining its last known altitude estimate.

The manufacturer's performance specifications for the TNL-2100 are listed in Table 4.

Type	L1 frequency, C/A code six-channel receiver, continuous all-in-view tracking
Acquisition time	1.5 to 3.5 minutes
Position update rate	Once per second
Dynamics	800kt, 2g (tracking)
Accuracy	Position: 15m RMS * Velocity: 0.1kt steady-state * Altitude: 35m RMS * (msl) Time: UTC to nearest μ s *

* Selective Availability not implemented

Table 4 Manufacturer's Declared Performance for Trimble TNL-2100

A number of problems were experienced with the Trimble receiver during the trials programme which precluded its use for a significant number of the test flights. Some of the difficulties were compounded by the fact that the receiver was not available for use until very shortly before the first flight trial, as a result of the extended length of time involved in procuring the specially modified unit.

- (1) The receiver was initially supplied with incorrect firmware installed.

Once the problem had been identified, the manufacturer supplied a replacement EPROM module for installation into the receiver.

- (2) The signal level provided to the receiver by the initial design of the airborne system installation proved to be insufficient to allow the receiver to operate correctly.

This problem was traced to the fact that the Trimble antenna, which is normally used to supply GPS signals to the TNL-2100 receiver, provides a significantly increased level of amplification compared to the Navstar antenna and splitter combination which was in use on the trials aircraft.

At the suggestion of Navstar, this problem was resolved by installing an additional 20dB gain preamplifier immediately ahead of the signal splitter, which would apparently have no detrimental effect upon the operation of the Navstar receivers.

- (3) With the TNL-2100 receiver operating, it was discovered that the XR5-M12 receivers were unable to maintain satisfactory satellite lock. The problem disappeared if the TNL-2100 was switched off.

Investigation using a spectrum analyser revealed that a spurious RF signal was being continuously output on the TNL-2100 receiver's antenna port. This signal, which was located at a frequency of just over 1571MHz (consistent with the use of a 4MHz IF frequency within the Trimble receiver), was sufficient to inhibit the tracking functions of the XR5-M12 receivers to which the TNL-2100 was indirectly connected by means of the antenna splitter.

The intensity of the 1571MHz interfering signal was greatly in excess of the signal rejection characteristics specified in TSO-C129 and consequently it was concluded that the problem would not necessarily be confined to the use of a Navstar receiver.

Despite several attempts to communicate with Trimble with regard to resolving this problem, no relevant response was forthcoming. However, some experimentation identified that a satisfactory solution was to introduce an RF circulator (which operates as a one-way attenuator of RF energy) into the TNL-2100's antenna input connection. With the circulator in place, the spurious 1571MHz signal was attenuated sufficiently to remove any observable interference effects.

- (4) The TNL-2100's internal configuration settings became corrupted at one stage, preventing the input RTCM corrections from being decoded and applied.

The source of the event which was the cause of the corruption was never established. Attempts at communicating with the manufacturer to resolve the problem eventually produced a solution, which involved selecting a 'hidden' key sequence on the receiver's front panel. This procedure, which was not publicised in any of the available technical documentation, sets the receiver into an internal reconfiguration mode to allow the operator to modify the RTCM settings.

4.5 **RF Circulator and DC Block**

These items were introduced in order to resolve the Trimble receiver interference problem which was described in the previous section.

RF signals from the fourth port of the splitter unit were passed via a Microtek model IL14161 circulator before reaching the TNL-2100 receiver's antenna input. The circulator provided isolation of around 20dB in the reverse direction, sufficient to remove the effects of the interfering signal, with a forward direction loss of only around 0.5dB.

Owing to the presence of a DC bias voltage on the TNL-2100's antenna port, and to the low DC resistance of the circulator, it was found necessary to install a DC blocking capacitor between the two. Since there was already a DC block present at the output of the signal splitter, this ensured that the circulator was provided with DC isolation in both directions but had no effect upon the passage of RF signals.

4.6 **MF Datalink Receiver and Antenna**

A Communication Systems International (CSI) MBX-2 DGPS Radio Beacon Receiver was used to receive and decode differential corrections broadcast from marine radiobeacons on the Medium Frequency (MF) band.

Marine radiobeacons broadcasting DGPS corrections normally do so by transmitting a Minimum Shift Keying (MSK) encoded bit stream on a side band of the main carrier frequency. The MBX-2 is capable of accepting MSK rates of 25, 50, 100 or 200 bits-per-second from beacons operating on frequencies of between 283.5 and 325.0 kHz, and will decode the transmitted data to produce RTCM format differential corrections on its RS232 output port.

Prior to 1998, the marine radiobeacons in the United Kingdom and Ireland transmitted encrypted differential corrections to allow the service provider to recoup the operating costs via licence fees. The MBX-2 unit used for the trials programme incorporated the appropriate decryption software to enable these corrections to be utilised.

DGPS correction messages received by the MBX-2 were transmitted at 4800 baud to the ECU where they were decoded for recording purposes, and retransmitted to the two MF-corrected GPS receivers (GPS 2 and GPS 4).

Selection of the desired MF station could be accomplished either via the front panel of the MBX-2 receiver, or via the receiver's RS232 input port to which tuning messages could be transmitted by the ECU. In the course of the trials programme it was discovered that, owing to a feature of the MBX-2 software, it was not possible to change the receiver operation between non-encrypted (mainland European) and encrypted (UK/Ireland) beacons without access to the front panel. Owing to the location of the receiver in the rear baggage bay, this had the unfortunate effect of preventing this form of selection whilst the aircraft was in flight.

The receiver was also arranged to report its current operating frequency, signal strength, and signal-to-noise ratio via the RS232 connection at a 1Hz rate.

A CSI MBL-1 H-field loop antenna was fitted to the aircraft (Figure 11, page 53) on the underside of the tail boom, for operation with the MBX-2 receiver. This antenna is housed in a sealed composite enclosure, with no requirement for a ground plane, although the antenna mounting points were electrically bonded to the aircraft structure.

4.7 UHF Datalink Receiver, Relay and Antennas

A Navstar Systems DR5-96S receiver was used to receive and decode differential corrections transmitted on the Ultra High Frequency (UHF) band from the dedicated DGPS reference station used for the flight trials (section 5).

The DR5-96S is supplied in a similar enclosure to an XR5-M12 receiver and the two units are designed for operation together as an integrated DGPS package. The unit may be selected to operate on a frequency in the range 450 to 470 MHz, with data transmitted at either 9600 or 4800 bits-per-second.

DGPS correction messages received by the DR5-96S were transmitted at 4800 baud to the ECU where they were retransmitted to the UHF-corrected GPS receiver (GPS 3).

Selection of the receiver's operating frequency and modulation parameters was accomplished prior to flight by using a Navstar-supplied programming adapter and PC software. Once loaded into the receiver, the settings were retained in non-volatile memory.

A dedicated UHF frequency of 455.500 MHz was assigned by the UK Radiocommunications Agency and CAA for the purposes of the flight trials. This frequency was assigned specifically for the offshore trials, on the understanding that it would not be possible to provide any guarantee as to its future availability following completion of the trials programme.

A separate frequency of 460.4875 MHz was assigned by the Radiocommunications Agency for use at Cranfield during system development and testing. Neither frequency was expected to give rise to any harmonic interference problems with the GPS L1 carrier frequency of 1575.42MHz.

In order to eliminate any problems due to antenna masking by the airframe, two quarter-wave stub antennas were installed on the aircraft, one under the tail boom (Figure 11, page 53) and the second on the nose just forward of the cockpit windshield (Figure 12, page 53). In both of these locations, the surrounding structure was largely of composite construction and both installations incorporated a small ground plane, approximately 8cm square, which was electrically bonded to the aircraft structure.

Selection between the antennas was accomplished using a double-pole coaxial RF relay, which could be commanded by the ECU to connect one or the other antenna to the DR5-96S receiver input.

4.8 **Electronic Computer Unit (ECU)**

The purpose of the ECU, which was designed and built at Cranfield specifically for the DGPS trials programme, was to act as the central data acquisition and processing facility for all of the airborne trials equipment. The unit contained a high speed microprocessor running dedicated embedded software, together with a series of interface modules for communication with external devices. The interface capabilities of the unit were as follows:

- (1) An analogue-to-digital converter supporting up to eight analogue input channels, and their associated signal conditioning, with a sample rate of up to 1kHz.
- (2) A digital-to-analogue converter supporting up to eight analogue output channels with associated signal conditioning.
- (3) Eight bidirectional RS232 serial ports.
- (4) Eight ARINC 429 aircraft databus input ports.
- (5) Two ARINC 429 aircraft databus output ports.
- (6) Six discrete input port bits.
- (7) Four discrete output port bits.
- (8) A bidirectional 2.5Mbit/s high speed serial port.

Embedded software for the ECU was stored on EPROM modules housed on the microprocessor board. Software could also be uploaded to the ECU from the trials laptop PC (section 4.12).

The aircraft system ECU, in addition to providing a central data acquisition facility which obtained information from the other aircraft systems and handled the reformatting of data for recording, was also able to generate synthetic aircraft guidance information using real-time DGPS data. These two facilities were essentially independent, although the various software modules involved were necessarily closely interlinked.

Section 7 of this volume describes in detail the data acquisition and recording functions performed by the ECU software. The aircraft guidance functions, which were developed and extended in the course of the trials programme, are described in Volume 3 of this report.

4.9 **Data Recorder**

A microprocessor-based data recorder, designed and constructed at Cranfield, was connected to the ECU's high-speed serial port.

Data recording was performed using a PCMCIA format hard disc storage module with a total storage capacity of 130Mbyte, which was inserted into the Data Recorder prior to each trial. On completion of a flight the module was removed and inserted directly into a PC to offload the stored data for analysis.

4.10 **Vertical Gyro**

A free vertical gyro was installed on the trials pallet to enable measurements to be made of the aircraft attitude in the pitch and roll axes, since this information was not readily available from any other source.

Analogue signals representing pitch and roll attitude were connected directly to the ECU and the unit was calibrated to an accuracy of better than 1° within the range $\pm 40^\circ$ of pitch and $\pm 80^\circ$ of roll.

4.11 **Aircraft Interface Box**

A custom-designed interface box was used to provide various buffering and amplification functions between the ECU and the existing aircraft systems to which the trials pallet was connected. In particular, the interface box provided isolation between the trials equipment and certain flight-critical systems such as the radio altimeter.

4.12 **Laptop PC**

A cabin mounted laptop PC running dedicated software was used during each flight trial to monitor the operation of the trials pallet systems, and to provide various control functions. In particular, the PC was used to set the parameters for each of the approaches performed using the ECU's built-in guidance facilities, described in Volume 3 of this report.

4.13 **Radio Altimeter**

An analogue signal from the aircraft radio altimeter was connected, via the Aircraft Interface Box, to one of the ECU analogue inputs.

This enabled measurements to be made of the current aircraft radio altitude, to an accuracy of around ± 10 ft. Radio altitude was one of the primary parameters used in the generation of DGPS approach guidance and was continuously recorded.

4.14 **Air Data Computer**

An ARINC 429 databus link from the aircraft Air Data Computer was connected to one of the ECU ARINC 429 inputs.

This enabled the ECU to determine the pressure altitude and true air speed for recording purposes.

4.15 **Racal RNAV-2**

The S76C was fitted with a sophisticated area navigation system known as the RNAV-2.

In the basic aircraft configuration, the RNAV-2 provided the crew with a waypoint-based navigation facility which was primarily based upon data from the Decca Navigator Mk32 receiver. Navigational information could be selected for display on the RNAV-2 Control Display Unit (CDU) screen and as an overlay on the weather radar display, and could also be selected onto either or both pilots' primary navigation indicators (HSI and ADI).

During the test flights the RNAV-2 was also supplied with data derived from the trials DGPS equipment, using an ARINC 429 output from the ECU which was fed to the RNAV-2's normally unused GPS input. This enabled the pilot to select between the use of Decca Navigator and GPS data for navigation purposes via the RNAV-2 CDU, and also provided a very basic monitoring capability in case of failure of the cabin laptop PC.

ARINC 429 data from the RNAV-2 was received by the ECU, allowing the aircraft heading to be determined for recording purposes. Magnetic heading was derived from the aircraft slaved gyro compass system, and corrected to true heading by the RNAV-2 prior to transmission.

Throughout the trials programme the RNAV-2 was operated using the standard operating software and navigational database supplied by Racal Avionics.

4.16 **DME Indicator**

An RS232 serial output from the ECU was used, via an interface converter located in the Aircraft Interface Box, to drive the central cockpit-mounted DME indicator.

As part of the aircraft modifications the pilot was provided with a selector switch (inhibited in normal flight operations) for selection between the display of normal DME range on the central indicator, and information derived from the DGPS trials equipment.

With the selection switch in the 'GPS ON' position, normal DME indications were replaced by data generated by the ECU approach guidance software (described in Volume 3). This included not only the range to a defined waypoint but also a three-character mnemonic identifying the current approach segment, which was displayed in place of the normal DME ident.

4.17 **HSI/ADI/Autopilot**

The selector switch described in the previous section had a dual function in that, whenever it was selected to the 'GPS ON' position, the output indications from the No. 1 VHF navigation receiver were automatically replaced by indications generated within the DGPS system ECU.

This enabled any cockpit system which was capable of using data from the No. 1 NAV receiver to be selected to use data generated by the DGPS system instead. The systems in question were the horizontal situation indicators (HSI), attitude director indicators (ADI) and the aircraft autopilot.

The ECU analogue and discrete outputs were arranged, by means of buffer circuitry in the Aircraft Interface Box, to generate simulated Localiser (horizontal), Glide Slope (vertical), and associated warning flag signals which were compatible with those normally output by the No. 1 NAV receiver and which were therefore capable of being used to drive the HSI, ADI and autopilot.

This feature allowed the DGPS equipment to output fully synthetic approach guidance information which could then be displayed and used by the pilots in an identical manner to standard ILS indications.

4.18 **LED Indicators**

During the latter stages of the flight trials programme the need for the handling pilot to be provided with an indication of the present approach segment and status during synthetic DGPS approaches had become clear.

In order to avoid the need to undertake aircraft modifications, a small module consisting of four coloured LED indicators was constructed so as to be readily affixed within the pilot's instrument scan using hook-and-loop fasteners (Figure 13, page 54).

The drive signals for the LEDs were derived from the cabin laptop PC via its (otherwise unused) printer port. Minor modifications to the laptop and ECU software were required.

5 PLATFORM SYSTEM

Whilst the trials aircraft was performing flight manoeuvres at each offshore structure, a GPS reference and recording system was sited and operated at a suitable fixed point on the 'target' platform. This unit provided the following facilities:

- (1) An independent GPS receiver configured to provide raw satellite code and carrier phase measurements for later processing into the aircraft truth position solution.
- (2) A second GPS receiver, and associated UHF transmitter, configured as an RTCM base station generating real-time differential corrections.
- (3) A data processing and recording system configured to record information output by each of the two GPS receivers.

The platform reference and recording system was housed in a free-standing aluminium enclosure (Figure 14, page 54) which could be readily carried on board the trials aircraft. This avoided the need to arrange separate transportation for the unit to and from each offshore platform visited.

The unit included its own power supply based upon sealed lead-acid batteries and was designed to comply with the requirements of the offshore operators relating to the use of electrical equipment in hazardous areas. External switches were provided to enable the unit to be switched on and off, and to isolate the UHF datalink transmitter.

Figure 3 shows the components of the platform system in diagrammatic form, omitting the power supplies for clarity.

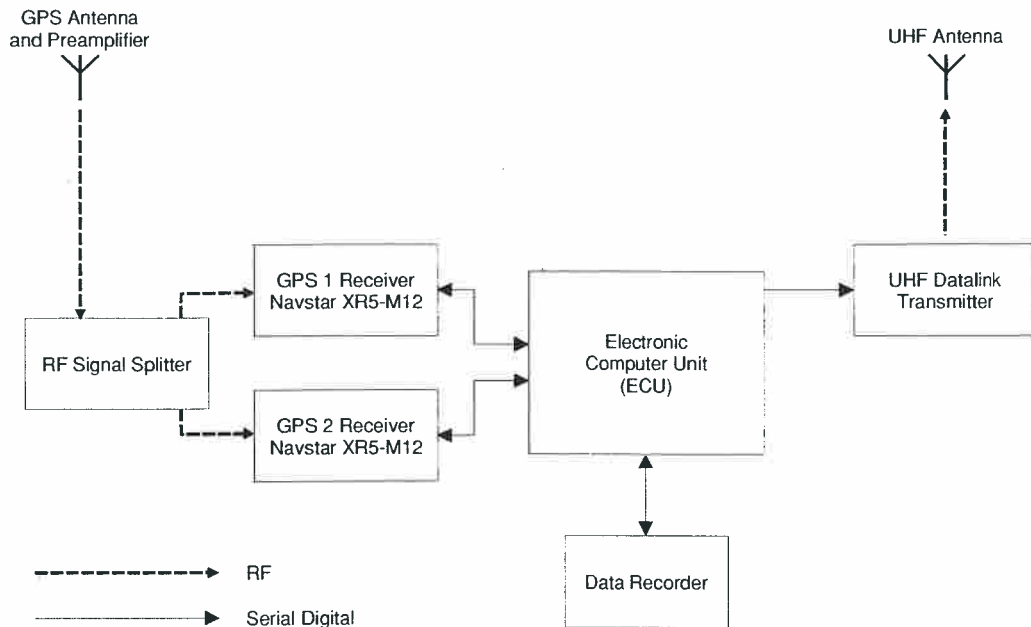


Figure 3 Platform System Equipment

5.1 **GPS Antenna**

GPS satellite signals were received via an Aeroantenna Technology model AT575-12 antenna, identical to the antenna used on the aircraft installation, and which was mounted centrally on the top surface of the platform system enclosure which acted as an extended ground plane for the antenna.

5.2 **RF Signal Splitter**

In order to divide the received RF signal equally between the two GPS receivers, a four-output passive signal splitter identical to that used on the aircraft installation was employed. The two unused outputs were left terminated.

5.3 **GPS 1 and 2 (Navstar XR5-M12)**

Two GPS receivers were employed within the platform system, both being Navstar XR5-M12 units identical to those used on the aircraft installation. The two receivers were configured for different functions.

The first receiver was configured to operate in stand-alone navigation mode (i.e. no differential corrections were applied to the receiver) and to output its position/velocity/time solution and status together with code and carrier phase measurements at a 1Hz rate for all satellites in view. This information was used along with similar information logged by the airborne and onshore systems to determine a truth position history for the aircraft. This receiver communicated with the Electronic Computer Unit (ECU) via an RS232 serial datalink operating at 9600 baud, using Navstar's proprietary Data Monitor format.

The second Navstar GPS receiver was set up to operate as an RTCM SC-104 differential base station, generating Type 1 and 2 corrections (ref 2) at a 1Hz rate. Corrections were output to the ECU for recording and onward transmission to the UHF transmitter via an RS232 datalink operating at 4800 baud. This receiver was required to be provided with an accurate estimate of its position in WGS84 co-ordinates in order to allow differential corrections to be determined.

5.4 **UHF Datalink Transmitter and Antenna**

A Navstar Systems DR5-96S transmitter was used to transmit the differential corrections generated by the second GPS receiver on the Ultra High Frequency (UHF) band.

The unit was effectively identical to that used on the aircraft installation, but was hardware configured for transmitter operation rather than for reception. Transmission power was approximately 2W (3dBW).

Selection of the receiver's operating frequency and modulation parameters was accomplished prior to flight by using a Navstar-supplied programming adapter and PC software. Once loaded into the receiver, the settings were retained in non-volatile memory.

A whip antenna, mounted in one corner of the platform system enclosure, was used to transmit the UHF corrections.

5.5 **Electronic Computer Unit (ECU)**

The platform system ECU was essentially identical to the unit used on the trials aircraft but operated with different software specific to the platform system recording task.

The data recording facilities provided by the ECU software are described in section 7.

5.6 **Data Recorder**

A data recorder identical to that used on the trials aircraft was connected to the ECU's high-speed serial port. Data was stored on an 85Mbyte PCMCIA hard disc module.

6 ONSHORE SYSTEM

To complement the aircraft and platform recording systems, a third reference system was sited and operated at a fixed onshore location whilst each offshore trial was being performed. This unit provided the following facilities:

- (1) An independent GPS receiver configured to provide raw satellite code and carrier phase measurements for later processing into the aircraft truth position solution.
- (2) A data processing and recording system configured to record information output by the GPS receiver.

The onshore recording system was located in an office environment and is shown in diagrammatic form in Figure 4.

Power supplies were derived from the mains via a low voltage adapter and are omitted from the diagram for clarity.

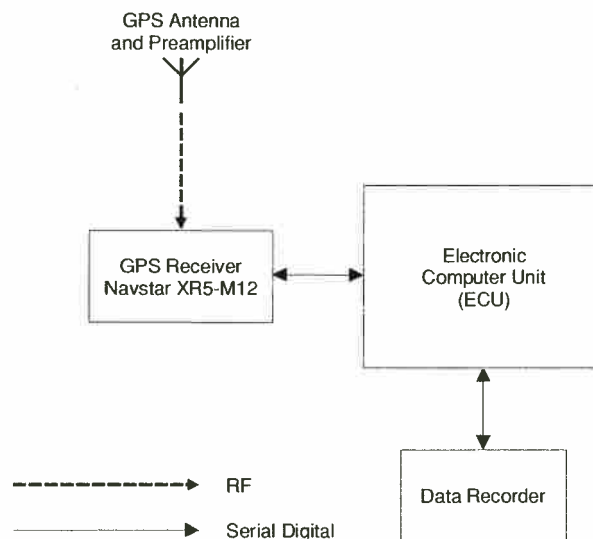


Figure 4 Onshore System Equipment

6.1 GPS Antenna

GPS satellite signals were received via an Aeroantenna Technology model AT575-12 antenna, identical to the antenna used on the aircraft installation, and which was mounted centrally on a metallic disc about 20cm in diameter which acted as a ground plane.

This assembly was located on the top of a metallic mast some 8m above the ground at the offices of Differential Technology Ltd (DiffTech) in Altens, to the south of Aberdeen city centre. This location was selected for the onshore system largely for practical reasons, such as the availability of personnel to switch on and monitor the system under the direction of the trials team, but also because it was believed that there was a lower probability of encountering interference sources than at the other locations (such as Aberdeen airport) which had been considered.

Figure 15 (page 55) shows the onshore system antenna installation, and the location of the DiffTech premises is shown on the map in Figure 16 (page 56).

Approximately fifteen metres of low-loss RF cabling (type RG58) were provided to interconnect the antenna with the GPS receiver.

6.2 **GPS Receiver (Navstar XR5-M12)**

A single GPS receiver was employed for the onshore system, being a Navstar XR5-M12 unit identical to those used on the aircraft installation and platform system.

The receiver was configured to operate in stand-alone navigation mode (i.e. no differential corrections were applied to the receiver) and to output its position/velocity/time solution and status together with code and carrier phase measurements at a 1Hz rate for all satellites in view. This information was used along with similar information logged from the airborne and platform systems to determine a truth position history for the aircraft. This receiver communicated with the Electronic Computer Unit (ECU) via an RS232 serial datalink operating at 9600 baud, using Navstar's proprietary Data Monitor format.

6.3 **Electronic Computer Unit (ECU)**

The onshore system ECU was essentially identical to the units used on the trials aircraft and platform system, but operated with different software specific to the onshore recording task.

The data recording facilities provided by the ECU software are described in section 7.

The unit, together with the onshore data recorder, was designed to be readily interchangeable with the similar units employed on the aircraft and/or platform systems in the event that a failure occurred. In this event, onshore data logging would have been performed using a desktop PC.

6.4 **Data Recorder**

A data recorder identical to those used on the trials aircraft and platform system was connected to the ECU's high-speed serial port. Data was stored on an 85Mbyte PCMCIA hard disc module.

7 DATA RECORDING

Each of the three data recording systems - aircraft, platform and onshore - included a pair of microprocessor-based units running custom software: the Electronic Computer Unit (ECU) and the Data Recorder.

The purpose of each ECU was to act as a central acquisition facility for all of the data which was required to be processed at that particular location, by means of a series of interconnections with each of the other subsystem units. Data to be recorded was generated within and transmitted by the ECU along the high speed link to the associated Data Recorder where it was stored without alteration on the PCMCIA hard disc module.

Although each of the three systems processed and recorded a different set of data, there proved to be sufficient similarity between the data formats to allow identical software to be utilised in each of the three Data Recorder units. Communications between each ECU and Data Recorder were confined to the transmission of data for recording in one direction, and to handshaking information in the other.

Data recording on each system was arranged to begin automatically when power was applied and to continue until power was removed, with all of the necessary setup tasks (such as initialising the data output specification for the GPS receivers) being performed autonomously by the ECU software. In the case of the aircraft and onshore recording systems, confirmation of correct operation could be achieved by means of a PC running diagnostic software. The nature of the platform reference system, however, was such that no action could be taken to rectify recording problems; hence the requirement for recording to proceed in a completely autonomous fashion.

7.1 Data Message Structure

The data recording scheme employed for the trials programme was based around sets of fixed-length messages.

Each individual message consisted of a fixed-length structure containing a consistent set of data items derived from one or more subsystems and output (typically) at a 1Hz rate. Lossless compression techniques were employed in order to reduce, as far as practicable, the overall message size.

Successive messages of the same type were assembled by the Data Recorder into a single data file, with each new message being appended to the end of the file immediately following its predecessor. Each system processed more than one type of output message and as a result a series of message files was generated within each Data Recorder.

Each set of message data files from a single recording session was automatically assigned a unique file name identifier, generated by the Data Recorder. The different message files within a recording session were identified by a series of three-letter file extensions.

A total of five distinct message formats (some of which were common to more than one message file) were employed and the structure of each message is defined later in this section. Tables 5, 6 and 7 list the message files recorded by each of the three systems, including in each case the message format used, the three-character file extension, and the source of the data included in the message.

Identifier	Message Format	Source	Update Rate
TRA	GPS Truth	GPS 1 (truth reference receiver)	1 Hz
EPA	GPS Ephemeris	GPS 1 (truth reference receiver)	Whenever an ephemeris update occurred
GD1	GPS Navigation	GPS 2 (MF-corrected Navstar real-time receiver)	1 Hz
GD2	GPS Navigation	GPS 3 (UHF-corrected Navstar real-time receiver)	1 Hz
GD3	GPS Navigation	GPS 4 (MF-corrected Trimble real-time receiver)	1 Hz
RTM	RTCM Correction	MF receiver data output	Whenever a new MF RTCM message arrived (typically every 5-6s)
NV1	Aircraft Data	Various (see section 7.6)	1 Hz

Table 5 Messages Recorded by Airborne Data System

Identifier	Message Format	Source	Update Rate
TRP	GPS Truth	GPS 1 (truth reference receiver)	1 Hz
EPP	GPS Ephemeris	GPS 1 (truth reference receiver)	Whenever an ephemeris updated occurred
RTU	RTCM Correction	GPS 2 (RTCM base station)	Whenever a new UHF RTCM message was generated (every 1s)

Table 6 Messages Recorded by Platform Data System

Identifier	Message Format	Source	Update Rate
TRS	GPS Truth	GPS truth reference receiver	1 Hz
EPS	GPS Ephemeris	GPS truth reference receiver	Whenever an ephemeris update occurred

Table 7 Messages Recorded by Onshore Data System

7.2 GPS Truth Message Format

Each of the three data recording systems included a Navstar GPS receiver configured to output code and carrier phase measurement data at a 1Hz rate. In each case the receiver in question was not supplied with differential corrections and accordingly operated in stand-alone navigation mode.

The information output by these receivers was processed following each flight by the truth reconstruction software described in Volume 2 of this report, which was capable of deriving an accurate estimate of the aircraft position history by comparing the data recorded on the aircraft with that obtained at a fixed location (platform or onshore) whose position was known.

An identical message format was employed to store the data output by each of the three truth GPS receivers. The three messages were distinguished by different file extensions: 'TRA' for aircraft receiver data, 'TRP' for platform receiver data, and 'TRS' for onshore data.

The information contained within the GPS Truth Message was as shown in Table 8. Where floating-point representation was used for the storage of data items, this was either double precision ('Double FP', accurate to better than one part in 10^{-15}) or single precision ('Single FP', accurate to better than one part in 10^{-7}).

Although the Navstar XR5-M12 receiver theoretically possessed twelve independent satellite tracking channels, data was only recorded from the first eleven channels. This constraint was imposed by the choice of Data Monitor output message utilised by the ECU for communication with the receiver (and recommended by the receiver manufacturer). The manufacturer stated that the receiver would never attempt to track more than eleven different satellites and that consequently no data loss would occur through the omission of the twelfth channel from the recording frame.

The receivers were configured to output a new set of data at one second intervals, at the start of the GPS second. Data was time-tagged (via the 'hhmmss' parameter) using the ECU's internal timing reference, described in section 7.7.

Data identifier	Number of data items	Description	Units	Resolution or FP format
hhmmss	1	UTC time-of-day (hours, minutes, seconds)	s	1s
mestim	1	Time-of-week when satellite measurements were taken	s	Double FP
mesckb	1	Receiver clock bias estimate for satellite measurement epoch	s	Double FP
nplat	1	Receiver latitude estimate	rad	12mm
nplon	1	Receiver longitude estimate	rad	≤12mm
npalt	1	Receiver altitude estimate	m	7.8mm
sltsv	11	Satellite PRN being tracked by each channel	1 to 32	n/a
sltazel	11	Satellite azimuth and elevation angles	deg	1 deg
iq11	11	Satellite measurement quality flag (0=no measurement, 4=code locked, 5=code and carrier locked)	n/a	n/a
ipr11	11	Satellite raw measured pseudorange	m	31mm
carcyc	11	Satellite carrier integer cycles counter	L1 cycles	1 cycle
carpha	11	Satellite carrier fractional phase	L1 cycles	1/65536 cycle
carlock	11	Number of satellite measurements since last detected cycle slip	s	0.25s
idr11	11	Satellite raw measured delta range	m/s	Single FP
npnedv	3	Receiver velocity estimates (north/east/down)	m/s	0.00391m/s
nknteh	1	Receiver estimated horizontal accuracy	m	0.0625m
nkntev	1	Receiver estimated vertical accuracy	m	0.0625m
nkntep	1	Receiver estimated 3-D positional accuracy	m	0.0625m
satlist	5	Satellite PRNs in use for navigation solution	1 to 32	n/a
gpsfix	1	Fix type (0=none, 1=2-D, 2=3-D)	n/a	n/a
swtow	1	GPS time-of-week	s	Double FP
icno	11	Satellite carrier-noise ratio	dB-Hz	1dB-Hz
idopp	11	Satellite raw measured doppler frequency	Hz	Single FP
pdopav	1	All-in-view PDOP	n/a	0.0625
prmadr	11	Satellite pseudorange minus accumulated delta range	m	16mm

Table 8 GPS Truth Message Format

7.3 GPS Ephemeris Message Format

The post-flight truth reconstruction software required, in addition to the raw satellite measurements contained within the GPS Truth Message structure, a valid set of ephemerides (orbital and clock parameters) for each satellite to be utilised during processing.

This requirement was satisfied by arranging for each of the data system ECUs to record a set of ephemeris parameters derived from its respective truth GPS receiver. New ephemeris data for a particular satellite was only stored whenever the ECU software observed a change in one or more of the ephemeris parameters reported by the receiver, an event which normally only occurred following the uploading of new data to the satellite by the GPS Control Segment at (typically) hourly intervals. As a

result, data was stored to the ephemeris file with a relatively slow rate, averaging around ten messages per hour.

An identical message format was employed to store the ephemeris data obtained from each of the three truth GPS receivers. The three messages were distinguished by means of the file extensions: 'EPA' for aircraft receiver data, 'EPP' for platform receiver data, and 'EPS' for onshore data.

The information contained within the GPS Ephemeris Message was as shown in Table 9. Definitions for the various satellite parameters are contained in ref 1. Data was time-tagged (via the 'hhmmss' parameter) using the ECU's internal timing reference, described in section 7.7. Where floating-point representation was used for the storage of data items, this was double precision ('Double FP', accurate to better than one part in 10^{-15}).

Data identifier	Description	Units	Resolution or FP format
hhmmss	UTC time-of-day (hours, minutes, seconds)	s	1s
swweek	Week number	week	1 week
ntxid	Satellite PRN to which ephemeris relates	1 to 32	n/a
ephsta	Satellite ephemeris status/source (0=invalid, 1=ephemeris, 2=almanac)	n/a	n/a
ephaf0	Satellite clock polynomial term a_{t_0}	s	Double FP
ephm0	Satellite ephemeris term M_0	rad	Double FP
ephe	Satellite ephemeris term e	n/a	Double FP
ephsqa	Satellite ephemeris term $(A)^{1/2}$	$m^{1/2}$	Double FP
ephw	Satellite ephemeris term ω	rad	Double FP
ephi0	Satellite ephemeris term i_0	rad	Double FP
ephom0	Satellite ephemeris term $(\text{OMEGA})_0$	rad	Double FP
ephomd	Satellite ephemeris term OMEGADOT	rad/s	Double FP
ephtgd	Satellite clock term T_{GD}	s	Double FP
ephaf2	Satellite clock polynomial term a_{t_2}	s/s^2	Double FP
ephaf1	Satellite clock polynomial term a_{t_1}	s/s	Double FP
ephcrs	Satellite ephemeris term C_{rs}	m	Double FP
ephmdn	Satellite ephemeris term Δn	rad/s	Double FP
ephcuc	Satellite ephemeris term C_{uc}	rad	Double FP
ephcus	Satellite ephemeris term C_{us}	rad	Double FP
ephcic	Satellite ephemeris term C_{rc}	rad	Double FP
ephcis	Satellite ephemeris term C_{is}	rad	Double FP
ephcrc	Satellite ephemeris term C_{rc}	m	Double FP
ephidt	Satellite ephemeris term IDOT	rad/s	Double FP
ephadc	Satellite clock parameter IODC counter	n/a	n/a
ephtoc	Satellite clock reference time t_{oc}	s	1s
ephtoe	Satellite ephemeris reference time t_{oe}	s	1s
ephfit	Satellite ephemeris fit interval (0=4hr, 1=6hr)	n/a	n/a
ephwno	Satellite ephemeris week number	week	1 week
ephacc	Satellite accuracy figure	0 to 15	n/a

Table 9 GPS Ephemeris Message Format

7.4 GPS Navigation Message Format

The aircraft trials instrumentation system incorporated three GPS receivers (GPS 2, 3 and 4) which were each configured to provide real-time differentially corrected position solutions. Data from these receivers was required both for use in real time by the ECU software modules which provided aircraft guidance facilities, and for recording purposes for use during post-flight analysis.

Data relating to the latest available position fix was extracted from each receiver at a 1Hz rate and recorded via the GPS Navigation Message format. The three receiver messages were distinguished by means of different file extensions: 'GD1' for the MF-corrected Navstar receiver, 'GD2' for the UHF-corrected Navstar receiver, and 'GD3' for the MF-corrected Trimble receiver.

The information contained within the GPS Navigation Message was as shown in Table 10. Data was time-tagged (via the 'hhmmss' and 'Time tag' parameters) using the ECU's internal timing reference, described in section 7.7. Where floating-point representation was used for the storage of data items, this was double precision ('Double FP', accurate to better than one part in 10^{15}).

The GD3 message was derived from the Trimble TNL-2100 receiver which employed a different serial interface protocol from that used by the Navstar receivers generating the GD1 and GD2 messages. As a result, and because the GPS Navigation Message was originally designed specifically for use with the Navstar equipment, it was not possible to extract and record the full set of parameters from the Trimble receiver. Where data was not available, null entries were made in the GD3 message frame and this is indicated in Table 10 via the 'Present in GD3?' column.

Data identifier	Number of data items	Description	Units	Resolution or FP format	Present in GD3?
hhmmss	1	UTC time-of-day (hours, minutes, seconds)	s	1s	Yes
Time tag	1	Navigation data validity time relative to integer second specified by 'hhmmss'	ms	1ms	Yes
nplat	1	Receiver latitude estimate	rad	12mm	Yes
nplon	1	Receiver longitude estimate	rad	≤12mm	Yes
npalt	1	Receiver altitude estimate	m	7.8mm	Yes
hz2tim	1	GPS time-of-week to which solution relates	s	Double FP	Yes
npnedv	3	Receiver velocity estimates (north/east/down)	m/s	0.00391m/s	Yes
nknteh	1	Receiver estimated horizontal accuracy	m	0.0625m	No
nkntev	1	Receiver estimated vertical accuracy	m	0.0625m	No
nkntep	1	Receiver estimated 3-D positional accuracy	m	0.0625m	No
satlist	5	Satellite PRNs used in navigation solution	1 to 32	n/a	Yes (4 only)
difage	1	Age of last valid differential corrections	s	1s	No
gpsfix	1	Bits 0-1: Fix type (0=none, 1=2-D, 2=3-D) Bit 2: DGPS status (0=no DGPS, 1=DGPS)	n/a	n/a	Yes

Table 10 GPS Navigation Message Format

7.5 RTCM Correction Message Format

Two alternative sources of differential corrections were available at the aircraft system, namely those received via the MF and UHF datalinks. In each case the differential corrections were recorded for later examination during post-flight analysis.

For reasons of convenience, differential corrections via the UHF datalink were recorded at their point of origin in the platform reference system rather than on board the aircraft. In the case of the MF differential corrections, which originated at a location independent of any of the trials equipment, corrections were recorded on board the aircraft.

As a result of this arrangement, a subtle difference existed between the corrections recorded for the MF and UHF systems. In the former case, a particular set of corrections was only recorded (and therefore available during post-flight analysis) if it had been satisfactorily decoded by the aircraft MF receiver. In the case of the UHF system, however, for which corrections were recorded directly at the reference base station, an entry would be present in the correction message file whether or not the data had actually been received on board the aircraft.

The airborne and platform system ECUs operated by examining the RTCM-SC104 serial data stream for the presence of RTCM Type 1 and/or 2 messages (ref 2). Following correct receipt of a complete message, free of parity errors, an RTCM Correction Message entry was added to the appropriate data file.

Corrections from the MF system recorded on board the aircraft were designated by the file extension 'RTM'. Corrections from the UHF system recorded within the platform system were designated 'RTU'. In each case, new messages were recorded at a rate determined by the correction source's update rate: 1Hz for the UHF corrections, and around every 5-6 seconds for the MF corrections.

The information contained within each RTCM Correction Message, which supported the storage of differential corrections for up to eleven satellites, was as shown in Table 11. Data was time-tagged (via the 'hhmmss' parameter) using the ECU's internal timing reference, described in section 7.7.

Data identifier	Number of data items	Description	Units	Resolution
hhmmss	1	UTC time-of-day (hours, minutes, seconds)	s	1s
Type	1	Message Type (only Type 1 and 2 recorded)	n/a	n/a
ID	1	DGPS Reference Station ID	0 to 1023	n/a
Z-count	1	Modified Z-count (message reference time)	s	0.6s
Health	1	Station health	0 to 7	n/a
SV	11	Satellite PRN to which correction relates	1 to 32	n/a
Scale	11	Scale factor (determines prc & rrc resolution)	0 or 1	n/a
UDRE	11	User differential range error	0 to 3	n/a
prc	11	Satellite pseudorange correction	m	0.02m or 0.32m
rrc	11	Range-rate correction	m/s	0.002m/s or 0.032m/s

Table 11 RTCM Correction Message Format

7.6 Aircraft Data Message Format

The aircraft recording system was arranged to record a series of data items relating to the operation of various aircraft systems via an Aircraft Data Message.

These messages were stored at a 1Hz rate, at the start of each new integer second as determined by the timing outputs from the aircraft GPS 1 receiver.

The structure of the Aircraft Data Message was as shown in Table 12. Data was time-tagged (via the 'hhmmss' and 'Time tag' parameters) using the ECU's internal timing reference, described in section 7.7.

Data identifier	Description	Units	Resolution
hhmmss	UTC time-of-day (hours, minutes, seconds)	s	1s
Heading	Aircraft true heading from RNAV-2	deg	1 deg
TAS	True airspeed, from air data computer	kt	1kt
Pressalt	Pressure altitude, from air data computer	ft	1ft
Radalt	Radio altitude (operative below 2000ft)	ft	1ft
Roll	Roll attitude, from vertical gyro	deg	0.01 deg
Pitch	Pitch attitude, from vertical gyro	deg	0.01 deg
UHFant	UHF antenna currently selected (0=nose, 1=tail)	0 or 1	n/a
MFfreq	MF receiver frequency	kHz	0.5kHz
MFss	MF receiver signal strength	dB μ V/m	1dB μ V/m
MFsnr	MF receiver signal-to-noise ratio	dB	1dB
ATD	Along track distance computed by ECU guidance	m	1m
XTD	Cross track distance computed by ECU guidance	m	1m
VtErr	Vertical error computed by ECU guidance module	ft	1ft
CDIh	VOR/loc deviation computed by ECU guidance	% fsd	1% fsd
CDIv	Glideslope deviation computed by ECU guidance	% fsd	1% fsd
Time tag	Pressure altitude validity time relative to integer second specified by 'hhmmss'	ms	1 ms

Table 12 Aircraft Data Message Format

7.7 Time Synchronisation

In designing the ECU hardware and software, careful consideration was given to the issue of ensuring that correct real-time synchronisation was maintained between the various data storage messages. The fact that the data was stored within a series of message files, rather than within one larger composite file, implied that any failure in relative time synchronisation would have significant implications during post-flight data processing which might attempt to perform a comparison between data messages which did not originate at the same instant in time.

The nature of the truth reconstruction process, which took as its inputs the raw satellite measurement data recorded concurrently at two separate locations, also implied that it was necessary to ensure that the data originating at each of the three measurement systems (aircraft, platform and onshore) was correctly time-tagged.

The fact that each of the three systems incorporated GPS receiver equipment meant that a ready source of timing information, derived from a common reference (the GPS Control Segment), was available at each location. Absolute timing accuracy was therefore only limited by the ability of the receivers to determine GPS time in the presence of the various GPS system errors. A discussion of the significance of errors in the GPS receivers' timing outputs is contained in Volume 2.

A decision was taken to employ as 'master' timing reference for each location the Navstar XR5-M12 GPS receiver which was providing raw satellite measurement data for subsequent truth processing. In the case of the aircraft and platform systems this was the receiver designated as GPS 1; and on the onshore system this was the only GPS receiver. Each of these receivers was operating in stand-alone mode (i.e. was not supplied with differential corrections), which removed the possibility of timing errors resulting from erroneous correction data.

Each of these receivers transmitted a data stream to the ECU at a 1Hz rate via an RS232 serial link, with each of the data items contained in the message being appropriate to the start of the integer second during which transmission occurred. Owing to the finite time necessary to transmit the message, this implied that data was not received by the ECU (and therefore available for processing) until some later point within 1s of the instant in time to which the data related.

To allow the receiver user to determine the validity epoch more precisely, the manufacturer provides a one-pulse-per-second output (1PPS) in the form of a digital discrete line. This output comprises a short-duration timing pulse which is output at a 1Hz rate, the leading edge of the pulse being synchronised to the start of the integer GPS second. According to the manufacturer, the 1PPS timing output is accurate to $\pm 50\text{ns}$ with SA off (and is understood to be of the order of $\pm 300\text{ns}$ with SA on).

By sampling the receiver 1PPS output, each measurement system ECU was able to determine the instant in time at which the subsequent data message was valid. This arrangement is shown diagrammatically in Figure 5.

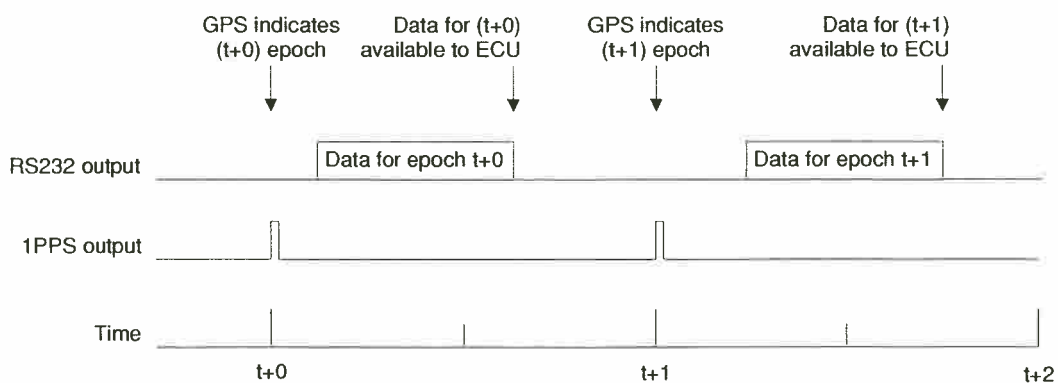


Figure 5 Temporal Relationship Between GPS Receiver 1PPS and RS232 Outputs (not to scale)

In order to provide an internal timing reference with a resolution in excess of that provided by the GPS 1PPS outputs, the software within each ECU was arranged to maintain an internal timing counter incremented continuously at a 1kHz rate. The counter was derived from the processor's 32MHz crystal oscillator which had a notional frequency stability of around ± 50 ppm (or a possible $\pm 50\mu\text{s}$ timing error over 1s, which was insignificant compared to the 1ms resolution of the counter).

An absolute timing reference within each ECU was derived by combining the internal 1ms counter with the absolute time update obtained at a 1Hz rate from the GPS receiver. This was achieved by maintaining an internal variable which stored the current offset, in 1ms units, between the value of the counter and the current absolute time. The offset variable was updated following the receipt of each new output sequence (comprising a 1PPS pulse followed several hundred milliseconds later by an RS232 data message) from the GPS.

The flowchart in Figure 6 is intended to illustrate this procedure and depicts, in simplified form, the algorithm executed by the ECU software every millisecond.

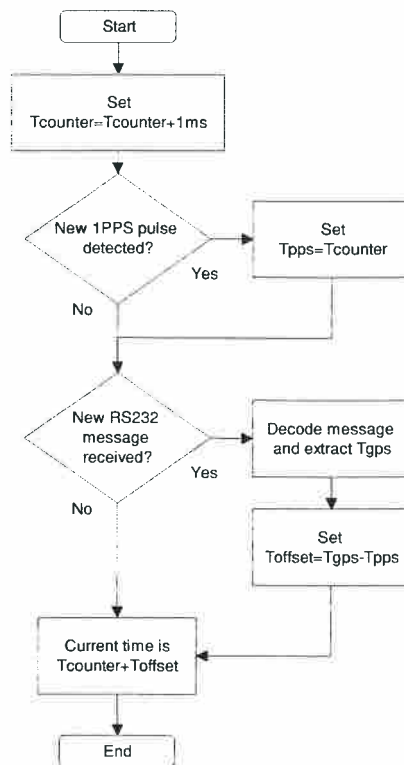


Figure 6 ECU Algorithm to Determine Absolute Time to 1ms Resolution (simplified)

Symbols used in the flowchart have the following meanings, all have units of seconds:

- T_{counter} current value of internal free-running timer (1ms resolution)
- T_{pps} value of internal timer at which last 1PPS pulse was detected
- T_{gps} time value contained in GPS RS232 data message
- T_{offset} offset between T_{counter} and absolute time

Additional logic, not shown in the flowchart, was incorporated in order to handle various possible scenarios which would affect the time synchronisation process, such as rejection of faulty data. For example, a 'missed' 1PPS pulse, or corruption in the RS232 data message preventing a new T_{gps} being extracted, would cause the ECU estimate of absolute time to continue to free-run using the internal oscillator until GPS timing was regained.

In practice, two different estimates of absolute time were obtained from the GPS receivers, namely GPS Time and UTC Time. The former is the timing reference system employed by the GPS Control Segment and satellite constellation whilst the latter corresponds to the internationally-recognised time standard ('Greenwich' or Zulu time). Differences are present between the two time references as a result of the periodic (every few years) inclusion of a 'leap second' into UTC. Throughout the trials programme a fixed relationship existed between GPS and UTC Time, namely

$$\text{GPS Time} = \text{UTC Time} + 11\text{s (exactly)}$$

Although this relationship remained constant throughout the trials programme, none of the real time or post-flight processing was reliant upon this being the case.

For convenience the ECU internal absolute timing reference employed UTC Time and this was used to provide basic time-tagging as the first item of each data message to a resolution of 1ms. The relationship between the time tag included in the messages and the source of the recorded data was as follows.

7.7.1 *Time Tagging of GPS Truth Messages*

A new GPS Truth Message was recorded every time the relevant data was transmitted by the Navstar XR5-M12. Since in each case this receiver also operated as the timing reference source for the ECU, the 'hhmmss' time tag parameter stored to disc was identical to the UTC Time value output by the GPS receiver.

Although the XR5-M12 was configured to output data consistent with the start of each new integer second, the precise instant at which the measurements were taken was also available, via the 'mestim' and 'swtow' parameters.

7.7.2 *Time Tagging of GPS Ephemeris Messages*

Each set of ephemerides was tagged with the value of UTC Time for the integer second during which the new data was received from the GPS receiver. Owing to the cyclic arrangement employed by the XR5-M12 for the output of ephemeris information, this could be up to 32s after the new ephemerides had been received from the relevant satellite.

The presence of a significant delay between receipt of new ephemerides and the time tag applied during storage to disc had no significant effect, since the truth reconstruction software ignored the time tag value and instead employed the time-of-clock and time-of-ephemeris parameters (t_{oc} , t_{oe}) when determining which set of ephemerides to use in processing the recorded data.

7.7.3 *Time Tagging of GPS Navigation Messages*

Each of the real-time differentially corrected GPS receivers employed on the trials aircraft possessed a 1PPS output which was used for time-tagging in a similar manner to the 1PPS from the truth reference receivers.

For the purposes of time-tagging it was assumed, as stated by the receiver manufacturers, that each RS232 serial data message transmitted by the receivers related to the instant in time at which the respective 1PPS pulse was output. No assumption was made, however, as to whether each receiver would output its 1PPS pulse at the same instant in time and hence the pulse output from each receiver was sampled separately, to a resolution of 1ms.

Once the RS232 data associated with an individual 1PPS pulse had been identified, the receiver data was stored to disc with an associated time tag comprised of two parts: an integer number of seconds ('hhmmss') and a fractional component ('Time tag') with resolution 1ms. These two values were related to the absolute instant at which the 1PPS pulse was detected by the expression:

$$\text{1PPS Output Time} = \text{hhmmss} + 0.001 \times \text{Time Tag}$$

For example, if one of the navigation receivers output its 1PPS pulse five milliseconds after the start of the UTC integer second 12:00:00 (as determined from the truth reference receiver), then the relevant Navigation Message would contain the values 12:00:00 for 'hhmmss' and 5 for 'Time Tag'. Similarly, if the 1PPS pulse was output five milliseconds in advance of 12:00:00, then the values stored would be 11:59:59 and 995 respectively.

This arrangement ensured that all of the information relating to the temporal relationship between the GPS receiver outputs was preserved and available for use during post-flight processing. The stored time tag had a basic resolution of 1ms and was subject to a maximum error (due to the effects of sampling, and then subtracting, the arrival instants of two 1PPS pulses) of no more than ± 1 ms.

7.7.4 *Time Tagging of RTCM Correction Messages*

A new RTCM Correction Message was recorded on each occasion that a complete RTCM Type 1 or Type 2 message was received by the ECU. The time tag applied, via the 'hhmmss' parameter, to the recorded data was the value of UTC Time appropriate to the start of the integer second during which the end of the message was received.

In the case of the UHF corrections, which were transmitted at a 1Hz rate, transmission of an individual RTCM Type 1 or 2 message both started and ended within the same integer second and consequently the 'hhmmss' time tag is sufficient to completely define, to a 1s resolution, the time of transmission.

The MF corrections, however, were transmitted at a much slower rate and consequently an RTCM Type 1 or 2 message typically took some five or six seconds to send. In this case the 'hhmmss' value related to the integer second during which the message ended: in effect, the instant at which the data would have been available for use by a GPS receiver; as opposed to the time at which the corrections were determined by the base station.

7.7.5 *Time Tagging of Aircraft Data Messages*

A new Aircraft Data Message was sequenced automatically for recording at the start of each integer second and all of the data stored related to the most up-to-date values received at the time of recording. Since the 'hhmmss' value stored was the UTC Time at the instant the recording was commenced, the offset between the stored time tag and the validity time of each data item in the message is directly dependent upon its respective update rate.

For the analogue parameters (radio altitude, pitch, and roll) which were sampled at a 1kHz rate, the maximum latency in a measurement was consequently less than 1ms.

For the parameters acquired from external sources via an ARINC 429 databus (pressure altitude, true air speed, and true heading) the maximum latency present in a recorded parameter was dependent upon the update rate with which the parameter was transmitted on the ARINC 429 bus. For the air data parameters this was never more than 100ms, but for true heading this could be up to around 1s.

The latency in the pressure altitude value was recorded by storing, as the altitude 'Time tag' value, the number of milliseconds since an ARINC 429 update was last received.

Parameters reported by the MF datalink receiver (frequency, signal strength and signal-to-noise ratio) possessed a latency of up to 1s.

Other stored parameters were derived from the aircraft guidance computation routines. These iterated at a fixed rate of 100Hz and consequently the latency in the recorded data was never in excess of 10ms.

8 TRIALS PROCEDURES

The aim of this section is to provide a summary of the procedures followed during each of the DGPS flight trials, including details of the pre-flight preparation and planning stages and of the post-flight analysis which was performed.

The flight trials outlined in this section were complemented by a series of ground-based trials over the course of the test programme. Ground trials were performed for a variety of purposes, including the development and testing of the three DGPS systems, the integration of the airborne DGPS system with the test airframe, the refinement of aircraft guidance algorithms, and the investigation of problems experienced during the flight trials programme.

A fully comprehensive description of the ground trials has not been included in this report owing to the diverse nature of the activities performed. Details have been provided, however (principally in Volume 2 of this report) of the procedures and results for those ground trials which are of particular significance to the trials programme. This category includes a series of activities which were performed at Cranfield shortly before the commencement of the flight test programme, and which are described in more detail in ref 4.

8.1 Flight Trials

A total of seven test flights were performed using the experimental DGPS equipment, each flight being performed on a different date and designated by a sequential reference number as shown in Table 13. Each test flight began and ended at Aberdeen (Dyce) aerodrome: the table includes a brief description of the destination used for each flight.

Flight	Date	Details
1	12th April 1996	Shakedown flight to and from Longside
2	8th May 1996	Offshore test flight: Beatrice C
3	19th June 1996	Ground trials at Longside
4	30th July 1996	Offshore test flight: Piper B
5	1st August 1996	Offshore test flight: Tartan A
6	26th September 1996	Offshore test flight: Buchan A
7	31st October 1996	Offshore demonstration flight: Beatrice A and C

Table 13 DGPS Flight Trials

Flights 2, 4, 5 and 6 in the programme were the principal offshore tests. Each of these four flights involved the execution of an essentially identical series of flight manoeuvres at one of four offshore structures which had been selected to offer a representative cross-section of the different types of offshore platform likely to be

encountered in the North Sea. The map in Figure 17 (page 57) depicts the location of the platforms used in the trials.

The results of these flights are presented in Volume 2 (where they relate to the performance of the GPS equipment) and Volume 3 (piloting and flyability aspects of the offshore approach manoeuvres).

The remaining flights in the programme were each devised for specific purposes which are described briefly below.

Flight 1 was essentially a 'shakedown' flight which was included in order to test the operation of the airborne systems prior to the main offshore flights, and to verify the compatibility of the trials equipment modifications with other aircraft systems. The flight comprised a sortie from Aberdeen to Peterhead (Longside) aerodrome (a private site, operated by Bond, about 20nm to the northeast of Aberdeen: Figures 16 and 17, pages 56–57) from where a number of test manoeuvres were performed. The return sortie included a series of test approaches to exercise the airborne guidance algorithms which were performed over the sea at an arbitrary location to the northeast of Aberdeen. Flight 1 identified a number of minor hardware and software problems which were rectified prior to the following flight. A limited quantity of data was recorded and analysed: where relevant the results have been included in Volumes 2 and 3 of this report.

The principal aim of Flight 3 was to perform a number of special purpose trials using the test airframe in a ground-based setting, with the airborne equipment configured in a slightly non-standard arrangement. To eliminate as far as possible the potential of interference from environmental factors, the trials were performed in the relatively featureless surroundings of Longside aerodrome. The results of these ground trials are presented in Volume 2. During the transit sorties to and from Longside, the opportunity was taken to perform a small number of test approaches at arbitrary points over the sea in order to investigate the effect of changes to the guidance algorithms (Volume 3).

The final test flight (number 7 in the series) was intended primarily as a demonstration flight. A number of invited representatives from industry bodies were offered the opportunity to witness typical DGPS approach manoeuvres, and to compare them with the existing procedures. These approaches were performed at the Beatrice A installation in a series of two consecutive sorties, with the aircraft returning to Aberdeen to exchange passengers in between. The opportunity was also taken on Flight 7 to gather some additional trials data on each sortie at the Beatrice C installation, on completion of the demonstration approaches and before returning to Aberdeen. Results of the analysis of this data are included in Volume 2, and a summary of the demonstration flight profiles appears in Volume 3.

Full details of the manoeuvres undertaken, and results obtained, on each of the seven test flights are contained in refs 5 to 16. The results presented in Volumes 2 and 3 of this report represent an attempt to summarise the results obtained during the flight trials programme and to comment upon their significance.

8.2 **DGPS Equipment Configuration**

Certain items included in the airborne equipment description of section 4 were not available, for a variety of reasons, for all of the test flights. These reasons included

the problems experienced with the operation of the Trimble GPS receiver (section 4.4) and the decision to add the LED indicator panel to assist the handling pilot during experimental approaches (section 4.18).

For completeness, Table 14 lists the differences between the airborne equipment utilised on each of the test flights and the description in section 4.

Flight	Differences between equipment configuration and section 4 description
1	Trimble receiver (GPS 4): present but disabled (no power applied) due to incorrect firmware and RF interference problem Antenna preamplifier, circulator and DC block: not present LED indicators: not present
2	Trimble receiver (GPS 4): present but disabled (no power applied) due to incorrect firmware and RF interference problem Antenna preamplifier, circulator and DC block: not present LED indicators: not present
3	Trimble receiver (GPS 4): present but disabled (no power applied) due to RF interference problem UHF-corrected Navstar receiver (GPS 3) reconfigured to act as second truth reference, for use with nose antenna (Volume 2 refers) Antenna preamplifier, circulator and DC block: not present LED indicators: not present
4	Trimble receiver (GPS 4): present but disabled (no power applied) due to internal configuration problem LED indicators: only active for second half of flight following ECU software change
5	Trimble receiver (GPS 4): present but disabled (no power applied) due to internal configuration problem
6	No differences
7	No differences

Table 14 Airborne Equipment Configuration on Each Flight

On a significant number of the test flights, the Trimble GPS receiver was not able to operate owing to a variety of problems. In each case the receiver was physically present (to avoid airworthiness problems, the equipment pallet having been approved as a complete assembly) but was disabled by removing the DC power

input. With the Trimble receiver disabled (with or without the circulator installed) it had been demonstrated that no detrimental effects occurred to the other GPS receivers.

As part of the permanent record of the system configuration, Table 15 lists the part number, serial number and software version of the principal items of aircraft equipment which were employed on each of the trials.

Item	Part Number	Serial Number	Software Version
Airborne ECU	FS-3024	001	004 (Flight 1) 005 (Flight 2) 006 (Flight 3) 007/008 (Flight 4) 009 (Flight 5) 010 (Flights 6-7)
Data Recorder	FS-3025	001	1.00
GPS 1 (Navstar)	A123-001G1	72014	3.9
GPS 2 (Navstar)	A123-001G1	69541	3.9
GPS 3 (Navstar)	A123-001G1	70715	3.9
GPS 4 (Trimble)	80265-01-0404C	6123000	D08
MF Receiver	MBX-2/02-00-05	37-1090 (Flights 1-6) Y18-1012 (Flight 7)	n/a
UHF Receiver	A141-001G1	73981	n/a

Table 15 Airborne Equipment Part, Serial and Version Numbers

The only item of aircraft equipment which was physically changed during the course of the trials was the MF datalink receiver, which developed a power supply fault (for reasons unconnected with the flight trials) between Flights 6 and 7. A replacement unit was provided by the supplier for the final trial, whilst the receiver was undergoing warranty repair.

The embedded software was updated at frequent intervals to introduce new guidance facilities on successive trials. The modifications did not affect the sections of the software responsible for data recording.

The configuration of the platform and onshore DGPS equipment was straightforward compared with the airborne system, as it remained essentially unchanged throughout the trials programme. Minor maintenance changes were introduced to the ECU code at intervals to maintain compatibility with the modules shared with the airborne system. Tables 16 and 17 list the relevant part, serial and version numbers.

Item	Part Number	Serial Number	Software Version
Platform ECU	FS-3024	002	004 (Flight 1) 005 (Flights 2-5) 010 (Flight 6-7)
Data Recorder	FS-3025	002	1.00
GPS 1 (Navstar)	A123-001G1	67661	3.9
GPS 2 (Navstar)	A123-001G1	69535	3.9
UHF Transmitter	A141-001G1	73973	n/a

Table 16 Platform System Part, Serial and Version Numbers

Item	Part Number	Serial Number	Software Version
Onshore ECU	FS-3024	003	004 (Flight 1) 005 (Flights 2-5) 010 (Flights 6-7)
Data Recorder	FS-3025	003	1.00
GPS (Navstar)	A123-001G1	72004	3.9

Table 17 Onshore System Part, Serial and Version Numbers

8.3 Pre-Flight Preparation

A defined procedure was followed in advance of each test flight so as to verify the correct operation of the processing and recording equipment. The following represents a summary of the operations that were performed.

8.3.1 Airborne System

Following completion of its last line flight before each trial the aircraft was converted to the DGPS role. This procedure, accomplished by Bond and Cranfield engineers, entailed installing the airborne equipment pallet in the rear baggage bay together with the demountable antenna installations. A programming pin change was necessary to enable the RNAV-2 computer to accept GPS data.

Equipment was also installed in the aircraft cabin, comprising the trials laptop PC and associated power supply, data interconnection leads and (on later flights) LED indicators. A cassette tape recorder was also installed, connected to the aircraft intercom system, to allow crew communications and R/T traffic to be recorded during the flight.

Following satisfactory completion of the aircraft modifications, an installation test procedure was performed using a predefined schedule. This served to exercise each of the items of equipment and aircraft interfaces to verify their correct operation, and

in particular it involved the operation of each of the onboard GPS receivers for a sufficient length of time to ensure that the stored almanac data was up-to-date, and that the position data held in non-volatile storage was correct for Aberdeen to minimise acquisition times.

Correct operation of the MF datalink receiver was tested using the Girdle Ness and Sumburgh beacons (Figures 16 and 17, 56–57) and Sumburgh beacons, and the UHF datalink receiver tested using the platform reference system (section 8.3.2).

The configuration of the aircraft RNAV-2 was modified, using the CDU, to ensure that the principal navigation data source was selected to GPS.

A test data recording was performed and its contents examined to verify correct operation.

8.3.2 *Platform System*

The frequency of the UHF transmitter within the platform reference system was set to the appropriate frequency (455.5MHz), using the Navstar programming adapter. This procedure was also performed on the corresponding UHF receiver which formed part of the airborne installation.

A test transmission of differential correction data was performed, by setting the GPS 2 (base station) parameters using the Navstar monitor software to indicate the unit's current location, and a transmission test performed to verify correction reception by the airborne equipment. Data for the initial position was derived from large-scale OS aerodrome maps.

Both receivers were operated for a sufficient length of time to ensure that their stored almanac data was up-to-date. A test data recording was performed and its contents examined.

The base station reference position at which the platform unit would be operating during the trial was then downloaded into each of the receivers using the Navstar monitor software. In the case of the base station receiver (GPS 2) this information was required in order for the unit to be able to generate the correct DGPS messages. Downloading a position to the truth unit (GPS 1) was performed so as to minimise the receiver acquisition time once the unit was positioned on the platform.

The platform system's internal batteries were fully charged (normally overnight) using a mains lead-acid charger, and the unit loaded in its transit condition into the aircraft baggage bay.

8.3.3 *Onshore System*

Testing and configuration of the onshore system was straightforward, and consisted of operating the system for a sufficient length of time to ensure that the GPS receiver contained up-to-date almanac and stored position, to minimise acquisition time. A test data recording was performed and its contents verified.

Once the onshore system configuration was complete, responsibility for the unit was transferred to the staff of DiffTech, at whose premises it was located, for the duration of the trial.

8.4 **Flight Trial Procedure**

With the exception of Flight 7, the aircraft crew for the DGPS test flights consisted of the following personnel:

Senior Training Captain, Bond (ND Mortimer).

Senior Test Pilot, CAA (N Talbot).

Flight Test Engineer/Observer, Cranfield (JRA Stevens).

Flight Test Observer, CAA (KM Dodson).

The Bond Senior Training Captain acted as aircraft commander and shared flying duties with the CAA Senior Test Pilot. In particular, evaluation of the offshore DGPS approaches was performed by each of the pilots, in an effort to obtain opinions on the suitability of the various approach profiles from both the operational and flight test aspects.

The Cranfield FTE was responsible for monitoring the operation of the DGPS recording equipment throughout each test flight and for making modifications to the system parameters (in particular those governing the experimental approaches) in consultation with the pilots. These activities were performed using the laptop PC, which provided facilities to both monitor and modify a comprehensive set of ECU parameters, but carried out no real-time processing of its own (other than for the purposes of driving the LED indicators).

Both observers were responsible for recording the progress of the flight and any pilot comments relating to the DGPS approaches or other system aspects. Recordings were obtained both in longhand and in audio form, via the intercom cassette tape recorder.

On Flight 4 an additional CAA operational pilot flew on the aircraft and had the opportunity to evaluate a proportion of the experimental DGPS approaches.

Additional Cranfield, Bond and CAA personnel were carried on some of the flights but had no active involvement in the execution of the trials.

On the final flight, a number of invited industry representatives were carried on the aircraft in two sorties, with two industry pilots replacing the CAA Senior Test Pilot and each able to undertake a small number of approaches. The FTE's duties were extended to include the provision of a commentary to the invited personnel regarding the course of the flight and, in particular, the approach profiles flown.

The following series of events represents the basic flight schedule undertaken on the main offshore trials (Flights 2, 4, 5 and 6) and was modified where necessary to accommodate the requirements of the other test flights.

- (1) The aircraft recording system was switched on, using an external ground power source, and correct operation of the recording systems was verified. A brief systems check was performed to exercise each of the aircraft interfaces, serving as confirmation that no changes had occurred since the pre-flight preparation (section 8.3.1).

- (2) A request was made to DiffTech personnel to start the onshore recording system, and to verify that recording was taking place.
- (3) The aircraft was left in a stationary condition, powered by an external ground supply, for between 20 and 30 minutes. This procedure was required in order to gather static GPS data for subsequent truth processing.
- (4) A normal engine and rotor start was performed, in the course of which the data system power source was transferred from external to internal power. The airborne system operation was monitored throughout this procedure.
- (5) The aircraft ground taxied to a predefined point at the intersection of Aberdeen runways 16/34 and 05/23, where it remained stationary for a period of at least 60 seconds. The purpose of this procedure was to provide a set of GPS data from a known static location prior to takeoff.
- (6) A normal takeoff and departure was performed, employing visual or instrument procedures as appropriate for the prevailing weather conditions.
- (7) The aircraft proceeded (using normal en-route procedures) to the 'target' offshore platform. The FTE continued to monitor the operation of the DGPS equipment and, in particular, verified that valid MF corrections were being received. The Girdle Ness reference station was used as the default correction source, with others being selected only if reception difficulties were experienced with Girdle Ness. No UHF correction data was received during this period as the platform reference system had not yet been set up on the platform.
- (8) On arrival at the platform, a visual or instrument approach was performed according to the weather conditions. The aircraft landed on the platform helideck and rotors were left running in accordance with standard offshore procedures.
- (9) The platform reference system was unloaded from the aircraft and positioned, by platform personnel and/or the flight test observers, at a prearranged point on the edge of the platform helideck. The unit was switched on.
- (10) The aircraft remained stationary on the helideck for a period of at least 20 minutes. During this time the FTE monitored the reception of satisfactory UHF corrections from the platform system.
- (11) On completion of the 20 minute period, the aircraft lifted from the helideck and commenced the first of a series of 'Modified Aerad' approaches (Volume 3) which were defined by parameters entered into the RNAV-2 by the pilot, and entered into the airborne system guidance algorithms by the FTE.
- (12) Each of these approaches consisted of an outbound leg commencing overhead the platform at 1500ft altitude. The aircraft proceeded downwind to a distance of approximately 4nm from the platform and descended to 800ft, before turning through 200° to establish on an inbound track to the platform.
- (13) Once the inbound track was established the aircraft intercepted a synthetic localiser and glideslope generated by the airborne DGPS equipment. The

aircraft descended to be level at a radial height of 200ft, with the approach track aligned to pass a fixed distance to one side of the platform.

- (14) Once past the platform the aircraft climbed back to 1500ft at a defined 'go around' point, before positioning for the next 'Modified Aerad' approach. A total of four such approaches were performed, with approach tracks aligned at 90° intervals to provide one into-wind, one downwind, and two crosswind approaches.
- (15) A series of orbital manoeuvres around the platform at predefined ranges and altitudes was performed. Standard ranges were 2nm, 1nm, 0.5nm, 0.2nm and (subject to wind conditions) as close to the platform as was practicable, and the standard radio altitude was 200ft.
- (16) A series of 'experimental approaches' (Volume 3) was performed, with parameters defined by the FTE via the laptop PC. Each of these was similar in concept to the 'Modified Aerad' approach, but typically dispensed with the overhead leg and was intended to allow experimentation with a wider variety of approach parameters.
- (17) Throughout stages 11 to 16, the FTE continued to monitor the operation of the aircraft DGPS equipment to detect any problems or malfunctions.
- (18) Typically, one or more landings on the platform were required in the course of stages 11 to 16 for refuelling purposes. In the case of the Beatrice C platform visited on Flight 2, at which fuel is not available, a transit flight to Wick aerodrome for refuelling was necessary.
- (19) On completion of the flight test manoeuvres, the aircraft landed on the platform where the platform reference system was switched off and reloaded into the baggage bay.
- (20) The aircraft took off and returned to Aberdeen following normal en-route procedures, with the FTE continuing to monitor the DGPS system performance.
- (21) After landing and before engine shutdown, ground power was applied to the aircraft to ensure that the airborne system continued running.
- (22) Following engine shutdown, the airborne system was arranged to continue to record data for a period of 20 to 30 minutes, on completion of which it was switched off.
- (23) A request was made to DiffTech personnel to switch off the onshore recording system.

8.5 Constraints on Flight Trial Manoeuvres

It was the original intention that each of the flight trials should be performed using standard aircraft operating procedures and that, consequently, there should be no constraints artificially imposed upon the choice of flight manoeuvres, other than those due to the limitations of the airframe or the onboard equipment.

Following the first offshore trial (Flight 2) to the Beatrice C platform, however, it became apparent that the truth reconstruction software was being affected by loss of satellite carrier lock at the airborne GPS 1 receiver during periods when the aircraft was in a significant starboard roll attitude.

The source of this problem, which is discussed in more detail in Volume 2, was traced to the fact that the GPS antenna (which was mounted on the top of the tail fin) was being masked by the tail rotor to an excessive degree whilst the aircraft was in this attitude. The problem did not occur in port roll attitudes due to the asymmetric nature of the tail rotor (located on the port side of aircraft).

The loss of carrier lock caused the accuracy of the truth position solution to be seriously compromised although it did not appear to affect the real-time code based solutions from the other GPS receivers. Various alternative antenna mounting locations were considered but it was expected that they might suffer from similar problems due to masking by either the tail or main rotor.

To reduce as far as possible the effects of the tail rotor masking problem upon the carrier-phase truth solution, it was decided that future flight trials would be performed with all turns being made, so far as practicable, in the direction in which the problem did not occur. It was not expected that this constraint would give rise to any significant operational disadvantages or affect the validity of the trials results in any way.

As a result, Flights 3 to 7 were performed with all turns, and in particular all of the DGPS approach patterns, being made to port. Where starboard turns were unavoidable, efforts were made to ensure that the bank angle was kept as low as possible.

8.6 **Post-Flight Activities**

On completion of a test flight the PCMCIA data storage modules were removed from the three DGPS systems as soon as practicable, and their contents transferred to a more permanent storage medium using a laptop PC.

The airborne installations were removed by Bond and Cranfield engineers and the aircraft returned to its normal configuration to allow resumption of line flying.

The final post-flight activity performed was to download, using a Navstar software utility, a copy of the almanac data held within each of the three truth reference GPS receivers. This data was archived in 'Yuma' format for use during later analysis if required.

8.7 **Post-Flight Processing**

Processing and analysis of the trials data was performed at Cranfield following each flight trial undertaken at Aberdeen, using office-based PC equipment. As the results of the analysis are presented in detail in Volumes 2 and 3, this section will be restricted to a brief description of the data processing techniques which were employed.

Data recorded from the three truth reference GPS receivers consisted of a series of GPS Truth messages and associated GPS Ephemeris data. These were contained in

the TRA and EPA files (airborne system), TRP and EPP files (platform system) and TRS and EPS files (onshore system).

Each pair of truth receiver files was processed in turn by a dedicated conversion utility program, which in effect reconstructed the original series of RS232 data messages output by the Navstar receiver. This intermediate file was then processed by the Navstar data capture utility which forms part of the truth processing suite (Premier GPS Inc GRAFNAV version 4.0), to produce a series of binary format data files suitable for further processing by the Premier software.

Each set of Premier format files was assigned a unique identifier associating it with the relevant system (aircraft, platform or onshore) and the trial date.

The Premier software was used to perform carrier phase based processing of the recorded data, as described in detail in Volume 2 of this report. The end result was the generation of one or more text format output files, containing a series of truth estimates for the aircraft position and velocity at each measurement epoch.

Comparisons between the real-time differentially corrected GPS data contained in the GD1, GD2 and GD3 files, and the truth position history for the aircraft, were performed using a further set of dedicated utility programs. Results of the comparisons were generated in a format suitable for input into a Microsoft Excel spreadsheet, which was used to perform statistical analysis and to present the results in graphical form.

Conversion programs were also written to decode the contents of the other recorded data files (RTCM data in the RTM and RTU files, and Aircraft data in the NV1 file) into a form suitable for import into Microsoft Excel, for use as required during the data processing.



Figure 7 Trials Airframe, Sikorsky S76C G-SSSC

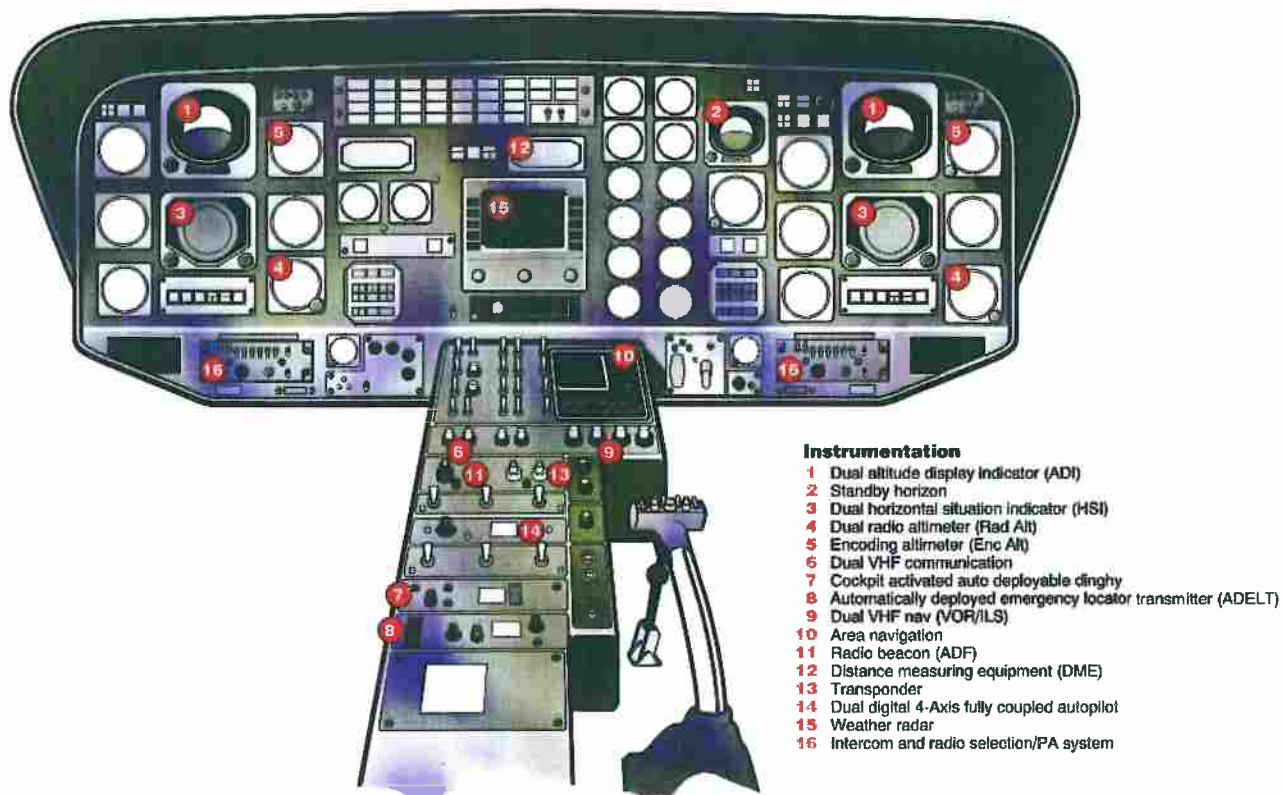


Figure 8 G-SSSC Cockpit Layout (source: Bond Helicopters Ltd)

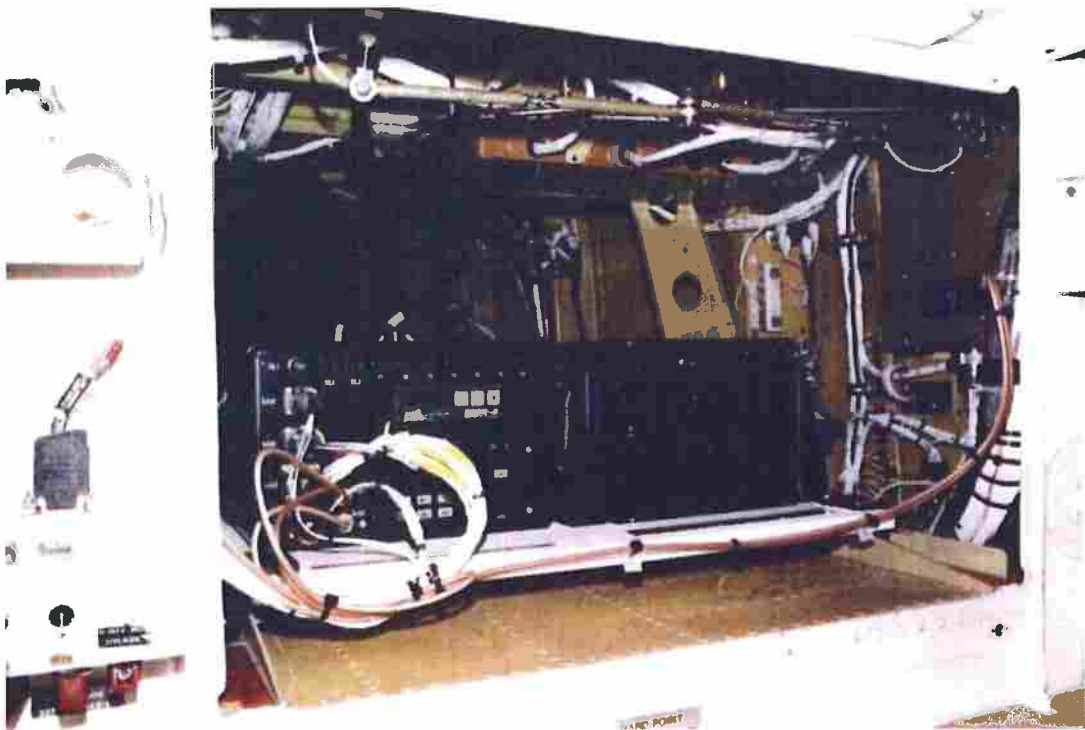


Figure 9 DGPS Trials Pallet Installation



Figure 10 GPS Antenna Installation

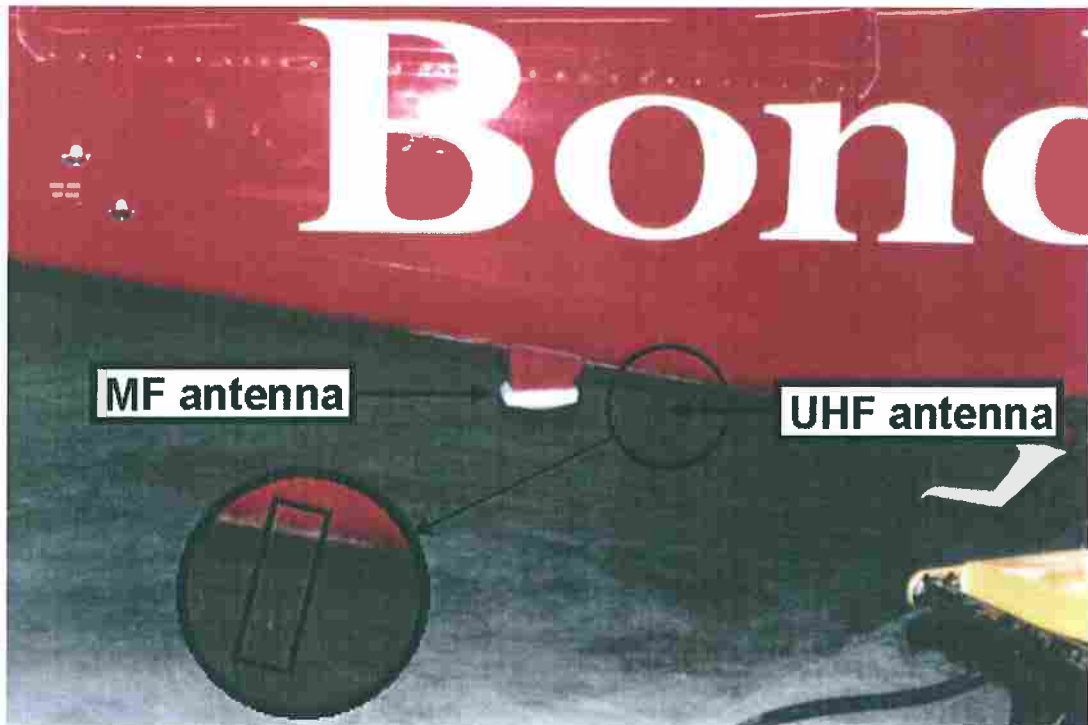


Figure 11 MF and Tail UHF Antenna Installation

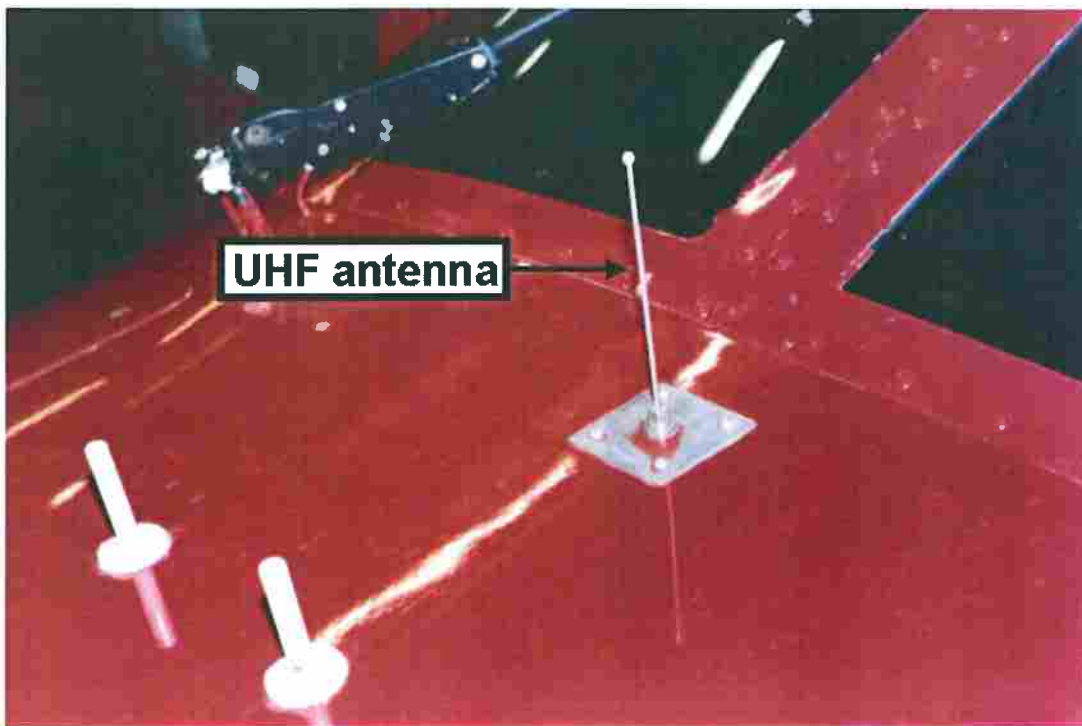


Figure 12 Nose UHF Antenna Installation



Figure 13 Cockpit LED Indicators

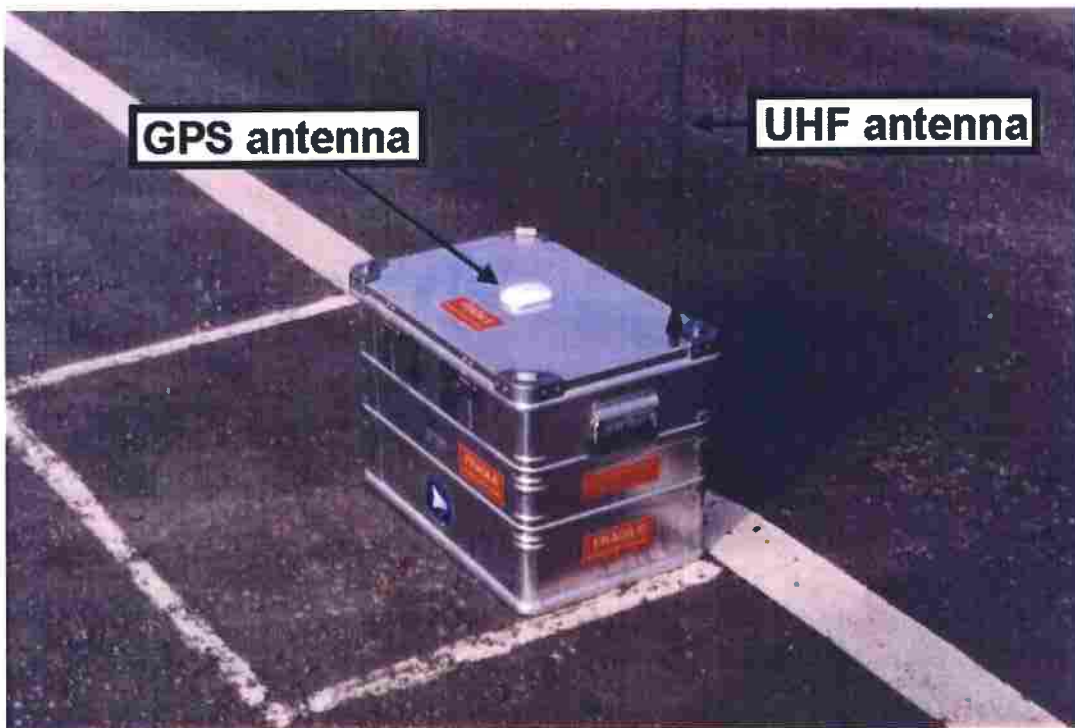


Figure 14 Platform Reference System



Figure 15 Onshore System Antenna

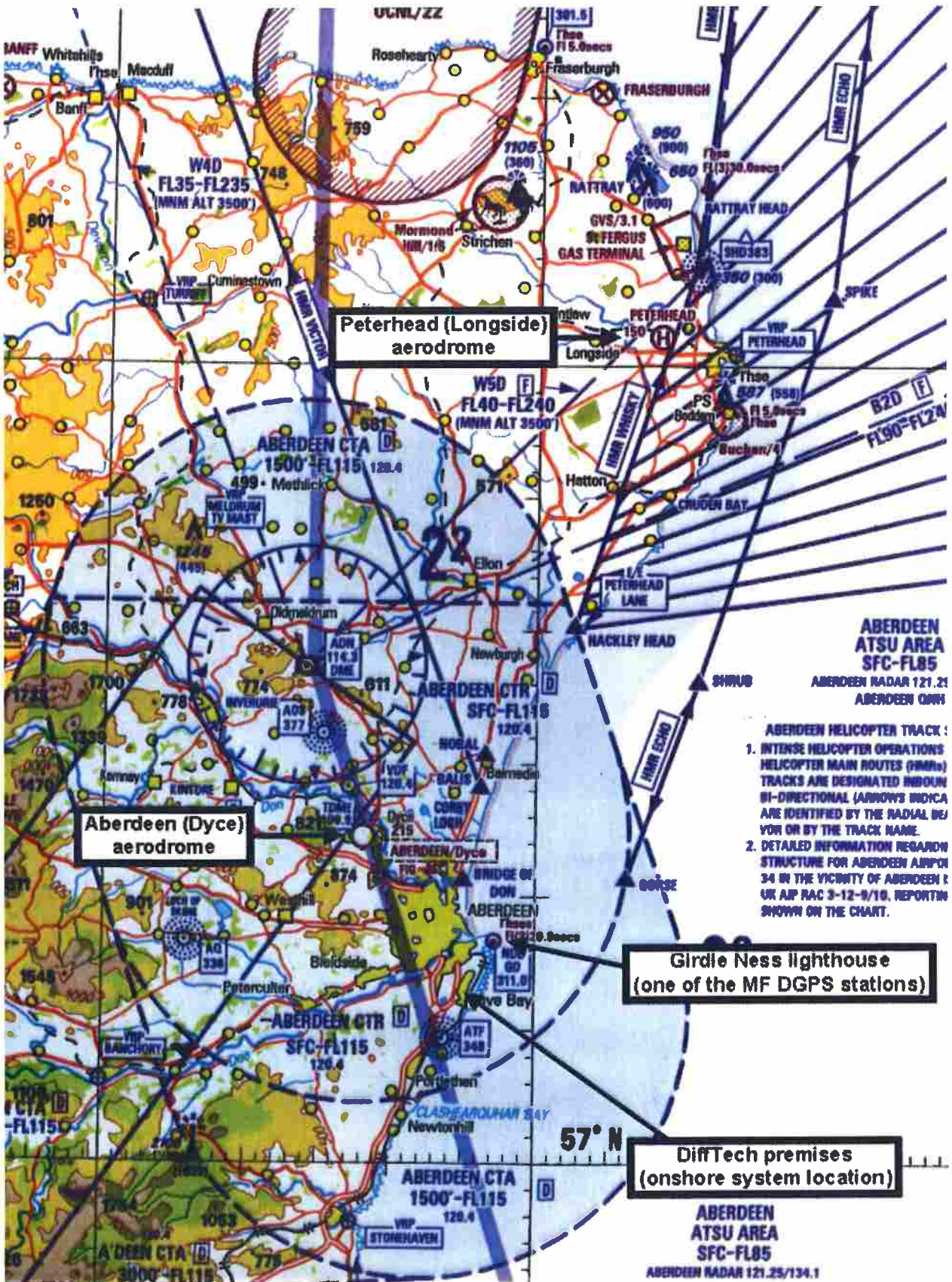


Figure 16 Aberdeen and Longside

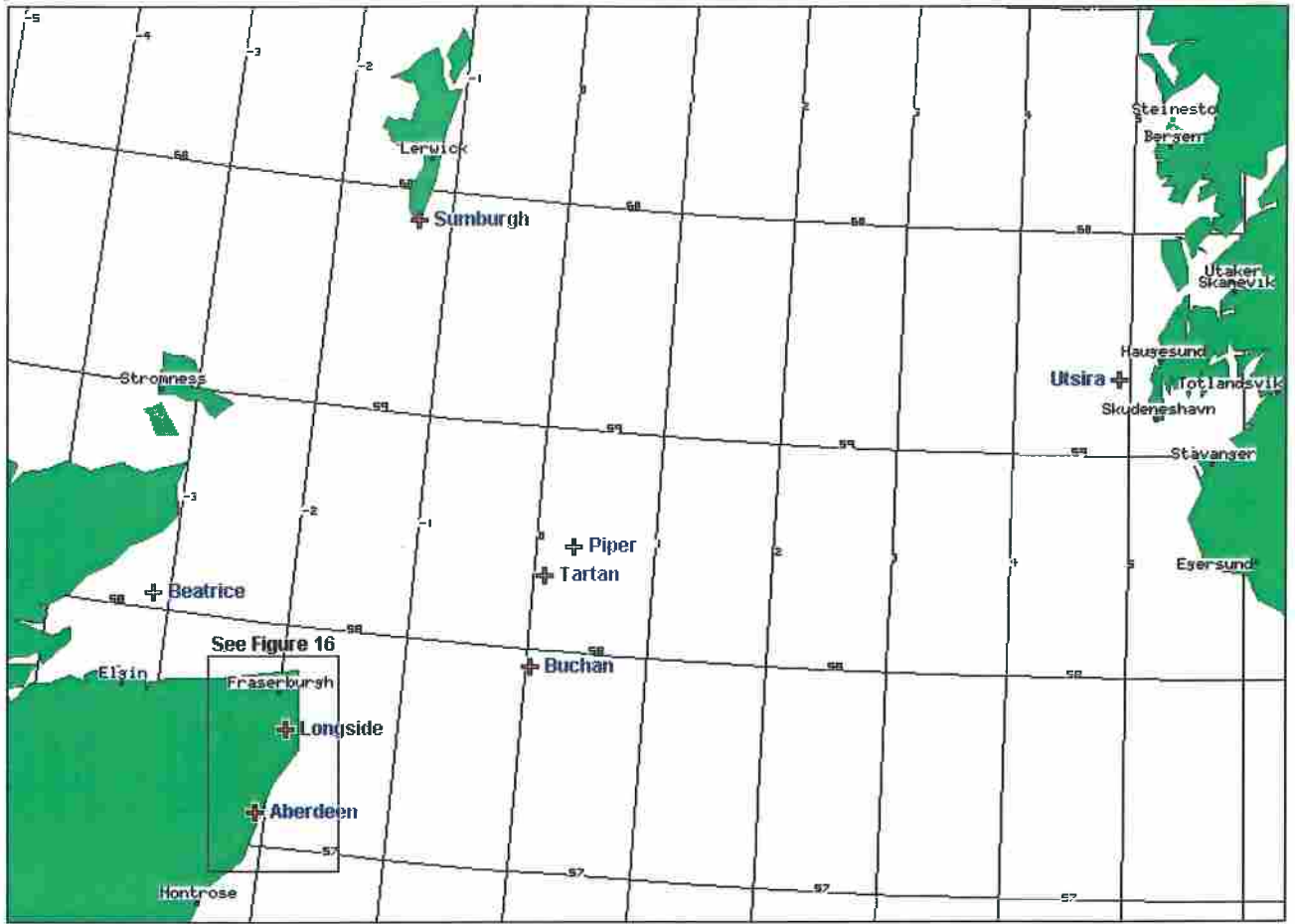


Figure 17 Northern North Sea

Volume 2

DGPS Equipment Performance

Contents

	<i>Page</i>
1 INTRODUCTION	1
2 REFERENCES	3
3 ABBREVIATIONS	4
4 TRUTH REFERENCE COMPUTATION	6
4.1 Post-Processing of Pseudorange Measurements	6
4.2 Post-Processing of Carrier Phase Measurements	12
4.3 Onshore System Survey-In	15
4.4 Platform System Survey-In	16
4.5 Aircraft Truth Position Computation	21
5 OTHER ISSUES AFFECTING GPS PERFORMANCE	25
5.1 GPS Satellite Constellation and Signals-in-Space	25
5.2 Time Synchronisation	26
5.3 Airborne Antenna Installation	29
6 DGPS PRECISION RESULTS FROM OFFSHORE TRIALS	34
6.1 MF-Corrected Navstar (GD1) Receiver	37
6.2 UHF-Corrected Navstar (GD2) Receiver	60
6.3 MF-Corrected Trimble (GD3) Receiver	91
7 DIFFERENTIAL CORRECTION DATALINKS	102
7.1 MF Correction Datalink	104
7.2 UHF Correction Datalink	108
8 DISCUSSION OF RESULTS	110
8.1 MF-Corrected Navstar (GD1) Receiver	112
8.2 UHF-Corrected Navstar (GD2) Receiver	115
8.3 MF-Corrected Trimble (GD3) Receiver	118
8.4 Overall Statistics	120
9 SUMMARY OF CONCLUSIONS	121

LIST OF ILLUSTRATIONS

Figure 1	Distribution of Platform System Positions, Flight 6, Buchan A	19
Figure 2	Statistics of Platform System Positions, Flight 6, Buchan A	19
Figure 3	Distribution of Platform System Positions, Flight 7, Beatrice C	20
Figure 4	Statistics of Platform System Positions, Flight 7, Beatrice C	20
Figure 5	Temporal Alignment Check: Average 2-D Error versus Time Offset	29
Figure 6	Longside Trial: Distribution of 2-D Difference Between Nose/Tail Fixes	31
Figure 7	Cumulative Probability of GD1 Error, Aerad Approaches, Beatrice C	38
Figure 8	Scatter Plot of GD1 Error, Aerad Approaches, Beatrice C	39
Figure 9	GD1 Error versus Range, Aerad Approaches, Beatrice C	39
Figure 10	Cumulative Probability of GD1 Error, Platform Orbits, Beatrice C	40
Figure 11	Scatter Plot of GD1 Error, Platform Orbits, Beatrice C	41
Figure 12	GD1 Error versus Range, Platform Orbits, Beatrice C	41
Figure 13	Cumulative Probability of GD1 Error, Aerad Approaches, Piper B	42
Figure 14	Scatter Plot of GD1 Error, Aerad Approaches, Piper B	43
Figure 15	GD1 Error versus Range, Aerad Approaches, Piper B	43
Figure 16	Cumulative Probability of GD1 Error, Platform Orbits, Piper B	44
Figure 17	Scatter Plot of GD1 Error, Platform Orbits, Piper B	45
Figure 18	GD1 Error versus Range, Platform Orbits, Piper B	45
Figure 19	Cumulative Probability of GD1 Error, Experimental Approaches, Piper B	46
Figure 20	Scatter Plot of GD1 Error, Experimental Approaches, Piper B	47
Figure 21	GD1 Error versus Range, Experimental Approaches, Piper B	47
Figure 22	Cumulative Probability of GD1 Error, Aerad Approaches, Tartan A	48
Figure 23	Scatter Plot of GD1 Error, Aerad Approaches, Tartan A	49
Figure 24	GD1 Error versus Range, Aerad Approaches, Tartan A	49
Figure 25	Cumulative Probability of GD1 Error, Platform Orbits, Tartan A	50
Figure 26	Scatter Plot of GD1 Error, Platform Orbits, Tartan A	51
Figure 27	GD1 Error versus Range, Platform Orbits, Tartan A	51
Figure 28	Cumulative Probability of GD1 Error, Experimental Approaches, Tartan A	52
Figure 29	Scatter Plot of GD1 Error, Experimental Approaches, Tartan A	53
Figure 30	GD1 Error versus Range, Experimental Approaches, Tartan A	53
Figure 31	Cumulative Probability of GD1 Error, Aerad Approaches, Buchan A	54
Figure 32	Scatter Plot of GD1 Error, Aerad Approaches, Buchan A	55
Figure 33	GD1 Error versus Range, Aerad Approaches, Buchan A	55
Figure 34	Cumulative Probability of GD1 Error, Platform Orbits, Buchan A	56
Figure 35	Scatter Plot of GD1 Error, Platform Orbits, Buchan A	57
Figure 36	GD1 Error versus Range, Platform Orbits, Buchan A	57
Figure 37	Cumulative Probability of GD1 Error, Experimental Approaches, Buchan A	58
Figure 38	Scatter Plot of GD1 Error, Experimental Approaches, Buchan A	59
Figure 39	GD1 Error versus Range, Experimental Approaches, Buchan A	59
Figure 40	Cumulative Probability of GD2 Error, Aerad Approaches, Beatrice C	62
Figure 41	Scatter Plot of GD2 Error, Aerad Approaches, Beatrice C	63
Figure 42	GD2 Error versus Range, Aerad Approaches, Beatrice C	63
Figure 43	Cumulative Probability of GD2 Error, Platform Orbits, Beatrice C	64
Figure 44	Scatter Plot of GD2 Error, Platform Orbits, Beatrice C	65
Figure 45	GD2 Error versus Range, Platform Orbits, Beatrice C	65

	<i>Page</i>
Figure 46	Cumulative Probability of GD2 Error, Aerad Approaches, Piper B 66
Figure 47	Scatter Plot of GD2 Error, Aerad Approaches, Piper B 67
Figure 48	GD2 Error versus Range, Aerad Approaches, Piper B 67
Figure 49	Cumulative Probability of GD2 Error, Platform Orbits, Piper B 68
Figure 50	Scatter Plot of GD2 Error, Platform Orbits, Piper B 69
Figure 51	GD2 Error versus Range, Platform Orbits, Piper B 69
Figure 52	Cumulative Probability of GD2 Error, Experimental Approaches, Piper B 70
Figure 53	Scatter Plot of GD2 Error, Experimental Approaches, Piper B 71
Figure 54	GD2 Error versus Range, Experimental Approaches, Piper B 71
Figure 55	Cumulative Probability of GD2 Error, Aerad Approaches, Tartan A 72
Figure 56	Scatter Plot of GD2 Error, Aerad Approaches, Tartan A 73
Figure 57	GD2 Error versus Range, Aerad Approaches, Tartan A 73
Figure 58	Cumulative Probability of GD2 Error, Aerad Approaches, Tartan A (no bias) 74
Figure 59	Scatter Plot of GD2 Error, Aerad Approaches, Tartan A (no bias) 75
Figure 60	GD2 Error versus Range, Aerad Approaches, Tartan A (no bias) 75
Figure 61	Cumulative Probability of GD2 Error, Platform Orbits, Tartan A 76
Figure 62	Scatter Plot of GD2 Error, Platform Orbits, Tartan A 77
Figure 63	GD2 Error versus Range, Platform Orbits, Tartan A 77
Figure 64	Cumulative Probability of GD2 Error, Platform Orbits, Tartan A (no bias) 78
Figure 65	Scatter Plot of GD2 Error, Platform Orbits, Tartan A (no bias) 79
Figure 66	GD2 Error versus Range, Platform Orbits, Tartan A (no bias) 79
Figure 67	Cumulative Probability of GD2 Error, Experimental Approaches, Tartan A 80
Figure 68	Scatter Plot of GD2 Error, Experimental Approaches, Tartan A 81
Figure 69	GD2 Error versus Range, Experimental Approaches, Tartan A 81
Figure 70	Cumulative Probability of GD2 Error, Experimental Apps, Tartan A (no bias) 82
Figure 71	Scatter Plot of GD2 Error, Experimental Approaches, Tartan A (no bias) 83
Figure 72	GD2 Error versus Range, Experimental Approaches, Tartan A (no bias) 83
Figure 73	Cumulative Probability of GD2 Error, Aerad Approaches, Buchan A 84
Figure 74	Scatter Plot of GD2 Error, Aerad Approaches, Buchan A 85
Figure 75	GD2 Error versus Range, Aerad Approaches, Buchan A 85
Figure 76	Cumulative Probability of GD2 Error, Platform Orbits, Buchan A 86
Figure 77	Scatter Plot of GD2 Error, Platform Orbits, Buchan A 87
Figure 78	GD2 Error versus Range, Platform Orbits, Buchan A 87
Figure 79	Cumulative Probability of GD2 Error, Experimental Approaches, Buchan A 88
Figure 80	Scatter Plot of GD2 Error, Experimental Approaches, Buchan A 89
Figure 81	GD2 Error versus Range, Experimental Approaches, Buchan A 89
Figure 82	Cumulative Probability of GD3 Error, Aerad Approaches, Beatrice C 92
Figure 83	Scatter Plot of GD3 Error, Aerad Approaches, Beatrice C 93
Figure 84	GD3 Error versus Range, Aerad Approaches, Beatrice C 93
Figure 85	Cumulative Probability of GD3 Error, Platform Orbits, Beatrice C 94
Figure 86	Scatter Plot of GD3 Error, Platform Orbits, Beatrice C 95
Figure 87	GD3 Error versus Range, Platform Orbits, Beatrice C 95
Figure 88	Cumulative Probability of GD3 Error, Aerad Approaches, Buchan A 96

	<i>Page</i>
Figure 89 Scatter Plot of GD3 Error, Aerad Approaches, Buchan A	97
Figure 90 GD3 Error versus Range, Aerad Approaches, Buchan A	97
Figure 91 Cumulative Probability of GD3 Error, Platform Orbits, Buchan A	98
Figure 92 Scatter Plot of GD3 Error, Platform Orbits, Buchan A	99
Figure 93 GD3 Error versus Range, Platform Orbits, Buchan A	99
Figure 94 Cumulative Probability of GD3 Error, Experimental Approaches, Buchan A	100
Figure 95 Scatter Plot of GD3 Error, Experimental Approaches, Buchan A	101
Figure 96 GD3 Error versus Range, Experimental Approaches, Buchan A	101
Figure 97 Beatrice C Platform Layout	125
Figure 98 Piper B Platform Layout	126
Figure 99 Tartan A Platform Layout	127
Figure 100 Buchan A Platform Layout	128
Figure 101 Beatrice C Platform	129
Figure 102 Piper B Platform	129
Figure 103 Tartan A Platform	130
Figure 104 Buchan A Platform	130
Figure 105 Carrier-Phase Convergence for Platform Station Survey, Beatrice C	131
Figure 106 Comparison of OTruth with PTruth, Flight 7, Beatrice C	132
Figure 107 Comparison of OTruth with PTruth, Flight 7, Beatrice C (Reverse)	133
Figure 108 Comparison of OTruth with PTruth, Flight 2, Beatrice C	134
Figure 109 Comparison of OTruth with PTruth, Flight 4, Piper B	135
Figure 110 Comparison of OTruth with PTruth, Flight 5, Tartan A	136
Figure 111 Comparison of OTruth with PTruth, Flight 6, Buchan A	137
Figure 112 Comparison of OTruth with PTruth, Flight 6, Buchan A (Expanded)	138
Figure 113 Longside Trial: OTruth Solutions for Nose and Tail Antenna Installations	139
Figure 114 Longside Trial: 2-D Difference Between Nose/Tail Fixes versus Heading	140
Figure 115 Longside Trial: Variation of CNR with Azimuth/Elevation for Nose Antenna	141
Figure 116 Longside Trial: Variation of CNR with Azimuth/Elevation for Tail Antenna	142
Figure 117 Cumulative Probability of GD1, GD2 and GD3 2-D Error	143

LIST OF TABLES

Table 1	GPS Satellite Status During Trials Programme	25
Table 2	Statistical Distribution of Pseudorange Errors Measured Onshore	26
Table 3	Distribution of 1PPS Time Synchronisation for GPS Receivers	28
Table 4	Statistics of GD1 Error, Aerad Approaches, Beatrice C	38
Table 5	Statistics of GD1 Error, Platform Orbits, Beatrice C	40
Table 6	Statistics of GD1 Error, Aerad Approaches, Piper B	42
Table 7	Statistics of GD1 Error, Platform Orbits, Piper B	44
Table 8	Statistics of GD1 Error, Experimental Approaches, Piper B	46
Table 9	Statistics of GD1 Error, Aerad Approaches, Tartan A	48
Table 10	Statistics of GD1 Error, Platform Orbits, Tartan A	50
Table 11	Statistics of GD1 Error, Experimental Approaches, Tartan A	52
Table 12	Statistics of GD1 Error, Aerad Approaches, Buchan A	54
Table 13	Statistics of GD1 Error, Platform Orbits, Buchan A	56
Table 14	Statistics of GD1 Error, Experimental Approaches, Buchan A	58
Table 15	Statistics of GD2 Error, Aerad Approaches, Beatrice C	62
Table 16	Statistics of GD2 Error, Platform Orbits, Beatrice C	64
Table 17	Statistics of GD2 Error, Aerad Approaches, Piper B	66
Table 18	Statistics of GD2 Error, Platform Orbits, Piper B	68
Table 19	Statistics of GD2 Error, Experimental Approaches, Piper B	70
Table 20	Statistics of GD2 Error, Aerad Approaches, Tartan A	72
Table 21	Statistics of GD2 Error, Aerad Approaches, Tartan A (no bias)	74
Table 22	Statistics of GD2 Error, Platform Orbits, Tartan A	76
Table 23	Statistics of GD2 Error, Platform Orbits, Tartan A (no bias)	78
Table 24	Statistics of GD2 Error, Experimental Approaches, Tartan A	80
Table 25	Statistics of GD2 Error, Experimental Approaches, Tartan A (no bias)	82
Table 26	Statistics of GD2 Error, Aerad Approaches, Buchan A	84
Table 27	Statistics of GD2 Error, Platform Orbits, Buchan A	86
Table 28	Statistics of GD2 Error, Experimental Approaches, Buchan A	88
Table 29	Statistics of GD3 Error, Aerad Approaches, Beatrice C	92
Table 30	Statistics of GD3 Error, Platform Orbits, Beatrice C	94
Table 31	Statistics of GD3 Error, Aerad Approaches, Buchan A	96
Table 32	Statistics of GD3 Error, Platform Orbits, Buchan A	98
Table 33	Statistics of GD3 Error, Experimental Approaches, Buchan A	100
Table 34	Statistics of GD1 2-D Error by Manoeuvre Type and Platform	112
Table 35	Statistics of GD2 2-D Error by Manoeuvre Type and Platform	115
Table 36	Ratio of GD2 to GD1 95% Confidence Statistics	116
Table 37	Statistics of GD3 and GD1 2-D Error by Manoeuvre Type and Platform	119
Table 38	Summary of Statistics of GD1, GD2 and GD3 2-D Error	120

1 INTRODUCTION

During 1996 a series of flight trials was undertaken in the North Sea to examine the use of Differential Global Positioning System (DGPS) equipment as an approach aid for offshore installations. The flight trials had three basic objectives:

- (1) To acquire knowledge and experience to support the development of both generic, and DGPS-specific, airworthiness and operational requirements and associated advisory material, for the conduct of offshore approaches.
- (2) To quantify by scientific means the accuracy which may be achieved in a DGPS system operating to/from offshore platforms.
- (3) To assess the flyability of the system in the applicable environment.

The flight trials programme was undertaken by the Flight Systems and Measurement Laboratories (now incorporated into Cranfield Aerospace Ltd) of the College of Aeronautics, Cranfield University in the role of prime contractor on behalf of the UK Civil Aviation Authority.

Flight trials were performed using a Sikorsky S76C helicopter chartered by Cranfield from Bond Helicopters Ltd. The aircraft was fitted with a special purpose experimental DGPS installation which was complemented by additional recording equipment sited at fixed locations.

In the course of seven test flights totalling 36 hours, over 70 predefined manoeuvres were performed at a set of four offshore production platforms with differing topside layouts. At each platform, approach trajectories and guidance presentations based upon the use of DGPS data were evaluated by the trials team which comprised representatives from CAA, Bond and Cranfield.

Post-flight processing of the data recorded during each trial enabled an assessment to be made of the performance of the real-time airborne DGPS equipment, and an understanding to be gained of some of the issues likely to affect GPS performance in the offshore environment. The trials installation allowed a comparison to be made between two alternative sources of differential corrections and between receivers produced by two different manufacturers.

The Final Report on the trials programme consists of three volumes, of which this document ('DGPS Equipment Performance') represents Volume 2. The three volumes are structured as follows:

Volume 1 ('Experimental Procedures') contains a description of the three measurement systems employed and of the data recorded by each system, and includes details of the experimental procedures employed on each of the flight trials.

Volume 2 (this document) presents and discusses the results of a comparison between the real-time DGPS data and a 'truth' reference which was derived, using techniques described in the report, from post-processed GPS measurements. A discussion is included of various factors which were found to affect the availability and precision of the real-time DGPS data, and these results are summarised in the form of a series of conclusions and suggestions for future work.

Volume 3 ('DGPS Approach Guidance') describes how the approach guidance information was generated and presented to the aircraft pilots over the course of the trials programme. Details are presented of the offshore approaches which were undertaken using the experimental installation, together with a comprehensive discussion of the flyability results which includes a series of conclusions and suggestions for future work.

2 REFERENCES

- 1 'Introductory Manual for GPS Surveying', Premier GPS Inc, 1993.
- 2 'Reference Manual for GPS_PROC & Utilities', Premier GPS Inc, 1994.
- 3 'Global Positioning System Standard Positioning Service Signal Specification', DoD, 1995.
- 4 'RTCM Recommended Standards for Differential Navstar GPS Service', Radio Technical Commission for Maritime Services, 1998.
- 5 ICD-GPS-200, 'NAVSTAR GPS Space Segment and Navigation User Interfaces', Arinc Research Corporation, 1997.
- 6 Williams DA, CoA-FS-96-416, 'Report on Initial Ground Trials', FSML, 1996.
- 7 Williams DA, CoA-FS-96-418, 'Report on Test Flight 1', FSML, 1996.
- 8 Williams DA, CoA-FS-96-422, 'Report on Test Flight 2', FSML, 1996.
- 9 Williams DA, CoA-FS-95-423, 'Note on Antenna Reception Properties', FSML, 1996.
- 10 Williams DA, CoA-FS-96-426, 'Report on Test Flight 4', FSML, 1996.
- 11 Williams DA, CoA-FS-96-427, 'Report on Test Flight 5', FSML, 1996.
- 12 Stevens JRA, CA/CSG/7047, 'Report on Test Flight 6', CAe, 1997.
- 13 Stevens JRA, CA/CSG/7048, 'Report on Test Flight 7', CAe, 1997.
- 14 'Standardization in the Methods of Expressing Navigational Accuracies', Royal Institute of Navigation, 1996.

3 ABBREVIATIONS.

Bond	Bond Helicopters Ltd
C/A	Coarse/Acquisition
CAA	Civil Aviation Authority
CAe	Cranfield Aerospace Ltd
CEP	Circular Error Probable
CNR	Carrier-to-Noise Ratio
Cranfield	Cranfield University, Cranfield Aerospace Ltd
dB	Decibel
DGPS	Differential Global Positioning System
DiffTech	Differential Technology Ltd
DoD	Department of Defense
drms	Distance RMS
FSML	Flight Systems and Measurement Laboratories
ft	Foot
GD1	Identifier for MF-corrected Navstar GPS Navigation data
GD2	Identifier for UHF-corrected Navstar GPS Navigation data
GD3	Identifier for MF-corrected Trimble GPS Navigation data
GPS	Global Positioning System
H-field	Magnetic Field
Hz	Hertz
IODE	Issue of Data Ephemeris
L-band	Region of electromagnetic spectrum around 1.5GHz
L1	GPS Link 1 Frequency (1575.42 MHz)
L2	GPS Link 2 Frequency (1227.60 MHz)
m	Metre
MF	Medium Frequency
MS-DOS	Microsoft Disk Operating System
MSK	Minimum Shift Keying
NANU	Notice Advisory to Navstar Users
Navstar	Navstar Systems Ltd
NDB	Non-Directional Beacon
nm	Nautical Mile
OS	Ordnance Survey
OTruth	Aircraft truth position history using onshore system as reference
PC	Personal Computer
PRN	Pseudo-Random Noise (GPS Satellite Identifier)
PTruth	Aircraft truth position history using platform system as reference
Radalt	Radio altimeter
ref	Reference
RF	Radio Frequency
RMS	Root Mean Square
RTCM	Radio Technical Commission for Maritime Services
RTCM-SC104	RTCM Special Committee Number 104
s	Second
SA	Selective Availability
std dev	Standard deviation
Trimble	Trimble Navigation Ltd
UHF	Ultra High Frequency
UK	United Kingdom
US	United States
UTC	Universal Time Co-ordinated

WGS84	World Geodetic System 1984
°T	Degrees True
1PPS	One Pulse-Per-Second
2-D	Two dimensional
3-D	Three dimensional

4 TRUTH REFERENCE COMPUTATION

In order to evaluate the performance of the airborne real-time DGPS equipment, it was first necessary to determine a truth position history for the aircraft against which the recorded data from the real-time equipment could be compared.

The truth system selected for the trials used recordings of the GPS L1 carrier phase, which were combined during post-flight analysis using a commercial post-processing software package.

During each trial, recordings of carrier phase data were made using dedicated GPS receiver equipment on board the aircraft and at two fixed sites (one onshore, the other offshore). Full details of the operation of the three recording systems are contained in Volume 1.

The software package employed for carrier phase processing is known as GRAFNAV and is produced by a Canadian company, Premier GPS Inc. All of the trials data was processed using version 4.0 of GRAFNAV, running under the MS-DOS operating system on a desktop PC.

A full description of the operation of the GRAFNAV software is contained in refs 1 and 2.

Sections 4.1 and 4.2 provide a summary of the mechanisms underlying the operation of the GRAFNAV software when processing carrier-phase based GPS recordings, and are partially based upon the description provided in ref 1.

4.1 Post-Processing of Pseudorange Measurements

GPS receivers intended for the computation of navigation solutions employ pseudorange ('code') measurements to each of a number of GPS satellites. Each pseudorange measurement can be expressed in the form

$$\rho = c\Delta t + v$$

where

ρ is the pseudorange measurement

c is the velocity of light

Δt is the transmission time of the radio signal from satellite to receiver

v is the sum of the error terms inherent in the measurement

In order to compute a navigation solution, a GPS receiver will perform a series of such measurements to each of a number of satellites. Provided that the position of each satellite is known (this can be determined using the ephemeris data transmitted by the satellite in question), knowledge of the transmission time Δt for each satellite would, in theory, allow the user's position to be computed from any three satellite measurements.

Unfortunately, the receiver is unable to measure Δt for each satellite directly but must instead rely upon the pseudorange measurements ρ , each of which is corrupted

by an error term v . The latter arises from a number of sources which include errors in the broadcast ephemeris and in the satellite clock; propagation errors due to the ionosphere (the region of charged particles between 50km and 1000km above the earth's surface) and troposphere (the portion of the atmosphere below 10km, whose refractive index varies according to the amount of water vapour and other trace gases present); multipath propagation due to the environment surrounding the receiver antenna; electrical noise sources in the antenna and receiver circuitry; receiver clock bias (arising from synchronisation differences between the receiver and satellite clocks); plus any deliberate degradation applied to the satellite signals (Selective Availability, SA).

The only one of these error sources which can be guaranteed to be identical for each satellite is the receiver clock bias term. As a result, it is possible to eliminate this unknown quantity from the computation by, for example, subtracting one pseudorange measurement from another.

This technique forms the basis for the computation of a GPS navigation solution using pseudorange measurements to four satellites. The additional satellite and pseudorange measurement is necessary in order to provide a uniquely determined solution (four equations with four unknowns: the four unknown quantities being the user's 3-D position and the clock bias term).

Additional pseudorange measurements may be included in the position computation provided that an appropriate mechanism is available to handle the over-determined nature of the solution. This is commonly achieved through the use of a Kalman filter in which a series of dynamically varying weightings is applied to each of the pseudorange measurements.

The effects of the other error contributions contained in v cannot, in general, be eliminated from the resulting position solution in a stand-alone navigation receiver. Partial exceptions are some of the atmospheric effects, for which an approximate correction can be applied in the receiver to remove a portion of the error.

The residual navigation error in this type of receiver, using only L1 code-based measurements, is normally quoted in the form of a 95% horizontal error confidence limit of 100m. A more detailed discussion of the characteristics of these errors is contained in ref 3.

Much of this error can be eliminated if a second receiver is used, placed at a known position. By inverting the position computation equations it is possible to determine the residual error v for each satellite pseudorange measurement taken by this second ('reference' or 'base station') receiver.

Assuming that the residual errors v for the mobile (unknown position) receiver are identical to those determined at the reference receiver, it is possible to remove these errors from the mobile receiver's position computation, either post mission or in real-time.

When used in real time, this technique forms the basis for Differential GPS (DGPS) in which the residual errors in v ('differential corrections') for each satellite are transmitted from the reference to the mobile receiver using whatever form of datalink is most appropriate. An industry standard, known as RTCM-SC104, exists for the transmission of differential corrections and is documented in ref 4 (which also

contains additional information relating to the performance of typical DGPS systems).

Through the use of DGPS techniques, it is possible to virtually eliminate the errors arising from the ephemeris, satellite clock, and Selective Availability since these effects should be independent of receiver location. Compensation for the remaining two significant error sources (ionospheric and tropospheric propagation) will be almost complete if the two receivers are close together; however as the baseline separation between them is increased the correction will become less valid as the difference in the atmospheric paths to the satellites increases.

Ref 4 suggests that DGPS equipment offers the possibility of 'accuracies of 2-10 metres for dynamic navigation applications', with an additional degradation with increasing baseline length of the order of 'a few metres' in several hundred kilometres.

DGPS techniques cannot compensate for the effects of any errors which are not common to and correlated between the two receivers involved: these include receiver noise, and any multipath propagation of the satellite signals due (for example) to the presence of significant metallic structures in the vicinity of the L-band antennas connected to the reference and mobile receivers.

The choice of frequency band and modulation technique employed for the DGPS datalink does not directly affect positional accuracy, since the datalink is simply a mechanism for transmitting a digital bit stream to a remote site. As a minimum, it should possess a data rate of at least 240 bits per second (ref 4): as the bit rate is increased, the interval between successive correction messages reduces.

Increasing the update rate for the differential corrections minimises the latency between their computation at the reference station, and their application at the mobile receiver: as this latency increases, the correction data becomes increasingly 'stale' and the positional accuracy reduces slightly (ref 4 suggests that the increased error will be of the order of a couple of metres after ten seconds). Many operational DGPS systems transmit new correction data at a 1Hz rate.

Since most forms of datalink are not immune to the possibility of data corruption during transmission, it is essential that corrupted messages can be identified and rejected before an attempt is made to apply the erroneous correction data in a navigation solution. It is for this reason that a strong parity-detection algorithm is an integral part of the RTCM-SC104 standard: if occasional data corruption occurs then the affected correction message will be rejected, and the previous message used (resulting in a temporary increase in message latency). Clearly, the datalink design should ensure that the occurrence of corrupted messages is kept to a minimum, in order to prevent the latency increasing to unacceptable levels.

As an alternative to the computation and transmission of the differential corrections in real time, it is possible to perform a post-mission computation using the pseudorange measurements from the base station and the mobile receivers. If this approach is used, then it is not necessary to perform an explicit computation of the correction terms: instead, these quantities can be removed by differencing the two sets of pseudorange measurements.

This operation can be explained mathematically as follows: the subscripts 'R' and 'M' denoting the measurements from the reference and mobile GPS receivers respectively.

The pseudorange measurements to a common satellite from the two receivers are:

$$\rho_R = c\Delta t_R + v_R$$

$$\rho_M = c\Delta t_M + v_M$$

Each of the error terms v can be expressed as follows:

$$v_R = C_R + v_C + R_R$$

$$v_M = C_M + v_C + R_M$$

where

C_R and C_M are the clock bias unknowns for the two receivers

v_C is the pseudorange error common to the two receivers (e.g. satellite clock)

R_R and R_M are the residual pseudorange errors specific to each receiver (e.g. multipath, receiver noise)

The difference between the two pseudorange measurements is then

$$\rho_R - \rho_M = c(\Delta t_R - \Delta t_M) + (C_R - C_M) + (R_R - R_M)$$

in which the common element of the pseudorange error has cancelled, leaving only the residual portion specific to each receiver.

If a similar operation is then performed on a pair of pseudorange measurements for a different satellite, then by subtracting the two results the clock bias terms also cancel each other. If the two satellites are denoted by subscripts '1' and '2' then

$$\rho_{R1} - \rho_{M1} = c(\Delta t_{R1} - \Delta t_{M1}) + (C_{R1} - C_{M1}) + (R_{R1} - R_{M1})$$

$$\rho_{R2} - \rho_{M2} = c(\Delta t_{R2} - \Delta t_{M2}) + (C_{R2} - C_{M2}) + (R_{R2} - R_{M2})$$

and, using the fact that the receivers' clock biases will be identical for each satellite, i.e.

$$C_{R1} = C_{R2}$$

$$C_{M1} = C_{M2}$$

then the so-called 'double-difference' is

$$(\rho_{R1} - \rho_{M1}) - (\rho_{R2} - \rho_{M2}) = c(\Delta t_{R1} - \Delta t_{M1}) - c(\Delta t_{R2} - \Delta t_{M2}) + (R_{R1} - R_{M1}) - (R_{R2} - R_{M2})$$

The assumption is now made that the residual double-difference error

$$(R_{R1} - R_{M1}) - (R_{R2} - R_{M2})$$

is small and can be ignored. The pseudorange measurements to four satellites then lead to three double-differences which are:

$$(\rho_{R1} - \rho_{M1}) - (\rho_{R2} - \rho_{M2}) = c(\Delta t_{R1} - \Delta t_{M1}) - c(\Delta t_{R2} - \Delta t_{M2})$$

$$(\rho_{R1} - \rho_{M1}) - (\rho_{R3} - \rho_{M3}) = c(\Delta t_{R1} - \Delta t_{M1}) - c(\Delta t_{R3} - \Delta t_{M3})$$

$$(\rho_{R1} - \rho_{M1}) - (\rho_{R4} - \rho_{M4}) = c(\Delta t_{R1} - \Delta t_{M1}) - c(\Delta t_{R4} - \Delta t_{M4})$$

These may be rewritten as:

$$(\rho_{R1} - \rho_{R2}) - (\rho_{M1} - \rho_{M2}) = c(\Delta t_{R1} - \Delta t_{R2}) - c(\Delta t_{M1} - \Delta t_{M2})$$

$$(\rho_{R1} - \rho_{R3}) - (\rho_{M1} - \rho_{M3}) = c(\Delta t_{R1} - \Delta t_{R3}) - c(\Delta t_{M1} - \Delta t_{M3})$$

$$(\rho_{R1} - \rho_{R4}) - (\rho_{M1} - \rho_{M4}) = c(\Delta t_{R1} - \Delta t_{R4}) - c(\Delta t_{M1} - \Delta t_{M4})$$

which for each equation provides four terms, each in its own bracket.

The first bracketed term may be computed from knowledge of the reference station co-ordinates and the satellite positions, as determined from the transmitted ephemerides. The second term represents the unknown (the mobile receiver position). The third and fourth terms represent measurements taken at the reference station, and mobile receiver, respectively.

The core of the GRAFNAV software is a proprietary Kalman filter algorithm which uses double-difference techniques to form a post-processed differential position solution from a set of two concurrent recordings. One of these recordings must be from a reference GPS receiver whose position is known (and supplied to the software), the second recording being derived at the mobile receiver.

The software operates by forming a series of double-differences between pairs of satellites: the number of satellite pairs employed being one less than the total number of satellites tracked by both receivers. For example, if a total of six satellites were visible to both receivers, then five double-differences would be computed (two more than the minimum of three necessary for a 3-D position solution). Weightings are assigned automatically by the Kalman filter to each double-difference to assist in the computation of the overdetermined solution.

When operating using pseudorange (code) measurements alone, it is claimed that the GRAFNAV software is capable of computing the mobile receiver position to the '2 to 10 metre level'. This accuracy can, however, only be attained if the receiver-specific pseudorange error terms (denoted R_R and R_M above) are sufficiently small.

The principal factors which are likely to contribute to the receiver-specific pseudorange errors are receiver noise, and multipath propagation of the satellite signals. In both cases these are effectively baseline-independent (ignoring the trivial case of the two antennas being co-located); as the baseline increases the other error

terms, such as differences in ionospheric delay between the two sites, will become larger and will eventually dominate.

The receiver noise contribution to the pseudorange error represents the extent to which the receiver's measurement would differ from the expected value in the presence of a 'perfect' input signal. This results from the basic uncertainty which is inherent in the mechanisms used by the receiver to track the L1 C/A code and perform pseudorange measurements; and includes the contribution of thermal noise within the receiver, antenna, and cabling.

The receiver noise would normally be expected to be essentially independent of the antenna location and relative satellite position, although there might be expected to be a small degree of variation with incoming signal field strength and carrier-to-noise ratio. Receiver noise could be determined by using a GPS satellite simulator to generate defined input signals; and can also be estimated by techniques such as feeding two identical receivers from a common antenna (the difference between the resulting pseudorange measurements provides an estimate of the receiver noise effects, assuming that the latter are random and uncorrelated) - the latter technique does not, however, allow the contributions from the antenna to be measured.

Multipath effects are related to the relative geometry of the GPS antenna, the satellite(s), and the presence of any surrounding structures which affect the propagation of the satellite signals in such a way that the antenna receives a reflected and/or refracted signal in addition to the 'line of sight' satellite transmission. Any multipath signals arriving at the receiver antenna will necessarily be delayed relative to the direct (line of sight) transmission, and will combine with the latter so as to introduce an additional error, with a positive sign, into the pseudorange measurement (this can be thought of as the multipath signal 'dragging' the measured pseudorange towards it).

The extent of this error could, in theory, be computed from knowledge of the geometry between satellite, antenna and multipath source; together with information regarding the relative amplitudes and phase relationships between the direct and indirect signals. In practice there is generally insufficient information available to carry out a precise calculation: a complication is the fact that the relative geometry will be constantly changing due to the orbital motion of the satellites and (for a mobile receiver) the trajectory followed by the antenna.

From basic electromagnetic theory, it can be deduced that GPS multipath can be generated by almost any object within the field of view of the receiver antenna. These would include the ground or sea surface, the helicopter airframe and rotor blades, and (most significantly for this project) any large metallic objects, such as an offshore structure, in the vicinity of the receiver.

One of the primary aims of the project was therefore to determine whether multipath due to platform structures was a significant contribution to the errors in real-time DGPS equipment being used for offshore approaches. Estimates of the effect of multipath provided by the receiver manufacturers were interpreted as suggesting that a 'worst case' platform multipath scenario could involve errors which were a significant fraction of a C/A code chip: since the latter is equivalent to 300m (refs 3 and 5) the implication was that multipath-induced errors in excess of 100m might be observed.

It was also suggested that the extent of multipath errors was likely to be affected by the type of correlator design employed in the GPS receiver: the 'narrow correlator' type of receiver was likely to provide an increased degree of multipath immunity, although possibly at the expense of other factors affecting its overall performance. Unfortunately it was not possible to explore these issues using the receivers employed for the trials.

It was considered likely that, in general, the impact of multipath would fall as the distance from the platform increased. However, since the information about the form and size of reflective surfaces was insufficient to allow reflective levels to be estimated theoretically, it was considered important to fly the receivers at a variety of different ranges from the platforms.

The possibility of multipath corruption being encountered on the trial flights, and possibly affecting both the real-time DGPS equipment and the truth reference system, led to the need to provide the truth system with some form of multipath immunity.

4.2 Post-Processing of Carrier Phase Measurements

In addition to providing pseudorange measurements, the Navstar XR5-M12 receivers used for the flight trials also possessed the ability to generate carrier phase measurements for each satellite signal.

Each carrier phase measurement can be expressed in the form

$$\Phi = \Theta + \Sigma\Theta + N + \nu$$

where

- Φ is the distance between receiver and satellite, expressed in L1 wavelengths (approximately 0.19m)
- Θ is between 0 and 1 and represents the instantaneous carrier-phase measurement as a fraction of the L1 wavelength, derived by mixing a reference frequency generated by the receiver with the incoming GPS carrier signal
- $\Sigma\Theta$ is an integer counter of the total number of complete cycles in the incoming carrier since the receiver locked onto the satellite, derived by counting the number of times Θ passes through zero
- N is the (initially unknown) number of integer cycles from the receiver to the satellite at the instant of lock-on: it will remain constant for successive measurements provided that carrier lock is maintained
- ν is the sum of the error terms inherent in the measurement

Provided that the receiver maintains continuous lock onto the satellite signal, it is possible to determine Θ and $\Sigma\Theta$ to an accuracy of some small fraction of a wavelength (e.g. a few millimetres). $\Sigma\Theta$ is set to zero at the instant of initial lock-on, which can occur at any point in the carrier cycle (there is no requirement for Θ to be zero at lock-on).

These measurements cannot, however, be used directly without knowledge of the initial integer distance N to the satellite. Unfortunately, this so-called 'phase ambiguity' is not a measurable quantity but must instead be computed from a series of other observations.

Provided that the phase ambiguities can be determined, it is possible to employ carrier phase observations in a single- or double-differenced process to determine the vector displacement between two receivers to a high level of accuracy. The use of two receivers eliminates the majority of the contributions to the error terms v , leaving only the residual error terms (receiver noise, multipath, and baseline effects) which are not common to both receivers.

For carrier phase measurements, the receiver noise is effectively a small fraction of a wavelength provided that continuous lock on the satellite is maintained.

Provided that continuous phase tracking can be achieved, the effect of multipath corruption upon carrier phase measurements has an upper bound which arises from the fact that the error on any single measurement cannot be greater than one wavelength. This is because an indirect signal arising from multipath will, as far as the phase tracking circuitry is concerned, appear to be another carrier waveform of the same frequency (even if it is significantly delayed, perhaps by several hundred wavelengths) since it is not directly possible to distinguish individual carrier cycles. Even at maximum amplitude, the indirect signal will combine with the main carrier to produce a resultant signal which is identical to the carrier, with the exception of a small phase difference.

The modulating pseudo-random noise (PRN) code signal which is imposed on the carrier has a basic frequency of 1.023MHz, the so-called 'chipping rate', which is several orders of magnitude lower than the carrier frequency itself (1575.42MHz). This wide frequency separation allows the carrier to be tracked without being corrupted by the code signal: for example by multiplying the carrier signal by itself, known as the 'squaring' technique.

Carrier phase measurements can hence provide a truth reference system which is largely immune to multipath effects, provided that the phase ambiguity (represented by N in the above equations) associated with each set of measurements can be determined. Loss of carrier lock (which causes the cycle counter $\Sigma\Theta$ to 'lose count') at either the reference or mobile receiver, will require the redetermination of the new phase ambiguity.

A variety of techniques currently exist for the determination of phase ambiguities in GPS carrier-phase processing. For example, if the starting position of the mobile receiver relative to the reference is precisely known, then the ambiguities can be determined directly from an examination of the corresponding carrier-phase measurements.

If the antenna starting position is not precisely known, then the ambiguities can be determined by means of a comparison between other GPS measurements and the carrier phase observations over a period of time. The L1 C/A pseudorange can be used for this purpose; in some of the more sophisticated survey systems, observations derived from the L2 carrier can also be used.

With all these techniques, problems occur if there is any form of interruption to the signal received from a particular satellite: the resulting loss of 'carrier lock' normally causes the receiver to lose count of the number of carrier cycles. If carrier lock is subsequently regained, it is necessary to recompute the phase ambiguity for the satellite in question.

It should be noted that brief interruptions to the satellite signals can result in an immediate loss of carrier lock, even if no undue effects are observed on the corresponding code measurements (the latter are derived by averaging over a substantial period of time compared to the carrier frequency).

Provided that sufficient alternative satellites are available for which the phase ambiguities have been determined, it is possible to recover almost instantaneously from a brief loss of carrier lock. This is because the knowledge of the other satellite ambiguities implies that an accurate instantaneous position can be computed, which can then in turn be used to derive an updated ambiguity value for the problematic measurement.

For the processing of data recorded during the flight trials, the GRAFNAV software was employed to derive a combined code/carrier phase-based double-differenced position solution, using a mode termed 'Float Solution' by the software supplier. This involves the use of a proprietary Kalman filter to combine the code and carrier phase measurements from each satellite, and is essentially an extension of the code-only processing mode described in section 4.1 above.

The GRAFNAV 'Float Solution' uses the Kalman filter to continuously refine the software's estimates of the carrier phase ambiguity values. Initially, the performance of the software is similar to that when operating with C/A code only, but as the estimates of the ambiguities are refined the software begins to improve the relative weightings of the carrier phase measurements. The effect can be observed as a gradual convergence of the solution over a period of around 20 minutes of recorded data, on completion of which the computed ambiguities can be seen to stabilise at, or close to, integer values.

In the event of any disturbance to the carrier phase measurements (such as losing and regaining carrier lock on a satellite) the software attempts to recompute a new ambiguity value for the satellite as soon as possible.

This dynamic ambiguity recomputation is only possible if continuous lock was maintained on at least four satellites for the duration of the interruption. If fewer than four satellites were available, the solution reverts immediately to the C/A code level and a further convergence period is then required.

A useful facility incorporated into the software is the ability to process data in reverse: i.e. by beginning the convergence period at the end of the recorded data. This allows attempts to be made at mitigating the effect of significant losses of lock, by employing reverse-processed data for the period immediately following the event in question.

An example of the convergence of a carrier phase GRAFNAV solution, over an appreciable baseline, is shown in Figure 105 (page 131). This represents the time history of the position deviations in three axes about the mean, for two stationary Navstar XR5-M12 receivers separated by a baseline of approximately 70nm. It can be seen that the solution has converged to within half a metre in the first 20 minutes.

The GRAFNAV software does not require the mobile receiver to remain stationary for the duration of the convergence period, and is capable of resolving the carrier phase ambiguities whilst the receiver is in motion. However, if the mobile receiver has remained stationary for an extended period of time, it is possible to indicate this fact to the program. This allows the software to utilise a simpler form of Kalman filter (since the filter states connected with the mobile receiver velocity can be set to zero) which can, in turn, aid the ambiguity resolution process.

In the processing of the flight trials data, the GRAFNAV software was used for a variety of different purposes which are described in the following sections. In each case, the software was supplied with pairs of data files derived from two of the GPS recording systems (airborne, platform and onshore, described in Volume 1), together with co-ordinates of a known position for one or other of the receivers. Details of the procedure for converting the data files for use with GRAFNAV are outlined in Volume 1.

4.3 Onshore System Survey-In

As described in Volume 1 of this report, the onshore reference station was sited at a fixed location at the offices of DiffTech in Aberdeen for the duration of the trials programme.

In order to allow this station to be used as the primary reference for all of the remaining GPS data processing, it was necessary to determine the location of the onshore reference station antenna to a high degree of accuracy.

This survey-in process was achieved as a one-off exercise by taking concurrent recordings of GPS data at the onshore reference station, and at the Ordnance Survey triangulation pillar sited at Brimmond Hill close to Aberdeen (Dyce) aerodrome. Data was recorded at both sites for a period of approximately one hour.

A set of WGS84 position co-ordinates for the Brimmond Hill pillar, with estimated accuracy of $\pm 1\text{m}$ in each axis, was obtained by DiffTech from the OS. These co-ordinates were supplied to the GRAFNAV software, together with the data files from the two sites, and the software used to calculate a set of mean WGS84 co-ordinates for the onshore reference station:

Latitude	N 57° 06' 37.4198"
Longitude	W 002° 05' 06.0329"
Ellipsoidal height	144.975m

Previous experience with the use of the GPS equipment to perform surveys of this nature, together with details provided by the receiver manufacturer and software supplier, suggested that the accuracy of the carrier-phase solution over the baseline in question (approximately 6nm) should be better than one metre in each axis. This, when combined with the estimated accuracy of the OS data yielded an overall bound upon the co-ordinate accuracy of $\pm 2\text{m}$ in each axis.

As an independent check, these figures were compared against a set of co-ordinates derived by DiffTech for the antenna position using their own carrier-phase survey system (which used equipment and software produced by a competing manufacturer). It transpired that the horizontal separation between the two sets of

co-ordinates was of the order of 1.1m, showing an excellent degree of consistency between the two estimates.

The set of co-ordinates shown above was used in all subsequent data processing as the reference position for the onshore station, from which all truth position computations were (directly or indirectly) derived.

4.4 Platform System Survey-In

As described in Volume 1 of this report, the platform system was operated at defined locations on the helideck of each of the four offshore platforms visited for the duration of the corresponding flight trials.

For Flight 1 and Flight 3, where offshore platforms were not involved, the platform system was operated at set locations on, or close to, the runway at Longside aerodrome.

For each trial, the first data processing activity undertaken using the GRAFNAV software was to determine an estimate of the position at which the platform station had been located. This was achieved by treating the data recorded at the onshore station, together with the set of co-ordinates listed in section 4.3, as the reference and using the software to calculate a set of mean WGS84 co-ordinates for the platform reference station.

The resulting sets of platform system co-ordinates for the five offshore flight trials are as follows:

Flight 2 (Beatrice C):

	Computed position	Standard deviation
Latitude	N 58° 05' 38.8922"	0.07m
Longitude	W 003° 09' 11.7196"	0.05m
Ellipsoidal height	76.878m	0.07m

Flight 4 (Piper B):

	Computed position	Standard deviation
Latitude	N 58° 27' 37.0600"	0.13m
Longitude	E 000° 14' 56.8054"	0.12m
Ellipsoidal height	106.585m	0.26m

Flight 5 (Tartan A):

	Computed position	Standard deviation
Latitude	N 58° 22' 09.6212"	0.14m
Longitude	E 000° 04' 16.8361"	0.13m
Ellipsoidal height	109.931m	0.08m

Flight 6 (Buchan A):

	Computed position	Standard deviation
Latitude	N 57° 54' 09.6220"	0.55m
Longitude	E 000° 01' 52.1967"	0.27m
Ellipsoidal height	65.082m	0.30m

Flight 7 (Beatrice C):

	Computed position	Standard deviation
Latitude	N 58° 05' 38.8887"	0.08
Longitude	W 003° 09' 11.7177"	0.17
Ellipsoidal height	76.947m	0.08

The Beatrice C platform was visited twice, once on Flight 2 (8th May 1996) and again on Flight 7 (31st October 1996). Photographic records taken on the earlier flight of the platform box position relative to helideck features, were employed on the later trial in an effort to ensure that it was set up as closely as possible in the same position (the uncertainty associated with repositioning the box was estimated to be less than $\pm 0.1\text{m}$).

Comparison of the co-ordinates listed above for Flights 2 and 7 reveals that the difference between them is as follows:

-0.1m North, +0.0m East, +0.1m Up

The fact that the two sets of co-ordinates are in agreement to this level of accuracy is taken as evidence for the repeatability of the GRAFNAV software when computing carrier phase solutions, despite the existence of a significant baseline (circa 70nm).

For each of the platforms visited, information was sought from the relevant operator's survey department as to whether any independent survey data, with accuracy comparable to that expected from the GRAFNAV system, could be made available.

The requested information proved to be available only for the Piper B platform, where it transpired that a so-called 'GPS Reference Point' existed in one corner of the helideck, identified by a small metal plate. Fortunately it proved possible to locate the platform reference system directly over this reference point, enabling a direct comparison between the two sets of co-ordinates to be undertaken, with the following result:

-1.5m North, +0.6m East, +2.3m Up

The information provided by the operators unfortunately does not include an accuracy estimate for their co-ordinate figures. However, since the accuracy of the onshore system co-ordinates upon which the GRAFNAV-computed position is estimated to be of the order of $\pm 2\text{m}$, this result is taken as providing independent evidence for the absence of any gross errors in the truth position computations when operating over this extended baseline (circa 110nm).

Examination of the standard deviation figures shown above for each of the platform system positions reveals that there is a significantly greater variation in the computed position for Buchan A than for any of the other platforms. This can also be observed by comparing the error distribution and cumulative probability plots in Figures 1 to 4 (pages 19 to 20): Figures 1 and 2 show the Buchan A data from Flight 6 whereas Figures 3 and 4 show the Beatrice C data from Flight 7; the latter are typical of all the other platforms.

This discrepancy was attributed to the fact that the Buchan A platform is not, unlike the other structures visited, rigidly anchored to the seabed but is a floating semi-submersible platform. As discussed in ref 12, the platform is subject to the effect of localised tidal, wind and wave conditions which result in a small degree of platform motion.

The reported wind at the time of the Buchan A trial was a steady 150° at 30kt. Tidal predictions based upon two nearby platforms suggest that the tide fell by approximately 0.5m during the trial. Observers on the platform noted that there was an observable motion due to the waves, with amplitude of around ± 2 m and period of a few seconds.

The data in both Figure 1 and Figure 3 exhibit a bias in the distribution which extends in an approximately north-easterly or northerly direction from the computed mean platform position. Examination of the associated time domain data reveals that only a small number of data points are involved, and that these all appear at the start of the data set where the GRAFNAV solution is converging. It may be significant that these asymmetries extend in a similar direction to the onshore-to-platform displacement vector, suggesting that the software might be employing an initial estimate for the equipment baseline which proves to be slightly too large.

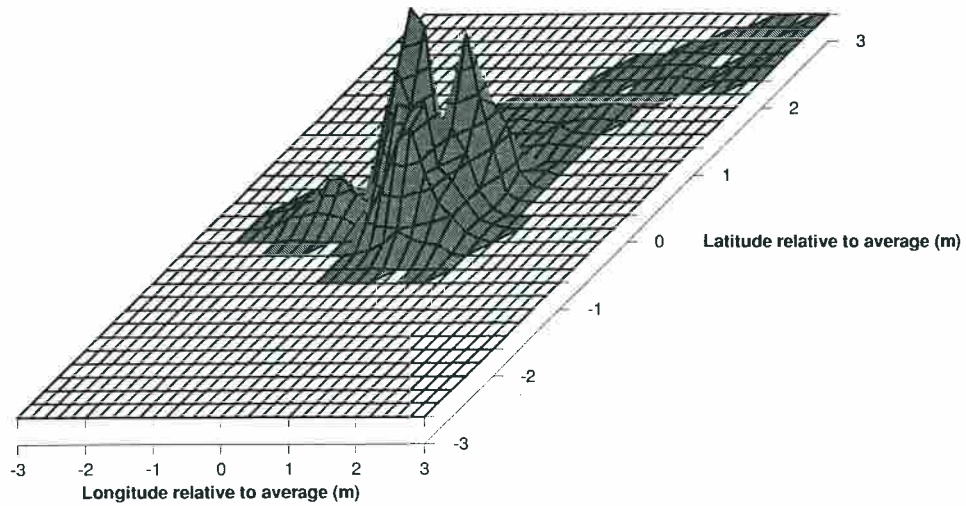


Figure 1 Distribution of Computed Platform System Positions Relative to Average, Flight 6, Buchan A

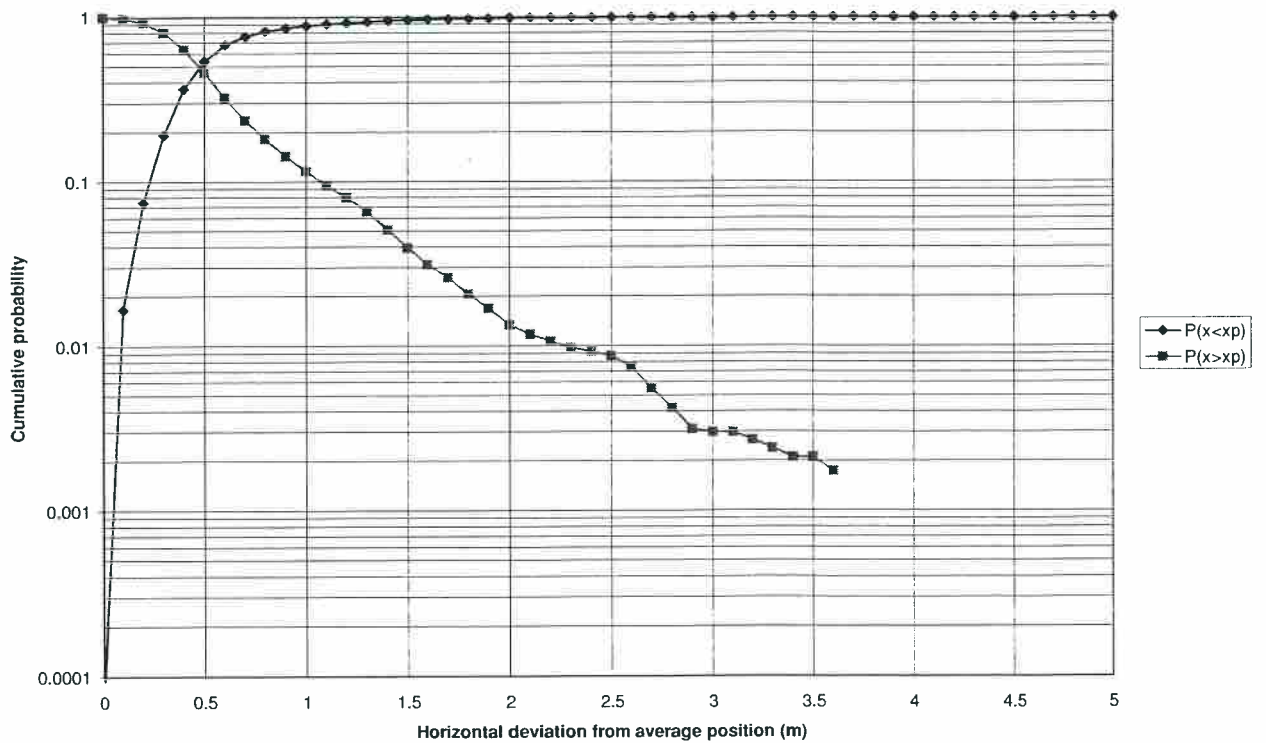


Figure 2 Statistics of Computed Platform System Positions Relative to Average, Flight 6, Buchan A (13,753 samples)

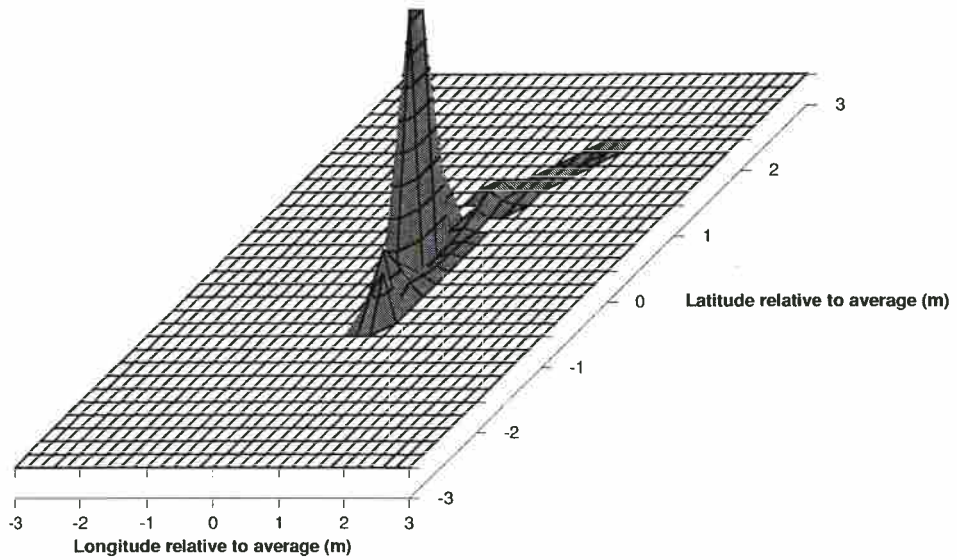


Figure 3 Distribution of Computed Platform System Positions Relative to Average, Flight 7, Beatrice C

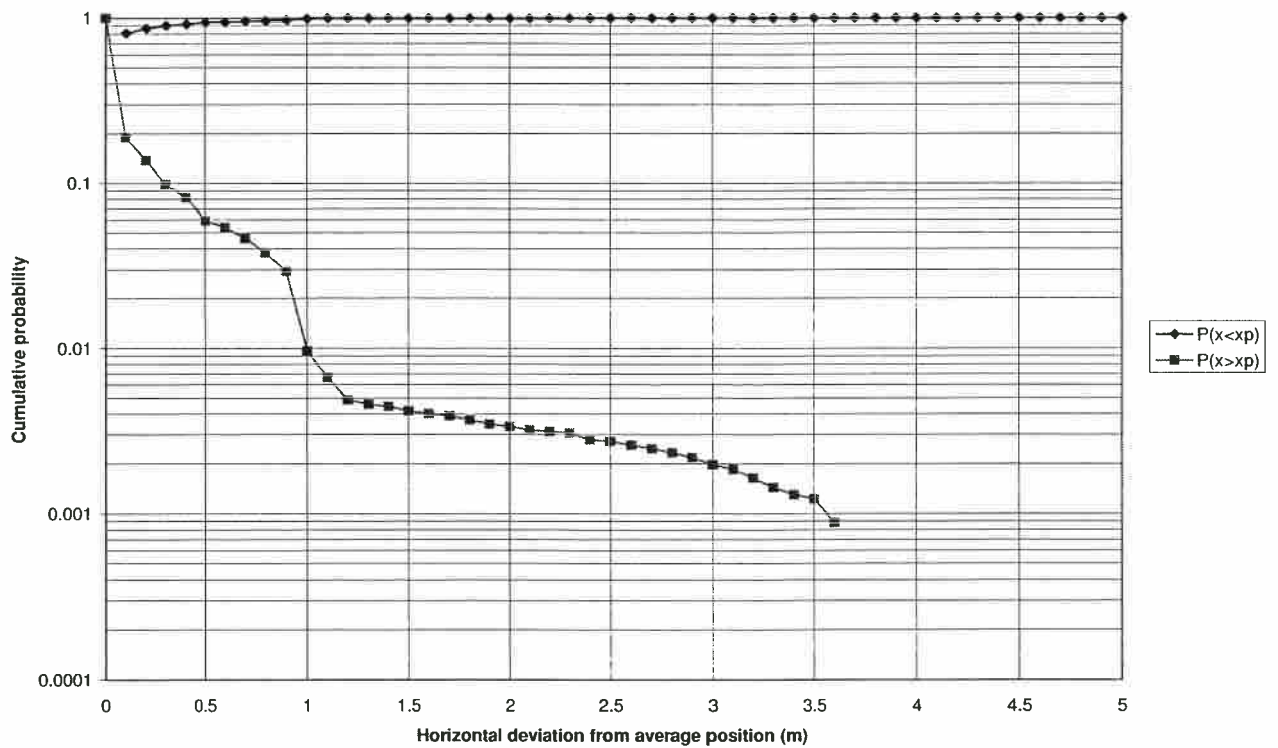


Figure 4 Statistics of Computed Platform System Positions Relative to Average, Flight 7, Beatrice C (14,629 samples)

4.5 Aircraft Truth Position Computation

Due to the fact that GPS data was recorded during each flight trial at two separate fixed locations, the GRAFNAV software could be used to derive two sets of truth position histories for the aircraft.

The first position history used the onshore system as a reference: data recorded onshore, together with the onshore system co-ordinates listed in section 4.3, were provided to the software together with the data recorded from the aircraft truth reference receiver. The resulting 'onshore-to-aircraft' position history was termed 'OTruth'.

The second position history used the platform system as reference: data recorded at the platform system was used, together with the appropriate co-ordinates derived in section 4.4 and the carrier phase data from the aircraft to generate a 'platform-to-aircraft' position history termed 'PTruth'.

Differences between the OTruth and PTruth position histories would be expected to arise as a result of various factors, including:

- (1) Different baselines.

With the aircraft in the vicinity of the platform, the baseline for the PTruth solution was relatively small (less than 10nm) compared with the OTruth baseline which could be up to 130nm. A shorter baseline would be expected to improve the resolution of carrier phase ambiguities, and might also speed the convergence process.

- (2) Bias in 'reference' co-ordinate data.

The sets of co-ordinates derived for the onshore system (section 4.3) and the platform system (section 4.4) both contain small unknown errors whose magnitude was estimated to be no more than a few metres. Any such error will propagate into the appropriate aircraft truth solution, appearing as a constant position bias with magnitude and direction equal (in the first order) to the error in the original co-ordinate data.

- (3) Different combinations of satellites tracked.

Owing to the separation between the two receivers, and to the presence of a different obstacle environment at the two sites, it would be expected that the two systems would not receive exactly the same set of satellites at all times. For example, a satellite at very low elevation would become visible to one station a short time before the other (the two receivers were both configured to attempt to track all satellites with elevation greater than 5°, although any satellite below 10° would be ignored by GRAFNAV).

The fact that a different number and/or combination of satellites could be tracked by the two reference stations, and thus available for use in the computation of the two truth solutions, would be expected to cause small variations between the results due to the weighting effect of the Kalman filter. This could be particularly significant during periods when the software was attempting to resolve the carrier phase ambiguities.

Although there was no independent position reference against which the data derived from either of the truth solutions could be compared, the fact that the two position histories were available led naturally to the concept of performing a direct comparison between the two. It was found that this comparison served as a useful indicator as to the stability of the two solutions: the presence of any significant discrepancy between OTruth and PTruth, and in particular of any significant deviation occurring over a short period of time, was generally found to result from a loss of precision in one or both solutions.

An example of a comparison between OTruth and PTruth is shown in Figure 106 (page 132). The gradual decrease in difference between the two solutions over the first 30 minutes corresponds to the convergence of the PTruth solution after the platform reference station has been switched on (the OTruth solution has converged earlier in the flight).

The consistency between the two solutions then remains below $\pm 1\text{m}$ in each axis for the remainder of the trial, with the exception of a short transient event occurring at around 12:45 UTC. Following this event, the consistency rapidly returns to below $\pm 1\text{m}$ but there is evidence of a repetition of the convergence process.

Examination of the raw carrier phase data reveals that the aircraft system operated for a short time with less than four satellites being tracked shortly after 12:45 UTC, due to loss of carrier lock. This caused both the OTruth and PTruth computations to attempt to redetermine the integer ambiguities, which in this instance was achieved fairly rapidly to bring the solution back within the $\pm 1\text{m}$ level.

An interesting comparison can be seen in Figure 107 (page 133), which represents exactly the same data but with GRAFNAV selected to process in reverse (i.e. to start with the most recent data). It can be seen that the effect of the loss of carrier lock at 12:45 is much more significant, in that the difference between OTruth and PTruth becomes greater than five metres for a short time and then reconverges over the following 45 minutes back to what appears to be a steady-state situation.

GRAFNAV's reverse processing capability proved to be a useful tool to mitigate the effects of this type of disturbance, by selecting the 'better' of the two (forward or reverse) solutions for particular time segments to produce one composite file covering the whole time span of interest.

Figures 108 to 111 (pages 134 to 137) depict the results of the comparison between OTruth and PTruth for Flights 2, 4, 5 and 6 respectively.

On the first offshore flight (Flight 2), it became apparent that the aircraft position truth solutions were not performing as expected, owing to the fact that there were frequent occasions when the aircraft receiver failed to maintain carrier lock on at least four GPS satellites. As a result, the software was frequently commencing fresh ambiguity resolution exercises during processing and the resultant effect upon truth performance can be observed on Figure 108 (page 134).

Examination of the events where major carrier lock loss occurred revealed that they exhibited a correlation with the aircraft being in a banked turn to the right. This resulted in the elevation of the tail rotor (which is located on the port side of the airframe) increasing relative to the GPS antenna, which was mounted centrally on top of the tail fin. Consideration of the geometry involved revealed that as the

aircraft was turning, the tail rotor disc was found to be progressively blocking the direct signal from those satellites which were not at a sufficiently high elevation. As the bank angle was increased, the receiver was able to maintain continuous carrier lock on fewer satellites.

The same effect did not occur in banked turns in the opposite direction, since the tail rotor was then at a lower elevation relative to the GPS antenna, thereby masking a smaller portion of the sky. It was also observed that the tail rotor masking appeared to be having little detrimental effect upon the operation of the real-time DGPS receivers, but was instead only affecting the truth reference receiver which, as discussed in section 4.2, was more susceptible to brief signal interruptions due to the necessity of maintaining continuous carrier lock.

After the flight, it was decided that in order to minimise the effect of this problem on future trials the pilots would be requested to perform turns to port wherever possible: in the event that a right-hand turn was unavoidable, then it was to be performed keeping the bank angle as low as possible. This restriction proved to have little detrimental effect upon the remainder of the trials programme: the approach manoeuvres described in Volume 3 were all symmetrical and could be performed with turns in either direction.

Examination of Figure 111 (page 137) reveals that a sinusoidal waveform, with period of a few seconds, appears to be superimposed upon the underlying OTruth/PTruth comparison for the Buchan A trial. The nature of this waveform can be observed more clearly on Figure 112 (page 138) which depicts an expanded portion of the same data.

This effect was only observed at the Buchan A platform and it was concluded that it resulted from the effect of the platform motion (described in 4.4 above) upon the PTruth solution: the processing software was assuming that the platform reference receiver was stationary, at the co-ordinates supplied by the user; whereas it was in fact moving with the platform. The resultant error was then propagating through into the PTruth position history for the aircraft.

Figure 113 (page 139) shows the results obtained by using the GRAFNAV software to process carrier phase data recorded in the course of the Longside ground trial (Flight 3). For this trial, the airborne recording system was reconfigured to provide an additional carrier phase receiver which was connected to a second (temporary) GPS antenna installation on the aircraft nose.

The trial was performed with rotors running, but the aircraft remaining stationary on the runway at Longside for periods of approximately 20 minutes. At the conclusion of each period, the pilot ground taxied the aircraft through two complete rotations, aiming to come to rest on approximately the same heading. A total of six rotations, with a 20 minute interval between each one, were undertaken.

For each 20 minute period, the post-processing software was arranged to perform two OTruth-like computations, one for each receiver/antenna pair. In each case, the program was requested to ignore data from previous periods, thereby ensuring that the Kalman filters were initialised from scratch for each of the twelve sets of solutions.

The plot shows in plan view the distribution of the horizontal position solutions returned by the GRAFNAV software. Each of the six 20-minute data periods is shown in a different colour (these can be thought of as six independent repetitions of the same experiment).

Whilst the aircraft was stationary for each 20 minute period, a series of photographic records was taken showing the aircraft's position relative to markings on the runway. By analysing these records, it was possible to determine an estimate of the position of each antenna and to overlay this information onto the drawing. This has been carried out using two black squares, joined by a colour-coded line, which represent the estimated positions (to within $\pm 0.5\text{m}$) of the nose and tail antennas.

The object of this exercise was to investigate the performance of the truth processing technique in an environment which was as close to flight as possible (i.e. with rotors and all aircraft systems running). If, for example, any degradation of the carrier phase recording and processing system existed due to interference from the aircraft main and/or tail rotor, then it would be expected to manifest itself in the results. The fact that all of the truth positions computed by the software were within 1.5m horizontal distance of the estimated antenna position is believed to provide compelling evidence in support of the validity of the selected truth system.

5 OTHER ISSUES AFFECTING GPS PERFORMANCE

5.1 GPS Satellite Constellation and Signals-in-Space

Throughout the trials programme, the status of the GPS satellite constellation was monitored by examining Notice Advisory to Navstar Users (NANU) and other public domain material issued by US Department of Defense (DoD) agencies.

Table 1 below provides a summary of the satellite status during the trials. Each operational satellite, identified by a unique Pseudo-Random Noise (PRN) number, occupied a different orbital position. The latter is identified by an orbital plane (of which there are six, A to F) and slot number within the plane, with a minimum of four satellites occupying slot positions within each plane.

	Slot 1	Slot 2	Slot 3	Slot 4	Slot 5
Plane A	9	25	27	19	-
Plane B	22	30*	2	5	20*
Plane C	6	3	31	7	28
Plane D	24	15	17	4	-
Plane E	14	21	10*	23	16
Plane F	1*	26	18*	29	-

Table 1 GPS Satellite Status During Trials Programme

Five of the satellites, whose PRNs are identified by asterisks in the table, were not operational for the full duration of the trials programme:

- PRN 1 was unusable for a period on the 12th April 1996 (07:55 to 14:15 UTC, NANU 069 of 1996 refers) and as a result was unavailable during Flight 1.
- PRN 18 was unusable from 7th May 1996 at 04:06 UTC until 9th May 1996 at 17:37 UTC (NANU 089 of 1996 refers) and as a result was unavailable during Flight 2.
- PRN 20 was removed from operational service on the 10th May 1996, and as a result was only available during Flights 1 and 2.
- PRN 10 was launched on the 16th July 1996 and became operational on the 15th August 1996: as a result it was only available during Flight 6 and Flight 7.
- PRN 30 was launched on the 12th September 1996 and became operational on the 1st October 1996: as a result it was only available during Flight 7.

The net effect was that the total number of operational satellites during each flight test was as follows:

- Flights 1 to 5: 24 satellites.
- Flight 6: 25 satellites.
- Flight 7: 26 satellites.

There was hence a minimum of 24 operational GPS satellites available in the constellation during the trials programme, and it is believed that Selective Availability (SA) was activated throughout this period.

Specific analysis of the GPS satellite geometry at the time of each trial, and of its likely effects upon navigation performance, was outside the terms of reference for the trials contractor. It is understood, however, that simulation tools are available to the CAA which permit studies of this nature to be undertaken, and which will also allow the trials data to be re-processed to examine the effects of individual satellite failures upon navigation performance.

In an attempt to determine whether any significant anomalies existed in GPS signal-in-space during the offshore platform trials, an examination was made of the pseudorange corrections generated by the onshore MF station as recorded on the aircraft.

The results of this analysis are presented in Table 2, which shows the statistics of the absolute value of the pseudorange errors (the sign of the correction has been ignored) for each of the five offshore flight trials. Similar data for Flights 1 and 3 was not available.

The 95% error figure of 77.8m and the maximum error of 229.1m suggest that no major signal-in-space anomalies occurred in the course of the trials.

	Flight 2 Beatrice C	Flight 4 Piper B	Flight 5 Tartan A	Flight 6 Buchan A	Flight 7 Beatrice C	All five flights
Samples	27873	19985	24392	28072	22643	122965
50%	20.5	15.7	15.4	16.7	25.0	18.7
95%	81.6	69.7	70.6	46.5	101.1	77.8
Maximum	163.5	163.5	163.5	79.4	229.1	229.1

Table 2 Statistical Distribution of Pseudorange Errors Measured Onshore (metres)

5.2 Time Synchronisation

In order for the analysis whose results are summarised in section 6 to be valid, it was important to ensure that the position fixes output by the three real-time GPS receivers were temporally consistent with the post-processed truth position solutions.

A failure to maintain temporal consistency would imply that the two position solutions which were under comparison did not relate to the same instant in time. Unless the aircraft was stationary, an error would be introduced into the position comparison equal to the product of aircraft velocity and the difference in validity time of the real-time and truth solutions.

Since the positional data in question originated from several different sources (i.e. the different GPS receivers mounted on the trials aircraft), care was taken in the design of the airborne recording system to ensure that time synchronisation was maintained (Volume 1 includes a summary of the techniques used). The recorded data also included sufficient information to enable any breakdown in time synchronisation during the trials to be identified.

Two forms of analysis were employed to confirm that time synchronisation had been maintained during the test flights.

The first technique was based upon an examination of the temporal relationship between the one pulse-per-second (1PPS) outputs generated by the aircraft truth receiver and each of the three differentially-corrected navigation receivers. As described in Volume 1, each receiver uses its 1PPS output to identify the specific instance in time at which each successive position solution is deemed to be valid. The 1PPS pulses should be synchronised to the start of the UTC second, via the medium of the GPS satellite timing reference.

Any difference (whether positive or negative) in time between two receivers' 1PPS outputs would imply that one receiver's position solution was valid in advance of the other receiver's, and that consequently it would not be possible to perform a legitimate position comparison by subtracting one position fix from the other.

The airborne instrumentation system was capable of identifying the occurrence of individual 1PPS pulses with a resolution of one millisecond. Comparison of the output times of the 1PPS pulses from any pair of receivers could be achieved, subject to an inherent uncertainty of $\pm 1\text{ms}$ which resulted from the hardware and software arrangement employed to identify the pulses.

An analysis was performed using the complete data set recorded during the flight trials programme, with the object of determining the statistical distribution of the δt parameter for each of the three differentially corrected receivers (GD1 GD2, and GD3). The parameter δt was defined as the elapsed time (positive or negative) between detection of a 1PPS pulse from the receiver in question, and the detection of the nearest 1PPS pulse from the airborne truth receiver. For example, a positive value of δt would imply that the receiver's 1PPS pulse (and hence its computed position solution) had occurred later than the truth receiver's 1PPS.

Table 3 shows the statistical distribution of δt for each of the three receivers, both in terms of individual samples and as a percentage of the total number of samples obtained from the receiver in question.

δt (ms)	GD1 receiver (MF-corrected Navstar)		GD2 receiver (UHF-corrected Navstar)		GD3 receiver (MF-corrected Trimble)	
	Number of samples	Percentage	Number of samples	Percentage	Number of samples	Percentage
< -2	0	0	0	0	0	0
-2	0	0	0	0	5189	9.8%
-1	11106	9.7%	11190	9.7%	39666	75.3%
0	98824	86.3%	98799	86.3%	7829	14.9%
+1	4561	4.0%	4552	4.0%	0	0
> +1	0	0	0	0	0	0

Table 3 Distribution of 1PPS Time Synchronisation for GPS Receivers

In the case of the two Navstar receivers, the table shows no evidence of any time synchronisation difference between the receivers' 1PPS outputs (no significance can be attached to the small proportion of samples at $\delta t = \pm 1\text{ms}$, since this is within the error bound associated with the measurement technique employed).

The results for the Trimble receiver imply that its 1PPS pulse was occurring consistently about a millisecond (plus or minus one millisecond) ahead of the reference Navstar receiver. Owing to the uncertainty involved in the measurement, it is perhaps debatable whether any significance can be attached to this result - in any event, at the approach speeds used during the trials, a one millisecond difference corresponds to a potential positional error of approximately five centimetres, which is significantly less than the anticipated accuracy of the truth system.

For all three receivers there are no outlying samples with larger values of δt , and therefore no evidence of any temporary failure of time synchronisation.

The second analysis technique which was used to examine temporal consistency was based upon the examination of a segment of data associated with a period of straight and level flight, to avoid any effects due to aircraft acceleration during manoeuvres.

Approximately 30 minutes' worth of data from Flight 4 was analysed by comparing the MF-corrected Navstar (GD1) position estimates with the post-processed OTruth truth solution. A process of linear interpolation was applied to the latter, to allow a defined and constant temporal shift to be introduced so as to simulate the effect of a failure of time synchronisation.

The interpolated position fixes were subtracted from the unmodified GD1 positions to provide a set of 2-D error estimates. The average of the latter over the whole data segment was then computed, and plotted as a function of the time shift (Figure 5).

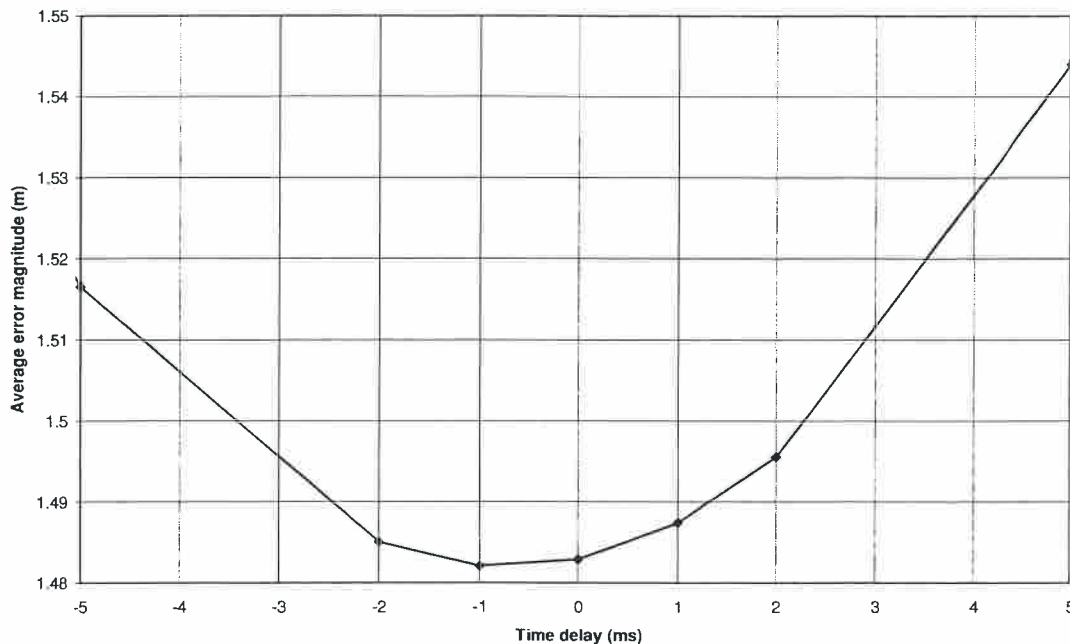


Figure 5 Temporal Alignment Check: Average 2-D Error versus Simulated Time Offset δt

From a consideration of the position of the minimum on the graph, it was concluded that the average temporal alignment between the two position sources was of the order of one millisecond, and was therefore insignificant at the approach speeds employed for the trials.

5.3 Airborne Antenna Installation

The choice of position for the aircraft L-band antenna was necessarily constrained by the very limited availability of locations on the upper fuselage offering the necessary visibility to the GPS satellite constellation. Whichever location were chosen, the signal path to the antenna from at least a portion of the visible hemisphere would be affected by the helicopter's main and/or tail rotor.

In an attempt to quantify the effect of the airframe and rotors upon the receiver performance with the selected antenna position, a special purpose ground trial was performed at Longside as part of Flight 3. The following is a summary of the method and results from this trial, full details of which can be found in ref 9. Data from this trial was also used to substantiate the performance of the truth reference system, as described in section 4.5.

The trial was performed with rotors running, but the aircraft remaining stationary on the runway at Longside for periods of approximately 20 minutes. At the conclusion of each period, the pilot ground taxied the aircraft through two complete rotations, aiming to come to rest on approximately the same heading. A total of six rotations, with a 20 minute interval between each one, were undertaken.

The airborne recording system was reconfigured in such a manner that identical data was recorded by two Navstar XR5-M12 receivers; one of which remained connected to the L-band antenna on the tail fin; and with the other receiver connected to a

second, identical, antenna which was mounted on the aircraft nose in place of the quarter-wave UHF antenna. Although this installation was of a temporary nature and only intended for use on the ground, the intention was that it would be fully representative of an operational antenna installation in this location.

Although the tail mounted GPS antenna was above the level of the helicopter's main rotor, it was relatively close to the tail rotor and the detrimental effect thus introduced upon the carrier phase truth system operation, described in section 4.5, had already been established. Although the problems with loss of carrier lock did not directly inhibit the code-based pseudorange measurements required for a real-time (D)GPS fix, it was considered likely that these measurements were being degraded by the rotor and one of the objectives of the trial was to estimate the extent of this degradation.

It was assumed that the nose-mounted GPS antenna would be relatively unaffected by the tail rotor, but that signal interference would instead be introduced by the main rotor due to the fact that the signal path to this antenna from a substantial portion of the visible hemisphere intersected the main rotor disc. Although the performance of the GPS receivers connected to both antennas would be affected by the rotors, it was considered likely that these effects would remain largely uncorrelated between the two receivers.

A direct comparison of the pseudorange measurements derived from the two receivers, although theoretically possible, would have involved the need to correct for the relative geometry associated with the two different antenna positions: this, of course, varied not only with satellite motion but also changed as the aircraft was rotated.

Fortunately, it proved possible to perform an essentially equivalent comparison by considering the difference between the position fixes output by the two receivers. Each receiver was artificially constrained to use an identical set of four satellite PRNs which had been predicted to offer good geometry over a one hour period: this ensured that the two position solutions would be based upon pseudorange measurements to the same satellites, and would therefore be identically affected by clock, SA, ephemeris and atmospheric errors.

The position solutions output by the two receivers were then differenced, to determine the horizontal separation between them. The distribution of these samples was examined, and compared with the physical horizontal separation between the two antenna positions which was measured as 10.8 ± 0.2 m.

A probability density plot of the difference between the two GPS solutions, based upon a sample size of 3,600, is shown in Figure 6. The average 2-D difference was computed as 10.8m, and all samples fell within the range (10.8 ± 3.5) m.

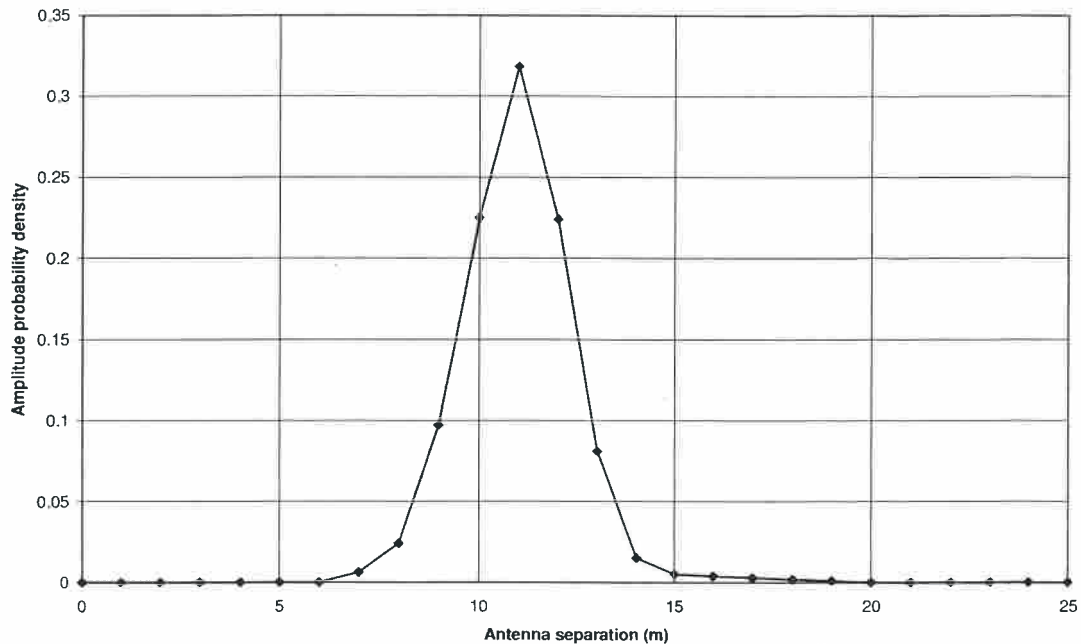


Figure 6 Longside Ground Trial: Distribution of 2-D Difference Between Nose and Tail Antenna Position Fixes (3,600 samples)

The difference between the receiver outputs during the rotations as a function of aircraft heading is shown in Figure 114 (page 140). Each rotation was undertaken in a clockwise direction through 720° at a rate of approximately $10^\circ/\text{s}$, beginning and ending on a heading close to 090° .

The plot exhibits signs of a 'weave' effect, with a relatively low period and which dominates over any random scatter. There is evidence of some correlation being present (around a heading of 045°) between the positions of the maxima of the weave on successive rotations, but there is also evidence of a phase shift in the positions of the maxima and minima within the sector 180° to 360° .

The presence of the weave suggests that a small degree of multipath corruption from the airframe was being encountered, with amplitude greater than the receiver noise, but with the maximum amplitude of the excursions due to both of these effects being no more than $\pm 1\text{m}$. The observed phase shift may be due to the relative motion of the four satellites in question during the 20 minute periods between rotations, which may have resulted in a slight shift in the multipath pattern surrounding the airframe.

Provided that the assumption regarding a lack of correlation between the effects of the airframe and surrounding environment upon the two GPS antennas is valid, the conclusion was drawn from Figures 6 and 114 that the net effect upon the 2-D position solutions output by the Navstar receivers was relatively small, i.e. no more than $\pm 2\text{m}$.

It was expected that interference to the GPS satellite signals from the airframe, rotors or any other localised source would, in addition to introducing errors into the pseudorange measurements, have the effect of reducing the signal-to-noise ratio of the satellite signal. Since the Navstar receiver data included a Carrier-to-Noise Ratio

(CNR) figure for each satellite in view, it proved possible to investigate these effects directly.

The analysis was performed by plotting the measured satellite CNR figures as a function of azimuth and elevation relative to the aircraft axes. From an examination of these plots, it was possible to investigate whether the CNR variations could be correlated with specific directions, which might relate to particular features of the airframe.

Figures 115 and 116 (pages 141 and 142) depict the variation of the mean CNR figures with azimuth and elevation, for the nose and tail antenna positions respectively.

The CNR values were first normalised, using measurements taken from a separate GPS receiver ('Platform Receiver') whose antenna was located in a open location several hundred metres from the aircraft, in an attempt to depict only those CNR variations resulting from the local environment at the aircraft.

The normalisation process involved subtracting, for each visible satellite in turn, the CNR value reported by the platform receiver from the corresponding aircraft receiver measurement. The resulting set of values expressed the difference between the performance of the aircraft and platform receiver installations when receiving satellite signals from a particular direction.

The normalised CNR figures were then assigned to a series of bins, according to the azimuth and elevation of the GPS satellite. Bins were set up in 10° increments in both azimuth and elevation, with any elevation angles less than 10° and greater than 80° being ignored.

By means of colour-coding, the polar plots depict the mean value of the normalised CNR figures assigned to each individual azimuth/elevation bin. Due to the satellite geometry and aircraft headings employed during the trial the number of samples assigned to each bin varied: at least 90% of bins contained at least six samples, and approximately 50% of bins contained more than 25 samples.

For the nose antenna the highest average CNR values were experienced at low forward elevations, and were lowest (less than -24dB) at low rearward elevations presumably due to signal masking by the aircraft fuselage. At higher elevations, under the main rotor, the reception quality was found to be relatively poor (e.g. -9dB loss at elevations of between 60° and 70°). There was a slight improvement at elevations above 70° .

For the tail antenna, reception was generally good in the starboard direction, exhibiting much less directional variation than the corresponding nose antenna results (presumably due to the fact that there are no obstructions from parts of the airframe in this direction). The average CNR was found to be lowest (less than -9dB) at low elevations to port, in directions which correlated precisely with the position of the tail rotor.

The presence of these large CNR reductions suggests that the passage of signals through the main and tail rotor discs could have a significant impact upon the receiver's ability to acquire and track satellites. The reason for the large variation in CNR is, at present, unclear although it is possible that a modulation effect, associated

with the rotor blade passing frequency (approximately 20Hz for the main rotor and 80Hz for the tail rotor), is involved. The effects are too severe to be attributed solely to the partial masking effect of the sky by the rotor blades, since the latter would be likely to cause a loss of only a few dB.

Additional experimentation, such as repeating the trial with the rotors stationary and/or rotating at varying speeds, would be necessary to explore this effect in more detail.

6 DGPS PRECISION RESULTS FROM OFFSHORE TRIALS

As discussed in Volume 1 of this report, the aircraft measurement system incorporated three separate GPS receivers, each of which was supplied with real-time differential corrections from one of two alternative sources. The resulting position solution from each receiver was recorded for post-flight comparison against the post-processed truth position history.

Two different receiver designs were employed (Navstar XR5-M12 and Trimble TNL-2100), combined with two alternative sources of differential corrections (MF, from commercially operated correction stations colocated with marine radiobeacons; and UHF, via a private datalink from the platform reference station). The three GPS receivers and their associated data identifiers were as follows:

GD1: MF-corrected Navstar.

GD2: UHF-corrected Navstar.

GD3: MF-corrected Trimble (only operational on Flights 6 and 7).

In order to perform an objective comparison of the performance of these three receivers, four offshore structures predicted to possess differing multipath characteristics were selected for the trials programme. A (notionally) identical series of flight manoeuvres was then performed at each platform.

Photographs of the four platforms, and copies of the platform layout diagrams employed by the helicopter operators, are shown in Figures 97 to 104 (pages 125 to 130).

- (1) Beatrice C (Flight 7 - data from Flight 2 has not been included).

The Beatrice is a small, unmanned, water injection platform with the particular, and unusual for the northern North Sea, characteristic that the helideck is the highest point of the structure. It was expected that this platform would provide a low multipath environment, which could be used as a baseline against which to compare results from other structures.

- (2) Piper B (Flight 4).

This platform (the replacement for Piper A) is a large oil and gas production platform typical of the northern North Sea. For safety reasons, the platform was designed with the accommodation module (the roof of which forms the helideck) separated as far as practicable from the derricks and other production equipment. The only significant vertical structures close to the helideck are a pair of gas turbine exhausts. This structure was expected to provide a medium level multipath environment.

- (3) Tartan A (Flight 5).

Tartan is broadly similar to Piper B, but with less separation between the accommodation and production modules. The derrick is partially clad in sheet metal and is relatively close to the helideck, thus the platform was anticipated to provide a medium to high multipath environment.

(4) Buchan A (Flight 6).

The Buchan is a former drilling rig which was converted into a production platform by the installation of additional equipment. The platform is semi-submersible, anchored to the seabed by chains; it is therefore subject to the effects of local tidal, wave and wind forces. In common with many mobile installations the helideck is located at a low level, close to the main superstructure which includes a derrick and twin flare booms. For this reason the platform was expected to provide a high multipath environment.

The manoeuvres undertaken at each platform are described in more detail in Volumes 1 and 3 of this report, but essentially they comprised:

- (1) A series of so-called 'Modified Aerad' approaches, which included an outbound leg passing overhead the platform at 1500ft, an inbound turn at a range of approximately 4nm, and a GPS-guided approach to pass abeam the platform at a range of 200-250m.
- (2) A series of orbits at varying ranges around the platform: 2nm, 1nm, 0.5nm, 0.2nm, and (subject to wind conditions) one or more passes as close to the platform structure as was practical. These were all undertaken at 200ft radalt height.
- (3) A number of 'experimental' approaches, which omitted the overhead outbound leg of the modified Aerad procedure, and were intended to allow the pilots to experiment with different approach guidance settings.

In this section, a summary of the performance of the three DGPS receivers during each of these tests is presented. The results have been grouped firstly by receiver (GD1, GD2 and GD3); secondly by platform (Beatrice C, Piper B, Tartan A and Buchan A); and thirdly by manoeuvre type (Aerad approaches, platform orbits, and experimental approaches).

All of the results in this section have been based upon the two-dimensional (horizontal) error between the DGPS receiver output, and the OTruth position history determined during post-processing. With the exception of a short period during the experimental approaches on Flight 6 (during which the both truth solutions are believed to have been affected by a carrier lock loss), the OTruth position provided a stable reference against which to compare the real-time solutions from the manoeuvres in question.

Periods during which the DGPS receiver reverted to non-differential operating mode, for whatever reason, have been excluded from the analysis. Section 7 includes a discussion of the circumstances under which reversion to non-differential operation was observed to occur.

For each of the combinations of receiver, platform and manoeuvre type which were investigated during the trials programme; the results have been presented in the form of a table followed by three graphical plots.

The table presents a summary of the statistics (number of samples, minimum, mean, standard deviation, 50% and 95% confidence levels, and maximum) of the 2-D errors;

broken down according to the horizontal range from the platform. Twelve range bins are employed, organised according to a logarithmic scale. Statistics are also presented in the table based upon the complete data set, irrespective of range from the platform.

The first graph in each set of results presents a cumulative probability distribution of the 2-D errors, irrespective of range from the platform; with a horizontal scale representing errors between 0 and 35m. The ' $P(x < x_p)$ ' curve represents the probability that the 2-D error will be less than the abscissa; and the ' $P(x > x_p)$ ' curve the probability that the error will be greater than the abscissa.

The second graph in each set is a scatter plot of 2-D error against range from the platform: this provides an indication of the distribution of sample points at different ranges (the 'Aerad' and experimental approaches consist of samples which are relatively evenly distributed, whereas the platform orbit samples are necessarily concentrated around the various orbit radii employed) and enables an impression to be gained of any correlation between error magnitude and range.

The third and final graph in each set of results displays a selection of the statistical data from the table for each individual range 'bin' (using a logarithmic horizontal scale) to provide a more qualitative indication of any significant variation of these statistics with range. As the graph does not display the number of samples contained within each 'bin', caution should be taken to avoid placing undue emphasis on any data for which the sample size is unduly low (e.g. just a handful of samples): this information may be readily obtained by cross-referring to the contents of the table.

6.1 **MF-Corrected Navstar (GD1) Receiver**

This receiver was a Navstar XR5-M12 which was supplied with differential corrections originating at commercially operated onshore reference stations, and broadcast in the MF (300kHz) band.

The receiver was operational on all of the offshore flight trials; the results on the following pages are derived from data gathered on Flights 4, 5, 6 and 7.

For a variety of reasons, the GD1 receiver periodically reverted to non-differential mode: this occurred in particular during portions of Flights 6 and 7 at the Beatrice C and Buchan A platforms. These problems are described in section 7.

Data relating to periods during which the receiver reverted to non-differential mode have been excluded from the analysis.

Distance to platform (metres)	Number of samples	Minimum	Mean	Standard deviation	50% of samples less than	95% of samples less than	Maximum
>3162	719	0.2	3.9	1.8	3.5	8.0	17.7
3162-1778	277	0.1	3.2	1.5	3.0	6.1	7.2
1778-1000	166	1.1	4.3	2.3	3.5	9.1	13.1
1000-562	88	1.6	3.5	1.1	3.4	5.4	6.4
562-316	58	1.8	3.4	0.8	3.2	5.3	5.6
316-178	51	1.9	3.4	0.5	3.5	4.3	4.5
178-100	4	2.9	3.5	0.5	3.8	3.9	3.9
100-56	4	1.3	2.2	0.7	2.5	2.7	2.7
56-32	0						
32-18	0						
18-10	0						
<10	0						
All ranges	1367	0.1	3.7	1.8	3.4	7.3	17.7

Table 4 Statistics of GD1 2-D Error (metres), Aerad Approaches, Flight 7, Beatrice C

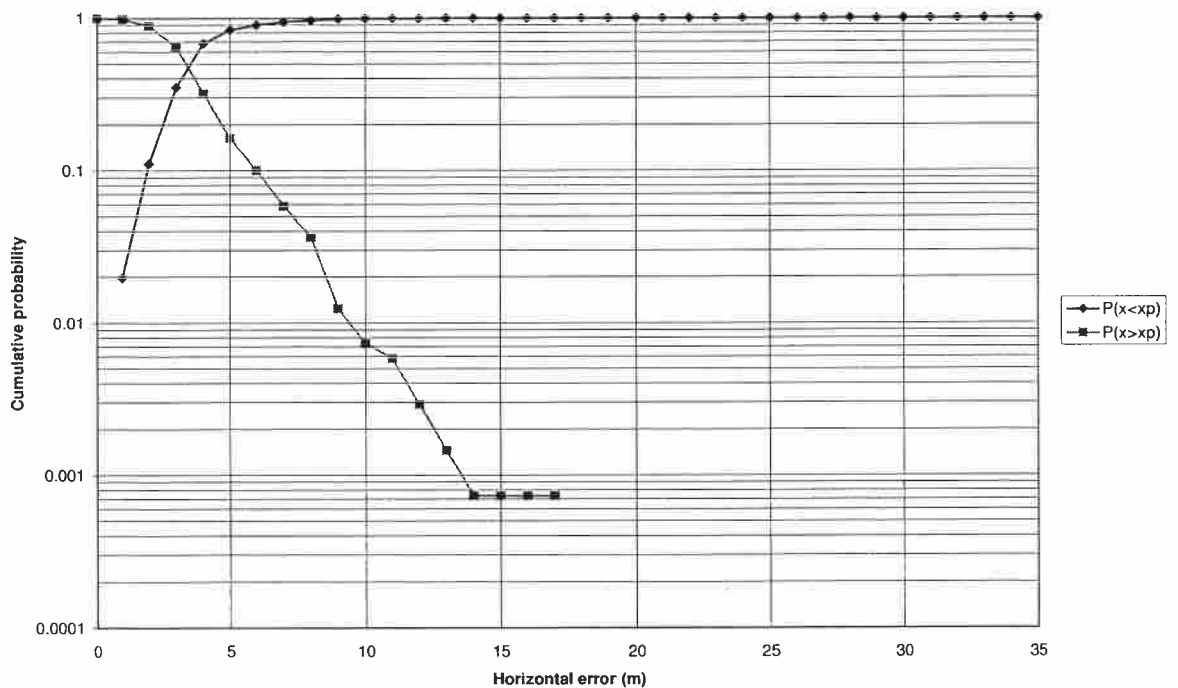


Figure 7 Cumulative Probability of GD1 2-D Error Irrespective of Range from the Platform, Aerad Approaches, Flight 7, Beatrice C

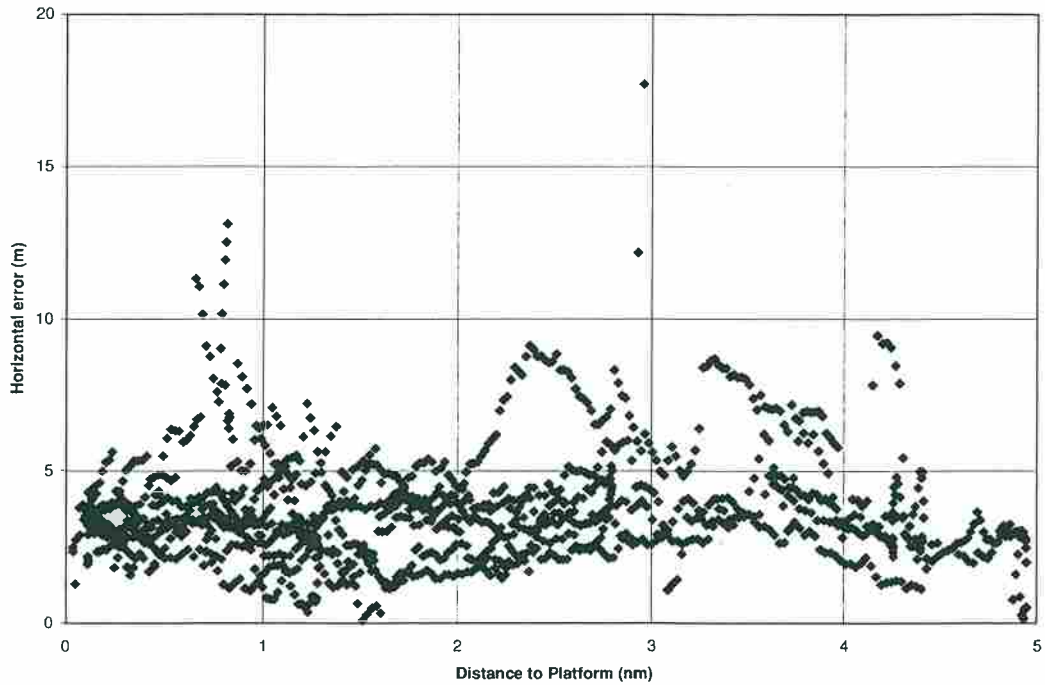


Figure 8 Scatter Plot of GD1 2-D Error Against Range from the Platform, Aerad Approaches, Flight 7, Beatrice C

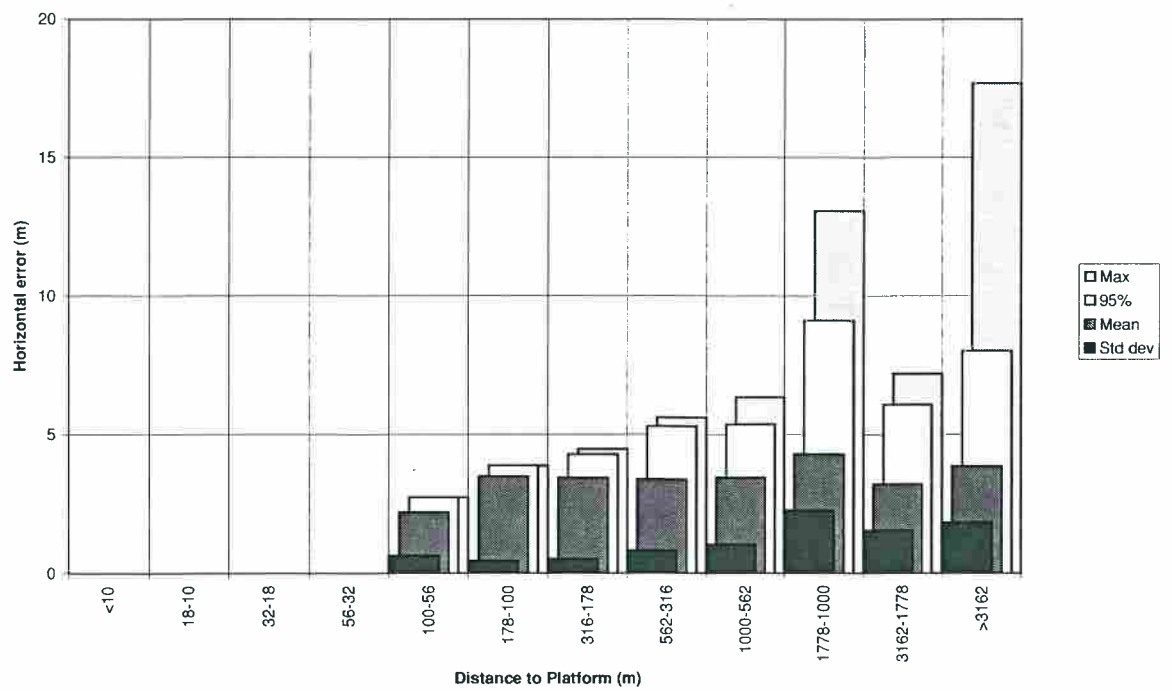


Figure 9 Variation of GD1 2-D Error Statistics with Range from the Platform, Aerad Approaches, Flight 7, Beatrice C

Distance to platform (metres)	Number of samples	Minimum	Mean	Standard deviation	50% of samples less than	95% of samples less than	Maximum
>3162	296	0.4	2.8	1.6	2.6	6.1	9.9
3162-1778	230	0.2	3.4	2.2	2.8	8.7	11.3
1778-1000	121	2.2	3.7	1.0	3.4	5.4	8.8
1000-562	141	1.5	3.2	0.9	3.2	5.0	5.8
562-316	164	0.3	3.1	1.4	2.9	5.1	5.7
316-178	114	1.3	2.9	1.0	2.7	4.8	5.7
178-100	63	1.2	3.2	1.2	3.1	5.1	5.4
100-56	56	1.1	3.0	1.4	2.6	5.0	5.3
56-32	38	1.7	2.6	0.9	2.3	5.0	5.1
32-18	5	2.8	3.2	0.3	3.3	3.4	3.4
18-10	4	2.7	2.9	0.3	3.1	3.3	3.3
<10	0						
All ranges	1232	0.2	3.1	1.5	2.9	5.4	11.3

Table 5 Statistics of GD1 2-D Error (metres), Platform Orbits, Flight 7, Beatrice C

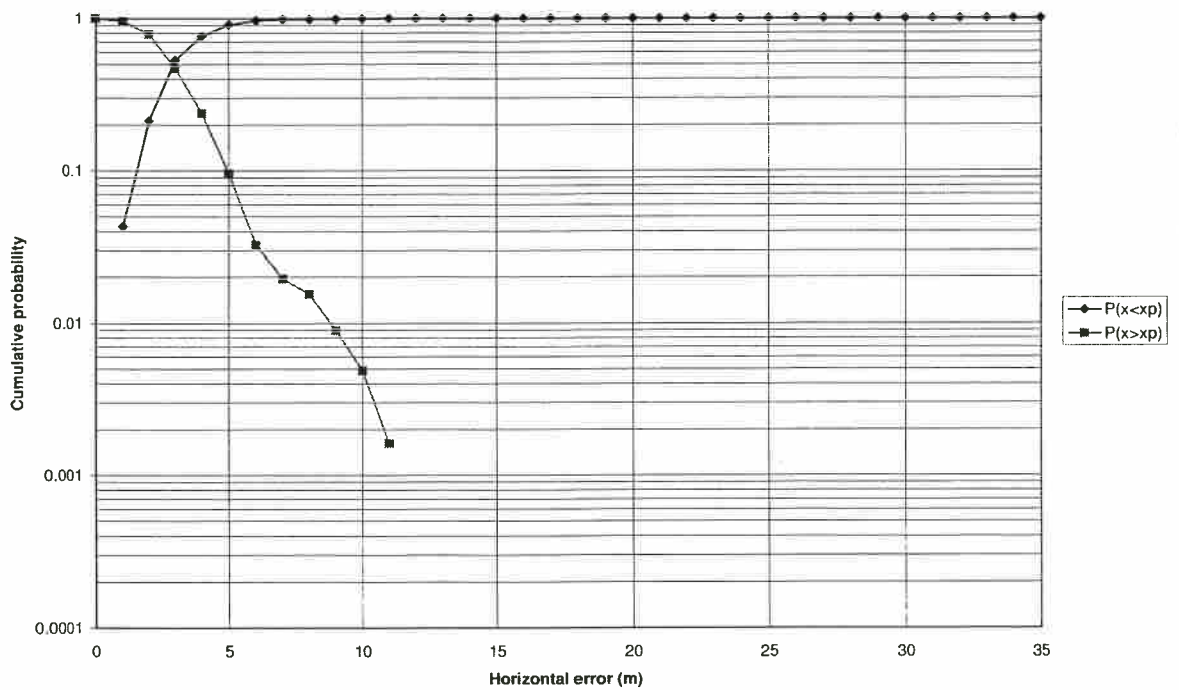


Figure 10 Cumulative Probability of GD1 2-D Error Irrespective of Range from the Platform, Platform Orbits, Flight 7, Beatrice C

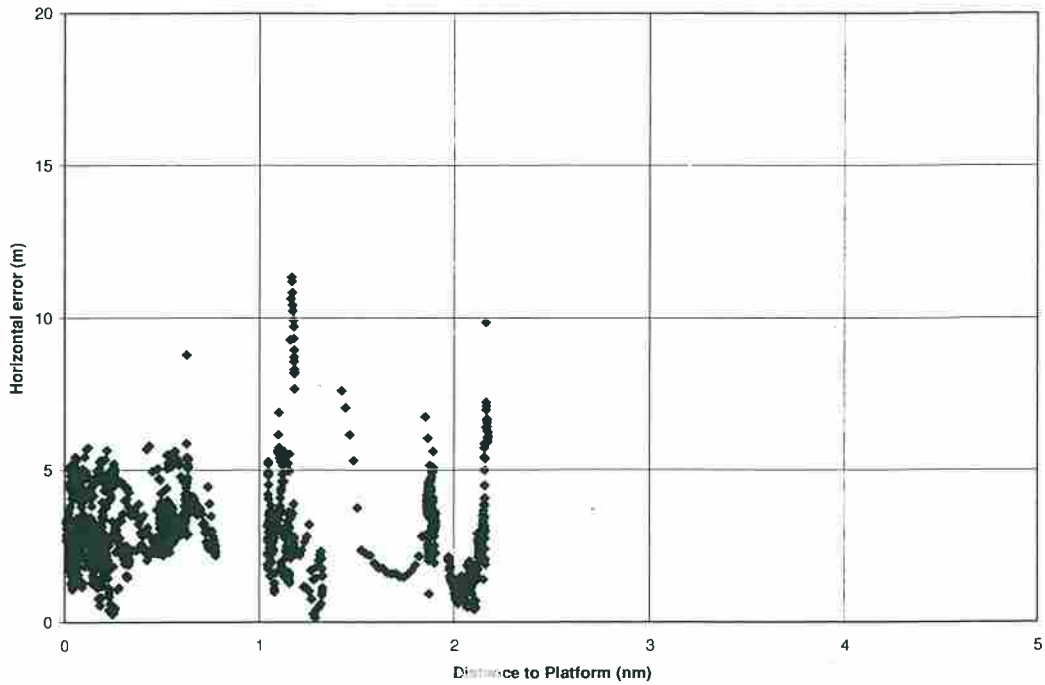


Figure 11 Scatter Plot of GD1 2-D Error Against Range from the Platform, Platform Orbits, Flight 7, Beatrice C

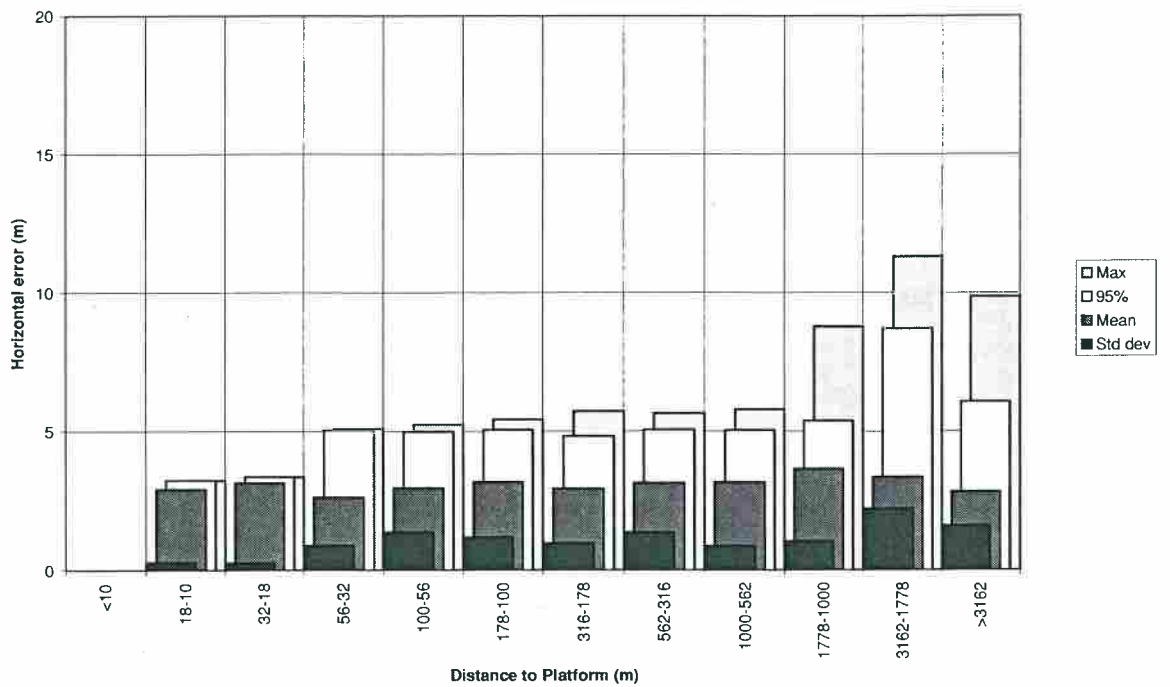


Figure 12 Variation of GD1 2-D Error Statistics with Range from the Platform, Platform Orbits, Flight 7, Beatrice C

Distance to platform (metres)	Number of samples	Minimum	Mean	Standard deviation	50% of samples less than	95% of samples less than	Maximum
>3162	2221	0.1	2.6	1.2	2.7	4.5	7.4
3162-1778	570	0.1	2.8	1.2	2.8	4.7	5.9
1778-1000	351	0.4	2.4	1.2	2.5	5.0	5.7
1000-562	196	0.2	2.5	1.1	2.7	4.2	5.7
562-316	112	0.2	2.5	1.3	2.7	4.4	4.6
316-178	61	1.0	2.8	0.8	2.8	4.4	4.9
178-100	14	1.7	3.4	0.9	3.7	4.5	4.5
100-56	8	2.8	3.5	0.4	3.6	4.0	4.0
56-32	2	3.3	3.5	0.3	3.7	3.7	3.7
32-18	1	3.1	3.1		3.1	3.1	3.1
18-10	1	3.6	3.6		3.6	3.6	3.6
<10	0						
All ranges	3537	0.1	2.6	1.2	2.7	4.6	7.4

Table 6 Statistics of GD1 2-D Error (metres), Aerad Approaches, Flight 4, Piper B

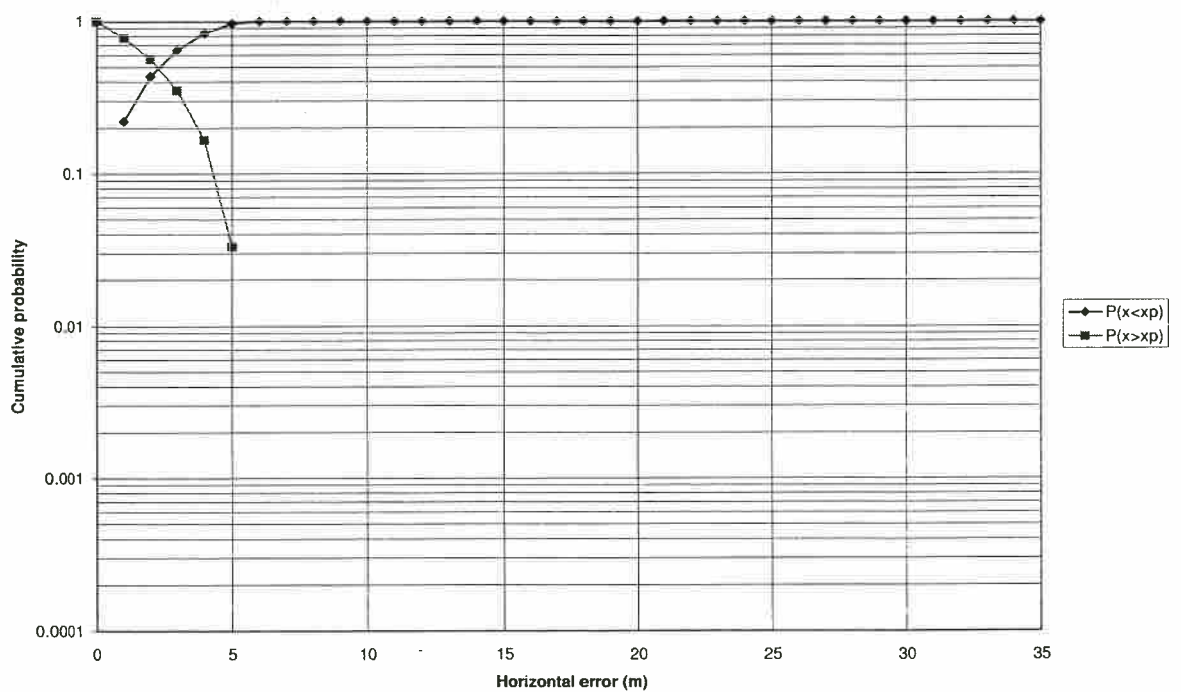


Figure 13 Cumulative Probability of GD1 2-D Error Irrespective of Range from the Platform, Aerad Approaches, Flight 4, Piper B

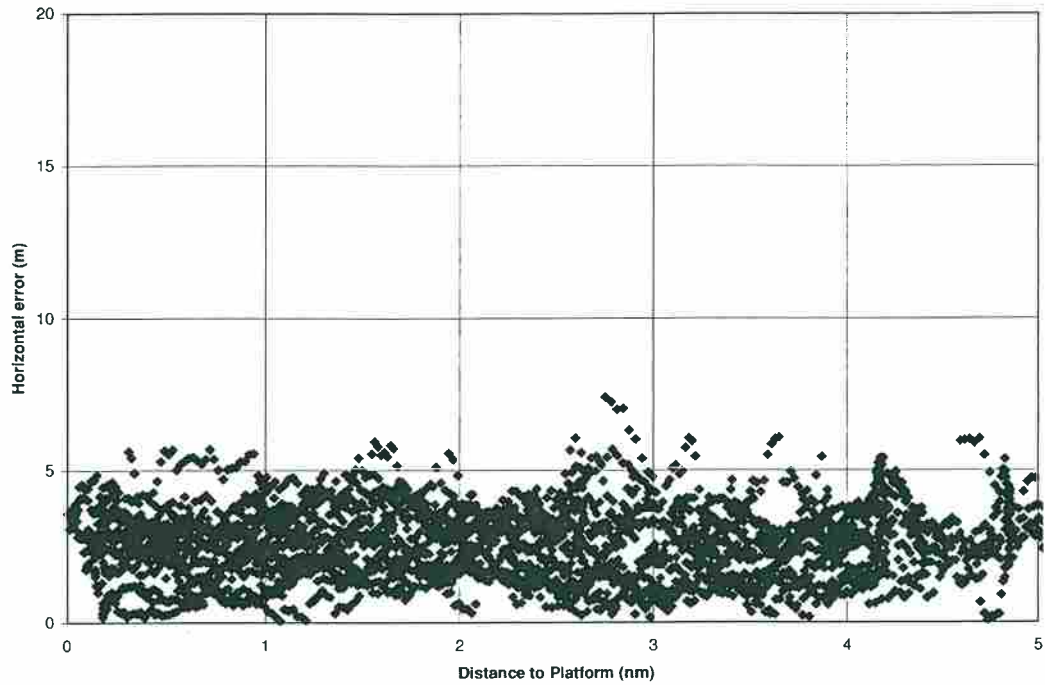


Figure 14 Scatter Plot of GD1 2-D Error Against Range from the Platform, Aerad Approaches, Flight 4, Piper B

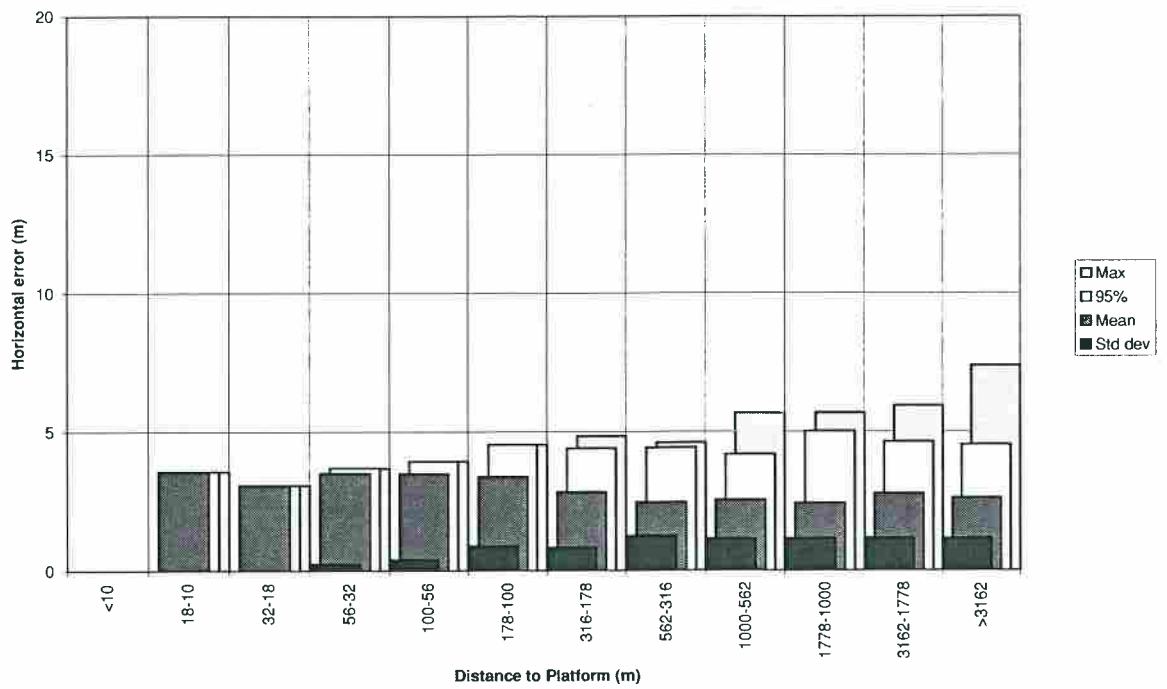


Figure 15 Variation of GD1 2-D Error Statistics with Range from the Platform, Aerad Approaches, Flight 4, Piper B

Distance to platform (metres)	Number of samples	Minimum	Mean	Standard deviation	50% of samples less than	95% of samples less than	Maximum
>3162	435	1.7	3.6	0.8	3.6	4.8	5.3
3162-1778	330	2.5	4.2	0.8	4.1	5.7	6.3
1778-1000	178	1.4	3.9	1.2	3.8	6.2	6.6
1000-562	161	0.3	3.4	1.6	3.2	5.9	6.9
562-316	153	0.2	3.2	1.6	2.8	5.9	6.5
316-178	63	0.7	3.5	1.8	3.9	6.2	6.9
178-100	38	2.1	4.8	1.3	4.5	7.4	7.6
100-56	22	2.3	3.4	1.4	3.0	6.9	7.0
56-32	7	0.2	1.1	0.7	1.0	2.0	2.0
32-18	3	0.3	4.7	7.3	0.7	13.0	13.0
18-10	0						
<10	0						
All ranges	1390	0.2	3.7	1.2	3.8	5.8	13.0

Table 7 Statistics of GD1 2-D Error (metres), Platform Orbits, Flight 4, Piper B

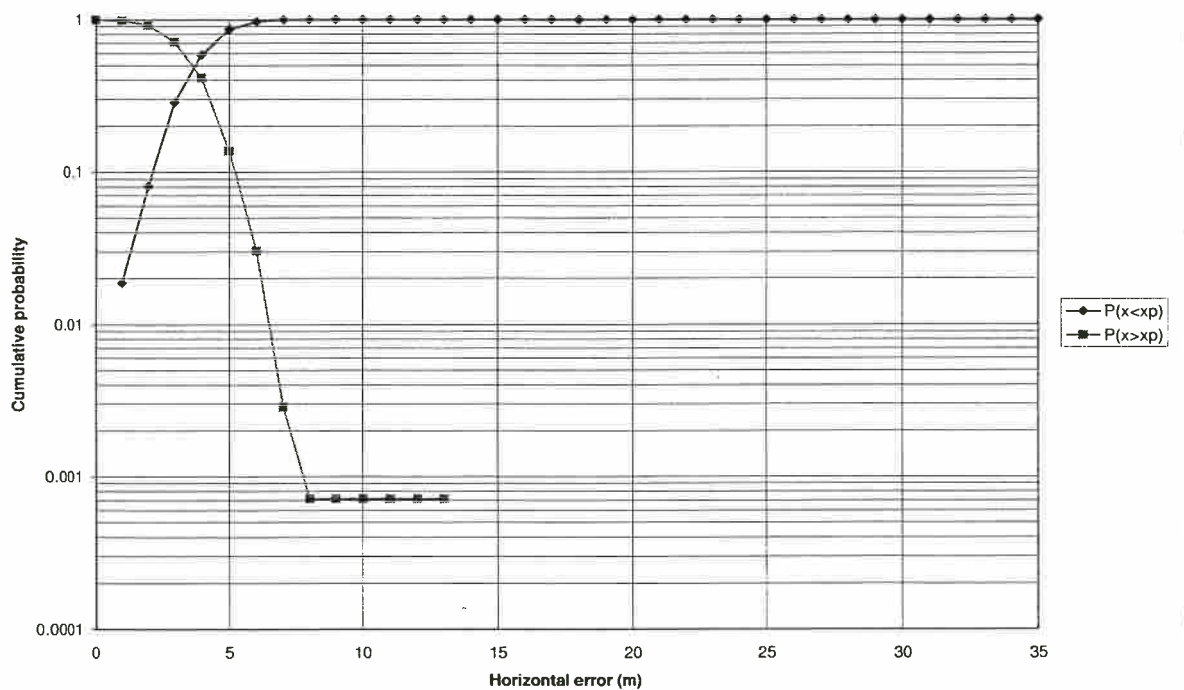


Figure 16 Cumulative Probability of GD1 2-D Error Irrespective of Range from the Platform, Platform Orbits, Flight 4, Piper B

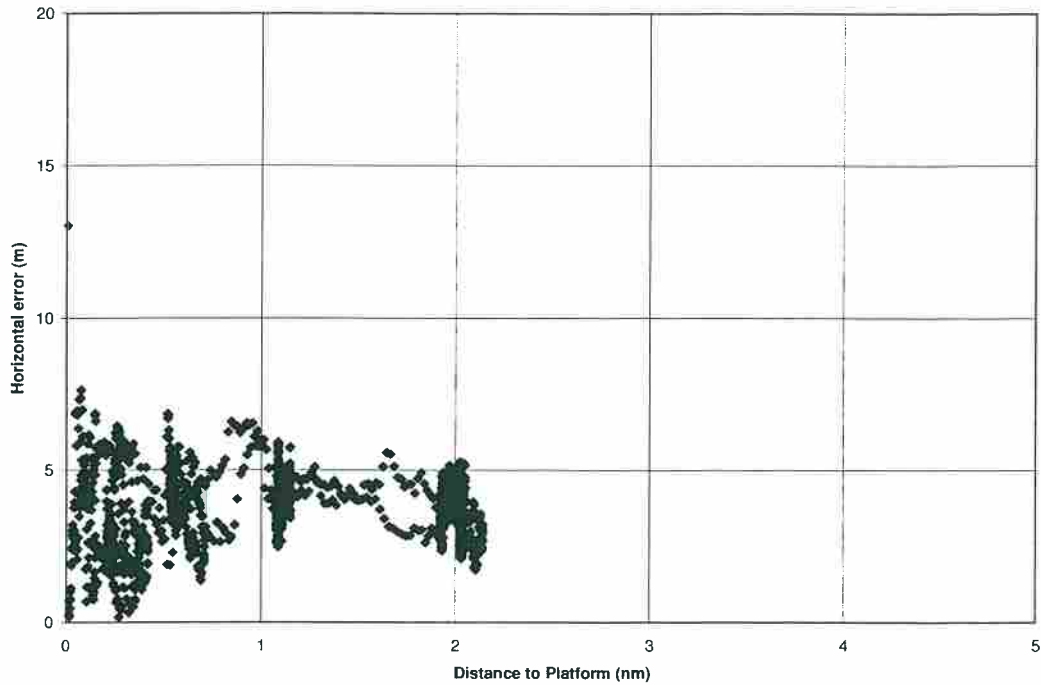


Figure 17 Scatter Plot of GD1 2-D Error Against Range from the Platform, Platform Orbits, Flight 4, Piper B

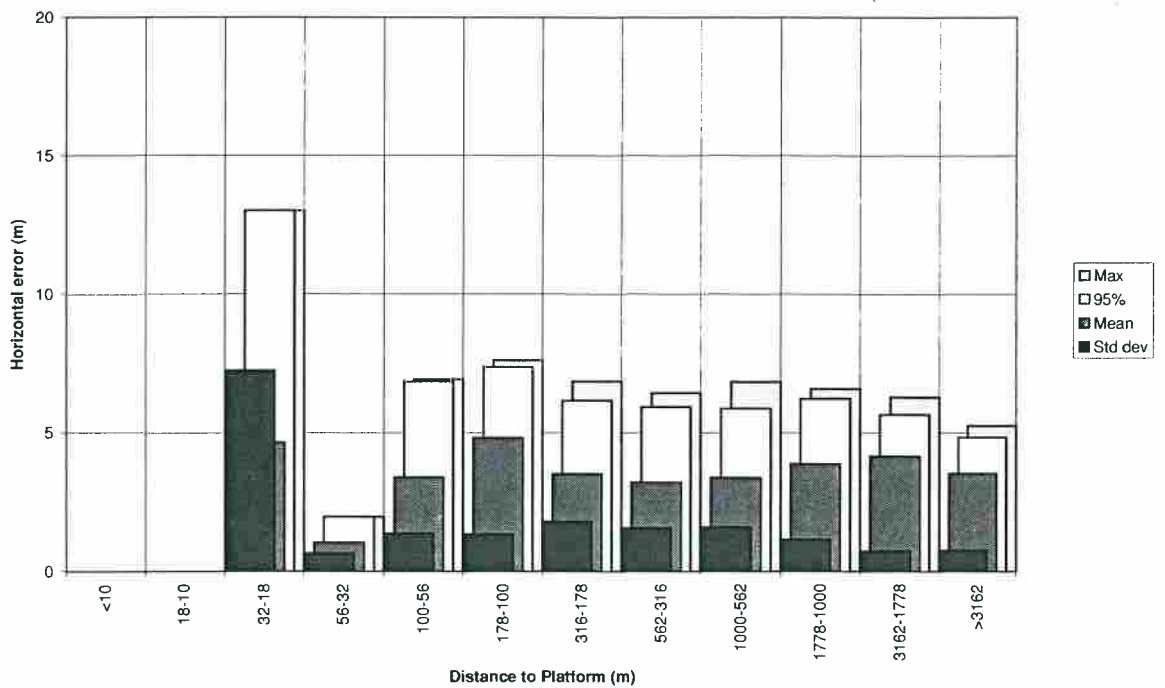


Figure 18 Variation of GD1 2-D Error Statistics with Range from the Platform, Platform Orbits, Flight 4, Piper B

Distance to platform (metres)	Number of samples	Minimum	Mean	Standard deviation	50% of samples less than	95% of samples less than	Maximum
>3162	1103	0.2	2.7	1.4	2.5	5.2	7.9
3162-1778	224	0.3	3.0	1.9	2.3	6.1	7.4
1778-1000	139	0.1	3.3	2.1	3.8	6.7	7.4
1000-562	82	0.0	3.4	2.2	3.4	7.6	8.9
562-316	53	0.5	3.7	1.9	3.2	7.2	7.6
316-178	42	0.1	3.7	3.1	3.4	11.4	12.7
178-100	15	3.5	4.9	2.1	3.9	9.2	9.2
100-56	11	4.1	5.2	1.0	5.1	7.6	7.6
56-32	9	5.1	5.6	0.3	5.6	5.9	5.9
32-18	22	4.5	6.2	1.4	5.8	8.3	10.4
18-10	3	7.6	7.6	0.1	7.6	7.8	7.8
<10	0						
All ranges	1703	0.0	3.0	1.8	2.8	6.0	12.7

Table 8 Statistics of GD1 2-D Error (metres), Experimental Approaches, Flight 4, Piper B

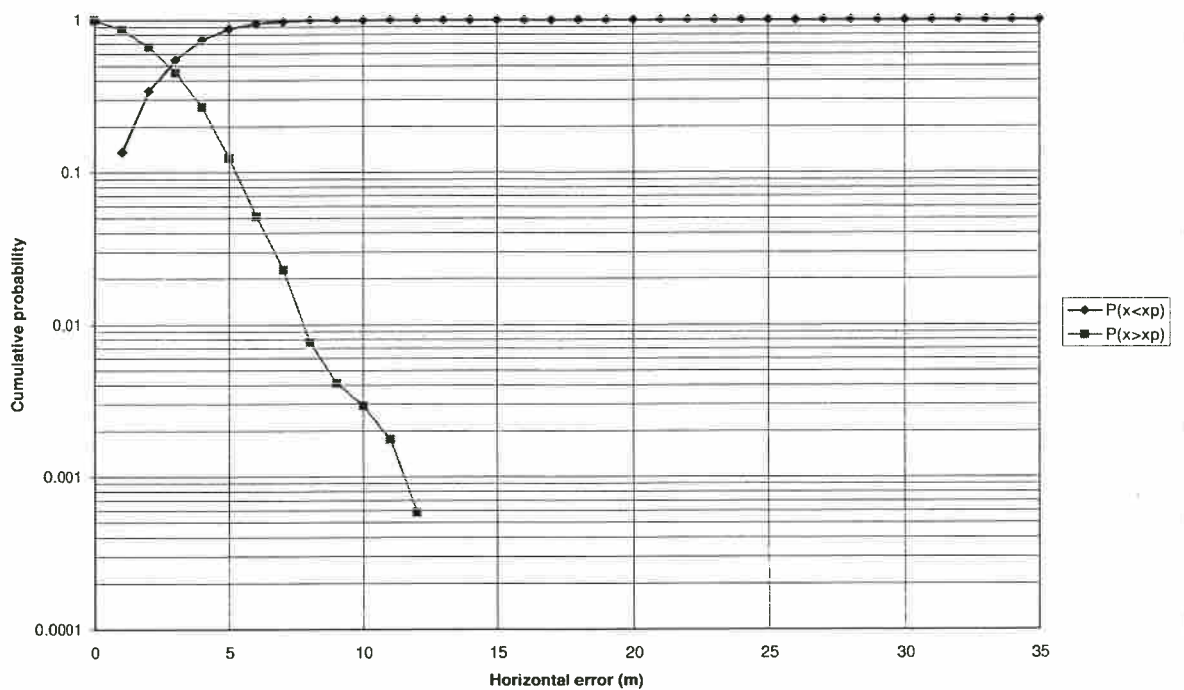


Figure 19 Cumulative Probability of GD1 2-D Error Irrespective of Range from the Platform, Experimental Approaches, Flight 4, Piper B

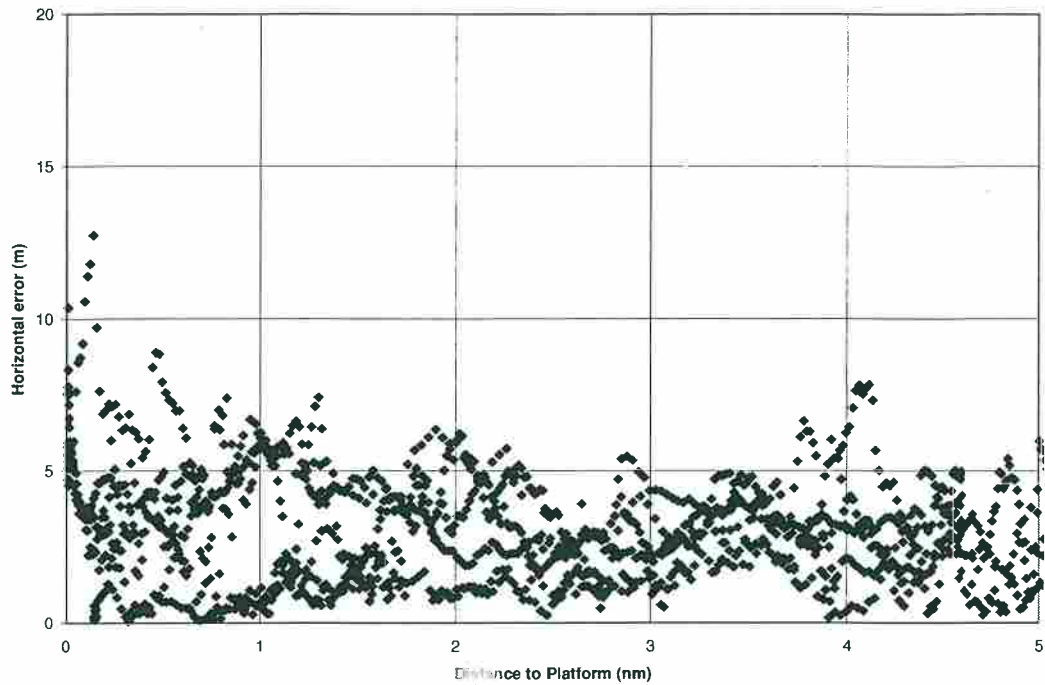


Figure 20 Scatter Plot of GD1 2-D Error Against Range from the Platform, Experimental Approaches, Flight 4, Piper B

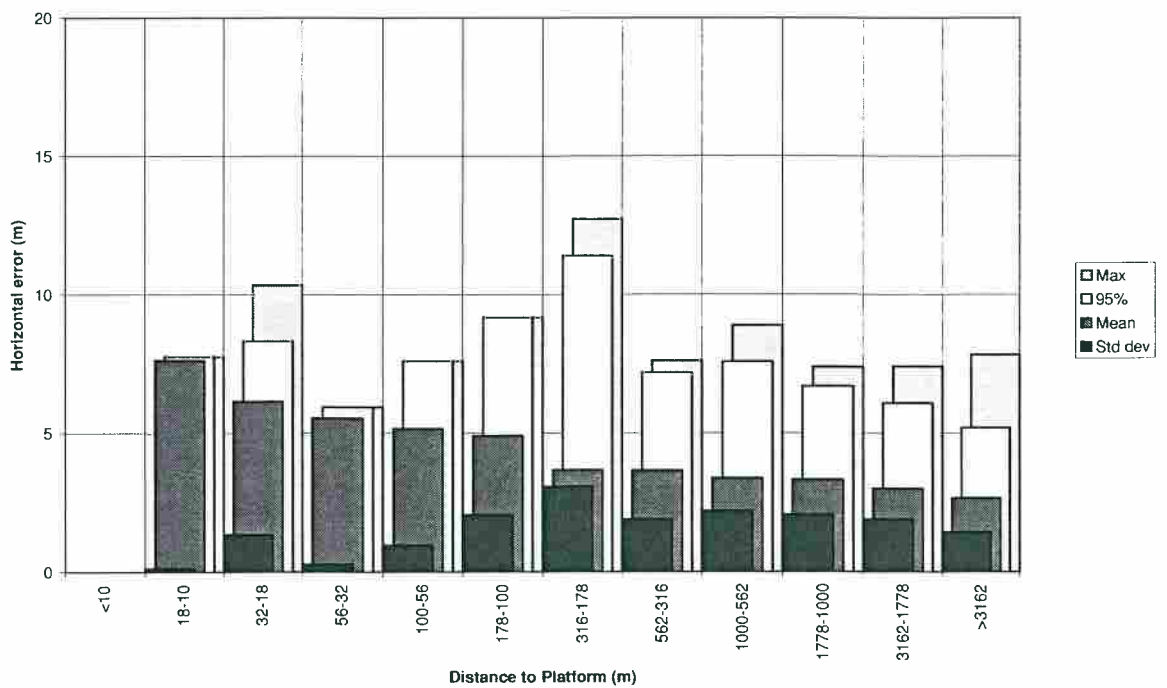


Figure 21 Variation of GD1 2-D Error Statistics with Range from the Platform, Experimental Approaches, Flight 4, Piper B

Distance to platform (metres)	Number of samples	Minimum	Mean	Standard deviation	50% of samples less than	95% of samples less than	Maximum
>3162	2343	0.1	2.9	1.7	2.6	6.0	10.6
3162-1778	580	0.2	3.1	1.5	2.9	6.2	8.1
1778-1000	353	0.5	3.7	1.9	3.4	8.3	10.3
1000-562	200	0.2	3.8	2.2	3.1	8.3	10.0
562-316	128	0.2	3.5	2.1	2.8	7.3	8.0
316-178	73	0.9	3.2	1.7	2.9	6.7	7.4
178-100	6	0.4	1.0	0.6	0.8	2.0	2.0
100-56	0						
56-32	0						
32-18	0						
18-10	0						
<10	0						
All ranges	3683	0.1	3.1	1.7	2.8	6.4	10.6

Table 9 Statistics of GD1 2-D Error (metres), Aerad Approaches, Flight 5, Tartan A

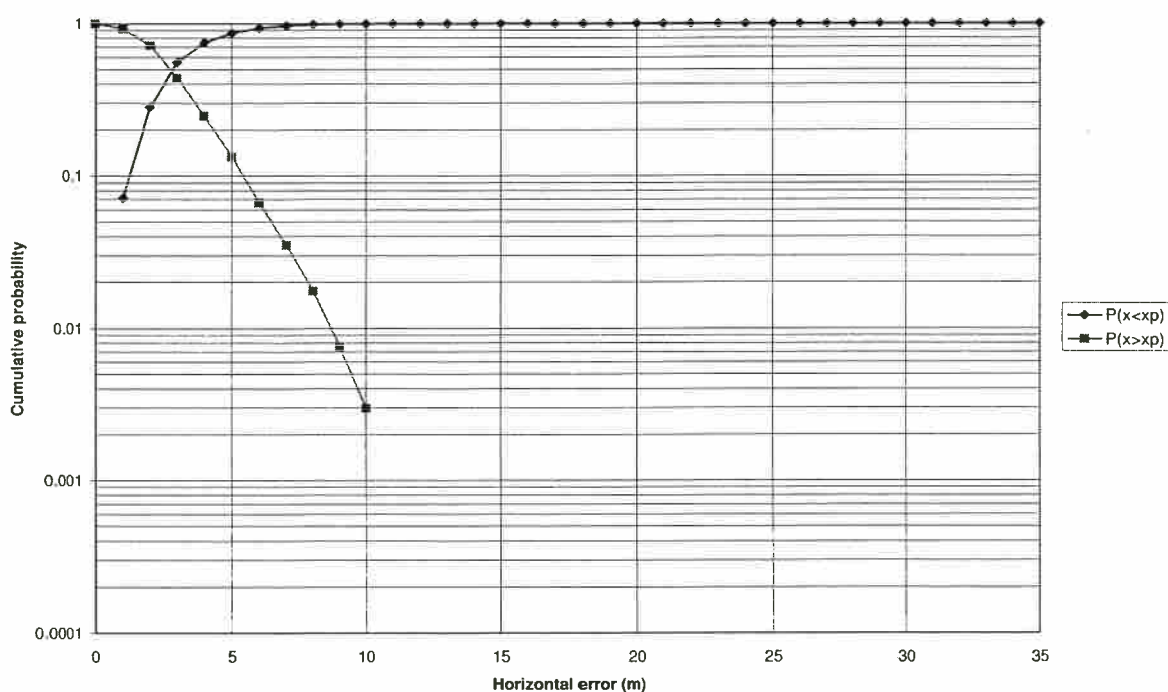


Figure 22 Cumulative Probability of GD1 2-D Error Irrespective of Range from the Platform, Aerad Approaches, Flight 5, Tartan A

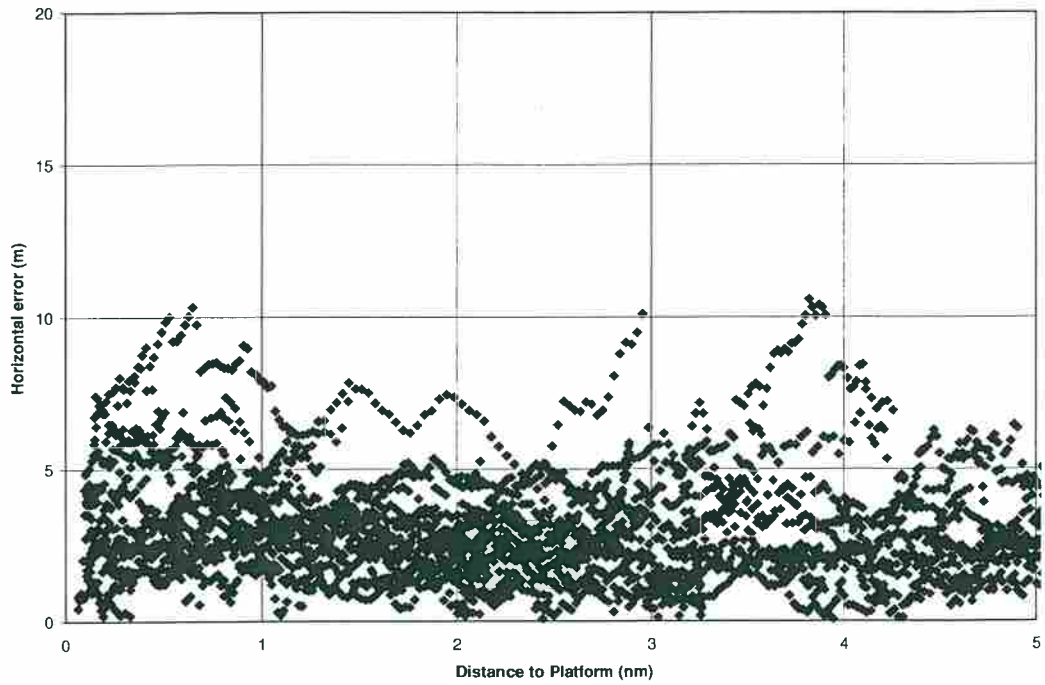


Figure 23 Scatter Plot of GD1 2-D Error Against Range from the Platform, Aerad Approaches, Flight 5, Tartan A

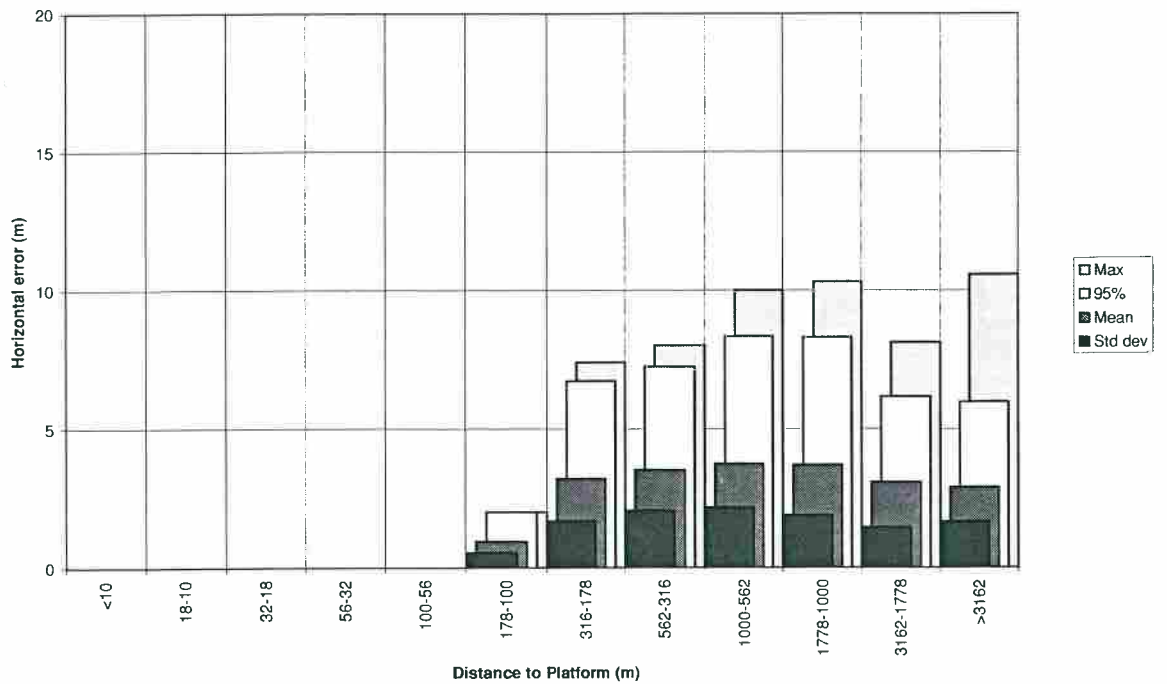


Figure 24 Variation of GD1 2-D Error Statistics with Range from the Platform, Aerad Approaches, Flight 5, Tartan A

Distance to platform (metres)	Number of samples	Minimum	Mean	Standard deviation	50% of samples less than	95% of samples less than	Maximum
>3162	722	1.3	3.9	1.0	4.0	5.4	6.5
3162-1778	275	2.1	4.0	0.9	3.9	5.7	6.8
1778-1000	239	1.7	4.8	1.4	4.7	7.5	9.1
1000-562	279	2.1	5.2	1.3	5.1	7.1	12.1
562-316	253	0.6	4.7	1.5	4.8	6.9	9.0
316-178	123	2.1	5.2	1.5	5.5	7.1	8.2
178-100	74	2.3	4.6	1.2	4.7	6.6	7.1
100-56	44	2.7	4.5	1.0	4.5	6.4	6.8
56-32	24	4.0	5.3	0.7	5.3	6.8	6.9
32-18	17	4.8	5.8	0.5	5.8	7.0	7.0
18-10	13	5.5	6.6	0.6	6.6	7.5	7.5
<10	3	6.8	6.9	0.2	6.8	7.2	7.2
All ranges	2066	0.6	4.5	1.3	4.4	6.7	12.1

Table 10 Statistics of GD1 2-D Error (metres), Platform Orbits, Flight 5, Tartan A

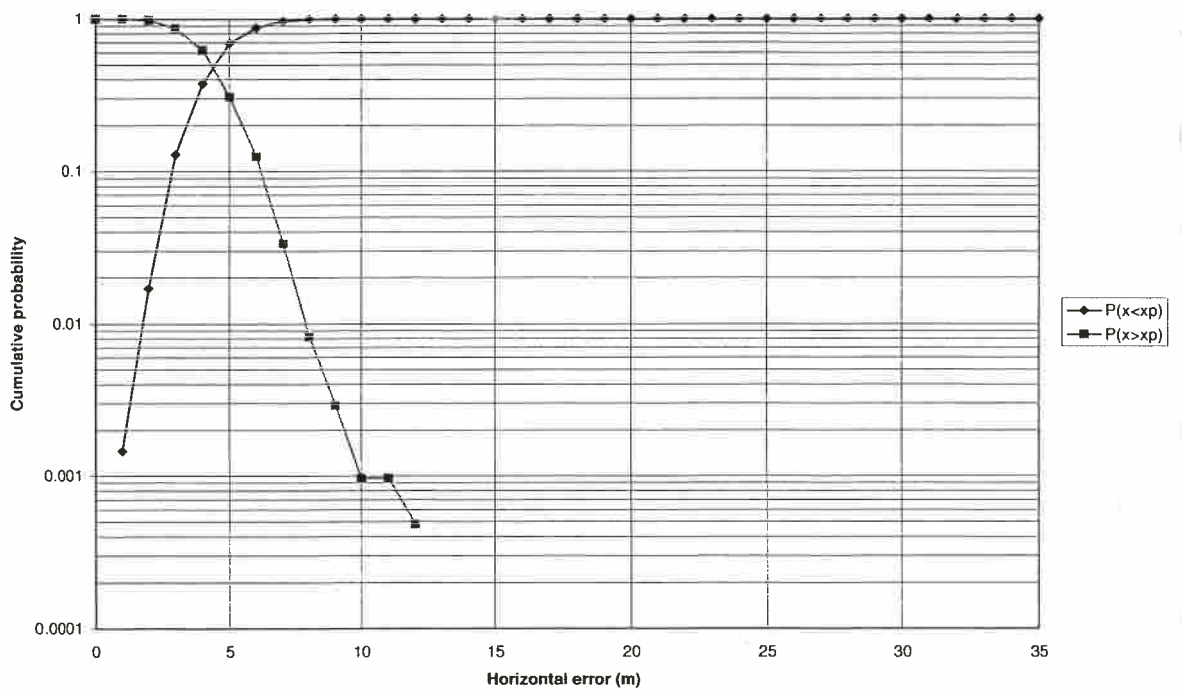


Figure 25 Cumulative Probability of GD1 2-D Error Irrespective of Range from the Platform, Platform Orbits, Flight 5, Tartan A

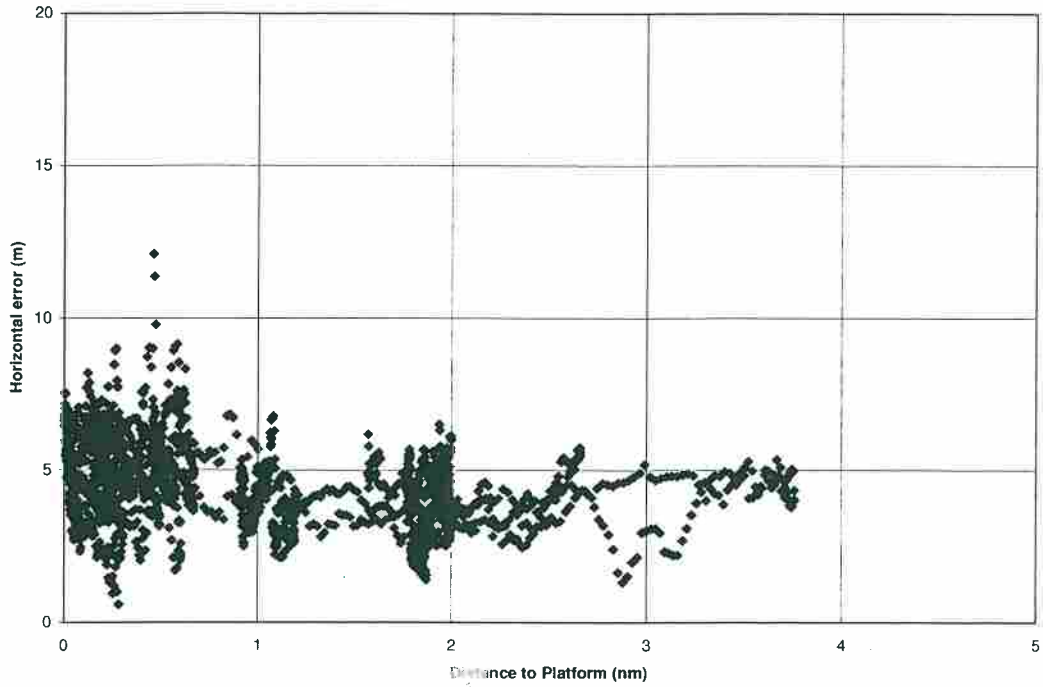


Figure 26 Scatter Plot of GD1 2-D Error Against Range from the Platform, Platform Orbits, Flight 5, Tartan A

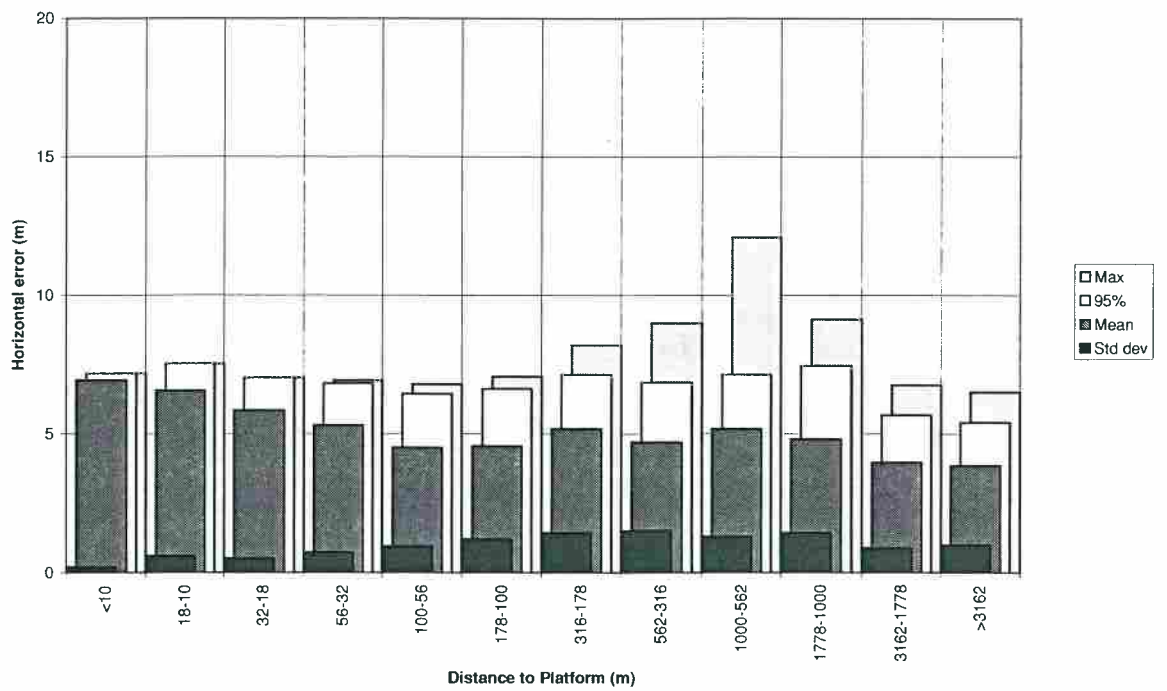


Figure 27 Variation of GD1 2-D Error Statistics with Range from the Platform, Platform Orbits, Flight 5, Tartan A

Distance to platform (metres)	Number of samples	Minimum	Mean	Standard deviation	50% of samples less than	95% of samples less than	Maximum
>3162	2467	0.0	2.2	1.3	2.1	4.8	7.9
3162-1778	757	0.1	2.2	1.1	2.2	4.1	5.0
1778-1000	478	0.2	2.5	1.3	2.4	4.7	8.0
1000-562	342	0.2	2.9	1.3	2.8	5.0	6.8
562-316	202	0.1	2.2	1.3	2.2	4.9	5.1
316-178	123	0.1	2.4	1.5	2.4	5.4	5.7
178-100	11	2.0	4.9	3.4	3.5	10.4	10.4
100-56	10	1.5	4.8	3.1	3.6	9.7	9.7
56-32	6	1.1	2.7	2.7	1.9	8.1	8.1
32-18	7	2.0	4.2	2.5	3.0	7.8	7.8
18-10	23	1.0	3.8	2.8	3.0	10.2	10.7
<10	9	4.8	7.0	1.5	6.8	9.0	9.0
All ranges	4435	0.0	2.4	1.3	2.2	4.8	10.7

Table 11 Statistics of GD1 2-D Error (metres), Experimental Approaches, Flight 5, Tartan A

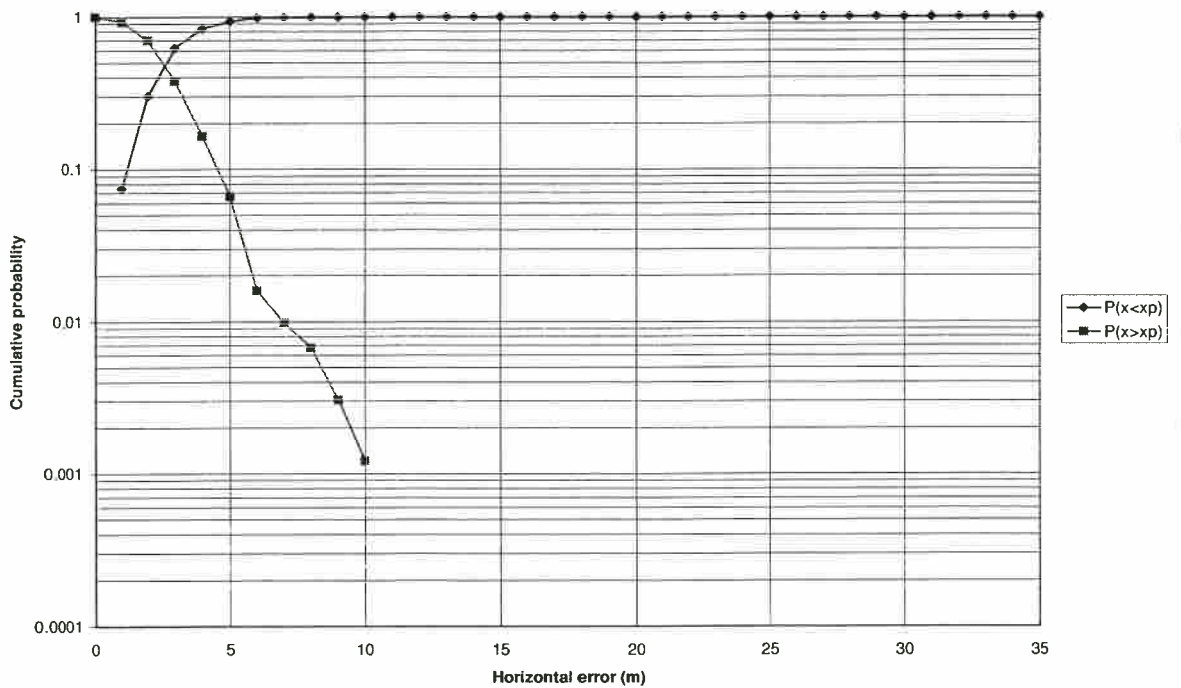


Figure 28 Cumulative Probability of GD1 2-D Error Irrespective of Range from the Platform, Experimental Approaches, Flight 5, Tartan A

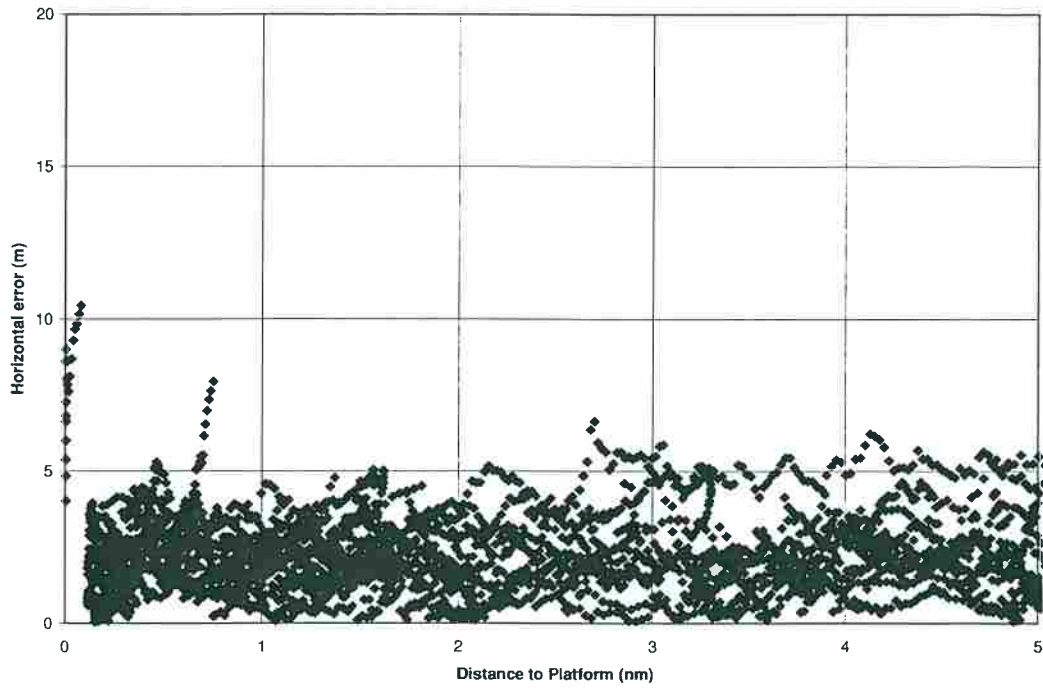


Figure 29 Scatter Plot of GD1 2-D Error Against Range from the Platform, Experimental Approaches, Flight 5, Tartan A

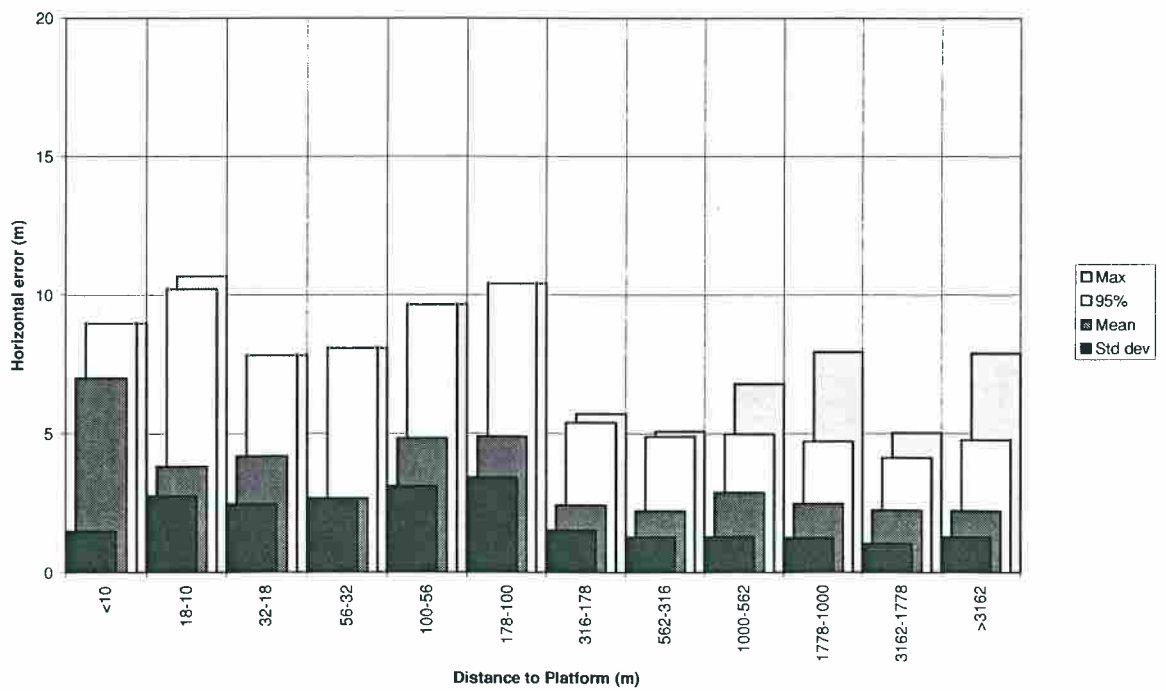


Figure 30 Variation of GD1 2-D Error Statistics with Range from the Platform, Experimental Approaches, Flight 5, Tartan A

Distance to platform (metres)	Number of samples	Minimum	Mean	Standard deviation	50% of samples less than	95% of samples less than	Maximum
>3162	2693	0.1	3.4	2.2	3.0	7.1	14.1
3162-1778	492	0.1	4.0	1.8	3.9	6.9	9.8
1778-1000	251	0.6	4.0	1.8	4.1	7.6	8.1
1000-562	151	0.7	3.9	1.7	3.7	7.5	7.8
562-316	100	0.9	3.8	1.8	3.6	7.4	8.3
316-178	67	1.0	3.9	2.3	3.8	8.2	8.4
178-100	27	1.3	3.5	0.9	3.9	4.2	4.3
100-56	7	3.0	3.6	0.5	3.9	4.0	4.0
56-32	0						
32-18	0						
18-10	0						
<10	0						
All ranges	3788	0.1	3.6	2.1	3.3	7.1	14.1

Table 12 Statistics of GD1 2-D Error (metres), Aerad Approaches, Flight 6, Buchan A

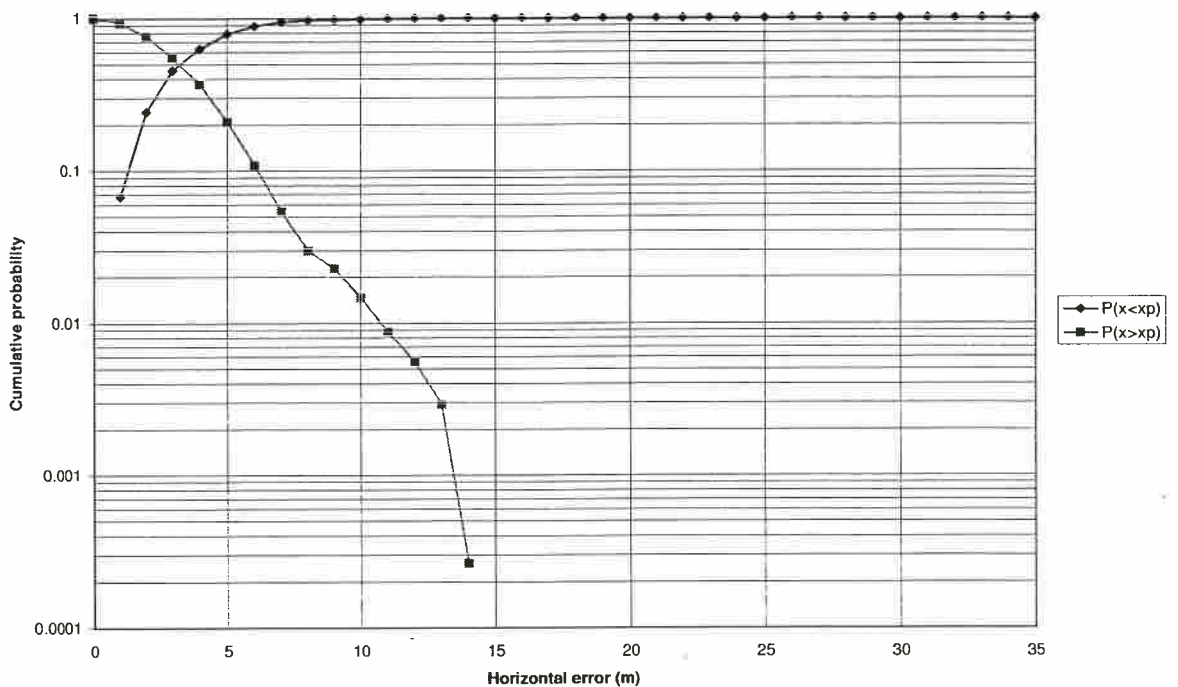


Figure 31 Cumulative Probability of GD1 2-D Error Irrespective of Range from the Platform, Aerad Approaches, Flight 6, Buchan A

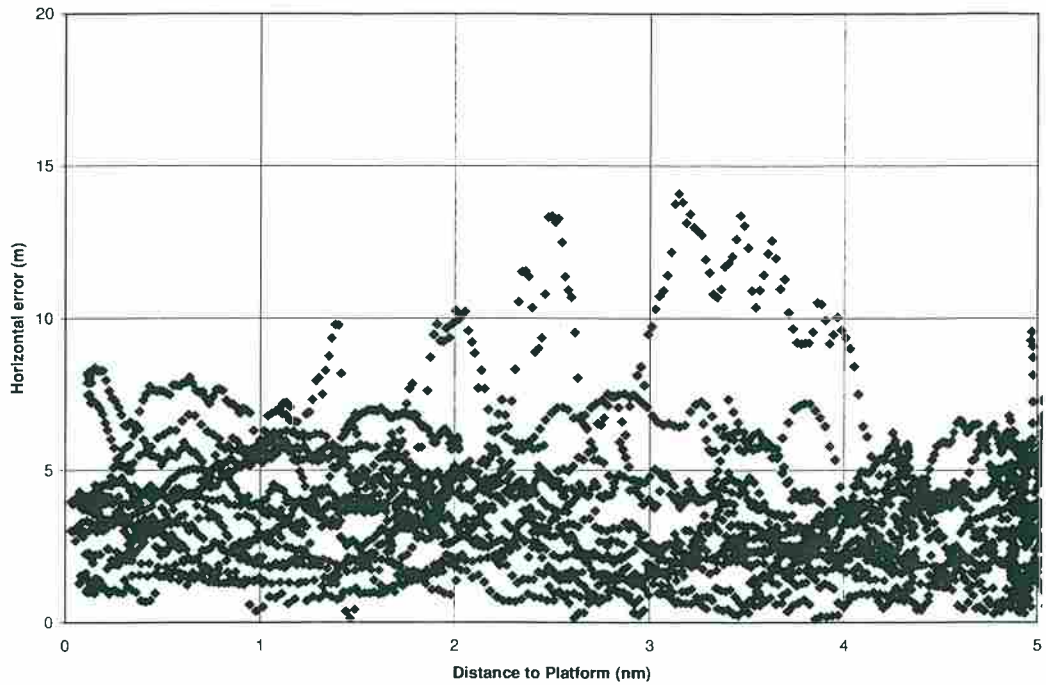


Figure 32 Scatter Plot of GD1 2-D Error Against Range from the Platform, Aerad Approaches, Flight 6, Buchan A

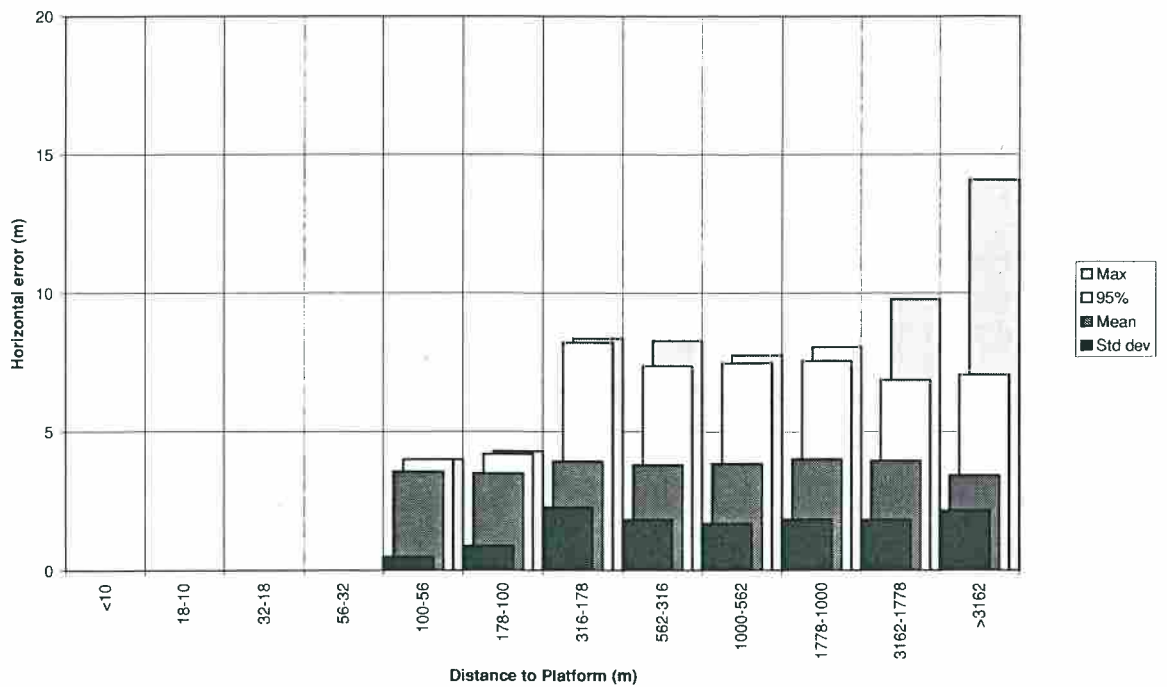


Figure 33 Variation of GD1 2-D Error Statistics with Range from the Platform, Aerad Approaches, Flight 6, Buchan A

Distance to platform (metres)	Number of samples	Minimum	Mean	Standard deviation	50% of samples less than	95% of samples less than	Maximum
>3162	686	0.1	2.6	1.0	2.6	4.2	4.8
3162-1778	205	0.3	3.2	0.9	3.2	4.9	5.7
1778-1000	321	0.2	2.3	1.2	2.3	4.0	5.6
1000-562	237	0.3	2.6	1.4	2.6	5.0	7.2
562-316	284	0.2	3.5	1.8	3.4	7.0	10.6
316-178	110	0.4	3.8	2.1	3.7	7.4	8.4
178-100	41	2.6	4.2	0.9	4.2	5.7	6.5
100-56	22	2.9	4.1	0.8	4.2	5.2	6.8
56-32	6	3.4	3.8	0.4	3.7	4.6	4.6
32-18	5	4.6	5.5	0.8	5.3	6.3	6.3
18-10	0						
<10	0						
All ranges	1917	0.1	2.9	1.4	2.9	5.1	10.6

Table 13 Statistics of GD1 2-D Error (metres), Platform Orbits, Flight 6, Buchan A

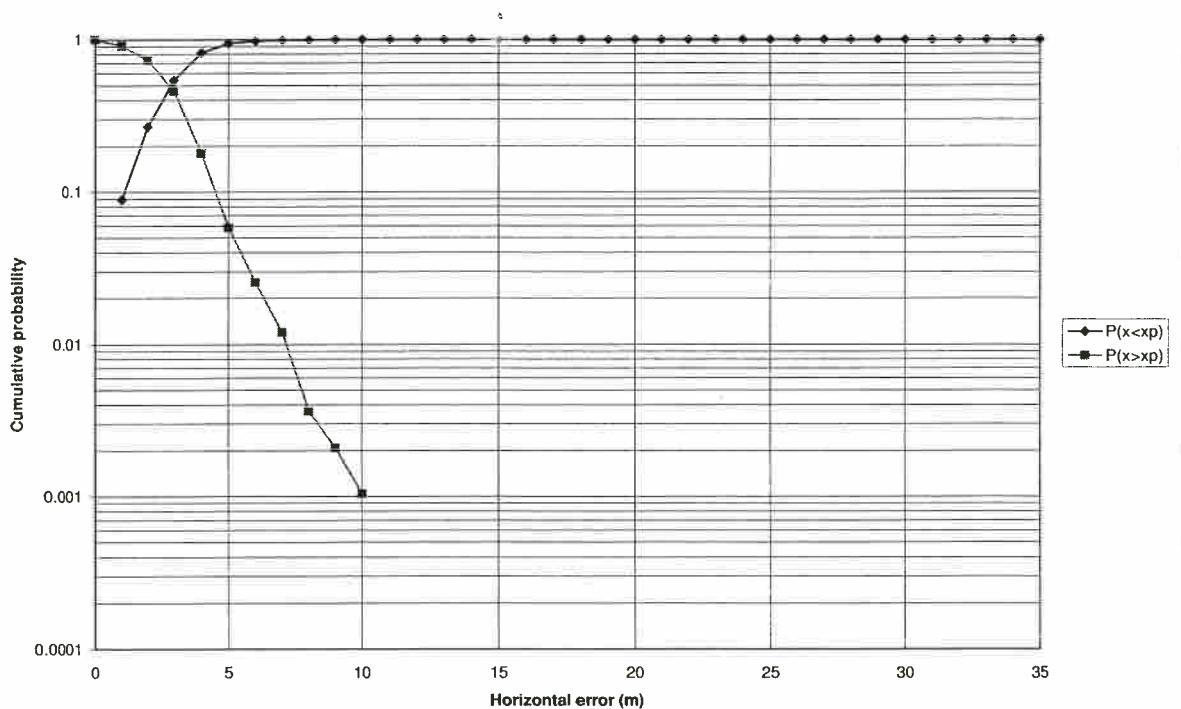


Figure 34 Cumulative Probability of GD1 2-D Error Irrespective of Range from the Platform, Platform Orbits, Flight 6, Buchan A

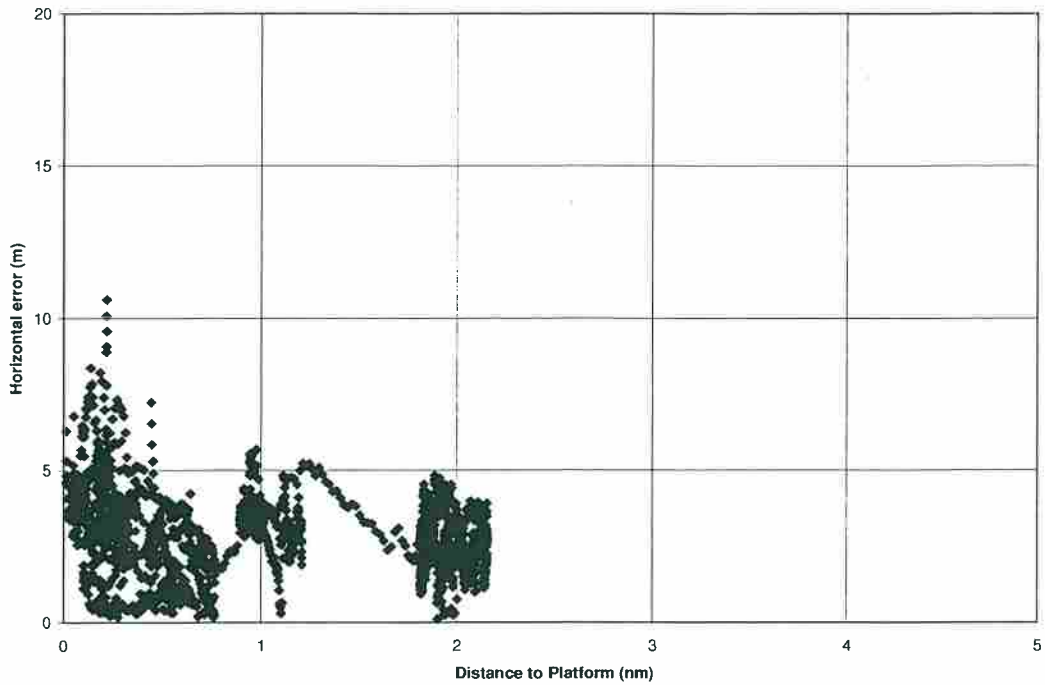


Figure 35 Scatter Plot of GD1 2-D Error Against Range from the Platform, Platform Orbits, Flight 6, Buchan A

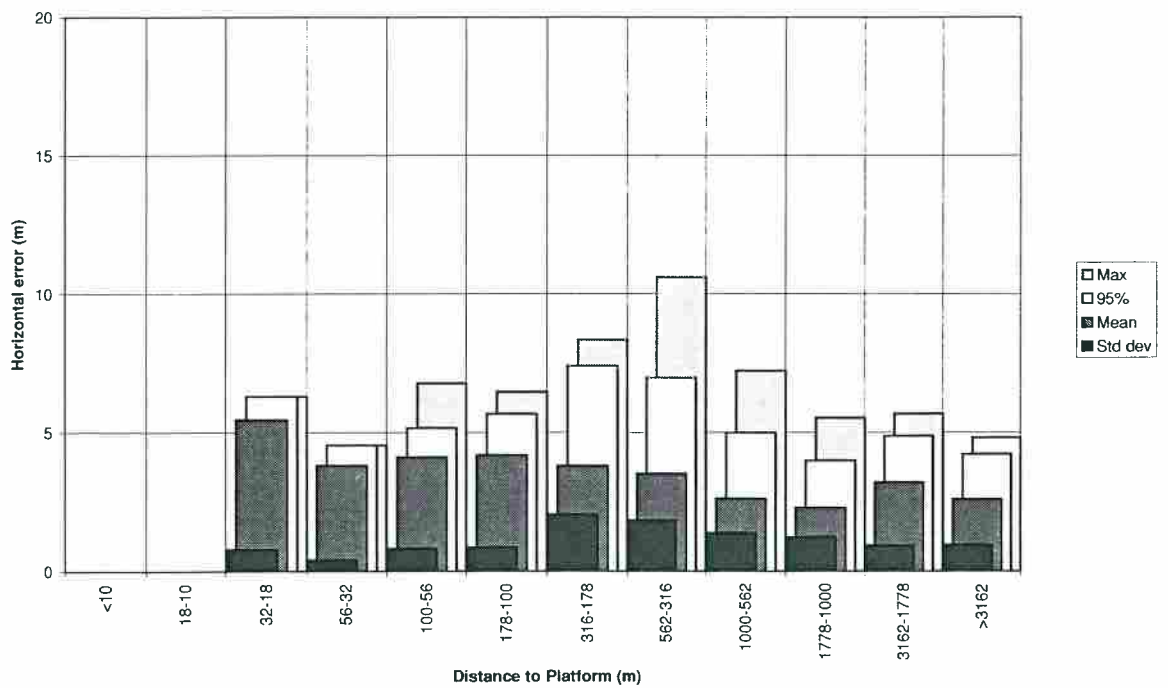


Figure 36 Variation of GD1 2-D Error Statistics with Range from the Platform, Platform Orbits, Flight 6, Buchan A

Distance to platform (metres)	Number of samples	Minimum	Mean	Standard deviation	50% of samples less than	95% of samples less than	Maximum
>3162	472	0.4	8.7	6.1	10.2	16.3	17.1
3162-1778	121	0.4	5.6	2.8	4.8	9.8	10.6
1778-1000	45	1.7	5.9	2.9	7.2	10.0	10.2
1000-562	28	3.5	6.2	1.7	6.6	9.2	11.1
562-316	13	5.6	6.6	0.6	6.6	7.6	7.6
316-178	17	5.6	6.3	0.6	6.4	7.3	7.3
178-100	9	6.5	6.7	0.1	6.7	6.9	6.9
100-56	4	6.2	6.6	0.6	6.5	7.5	7.5
56-32	4	5.8	6.3	0.5	6.6	7.0	7.0
32-18	0						
18-10	0						
<10	0						
All ranges	713	0.4	7.8	5.3	6.6	16.0	17.1

Table 14 Statistics of GD1 2-D Error (metres), Experimental Approaches, Flight 6, Buchan A

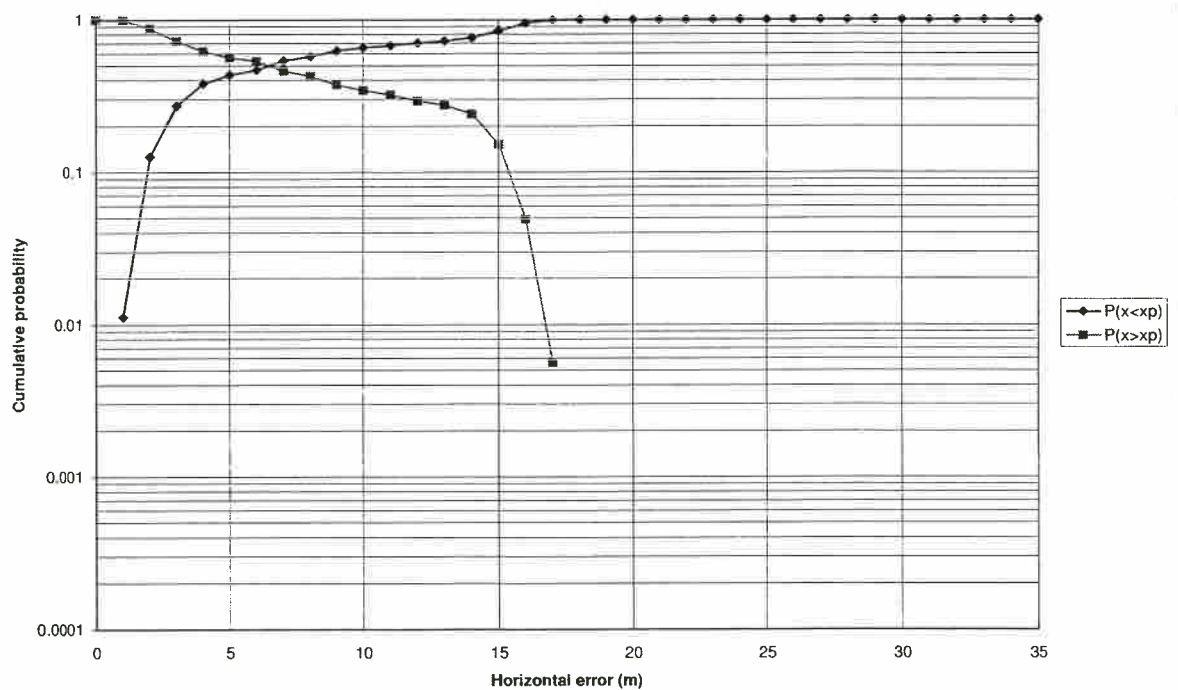


Figure 37 Cumulative Probability of GD1 2-D Error Irrespective of Range from the Platform, Experimental Approaches, Flight 6, Buchan A

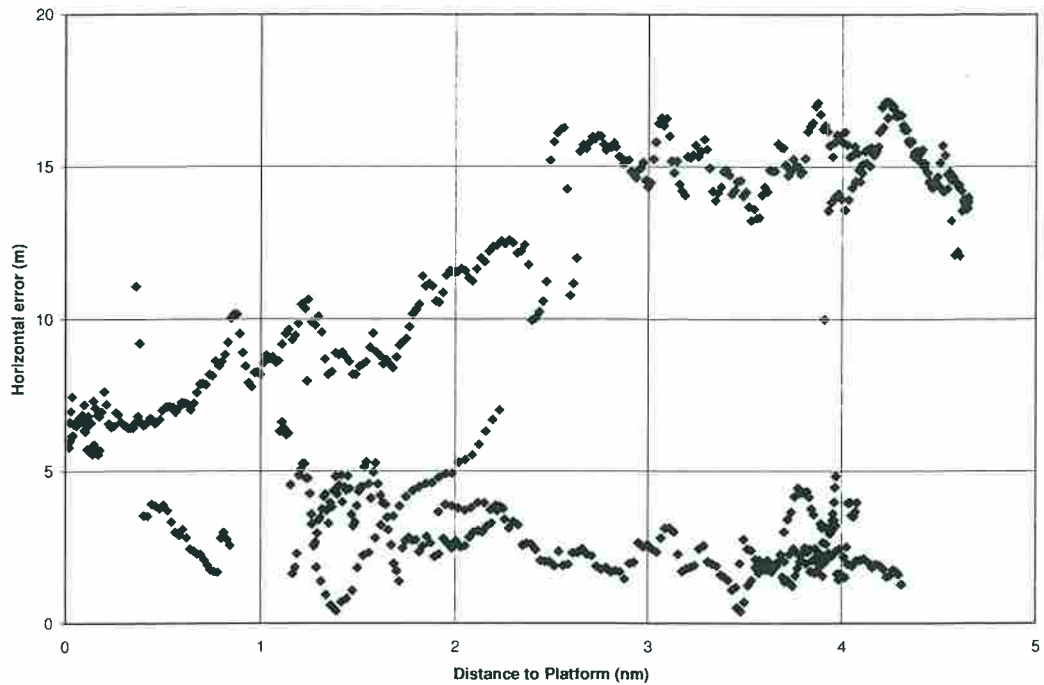


Figure 38 Scatter Plot of GD1 2-D Error Against Range from the Platform, Experimental Approaches, Flight 6, Buchan A

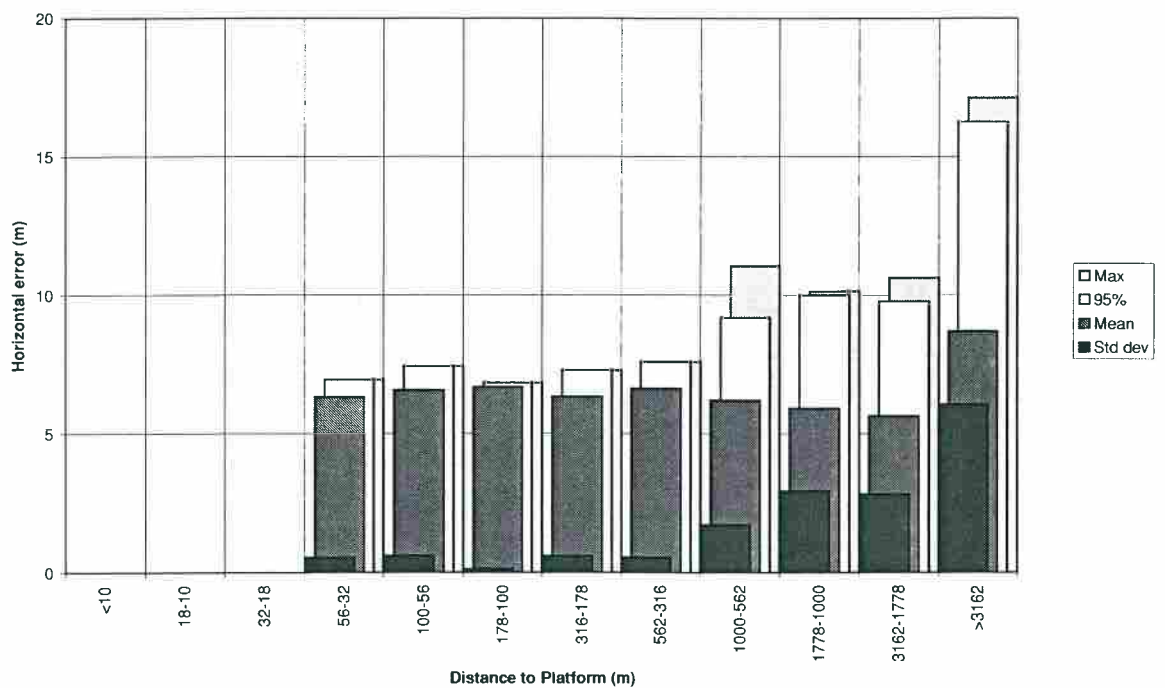


Figure 39 Variation of GD1 2-D Error Statistics with Range from the Platform, Experimental Approaches, Flight 6, Buchan A

6.2 UHF-Corrected Navstar (GD2) Receiver

This receiver was a Navstar XR5-M12, identical to the GD1 unit, which was supplied with differential corrections originating at the platform reference system and transmitted on a 'private' UHF datalink frequency.

The receiver was operational on all of the offshore flight trials; the results on the following pages are derived from data gathered on Flights 4, 5, 6 and 7.

Before commencing each flight trial it was necessary to provide the platform reference system with details of its location, to enable it to generate differential correction messages. Owing to the limitations of the survey data available to the platform operators there was generally a small difference between the co-ordinates calculated prior to the flight (and loaded into the reference station's memory), and the more accurate position which was calculated following the trial (section 4.4).

The differences between these two sets of positions, for each of the platforms visited, are as follows:

Flight 4 (Piper B):

	Computed Position	Position Used for Init	Difference
Latitude	N 58° 27' 37.0600"	N 58° 27' 37.0100"	+1.5m North
Longitude	E 000° 14' 56.8054"	E 000° 14' 56.8400"	-0.6m East
Ellipsoidal height	106.585m	109.000m	-2.4m Up

Flight 5 (Tartan A):

	Computed Position	Position Used for Init	Difference
Latitude	N 58° 22' 09.6212"	N 58° 22' 09.0000"	+19.2m North
Longitude	E 000° 04' 16.8361"	E 000° 04' 15.0000"	+29.8m East
Ellipsoidal height	109.931m	110.000m	+0.0m Up

Flight 6 (Buchan A):

	Computed Position	Position Used for Init	Difference
Latitude	N 57° 54' 09.6220"	N 57° 54' 09.4900"	+4.1m North
Longitude	E 000° 01' 52.1967"	E 000° 01' 52.3000"	-3.1m East
Ellipsoidal height	65.082m	67.000m	-1.9m Up

Flight 7 (Beatrice C):

	Computed Position	Position Used for Init	Difference
Latitude	N 58° 05' 38.8887"	N 58° 05' 38.6220"	+8.2m North
Longitude	W 003° 09' 11.7177"	W 003° 09' 11.9268"	+3.4m East
Ellipsoidal height	76.947m	75.000m	-1.9m Up

It may be observed that a significant difference (approximately 35m horizontally) was present between the two sets of co-ordinates in the case of the Tartan trial, and this difference was propagated into the resulting GD2 position solutions from that flight in the form of a fixed co-ordinate bias.

The effect of this 35m bias may be observed on the Tartan GD2 results, which are presented twice: firstly with the co-ordinate bias present, and then with the bias removed to provide an estimate of the position accuracy which might have been achievable had the assumed platform system position not been in error to such a significant extent.

As the co-ordinate differences for all of the other platforms were significantly lower, no attempt has been made to remove the bias on any of the other data sets.

Distance to platform (metres)	Number of samples	Minimum	Mean	Standard deviation	50% of samples less than	95% of samples less than	Maximum
>3162	840	5.2	9.3	1.3	9.3	11.5	13.7
3162-1778	317	6.7	9.1	1.2	8.8	11.4	13.5
1778-1000	197	5.4	9.2	1.4	9.4	11.4	11.9
1000-562	104	6.0	9.2	1.6	9.4	11.8	12.6
562-316	65	6.2	9.1	1.5	9.5	11.3	11.4
316-178	52	5.8	8.9	1.5	9.5	11.2	11.4
178-100	4	5.8	6.0	0.1	6.0	6.1	6.1
100-56	4	5.6	5.7	0.1	5.7	5.8	5.8
56-32	0						
32-18	0						
18-10	0						
<10	0						
All ranges	1583	5.2	9.2	1.3	9.2	11.4	13.7

Table 15 Statistics of GD2 2-D Error (metres), Aerad Approaches, Flight 7, Beatrice C

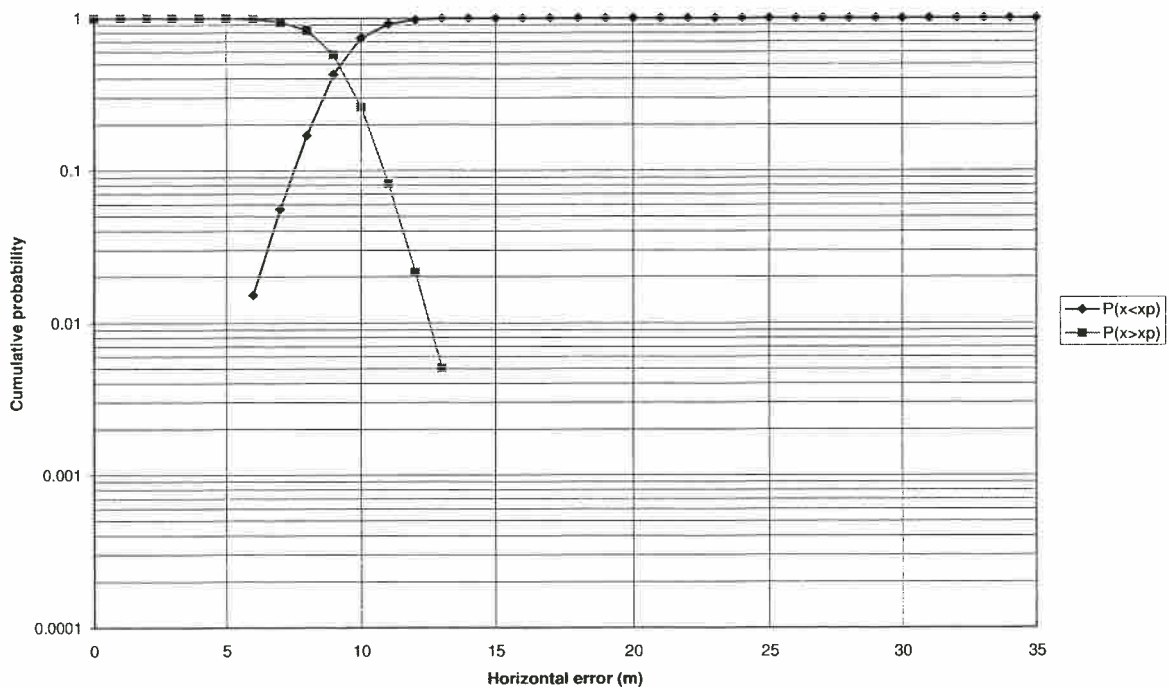


Figure 40 Cumulative Probability of GD2 2-D Error Irrespective of Range from the Platform, Aerad Approaches, Flight 7, Beatrice C

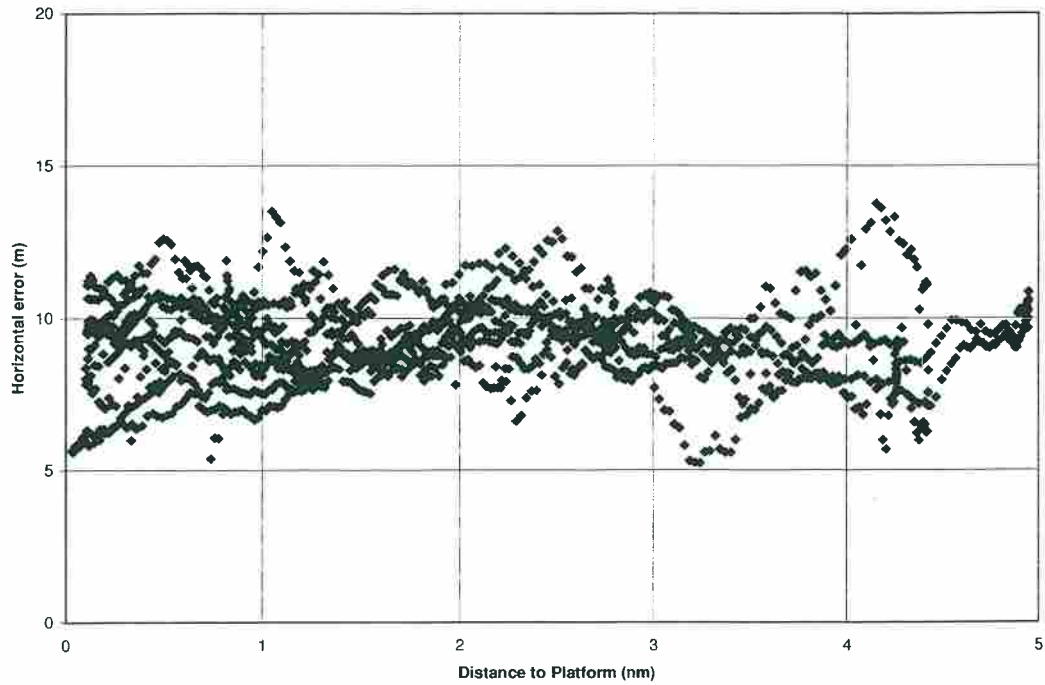


Figure 41 Scatter Plot of GD2 2-D Error Against Range from the Platform, Aerad Approaches, Flight 7, Beatrice C

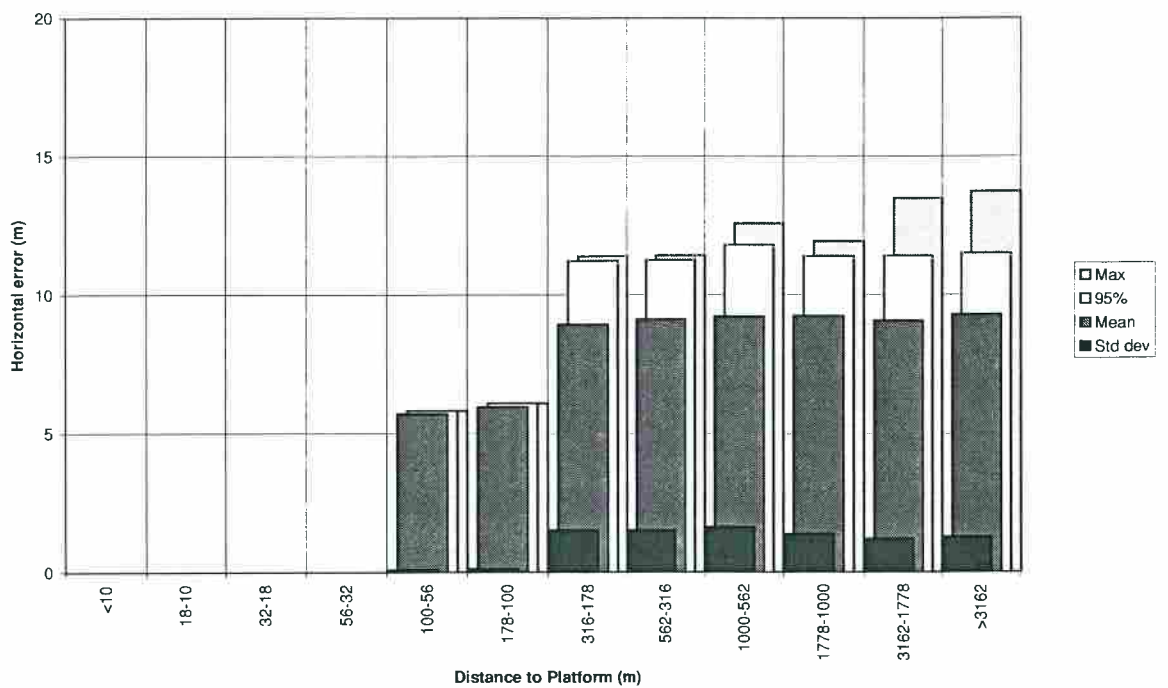


Figure 42 Variation of GD2 2-D Error Statistics with Range from the Platform, Aerad Approaches, Flight 7, Beatrice C

Distance to platform (metres)	Number of samples	Minimum	Mean	Standard deviation	50% of samples less than	95% of samples less than	Maximum
>3162	362	8.0	10.2	0.9	10.1	12.0	13.0
3162-1778	299	7.3	9.6	1.3	9.4	11.9	12.4
1778-1000	123	6.7	8.6	1.0	8.9	9.9	10.3
1000-562	154	6.6	9.4	1.0	9.4	11.0	11.4
562-316	164	6.5	10.0	1.3	10.3	11.9	12.3
316-178	114	7.2	9.7	1.0	9.4	11.3	11.7
178-100	63	8.4	10.0	0.8	10.1	11.1	11.5
100-56	56	8.1	10.0	1.0	10.2	11.6	11.7
56-32	38	8.0	9.1	0.8	9.0	10.8	11.0
32-18	5	10.5	10.9	0.2	10.9	11.2	11.2
18-10	4	9.7	10.0	0.3	10.2	10.3	10.3
<10	0						
All ranges	1382	6.5	9.7	1.2	9.7	11.7	13.0

Table 16 Statistics of GD2 2-D Error (metres), Platform Orbits, Flight 7, Beatrice C

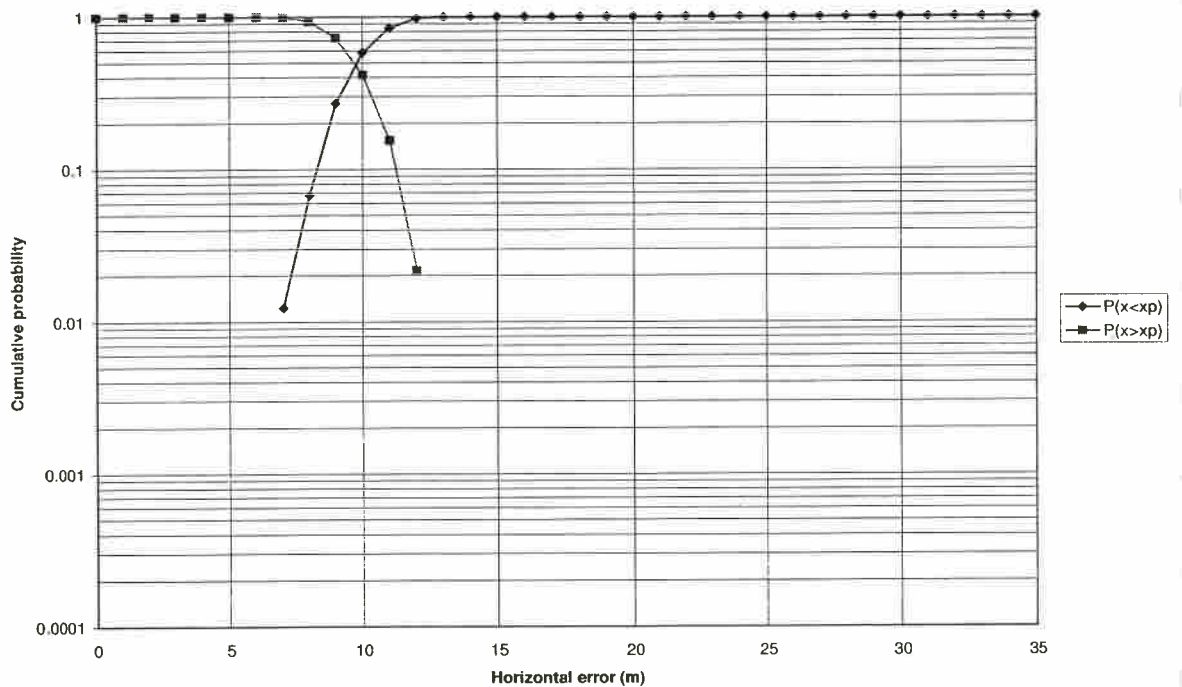


Figure 43 Cumulative Probability of GD2 2-D Error Irrespective of Range from the Platform, Platform Orbits, Flight 7, Beatrice C

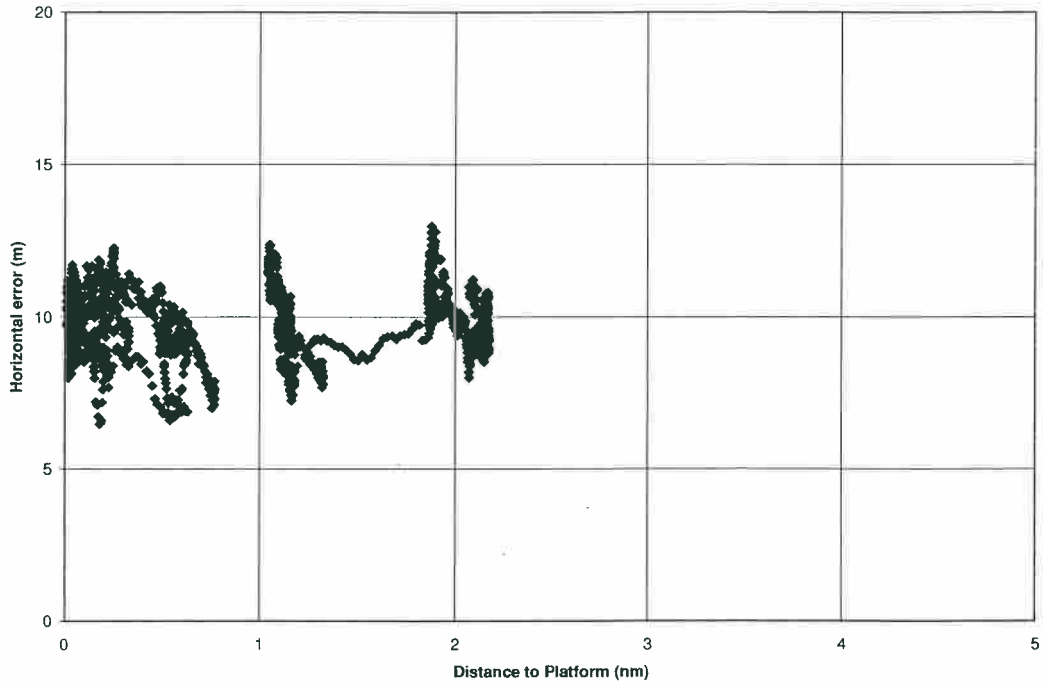


Figure 44 Scatter Plot of GD2 2-D Error Against Range from the Platform, Platform Orbits, Flight 7, Beatrice C

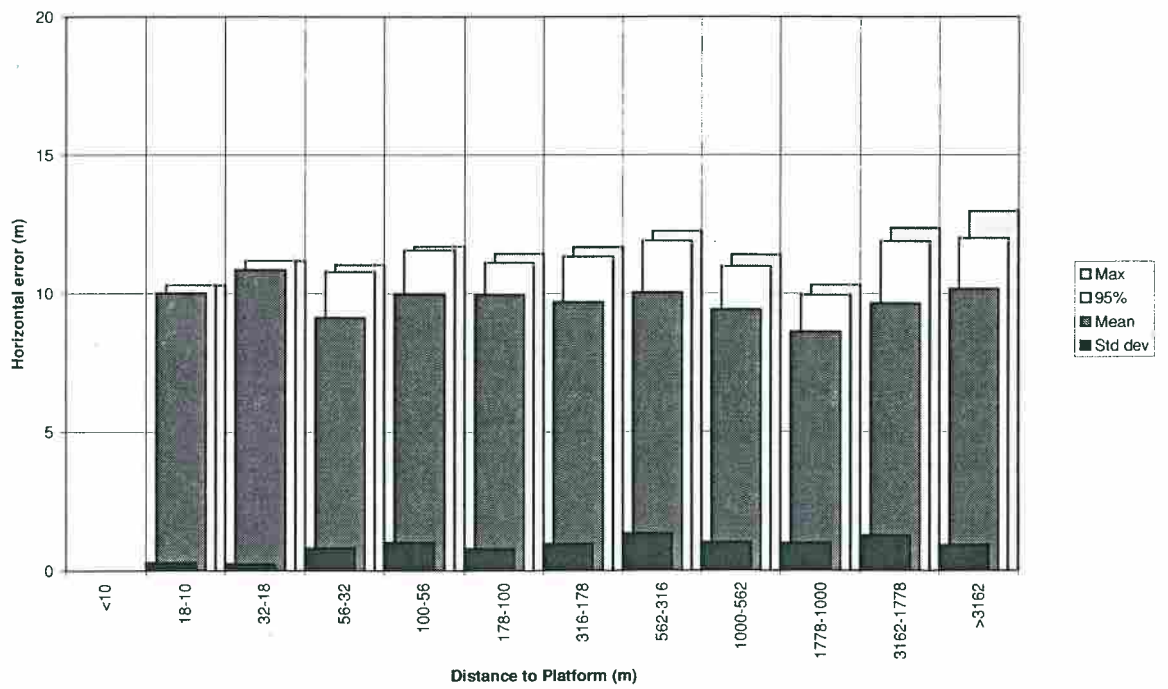


Figure 45 Variation of GD2 2-D Error Statistics with Range from the Platform, Platform Orbits, Flight 7, Beatrice C

Distance to platform (metres)	Number of samples	Minimum	Mean	Standard deviation	50% of samples less than	95% of samples less than	Maximum
>3162	2221	0.1	5.8	5.2	5.0	12.5	99.8
3162-1778	570	0.2	6.0	6.7	4.3	14.0	72.8
1778-1000	351	0.3	10.6	18.7	5.1	50.2	117.3
1000-562	196	0.4	12.7	23.9	5.9	76.0	123.1
562-316	121	0.5	6.7	5.4	4.8	17.5	26.6
316-178	62	0.7	5.9	4.7	4.4	15.6	23.6
178-100	14	1.7	3.4	1.4	3.5	6.4	6.4
100-56	8	2.3	2.9	0.5	3.1	3.7	3.7
56-32	2	2.7	2.8	0.2	3.0	3.0	3.0
32-18	1	2.7	2.7		2.7	2.7	2.7
18-10	1	2.7	2.7		2.7	2.7	2.7
<10	0						
All ranges	3547	0.1	6.7	9.8	4.9	14.5	123.1

Table 17 Statistics of GD2 2-D Error (metres), Aerad Approaches, Flight 4, Piper B

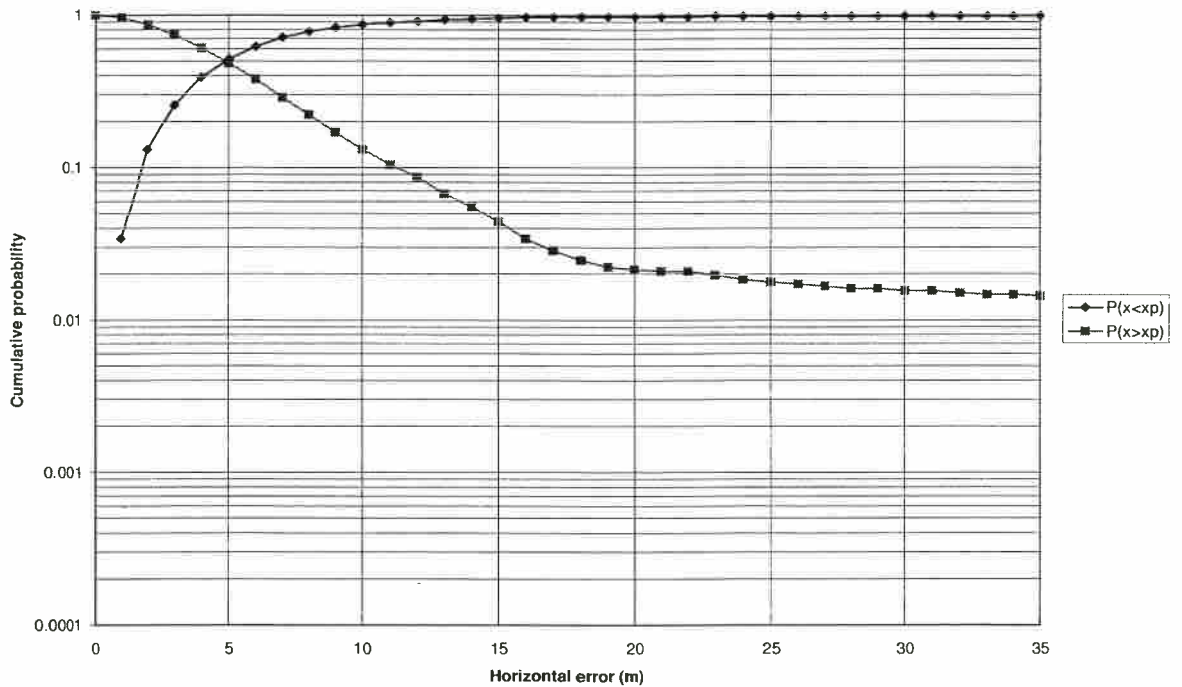


Figure 46 Cumulative Probability of GD2 2-D Error Irrespective of Range from the Platform, Aerad Approaches, Flight 4, Piper B

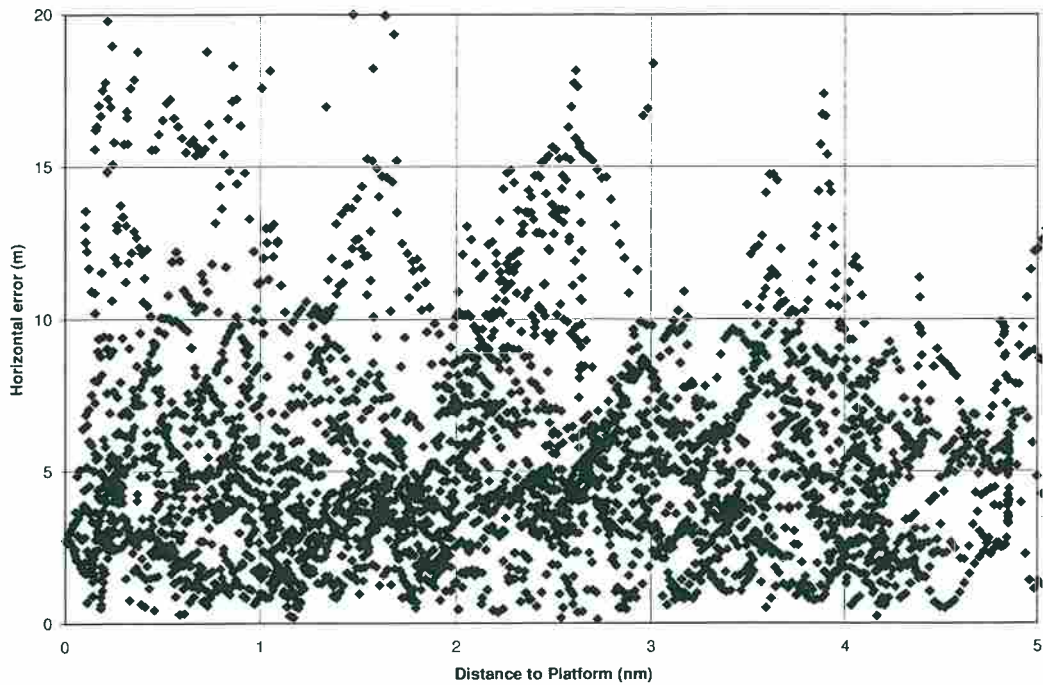


Figure 47 Scatter Plot of GD2 2-D Error Against Range from the Platform, Aerad Approaches, Flight 4, Piper B

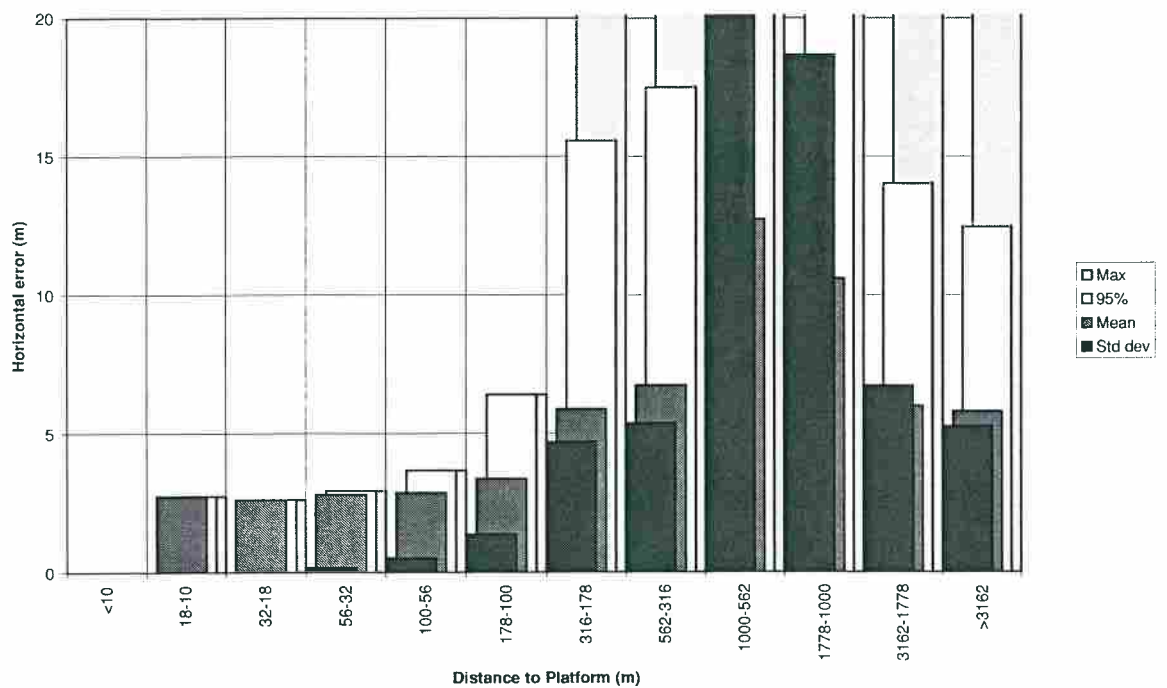


Figure 48 Variation of GD2 2-D Error Statistics with Range from the Platform, Aerad Approaches, Flight 4, Piper B

Distance to platform (metres)	Number of samples	Minimum	Mean	Standard deviation	50% of samples less than	95% of samples less than	Maximum
>3162	435	0.6	8.7	5.6	7.1	20.0	24.1
3162-1778	330	0.2	6.8	3.7	6.4	13.1	20.6
1778-1000	178	1.8	8.9	3.6	8.9	14.6	16.0
1000-562	161	0.3	9.4	7.1	7.8	28.2	30.6
562-316	150	1.3	10.3	5.9	10.5	21.2	30.5
316-178	63	3.7	8.6	3.2	8.7	13.8	16.3
178-100	38	6.0	15.5	5.4	16.0	24.7	24.8
100-56	22	3.2	10.1	3.1	9.7	14.3	14.6
56-32	7	1.9	2.6	0.8	2.2	4.1	4.1
32-18	3	5.1	8.5	5.0	6.3	14.2	14.2
18-10	0						
<10	0						
All ranges	1387	0.2	8.7	5.4	7.7	19.3	30.6

Table 18 Statistics of GD2 2-D Error (metres), Platform Orbits, Flight 4, Piper B

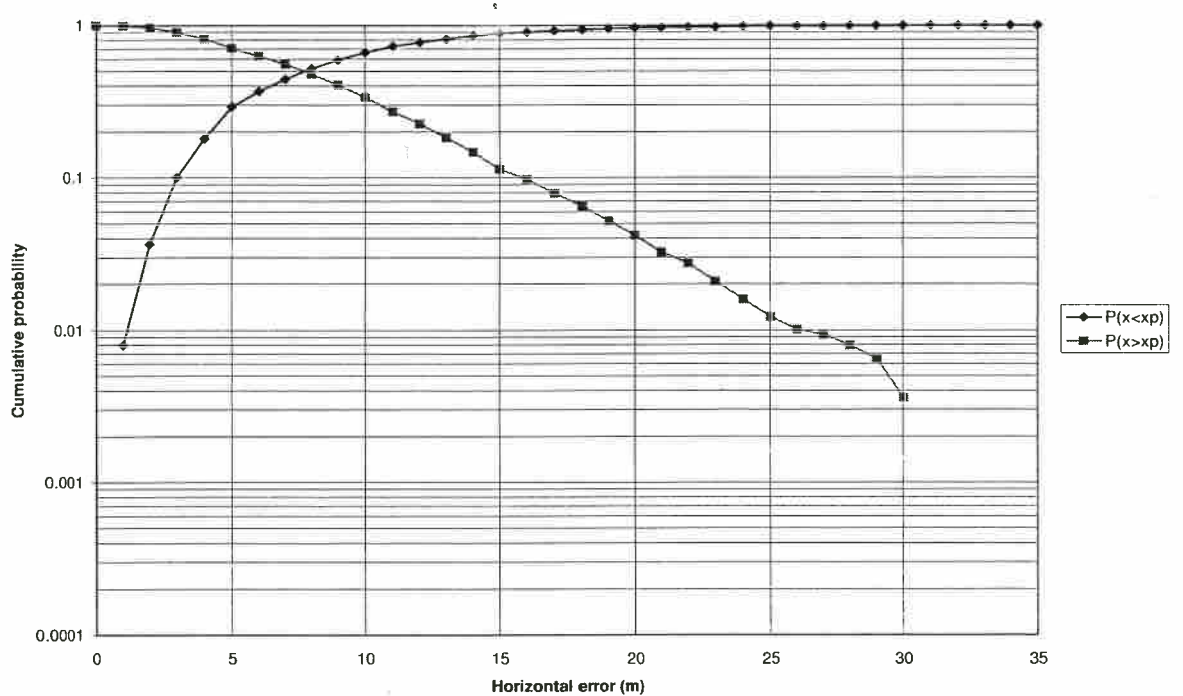


Figure 49 Cumulative Probability of GD2 2-D Error Irrespective of Range from the Platform, Platform Orbits, Flight 4, Piper B

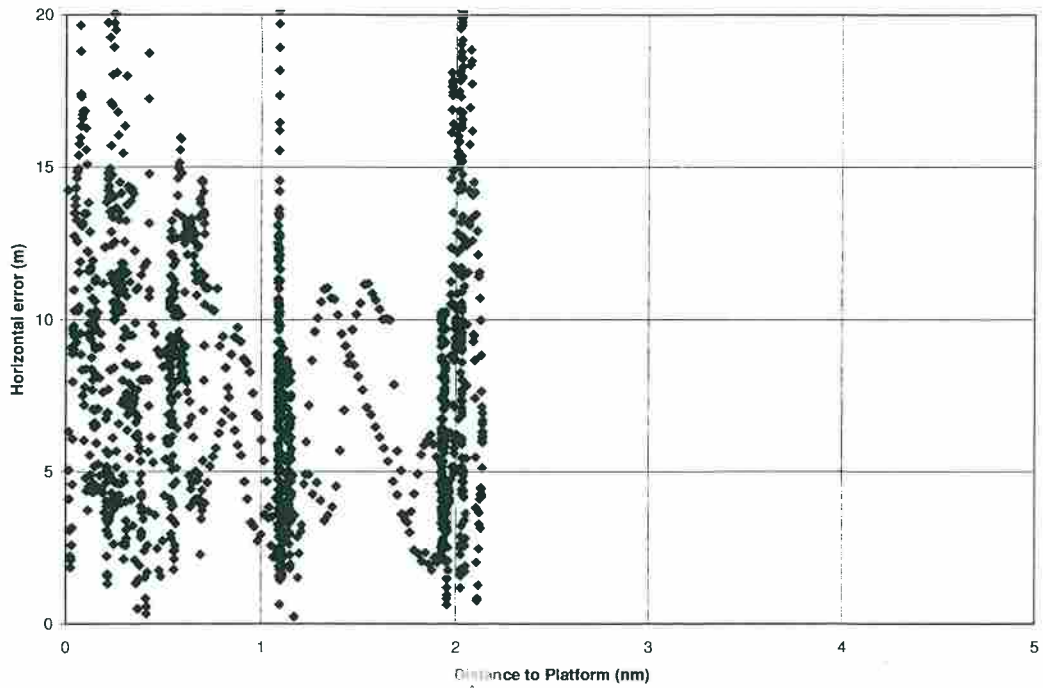


Figure 50 Scatter Plot of GD2 2-D Error Against Range from the Platform, Platform Orbits, Flight 4, Piper B

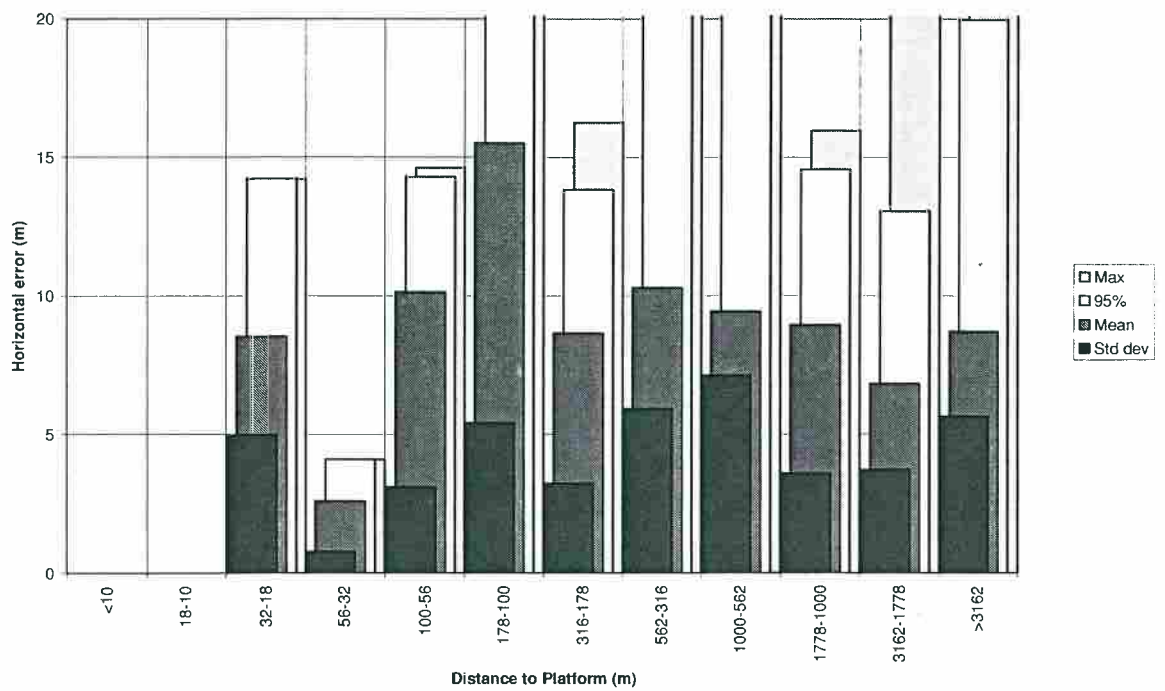


Figure 51 Variation of GD2 2-D Error Statistics with Range from the Platform, Platform Orbits, Flight 4, Piper B

Distance to platform (metres)	Number of samples	Minimum	Mean	Standard deviation	50% of samples less than	95% of samples less than	Maximum
>3162	1103	0.1	6.2	3.8	5.3	13.3	18.5
3162-1778	224	0.2	6.2	3.1	5.9	12.5	14.3
1778-1000	139	0.4	4.9	3.7	3.5	13.6	16.3
1000-562	82	0.4	3.0	1.9	2.6	7.9	9.4
562-316	53	0.4	5.0	3.5	3.9	10.4	11.3
316-178	42	1.3	5.7	6.7	3.5	23.7	27.4
178-100	15	3.7	8.6	8.0	5.2	28.2	28.2
100-56	11	0.1	4.3	5.4	2.7	14.9	14.9
56-32	9	0.1	4.3	5.4	2.2	14.1	14.1
32-18	22	1.0	3.7	2.5	3.3	10.0	12.0
18-10	3	4.5	6.4	1.9	6.6	8.2	8.2
<10	0						
All ranges	1703	0.1	5.9	3.9	4.9	13.2	28.2

Table 19 Statistics of GD2 2-D Error (metres), Experimental Approaches, Flight 4, Piper B

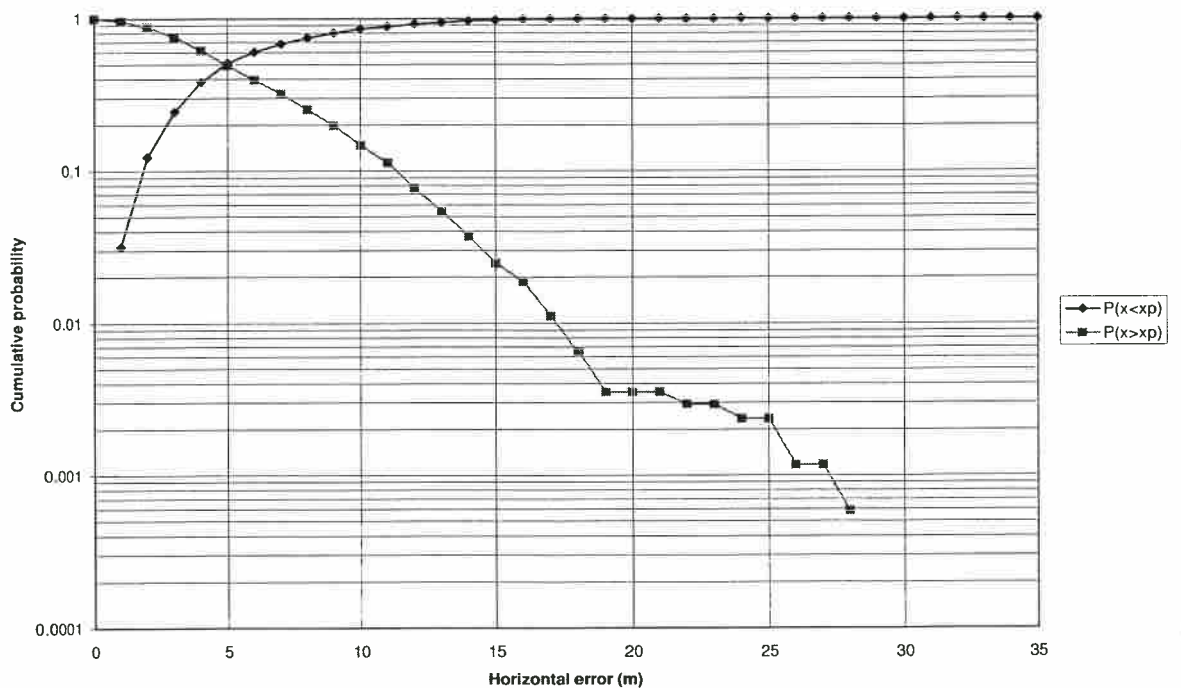


Figure 52 Cumulative Probability of GD2 2-D Error Irrespective of Range from the Platform, Experimental Approaches, Flight 4, Piper B

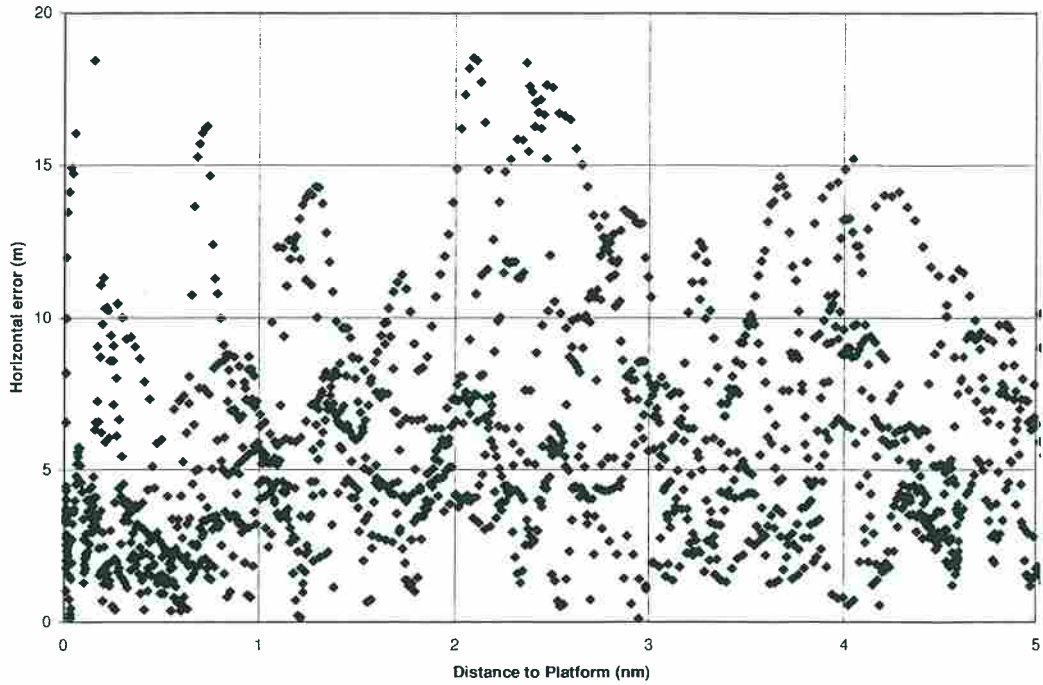


Figure 53 Scatter Plot of GD2 2-D Error Against Range from the Platform, Experimental Approaches, Flight 4, Piper B

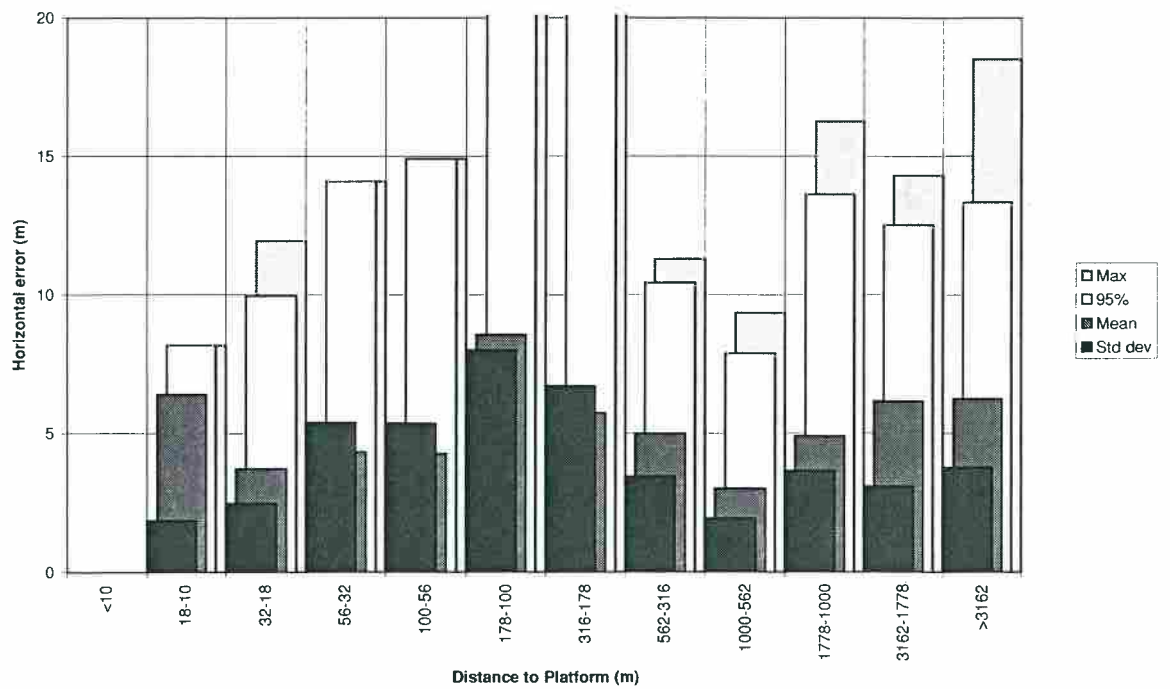


Figure 54 Variation of GD2 2-D Error Statistics with Range from the Platform, Experimental Approaches, Flight 4, Piper B

Distance to platform (metres)	Number of samples	Minimum	Mean	Standard deviation	50% of samples less than	95% of samples less than	Maximum
>3162	2332	26.9	35.7	2.8	35.7	39.9	45.9
3162-1778	580	31.2	35.5	2.2	35.1	40.7	41.9
1778-1000	353	31.2	36.1	2.0	36.1	39.5	41.9
1000-562	200	31.0	35.8	2.2	36.0	39.4	40.6
562-316	128	30.2	35.5	2.8	35.9	39.7	40.4
316-178	73	30.1	35.8	2.5	36.8	38.6	39.3
178-100	6	38.3	38.7	0.3	38.7	39.0	39.0
100-56	0						
56-32	0						
32-18	0						
18-10	0						
<10	0						
All ranges	3672	26.9	35.7	2.6	35.7	39.9	45.9

Table 20 Statistics of GD2 2-D Error (metres), Aerad Approaches, Flight 5, Tartan A

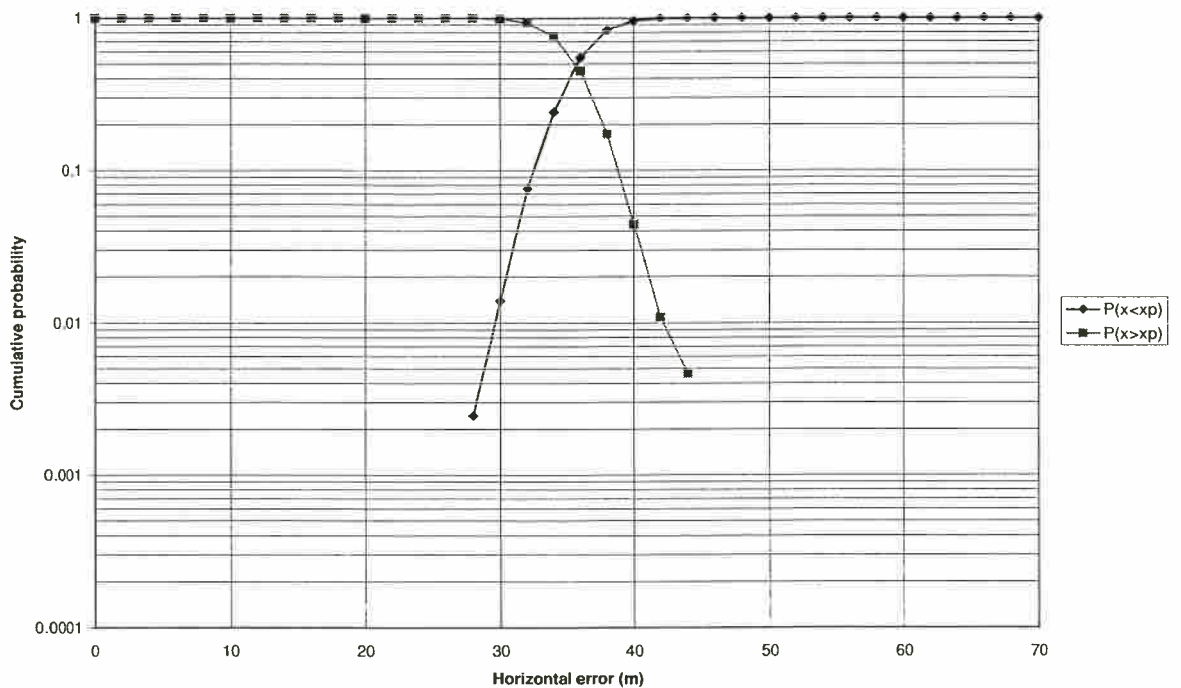


Figure 55 Cumulative Probability of GD2 2-D Error Irrespective of Range from the Platform, Aerad Approaches, Flight 5, Tartan A (non-standard horizontal scale employed due to large bias)

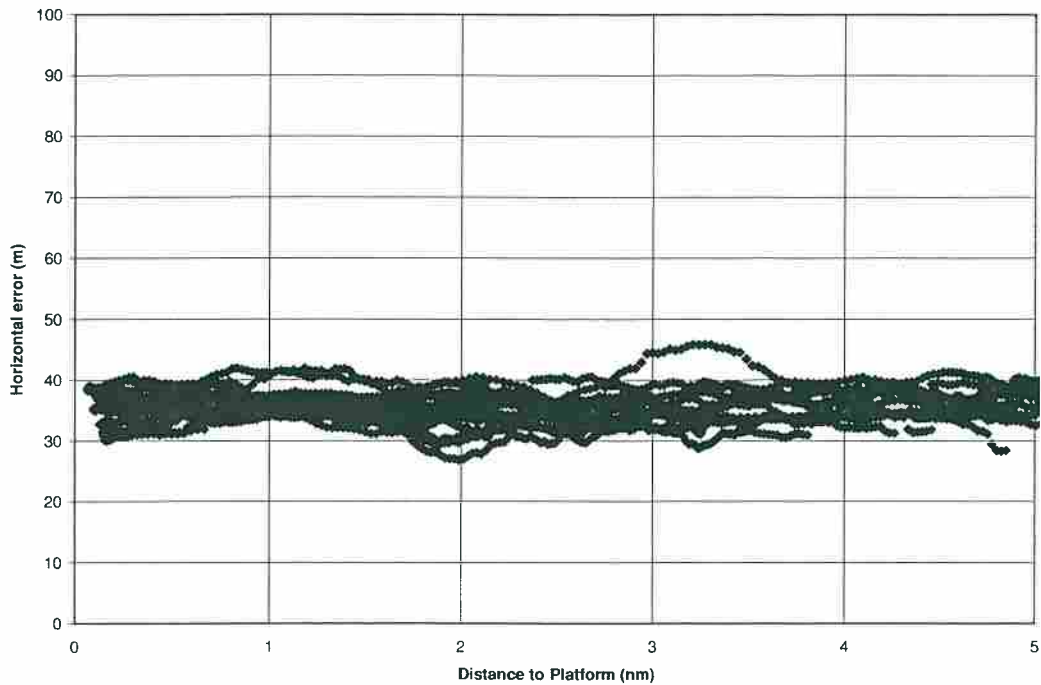


Figure 56 Scatter Plot of GD2 2-D Error Against Range from the Platform, Aerad Approaches, Flight 5, Tartan A (non-standard vertical scale employed due to large bias)

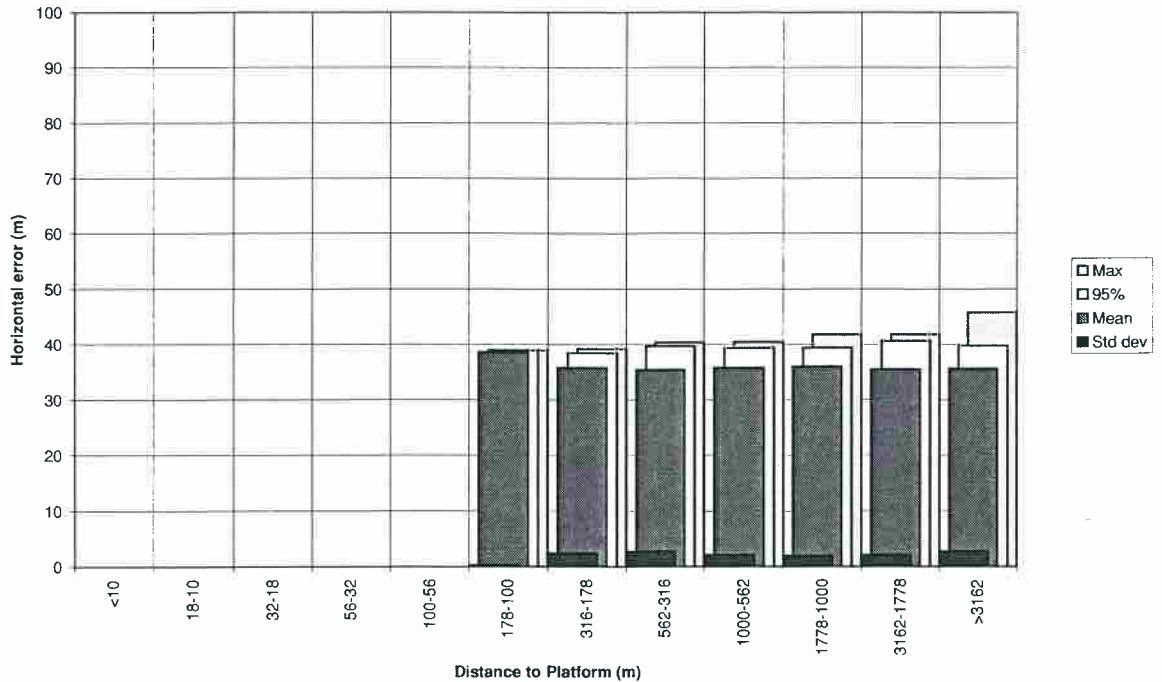


Figure 57 Variation of GD2 2-D Error Statistics with Range from the Platform, Aerad Approaches, Flight 5, Tartan A (non-standard vertical scale employed due to large bias)

Distance to platform (metres)	Number of samples	Minimum	Mean	Standard deviation	50% of samples less than	95% of samples less than	Maximum
>3162	2332	0.1	3.9	2.4	3.4	8.9	14.0
3162-1778	580	0.1	3.4	2.2	2.8	8.0	10.6
1778-1000	353	0.1	3.5	2.6	2.5	9.1	10.6
1000-562	200	0.2	3.7	2.5	3.2	9.3	10.3
562-316	128	0.3	4.4	2.1	3.8	8.4	9.7
316-178	73	1.9	4.0	1.3	4.0	5.8	6.9
178-100	6	2.8	3.3	0.4	3.2	3.7	3.7
100-56	0						
56-32	0						
32-18	0						
18-10	0						
<10	0						
All ranges	3672	0.1	3.8	2.4	3.3	8.7	14.0

Table 21 Statistics of GD2 2-D Error (metres), Aerad Approaches, Flight 5, Tartan A (bias removed)

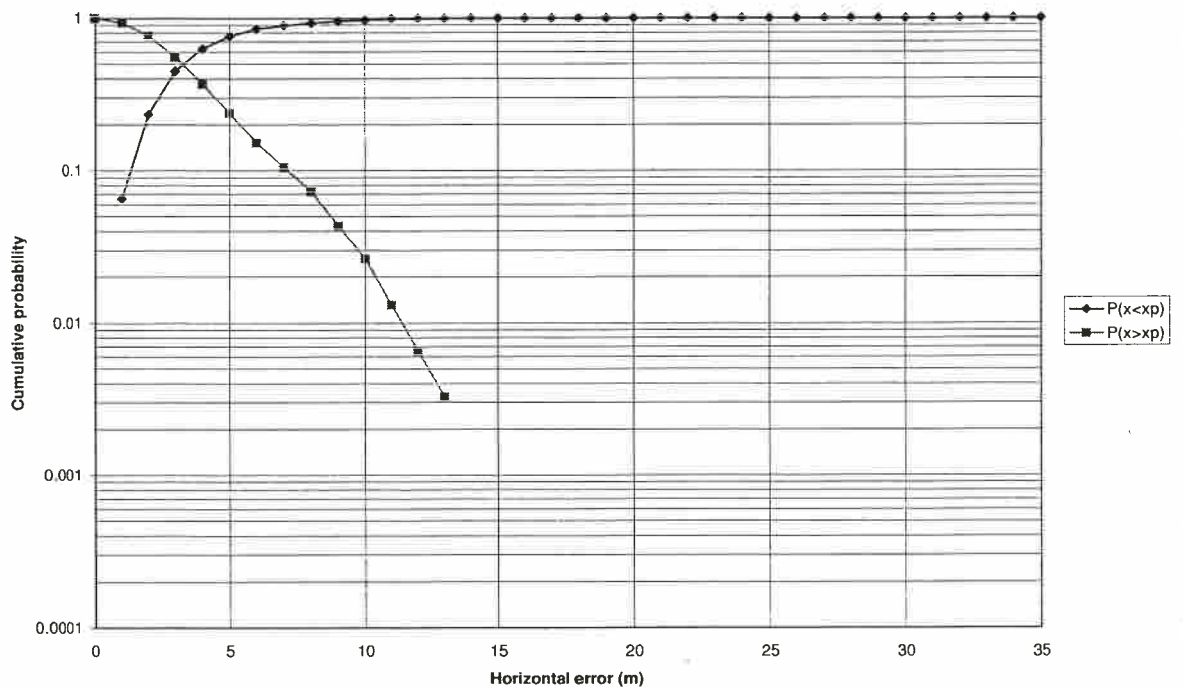


Figure 58 Cumulative Probability of GD2 2-D Error Irrespective of Range from the Platform, Aerad Approaches, Flight 5, Tartan A (bias removed)

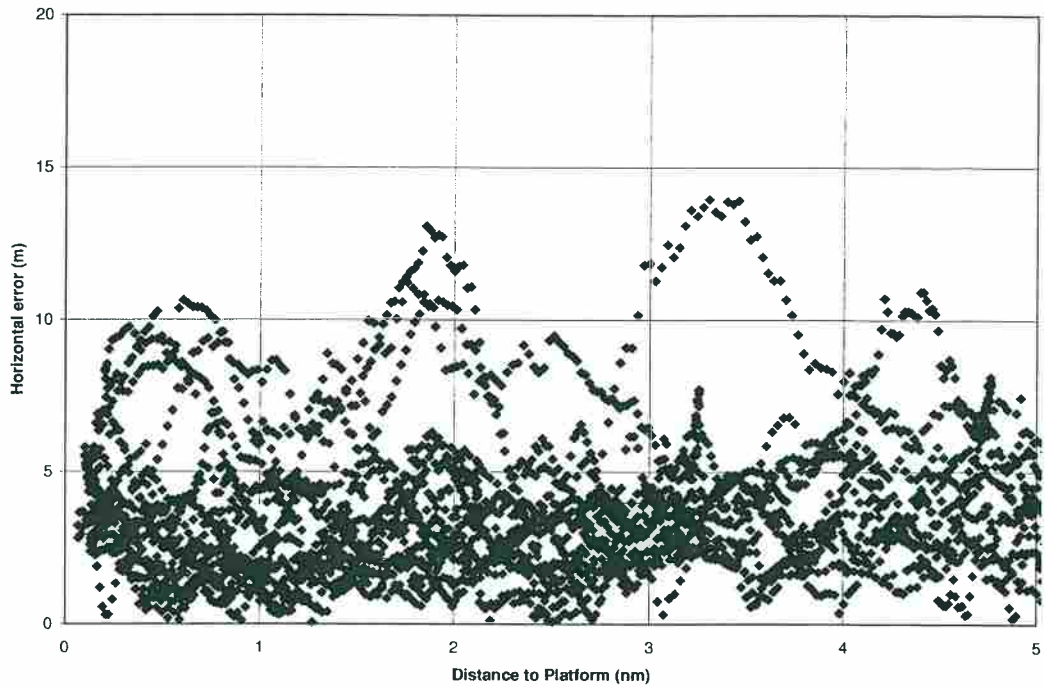


Figure 59 Scatter Plot of GD2 2-D Error Against Range from the Platform, Aerad Approaches, Flight 5, Tartan A (bias removed)

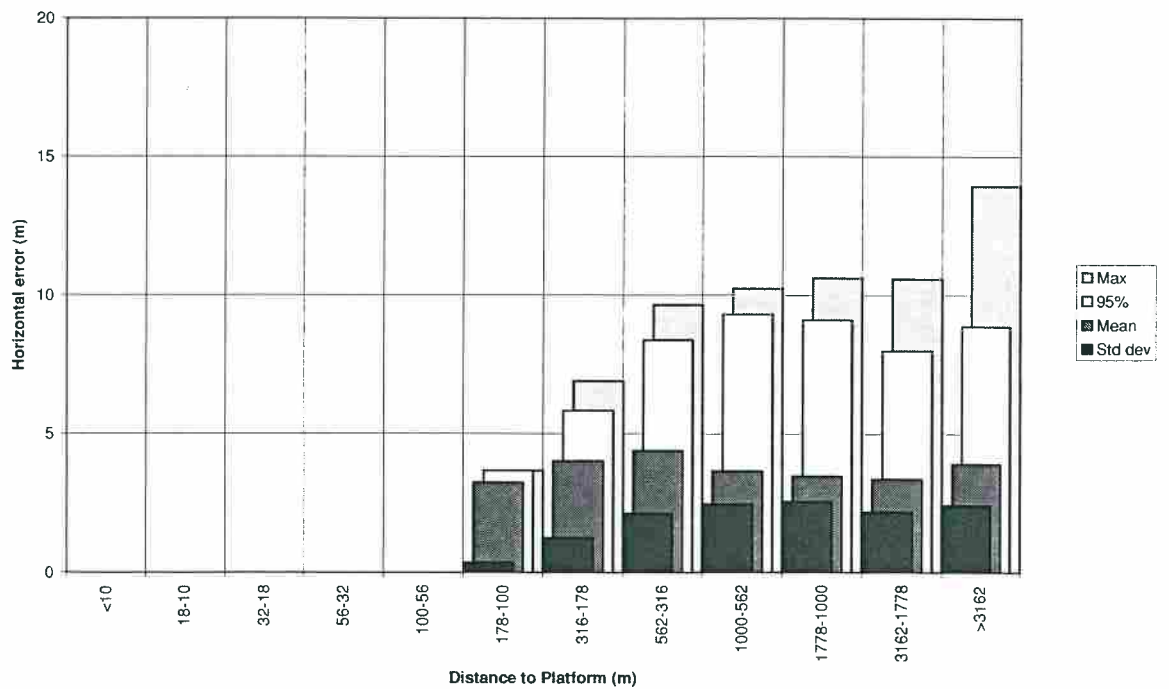


Figure 60 Variation of GD2 2-D Error Statistics with Range from the Platform, Aerad Approaches, Flight 5, Tartan A (bias removed)

Distance to platform (metres)	Number of samples	Minimum	Mean	Standard deviation	50% of samples less than	95% of samples less than	Maximum
>3162	722	29.0	35.7	2.2	35.6	40.3	41.4
3162-1778	275	21.9	30.7	5.1	32.4	37.5	39.5
1778-1000	239	24.9	32.4	3.6	32.7	38.4	39.1
1000-562	279	22.4	36.5	5.7	37.1	46.5	47.4
562-316	253	22.4	36.3	6.3	37.4	44.9	46.9
316-178	123	22.6	36.2	5.4	37.1	43.9	44.8
178-100	74	31.7	36.6	3.0	37.0	42.3	42.4
100-56	44	33.8	36.8	2.2	36.1	40.9	41.9
56-32	24	34.3	38.1	2.8	39.3	41.3	41.7
32-18	17	34.2	39.8	3.1	41.3	42.2	42.2
18-10	13	29.3	33.4	3.2	34.1	39.5	39.5
<10	3	32.5	34.8	3.6	33.0	39.0	39.0
All ranges	2066	21.9	35.0	4.8	35.4	42.1	47.4

Table 22 Statistics of GD2 2-D Error (metres), Platform Orbits, Flight 5, Tartan A

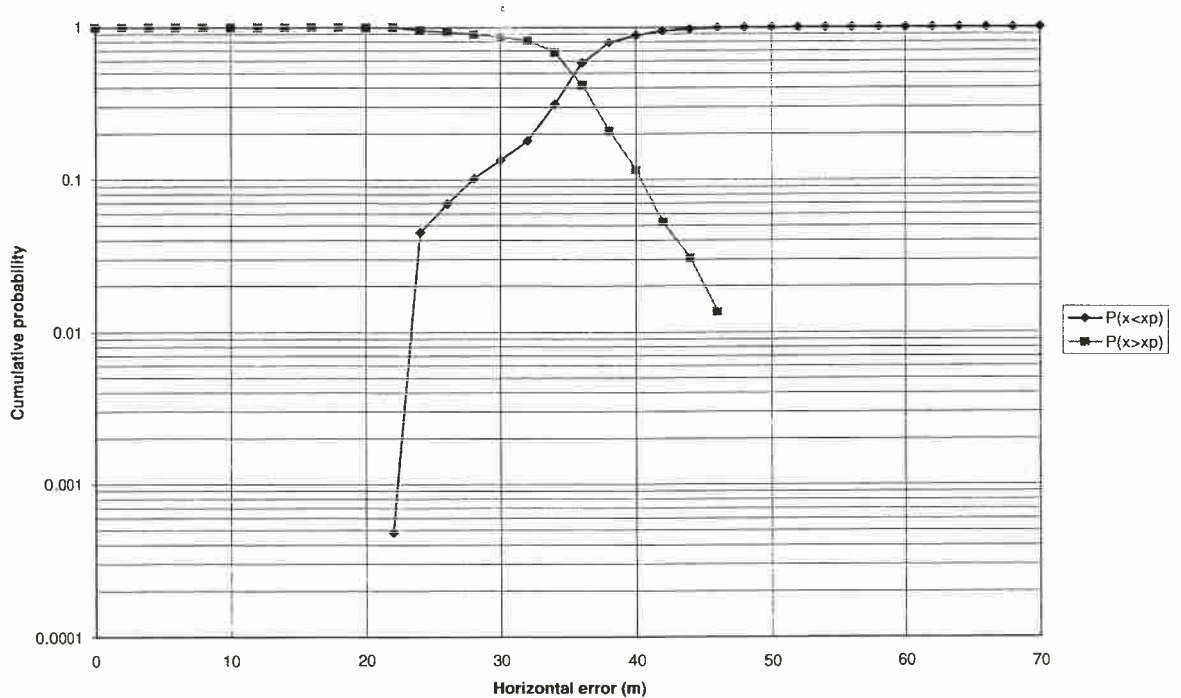


Figure 61 Cumulative Probability of GD2 2-D Error Irrespective of Range from the Platform, Platform Orbits, Flight 5, Tartan A (non-standard horizontal scale employed due to large bias)

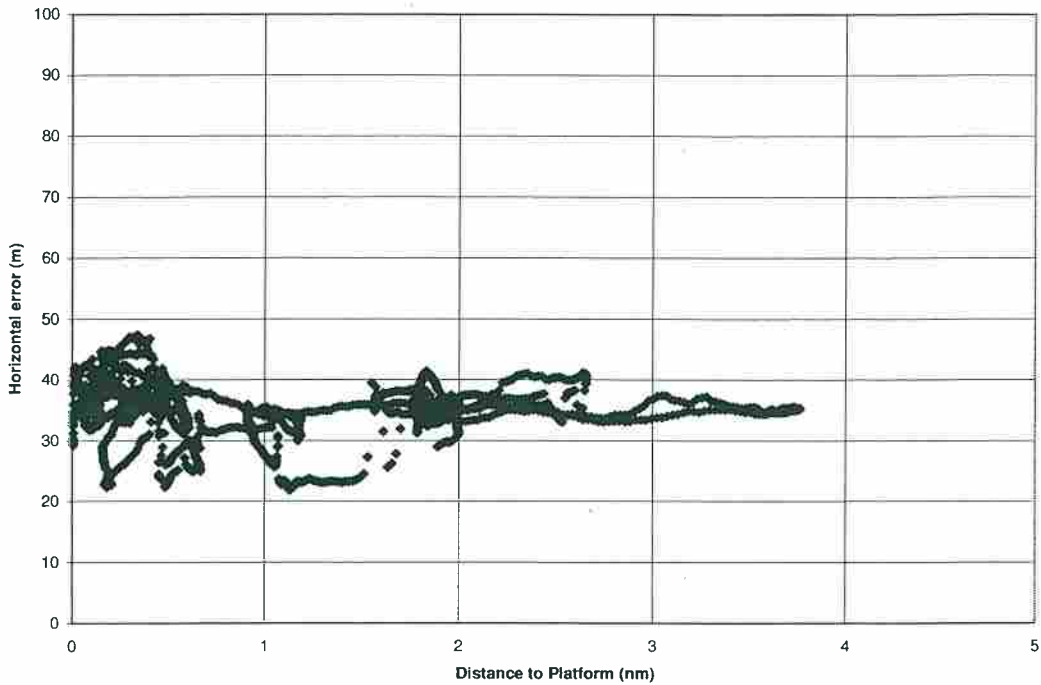


Figure 62 Scatter Plot of GD2 2-D Error Against Range from the Platform, Platform Orbits, Flight 5, Tartan A (non-standard vertical scale employed due to large bias)

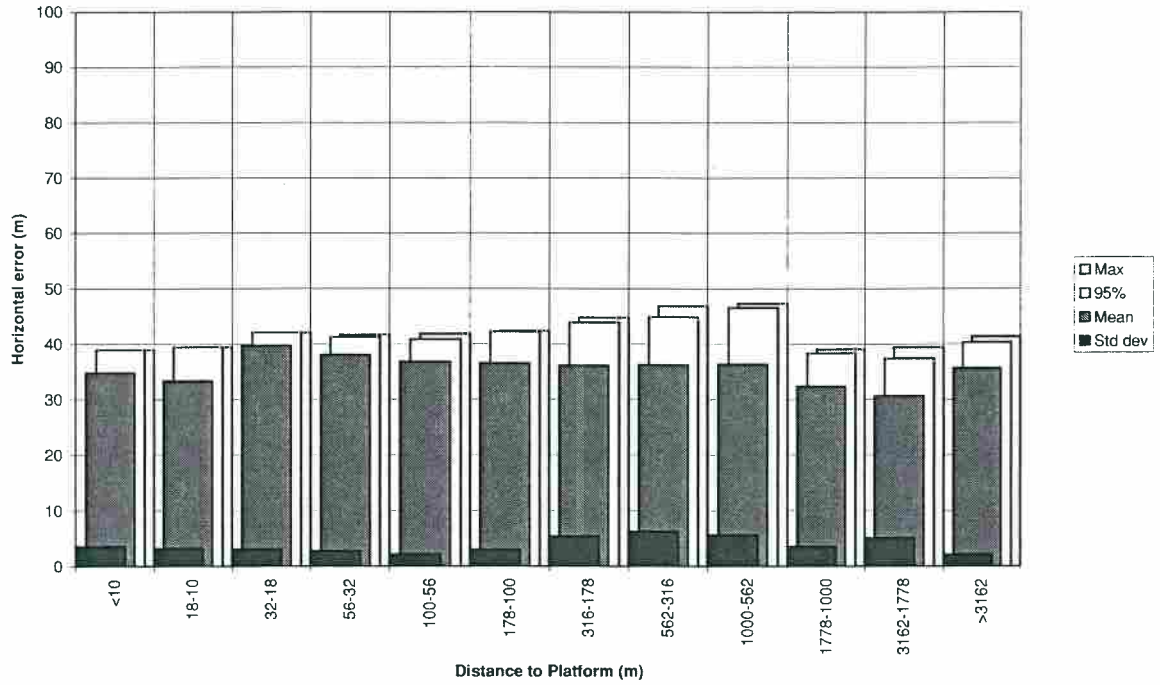


Figure 63 Variation of GD2 2-D Error Statistics with Range from the Platform, Platform Orbits, Flight 5, Tartan A (non-standard vertical scale employed due to large bias)

Distance to platform (metres)	Number of samples	Minimum	Mean	Standard deviation	50% of samples less than	95% of samples less than	Maximum
>3162	722	0.2	3.5	1.9	3.3	6.6	11.8
3162-1778	275	0.1	8.9	7.3	5.0	20.9	21.4
1778-1000	239	0.3	6.6	5.3	4.7	19.8	22.0
1000-562	279	0.1	8.0	5.8	6.1	21.6	23.1
562-316	253	0.3	7.9	6.3	5.5	21.2	23.8
316-178	123	1.9	7.3	4.6	5.6	15.4	23.7
178-100	74	0.5	3.9	2.0	3.3	7.5	7.7
100-56	44	0.4	2.7	2.0	2.1	7.1	7.6
56-32	24	0.6	4.3	2.5	4.9	7.4	7.4
32-18	17	2.7	6.3	1.9	7.1	7.6	7.6
18-10	13	2.8	4.6	1.6	4.3	7.0	7.0
<10	3	4.4	5.0	0.9	4.6	6.1	6.1
All ranges	2066	0.1	6.0	5.2	4.2	19.6	23.8

Table 23 Statistics of GD2 2-D Error (metres), Platform Orbits, Flight 5, Tartan A (bias removed)

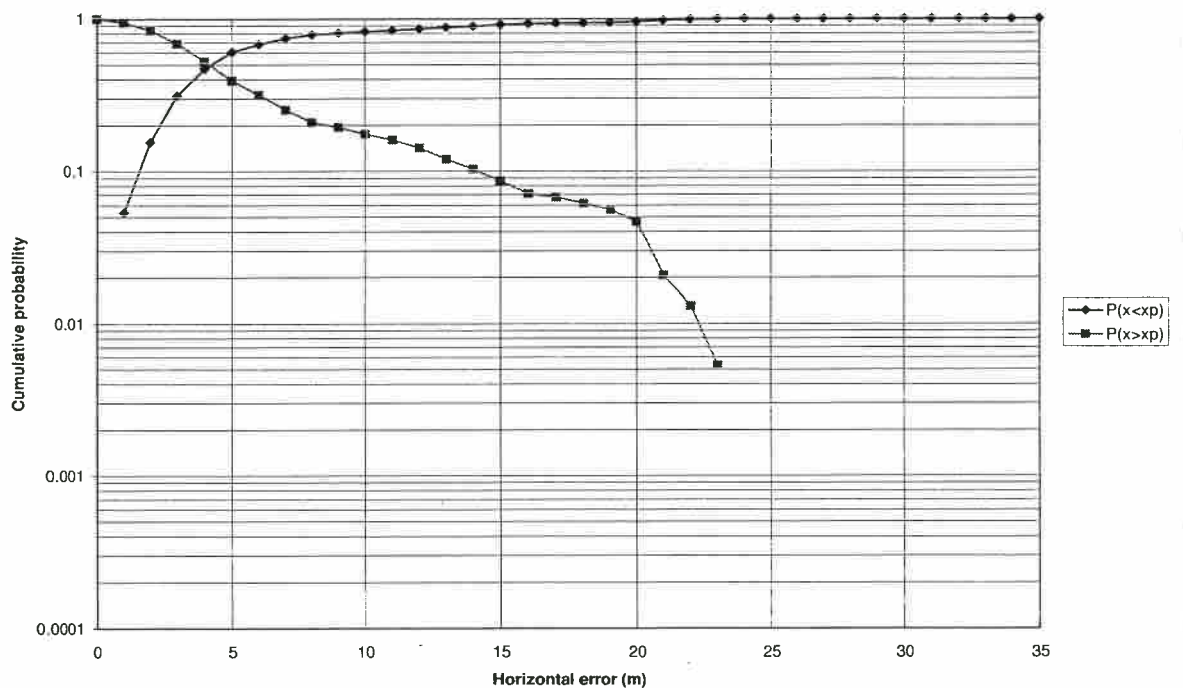


Figure 64 Cumulative Probability of GD2 2-D Error Irrespective of Range from the Platform, Platform Orbits, Flight 5, Tartan A (bias removed)

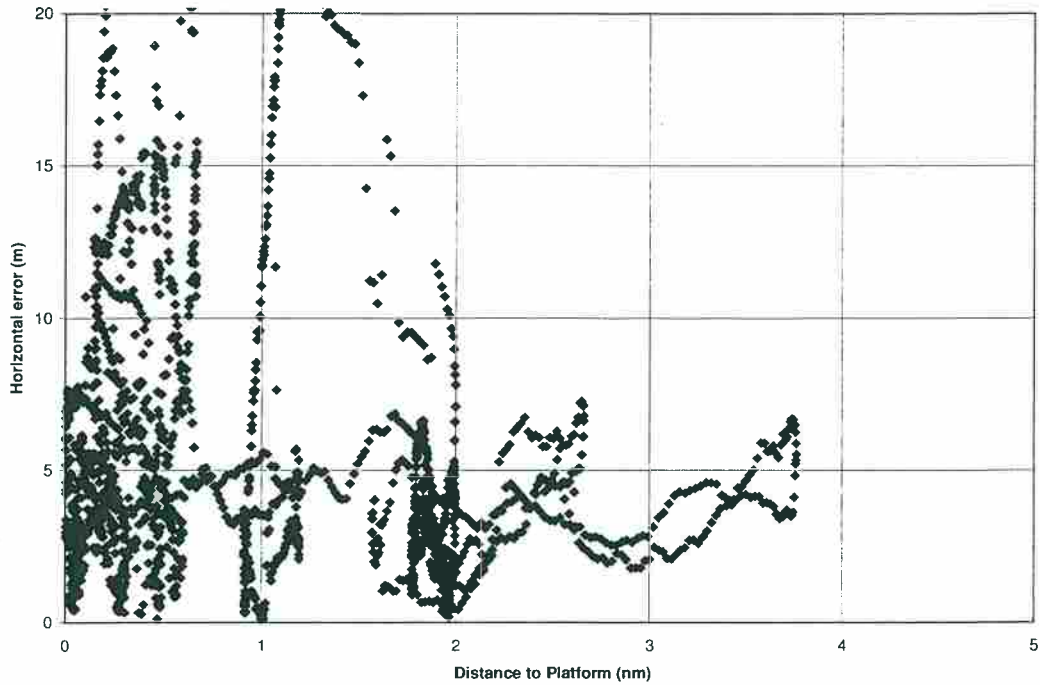


Figure 65 Scatter Plot of GD2 2-D Error Against Range from the Platform, Platform Orbits, Flight 5, Tartan A (bias removed)

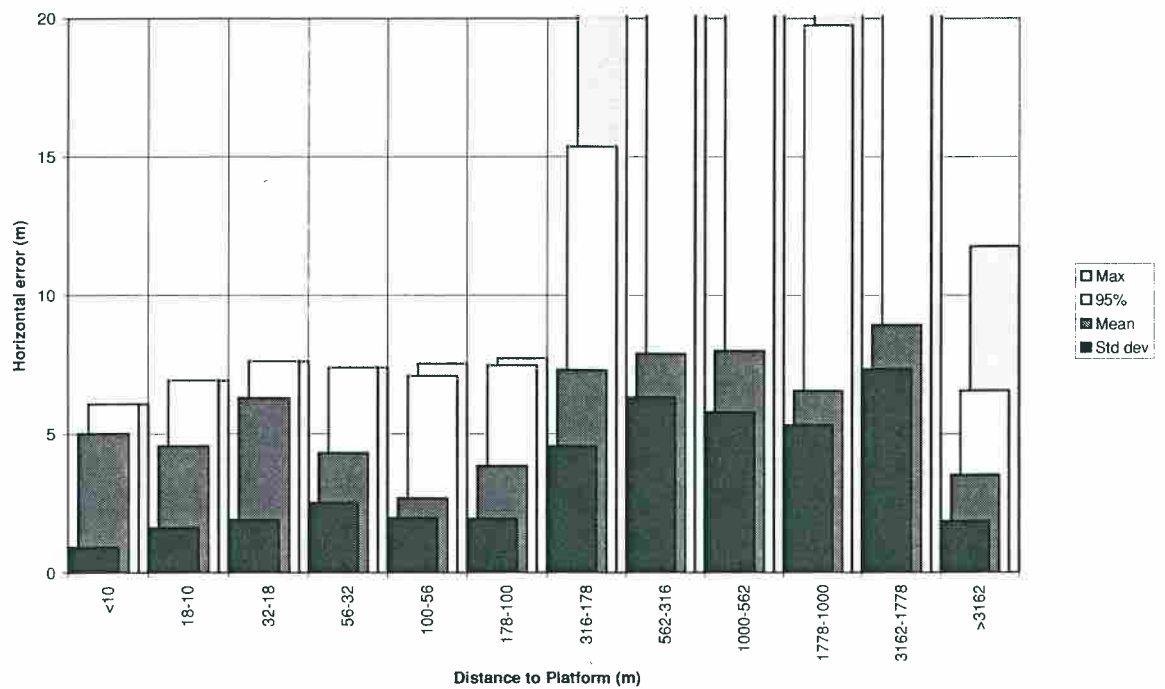


Figure 66 Variation of GD2 2-D Error Statistics with Range from the Platform, Platform Orbits, Flight 5, Tartan A (bias removed)

Distance to platform (metres)	Number of samples	Minimum	Mean	Standard deviation	50% of samples less than	95% of samples less than	Maximum
>3162	2654	26.5	37.1	10.9	35.0	44.0	122.4
3162-1778	757	27.2	38.3	8.0	36.2	56.9	80.6
1778-1000	482	23.0	41.1	15.9	35.3	86.5	89.8
1000-562	353	20.4	40.3	16.9	36.1	87.1	94.6
562-316	220	26.2	45.9	18.7	36.8	93.6	96.4
316-178	140	31.0	45.4	18.4	36.7	94.8	95.7
178-100	12	35.0	52.2	12.8	58.4	65.8	65.8
100-56	10	35.5	58.1	16.0	65.3	74.9	74.9
56-32	6	35.7	62.0	12.9	67.6	68.7	68.7
32-18	12	12.4	19.4	9.3	14.5	35.3	35.3
18-10	342	7.7	35.9	12.6	35.2	57.0	63.2
<10	9	34.9	36.6	1.1	37.2	37.5	37.5
All ranges	4997	7.7	38.5	12.8	35.5	63.6	122.4

Table 24 Statistics of GD2 2-D Error (metres), Experimental Approaches, Flight 5, Tartan A

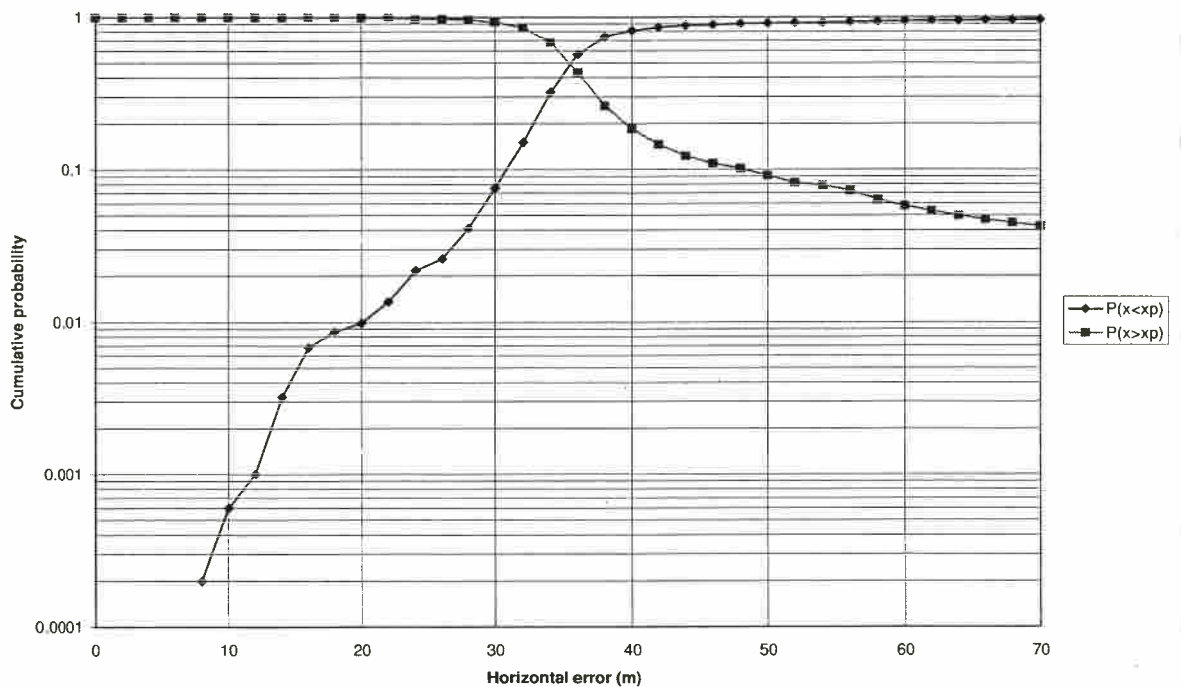


Figure 67 Cumulative Probability of GD2 2-D Error Irrespective of Range from the Platform, Experimental Approaches, Flight 5, Tartan A (non-standard horizontal scale employed due to large bias)

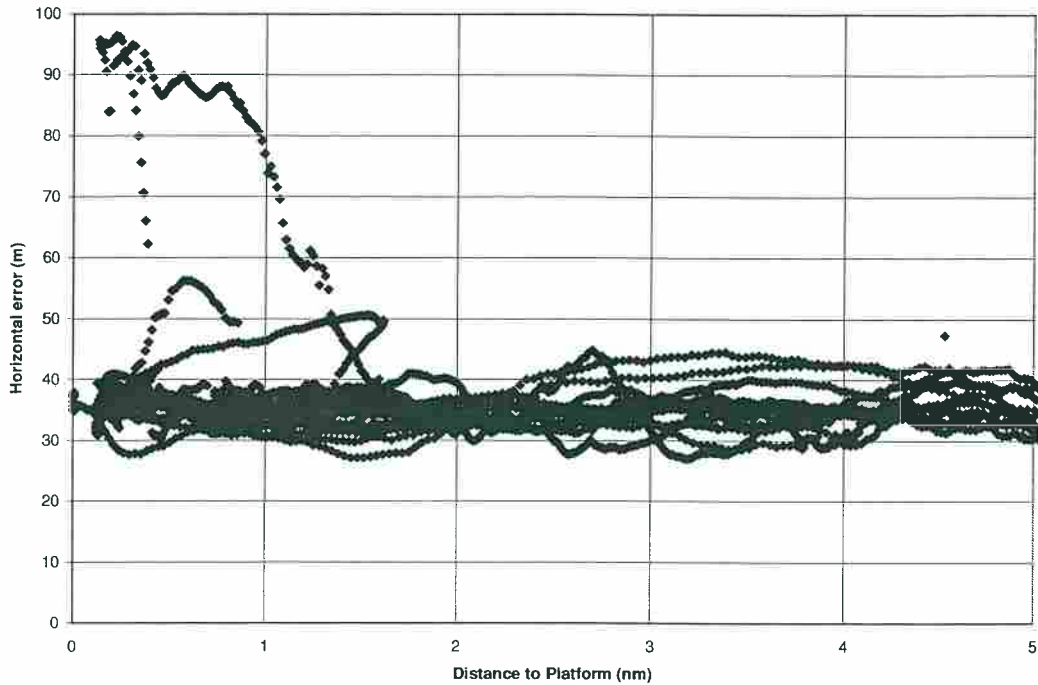


Figure 68 Scatter Plot of GD2 2-D Error Against Range from the Platform, Experimental Approaches, Flight 5, Tartan A (non-standard vertical scale employed due to large bias)

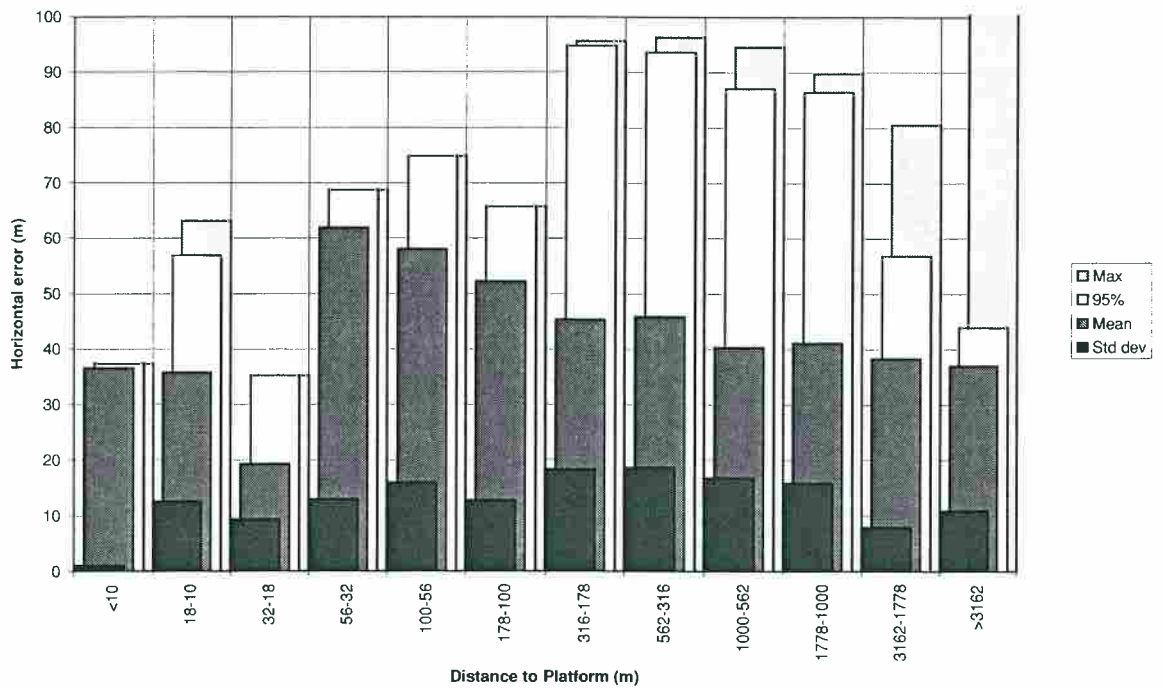


Figure 69 Variation of GD2 2-D Error Statistics with Range from the Platform, Experimental Approaches, Flight 5, Tartan A (non-standard vertical scale employed due to large bias)

Distance to platform (metres)	Number of samples	Minimum	Mean	Standard deviation	50% of samples less than	95% of samples less than	Maximum
>3162	2654	0.0	6.4	11.2	3.8	17.4	95.5
3162-1778	757	0.2	7.5	9.2	3.5	28.6	49.1
1778-1000	482	0.2	12.5	17.5	4.0	55.3	63.1
1000-562	353	0.6	13.1	17.9	4.0	58.0	63.6
562-316	220	0.5	14.3	19.6	4.4	63.0	66.4
316-178	140	0.5	13.2	19.0	4.1	65.6	66.5
178-100	12	0.5	26.2	18.8	37.5	42.9	42.9
100-56	10	2.0	34.9	22.3	48.2	53.2	53.2
56-32	6	4.1	43.0	19.1	51.1	52.3	52.3
32-18	12	4.4	20.2	11.0	23.8	33.2	33.2
18-10	342	4.4	35.3	12.8	34.9	56.9	63.2
<10	9	3.3	6.1	2.0	6.9	8.2	8.2
All ranges	4997	0.0	10.3	15.1	4.1	48.9	95.5

Table 25 Statistics of GD2 2-D Error (metres), Experimental Approaches, Flight 5, Tartan A (bias removed)

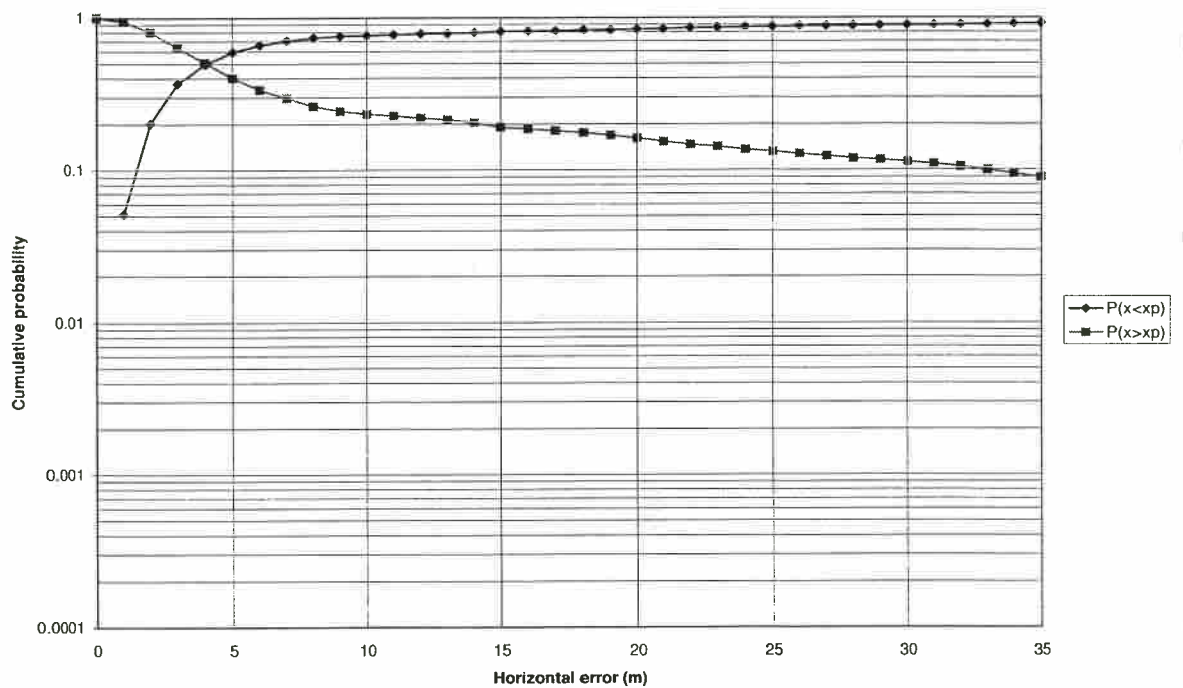


Figure 70 Cumulative Probability of GD2 2-D Error Irrespective of Range from the Platform, Experimental Approaches, Flight 5, Tartan A (bias removed)

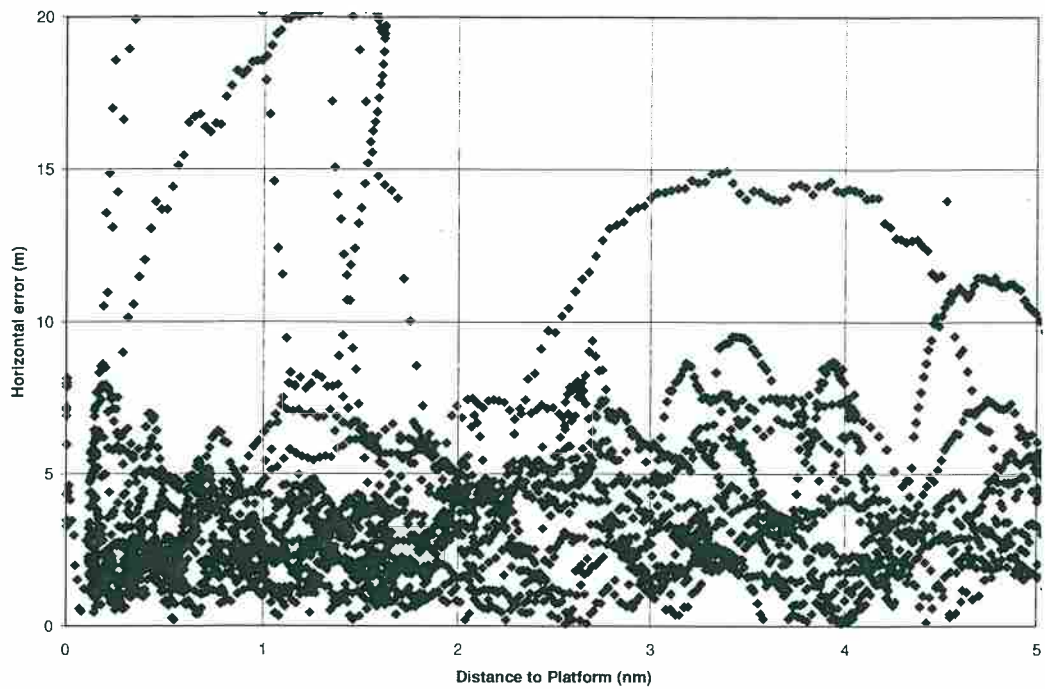


Figure 71 Scatter Plot of GD2 2-D Error Against Range from the Platform, Experimental Approaches, Flight 5, Tartan A (bias removed)

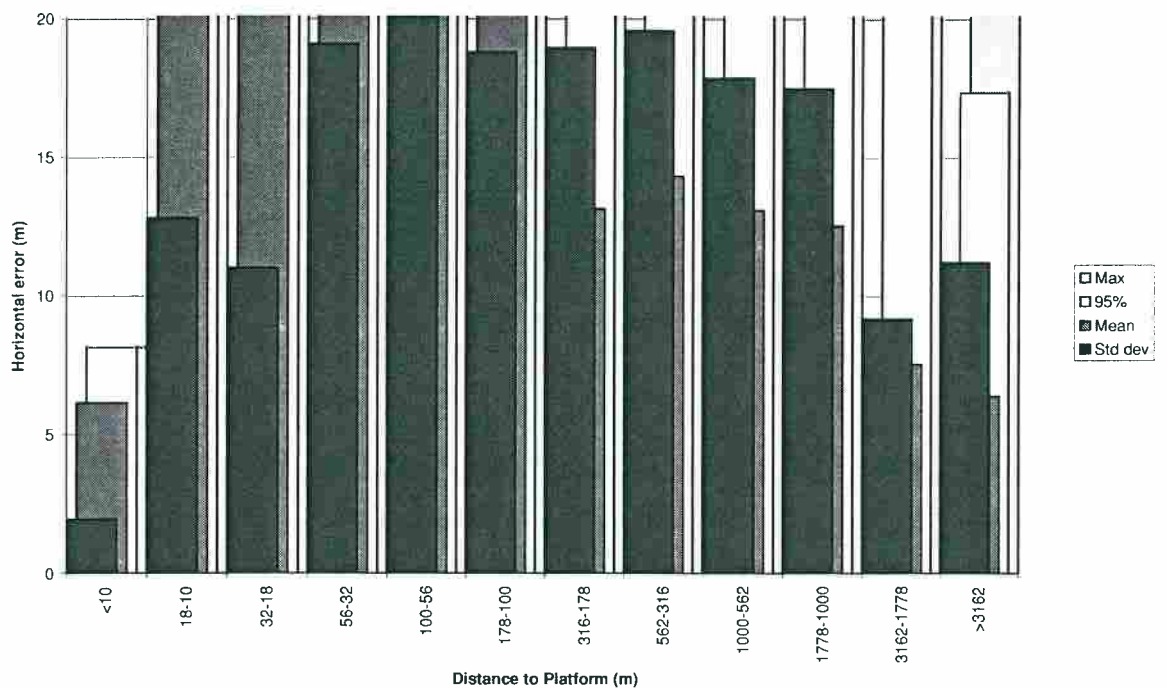


Figure 72 Variation of GD2 2-D Error Statistics with Range from the Platform, Experimental Approaches, Flight 5, Tartan A (bias removed)

Distance to platform (metres)	Number of samples	Minimum	Mean	Standard deviation	50% of samples less than	95% of samples less than	Maximum
>3162	3370	0.3	5.5	3.2	4.7	12.2	20.3
3162-1778	751	0.4	5.1	2.5	4.9	9.6	15.4
1778-1000	406	0.1	4.5	2.4	4.2	8.8	14.3
1000-562	235	0.6	5.3	2.3	5.2	8.7	13.1
562-316	145	0.6	5.2	2.5	5.4	9.3	13.2
316-178	106	0.0	4.8	2.6	4.7	9.0	10.5
178-100	27	1.6	5.7	3.0	5.2	10.6	11.0
100-56	7	3.2	5.6	2.2	4.3	8.1	8.1
56-32	0						
32-18	0						
18-10	0						
<10	0						
All ranges	5047	0.0	5.3	3.0	4.7	11.1	20.3

Table 26 Statistics of GD2 2-D Error (metres), Aerad Approaches, Flight 6, Buchan A

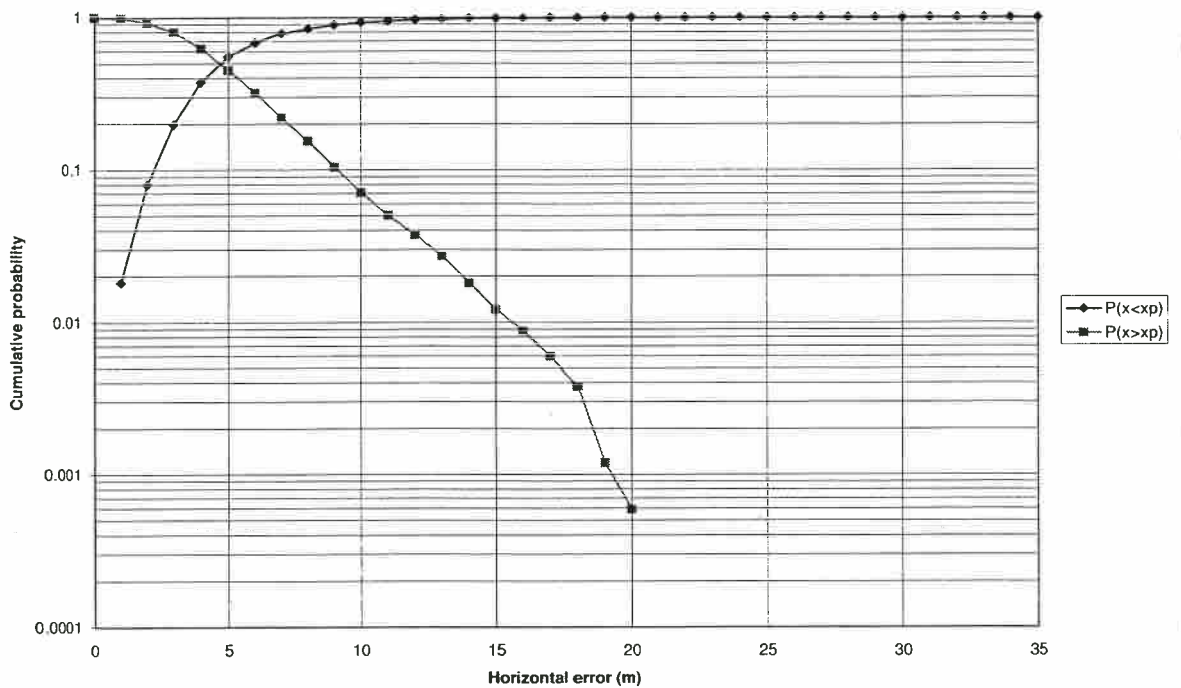


Figure 73 Cumulative Probability of GD2 2-D Error Irrespective of Range from the Platform, Aerad Approaches, Flight 6, Buchan A

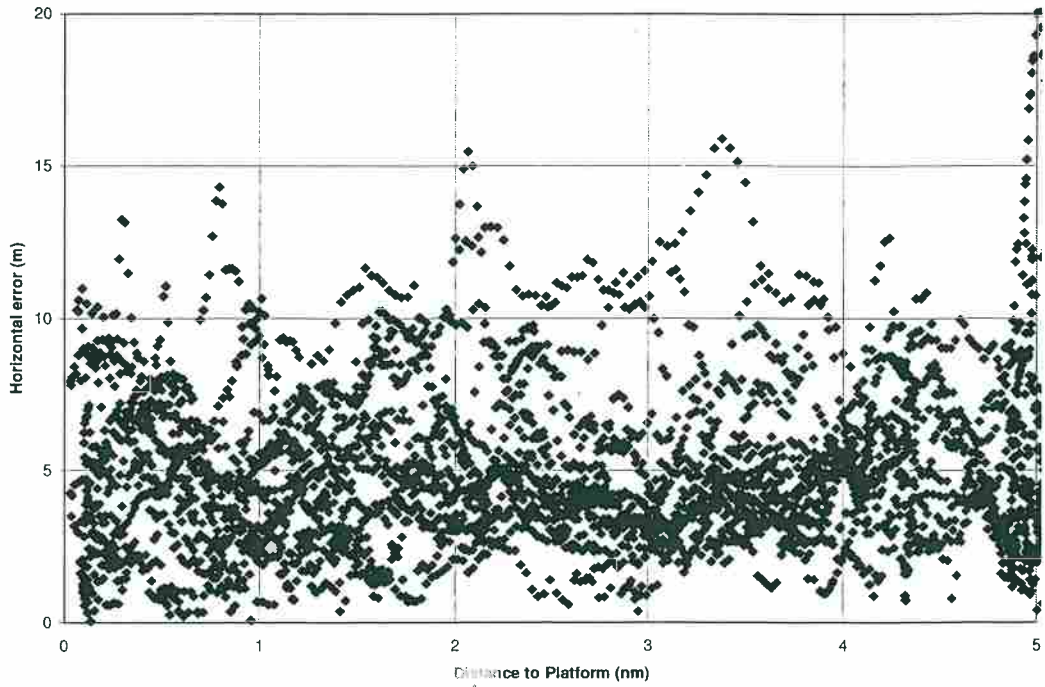


Figure 74 Scatter Plot of GD2 2-D Error Against Range from the Platform, Aerad Approaches, Flight 6, Buchan A

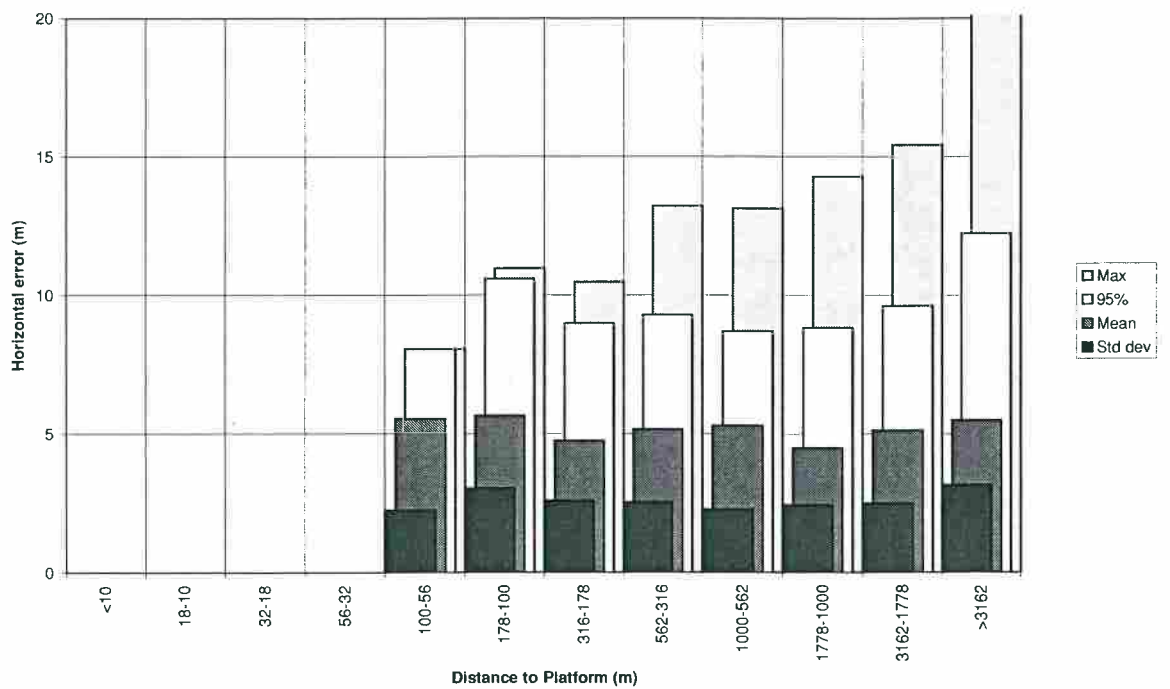


Figure 75 Variation of GD2 2-D Error Statistics with Range from the Platform, Aerad Approaches, Flight 6, Buchan A

Distance to platform (metres)	Number of samples	Minimum	Mean	Standard deviation	50% of samples less than	95% of samples less than	Maximum
>3162	686	1.4	6.6	2.5	6.4	10.9	14.1
3162-1778	215	0.4	6.6	3.0	6.8	12.8	15.2
1778-1000	321	1.9	6.4	2.5	6.4	10.7	12.4
1000-562	237	1.0	6.1	3.4	5.7	13.2	22.0
562-316	290	0.5	6.5	3.4	5.8	13.3	15.2
316-178	110	0.8	6.7	2.6	7.3	9.9	12.2
178-100	45	1.6	7.3	2.3	7.9	10.5	10.6
100-56	30	5.8	8.0	1.3	7.8	10.0	10.1
56-32	6	2.8	4.5	1.1	4.7	6.1	6.1
32-18	4	2.4	3.3	0.7	3.8	3.9	3.9
18-10	0						
<10	0						
All ranges	1944	0.4	6.5	2.8	6.4	11.5	22.0

Table 27 Statistics of GD2 2-D Error (metres), Platform Orbits, Flight 6, Buchan A

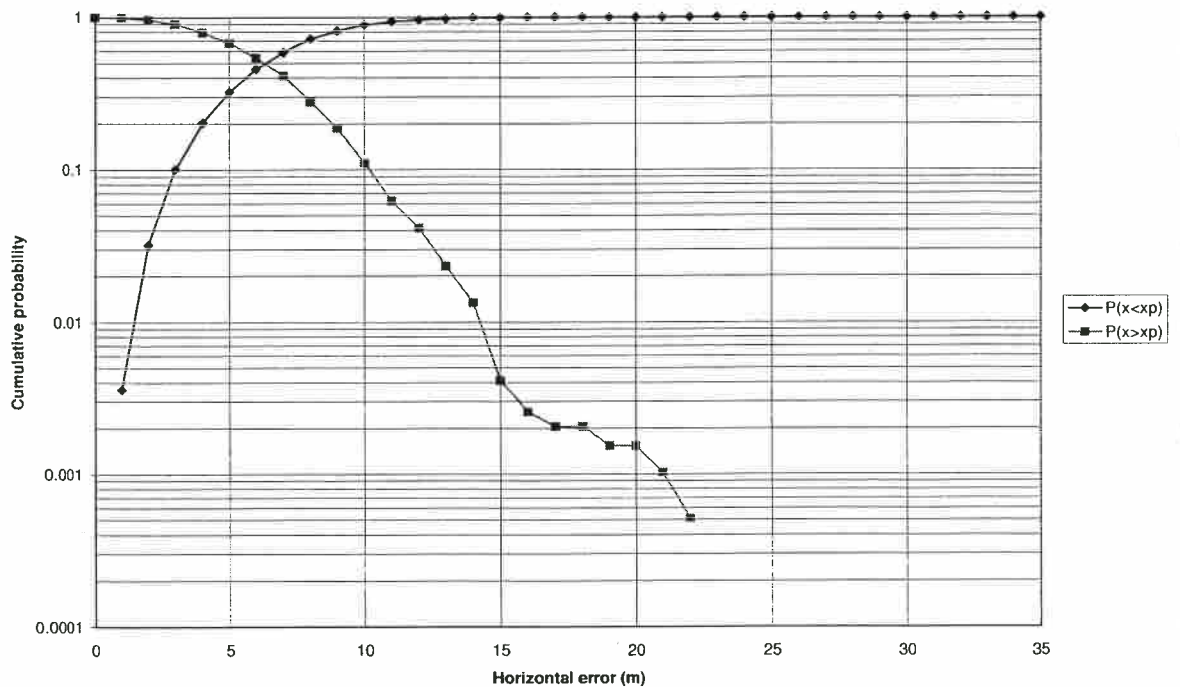


Figure 76 Cumulative Probability of GD2 2-D Error Irrespective of Range from the Platform, Platform Orbits, Flight 6, Buchan A

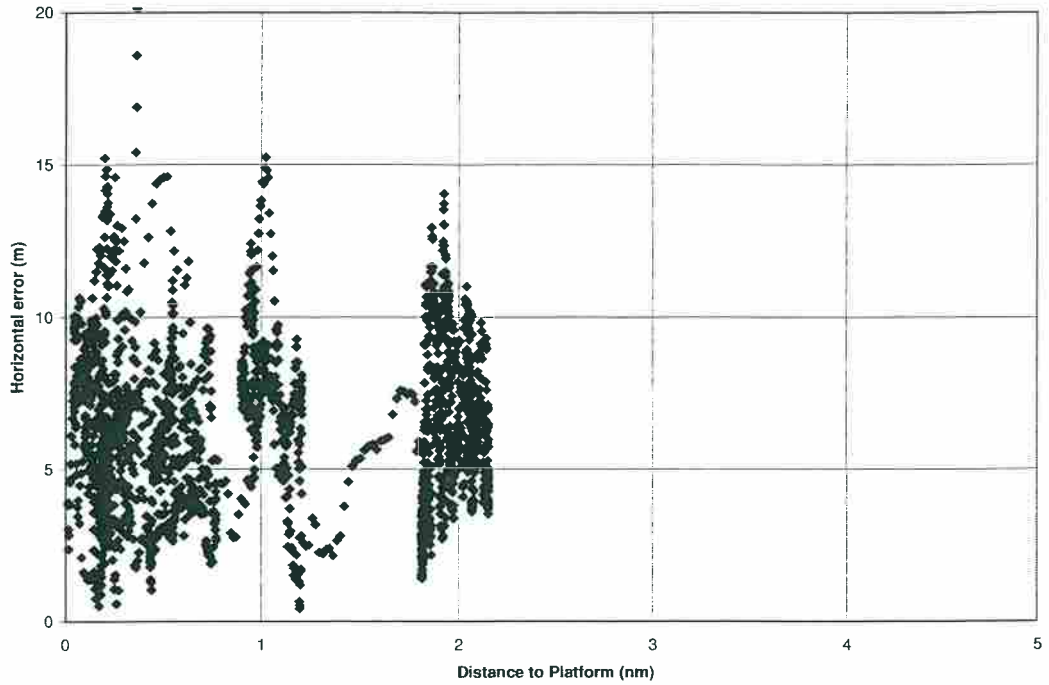


Figure 77 Scatter Plot of GD2 2-D Error Against Range from the Platform, Platform Orbits, Flight 6, Buchan A

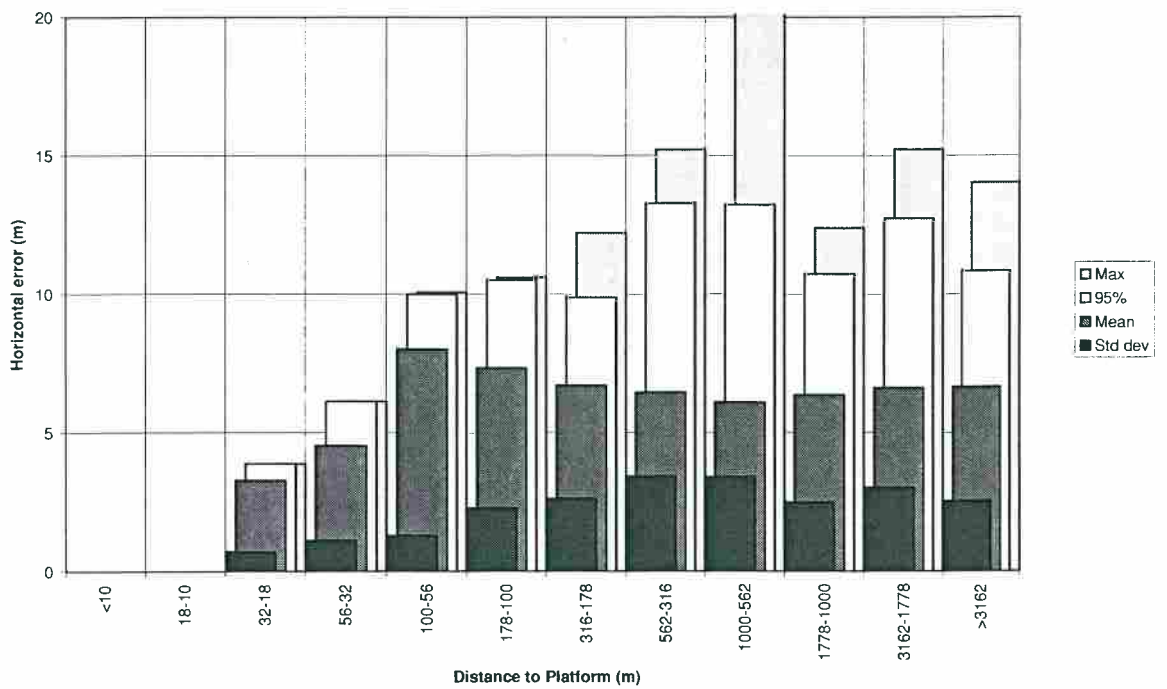


Figure 78 Variation of GD2 2-D Error Statistics with Range from the Platform, Platform Orbits, Flight 6, Buchan A

Distance to platform (metres)	Number of samples	Minimum	Mean	Standard deviation	50% of samples less than	95% of samples less than	Maximum
>3162	1131	0.0	7.1	5.6	5.1	19.1	22.3
3162-1778	405	1.7	6.3	3.0	5.5	13.8	16.7
1778-1000	252	1.9	6.4	2.6	5.9	12.4	15.7
1000-562	137	2.8	6.6	2.6	6.1	12.8	13.4
562-316	87	2.0	6.4	2.1	6.3	10.7	11.2
316-178	75	4.1	6.9	1.2	7.0	8.7	10.1
178-100	15	7.7	8.7	0.6	8.7	9.8	9.8
100-56	9	7.0	8.0	0.7	7.9	8.9	8.9
56-32	5	6.3	9.1	1.6	9.6	10.2	10.2
32-18	0						
18-10	0						
<10	0						
All ranges	2116	0.0	6.8	4.5	5.5	17.9	22.3

Table 28 Statistics of GD2 2-D Error (metres), Experimental Approaches, Flight 6, Buchan A

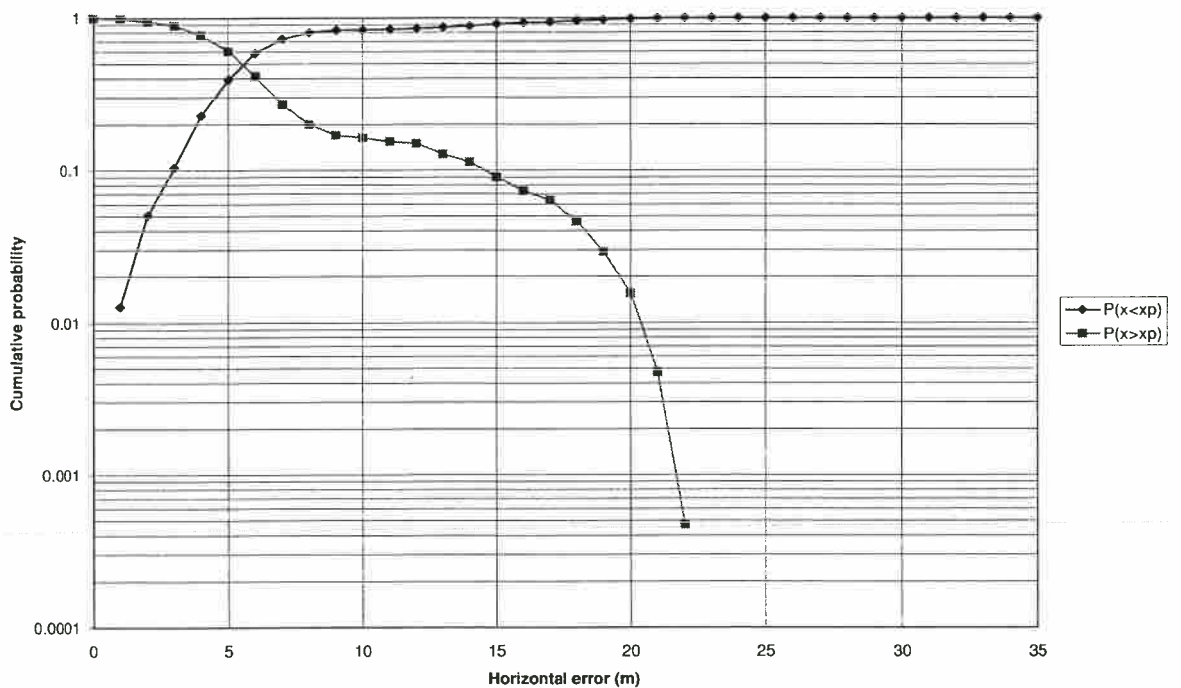


Figure 79 Cumulative Probability of GD2 2-D Error Irrespective of Range from the Platform, Experimental Approaches, Flight 6, Buchan A

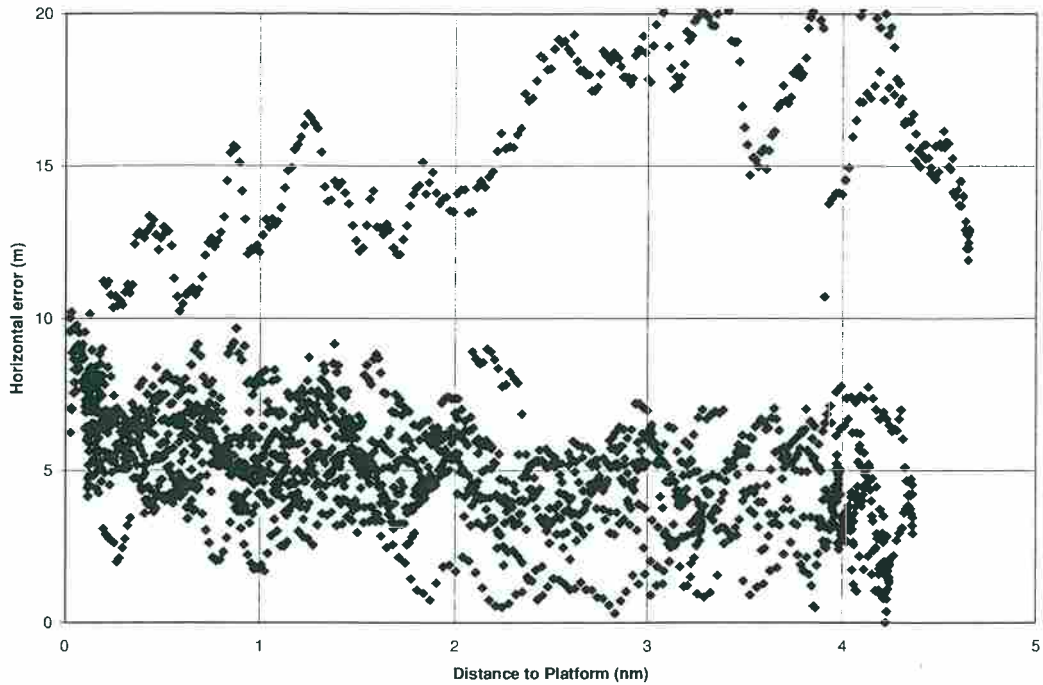


Figure 80 Scatter Plot of GD2 2-D Error Against Range from the Platform, Experimental Approaches, Flight 6, Buchan A

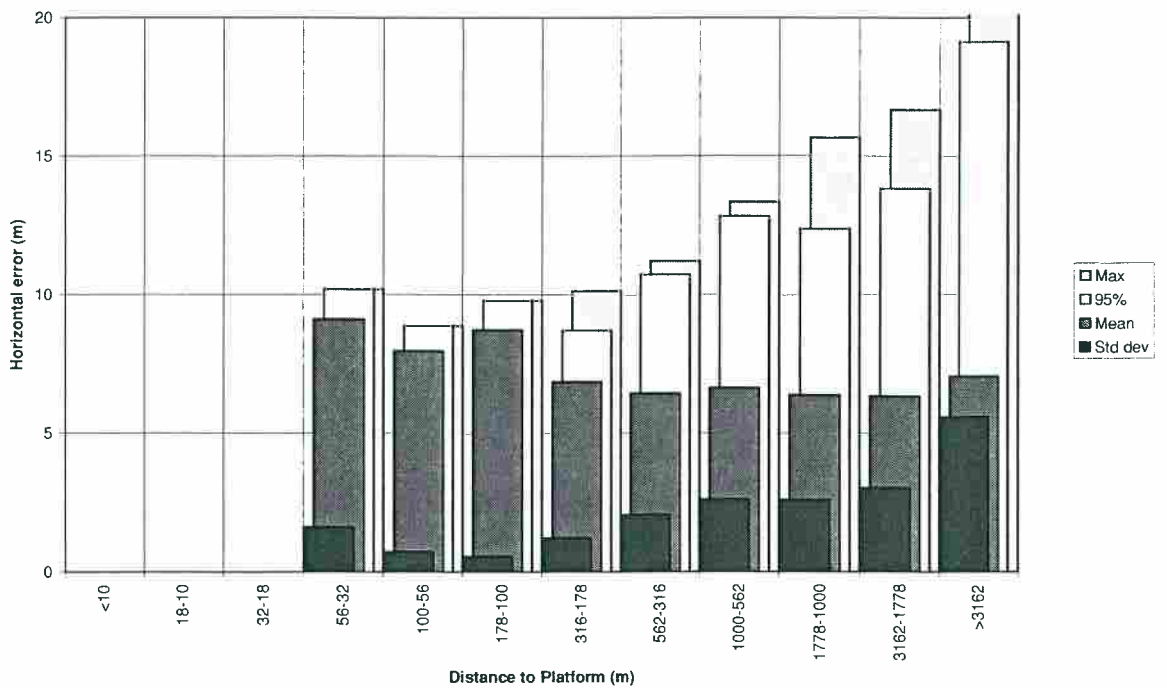


Figure 81 Variation of GD2 2-D Error Statistics with Range from the Platform, Experimental Approaches, Flight 6, Buchan A

6.3 **MF-Corrected Trimble (GD3) Receiver**

This receiver was a Trimble TNL-2100 which was supplied with differential corrections originating from the same MF source as the GD1 receiver.

Owing to a variety of technical difficulties, described in Volume 1 of this report, the receiver was only operational on the last two flight trials (Flights 6 and 7). As a result, data from the receiver is only available for the Beatrice C and Buchan A platforms.

On these two flights, the receiver was not able to operate in differential mode for a substantial proportion of the trial (the reasons are outlined in section 7). Data relating to these periods has been excluded from the analysis.

Distance to platform (metres)	Number of samples	Minimum	Mean	Standard deviation	50% of samples less than	95% of samples less than	Maximum
>3162	329	0.8	2.3	1.0	2.2	4.1	5.6
3162-1778	166	0.2	1.8	0.9	1.7	4.0	4.1
1778-1000	79	0.5	2.0	0.5	2.0	2.8	3.0
1000-562	50	0.9	1.8	0.4	1.9	2.3	2.4
562-316	29	1.1	1.8	0.3	1.9	2.1	2.1
316-178	25	1.1	2.7	1.4	2.0	5.0	5.1
178-100	4	1.0	1.3	0.6	1.2	2.2	2.2
100-56	4	0.9	1.1	0.2	1.2	1.3	1.3
56-32	0						
32-18	0						
18-10	0						
<10	0						
All ranges	686	0.2	2.1	0.9	1.9	4.0	5.6

Table 29 Statistics of GD3 2-D Error (metres), Aerad Approaches, Flight 7, Beatrice C

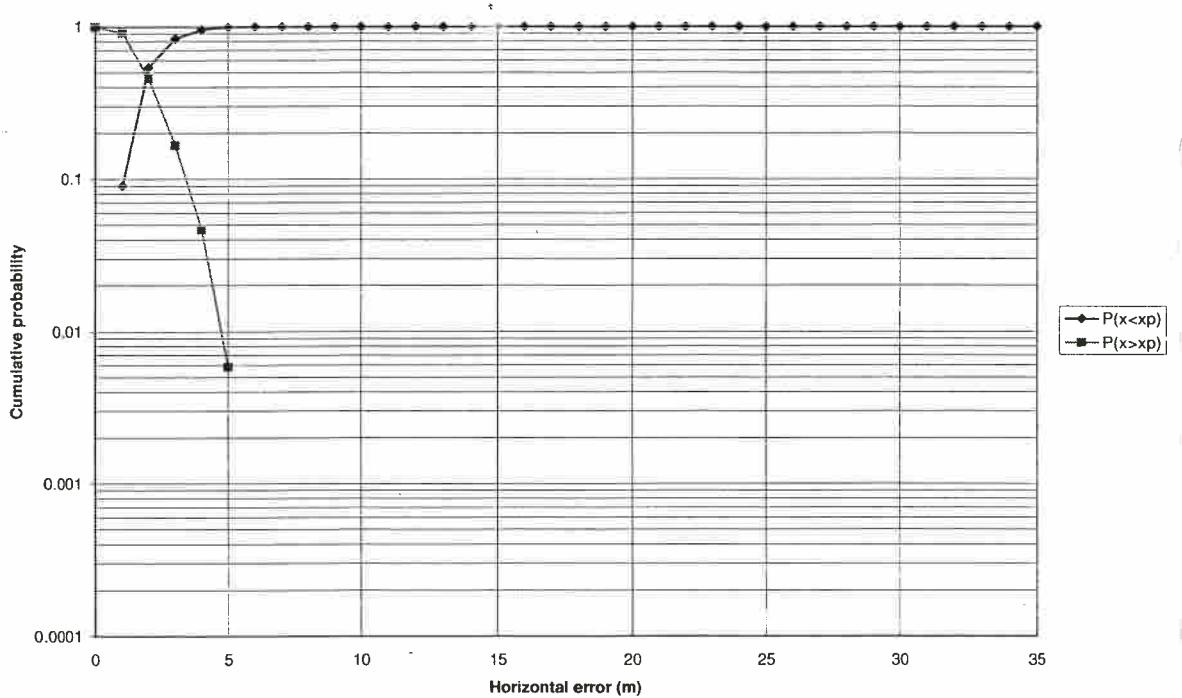


Figure 82 Cumulative Probability of GD3 2-D Error Irrespective of Range from the Platform, Aerad Approaches, Flight 7, Beatrice C

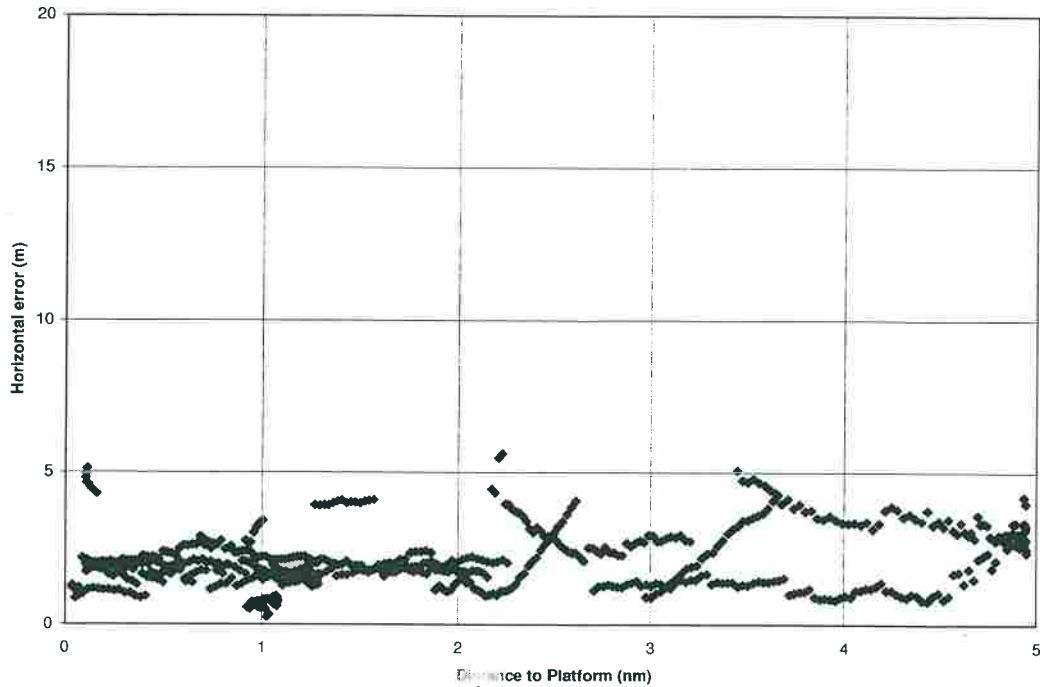


Figure 83 Scatter Plot of GD3 2-D Error Against Range from the Platform, Aerad Approaches, Flight 7, Beatrice C

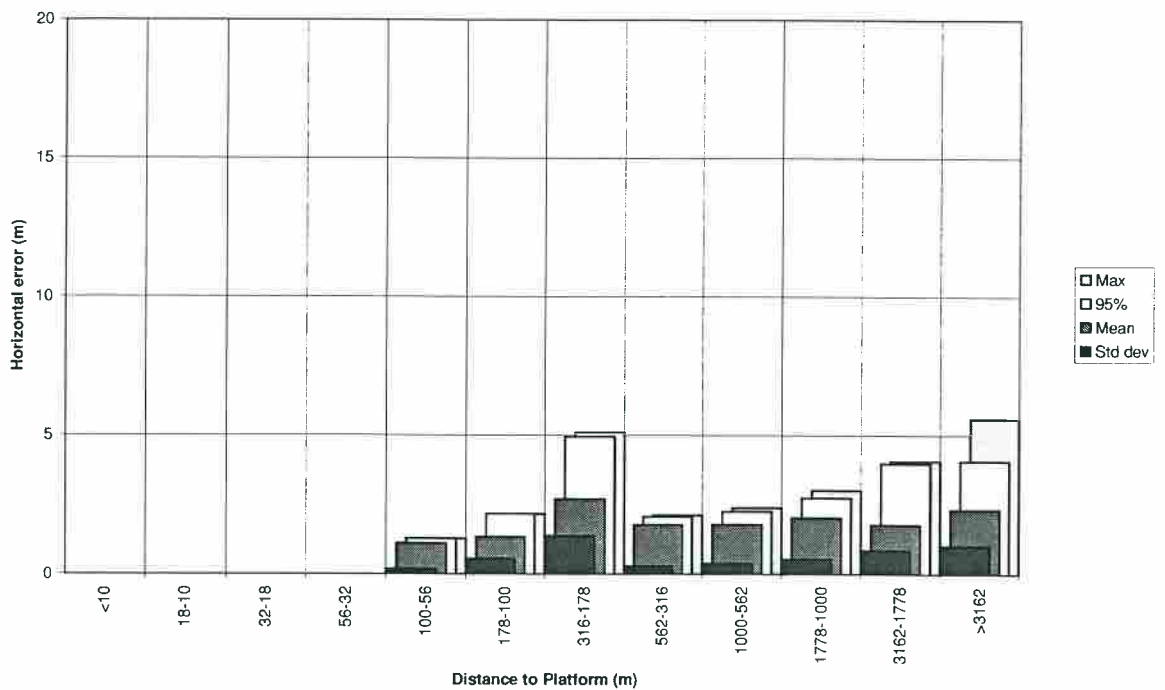


Figure 84 Variation of GD3 2-D Error Statistics with Range from the Platform, Aerad Approaches, Flight 7, Beatrice C

Distance to platform (metres)	Number of samples	Minimum	Mean	Standard deviation	50% of samples less than	95% of samples less than	Maximum
>3162	0						
3162-1778	0						
1778-1000	83	0.2	2.0	1.3	1.9	4.4	5.3
1000-562	84	0.2	2.5	1.6	2.2	4.9	5.5
562-316	123	2.1	5.4	1.4	5.9	7.1	7.2
316-178	105	0.6	4.5	2.0	4.3	7.5	7.6
178-100	63	3.0	5.4	1.1	5.7	6.9	7.4
100-56	56	2.3	5.3	1.4	5.6	7.1	7.2
56-32	38	3.7	6.1	1.1	6.4	7.4	7.5
32-18	5	3.0	3.5	0.5	3.8	3.9	3.9
18-10	4	2.9	2.9	0.1	2.9	3.0	3.0
<10	0						
All ranges	561	0.2	4.3	2.0	4.3	7.1	7.6

Table 30 Statistics of GD3 2-D Error (metres), Platform Orbits, Flight 7, Beatrice C

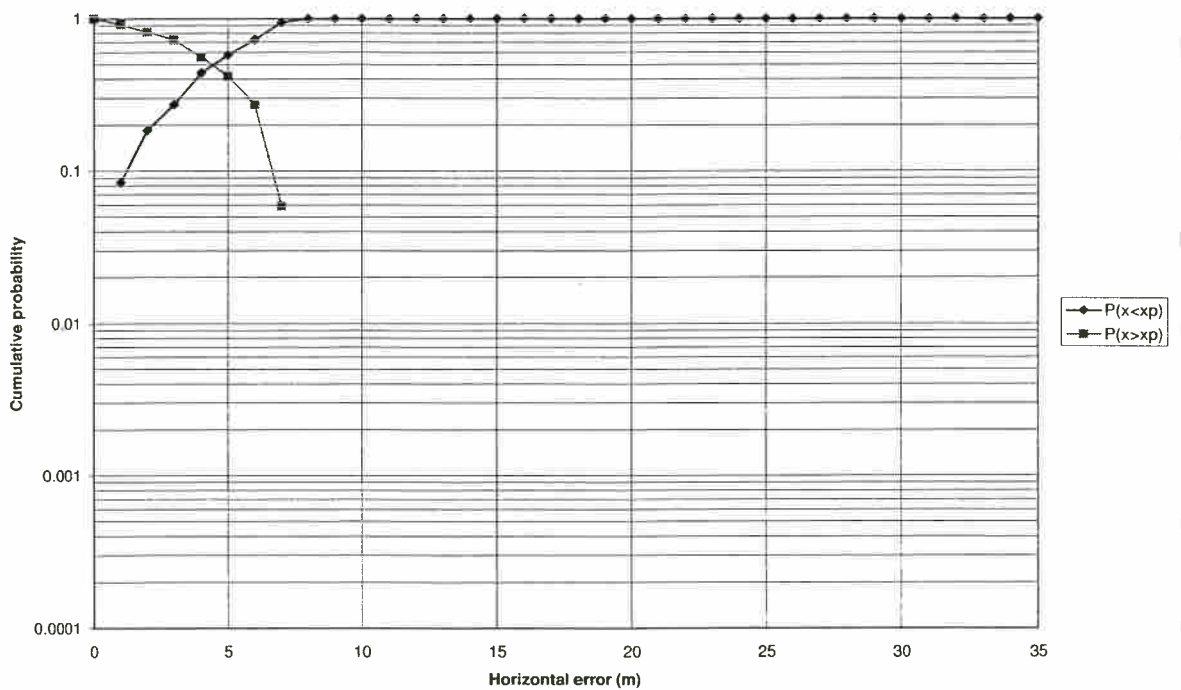


Figure 85 Cumulative Probability of GD3 2-D Error Irrespective of Range from the Platform, Platform Orbits, Flight 7, Beatrice C

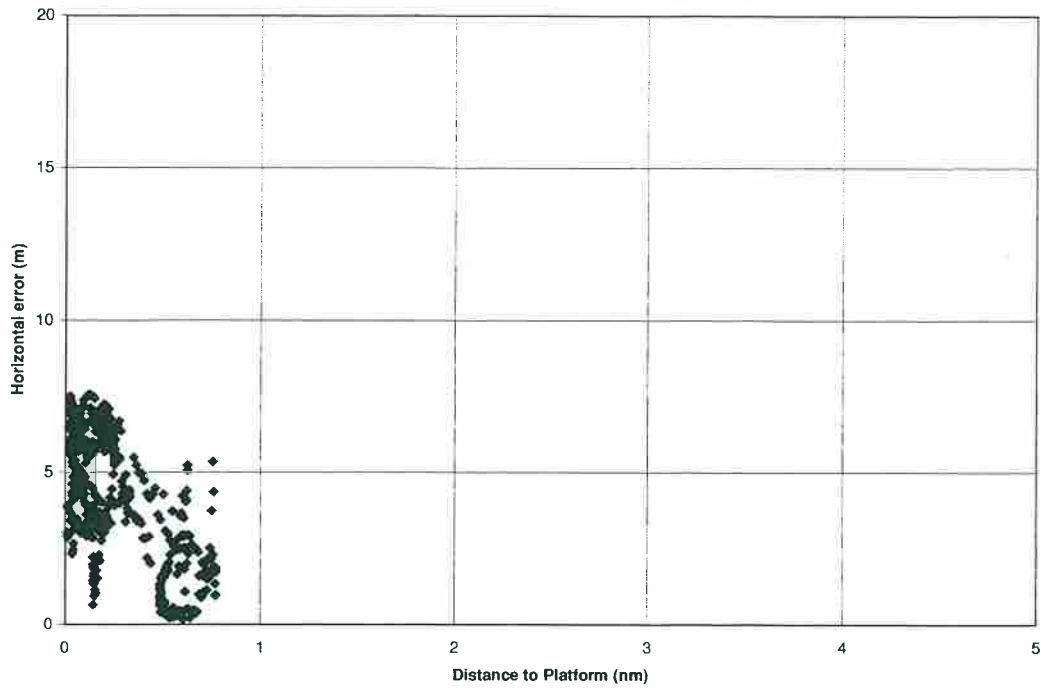


Figure 86 Scatter Plot of GD3 2-D Error Against Range from the Platform, Platform Orbits, Flight 7, Beatrice C

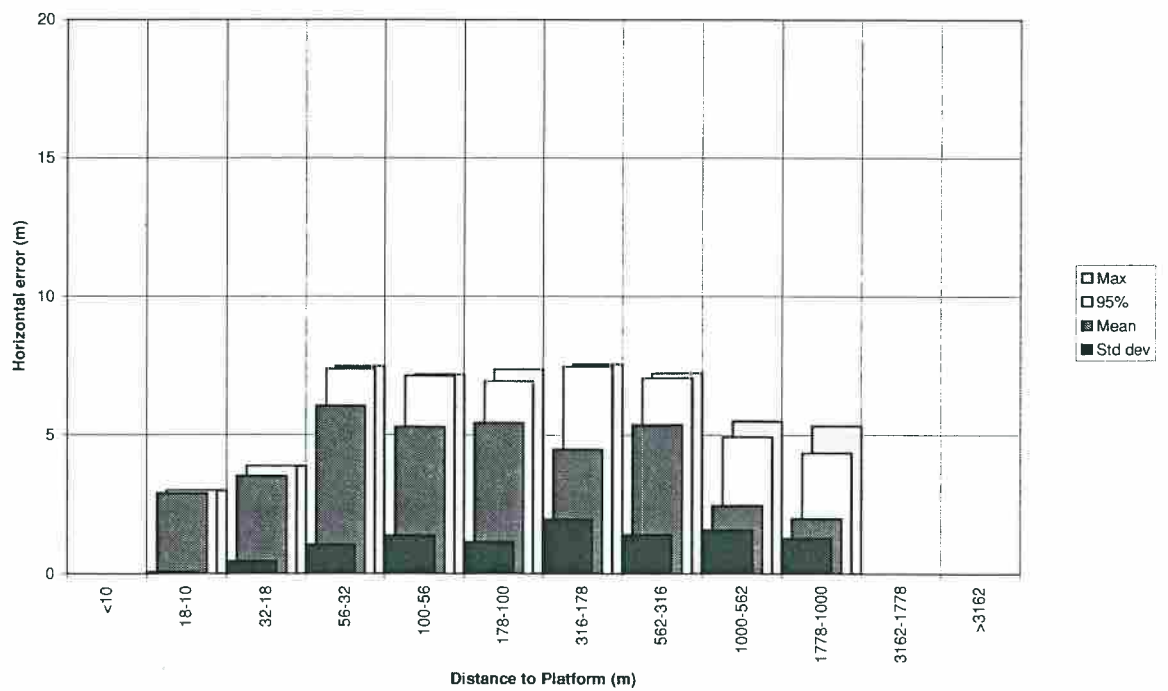


Figure 87 Variation of GD3 2-D Error Statistics with Range from the Platform, Platform Orbits, Flight 7, Beatrice C

Distance to platform (metres)	Number of samples	Minimum	Mean	Standard deviation	50% of samples less than	95% of samples less than	Maximum
>3162	2578	0.1	4.5	2.1	4.4	8.2	21.0
3162-1778	483	0.7	5.0	1.6	5.0	7.4	8.4
1778-1000	261	1.9	4.6	1.3	4.9	6.7	7.4
1000-562	155	1.5	4.4	1.5	4.7	6.5	7.2
562-316	95	1.2	4.4	1.7	3.9	6.6	7.8
316-178	67	1.4	4.1	1.6	4.1	6.4	6.5
178-100	27	1.2	3.6	1.3	3.6	5.8	5.9
100-56	7	1.3	2.7	1.2	3.6	3.7	3.7
56-32	0						
32-18	0						
18-10	0						
<10	0						
All ranges	3673	0.1	4.5	2.0	4.5	7.8	21.0

Table 31 Statistics of GD3 2-D Error (metres), Aerad Approaches, Flight 6, Buchan A

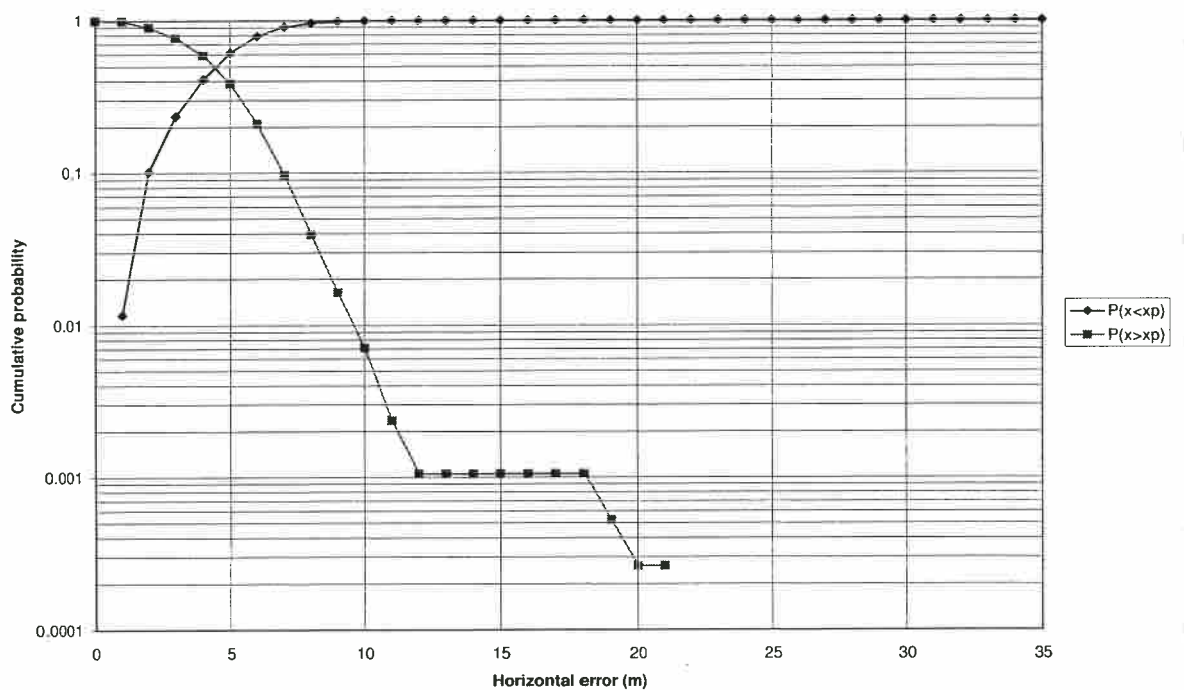


Figure 88 Cumulative Probability of GD3 2-D Error Irrespective of Range from the Platform, Aerad Approaches, Flight 6, Buchan A

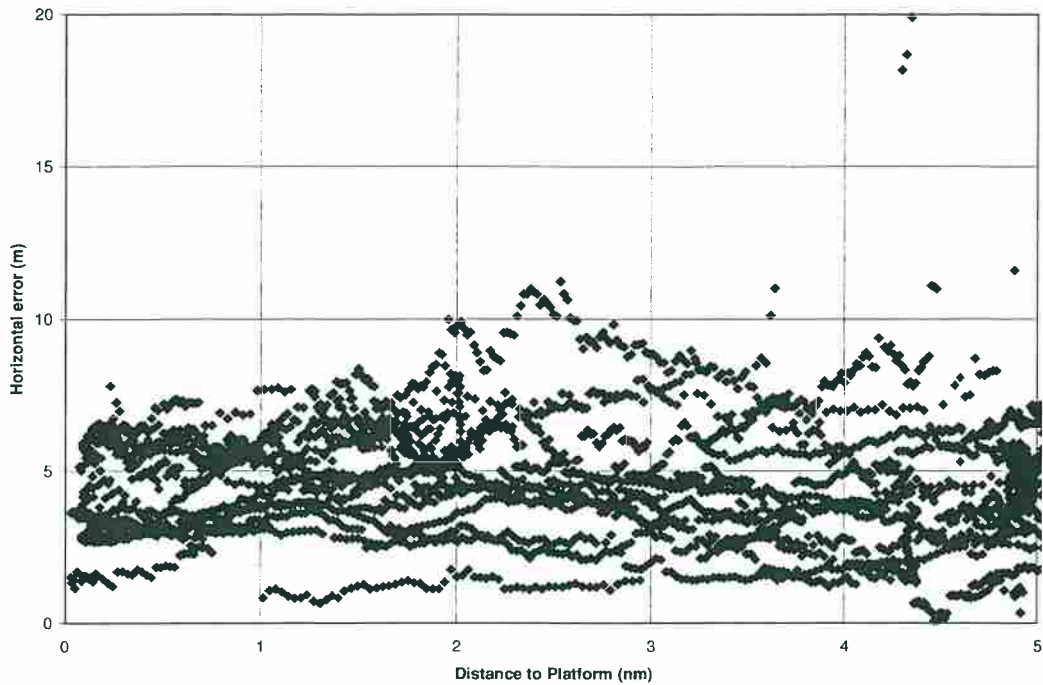


Figure 89 Scatter Plot of GD3 2-D Error Against Range from the Platform, Aerad Approaches, Flight 6, Buchan A

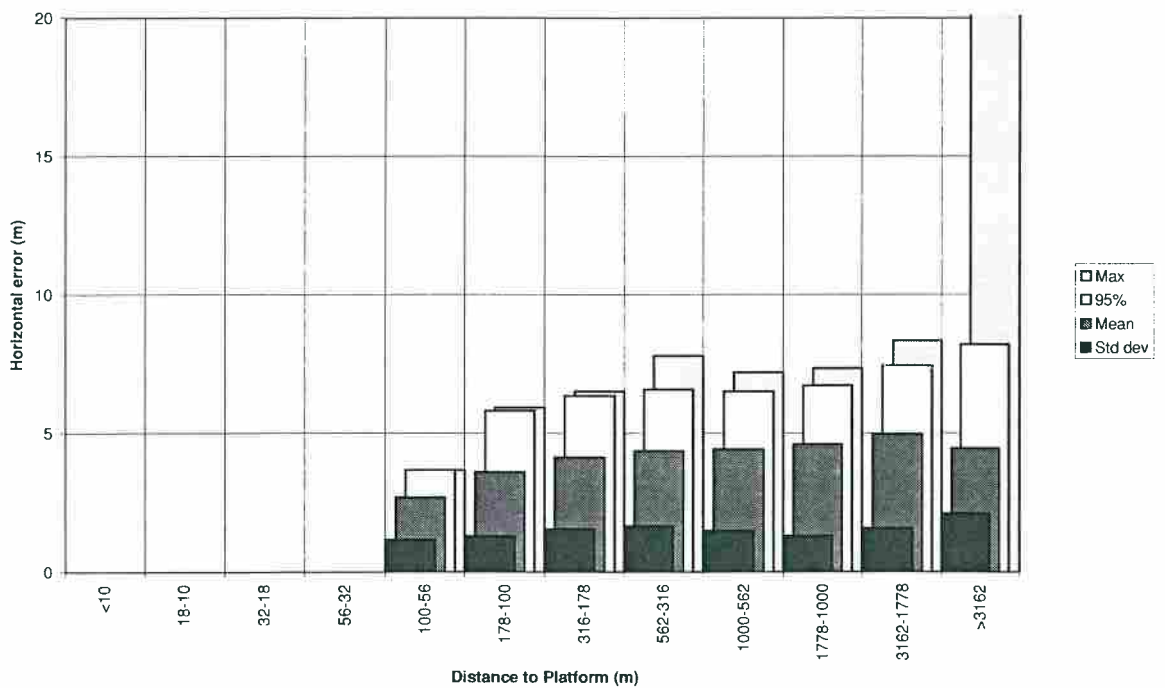


Figure 90 Variation of GD3 2-D Error Statistics with Range from the Platform, Aerad Approaches, Flight 6, Buchan A

Distance to platform (metres)	Number of samples	Minimum	Mean	Standard deviation	50% of samples less than	95% of samples less than	Maximum
>3162	675	1.3	3.8	1.0	3.8	5.4	9.4
3162-1778	203	0.6	2.6	1.1	2.7	4.2	7.5
1778-1000	309	0.1	2.6	1.1	2.5	4.6	5.5
1000-562	235	0.3	3.0	1.7	2.8	6.6	7.6
562-316	283	0.4	3.8	1.6	3.6	6.6	8.6
316-178	106	0.8	4.0	1.8	3.8	6.8	7.0
178-100	44	1.7	5.0	1.5	5.5	7.0	7.1
100-56	29	2.2	5.1	1.3	5.7	6.5	6.7
56-32	6	6.1	6.3	0.1	6.3	6.4	6.4
32-18	4	5.6	6.0	0.3	6.1	6.2	6.2
18-10	0						
<10	0						
All ranges	1894	0.1	3.5	1.5	3.5	6.1	9.4

Table 32 Statistics of GD3 2-D Error (metres), Platform Orbits, Flight 6, Buchan A

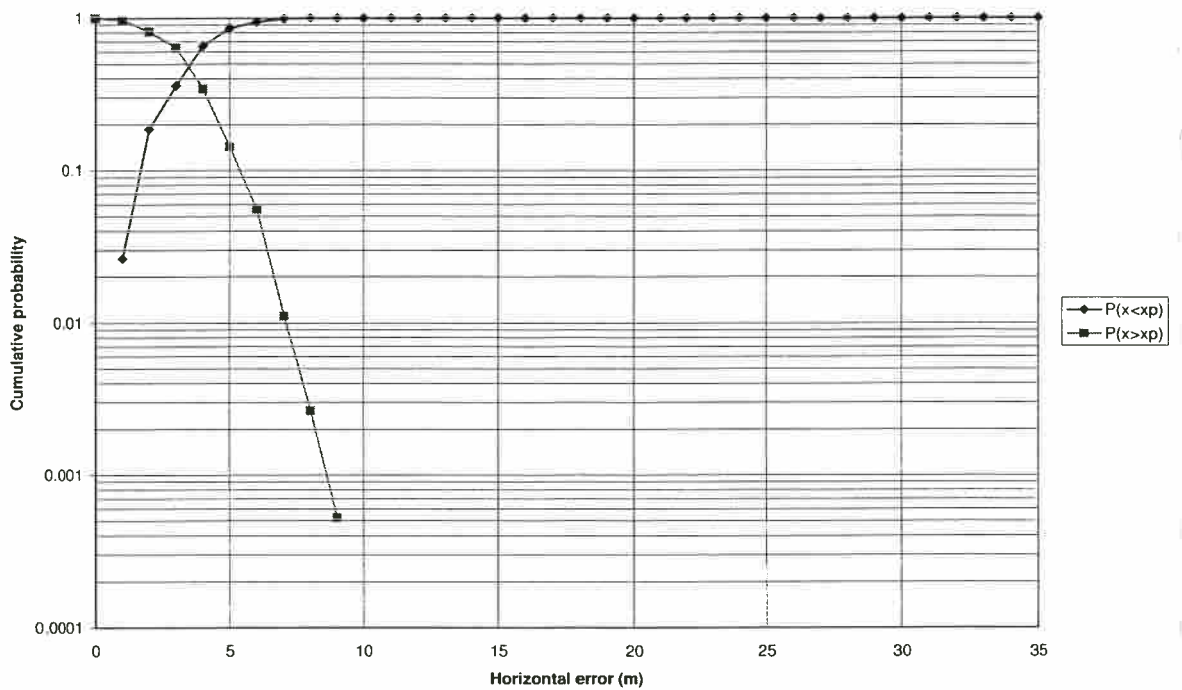


Figure 91 Cumulative Probability of GD3 2-D Error Irrespective of Range from the Platform, Platform Orbits, Flight 6, Buchan A

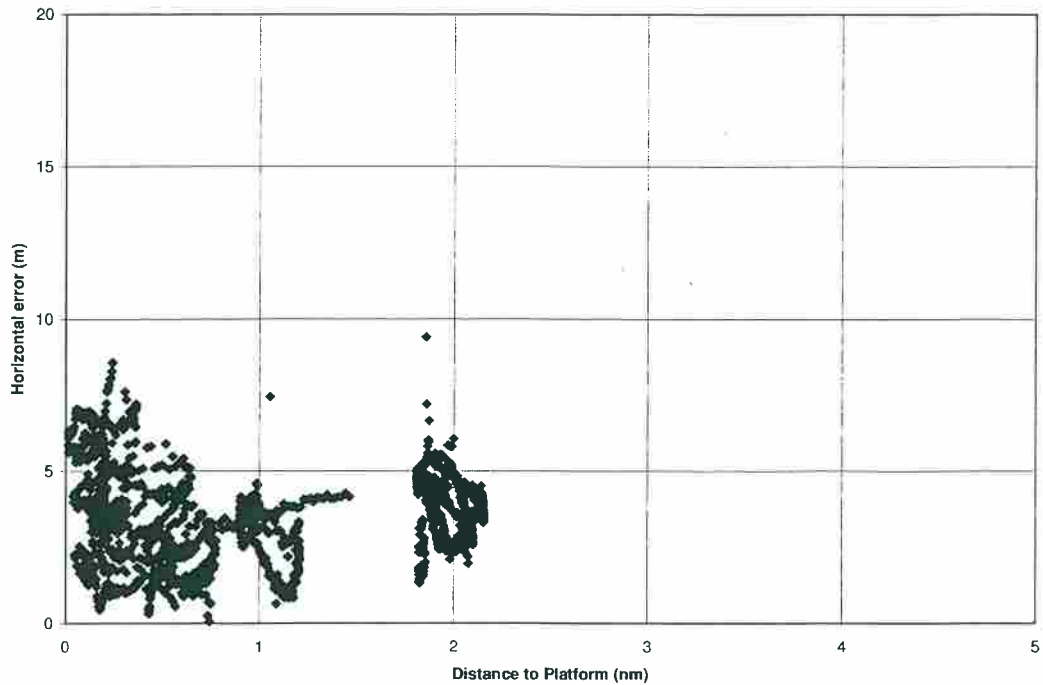


Figure 92 Scatter Plot of GD3 2-D Error Against Range from the Platform, Platform Orbits, Flight 6, Buchan A

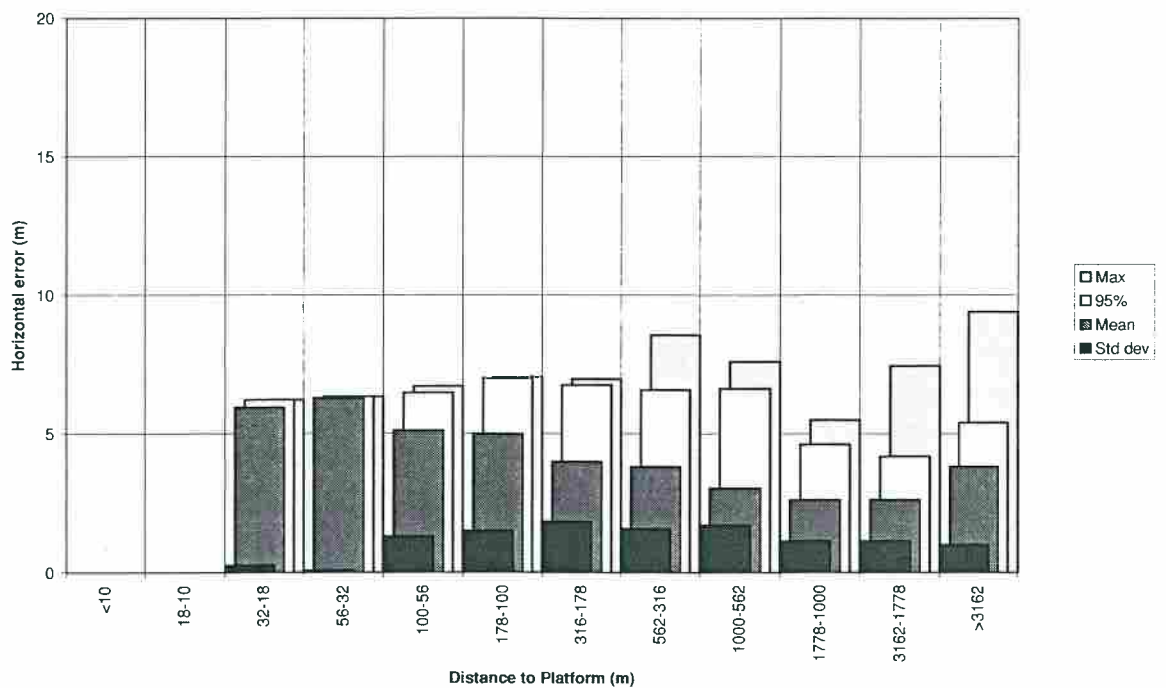


Figure 93 Variation of GD3 2-D Error Statistics with Range from the Platform, Platform Orbits, Flight 6, Buchan A

Distance to platform (metres)	Number of samples	Minimum	Mean	Standard deviation	50% of samples less than	95% of samples less than	Maximum
>3162	624	0.1	7.3	5.2	4.9	14.6	15.3
3162-1778	159	0.6	5.1	2.8	4.1	9.8	10.2
1778-1000	111	2.5	5.3	1.8	5.0	8.4	8.6
1000-562	50	2.9	5.6	1.5	5.5	7.5	7.5
562-316	35	3.8	5.7	0.9	5.8	6.7	6.7
316-178	31	4.3	5.6	0.8	6.2	6.5	6.5
178-100	15	4.1	5.6	0.9	6.1	6.3	6.3
100-56	9	4.5	5.3	0.8	4.8	6.3	6.3
56-32	5	4.8	5.9	0.6	6.1	6.3	6.3
32-18	0						
18-10	0						
<10	0						
All ranges	1039	0.1	6.5	4.4	4.9	14.6	15.3

Table 33 Statistics of GD3 2-D Error (metres), Experimental Approaches, Flight 6, Buchan A

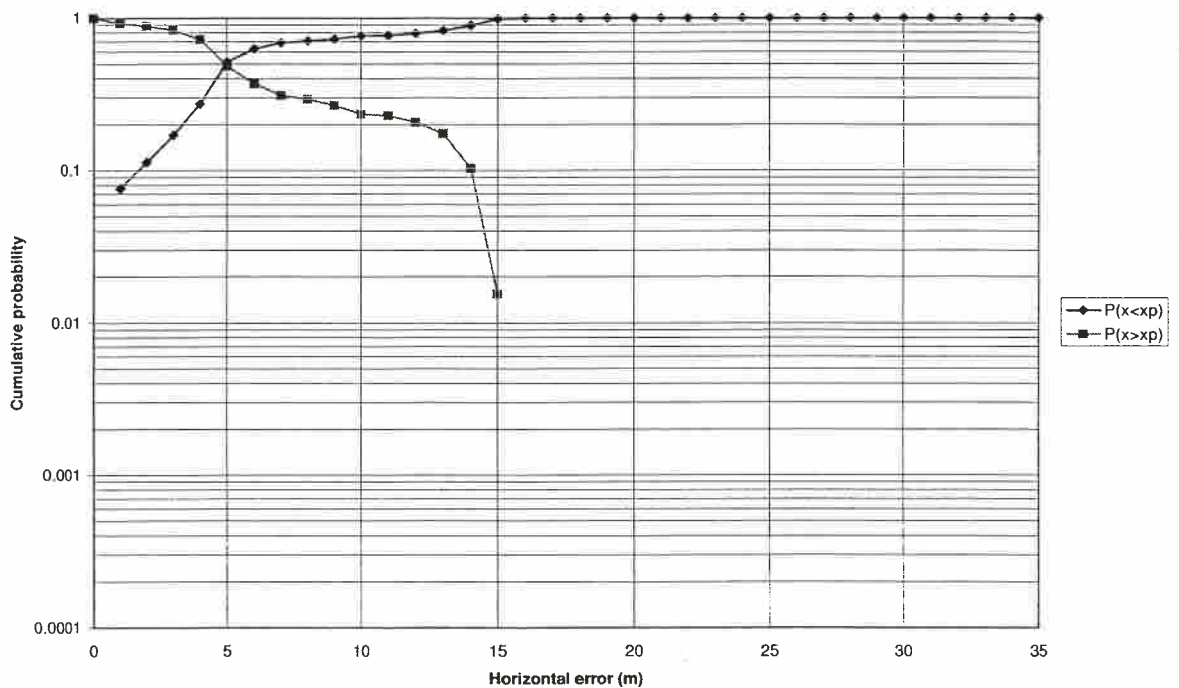


Figure 94 Cumulative Probability of GD3 2-D Error Irrespective of Range from the Platform, Experimental Approaches, Flight 6, Buchan A

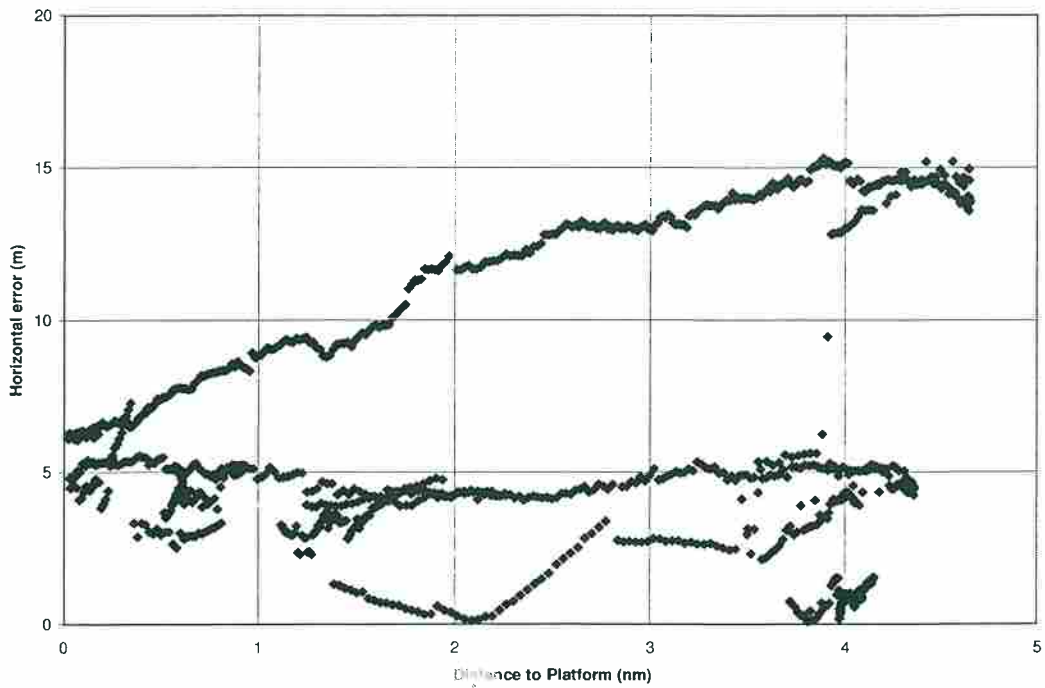


Figure 95 Scatter Plot of GD3 2-D Error Against Range from the Platform, Experimental Approaches, Flight 6, Buchan A

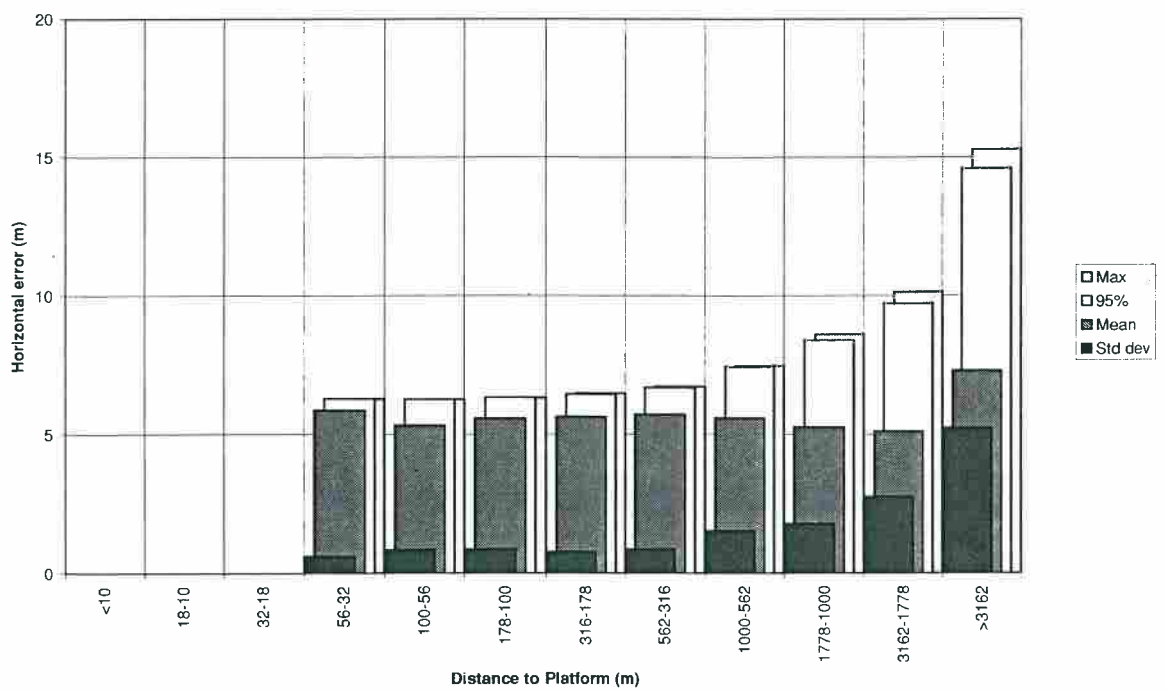


Figure 96 Variation of GD3 2-D Error Statistics with Range from the Platform, Experimental Approaches, Flight 6, Buchan A

7 DIFFERENTIAL CORRECTION DATALINKS

The results presented in section 6 were derived by comparing the position solutions output by the three real-time DGPS receivers at each 1Hz epoch, with the corresponding 'truth' position fixes. Each real-time solution (the recording format is described in Volume 1) included an indication of the current operating mode of the receiver in terms of the GPS fix type and DGPS status.

The GPS fix type indicator could take one of three values: in normal operation '3-D Fix' was indicated, implying that data from a minimum of four usable satellites was available. With three satellites, the receivers were capable of reverting to the '2-D Fix' mode in which the aircraft altitude was not computed as part of the position solution – instead, the last known valid altitude solution was retained. The third possible indication was 'No Fix', which implied that the position data was invalid and should be ignored.

Since the analysis in section 6 was based solely upon two-dimensional (horizontal) position solutions, no distinction was made between the 3-D and 2-D operating modes. However, any 'No Fix' epochs were excluded from the analysis.

The DGPS status indicator was a binary flag whose purpose was to identify whether or not the position solution computation had been based upon differentially-corrected satellite measurements. It is a requirement of the RTCM specification (ref 4) that, if differential corrections are to be used, then valid correction data must be available for all satellites to be employed (implying that it is not possible to achieve a 'partial' DGPS solution for which only a subset of the satellite measurements have had corrections applied).

In preparing the results in section 6, data from epochs where the position solution was not differentially corrected were excluded from the analysis. Failure to operate in differential mode could occur as a result of any of a number of factors, which can be divided into two main cases:

- (1) Valid RTCM data stream not available to GPS receiver.

Under the test arrangement employed for the trials, the GPS receivers' differential correction inputs were permanently connected to the outputs of the appropriate radio datalink receivers. However, there was no guarantee that valid RTCM data would be available to the receivers at all times: data reception was clearly conditional upon the correct operation of the transmitting station, and upon the datalink receiver antenna being suitably positioned to receive the transmission.

The strong parity checking inherent in the RTCM message structure should have ensured that any corruption of the received data would cause the message in question to be rejected rather than misinterpreted. Since no explicit indication of parity failures was provided, this situation would be indistinguishable, as far as the GPS receiver outputs were concerned, from the absence of correction data.

In order to avoid nuisance reversions to non-differential mode in response to short-duration 'outages' on the correction input (perhaps as a result of data corruption) the GPS receivers include a 'timeout' period during which the most

recent valid correction message is assumed to remain valid. For all three receivers employed on the trials, the timeout period was fixed by the manufacturer at 30s.

- (2) RTCM data stream present, but GPS receiver unable to use the corrections.

Even if the GPS receiver had acquired a valid RTCM input message which passed all of the parity tests, this would not in itself be a guarantee that the receiver would then operate in DGPS mode. This arises because of the requirement for there to be a valid differential correction, acceptable to the receiver, for each satellite used in the position solution.

In order for this condition to be true, both the reference and mobile receivers must be receiving data from a similar set of satellites, and with a minimum of four (preferably more) in common. This can become more of a problem as the baseline between the two receivers, and consequently the relative geometry to the satellites, is increased; but it can also present problems if either or both of the receiver antennas possesses a partially obstructed view of the sky, perhaps due to the proximity of other structures.

Both of the differential correction sources employed for the trials supplied Type 1 RTCM corrections, which essentially consist of a list of corrections, one for each satellite visible to the reference station receiver. Each Type 1 message contains a complete list of satellite corrections, repeating at a 1Hz rate in the case of the UHF source, and with a period of around 5-6s (dependent upon the number of satellites contained in the data message) for the MF source.

In order for the differential correction relating to a particular satellite to be considered acceptable by a GPS receiver, ref 4 also imposes a requirement that both the reference and mobile receivers shall be operating with the same Issue of Data Ephemeris (IODE).

The IODE is transmitted by the satellite as part of the ephemeris data defining its position in three-dimensional space, and serves as a tag identifying a particular set of ephemeris data: whenever a change is made to the satellite's transmitted ephemeris by the GPS Control Segment, the IODE counter is incremented. The requirement for there to be consistency between the IODEs employed by the reference and mobile receivers is imposed to ensure that both receivers are able to make the same assumptions regarding the satellite's position.

To allow this consistency test to be performed by the mobile receiver, the data in the Type 1 format RTCM message includes the IODE currently being employed by the reference receiver for each satellite.

Problems can arise, however, during the period immediately following an ephemeris update (and consequential incrementing of the satellite's transmitted IODE) if the two receivers do not both recognise and act on the change at precisely the same instant, perhaps as a result of interference or temporary loss of the satellite signal at one of the receivers. Ephemeris updates are only transmitted by the satellite every 30s, and therefore if an IODE mismatch occurs it will be a minimum of 30s before the situation can be corrected.

In an attempt to mitigate the effect of this problem, RTCM specify a second correction message (Type 2) which is intended for transmission for a short period following an ephemeris update. The Type 2 message contains data which is consistent with the 'old' IODE counter, which can be used by the mobile receiver in the event that it is still operating using the previous IODE.

The UHF reference source employed for the trials was arranged to transmit both Type 1 and (when required) Type 2 RTCM messages: the bit rate employed for this datalink allowed sufficient capacity for both messages to be transmitted whilst still maintaining a 1Hz update rate.

The MF reference source, however, was severely constrained by the low MSK data rate and as a result the service provider did not offer Type 2 corrections, which if transmitted would have doubled the interval between correction message updates to something in the region of 10s. The absence of Type 2 corrections from this source was found to give rise to problems, as described in section 7.1.

The data recorded from the real-time Navstar receivers included an indication of the age of differential corrections (essentially the time, in seconds, since the last valid RTCM message was received), which proved to be useful when examining recorded data to investigate the cause of reversion to non-differential mode. Loss of the correction message due to reception problems would cause this indicator to increment by one at each successive epoch, whereas if correction messages were still being received but were not (for whatever reason) being acted upon, the age indicator would remain close to zero.

7.1 MF Correction Datalink

The trials arrangement allowed the MF datalink receiver, whose output was fed to the GD1 and GD3 receivers, to be manually selected to any of a number of MF correction stations in flight.

It had been the original intention that UK-based MF correction stations would be used, the nearest being that at Girdle Ness near Aberdeen which was at a range of between 70nm and 100nm from each of the platforms visited. An alternative station was available at Sumburgh, at a range of approximately 120nm from each platform.

In the event, it proved necessary to also employ the Norwegian correction station at Utsira for a portion of the test flights. The operating range was approximately 175nm at the Buchan A platform, and 265nm at Beatrice C.

Each of these stations is co-located with a marine NDB operating in the MF band, the NDB having originally been installed for maritime direction finding purposes. Differential corrections are modulated onto the main NDB output frequency, or onto one of its sidebands, in such a manner that the basic direction finding capabilities are not compromised. As a result, and due to the requirement for international co-ordination of MF frequencies, there is a limit on the maximum possible output power (and hence the range) of the correction transmission from each station.

Previous experience had suggested that it should be possible to receive usable correction transmissions in the airborne environment at a range which considerably exceeded the published operating range of the marine NDB itself (for example the

published ranges for the Girdle Ness, Sumburgh and Utsira stations are 40nm, 56nm and 60nm, respectively). This is likely to arise from the published ranges having been set in a conservative manner to reflect the maximum distances at which the NDB should be relied upon for direction-finding in the marine environment, rather than the greatest range at which it is possible to receive the ground- or sky-wave signal from the station.

During the first five test flights, successful results were obtained using the two MF correction stations in the UK (Girdle Ness and Sumburgh). Reception of correction messages was virtually continuous throughout the trial at each platform, in spite of the extended range from the stations, and this appeared to confirm that there was not a range problem with the use of the MF transmissions.

On a very small number of occasions on these flights, correction signals were lost temporarily whilst in the vicinity of the offshore platform and the GD1 receiver reverted to non-differential mode. Since differential operation was regained on each occasion by switching to the other UK station, no attempt was made to investigate in detail the reason for the loss of corrections, it being assumed that the aircraft was operating at marginal range from the station in question.

The situation on the final two flight trials was, however, significantly different. Throughout both of these flights it proved difficult to obtain and maintain a continuous source of usable MF corrections from any of the available stations, with the GD1 and GD3 receivers reverting to non-differential mode for significant portions of the flights.

As a result of some experimentation performed in the course of these two flight trials, it was found that better results were achieved when the Norwegian station at Utsira was selected, in spite of its considerably greater range from the aircraft. Even with the Utsira station in use, there were still a number of occasions where the receivers were unable to use the received corrections and reverted to non-differential mode for periods ranging from a few seconds to several minutes.

Analysis of the recorded data revealed that the MF receiver claimed to be receiving a signal from the selected station throughout the trial, but that the output RTCM data stream was being subjected to corruption during those periods where outages were observed. This suggested that the GPS receivers were rejecting the incoming data for the reasons outlined above, and were hence reverting to non-differential operation.

The only significant change which had been made to the trials equipment between the first five and the last two flight trials had been the addition of a serviceable Trimble GPS receiver to provide the GD3 position solution. It was initially suspected that the presence of the Trimble receiver may have contributed to the problem, but this was not borne out by the results of ground experimentation on the aircraft, which showed good results with both receivers when using both the UK and Norwegian stations. Although the RTCM output of the MF correction receiver was now feeding two receivers rather than one, the data lines in question had been buffered in an effort to avoid any data transmission problems when driving the two receivers in parallel from a single source.

The possibility that the output power of the MF stations was lower than on previous trials, or that they were exhibiting problems transmitting the correct signals-in-space, was considered. However, discussions with the operator of the UK reference stations

revealed that there were no known problems with their operation during these flight trials.

Various ground experiments were performed using the MF antenna and receiver from the airborne installation, in an effort to discover whether they exhibited any degradation in performance relative to a second antenna/receiver pair. No significant differences in performance were observed.

Observations made during the flights suggested that there was a positive correlation between the occurrence of some of the MF correction outages and periods where the aircraft was flying in cloud and/or precipitation conditions. This led to the consideration of static build-up on the antenna as a candidate explanation for these problems.

The trials airframe, whose fuselage is constructed largely of composite material, was known to suffer with precipitation static affecting certain of the avionic systems; it was therefore considered possible that the MF antenna (which consists of a series of ferrite rod H-Field aeriels housed within a plastic radome) could have been adversely affected by a buildup of external static charge. This suggestion does not explain, however, why similar problems had not been observed on the earlier flight trials.

An explanation is also required as to why the MF receiver's performance was better when using the Norwegian Utsira station, even though the two UK stations at Girdle Ness and Sumburgh were considerably closer. This may have been due to the fact that, prior to 1998, the UK reference station transmissions were encrypted to allow the service provider to recoup costs via licence fees, whereas the Norwegian transmissions were unencrypted. Different frequencies were also at work.

Decryption of the UK correction signals, and translation into standard RTCM messages, took place within the MF datalink receiver and it is possible that the decryption algorithms may have been adversely affected by the presence of occasional corrupted data on the incoming MSK bit stream, with the result that the receiver was less immune to the effects of corrupted data when using the encrypted transmissions. This conclusion is supported by results reported by another operator.

It was also observed that, whenever corruption of the incoming MF signals occurred, the Trimble (GD3) receiver typically took longer to recover and return to differential operation than the Navstar (GD1) receiver. Since both receivers were provided with identical RTCM correction data, this possibly indicates a difference between the characteristics of the two receivers' internal software, with the Trimble firmware apparently taking longer to resynchronise following the detection and rejection of corrupted RTCM data.

A second, and unrelated, problem with the MF correction source was first observed at an early stage in the trials programme, and continued to give rise to difficulties on occasions throughout the flight trials.

This problem typically manifested itself as a reversion by the GD1 (MF-corrected Navstar) receiver to non-differential mode for a period of approximately 30s, normally commencing 20s after the start of a new UTC hour. This reversion would occur despite the fact that valid MF correction updates were being received (indicated by a low value in the 'age of corrections' counter).

Although these reversions were extremely constant (same duration, and same time after the start of a new hour) they did not take place every hour: on average, the probability of one of these 'start of the hour' dropouts occurring in any particular hour was around 30%.

A series of discussions with the receiver manufacturer led to the conclusion that these occurrences arose from the absence of Type 2 messages from the MF corrections, and that they were being triggered by the transmission of new ephemeris by one or more satellites (which was evidently arranged by the DoD to occur at the start of the hour).

Once the correction station had received and decoded the new satellite ephemeris, then an updated IODE would immediately appear in the transmitted Type 1 RTCM correction messages. If, for some reason, the aircraft receiver had not yet decoded the new ephemeris (perhaps due to a momentary loss of satellite signal for a portion of the transmission), then it would still be operating with the previous IODE and, following a strict interpretation of the RTCM specification, would revert to non-differential mode until the mismatch was corrected, normally following the next ephemeris transmission.

As previously discussed, this is exactly the situation which Type 2 correction messages were designed to overcome and it is believed that it would not have been observed had the MF stations been transmitting Type 2 corrections.

Due to these two problems of intermittent reception and dropouts following ephemeris updates, there were numerous occasions in the course of the flight trials where the MF-corrected GPS receivers reverted to non-differential mode and this generally affected the GPS indications displayed to the pilot, since the GD1 receiver was used as the source of guidance data for most of the programme.

The transitions between differential and non-differential mode normally resulted in a step change on the displayed indications, as the GPS position solution upon which they were based switched between the more accurate differential solution and the uncorrected solution. Due to the effects of SA, the error on the latter varied with time and hence the size of the step change was not constant. Step changes of several tens of metres were typically seen, although it was also possible for no discernable step change to be observed during periods of low SA.

It had originally been the intention that loss of differential mode would result in an immediate 'flag' indication to the pilot, signifying that the approach should be abandoned, as would be the case with an operational approach aid relying upon differential GPS. Owing to the frequency with which dropouts were found to occur, this facility was in fact disabled for much of the trials programme with the pilots preferring to accept the fact that step changes might appear on their indications, rather than risk having to abandon approaches due to loss of guidance.

This situation would be unacceptable for an operational approach aid, and as a result it is considered that solutions would need to be found and implemented to correct the two reliability problems before the MF correction source could be considered acceptable for this purpose.

7.2 UHF Correction Datalink

The UHF datalink receiver, whose output was fed to the GD2 (Navstar) GPS receiver, received signals transmitted by a dedicated correction station which was set up on the destination offshore platform for the duration of each trial.

The data rate of the UHF transmission was significantly greater than that of the MF correction stations, allowing a new set of corrections (including a set of Type 2 messages for the first few minutes following an ephemeris update) to be transmitted every second.

The UHF datalink proved to be extremely reliable, with the corresponding GD2 receiver remaining in differential mode for virtually 100% of the time that the transmitter was in operation. In particular, there were no ephemeris update problems similar to those experienced with the MF source, presumably due to the presence of the Type 2 correction messages.

On the majority of the flight trials, the aircraft remained in the vicinity of the offshore platform (within a 10nm radius) for the entire period that the transmitter was switched on, since the latter was transported to and from the platform by the trials aircraft. As a result, very little data is available to provide an indication of the maximum attainable range using the UHF equipment. Evidence from the two flights where the aircraft did move a significant distance away from the transmitter suggests that operation out to ranges in excess of 40nm was possible, but that reception was lost at extreme ranges before the aircraft ceased to be within line-of-sight of the transmitter.

The aircraft installation included two identical UHF antennas, one positioned under the tail boom, and the other located on the nose. The outputs from the two antennas were connected, via a changeover relay, to the RF input of the UHF receiver. The relay was arranged to switch between the two antennas once per second, with each antenna being used for the reception of alternate correction transmissions (the changeover was arranged to occur in the 'dead time' between successive transmissions).

It had been hoped that this arrangement would allow an analysis to be performed, from an examination of the recorded data, as to whether there was any significant difference in reception reliability between the two antenna installations, either generally or in specific situations. For example, it was conceivable that the tail antenna would be likely to suffer from reception problems due to the masking effect of the airframe during approaches towards the platform containing the UHF transmitter.

In the event, the performance of both antenna installations proved to be sufficiently reliable that no significant conclusions could be drawn as to whether one antenna installation was better than the other. It was therefore concluded that satisfactory performance could have been achieved using a single antenna in either location.

The only significant loss of UHF corrections occurred on the final flight trial where four outage periods, whose duration varied between 30s and 4.5 minutes, were observed. These outages occurred during periods where the reference station was transmitting Type 2 messages in addition to the basic Type 1 corrections.

During the outage periods, the GD2 receiver reported that no corrections were being received although examination of the reference station data showed that they were being generated and (presumably) transmitted. Since range was not thought to be an issue (the aircraft was within a few hundred metres of the transmitter for some of these periods) another explanation needed to be sought: either the GD2 receiver was experiencing some, unexplained, difficulty with interpreting the received corrections, or there was a problem in transmission. It is even possible that the antenna switching relay was to blame.

The most likely form of transmission problem is considered likely to be some effect which relates to the increase in the amount of data to be transmitted each second, resulting from the inclusion of Type 2 corrections in addition to the standard Type 1 messages. There is a possibility that conditions may have arisen to cause the UHF transmitter to, erroneously, truncate the transmitted data packet in conditions where Type 1 and Type 2 corrections for a large number of satellites were being generated, thereby causing the UHF receiver on the aircraft to discard the complete packet. Since it did not prove possible to replicate this condition during testing in controlled conditions on the ground, this must only be considered as one potential explanation for the outages.

8 DISCUSSION OF RESULTS

The installation on the trials aircraft included three GPS receivers supplied with differential corrections. All three receivers were shown to operate successfully in differential mode and to output real-time DGPS position solutions, which were in turn successfully employed to generate approach guidance information.

The results presented in section 6 are based upon an analysis of the horizontal position error for each receiver, determined by comparing the real-time DGPS position with the aircraft's truth position history derived from post-processed carrier phase measurements.

From an examination of the figures in section 6, it is apparent that the results are broadly consistent with those predicted by ref 4 ('accuracies of 2-10 metres for dynamic navigation applications'), but that a number of significant variations exist across the complete data set.

The factor with the most significant impact upon the horizontal error results proved to be the loss of differential corrections. This caused the receivers to revert to stand-alone GPS mode, where they were subject to the full effects of SA. Differential corrections were lost on a number of occasions, referred to in section 7, but in all cases the effect upon the receiver was a reversion to stand-alone mode rather than a complete loss of GPS information.

Since many of the candidate reasons for correction loss during the trials are believed to be preventable, and would therefore not be expected to be encountered in an operational installation, the effects of loss of corrections were deliberately excluded from the results in section 6. Excluding the stand-alone data should avoid the possibility of significant effects in the DGPS solution being overlooked through being 'swamped' by the much larger errors from the stand-alone solutions.

Aside from the loss of corrections, a number of other factors were identified which it was considered might affect the performance of the real-time DGPS receivers, and the results in section 6 have been broken down so as to allow the effects of these factors to be examined. They include:

- (1) Variation between different correction sources.

Two sources of differential corrections were available on the trials aircraft and were supplied to a pair of Navstar GPS receivers (MF corrections from an onshore provider to the GD1 receiver, and UHF corrections from a reference station on the platform to the GD2 receiver) which were in all other respects identical.

Not only did this arrangement allow a comparison to be made between the reliability of the two correction sources in the offshore environment, it also allowed a direct comparison to be made between the effect of the correction messages themselves upon a pair of identical receivers. Factors which potentially affected the accuracy of the differential corrections included variations in baseline, and differences between the signal reception environment at the two reference stations.

(2) Variation with range from the platform.

The requirement to investigate whether a GPS receiver would be significantly affected by multipath, when operating close to an offshore structure, was one of the primary objectives of the trials programme.

Due to the many and varied factors which were likely to impact upon the level of GPS multipath encountered, it was considered difficult (if not impossible) to predict the latter with any certainty in advance of a particular trial. However, consideration of basic electromagnetic theory suggested that the probability of encountering multipath was likely to increase significantly as the receiver's range to the platform was reduced. Accordingly, the trials were designed to allow the investigation of the effects of range upon position error.

(3) Variation with platform design.

The extent of GPS multipath caused by an offshore platform was also likely to vary according to the complexity of the structure in question. A set of four offshore structures of varying degrees of complexity, selected so as to provide a representative cross-section of those commonly encountered in the North Sea, was therefore chosen for the trials programme and a (notionally) identical set of manoeuvres performed at each location.

The target platforms (Figures 97 to 104, pages 125 to 130) ranged from the basic Beatrice C, of uncomplicated design and with uncluttered topside layout; through the Piper B and Tartan A, typical of the more complex structures encountered at larger production platforms; to the semi-submersible Buchan A with its unique problems of platform motion and complex metallic structure around the helideck.

The Beatrice C platform was considered as a baseline at which the lowest level of multipath would be experienced. Multipath effects were expected to become more significant at the other three platforms in turn.

(4) Variation with manoeuvre type.

Results in section 6 have been presented for each of the three manoeuvre types individually.

The 'Aerad' approaches were intended to be representative of a series of typical approach profiles, and comprised an overflight of the platform, an inbound turn at approximately 4nm, and a straight approach passing within a few hundred metres of the platform. This pattern was repeated four times, with the approach directions spaced 90° apart around the compass, and was intended to be flown as consistently as possible at the four platforms to allow direct comparison of the results.

Platform orbits were undertaken at varying ranges from the platform (2nm, 1nm, 0.5nm, 0.2nm, and as close as possible) and were specifically intended to investigate any multipath effects which might be observed close to the platform. The range distribution of the samples from the orbits was therefore uneven, and hence the statistical properties of the results from these manoeuvres might well differ from those obtained during the 'Aerad' profiles (especially if significant multipath was encountered at close ranges). Consistent orbits were intended to be performed at each of the platforms.

'Experimental' approaches were essentially a series of abbreviated versions of the 'Aerad' patterns, but with more variation between platforms because the form of the approach profiles, and the number of approaches undertaken, was not constant. The results from these manoeuvres can therefore be considered as representative of typical approaches, supplementing those from the 'Aerad' profiles, but any comparisons between the results from different platforms are likely to be less objective.

(5) Variation with receiver design.

Identical corrections (from the onshore MF source) were supplied to the GD1 and GD3 receivers; the former being a Navstar XR5-M12 and the latter a Trimble TNL-2100.

This allowed an attempt to be made at a comparison between the results obtained when two receivers of different manufacturer and design were employed in an identical environment.

8.1 **MF-Corrected Navstar (GD1) Receiver**

Table 34 contains a summary of the statistical results from the GD1 receiver (the Navstar unit supplied with corrections from the onshore MF correction stations), irrespective of range from the platform.

		Beatrice C	Piper B	Tartan A	Buchan A
Aerad approaches	Samples	1367	3537	3683	3788
	Mean	3.7	2.6	3.1	3.6
	Std dev	1.8	1.2	1.7	2.1
	50%	3.4	2.7	2.8	3.3
	95%	7.3	4.6	6.4	7.1
	Maximum	17.7	7.4	10.6	14.1
Platform orbits	Samples	1232	1390	2066	1917
	Mean	3.1	3.7	4.5	2.9
	Std dev	1.5	1.2	1.3	1.4
	50%	2.9	3.8	4.4	2.9
	95%	5.4	5.8	6.7	5.1
	Maximum	11.3	13.0	12.1	10.6
Experimental approaches	Samples	0	1703	4435	713
	Mean	n/a	3.0	2.4	7.8
	Std dev	n/a	1.8	1.3	5.3
	50%	n/a	2.8	2.2	6.6
	95%	n/a	6.0	4.8	16.0
	Maximum	n/a	12.7	10.7	17.1

Table 34 Statistics of GD1 2-D Error (metres) by Manoeuvre Type and Platform

It may be observed that the sample size for the Aerad approaches is very consistent across three of the platforms: the lower number of samples for the Beatrice C platform results from the MF datalink problems experienced on this flight, which caused many of the data points to be discarded during analysis.

The statistical results from the Aerad approaches, representing the manoeuvres which were executed most consistently at the various platforms, can be observed to vary little between the platforms. Only if the Beatrice data is excluded is there any evidence of an increasing error with degree of complexity of the platform structure (the latter increases across the table from left to right).

A similar statement can be made regarding the platform orbit manoeuvres, which can be seen to be broadly consistent between the different structures, and to be of very similar magnitude to the corresponding Aerad approach figures. There is less consistency between the number of samples at the different locations: again there are fewer samples from the Beatrice due to loss of MF datalink, but there are also fewer samples at the Piper B platform and it is believed that this is due to the aircraft having been flown around the orbits at higher speed on this trial. The first of these problems was beyond the direct control of the trials team, but the second was not and could have been avoided with more careful planning.

Considerable variation exists between the number of samples from the experimental approaches, but the results themselves are very similar to those from the Aerad approaches (to which the experimental manoeuvres were closely related).

The greatest degree of variation can be seen to occur with the maximum error values, although there is no clear evidence of a definite trend between different platforms. The presence of more variation between the maximum error figures may be explained by the fact that this statistic can be dominated by the effect of only a very small number of data points - for example at the Beatrice C platform, where the greatest error figure of 17.7m was observed, there were in fact only ten samples (or fewer than 1%) where the horizontal error exceeded ten metres (Figure 8, page 39). Even if an identical set of manoeuvres were to be repeated in an identical environment on a different occasion, it would be expected that more variation would be observed between the maximum error figures than between those from the other statistics.

In the analysis of navigation system errors, the statistics most commonly quoted are the 50% and 95% confidence limits: the former is sometimes termed Circular Error Probable (CEP), and the latter is often identified with the two-sigma (sometimes 2drms) figure although strictly this is only true if the errors follow a Gaussian distribution (ref 14). Maximum error statistics are quoted less frequently.

For the offshore approach application, the maximum error statistic was also considered to be of importance due to the impact that large position errors might have upon operational safety. The effect of such an error will depend not only upon its magnitude, but also upon its duration and rate of growth, and upon how the approach guidance information is being derived from the GPS position solution. For example, a large or sudden step change could be detected more easily than an error which increases smoothly over a period of time.

Another reason for paying particular attention to maximum errors in the trials results was the possibility that a multipath-related 'event' might be encountered, possibly

one which only occurred in a very localised region of space where the combination of the direct satellite signals, and those resulting from the presence of the platform, was such as to cause a large position error.

Consideration of the maximum error values observed during the trials is therefore important, and these figures (which ranged from 7.4m to 17.7m for the twelve manoeuvre/platform combinations studied) represent an estimate of the upper bound for the system error observed with the GD1 receiver.

Examination of Tables 4 to 14, and Figures 7 to 39 (pages 38 to 59), from which the results in the table have been extracted, but which show how the error distribution varies with range from the platform, reveal that there is little or no evidence of any increase in GPS position error as the range to the platform is reduced, even down to below ten metres: any such increase might have been an indication of the presence of a significant multipath effect due to signal corruption by the platform structure at close ranges.

The one possible exception to the above statement is Figure 18 (page 45) which shows, on first sight, a significant increase in the 95% and maximum error statistics at ranges below 32m during the orbit manoeuvres at Piper B. Examination, however, of the data in Table 7 (page 44) reveals that this increase has resulted from the presence of a single data point with 13.0m error (there being only three samples at ranges below 32m). Since this larger error, admittedly the largest GD1 error observed during the Piper B orbits, is smaller than the maximum errors observed elsewhere at much greater ranges, it was concluded that this represented insufficient evidence to identify it as having been caused by a multipath effect.

Some of the plots of error statistics against range (such as Figures 9, 33 and 39 on pages 39, 55 and 59 respectively) appear to show a significant increase in the 95% error at large ranges from the platform. This can be attributed to the fact that, due to the use of a logarithmic horizontal scale, the final couple of range bins tend to contain the majority of the data samples, thereby increasing the probability that any short-duration, randomly occurring error events (such as those at just below 3nm range on Figure 8) will be found to occur at the larger ranges. There is also some variation in the maximum error, but such values have less statistical significance.

Examination of the results for the experimental approaches at the Buchan A platform reveals a significant increase in many of the error statistics compared to all of the other platform/manoeuvre cases. It is unfortunate that, due to MF datalink loss, the number of samples involved is significantly smaller: in fact, although five experimental approaches were performed, data is only available for one complete approach plus portions of two others.

However, examination of the data from the complete approach (which appears as part of the plotted data in Figure 38, page 59) reveals that the GD1 errors were significantly greater than average for the entire duration of the approach: ranging from around fifteen metres at the beginning of the approach to five metres at the end. This was the period, referred to at the start of section 6, during which reduced confidence was available in the OTruth position owing to the recovery of the post-processed solution following a carrier lock loss event. Since increased errors with broadly similar characteristics were also observed on the corresponding results for GD2 (Figure 80, page 89) and GD3 (Figure 95, page 101), it is believed that the most likely explanation for this occurrence was a temporary reduction in truth system accuracy.

In summary, the results obtained using the GD1 receiver were found, when not subject to loss of differential corrections due to datalink or other problems, to be entirely in accordance with expectations for an airborne DGPS system. The manufacturer's stated accuracy figure for the Navstar receiver in differential mode was '1-3m CEP' (Volume 1) and this is in broad agreement with the 50% confidence error figures obtained during the trials. Ref 4 suggests that 'accuracies of 2-10 metres for dynamic navigation applications' are possible with DGPS (possibly with an increase of 'a few metres' due to baseline effects) and this is again in accordance with the observed results.

No significant evidence was observed for the presence of an increase in GPS errors in environments considered more conducive to multipath reception (namely an increase in platform complexity, and/or a decrease in aircraft range to the platform). This does not, however, guarantee that GPS multipath will not present a problem under all conditions in the offshore environment; merely that no evidence for it was observed during the trials programme.

8.2 UHF-Corrected Navstar (GD2) Receiver

Table 35 contains a summary of the statistical results from the GD2 receiver (the Navstar unit supplied with corrections from the offshore UHF reference station), irrespective of range from the platform.

		Beatrice C	Piper B	Tartan A	Buchan A
Aerad approaches	Samples	1583	3547	3672	5047
	Mean	9.2	6.7	3.8	5.3
	Std dev	1.3	9.8	2.4	3.0
	50%	9.2	4.9	3.3	4.7
	95%	11.4	14.5	8.7	11.1
	Maximum	13.7	123.1	14.0	20.3
Platform orbits	Samples	1382	1387	2066	1944
	Mean	9.7	8.7	6.0	6.5
	Std dev	1.2	5.4	5.2	2.8
	50%	9.7	7.7	4.2	6.4
	95%	11.7	19.3	19.6	11.5
	Maximum	13.0	30.6	23.8	22.0
Experimental approaches	Samples	0	1703	4997	2116
	Mean	n/a	5.9	10.3	6.8
	Std dev	n/a	3.9	15.1	4.5
	50%	n/a	4.9	4.1	5.5
	95%	n/a	13.2	48.9	17.9
	Maximum	n/a	28.2	95.5	22.3
Co-ordinate difference		8.9	1.6	35.4	5.1

Table 35 Statistics of GD2 2-D Error (metres) by Manoeuvre Type and Platform (co-ordinate bias removed from Tartan results)

The final row in the table, labelled 'Co-ordinate difference', represents the horizontal difference between the position fix which was loaded into the UHF reference station before the flight, and the actual position of the unit determined by post-flight analysis. These discrepancies, which were discussed at the start of section 6.2, result from limitations in the survey data which could be obtained by the trials contractors from the platform operators.

Any such error in the pre-loaded position resulted in the introduction of a constant bias, equal to the vector displacement between the two sets of co-ordinates, which was added to all of the position solutions returned by the GD2 receiver. With the exception of the Tartan A platform, the co-ordinate bias was determined to be less than ten metres and all of the statistical results shown in the table include the effect of the bias.

At Tartan A, the co-ordinate bias was determined to be in excess of 35m and this had a very significant effect upon the GD2 results obtained at this platform (as can be seen in section 6.2). If left uncorrected, this bias would have swamped most of the statistical variation on the results and accordingly a decision was taken to remove the co-ordinate bias in the analysis of the GD2 data from this flight.

It would be expected that, if an operational DGPS system were to be introduced which employed correction station receivers located at offshore platforms, it would prove possible to correctly determine the location of each reference station during system commissioning, by undertaking dedicated surveys if necessary and, as a result, the co-ordinate bias problem would not occur.

Examination of the data in Table 35, and comparison with the corresponding GD1 results from Table 34 using the MF-corrected receiver, reveals some significant differences even when the additional error contribution from the co-ordinate bias effect is taken into account.

The most significant differences may be seen on the Piper B and Tartan A results, where the maximum error and (to a lesser extent) the 95% confidence statistics are considerably greater than those observed with the GD1 receiver: in two of these cases, the maximum error is close to or exceeds 100m which represents almost an order of magnitude increase.

Ignoring the maximum error values and considering only the 95% confidence statistics, the differences between the GD2 and GD1 results are illustrated in Table 36 which presents the ratio of each GD2 95% statistic to the corresponding GD1 value.

	Beatrice C	Piper B	Tartan A	Buchan A
Aerad approaches	1.6	3.2	1.4	1.6
Platform orbits	2.2	3.3	2.9	2.3
Experimental approaches	n/a	2.2	10.2	1.1

Table 36 Ratio of GD2 to GD1 95% Confidence Statistics

The fact that each value in the table is greater than unity confirms that the GD2 results are consistently worse than those for GD1, with the greatest discrepancy being observed at the Piper B and Tartan A platforms.

The presence of results which were significantly worse at some of the more complex offshore platforms naturally led to the consideration of platform-induced multipath affecting the aircraft receivers as the most likely explanation. However, examination of the plots of error statistics against range revealed no evidence whatsoever for an increase in GPS error close to the platform, as would be expected if multipath was the cause.

This theory also does not explain why the aircraft GD2 receiver should have been significantly affected by platform multipath to such an extent that position errors in excess of 100m were observed, whilst the GD1 receiver which was of identical design and operating with a common antenna should have been completely unaffected.

The only difference between the two receivers was that they were receiving corrections from different sources, and this naturally led to the consideration of whether some aspect of the differential corrections could have been causing the large observed position errors.

Examination of the differential corrections recorded from the onshore MF station, and from the platform-based UHF station, revealed the true reason for the poor performance of the GD2 receiver at the Piper B and Tartan A platforms. It was discovered that significant disturbances were present on portions of the pseudorange corrections being transmitted by the UHF station, and that these disturbances correlated in the time domain with periods of large error in the GD2 position solution.

At the Beatrice C platform, the UHF reference station had been located at the edge of the helideck which at this location is the highest point of the structure: as a result, the reference station's GPS antenna had an unobstructed view of the sky, with no intervening metallic structure which could cause reflections or block the satellite signals.

At the Piper B and Tartan A, the reference station had again been placed on the helideck but at these two locations there are significant metallic structures above the level of, and relatively close to, the helideck as can be seen from the photographs and diagrams in Figures 97 to 104 (pages 125 to 130). It was concluded that the presence of these structures had adversely affected the operation of the reference GPS receiver causing it to transmit erroneous data, which was then propagated into the position solutions output by the airborne GD2 receiver.

Consideration of the relative geometry between the reference receiver, platform structure and satellites confirmed that there was a possibility of the satellite signals having been affected both by periodic blockages by the structure (causing loss of lock, and/or difficulty in maintaining adequate tracking), and by reflections from the structure giving rise to multipath corruption of the measured pseudoranges.

The reason why no such effects were observed at the Buchan A platform was unclear. The reference station had been placed in a similar location (deck edge) relative to the platform superstructure as at the other two locations where problems

were experienced, and this platform had been identified as, potentially, an even more likely candidate for affecting GPS reception owing to the size and nature of the vertical structures.

Examination of the large GD2 errors which occurred at the Piper B and Tartan A platforms revealed that they had only been present for a small fraction of the duration of the flight trial. It was concluded that the disturbances affecting the reference GPS receiver were likely to have been strongly dependent upon the relative geometry of the satellites and it is therefore possible that similar problems had not been observed at Buchan A, not because the platform structure was incapable of affecting the satellite signals, but rather because the geometry over the course of the trial happened to have been such as to avoid any significant reception difficulties.

A very similar argument could, of course, be applied to the Beatrice C platform to explain why no significant errors were observed at this location. This is, however, considered to be unlikely due to the total absence of any platform superstructure above the helideck level.

A comparison of the results from the GD1 and GD2 receivers led to the conclusion that, on the basis of the results observed during the trials programme, the platform structure had little or no detrimental effect upon aircraft GPS reception, even at relatively close range (less than 100m). It could, however, be observed to affect the operation of a platform-based differential reference receiver if metallic structures were present above the level of the reception antenna.

The obvious solution, if a platform-based reference station is required, would appear to be to locate the GPS antenna at the highest point on the platform structure, preferably using a well-designed ground plane to block any signals arriving from below the horizontal. The highest point would normally be the top of the derrick and might not, as a result, be particularly convenient due to the operational aspects of positioning an antenna in this location. In addition, problems might arise with the antenna location not remaining constant, perhaps due to derrick repositioning or to the platform motion experienced with semi-submersible structures.

8.3 **MF-Corrected Trimble (GD3) Receiver**

It is unfortunate that the GD3 (MF-corrected Trimble) receiver was only available for a small portion of the programme, largely due to delays in integrating the receiver with the remainder of the trials equipment. As a result, the unit was only operational for the Flight 6 and Flight 7 trials at the Buchan A and Beatrice C platforms, where it was also affected by the dropout problems experienced with the onshore MF differential correction datalink.

Table 37 summarises the results from the GD3 receiver, irrespective of range from the platform. The corresponding results from the GD1 receiver are also shown, to enable a direct comparison to be made.

		Beatrice C		Buchan A	
		GD3	GD1	GD3	GD1
Aerad approaches	Samples	686	1367	3673	3788
	Mean	2.1	3.7	4.5	3.6
	Std dev	0.9	1.8	2.0	2.1
	50%	1.9	3.4	4.5	3.3
	95%	4.0	7.3	7.8	7.1
	Maximum	5.6	17.7	21.0	14.1
Platform orbits	Samples	561	1232	1894	1917
	Mean	4.3	3.1	3.5	2.9
	Std dev	2.0	1.5	1.5	1.4
	50%	4.3	2.9	3.5	2.9
	95%	7.1	5.4	6.1	5.1
	Maximum	7.6	11.3	9.4	10.6
Experimental approaches	Samples	0	0	1039	713
	Mean	n/a	n/a	6.5	7.8
	Std dev	n/a	n/a	4.4	5.3
	50%	n/a	n/a	4.9	6.6
	95%	n/a	n/a	14.6	16.0
	Maximum	n/a	n/a	15.3	17.1

Table 37 Statistics of GD3 and GD1 2-D Error (metres) by Manoeuvre Type and Platform

Examination of the data in the table suggests that the statistical results from the Trimble receiver are very closely correlated with those from the Navstar receiver, to within better than 1.5m in almost all cases.

The greatest degree of variation was observed to occur in the maximum error figures, but with no clear pattern as to whether one receiver has a consistently lower maximum error than the other. The very limited size of the data set means that any comparison of this nature must be necessarily rather limited.

Examination of the results against range from the platform in section 6.3 reveals no evidence for any increased error at low ranges, suggesting that the platform structure has little or no effect upon the operation of the Trimble receiver.

With the benefit of hindsight, it would have been extremely useful to have been able to operate the Trimble receiver using the platform-based UHF corrections, and to investigate whether large position errors were observed in the conditions experienced at the Piper B and Tartan A platforms on Flights 4 and 5. Regrettably this did not prove possible, although it would be a prime candidate for any future work programme investigating the effect of different receiver designs.

The close agreement between the results from the Navstar and Trimble receivers suggests that, on the basis of the available data, there is little to choose between them for the purposes of providing a navigation solution for approach guidance. A future trials programme might benefit from a comparison between two receiver designs which differ more significantly than do the Navstar and Trimble models, such as by arranging to use a receiver with a different correlator design.

8.4 Overall Statistics

Table 38 summarises the precision statistics obtained from each of the three receivers over the course of the offshore trials programme. Data in the fourth column was derived by combining the GD1 and GD3 data (i.e. the results from both MF-corrected receivers).

	GD1 receiver (MF Navstar)	GD2 receiver (UHF Navstar)	GD3 receiver (MF Trimble)	GD1 plus GD3 (Both MF units)
Samples	25831	29444	7853	33684
Minimum	0.0	0.0	0.1	0.0
Mean	3.3	7.0	4.3	3.5
Std dev	2.0	8.0	2.5	2.2
50%	3.0	5.1	4.0	3.2
95%	6.5	16.7	8.5	7.0
99%	11.4	48.5	14.4	13.6
Maximum	17.7	123.1	21.0	21.0

Table 38 Summary of Statistics of GD1, GD2 and GD3 2-D Error (metres)

The distribution of the errors for the three receivers is shown on the cumulative probability plot in Figure 117 (page 143).

The close agreement between the results from the two MF-corrected receivers, alluded to in section 8.3, can be observed from the data in the table and from the form of the 'P(x>xp)' curves on the figure.

The corresponding curve for the UHF-corrected receiver clearly shows how the significantly increased 2-D errors which were observed on a small proportion of the data samples have affected the overall probability distribution.

9 SUMMARY OF CONCLUSIONS

The Measurement System

- (1) Recordings of the GPS C/A code carrier phase were successfully post-processed, in combination with similar data recorded at a fixed reference site, to yield a 'truth' position history for the trials aircraft.
- (2) The presence of data from a second reference site allowed two, semi-independent, aircraft truth position solutions to be determined. This provided additional redundancy in the truth data and also, from a comparison of the two solutions, provided a measure of confidence in the truth position accuracy.
- (3) Loss of carrier lock due to interference from the aircraft tail rotor proved to have a significant and detrimental impact upon the truth system performance. On this occasion it was possible to mitigate against this problem by careful design of the trials manoeuvres, but this might not always prove to be the case.
- (4) The results of ground-based testing suggest that the overall absolute position accuracy of the truth system was of the order of two metres, and all the indications suggest that a similar accuracy was maintained in flight.
- (5) Correct time synchronisation between the recorded data from the truth system, and that from the real-time DGPS receivers, was maintained to better than one millisecond.
- (6) The three DGPS receivers were operated successfully in an offshore environment using differential correction signals from an onshore chain of beacons operating in the MF band, and from a platform-based correction station which transmitted on a UHF datalink.

These facts demonstrate the suitability of the measurement system to investigate the issues which the trials programme was intended to address.

Receiver Performance.

- (7) The contributions of the airframe and rotors to errors in the position solutions output by the real-time DGPS receivers were estimated to be no more than two metres, following ground testing to compare the position solutions generated using two physically separate aircraft antenna installations. This low level of multipath does not justify repeating these tests on other helicopter types.
- (8) The aircraft main and tail rotors were found to have a significant impact upon the carrier-to-noise ratio reported by a GPS receiver, in situations where a satellite signal was obliged to pass through the rotor disc. Losses in excess of 12dB were experienced and, although additional experimentation is required to investigate the circumstances under which this effect occurs, it may have significant certification implications.
- (9) Subject to resolution of the datalink problems, the onshore MF correction source was found to provide an accurate real-time differential solution. The maximum horizontal error encountered was 21.0m (the corresponding sample size of 33,684 implies that the probability of encountering this maximum value

was 1/33,684, i.e. less than 3×10^{-5}); and the 95% and 99% confidence limits for position accuracy were 7.0m and 13.6m respectively.

- (10) No evidence was observed for an airborne GPS receiver being affected by L-band multipath effects from an offshore structure, even at ranges below 20 metres. However, more experimentation is required to increase the available sample size to provide additional confidence that this is the case.
- (11) A differential correction station located on the platform helideck was found to be subject to signal disturbances due to the platform structure. This affected the differential corrections from the platform, resulting in 2-D errors at the airborne GPS receiver of up to 123.1m. It is believed that these problems could be eliminated by siting the reference antenna at the highest point of the platform structure, provided that any associated operational difficulties can be overcome.
- (12) A comparison between two similar GPS receivers designed by different manufacturers, both using the onshore MF correction source, revealed no significant differences in their performance. However, the very limited number of data samples prevents more detailed conclusions from being drawn.

Implications of the Results.

- (13) A minimum of 24 operational GPS satellites were available throughout the trials programme, thereby suggesting that the results will remain reasonably valid for the future since this represents the minimum number of operational satellites planned to remain in the constellation.
- (14) Reception of MF corrections was found to be unreliable under certain conditions, to such an extent that the system would be unusable as an operational approach aid. These problems appeared to be associated with the extended operating range from the transmission stations (upwards of 70nm), and with flight in conditions conducive to the formation of precipitation static on the antenna installation, but further experimentation is required.
- (15) Compatibility problems were experienced between the MF correction source and the real-time receiver, relating to satellite ephemeris updates. Resolution of these problems (one solution to which is believed to be the use of RTCM-SC104 Type 2 differential corrections) would be required prior to the introduction of an operational approach aid.
- (16) The UHF datalink from the platform reference station was found to be reliable in operation, with the results implying that the dual nose/tail antenna installation could have been dispensed with.
- (17) At some locations it proved difficult to determine a sufficiently accurate estimate of the platform reference station's position using the available survey data. This suggests that a dedicated survey, with the results expressed in the WGS84 co-ordinate datum, should be undertaken before commissioning a differential reference station at an offshore location.

Future Work

The trials programme has identified a number of areas of uncertainty which could usefully be explored further, by means of additional theoretical and practical studies. These include the following:

- (18) Additional experimentation is needed into the effect of helicopter rotor blades upon GPS receiver carrier-to-noise performance, to examine how these effects are observed to vary with rotor speed, blade construction, and receiver design.
- (19) The reception problems observed with the shore-based MF correction source are such that the datalink is unacceptable as it currently stands. An experimental programme is required in order to provide a better understanding of the mechanisms involved, and to determine whether a practicable solution to them can be found. This should be preceded by an analysis of the data already gathered, to quantify the extent of the problem as a function of range from the MF station.
- (20) A solution is also required to the ephemeris update problems which were observed to result in the temporary loss of MF-corrected differential position. GPS receiver manufacturers, and the operators of the correction stations, should be consulted in order to determine how these problems could be overcome.
- (21) Before any further attempt is made to proceed with the development of a platform-based correction station, careful consideration is required of all of the interference issues related to the presence of the platform structure. Experimental GPS measurements from the site(s) in question, preferably derived from an extended period of operation, should ideally be used to provide the necessary degree of confidence.
- (22) The available sample size is insufficient to enable a definitive statement to be made regarding the presence of any significant GPS multipath effects when operating close to offshore structures. This can only be rectified by performing additional flight trials, which would be most cost-effective if undertaken in revenue-earning service.
- (23) Additional experimentation into the effect of different GPS receiver architectures, and their performance when operating with different correction sources, could usefully be undertaken.
- (24) The large amount of data recorded during the flight trials provides a useful source of information for further technical analysis, such as an investigation of the sensitivity of the GPS solutions to satellite failures and malfunctions.
- (25) The applicability of the trials results to a system in which the GPS sensor is not differentially corrected should be explored.

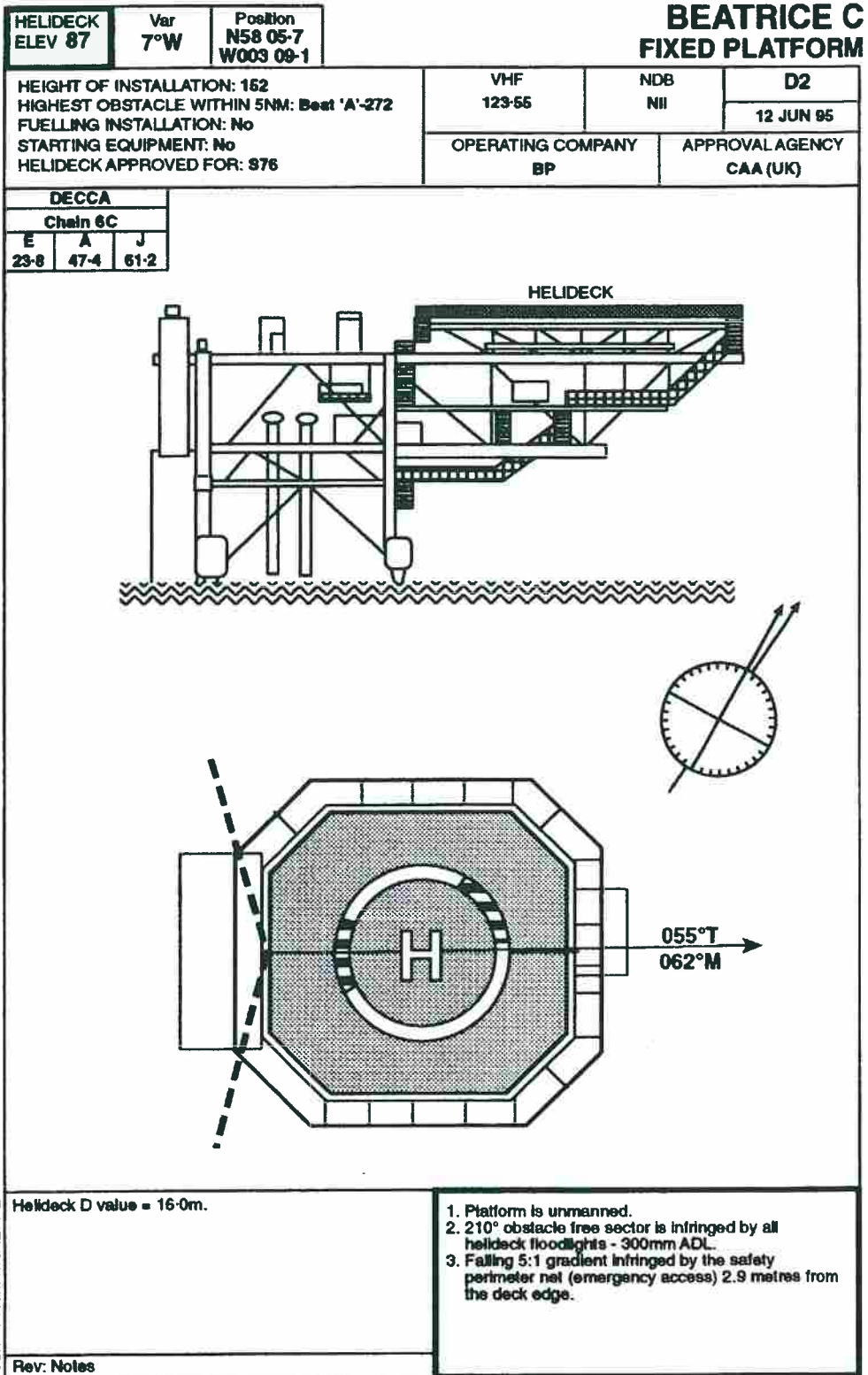


Figure 97 Beatrice C Platform Layout (reproduced by permission of British Airways AERAD)

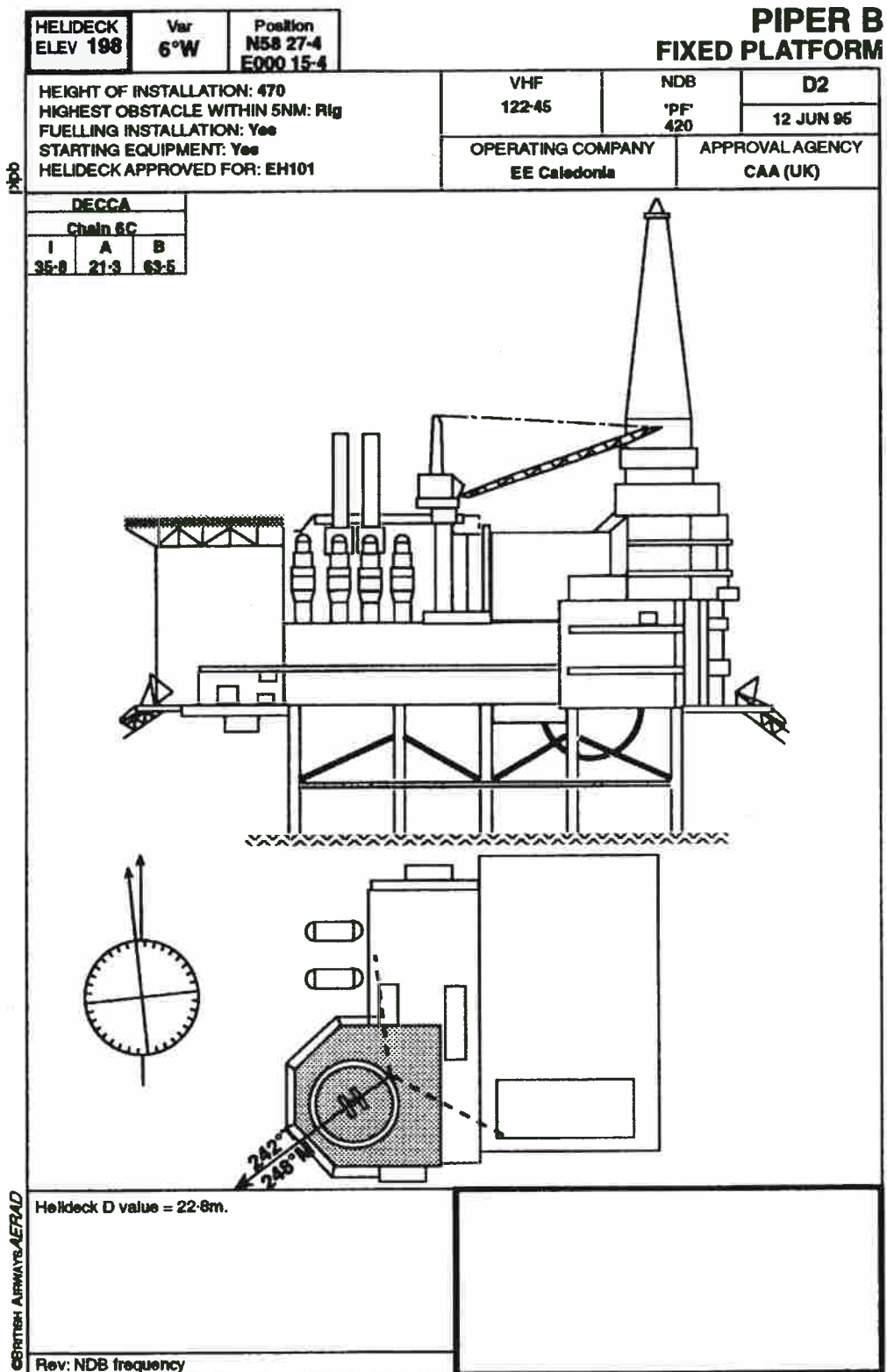


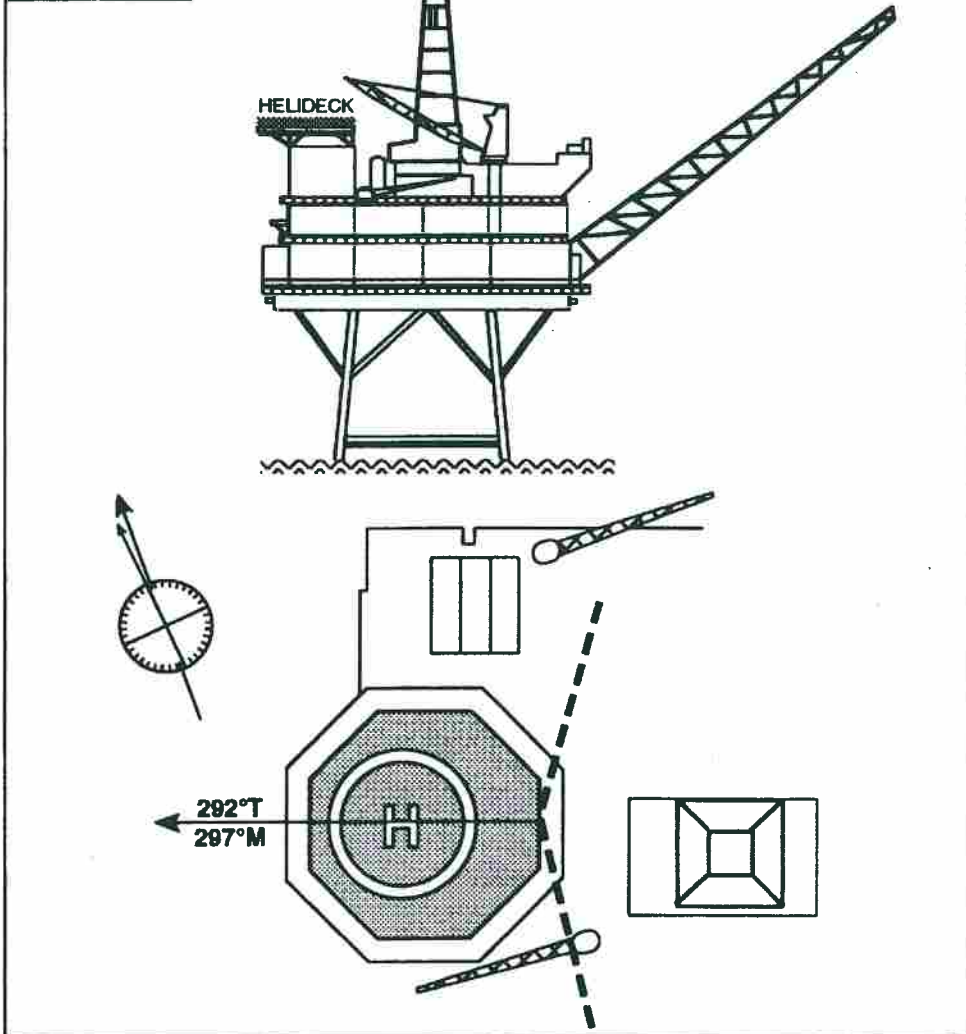
Figure 98 Piper B Platform Layout (reproduced by permission of British Airways AERAD)

HELIDECK ELEV 214	Var 5°W	Position N58 22.2 E000 04.4
----------------------	------------	-----------------------------------

TARTAN A FIXED PLATFORM

HEIGHT OF INSTALLATION: 419 HIGHEST OBSTACLE WITHIN 5NM: Top of rig FUELLING INSTALLATION: Yes STARTING EQUIPMENT: Yes HELIDECK APPROVED FOR: S61UR	VHF 122.45	NDB 'TAA' 402	D1 19 JUN 95
	OPERATING COMPANY Texaco		APPROVAL AGENCY CAA (UK)

DECCA		
Chain 6C		
B	H	C
1.4	43.9	74.8



HELIDECK D value = 22.2m

Rev: Minor

1. Turbulence from derrick.
2. The 5:1 falling gradient is swung 15° anti-clockwise (Independent of the 210° OFS).
3. Overflight of the accommodation module (platform north) should be avoided on take-off.
4. Helideck net removed.

Figure 99 Tartan A Platform Layout (reproduced by permission of British Airways AERAD)

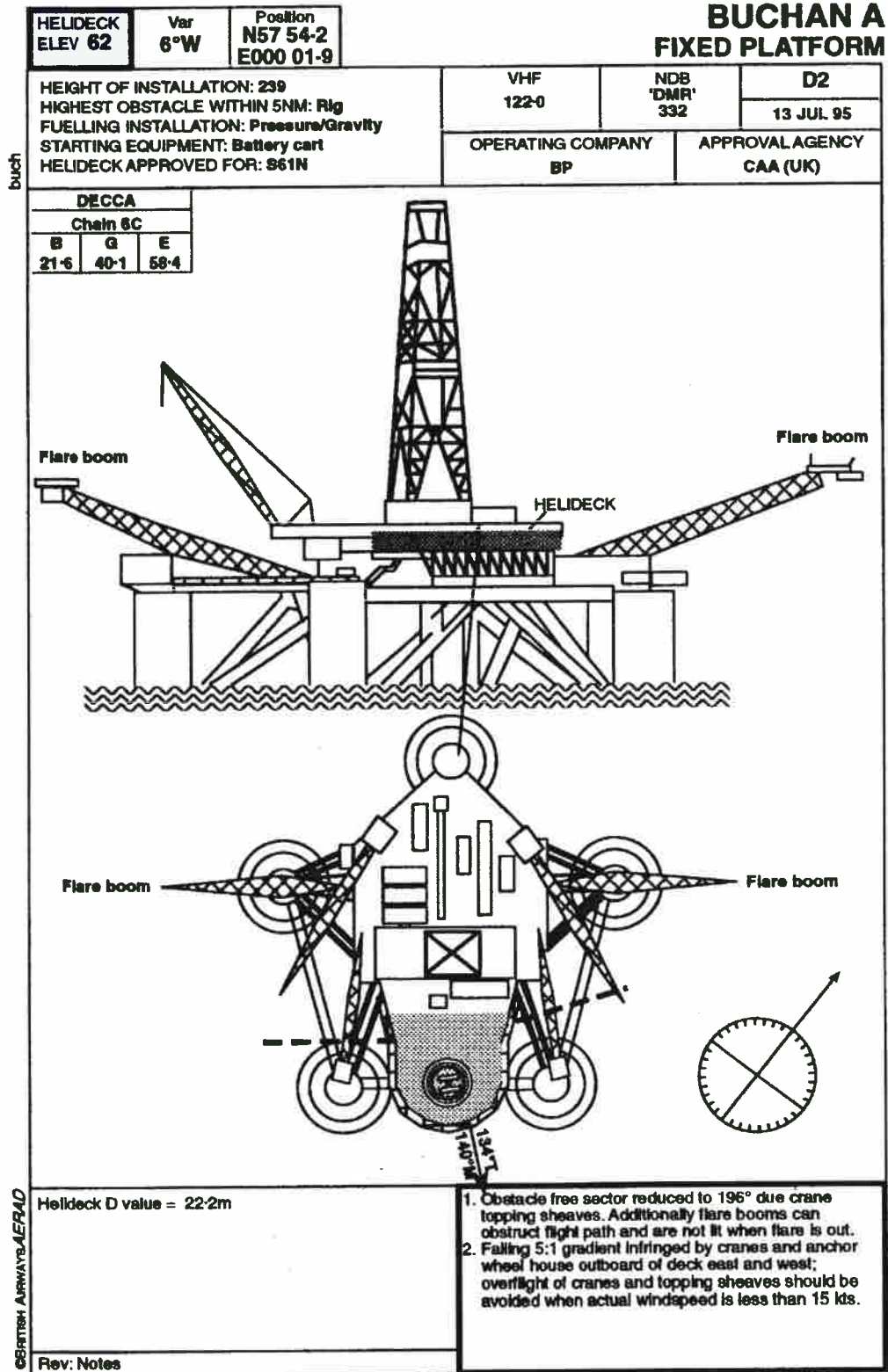


Figure 100 Buchan A Platform Layout (reproduced by permission of British Airways AERAD)



Figure 101 Beatrice C Platform



Figure 102 Piper B Platform



Figure 103 Tartan A Platform



Figure 104 Buchan A Platform

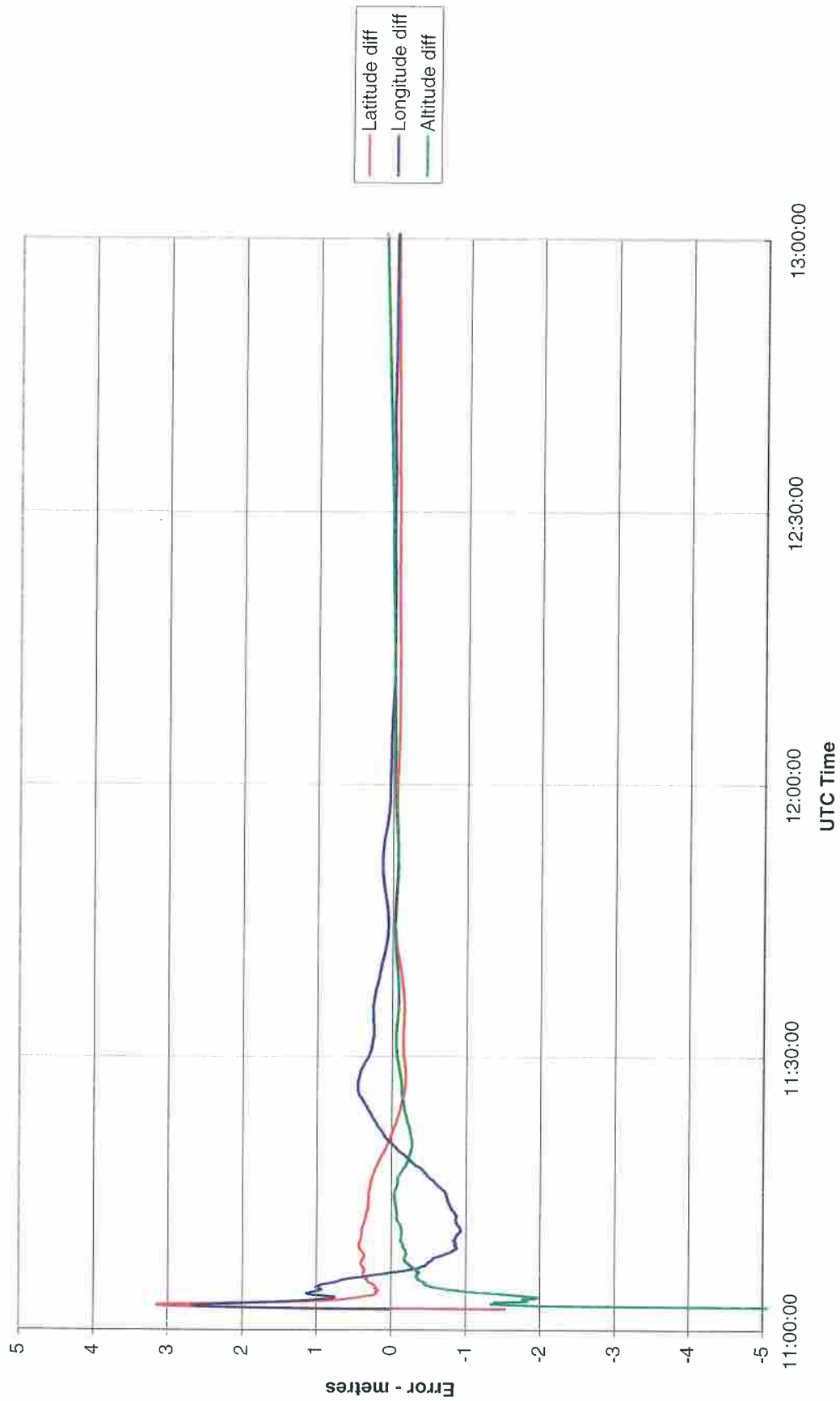


Figure 105 Carrier-Phase Solution Convergence for Platform Station Survey, Flight 7, Beatrice C



Figure 106 Comparison of OTruth with PTruth, Flight 7, Beatrice C

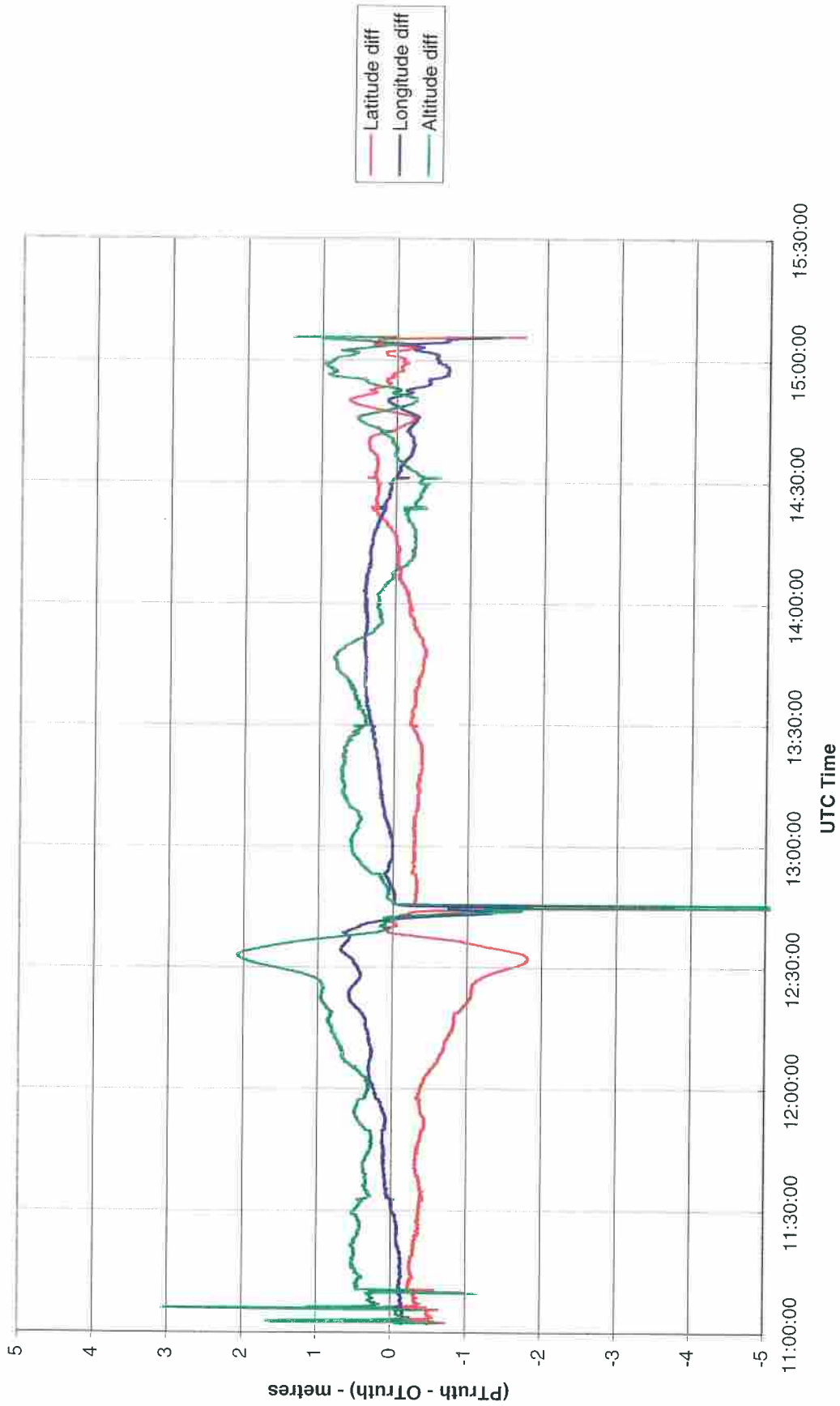


Figure 107 Comparison of OTruth with PTruth, Flight 7, Beatrice C (Reverse Processed)

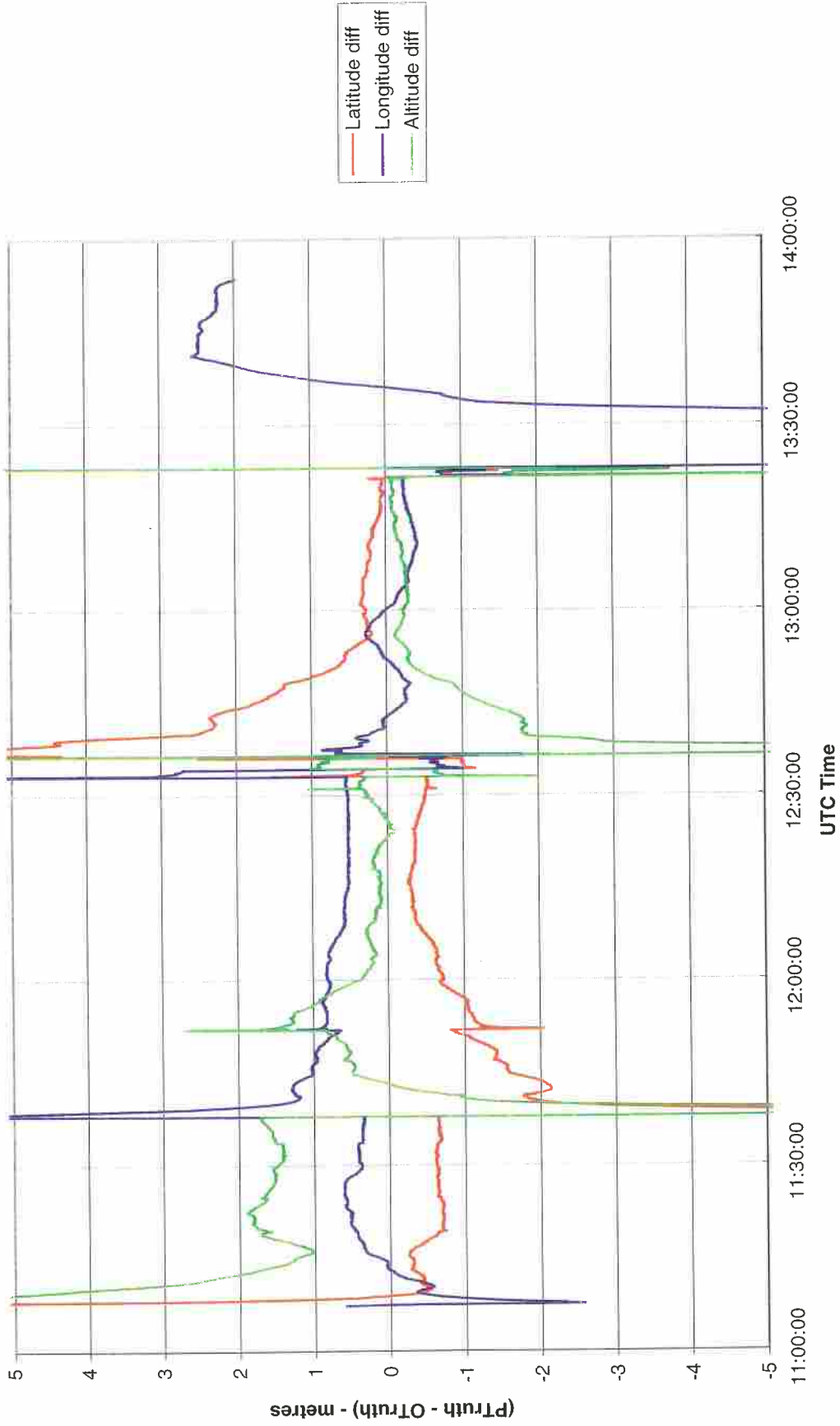


Figure 108 Comparison of OTruth with PTruth, Flight 2, Beatrice C

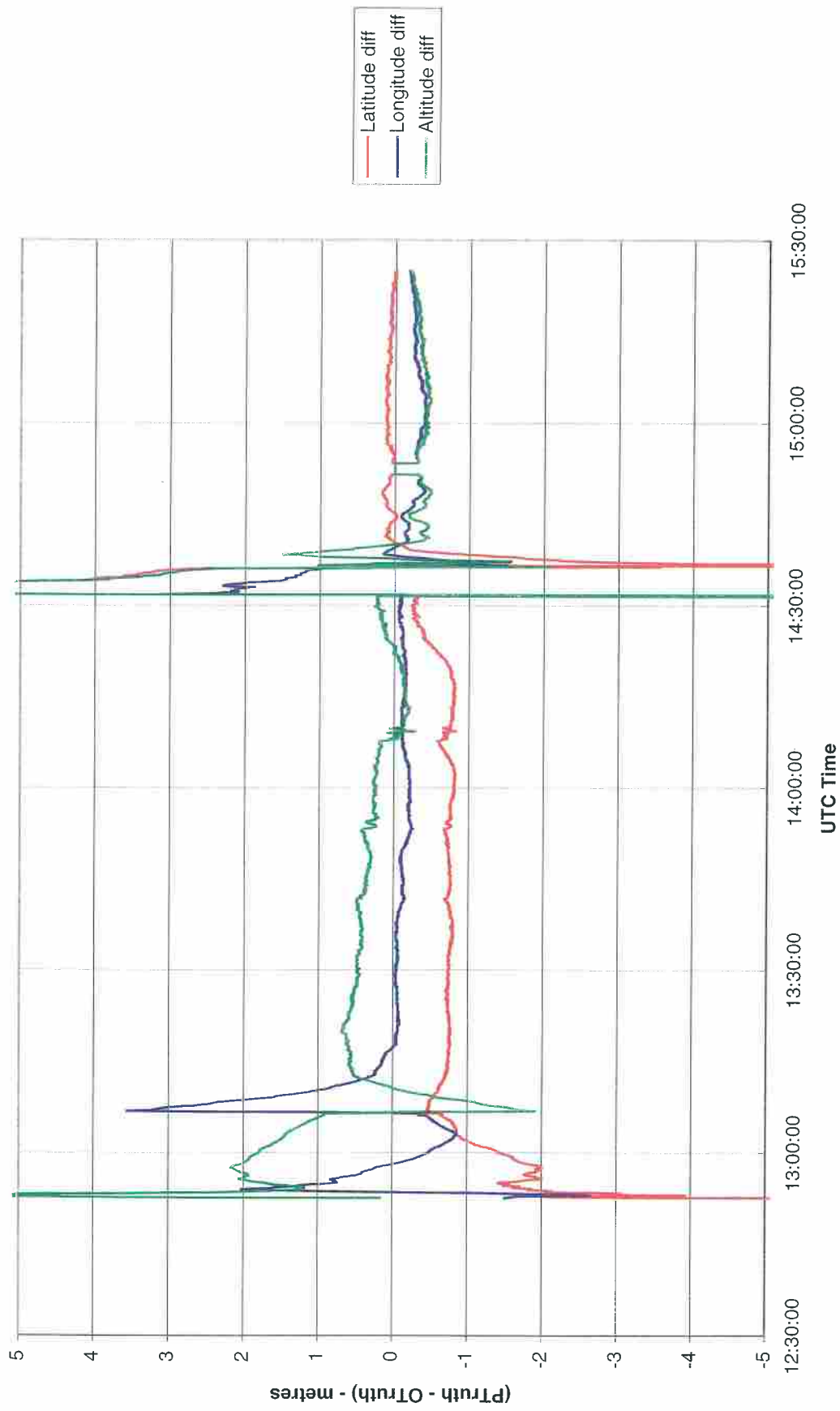


Figure 109 Comparison of OTruth with PTruth, Flight 4, Piper B



Figure 110 Comparison of OTruth with PTruth, Flight 5, Tartan A

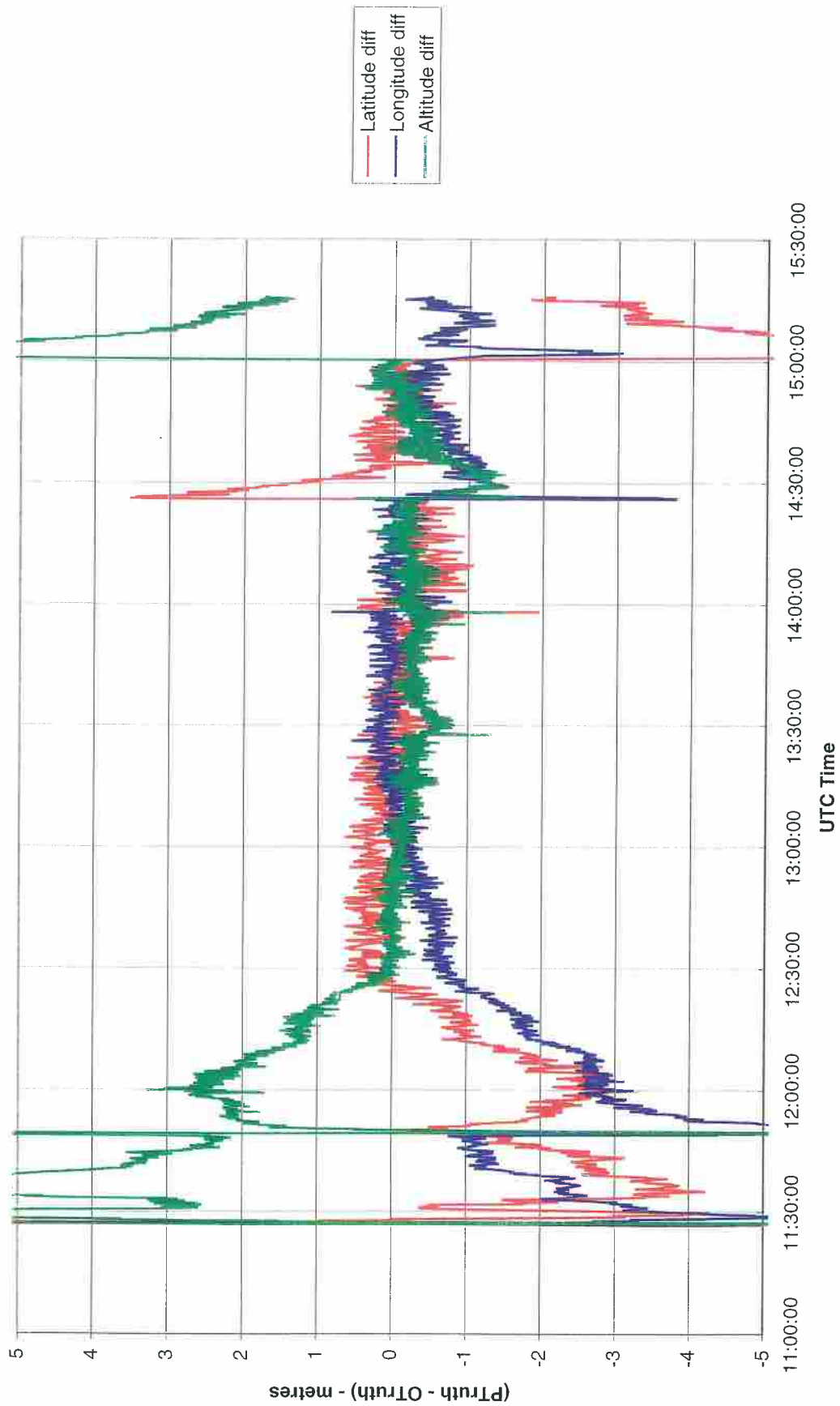


Figure 111 Comparison of OTruth with PTruth, Flight 6, Buchan A

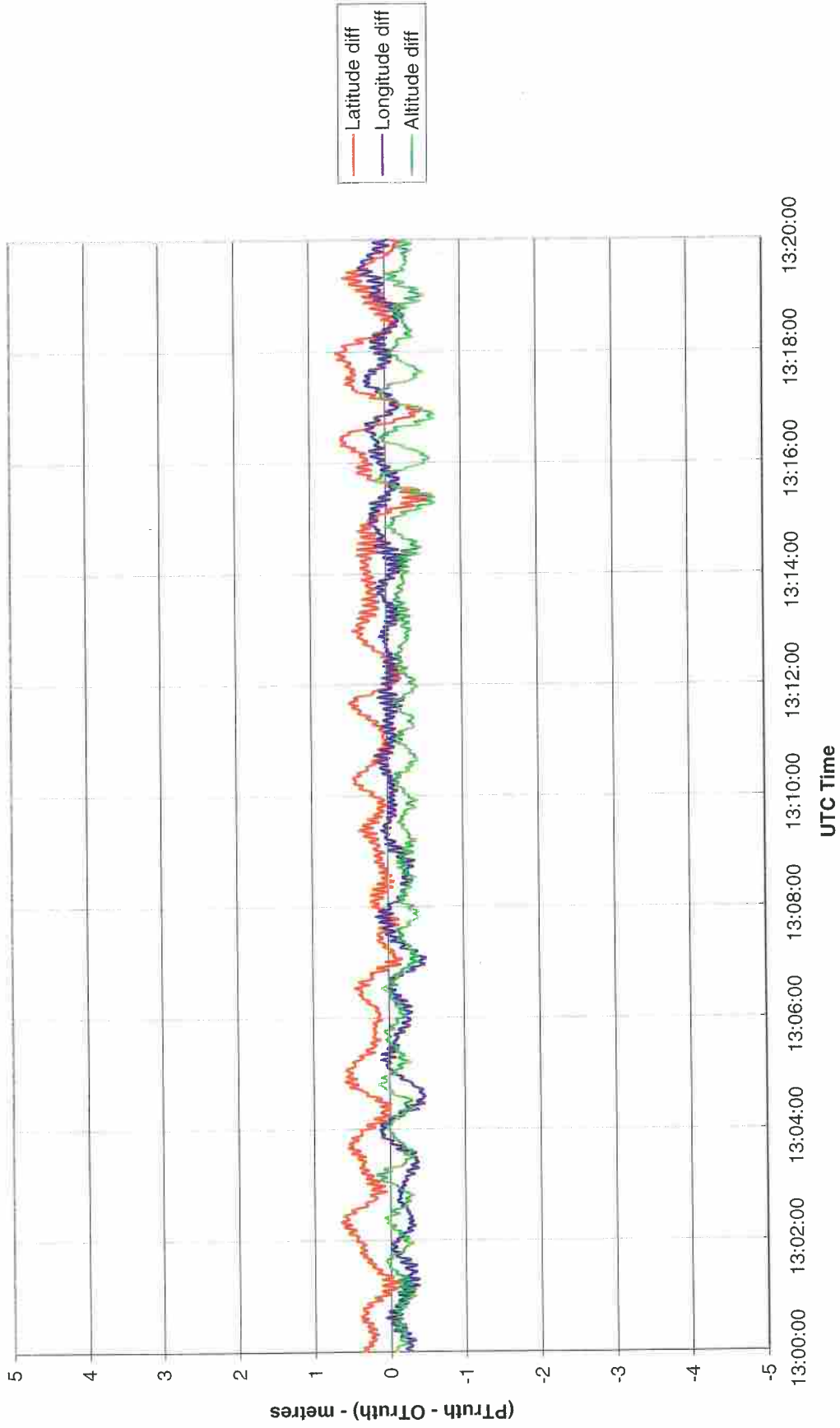


Figure 112 Comparison of OTruth with PTruth, Flight 6, Buchan A (Expanded)

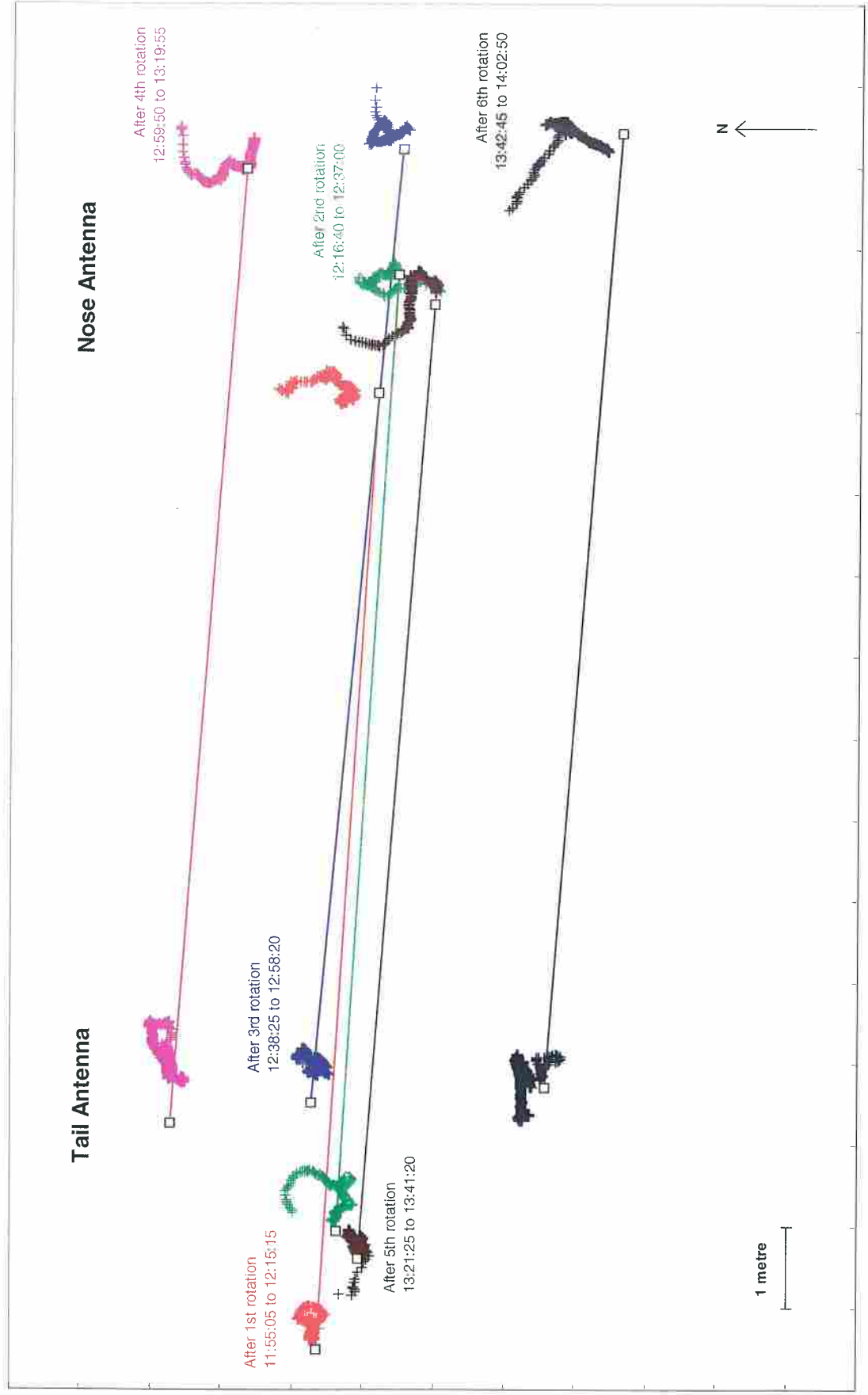


Figure 113 Longside Ground Trial: OTruth Solutions for Nose and Tail Antenna Installations

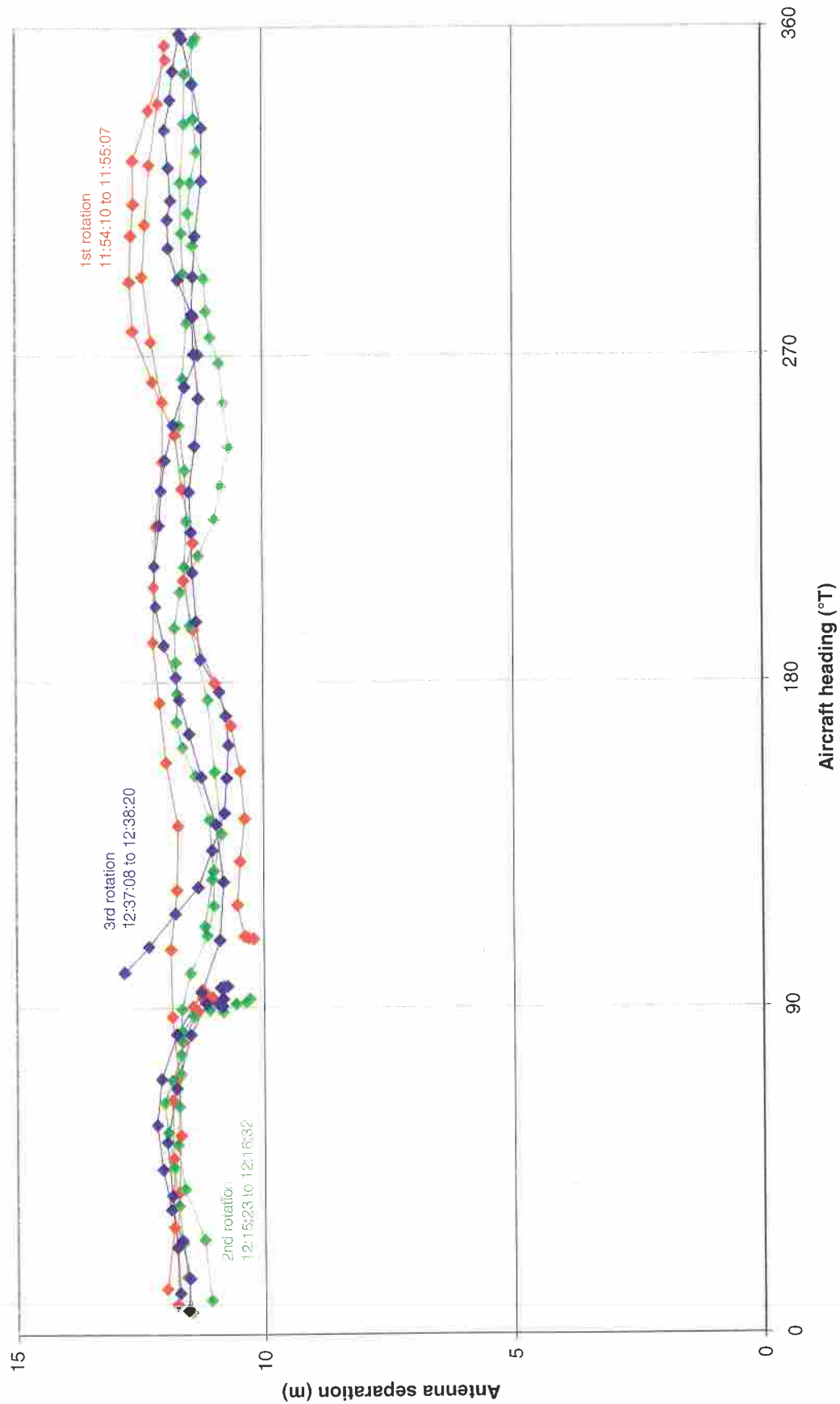


Figure 114 Longside Ground Trial: 2-D Difference Between Nose and Tail Antenna Position Fixes versus Heading

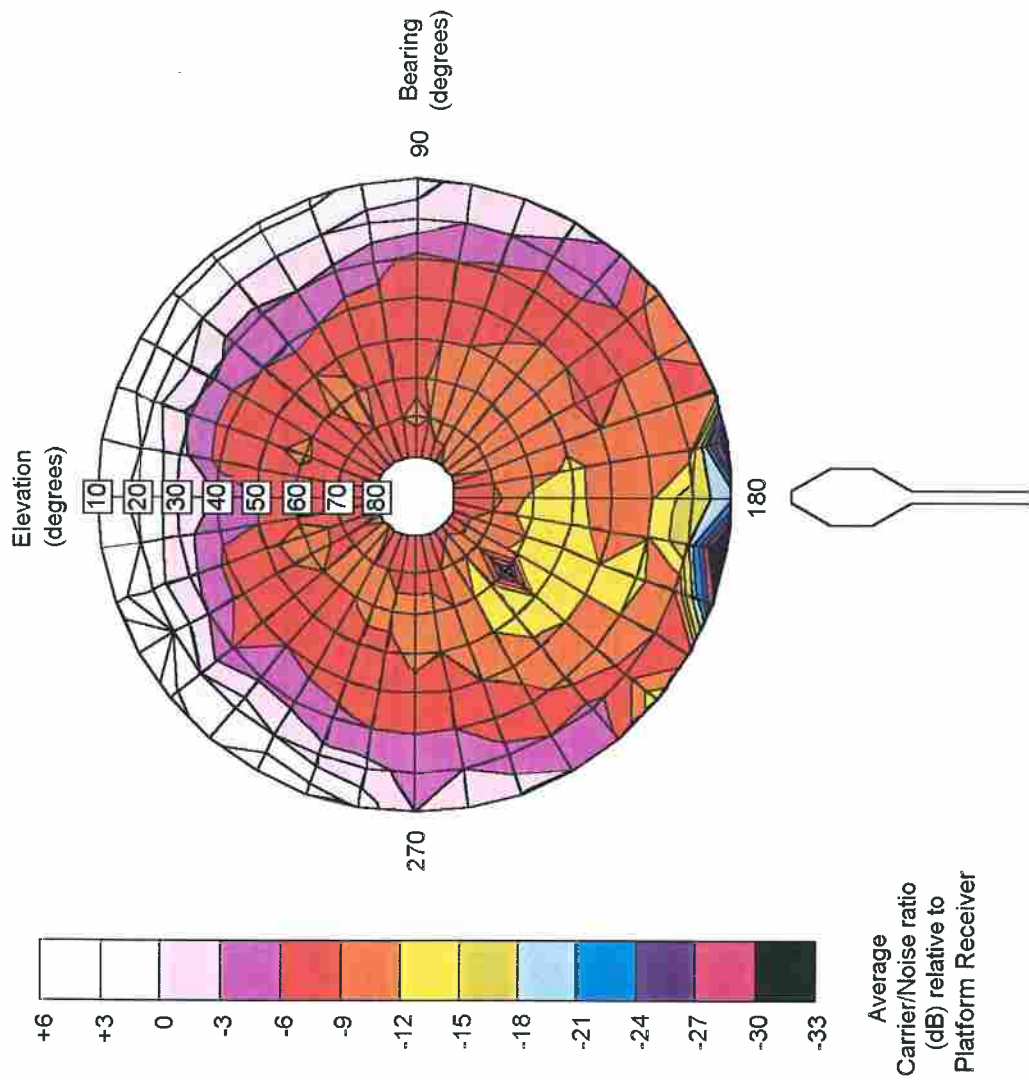


Figure 115 Longside Ground Trial: Variation of Average CNR with Azimuth and Elevation for Nose Antenna

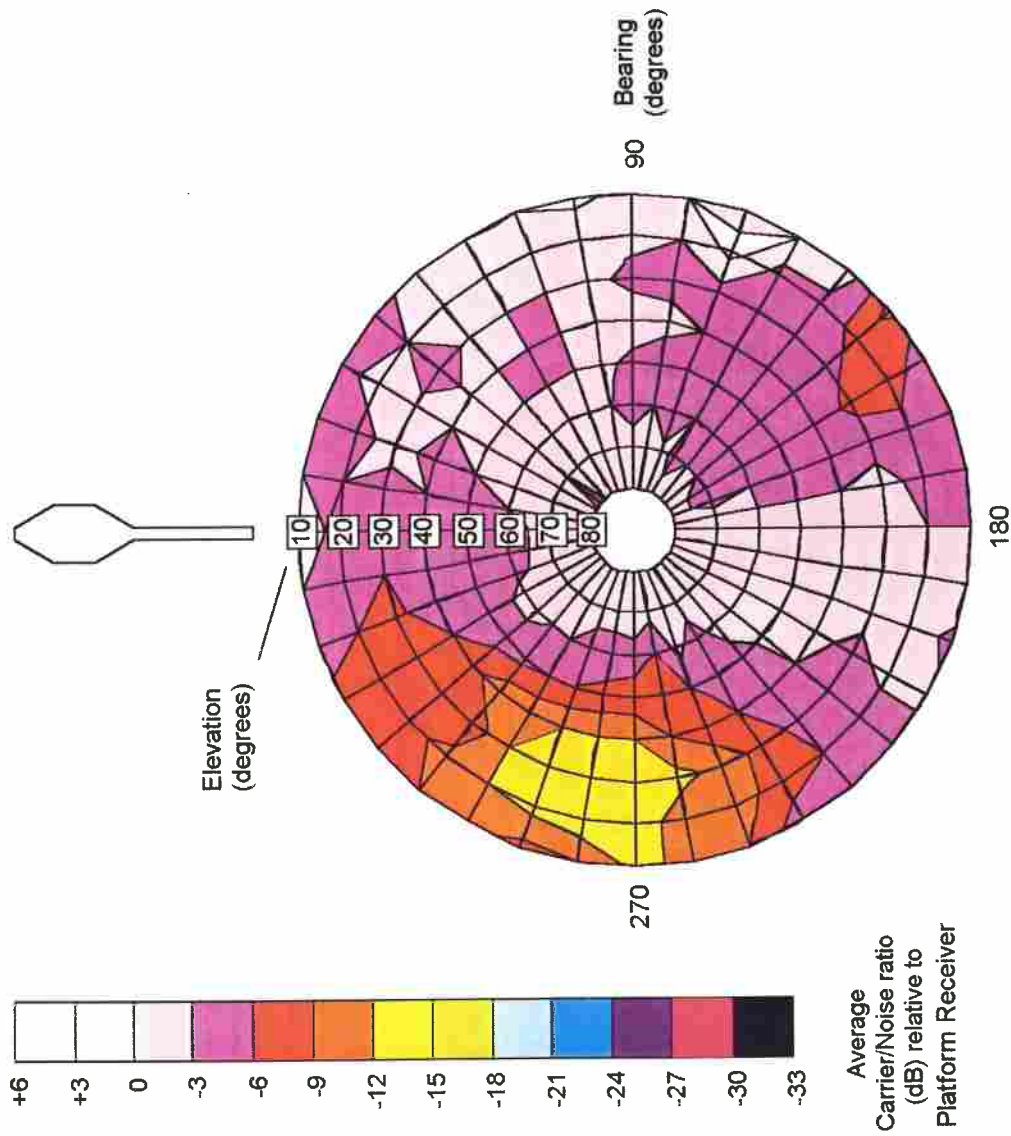


Figure 116 Longside Ground Trial: Variation of Average CNR with Azimuth and Elevation for Tail Antenna

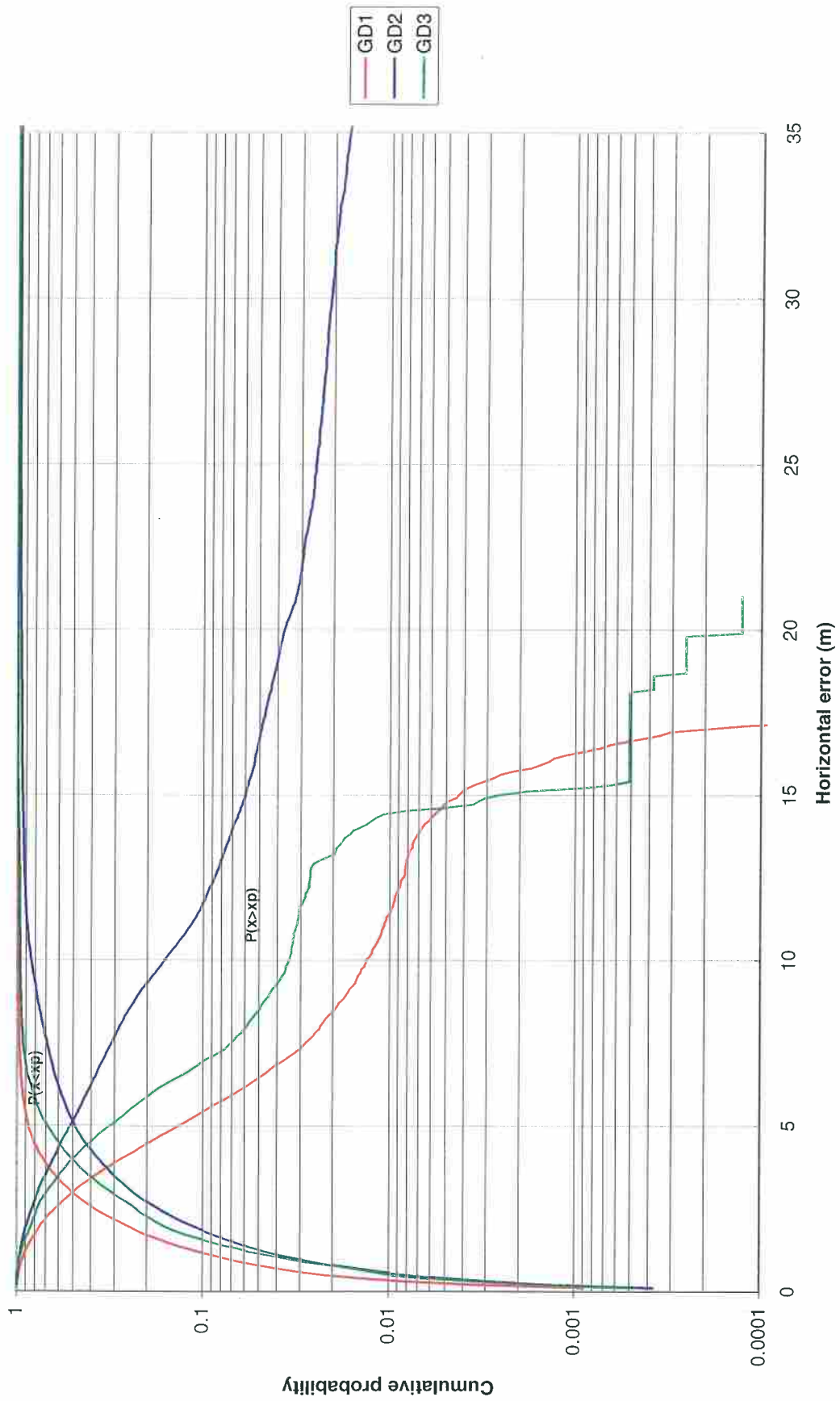


Figure 117 Cumulative Probability of GD1, GD2 and GD3 2-D Error

Volume 3
DGPS Approach Guidance

Contents

	<i>Page</i>
1 INTRODUCTION	1
2 REFERENCES	3
3 ABBREVIATIONS	4
4 DGPS APPROACH PROFILE AND GUIDANCE DISPLAYS	6
4.1 Existing Offshore Enroute and Approach Procedures	6
4.2 Airborne DGPS Equipment Installation	10
4.3 Designing the DGPS Approach Profile	15
4.4 ECU Implementation of Approach Guidance	22
4.5 Enhancements to the Basic Approach Guidance	24
5 EXPERIMENTAL DGPS APPROACHES	27
5.1 Flight Trial 1	30
5.2 Flight Trial 2	38
5.3 Flight Trial 3	51
5.4 Flight Trial 4	57
5.5 Flight Trial 5	65
5.6 Flight Trial 6	77
5.7 Flight Trial 7	89
6 DISCUSSION OF RESULTS	98
6.1 Initial Pilot Reactions	98
6.2 Pilot Confusion	98
6.3 Transition to Level Segment	99
6.4 Approach and Overshoot Angles	99
6.5 Range Indications	100
6.6 Mode Annunciation	100
6.7 Instrument Scalings	101
6.8 Crosswind and Reduced Speed Approaches	103
6.9 Autocoupled Approaches	103
6.10 Loss of GPS and Go-Around Techniques	104
6.11 Seamless GPS Navigation	105
6.12 Removal of Level Segment	105
6.13 Entry of Approach Data	106
6.14 Applicability to Other Aircraft	106
6.15 Applicability to Other Data Sources	107
7 SUMMARY OF CONCLUSIONS	108

LIST OF ILLUSTRATIONS.

Figure 1	Aircraft DGPS Guidance Equipment Installation	10
Figure 2	Localiser and Glideslope Displays on HSI and ADI	13
Figure 3	Distance and Ident Display on DME Indicator	14
Figure 4	LED Indicator Panel	14
Figure 5	Laterally Offset Approach Track	15
Figure 6	Definition of MAP	16
Figure 7	Vertical Approach Profile	18
Figure 8	Specification of Instrument Scalings	20
Figure 9	Introduction of Fairing into Vertical Profile	24
Figure 10	Introduction of Turnaway on Overshoot	26
Figure 11	Bond Helicopters Offshore Weather Radar Approach Plate	111
Figure 12	Experimental DGPS Approach Plate	112

LIST OF TABLES

Table 1	Principal Approach Guidance Parameters	22
Table 2	DGPS Flight Trials	28
Table 3	Cross-Track Statistics for Level Segment	102

1 INTRODUCTION.

During 1996 a series of flight trials was undertaken in the North Sea to examine the use of Differential Global Positioning System (DGPS) equipment as an approach aid for offshore installations. The flight trials had three basic objectives:

- (1) To acquire knowledge and experience to support the development of both generic, and DGPS-specific, airworthiness and operational requirements and associated advisory material, for the conduct of offshore approaches.
- (2) To quantify by scientific means the accuracy which may be achieved in a DGPS system operating to/from offshore platforms.
- (3) To assess the flyability of the system in the applicable environment.

The flight trials programme was undertaken by the Flight Systems and Measurement Laboratories (now incorporated into Cranfield Aerospace Ltd) of the College of Aeronautics, Cranfield University in the role of prime contractor on behalf of the UK Civil Aviation Authority.

Flight trials were performed using a Sikorsky S76C helicopter chartered by Cranfield from Bond Helicopters Ltd. The aircraft was fitted with a special purpose experimental DGPS installation which was complemented by additional recording equipment sited at fixed locations.

In the course of seven test flights totalling 36 hours, over 70 predefined manoeuvres were performed at a set of four offshore production platforms with differing topside layouts. At each platform, approach trajectories and guidance presentations based upon the use of DGPS data were evaluated by the trials team which comprised representatives from CAA, Bond and Cranfield.

Post-flight processing of the data recorded during each trial enabled an assessment to be made of the performance of the real-time airborne DGPS equipment, and an understanding to be gained of some of the issues likely to affect GPS performance in the offshore environment. The trials installation allowed a comparison to be made between two alternative sources of differential corrections and between receivers produced by two different manufacturers.

The Final Report on the trials programme consists of three volumes, of which this document ('DGPS Approach Guidance') represents Volume 3. The three volumes are structured as follows:

Volume 1 ('Experimental Procedures') contains a description of the three measurement systems employed and of the data recorded by each system, and includes details of the experimental procedures employed on each of the flight trials.

Volume 2 ('DGPS Equipment Performance') presents and discusses the results of a comparison between the real-time DGPS data and a 'truth' reference which was derived, using techniques described in the report, from post-processed GPS measurements. A discussion is included of various factors which were found to affect the availability and precision of the real-time DGPS data, and these results are summarised in the form of a series of conclusions and suggestions for future work.

Volume 3 (this document) describes how the approach guidance information was generated and presented to the aircraft pilots over the course of the trials programme. Details are presented of the offshore approaches which were undertaken using the experimental installation, together with a comprehensive discussion of the flyability results which includes a series of conclusions and suggestions for future work.

2 REFERENCES

- 1 Williams DA, CoA-FS-95-406, 'Approach Guidance Strategies: An Interim Report', FSML, 1996.
- 2 Williams DA, CoA-FS-96-418, 'Report on Test Flight 1', FSML, 1996.
- 3 Williams DA, CoA-FS-96-422, 'Report on Test Flight 2', FSML, 1996.
- 4 Dodson K, Mortimer ND, Talbot N, FTR 9793E, 'Flight Test Report (Beatrice Field)', CAA, 1996.
- 5 Dodson KM, Stevens JRA, Talbot N, FTR 10215E, 'Flight Test Report (Longside)', CAA, 1997.
- 6 Williams DA, CoA-FS-96-426, 'Report on Test Flight 4', FSML, 1996.
- 7 Dodson KM, Stevens JRA, Talbot N, FTR 10216E, 'Flight Test Report (Piper Bravo)', CAA, 1997.
- 8 Williams DA, CoA-FS-96-427, 'Report on Test Flight 5', FSML, 1996.
- 9 Dodson KM, Stevens JRA, Talbot N, FTR 10217E, 'Flight Test Report (Tartan)', CAA, 1997.
- 10 Stevens JRA, CA/CSG/7047, 'Report on Test Flight 6', CAe, 1997.
- 11 Dodson KM, Stevens JRA, Talbot N, FTR 10218E, 'Flight Test Report (Buchan A)', CAA, 1997.
- 12 Stevens JRA, CA/CSG/7048, 'Report on Test Flight 7', CAe, 1997.

3 ABBREVIATIONS

ADF	Automatic Direction Finder
ADI	Attitude Director Indicator
ARINC	Aeronautical Radio, Inc
ATC	Air Traffic Control
Bond	Bond Helicopters Ltd
CAA	Civil Aviation Authority
CAe	Cranfield Aerospace Ltd
Cranfield	Cranfield University, Cranfield Aerospace Ltd
dB	Decibel
deg	Degree
DGPS	Differential Global Positioning System
DME	Distance Measuring Equipment
ECU	Electronic Computer Unit
ED50	European Datum 1950
FAF	Final Approach Fix
FSML	Flight Systems and Measurement Laboratories
ft	Foot
FTE	Flight Test Engineer
GD1	Identifier for MF-corrected Navstar GPS Navigation data
GD2	Identifier for UHF-corrected Navstar GPS Navigation data
GNSS	Global Navigation Satellite System
GPS	Global Positioning System
HSI	Horizontal Situation Indicator
Hz	Hertz
IAS	Indicated Airspeed
ILS	Instrument Landing System
kt	Knot
LED	Light Emitting Diode
m	Metre
MAP	Missed Approach Point
mb	Millibar
MDH	Minimum Descent Height
MF	Medium Frequency
min	Minute
MSA	Minimum Safe Altitude
msl	Mean Sea Level
NAV	Navigation
Navstar	Navstar Systems Ltd
NDB	Non-Directional Beacon
nm	Nautical Mile
PC	Personal Computer
QDM	Approach track direction
QFE	Pressure setting which gives zero height reading at an aerodrome
QNH	Pressure setting which gives zero altitude reading at sea level
Radalt	Radio altimeter
ref	Reference
RNAV-2	Racal Avionics Area Navigation System 2
s	Second
SA	Selective Availability
std dev	Standard deviation
Trimble	Trimble Navigation Ltd

UHF	Ultra High Frequency
UK	United Kingdom
UTC	Universal Time Co-ordinated
V	Volt
VHF	Very High Frequency
VOR	VHF Omni Range
WGS84	World Geodetic System 1984
°M	Degrees magnetic
3-D	Three dimensional

4 DGPS APPROACH PROFILE AND GUIDANCE DISPLAYS.

4.1 Existing Offshore Enroute and Approach Procedures

The physical nature of offshore installations, combined with the limited availability of communication and navigation aids, has required the offshore helicopter industry to develop operating procedures which are substantially different in many respects from those employed in other areas of aviation.

Many of the North Sea platforms, in particular those in the Northern sector, are beyond the range of conventional ground-based navigation aids such as VOR/DME and are also beyond the coverage of primary and secondary ATC radar services. These facilities are, however, available in the area of the helicopters' main onshore operating bases (such as Aberdeen and Sumburgh) where the concentration of aircraft, and consequently the need to ensure safe separation, tends to be greatest. Standard terminal area ATC procedures are normally employed for this part of the flight.

For many years the only viable enroute navigational aid for offshore operations was the Decca Navigator system and, consequently, the majority of the North Sea helicopter fleet was equipped for Decca operations. Access to the Decca information was generally achieved by means of an area navigation system, such as the Racal RNAV-2 employed on the trials aircraft which provided a waypoint-based navigation facility.

Until recently, the chains of Decca Navigator transmitters in the British Isles, Scandinavia and the Low Countries provided satisfactory coverage for all North Sea operations. The system could, however, be subject to erratic operation in certain types of meteorological and ionospheric conditions, and the equipment could be affected by such factors as static buildup on the airframe.

Recent decisions to cease operating the Decca Navigator transmitters covering the North Sea have forced the offshore helicopter operators to consider the installation of an alternative enroute navigation aid. GPS equipment intended for the general and light commercial aviation market, of which a large number of different models have come onto the market in recent years, appears to have been the favoured choice of most operators.

In the northern North Sea, a system for enroute separation of aircraft has evolved based upon a series of radial tracks originating at onshore VOR/DME facilities. In the Aberdeen area, tracks are spaced at 3° intervals with alternate tracks being employed for outbound and inbound flights. For example, an aircraft routing to a platform whose bearing from the Aberdeen VOR was 051° would be expected to follow the 050° radial outbound and the 053° radial inbound.

Aircraft position reporting whilst following the radial track structure is based upon distances from the VOR/DME rather than specific reporting points: hence an aircraft might be requested to report on reaching 80nm from the beacon.

In practice, navigation along the track structure once the aircraft is beyond range of the VOR/DME would need to be performed using the available enroute aid (such as Decca Navigator or, more recently, GPS), with a degree of cross-checking being performed between the two systems before the point at which coverage was lost.

In the past, when the use of Decca equipment (rather than GPS) was more-or-less universal, there would appear to have been a commonly held belief that any perturbations of the Decca signal affecting its positioning accuracy would have an equal effect upon all aircraft in a particular area. Consequently, separation between aircraft would still be assured even if significant deviations occurred from the intended track. The justification for this belief is, perhaps, debatable.

On arrival in the vicinity of the destination platform the aircraft crew need firstly to address the issue of locating the structure itself, and secondly to perform an approach manoeuvre which will not result in a hazard to the aircraft, the destination platform, or other structures and shipping in the vicinity. This last category is particularly significant owing to its transient nature, and includes not only the normal support and safety vessels found offshore, but also such structures as crane barges and accommodation 'flotels' which can present a considerable obstruction owing to their large size.

The only navigational aid generally found on offshore platforms is the Non-Directional Beacon (NDB) which allows the aircraft crew to determine the relative bearing of the platform using their ADF equipment. Unlike onshore NDBs, those found offshore are generally only switched on when specifically requested by an inbound aircraft: this is partially due to the fact that the limited number of available frequencies implies that more than one platform will employ the same NDB frequency (multiple transmitters sharing a common frequency may be distinguished by their morse code identification).

Most offshore helicopters are fitted with a weather radar system which is designed to allow the crew to identify and avoid unfavourable weather conditions such as thunderstorms. The value of the weather radar as an aid to obstacle avoidance was recognised and the systems fitted to many aircraft have been modified by the manufacturers to provide additional short-range display modes, which allow returns from 5 to 10nm ahead of the aircraft to be displayed.

Procedures were developed by the offshore operators for the use of the weather radar in offshore approaches and an example is shown in Figure 11 (page 111). This approach procedure normally begins with the aircraft proceeding to a point directly overhead the destination at the desired Minimum Safe Altitude (MSA), typically chosen to be 1000ft above the highest known obstacle in the area (normally this is the platform itself).

Identification of the platform whilst passing through the overhead may be achieved in one of several ways and procedures normally require confirmation by two independent methods. The available techniques include:

- (1) Enroute navigation aid: the co-ordinates of the destination platform would normally have been entered into the area navigation system as a waypoint, allowing the range and bearing to the platform to be determined to an accuracy commensurate with that of the navigation sensor employed (e.g. Decca Navigator or GPS).
- (2) Weather radar: identification of the platform from its return on the radar display, possibly by reference to its relationship with other returns such as those from neighbouring platforms.

- (3) ADF: with the platform NDB activated and identified from its morse coding, flying overhead the structure will cause the ADF needle to pass through 180° as for a normal onshore beacon overflight.
- (4) Visually: if the visibility is sufficient to allow positive identification of the platform before or during passage through the overhead.

Some aircraft incorporate a weather radar overlay facility which allows a series of waypoints, stored in the area navigation computer, to be overlaid in their correct relative positions on the weather radar display: this allows a form of cross-checking to be achieved by confirming that the destination platform waypoint is coincident with its radar return.

Once identification of the platform has been achieved to the satisfaction of the crew, the weather radar approach procedure requires the aircraft to take up a track which is offset by 160° in either direction from the final approach track. Since the latter would normally be directly into wind (whose direction is generally reported to the aircraft crew by the platform radio operator), this results in a downwind track with a 20° offset.

The aircraft proceeds downwind to a range of (generally) 4nm from the platform, during which time the weather radar returns in the approach sector are examined and correlated with known obstacles (such as other platforms, shipping, etc.). Once satisfied that obstacle clearance can be maintained, a descent is commenced to an intermediate altitude of around 800ft at the end of the downwind leg.

At 4nm range a turn is commenced onto the final approach track and a further descent is commenced down to 200ft (normally determined from the radio altimeter). During this time the weather radar returns continue to be examined to confirm that the aircraft will remain clear of all obstacles. This also provides the only available source of information, other than dead reckoning (i.e. timing the approach), on the range to the destination platform.

During both the outbound (downwind) and inbound legs, a platform NDB may be used to provide additional confirmation that the correct track is being flown: ideally the ADF needle should indicate directly behind the aircraft during the downwind leg, and directly ahead of the approach track during the initial section of the inbound leg.

The approach procedure requires the aircraft to diverge from the direct approach track at a range of 1.5nm from the platform so as to maintain separation from the structure in the event that visual contact cannot be established. This is achieved by turning away from the approach track, initially by 10° at 1.5nm range and by a further 5° at 1nm range.

If visual contact is not established by the Missed Approach Point (MAP), defined to be at a range from the platform of 0.75nm, then a go-around manoeuvre is executed involving a climbing turn away from the structure to regain MSA.

The approach procedure is terminated as soon as visual contact is established with the platform during the inbound leg, with the aircraft then being manoeuvred as required to land on the platform. This may involve the aircraft circling the platform at

close range in order to approach the helideck from the optimum direction, which may be on the opposite side of the structure.

For an aircraft operated by two crew members, one pilot will typically fly the instrument procedure whilst the second is attempting to establish visual contact with the platform, taking over control of the aircraft once this has been achieved.

Slight modifications, such as an increase in altitude at the various stages, are made to the procedure described above to cater for various scenarios such as night approaches or lack of a serviceable radio altimeter. If the weather radar is unserviceable, a broadly similar approach may be performed using the NDB only, but involving correspondingly greater minima and descent heights.

The radar procedure, whilst offering the best method for undertaking an offshore approach in poor visibility with the available equipment, is generally held to be unsatisfactory owing to the fact that the weather radar is neither designed nor certificated as an obstacle detector or navigational aid. One of the primary objectives of the DGPS trials programme was therefore to devise and evaluate a generic approach procedure utilising an instrument-based approach aid.

4.2 Airborne DGPS Equipment Installation

For the offshore approach trials programme, the subject aircraft (Bond Helicopters Sikorsky S76C registration G-SSSC) was fitted with an experimental DGPS installation which is fully described in Volume 1 of this report.

Figure 1, which is a simplified version of the system diagram in Volume 1, shows only those elements of the experimental DGPS system which were relevant to the evaluation of experimental DGPS approaches.

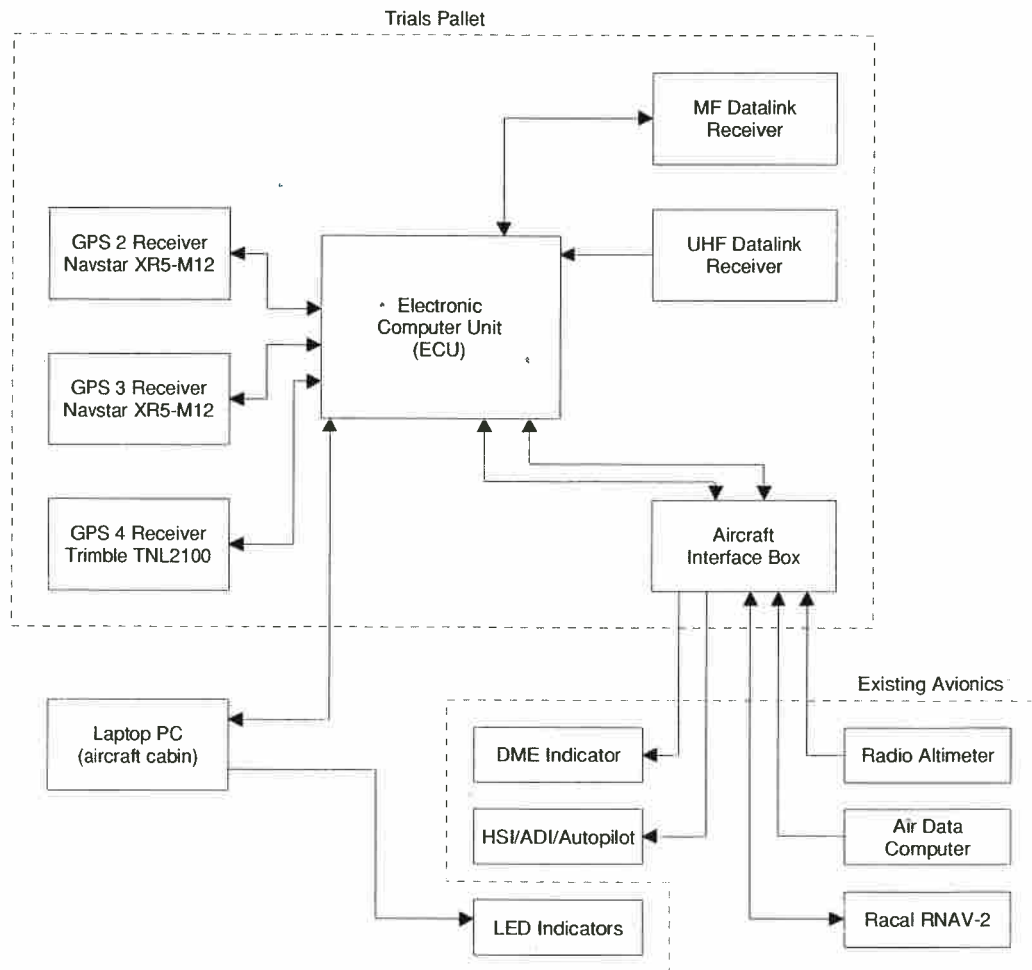


Figure 1 Aircraft DGPS Guidance Equipment Installation

4.2.1 Real-Time DGPS Receivers

The equipment pallet contained three GPS receivers which were configured to output real-time differentially corrected position solutions. A fourth GPS receiver formed part of the truth reference system against which the performance of the real-time DGPS equipment could be compared, and was not directly relevant to the conduct of the experimental approaches.

Each of the three differentially corrected GPS receivers was capable of producing a new data solution at a 1Hz rate. This solution included:

- (1) UTC Time, with a 1s resolution and with a pulse marker allowing the start of the second to be identified to ± 1 ms.
- (2) An estimate of aircraft position, in the form of separate latitude, longitude and altitude. Each of these was specified relative to the WGS84 ellipsoid (a simplified representation of the shape of the earth's surface).
- (3) An estimate of aircraft velocity, in the form of three velocity components (north, east and vertical).
- (4) An indication of the receiver status, including whether or not the receiver solution was valid, and whether or not differential correction data was being incorporated in the position solution. If no valid correction data had been received in a defined time period, typically 30s, each receiver would revert to stand-alone (uncorrected) navigation.
- (5) (Navstar receivers only) An indication of the receiver's estimated position accuracy in terms of horizontal, vertical and 3-D position.

Other data, such as the identifiers of the satellites used in the solution, were also available but were not considered to be directly relevant for real-time guidance purposes.

It was expected that each receiver would operate continuously throughout the trials programme, with a new solution output each second. The GPS solution would only be lost if the receiver was unable to receive satisfactory signals from sufficient satellites, or if an equipment malfunction occurred.

4.2.2 *Differential Correction Sources*

Two sources of differential corrections were available, one derived from a series of commercial land-based marine radiobeacons and received on an MF datalink, the other was generated from a 'private' base station located on the destination offshore platform and received via a dedicated UHF datalink.

Of the three guidance GPS receivers, two were identical units (Navstar XR5-M12), one of which was corrected by the MF data, and the other by the UHF data. The third was a dissimilar unit from a different manufacturer (Trimble TNL-2100) which was supplied with MF corrections.

Each of the two differential correction sources was expected to be available continuously throughout the experimental DGPS approaches at each platform.

With valid differential corrections available to a real-time receiver, position solution accuracy was expected to offer an order of magnitude improvement in accuracy compared to the corresponding stand-alone solution. Upon reversion to stand-alone operation after the defined time-out period, the receiver would immediately revert to the less accurate uncorrected solution.

4.2.3 *Electronic Computer Unit (ECU)*

The outputs of the GPS receivers were connected to a microprocessor-based Electronic Computer Unit (ECU) which was able to process the data to provide

usable guidance information. The ECU was also supplied, via a series of interfaces, with other aircraft data such as pressure and radio altitude, airspeed, heading, and pitch and roll attitude.

The ECU provided an output of GPS data which was fed to the existing aircraft area navigation computer (RNAV-2) via an ARINC 429 databus. This allowed GPS to be selected as the RNAV-2's primary navigation source in place of Decca Navigator. No processing of the GPS data supplied to the RNAV-2 was performed by the ECU other than that which was required to translate the various parameters (position, velocity, time and status) into the correct ARINC 429 format.

4.2.4 *Barometric and Radio Altitude*

The GPS receivers were not supplied with inputs of barometric or radio altitude but both of these parameters were continuously available to the ECU.

Barometric altitude, derived from the aircraft Air Data Computer, represented pressure altitude relative to the standard pressure setting of 1013.2mb and was updated at a rate in excess of 10Hz via an ARINC 429 databus.

The aircraft Radio Altimeter only operated below 2000ft and its output was sampled by the ECU every 1ms via an analogue-to-digital converter interface. There was a step change in the radalt's output scaling at 500ft (20mV/ft below this height, 3mV/ft above), which provided increased sensitivity and lower noise at low heights. The time constant of the radalt output was stated to be 90 ± 10 ms.

4.2.5 *Cockpit Displays*

The ECU was provided with the capability to drive, via analogue and digital outputs, various cockpit instruments directly whenever a special 'DGPS' switch selection had been made by the pilot. These outputs comprised localiser and glideslope deviations and their associated status flags, which were displayed directly in 'raw data' format on the HSI and ADI, and were also available for use by the flight director and autopilot. As far as the instrument electronics were concerned, the signals were indistinguishable from normal ILS signals.

The analogue outputs of localiser and glideslope deviation to the cockpit instruments were calibrated as part of the aircraft commissioning process in terms of full-scale needle deflection on the HSI. The HSI indicated the centre, half-scale and full-scale deflection points by means of 'dots' (Figure 2), with two dots corresponding to full-scale deflection.

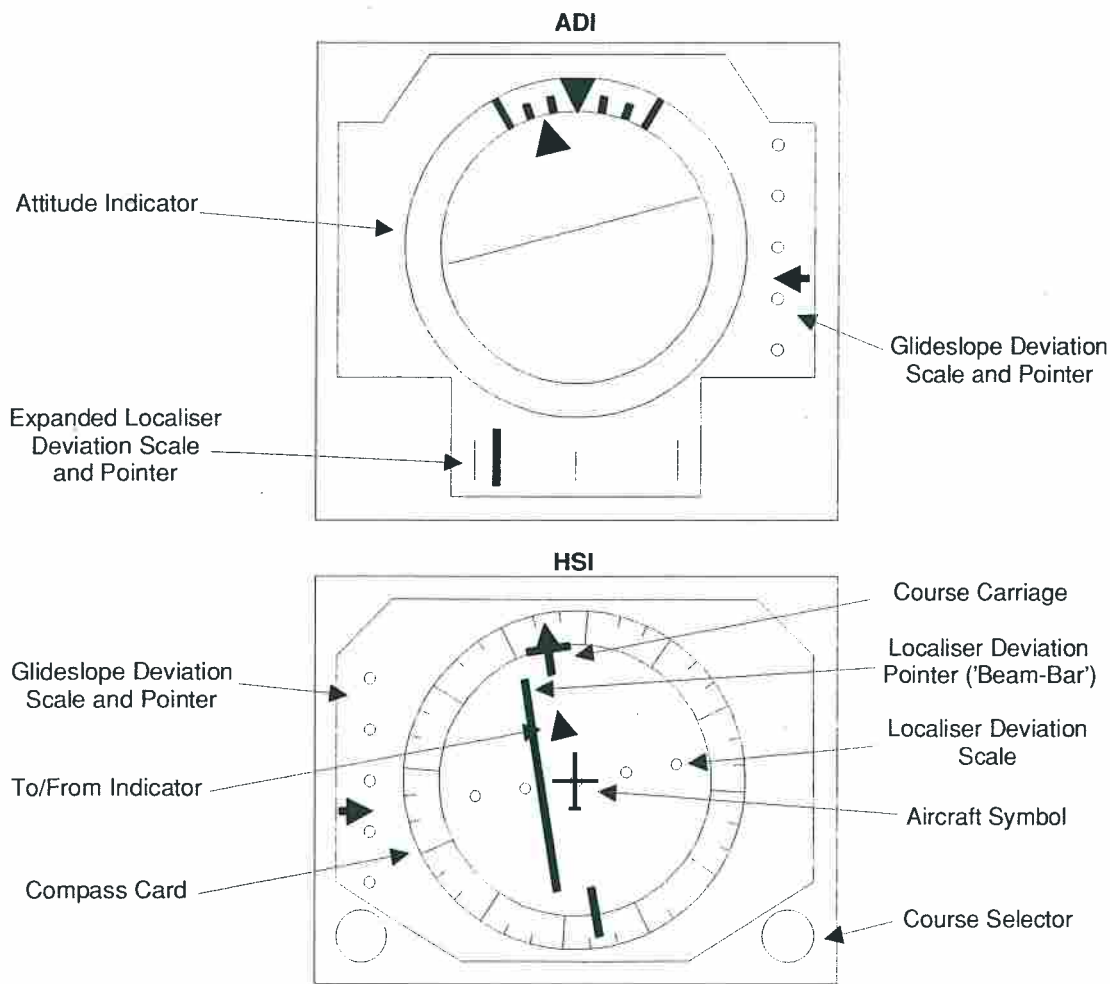


Figure 2 Localiser and Glideslope Displays on HSI and ADI (not to scale)

Expressing the deflections as a proportion of full-scale, rather than in terms of some of the other methods used to express ILS deviations (e.g. difference in depth of modulation, microamperes) avoided the possibility of confusion and allows the deviation signal to be directly related to the information presented to the pilot.

The deviation information displayed on the HSI was repeated on the ADI 'raw data' pointers. The scaling for the ADI glideslope pointer was identical to that of the HSI glideslope, but the ADI localiser was expanded (thereby providing increased sensitivity) relative to the corresponding HSI indication by a factor of approximately two.

Localiser and glideslope indications on both instruments were provided with validity flags, which could be driven independently by the DGPS equipment to signify the presence or absence of valid localiser and/or glideslope data.

A 'To/From' indication was also provided as part of the HSI course carriage: this could be driven to either the 'To' or 'From' state, or hidden from view, under the control of the ECU.

The navigation switching arrangements allowed each pilot to independently select DGPS-derived data for display on his own instruments, although the system design imposed a number of restrictions when in DGPS mode (most significantly, neither

pilot was able to obtain normal No. 1 NAV receiver (VOR/ILS) indications whilst DGPS data display was enabled). These restrictions were considered to be acceptable for the purposes of an experimental trial but would be undesirable in an operational installation.

The central cockpit DME display (Figure 3) was also capable of being driven by the ECU. This unit allowed distances to be displayed to two decimal places, and also provided an alphanumeric identifier (normally used to display the DME facility ident) which was displayed alongside the distance.



Figure 3 Distance and Ident Display on DME Indicator

Embedded software executing within the ECU at a 100Hz rate used the DGPS and aircraft data as inputs and computed output values for transmission to the cockpit systems. Software was developed using a high-level language, to allow full advantage to be taken of the processor's floating-point capabilities. The processor throughput (i.e. limitations due to the finite computing time available) was not expected to be an issue.

Parameters necessary to define the approach profiles were sent to the ECU via a cabin-mounted laptop PC computer, which was controlled by the FTE. This was also able to monitor the operation and performance of the various elements of the experimental systems throughout each flight trial.

Midway through the trials programme, a small addition was made to the cockpit display arrangements. This was a small detachable panel (Figure 4) containing four LED indicators, which could be attached by either pilot to a suitable location on the instrument panel using hook-and-loop fasteners.

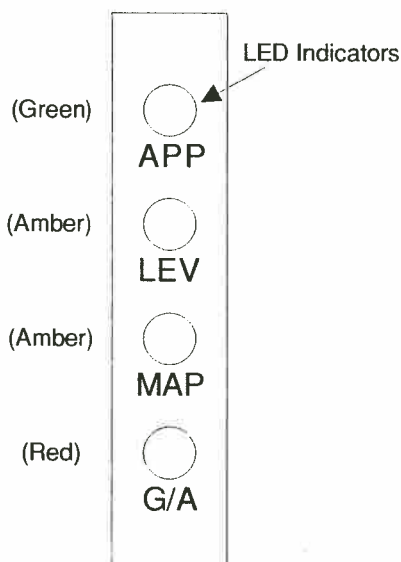


Figure 4 LED Indicator Panel

4.3 Designing the DGPS Approach Profile

In order to take best advantage of the capabilities and facilities provided by the experimental DGPS equipment installation, a new approach profile (summarised on the approach plate shown in Figure 12, page 112) was developed.

Over the course of the flight trials programme a considerable amount of experimentation was performed in an attempt to refine the DGPS approach profile. This was very much an iterative process, in which the results of each trial (including feedback from the pilots) were actively employed in the planning and execution of subsequent sorties.

4.3.1 Horizontal Profile

One of the greatest drawbacks of the existing weather radar based procedure is the inclusion of the 10° and 15° offsets into the final approach track. This manoeuvring is necessary to ensure that the aircraft will remain clear of the platform structure in the event that visual contact cannot be established.

The inclusion of an offset procedure recognises that separation between aircraft and platform cannot be maintained directly by reference to any of the sources of data generally available to the pilot (Decca Navigator, NDB, weather radar).

The availability of a sufficiently accurate method for the determination of aircraft position offered the potential to employ an alternative method for ensuring separation. Rather than introducing a change in direction, the entire final approach path could be offset laterally to remain clear of the platform structure (Figure 5).

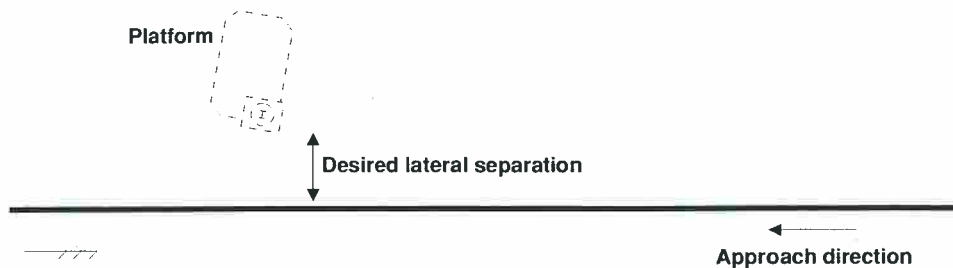


Figure 5 Laterally Offset Approach Track (plan view)

The extent of the lateral separation which is necessary at a particular location is dependent upon many factors, including the performance of the navigation data source itself, the presence of any error or uncertainty in the co-ordinate data defining the platform location, and the extent to which deviations of the aircraft ground track from the desired trajectory can be tolerated. An additional safety margin would also need to be added over and above all of the other error sources.

For the flight trials, it was decided to employ the smallest lateral offset which was envisaged to be viable for an operational approach guidance system. It was decided that the minimum acceptable lateral separation between the approach profile and the platform structure was of the order of 180m, which translated to a lateral offset relative to the platform centre of between 200m and 250m.

As is the case with the weather radar procedure, the lateral offset arrangement allows the approach to be carried out from any direction so as to be oriented into wind to

minimise the ground speed. It also allows the offset to be applied in either a left-hand or right-hand direction: the side chosen would be expected to be dependent upon such factors as the seating position of the handling pilot and the position of the helideck on the platform. Once satisfactory visual contact has been established, the aircraft would require to be manoeuvred to position for a landing and this might well favour one direction of lateral offset. The presence of additional obstacles (support vessels, crane barges etc.) might also dictate a preferred offset direction.

For the trials programme, approaches with both left and right-hand offsets were undertaken in approximately equal numbers, independently of the handling pilot's seating position. The lateral offset was 200m at the smaller platforms and 250m at the larger structures.

Having established the horizontal profile to be followed by the aircraft during an approach it is necessary to define the location at which a decision must be taken as to whether to continue with a landing (if visual contact has been established) or to go around. For the conventional weather radar approach, this Missed Approach Point (MAP) is defined in terms of a minimum range of 0.75nm from the platform.

With the laterally offset approach profile, the point on the approach at which minimum range is attained will be directly abeam the platform, assuming that no track changes are introduced during the go-around, and that the aircraft will continue to fly in a straight line. It was assumed that the aircraft would be flying level during this portion of the approach (section 4.3.2).

Consideration must, however, be given to the action to be taken by the aircraft crew in the event that visual contact with the platform is established. It is conceivable that, in marginal visibility conditions, a very late sighting might occur which, if it occurred at or shortly before reaching a MAP defined to be abeam the platform, could be too late for the crew to manoeuvre for a landing since the aircraft would effectively have passed the platform before a response could be made. Visual contact might also be lost again as the platform passed through the pilot's three o'clock or nine o'clock position.

It was decided that a more satisfactory location for the MAP would be a position at which the bearing of the platform relative to the approach track was still fairly small, e.g. of the order of 30° . In the event that the platform was sighted close to the MAP, this would allow the crew to manoeuvre for a landing without loss of visual contact (Figure 6).

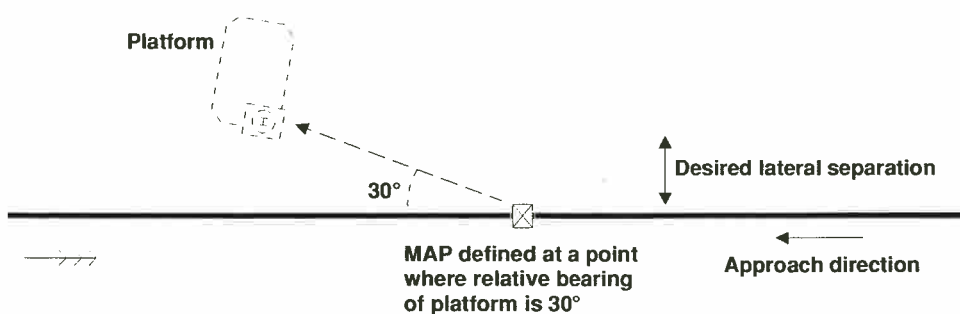


Figure 6 Definition of MAP (plan view)

For the purposes of the flight trials programme the MAP was defined in terms of a relative offset of exactly 30°, whilst recognising that it would not necessarily be practicable to complete a helideck landing from this MAP position at all offshore platforms due to location-specific differences in the relative orientation of the platform structure, helideck and approach track.

It was also necessary to define the point at which the aircraft would expect to be established on the approach track. A Final Approach Fix (FAF) at a range of around 4nm, as used for the weather radar approach, seemed to be appropriate and was selected for the trials programme.

4.3.2 *Vertical Profile*

The vertical profile to be followed by the aircraft during an offshore approach is subject to a number of constraints which are, to some extent, mutually exclusive.

- (1) Whilst the crew are attempting to obtain visual contact with the platform, the aircraft should be flying level at the chosen Minimum Descent Height (MDH). Assuming that the radio altimeter is servicable, a MDH of 200ft radalt is normally employed with the existing weather radar approach procedure.

The selection of the MDH does not appear to be influenced by the actual height of the platform helideck above the sea surface; instead it is normal practice for the aircraft to climb or descend as necessary to position for a landing, once visual contact had been established.

- (2) To minimise workload at this stage of the approach it is desirable for there to be no changes in height in the region of the missed approach point. In the weather radar case, the aircraft descends to MDH and remains level for a significant distance (about 2nm) before reaching the MAP.
- (3) To maintain the greatest degree of obstacle clearance it is desirable for the aircraft to remain at a safe altitude for as long as possible, and to only commence the descent to MDH at a comparatively short range from the platform.

In order to satisfy these requirements the vertical approach profile depicted in Figure 7 was developed. As in the case of the weather radar approach, the portion of the approach centred on the MAP would be flown level at MDH, satisfying requirements (1) and (2); however the availability of more accurate positional data would allow the horizontal extent of this 'level segment', extending equally either side of the MAP for a set distance, to be considerably smaller than in the weather radar case so as to satisfy requirement (3).

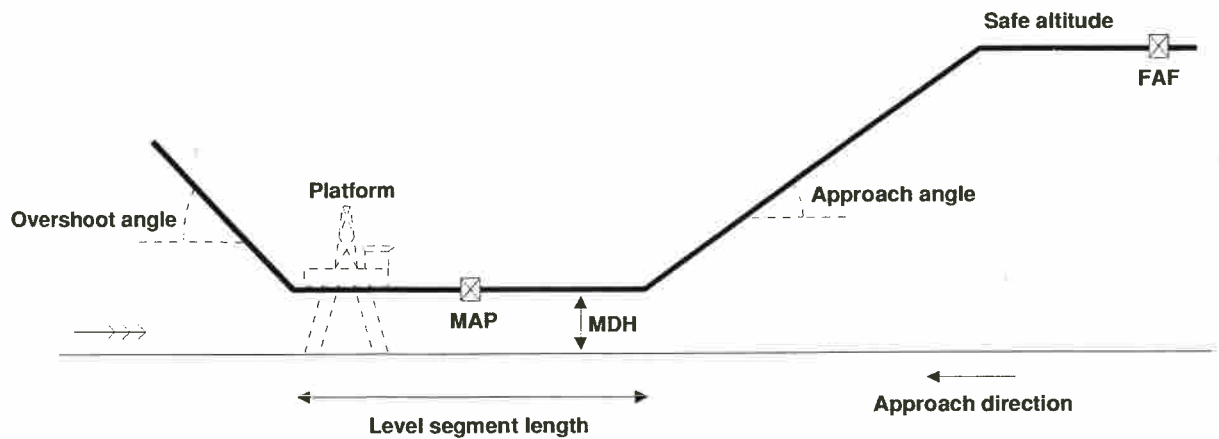


Figure 7 Vertical Approach Profile

The shortest operationally acceptable length for the level segment was determined to be somewhere in the region of 1500m: at a nominal 80kt ground speed this would correspond to approximately 35s of level flight. Accordingly, a level segment length of 1500m was selected for the trials programme.

For the transition from safe altitude down to MDH, it was possible to construct a fixed angle approach path which was similar in concept to an ILS glide slope. This 'approach segment' was arranged to end at the start of the level segment.

A similar concept was applied to produce a go-around or 'overshoot segment' (resembling a reverse glideslope), commencing at the end of the level segment. In the event that satisfactory visual contact with the platform could not be established prior to or upon arrival at the MAP, this arrangement would ensure that the aircraft would have passed safely abeam the platform before the go-around, with its associated climb demand and increase in pilot workload, was initiated.

A flight path angle of 3.5° was initially selected for the approach segment (in preference to the standard ILS glideslope angle of 3°) as this was comparable with the descent profile involved in the standard weather radar approach. It was expected, however, that this was one parameter whose value might require adjusting over the course of the trials programme.

For simplicity, the overshoot angle was initially set to 3.5° , identical to the approach angle.

4.3.3 *Guidance Presentation During the Approach*

Having decided upon the horizontal and vertical profiles described above as the basis for the experimental DGPS approach, it was then necessary to determine how the aircraft crew were to be provided with information to follow the approach trajectory, within the limitations of the experimental equipment installation.

The DGPS profile is broadly similar to a conventional onshore ILS approach in that it forms a locus of points representing the desired aircraft trajectory. An ILS system displays the position of the aircraft relative to this locus in the form of deviations in azimuth (localiser) and elevation (glideslope), which are directly related to the angular displacements in these two planes.

In the horizontal plane, both the DGPS approach profile and an ILS localiser are represented by a single straight line. The latter, however, terminates at a point (the localiser antenna position) shortly beyond the end of the runway, and the displayed ILS azimuth deviations are directly related to angles fanning out from this position.

In order to provide a continuous display of horizontal deviation throughout the DGPS approach, it was necessary for the displayed deviation to be based upon linear (cross-track) displacement rather than upon any form of angular measurement. There was, however, no reason why the linear scaling could not vary with position relative to the MAP, so as to provide both maximum sensitivity close to the platform and a wider 'capture band' at longer ranges.

In the vertical plane, the DGPS profile is composed of a series of straight-line segments rather than the single straight line of an ILS glideslope. The requirement for a continuous display throughout the approach dictated that the displayed vertical deviation would need to be based upon the aircraft's linear (vertical) displacement relative to this profile, possibly with variations in the linear scaling according to the distance from the MAP.

In an ILS installation, the localiser and glideslope equipment is frequently supplemented by a continuous digital DME readout of the range from a defined feature (normally the runway touchdown point). It was clear that a similar feature would be useful for the DGPS approach, although it was not immediately obvious which feature should be chosen as the 'origin' for the range display.

Owing to the segmented nature of the vertical DGPS profile, it was decided that situational awareness could be enhanced by providing an unambiguous indication of the current approach segment to supplement the DME-format range display.

It was therefore decided that the guidance information displayed to the pilot during an approach should consist of the following elements:

- (1) Localiser (azimuth) deviation, proportional to the lateral positional displacement of the aircraft from the desired approach track ('cross-track error').
- (2) Glideslope (elevation) deviation, proportional to the vertical positional displacement of the aircraft relative to the desired approach profile ('vertical error').
- (3) Distance to go indication (in miles to two decimal places), selectable between the following two alternative formats:

True distance from aircraft to platform ('true range'), or

Distance from aircraft to MAP, resolved along the approach direction ('along-track distance').

- (4) An alphanumeric indication of the current approach segment, to display one of the following four captions:
 - (a) Approach segment ('APP').

- (b) Level segment, between end of approach segment and MAP ('LEV').
- (c) Level segment, between MAP and start of overshoot segment ('MAP').
- (d) Overshoot segment ('G A').

The constant of proportionality implied in items (1) and (2) was specified, for convenience, in terms of the aircraft displacement which would result in a full scale deflection of the appropriate HSI indication. For example, if the full scale vertical sensitivity were $\pm 100\text{ft}$ then a 50ft vertical error would result in a half scale glideslope indication.

Instead of employing sensitivities which varied continuously with distance from the MAP, it was decided that it would be preferable to keep the scale factors fixed whilst the aircraft was in transit through the level segment. The necessity was also recognised of employing a reduced sensitivity at larger ranges from the MAP in order to facilitate the initial 'capture' of the horizontal and vertical profiles.

For convenience it was decided to employ three independent pairs of scaling values (Figure 8), the first of which would apply throughout the level segment. The other two would apply at distances of 4nm from the MAP on the approach and overshoot segments. Between the 4nm points and the ends of the level segment, the sensitivity would vary linearly with distance giving rise to a 'fanned' effect (as can be observed on the approach plots in section 5).

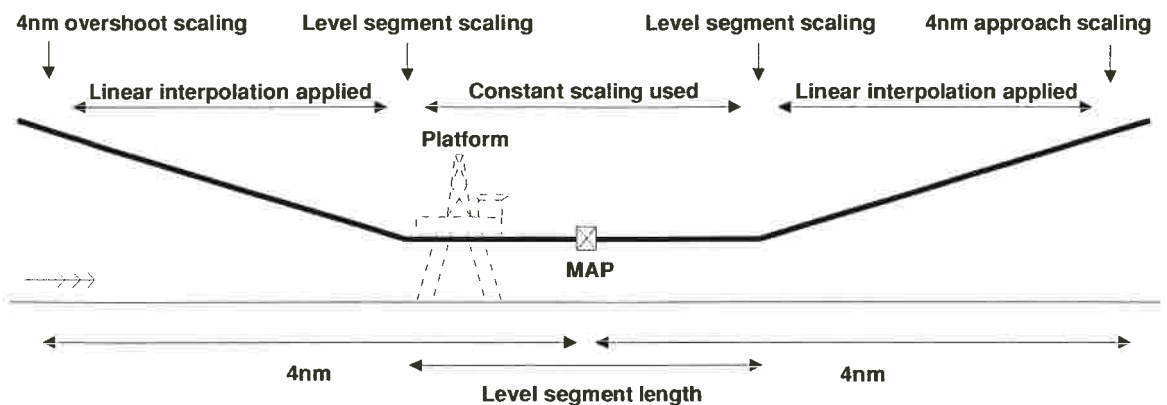


Figure 8 Specification of Instrument Scalings

Items (1), (3) and (4) could be computed directly from the horizontal position solution output by any of the DGPS receivers. The computation of item (2) required both a position solution, to provide the current along-track distance to the MAP from which the desired height could be determined, and data relating to the current aircraft height.

Three alternative sources of height data were available: these were DGPS altitude, radio altimeter height, and barometric altitude. It was felt that the radio altitude offered the most relevant information as it would provide a direct indication of the aircraft's vertical position relative to the sea surface. The other two parameters could be related to altitudes above mean sea level (from knowledge of the WGS84 geoid-ellipsoid separation, and of the current barometric pressure, respectively), but not to the actual sea conditions. As a result the radio altimeter was selected as the primary source of vertical data.

Whereas data from the radio altimeter was sampled at 1kHz, the DGPS receivers only provided new position fixes at 1s intervals. Using this information directly would have resulted in a disjointed form of approach guidance, with step changes occurring in the displayed indications at a 1Hz rate. This would, in particular, have prevented taking full advantage of the two decimal places available on the DME display.

Since both position and velocity data were available each second from the DGPS receivers, it was decided that some form of extrapolation technique would provide smoother indications. The simplest technique considered was a basic linear extrapolation, in which the last known position solution was supplemented by adding (in vector form) the last known velocity solution multiplied by the age, in seconds, of the fix data:

$$\text{Current Position} = \text{Last GPS Position} + \text{Last GPS Velocity} \times \text{Age of GPS Fix}$$

A number of higher-order extrapolation schemes, which potentially offered an improvement over the basic linear extrapolation, were also considered (ref 1). These were polynomial prediction functions based upon the last two (quadratic extrapolation) or three (cubic extrapolation) position/velocity solutions. The relative weightings of the various terms in the polynomials were determined by regression analysis.

Unfortunately, these higher-order extrapolation functions proved difficult to implement in software without giving rise to instabilities which significantly affected the guidance indications (this had been identified as a possible problem in ref 1). As a result, it was decided to employ the linear extrapolation method.

To minimise the effects of sampling quantization and other noise sources on the analogue radio altimeter input to the ECU, the acquired data was passed through a two-pole low pass filter (damping ratio 0.7) prior to its use in the computation of the glideslope deviation signal. A default value of 10Hz (at the -3dB point) was chosen for the filter bandwidth, consistent with the radalt sensor's time constant of 90ms.

4.4 ECU Implementation of Approach Guidance

The profiles and data presentation described in the previous section were implemented by means of custom software executing within the airborne ECU.

In order to fully specify the desired approach, a series of parameters was defined which could be set up and modified under FTE control using the cabin laptop PC. Table 1 lists the principal approach parameters.

Category	Parameter	Units	Default
Platform position	Platform waypoint latitude	deg	n/a
	Platform waypoint longitude	deg	n/a
	Magnetic variation	deg	n/a
Approach track definition	Approach QDM (magnetic)	deg	n/a
	Approach track offset (left or right)	m	200m
	MAP position	deg	30 deg
Level segment	Level segment length	m	1500m
Vertical profile	Approach angle	deg	3.5 deg
	Level segment height	ft	200ft
	Overshoot angle	deg	3.5 deg
Horizontal sensitivity (deviation resulting in full scale instrument deflection)	Horizontal sensitivity at 4nm on approach	m	±425m
	Horizontal sensitivity through level segment	m	±120m
	Horizontal sensitivity at 4nm on overshoot	m	±425m
Vertical sensitivity (deviation resulting in full scale instrument deflection)	Vertical sensitivity at 4nm on approach	ft	±350ft
	Vertical sensitivity through level segment	ft	±100ft
	Vertical sensitivity at 4nm on overshoot	ft	±350ft
DME display mode	Selectable between along-track distance to MAP, and true range to platform	n/a	Distance to MAP

Table 1 Principal Approach Guidance Parameters

The values shown in the 'Default' column in the table are those which were selected prior to the flight trials programme, and effectively defined the 'starting point' for experimentation with different approach parameters.

The ECU software was arranged to execute the guidance algorithm routine at a rate of 100Hz. This routine took as inputs the currently selected approach parameters,

together with details of the last DGPS solution and the current radio altitude, and executed a series of operations which can be summarised as follows:

- (1) On receipt of an updated DGPS position fix, compute and store the aircraft position in metres North and East relative to the platform waypoint using the defined platform latitude and longitude.

Since the guidance algorithms would only be used at short ranges from the platform, a basic conversion algorithm was employed based upon the WGS84 earth model radii of curvature. No attempt was made to correct for 'great circle' distances.

- (2) Multiply the last DGPS velocity fix by the age of the data, and add to the result of step (1) to determine the linearly extrapolated position.
- (3) Using the defined QDM, magnetic variation, track offset and MAP position, convert the result of step (2) to along-track and cross-track positions relative to the MAP and approach track.
- (4) Using the defined level segment length and the along-track distance computed at step (3), determine the current segment: approach, level or overshoot.
- (5) Determine the appropriate horizontal guidance sensitivity according to the result of step (4), and divide the cross-track distance by this sensitivity to yield the localiser deviation signal (limiting to \pm full scale deviation).
- (6) Compute the desired height at the present position using the along-track distance (3) and current segment (4).
- (7) Subtract the result of step 6 from the low-pass filtered radio altimeter signal to determine the vertical error.
- (8) Determine the appropriate vertical guidance sensitivity according to the result of step (4), and divide the vertical error (7) by this sensitivity to yield the glide slope deviation signal (limiting to \pm full scale deviation).
- (9) Determine the DME range using the results of steps (2) and/or (3) according to the selected display mode.
- (10) Determine the alphanumeric segment identifier for the DME display from the result of step (4).

4.5 Enhancements to the Basic Approach Guidance

During the course of the trials programme a number of additional features were added to the approach guidance software as a result of pilot feedback. These changes can be summarised as follows:

4.5.1 Vertical Fairing

The transition between the approach segment and level segment was modified by providing a short 'faired' section between the two straight-line segments.

The approach fairing was implemented by including a short parabolic section into the vertical profile, between the approach and level segments (Figure 9). The 'faired' section was arranged so that there was no discontinuity in rate of change of height at either end.

An additional approach parameter was added, which defined the size of the 'faired' segment. This was initially implemented as the height above MDH at which the faired section would commence, and was set to 50ft. To avoid the necessity of modifying this value if a different approach angle was selected, the parameter definition was subsequently changed to specify the horizontal distance in advance of the level segment at which the fairing would commence, with a default value of 500m which, for a 3.5° approach angle, is directly equivalent to a 50ft fairing height.

The facility was also included (not shown in Figure 9) to enable vertical fairing for the transition from the level to the overshoot segment. This operated in an identical manner to the approach fairing, with a separate parameter to define the extent of the fairing.

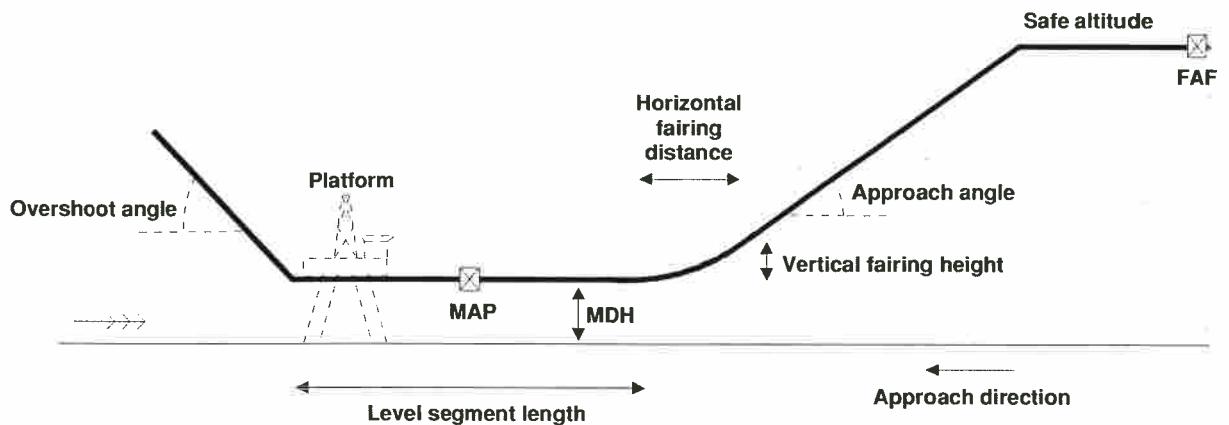


Figure 9 Introduction of Fairing into Vertical Profile

4.5.2 Approach Mode LEDs

A set of four LED indicators was added to the trials installation midway through the programme.

The LEDs were arranged to duplicate the approach mode information shown on the DME display, and were labelled as follows:

- (1) 'APP' (green): Approach segment.
- (2) 'LEV' (amber): Level segment, between end of approach segment and MAP.
- (3) 'MAP' (amber): Level segment, between MAP and start of overshoot segment.
- (4) 'G/A' (red): Overshoot segment.

Following the initial introduction of the LEDs, various minor changes were made to the software so as to vary the sequencing slightly (for example, to provide flashing indications). The sequencing arrangement eventually selected was as follows:

- (1) Approach: Continuous 'APP'.
- (2) On commencement of vertical fairing: Continuous 'APP' plus flashing 'LEV'.
- (3) From start of level segment: Continuous 'LEV'.
- (4) Once MAP reached: Continuous 'MAP'.
- (5) From start of overshoot segment: Flashing 'G/A'.

4.5.3 *Curved and Segmented Approaches*

Prior to the approach segment, an additional two flight segments were added to allow curved and segmented approaches to be evaluated. For these two segments, guidance was provided only in the horizontal plane.

The range at which these segments were joined to the straight-in approach was termed the Final Approach Fix (FAF) range and was implemented as a user-selectable parameter (typically 4nm).

In advance of the FAF a curved segment was added consisting of an arc of a circle, specified by means of its radius, included angle, and direction of turn. This was preceded by an additional straight segment.

These additional segments were introduced in an attempt to provide 'seamless' guidance through the overhead and downwind legs of a conventional weather radar approach, and around the turn to intercept the approach segment. This is illustrated on the approach plate shown in Figure 12 (page 112).

Setting the radius of the curved segment to zero resulted in a segmented horizontal approach profile. By default, the curved/segmented approach facility was disabled.

4.5.4 *Turnaway on Entry to Overshoot*

A facility was added to provide a turn on completion of the level segment, to allow for an overshoot which was not directly straight ahead.

The turnaway manoeuvre (Figure 10) was specified by means of the turn angle, direction of turn, and the horizontal distance over which the turn would be introduced.

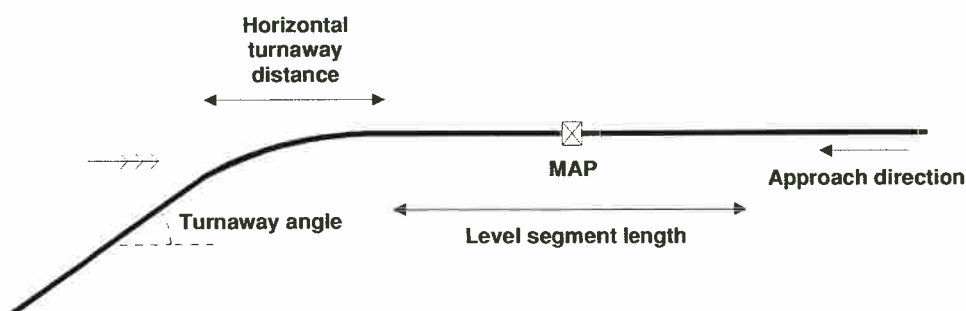


Figure 10 Introduction of Turnaway on Overshoot (plan view)

4.6 Platform Survey Data

Survey data relating to each platform to be visited was obtained from the relevant operator and used to derive latitude and longitude co-ordinates for a defined point on the platform. This information was typically not available directly with respect to the international WGS84 datum but was instead sourced in the relevant 'local' datum (European Datum 1950, ED50) and converted to WGS84 using a commercial software package. Failure to impose the correct co-ordinate conversion would have resulted in relatively large co-ordinate errors, typically of over 100m.

Owing to the limited availability of survey data for some of the platforms, in particular some of the older structures, it was not always possible to obtain WGS84 co-ordinates before the trial to an accuracy of better than around $\pm 50\text{m}$ in the horizontal axes. More accurate survey data was, however, obtained after the flight by post-processing the GPS data recorded by the platform measurement system (the processing involved is described in Volume 2 of this report).

Data relating to the helideck and overall structure height for each platform was also available from the relevant operator, expressed relative to mean sea level (msl). These msl heights differed from the corresponding WGS84 ellipsoidal heights by a fixed offset at each location (typically around 50m) whose value could be estimated from the available geodetic data to within a few metres.

Radio altimeter heights differed from msl heights as a result of prevailing tidal and wave conditions and the precise relationship was not known in advance of the trials.

Heights derived from barometric (pressure altitude) data could be related to msl heights from knowledge of the prevailing air pressure (QNH) and temperature reported by the platform.

5 EXPERIMENTAL DGPS APPROACHES

This chapter presents, in chronological order, details of each of the DGPS approaches flown over the course of the trials programme. Full details of the approach manoeuvres undertaken on each of the seven test flights are contained in refs 2 to 12.

The results have been grouped by flight trial, with a brief introduction to each flight providing details of any information which is specific to the trial itself rather than to particular approaches (e.g. equipment configuration). Any generic pilot comments, and a summary of the results from each trial, are also presented.

A single-page format has been adopted for each individual approach within a flight trial, containing details of the approach setup, pilot comments, and any other pertinent observations in tabular format. A series of plots is also shown, which represents the aircraft trajectory and guidance information displayed during each approach.

The approach data table contains the following information:

- (1) Flight number: 1 to 7 in the series - dates and locations are shown in Table 2.
- (2) Approach number: sequence number within the flight.
- (3) Location: point used as destination waypoint for the approach. 'Arbitrary' refers to locations over the sea at which no physical structure was present.
- (4) Wind: direction ($^{\circ}$ M) and speed (kt), normally as reported from the platform.
- (5) Approach track: direction ($^{\circ}$ M) and offset (left or right of platform).
- (6) Approach angle, Overshoot angle: segment angles in degrees.
- (7) DGPS source, Height source: selected sources of horizontal and vertical data.
- (8) Horizontal/vertical sensitivities: values which correspond to full-scale instrument deflection for the following three points: 4nm range from the MAP on the approach; level segment; and 4nm range from the MAP on the overshoot.
- (9) Entry technique: details of the manoeuvre used by the pilot to intercept the approach segment (see below).
- (10) Go-around technique: details of the manoeuvre flown by the pilot after the MAP.
- (11) Handling pilot: identification (by initials) of the pilot flying the approach.
- (12) Method: 'raw data' approaches were manually flown using the HSI/ADI deviations, 'flight director' approaches were manually flown using the ADI command bar information, and 'autopilot' approaches were autocoupled.

- (13) Start and end times: UTC times for start and end of the data plotted on the graphs.
- (14) Other details: any other pertinent information relating to the guidance setup used.
- (15) Pilot comments: a paraphrased version of any comments recorded by the handling pilot.
- (16) Observations: any other comments relating to the approach (e.g. in-flight observations by the FTE, or deductions following analysis of the data).

Flight	Date	Details
1	12th April 1996	Shakedown flight to and from Longside
2	8th May 1996	Offshore test flight: Beatrice C
3	19th June 1996	Ground trials at Longside
4	30th July 1996	Offshore test flight: Piper B
5	1st August 1996	Offshore test flight: Tartan A
6	26th September 1996	Offshore test flight: Buchan A
7	31st October 1996	Offshore demonstration flight: Beatrice A and C

Table 2 DGPS Flight Trials

For each approach a series of four graphs is shown, each of which has an identical horizontal scale which is based upon the along-track distance from the MAP. The plots commence at 7000m (3.8nm) range on the approach and end 1000m beyond the MAP.

The two left-hand plots represent the horizontal profile flown, in terms of the actual aircraft trajectory in plan view (upper) and the localiser deviations displayed (lower). These are derived, respectively, from the post-processed carrier-phase truth position history, and from the recorded horizontal HSI deviation data.

The two corresponding right-hand plots represent the vertical profile flown, depicting the aircraft trajectory in elevation (upper) and the glideslope deviations displayed (lower). These are derived from the recorded radio altitude data and from the recorded HSI vertical deviations, respectively.

On the two upper plots, a pair of 'fan lines' is shown which represents the locus of the points in space at which full-scale instrument deviation would have been displayed in the horizontal and vertical planes. The position of the fan lines varies according to the parameters used to specify the approach.

For many of the approaches (a minimum of four at each platform), the entry technique is described as 'modified Aerad'. This was essentially the manoeuvre

depicted in Figure 12 (page 112), incorporating an overflight of the platform at 1500ft, a descent to 800ft on the outbound leg, and a turn through 200° to intercept the inbound DGPS guidance. The term 'modified Aerad' derives from the fact that the overflight and outbound leg are identical to the weather radar procedure in Figure 11 (page 111).

For the majority of the 'modified Aerad' approaches, guidance during the outbound leg and around the turn was not provided by the DGPS equipment: instead, the pilot programmed appropriate waypoints into the RNAV-2 navigation computer and used the resulting guidance information in exactly the same manner as when flying a standard weather radar approach.

5.1. **Flight Trial 1**

The first test flight was intended primarily as a 'shakedown' of the airborne system. In the event a number of software and hardware problems were discovered and these were corrected prior to the subsequent test flight.

A series of DGPS approaches was undertaken along the coast to the northeast of Aberdeen, using a defined coastal feature (Blackdog Rock) as a simulated platform waypoint. On this trial only, a level segment height of 500ft was required in place of 200ft in order to comply with the low-flying regulations.

As a result of a programming error, the approach segment positioning was incorrect, with the result that discontinuities were present in the vertical profile and, to a lesser extent, in the horizontal profile.

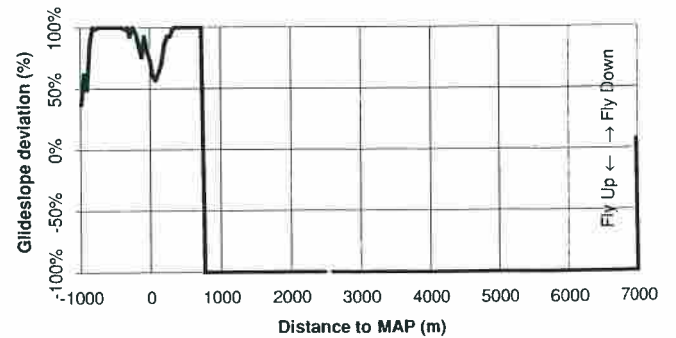
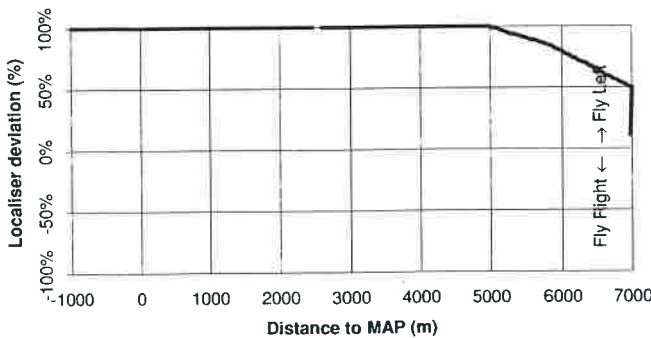
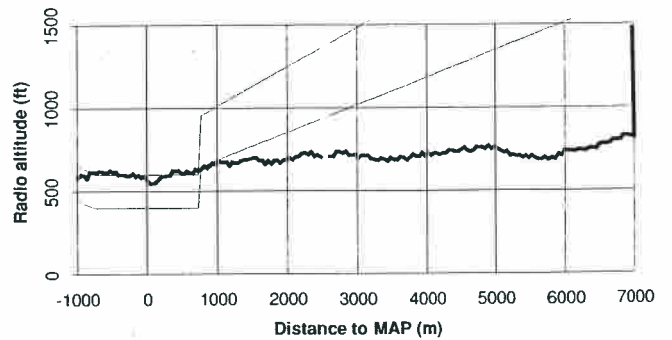
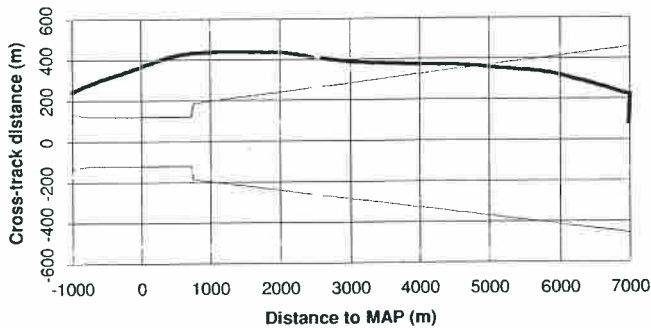
A hardware fault prevented the HSI localiser and glideslope flags from 'clearing', despite the presence of valid DGPS data. This was identified during the flight and the pilot was instructed to assume that the displays were, in fact, showing valid data.

The same fault prevented range data from being displayed on the central DME readout: in its absence the FTE was able to obtain this information from the laptop PC display and relay it to the pilot.

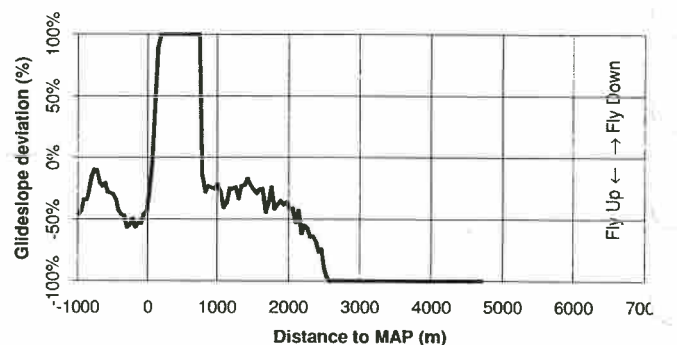
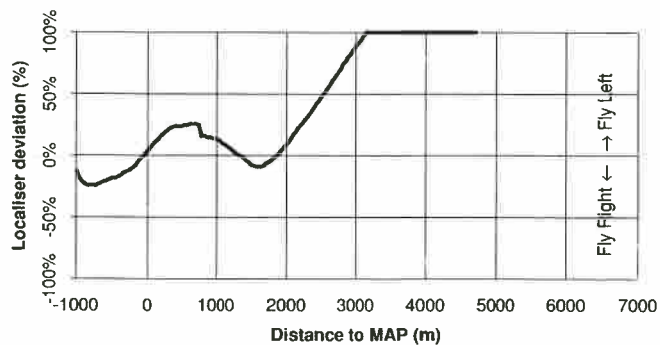
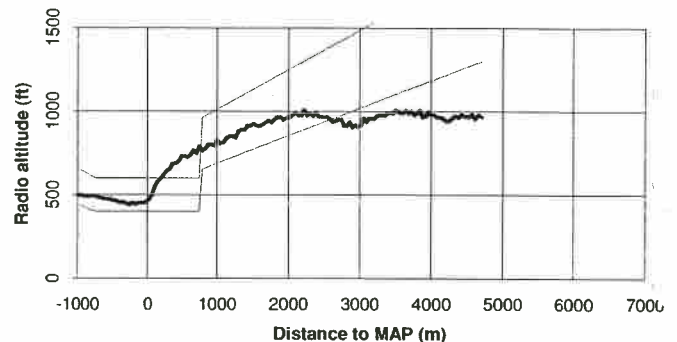
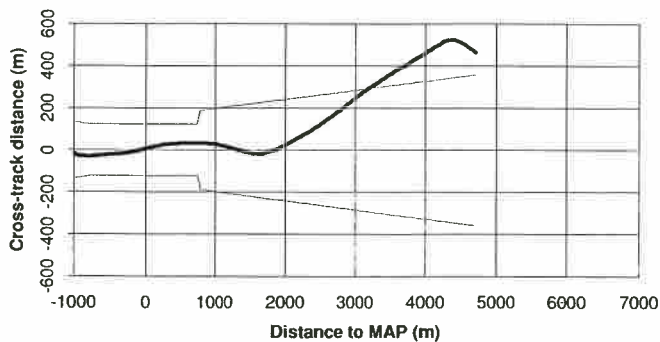
In spite of these difficulties, a series of DGPS approaches was successfully undertaken and served to prove that there were no fundamental difficulties with the basic concept of the new approach profiles.

The pilots were able to identify that the value initially chosen for the horizontal scaling at 4nm range appeared to be too low. Doubling this parameter (to $\pm 850\text{m}$) proved beneficial and a decision was taken to employ this new value on subsequent trials.

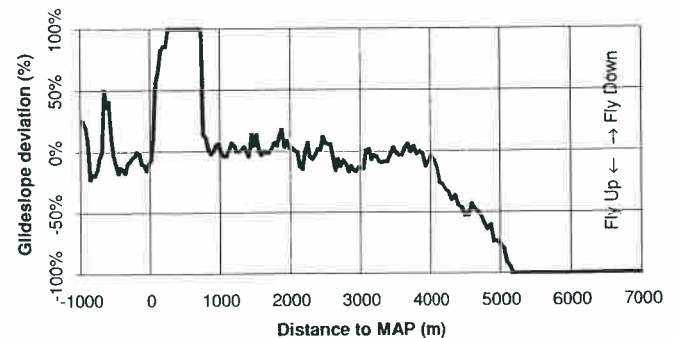
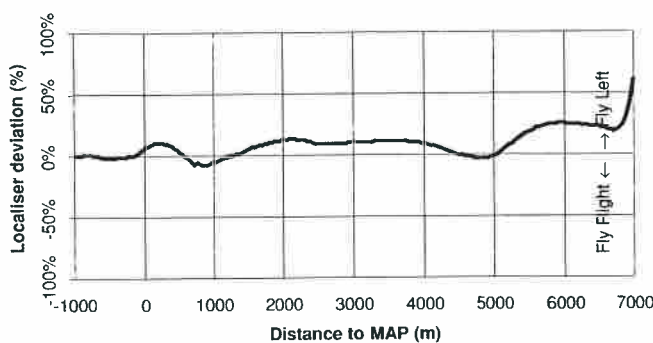
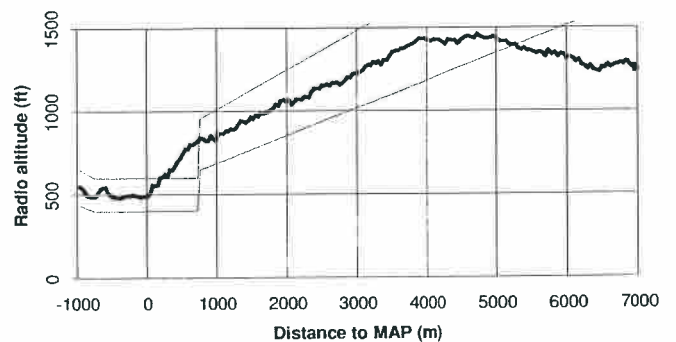
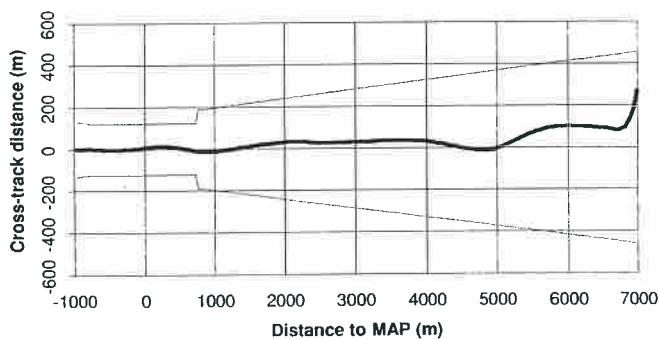
Flight number: 1	Approach number: 1	Location: Blackdog	Wind: 140-150°M, 20kt
Approach track: QDM 207°M, 200m left offset		Approach angle: 3.5°	Overshoot angle: 3.5°
DGPS source: GD1 (MF-corrected Navstar)		Height source: radio altimeter	
Horizontal sensitivities:	4nm approach: ±425m	Level segment: ±120m	4nm overshoot: ±425m
Vertical sensitivities:	4nm approach: ±350ft	Level segment: ±100ft	4nm overshoot: ±350ft
Entry technique: aircraft flown directly to a point at around 4nm range to intercept the approach.			
Go-around technique: straight ahead from MAP, climbing as directed by DGPS guidance.			
Handling pilot: NT	Method: Raw data	Start Time: 11:35:04	End Time: 11:38:05
Other details: As a result of a programming error the approach segment was incorrectly positioned relative to the level segment. Localiser and glideslope deviation indications were displayed to the pilot but were flagged as invalid owing to a failure of the interface hardware. This failure also prevented range indications being shown on the DME indicator.			
Pilot comments: No attempt was made to follow the HSI indications as these were shown as invalid: instead a manual visual approach to the target was flown.			
Observations: n/a.			



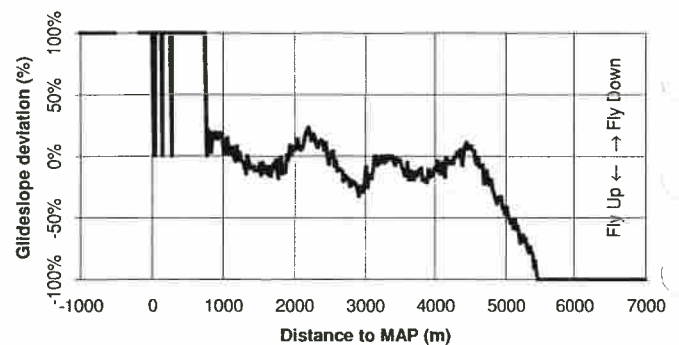
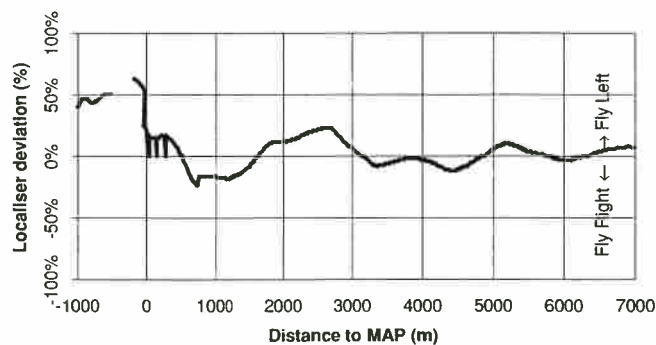
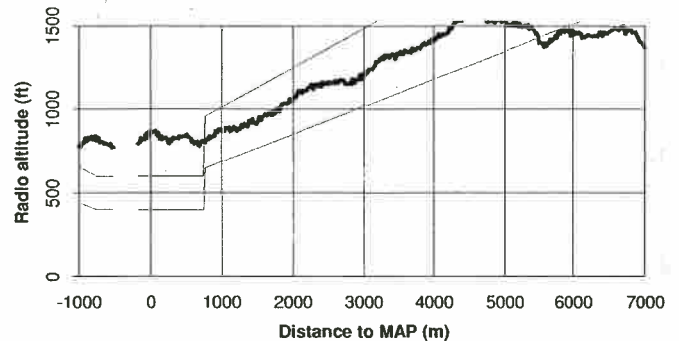
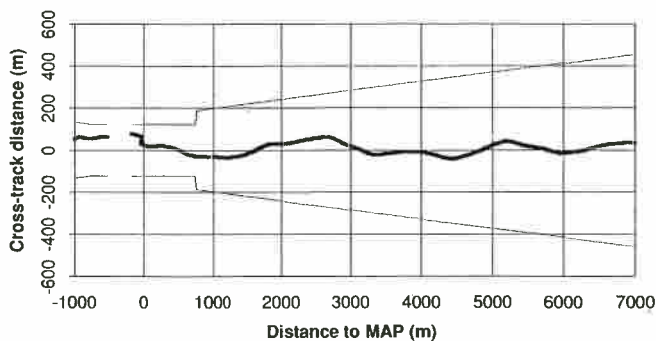
Flight number: 1	Approach number: 2	Location: Blackdog	Wind: 140-150°M, 20kt
Approach track: QDM 207°M, 200m left offset		Approach angle: 3.5°	Overshoot angle: 3.5°
DGPS source: GD1 (MF-corrected Navstar)		Height source: radio altimeter	
Horizontal sensitivities:	4nm approach: ±425m	Level segment: ±120m	4nm overshoot: ±425m
Vertical sensitivities:	4nm approach: ±350ft	Level segment: ±100ft	4nm overshoot: ±350ft
Entry technique: aircraft flown directly to a point at around 4nm range to intercept the approach.			
Go-around technique: straight ahead from MAP, climbing as directed by DGPS guidance.			
Handling pilot: NT	Method: Raw data	Start Time: 11:41:59	End Time: 11:44:19
Other details: As a result of a programming error the approach segment was incorrectly positioned relative to the level segment. Localiser and glideslope deviation indications were displayed to the pilot but were flagged as invalid owing to a failure of the interface hardware. This failure also prevented range indications being shown on the DME indicator.			
Pilot comments: The HSI indications were treated as valid despite the presence of the flag indications, and appeared to provide sensible guidance during the approach (but not the level) segment.			
Observations: On entry to the level segment the aircraft was not at the desired height, due to the incorrect positioning of the approach segment, causing a full-scale fly down indication on the glideslope.			



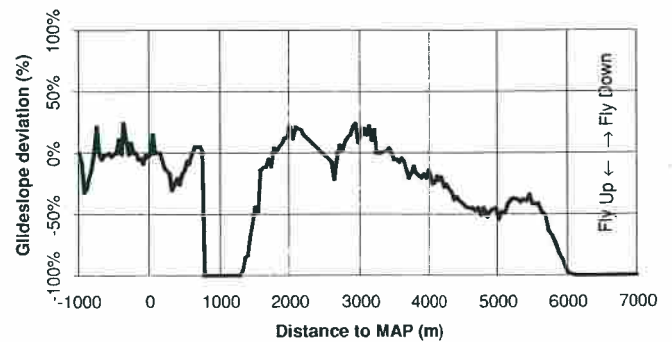
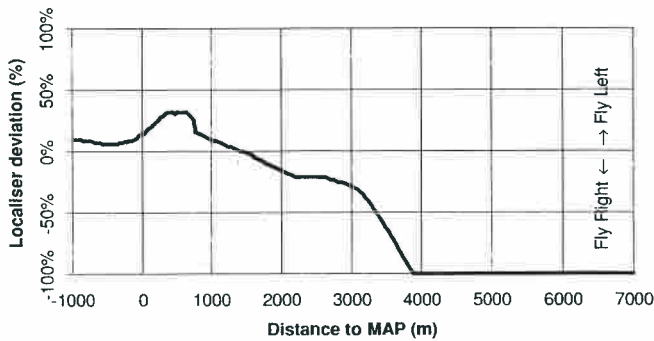
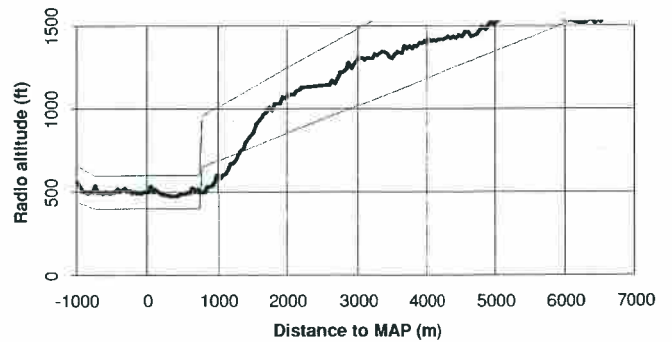
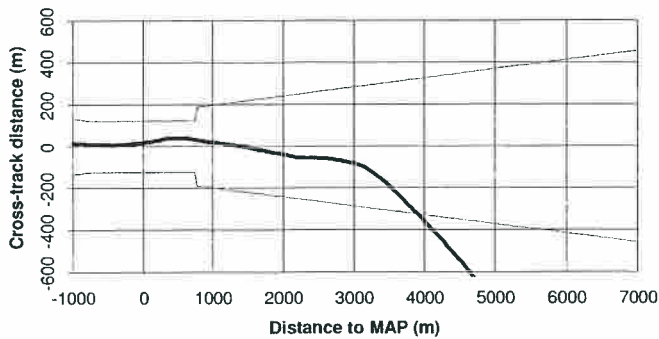
Flight number: 1	Approach number: 3	Location: Blackdog	Wind: 140-150°M, 20kt
Approach track: QDM 207°M, 200m left offset		Approach angle: 3.5°	Overshoot angle: 3.5°
DGPS source: GD1 (MF-corrected Navstar)		Height source: radio altimeter	
Horizontal sensitivities:	4nm approach: ±425m	Level segment: ±120m	4nm overshoot: ±425m
Vertical sensitivities:	4nm approach: ±350ft	Level segment: ±100ft	4nm overshoot: ±350ft
Entry technique: aircraft flown directly to a point at around 4nm range to intercept the approach.			
Go-around technique: straight ahead from MAP, climbing as directed by DGPS guidance.			
Handling pilot: NT	Method: Raw data	Start Time: 11:47:03	End Time: 11:50:34
Other details: As a result of a programming error the approach segment was incorrectly positioned relative to the level segment. Localiser and glideslope deviation indications were displayed to the pilot but were flagged as invalid owing to a failure of the interface hardware. This failure also prevented range indications being shown on the DME indicator.			
Pilot comments: Lateral guidance appeared to be 'about right'. On entry to the level segment the vertical guidance appeared to be demanding a height of 760ft and not 500ft as expected: there was then a sudden jump to a 500ft demand.			
Observations: The aircraft was not at the desired height on entry to the level segment as a result of the programming error.			



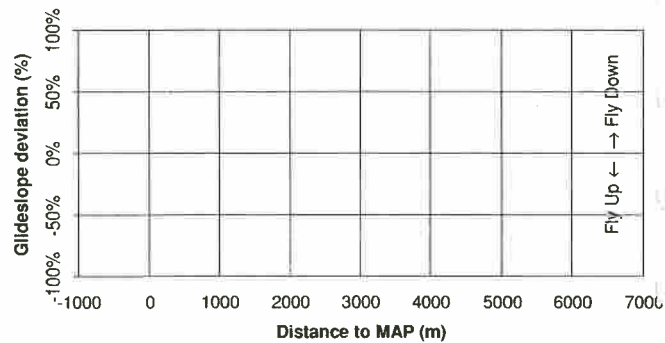
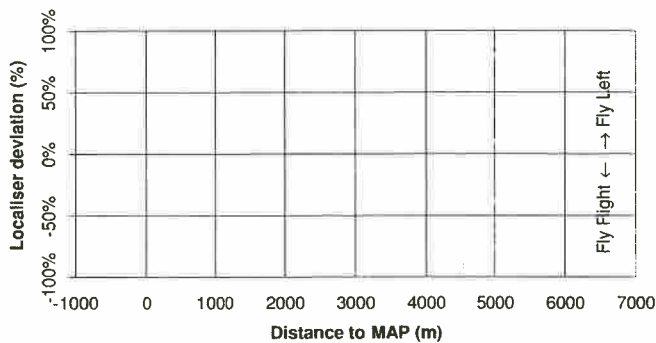
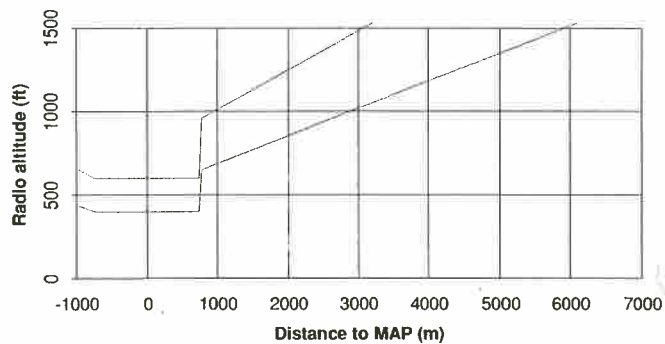
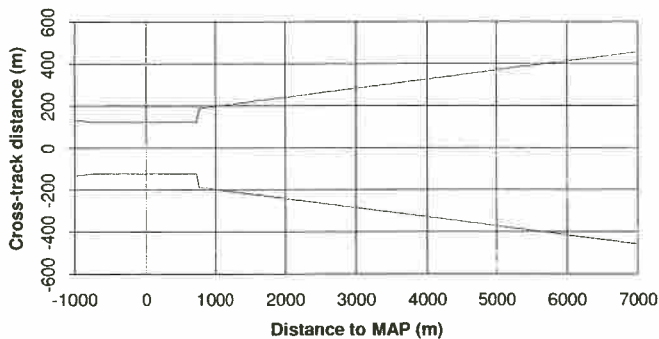
Flight number: 1	Approach number: 4	Location: Blackdog	Wind: 140-150°M, 20kt
Approach track: QDM 207°M, 200m left offset		Approach angle: 3.5°	Overshoot angle: 3.5°
DGPS source: GD1 (MF-corrected Navstar)		Height source: radio altimeter	
Horizontal sensitivities:	4nm approach: ±425m	Level segment: ±120m	4nm overshoot: ±425m
Vertical sensitivities:	4nm approach: ±350ft	Level segment: ±100ft	4nm overshoot: ±350ft
Entry technique: aircraft flown directly to a point at around 4nm range to intercept the approach.			
Go-around technique: straight ahead from MAP, climbing as directed by DGPS guidance.			
Handling pilot: NM	Method: Raw data	Start Time: 11:55:06	End Time: 12:01:16
Other details: As a result of a programming error the approach segment was incorrectly positioned relative to the level segment. Localiser and glideslope deviation indications were displayed to the pilot but were flagged as invalid owing to a failure of the interface hardware. This failure also prevented range indications being shown on the DME indicator.			
Pilot comments: The localiser sensitivity at 4nm range was too high: a greater sector width would be preferable. No attempt was made to follow the displayed vertical guidance through the level segment as this was obviously faulty.			
Observations: Erroneous vertical guidance was again presented during the level segment.			



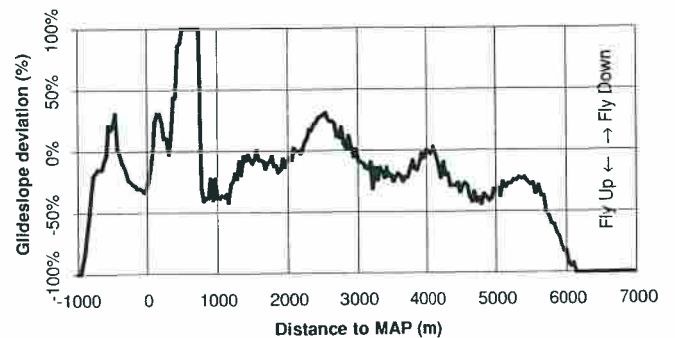
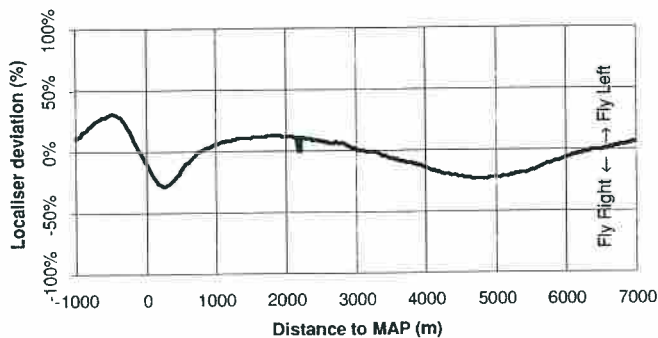
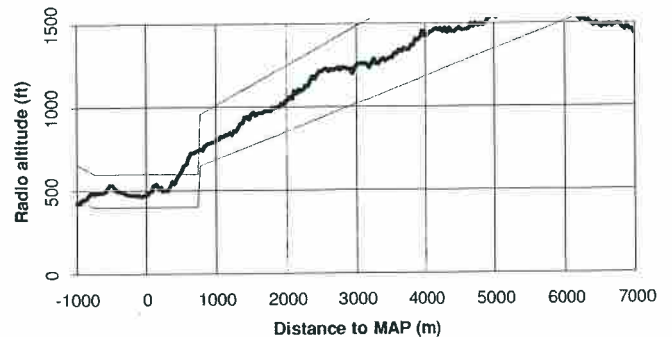
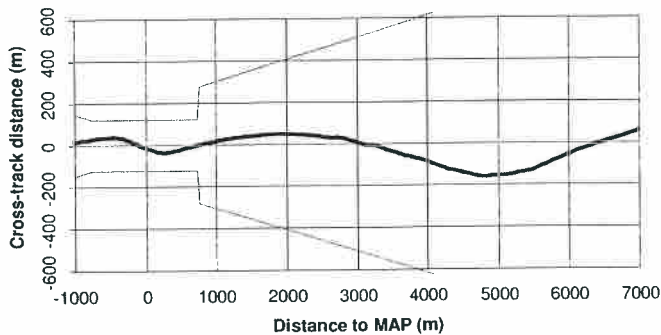
Flight number: 1	Approach number: 5	Location: Blackdog	Wind: 140-150°M, 20kt
Approach track: QDM 207°M, 200m left offset		Approach angle: 3.5°	Overshoot angle: 3.5°
DGPS source: GD1 (MF-corrected Navstar)		Height source: radio altimeter	
Horizontal sensitivities:	4nm approach: ±425m	Level segment: ±120m	4nm overshoot: ±425m
Vertical sensitivities:	4nm approach: ±350ft	Level segment: ±100ft	4nm overshoot: ±350ft
Entry technique: see below.			
Go-around technique: see below.			
Handling pilot: NM	Method: Raw data	Start Time: 12:09:37	End Time: 12:13:00
Other details: As a result of a programming error the approach segment was incorrectly positioned relative to the level segment. Localiser and glideslope deviation indications were displayed to the pilot but were flagged as invalid owing to a failure of the interface hardware. This failure also prevented range indications being shown on the DME indicator.			
Pilot comments: The lateral scaling at the start of the inbound leg was held to be too narrow.			
Observations: The approach was flown in the reverse direction (descending on the overshoot segment and climbing using the approach segment) in an attempt to investigate the vertical guidance problems. This revealed that the problem appeared to be a step change at the interface between the level segment and approach segment.			



Flight number: 1	Approach number: 6	Location: Blackdog	Wind: 140-150°M, 20kt
Approach track: QDM 207°M, 200m left offset		Approach angle: 3.5°	Overshoot angle: 3.5°
DGPS source: GD1 (MF-corrected Navstar)		Height source: radio altimeter	
Horizontal sensitivities:	4nm approach: ±425m	Level segment: ±120m	4nm overshoot: ±425m
Vertical sensitivities:	4nm approach: ±350ft	Level segment: ±100ft	4nm overshoot: ±350ft
Entry technique: aircraft flown directly to a point at around 4nm range to intercept the approach.			
Go-around technique: straight ahead from MAP, climbing as directed by DGPS guidance.			
Handling pilot: NM	Method: Raw data	Start Time: 12:14:14	End Time: 12:19:07
Other details: As a result of a programming error the approach segment was incorrectly positioned relative to the level segment. Localiser and glideslope deviation indications were displayed to the pilot but were flagged as invalid owing to a failure of the interface hardware. This failure also prevented range indications being shown on the DME indicator.			
Pilot comments: Sensitivities during the level segment appeared to be about correct for an approach conducted using a 200ft MDH.			
Observations: Data from this approach is not available due to a recording problem: indications were, in fact, presented throughout the approach.			



Flight number: 1	Approach number: 7	Location: Blackdog	Wind: 140-150°M, 20kt
Approach track: QDM 207°M, 200m left offset		Approach angle: 3.5°	Overshoot angle: 3.5°
DGPS source: GD1 (MF-corrected Navstar)		Height source: radio altimeter	
Horizontal sensitivities:	4nm approach: ±850m	Level segment: ±120m	4nm overshoot: ±850m
Vertical sensitivities:	4nm approach: ±350ft	Level segment: ±100ft	4nm overshoot: ±350ft
Entry technique: aircraft flown directly to a point at around 4nm range to intercept the approach.			
Go-around technique: straight ahead from MAP, climbing as directed by DGPS guidance.			
Handling pilot: NT	Method: Raw data	Start Time: 12:30:21	End Time: 12:34:18
Other details: As a result of a programming error the approach segment was incorrectly positioned relative to the level segment. Localiser and glideslope deviation indications were displayed to the pilot but were flagged as invalid owing to a failure of the interface hardware. This failure also prevented range indications being shown on the DME indicator.			
Pilot comments: Doubling the sector width at 4nm provided a much 'kinder' entry to the approach by easing the task of establishing on the localiser. Lateral scaling through the level segment was correct. It was difficult to evaluate the vertical scaling due to the presence of the step change but it appeared to be satisfactory.			
Observations: n/a.			



5.2 **Flight Trial 2**

The second test flight was performed at the Beatrice C platform and was the first offshore flight, allowing approaches to be performed with a level segment height of 200ft.

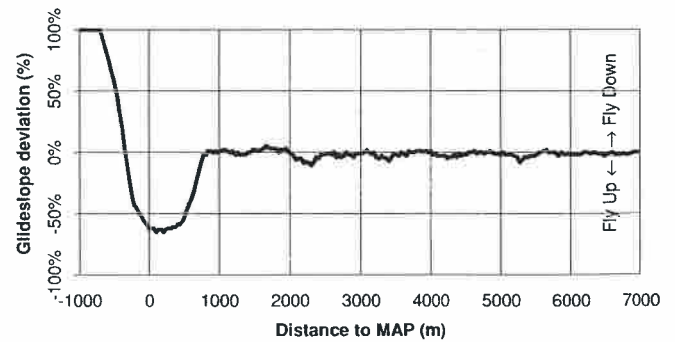
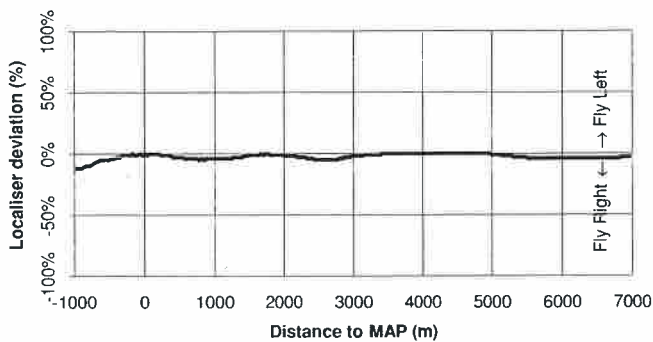
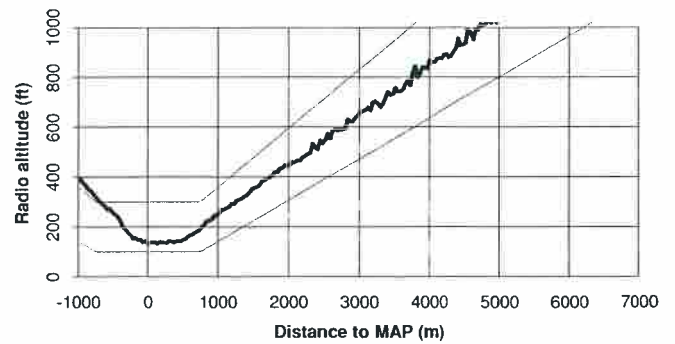
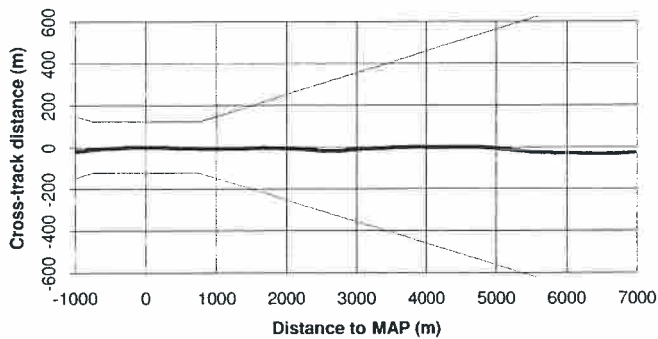
A small number of test approaches were also performed at arbitrary locations during the transit flights to and from the platform. On the outbound flight the objective was to verify that the hardware and software problems experienced on the preceding trial had been satisfactorily overcome. The approaches on the inbound transit flight were experiments with the use of barometric and GPS altitude data for vertical guidance.

Several approaches were performed using the default parameters, followed by some experimentation with increased (6° and 9°) approach angles. A 9° approach angle was considered to be unsatisfactory, but the 6° angle was usable.

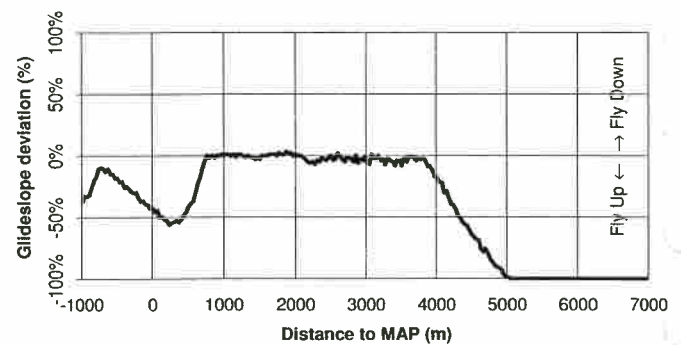
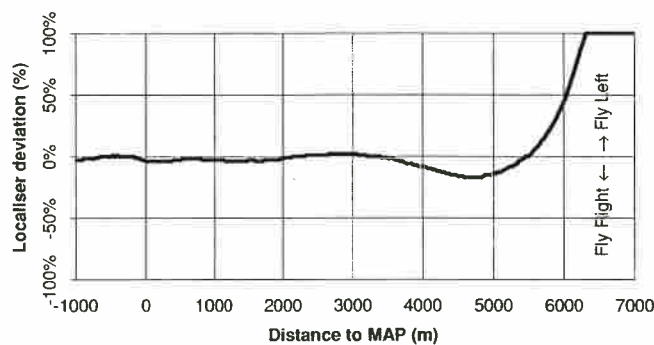
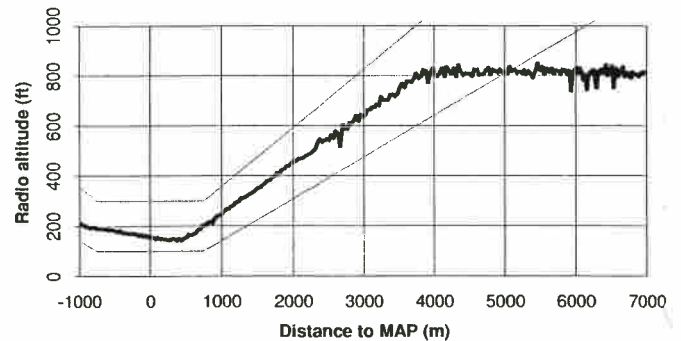
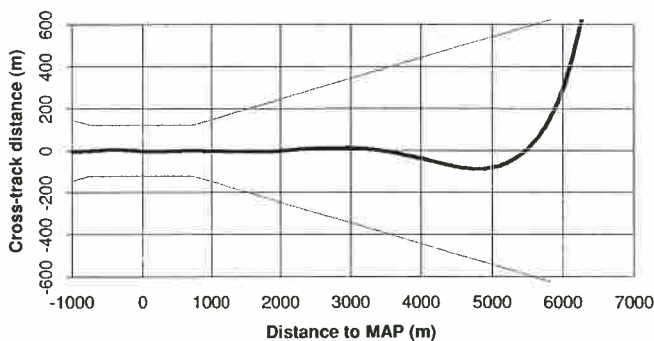
The sudden transition in the vertical profile on entry to the level segment was identified as the cause of altitude undershoots at the start of the level segment. This effect was most significant when performing an autocoupled approach, but it was also identified as being a potential problem (owing to the excessive attention which the pilot was required to pay to the vertical deviation indication) when approaches were flown manually.

The remoteness of the mode annunciation on the central DME display meant that this information was of little use to the pilot.

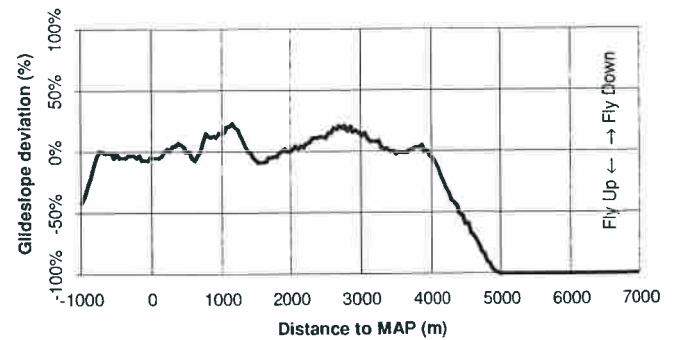
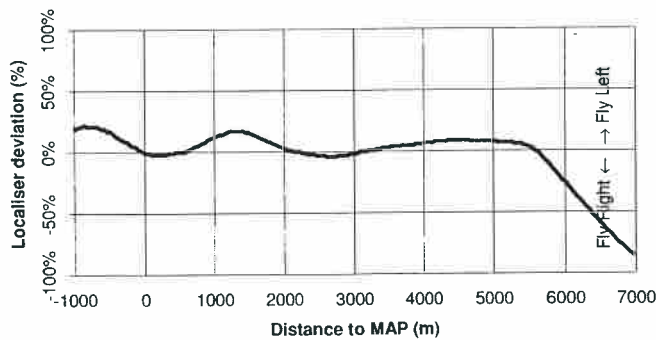
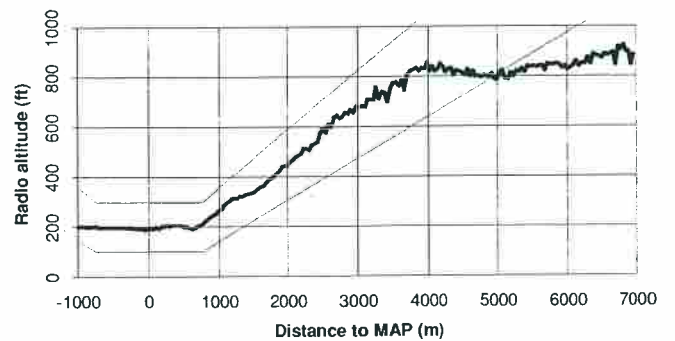
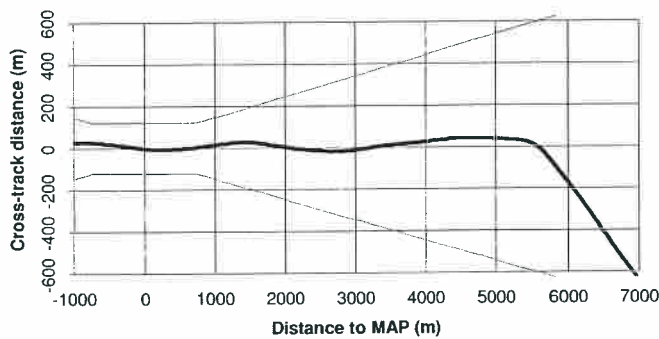
Flight number: 2	Approach number: 1	Location: arbitrary	Wind: 020-040°M, 15kt
Approach track: n/a		Approach angle: 3.5°	Overshoot angle: 3.5°
DGPS source: GD1 (MF-corrected Navstar)		Height source: radio altimeter	
Horizontal sensitivities:	4nm approach: ±850m	Level segment: ±120m	4nm overshoot: ±850m
Vertical sensitivities:	4nm approach: ±350ft	Level segment: ±100ft	4nm overshoot: ±350ft
Entry technique: approach commenced during enroute transit to Beatrice platform.			
Go-around technique: straight ahead from MAP, climbing using autopilot go-around function.			
Handling pilot: NM	Method: Autopilot	Start Time: 10:55:10	End Time: 10:58:41
Other details: n/a			
Pilot comments: Good capture onto the pseudo-ILS.			
Observations: This was the first approach undertaken with a fully functional trials installation and the first performed down to 200ft MDH. It was also the first auto-coupled approach. The aim was to test the operation of the DGPS guidance system at an arbitrary location over the sea, prior to arriving at the Beatrice platform.			



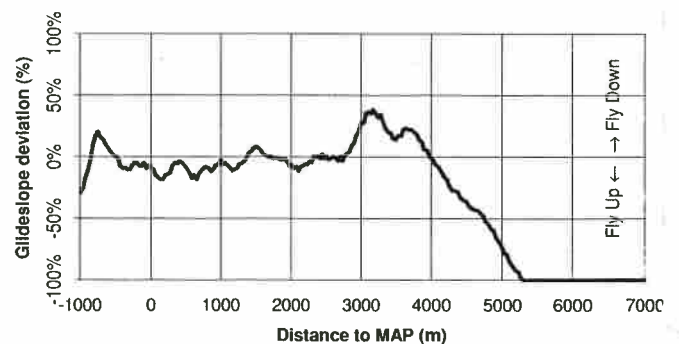
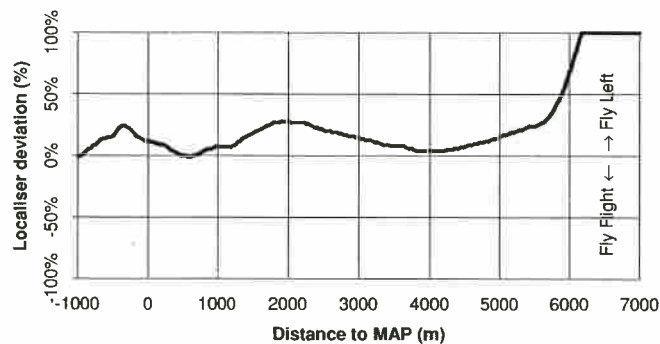
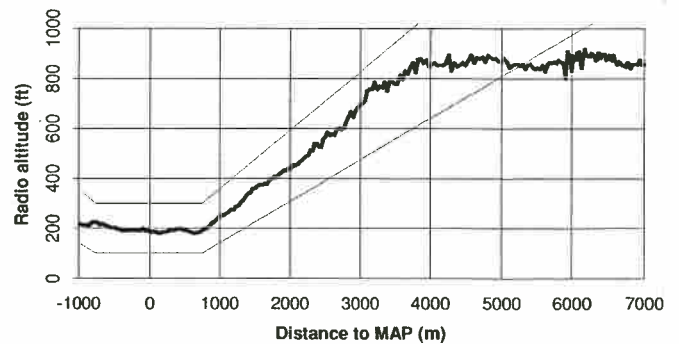
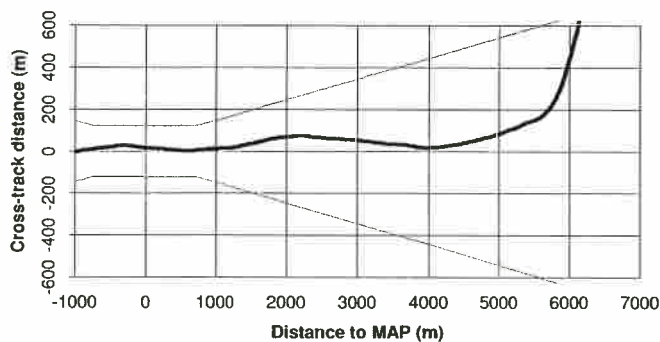
Flight number: 2	Approach number: 2	Location: Beatrice C	Wind: 020-040°M, 15kt
Approach track: QDM 020°M, 200m left offset		Approach angle: 3.5°	Overshoot angle: 3.5°
DGPS source: GD1 (MF-corrected Navstar)		Height source: radio altimeter	
Horizontal sensitivities:	4nm approach: ±850m	Level segment: ±120m	4nm overshoot: ±850m
Vertical sensitivities:	4nm approach: ±350ft	Level segment: ±100ft	4nm overshoot: ±350ft
Entry technique: Modified Aerad procedure commencing overhead the platform, with a right-hand outbound leg flown using RNAV-2 guidance and the turn commenced at 4nm range.			
Go-around technique: straight ahead from MAP, climbing as directed by DGPS guidance.			
Handling pilot: NM	Method: Autopilot	Start Time: 11:28:34	End Time: 11:32:51
Other details: approach flown at 80kt IAS (into-wind approach).			
Pilot comments: Excellent performance.			
Observations: This was the first approach undertaken at an offshore installation using the trials equipment. The localiser capture by the autopilot could not be faulted. On reaching the level segment the aircraft descended to around 60ft below the desired MDH and had almost recovered by the time the go-around point was reached. This was attributed to the autopilot gain being too low for this task.			



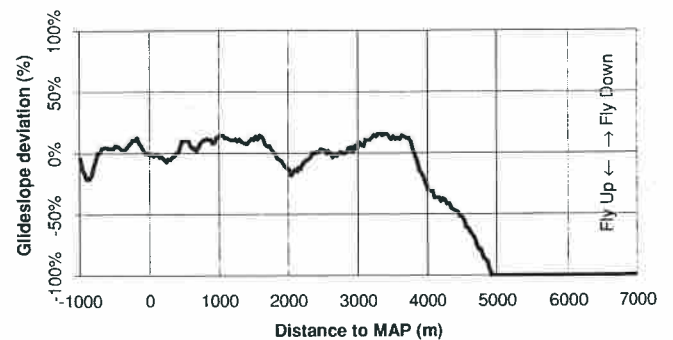
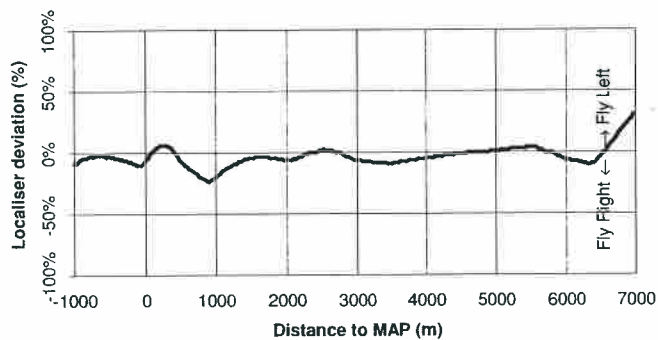
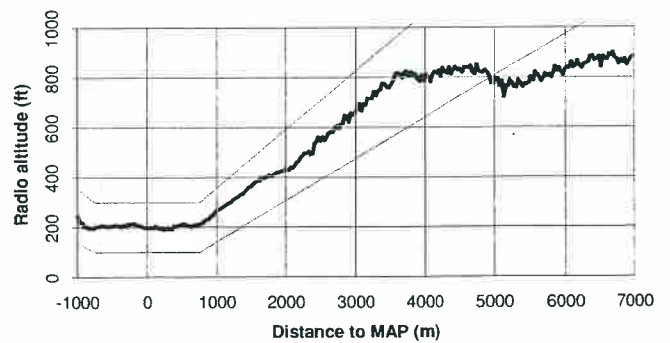
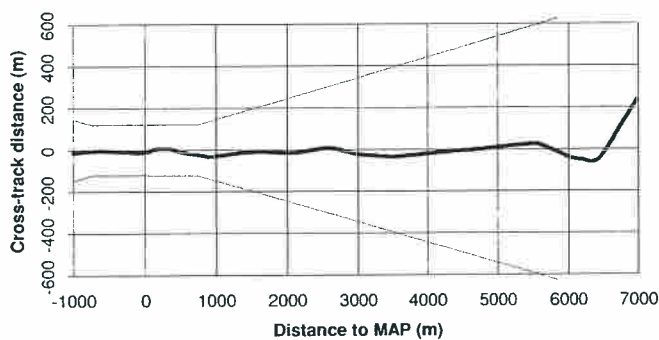
Flight number: 2	Approach number: 3	Location: Beatrice C	Wind: 020-040°M, 15kt
Approach track: QDM 110°M, 200m left offset		Approach angle: 3.5°	Overshoot angle: 3.5°
DGPS source: GD1 (MF-corrected Navstar)		Height source: radio altimeter	
Horizontal sensitivities:	4nm approach: ±850m	Level segment: ±120m	4nm overshoot: ±850m
Vertical sensitivities:	4nm approach: ±350ft	Level segment: ±100ft	4nm overshoot: ±350ft
Entry technique: modified Aerad procedure commencing overhead the platform, with a right-hand outbound leg flown using RNAV-2 guidance and the turn commenced at 4nm range.			
Go-around technique: straight ahead from MAP, climbing as directed by DGPS guidance.			
Handling pilot: NT	Method: Raw data	Start Time: 11:41:29	End Time: 11:44:50
Other details: approach flown at 80kt IAS.			
Pilot comments: Straightforward to fly. Annunciation of the system mode was not sufficiently compelling, resulting in the pilot missing the entry into the go around.			
Observations: n/a.			



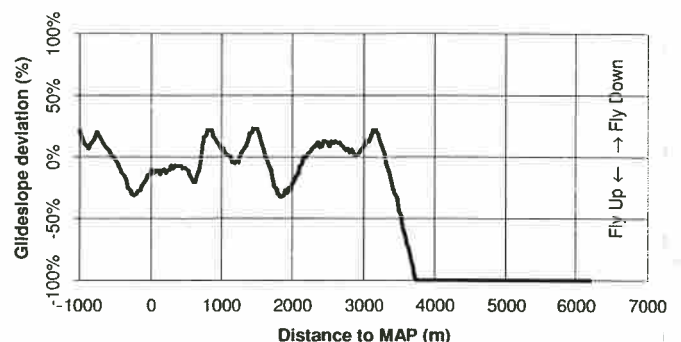
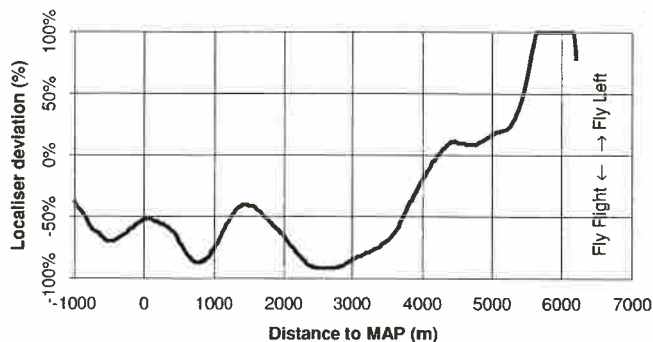
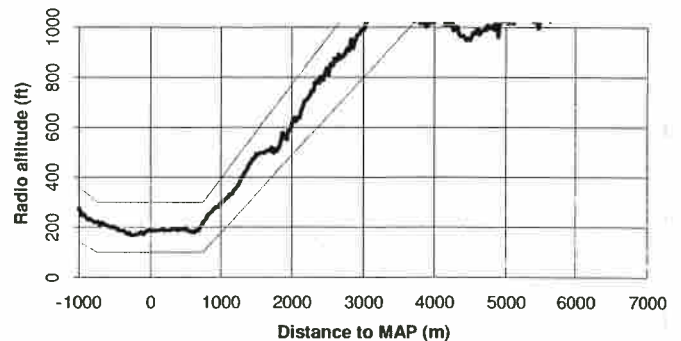
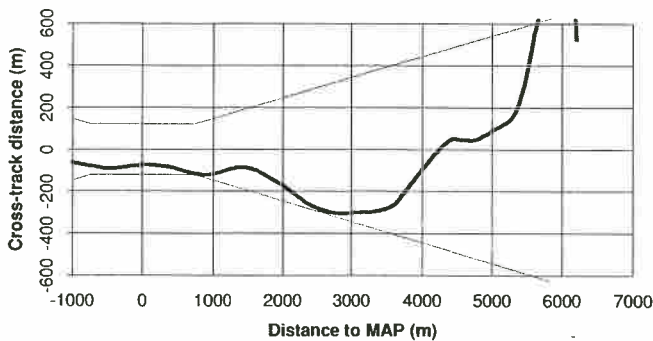
Flight number: 2	Approach number: 4	Location: Beatrice C	Wind: 020-040°M, 15kt
Approach track: QDM 200°M, 200m left offset		Approach angle: 3.5°	Overshoot angle: 3.5°
DGPS source: GD1 (MF-corrected Navstar)		Height source: radio altimeter	
Horizontal sensitivities:	4nm approach: ±850m	Level segment: ±120m	4nm overshoot: ±850m
Vertical sensitivities:	4nm approach: ±350ft	Level segment: ±100ft	4nm overshoot: ±350ft
Entry technique: modified Aerad procedure commencing overhead the platform, with a right-hand outbound leg flown using RNAV-2 guidance and the turn commenced at 4nm range.			
Go-around technique: straight ahead from MAP, climbing as directed by DGPS guidance.			
Handling pilot: NT	Method: Raw data	Start Time: 11:52:33	End Time: 11:56:39
Other details: approach flown at 60kt IAS to minimise groundspeed (downwind approach).			
Pilot comments: The technique attempted of performing a 90° 'cut' to intercept the localiser appeared to work quite well at 60kt IAS.			
Observations: n/a.			



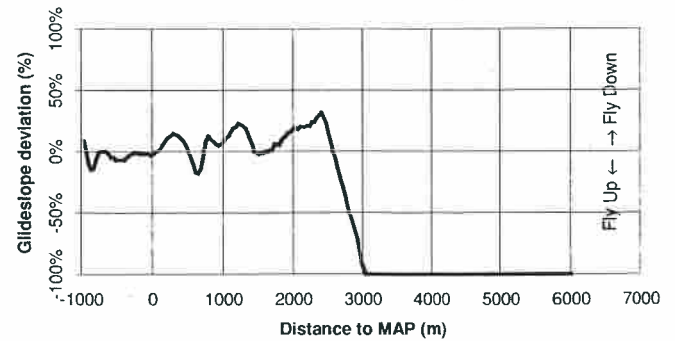
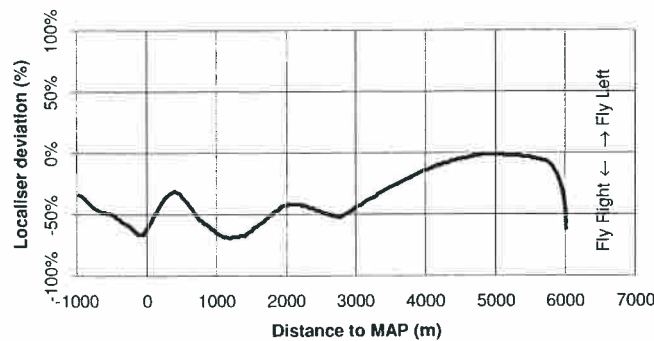
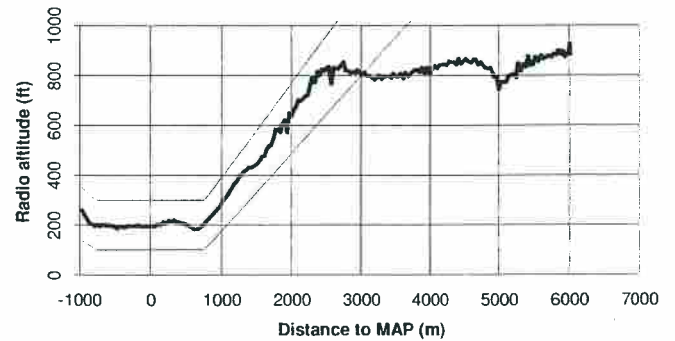
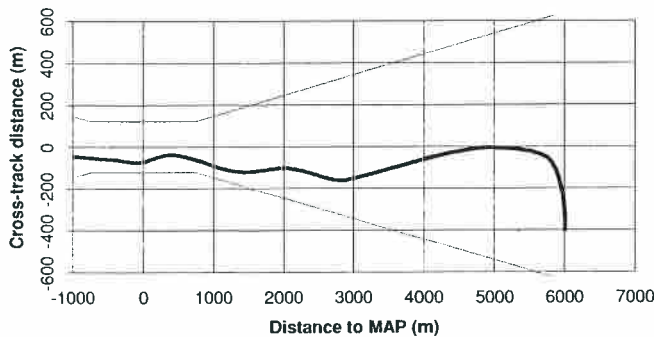
Flight number: 2	Approach number: 5	Location: Beatrice C	Wind: 020-040°M, 15kt
Approach track: QDM 290°M, 200m left offset		Approach angle: 3.5°	Overshoot angle: 3.5°
DGPS source: GD1 (MF-corrected Navstar)		Height source: radio altimeter	
Horizontal sensitivities:	4nm approach: ±850m	Level segment: ±120m	4nm overshoot: ±850m
Vertical sensitivities:	4nm approach: ±350ft	Level segment: ±100ft	4nm overshoot: ±350ft
Entry technique: modified Aerad procedure commencing overhead the platform, with a right-hand outbound leg flown using RNAV-2 guidance and the turn commenced at 4nm range.			
Go-around technique: straight ahead from MAP, climbing as directed by DGPS guidance.			
Handling pilot: NM	Method: Raw data	Start Time: 12:08:48	End Time: 12:13:16
Other details: n/a.			
Pilot comments: n/a.			
Observations: n/a.			



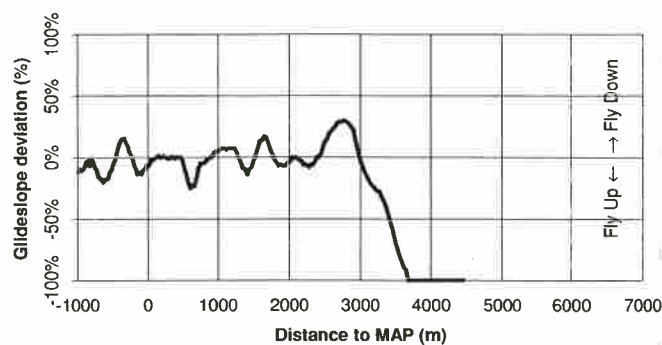
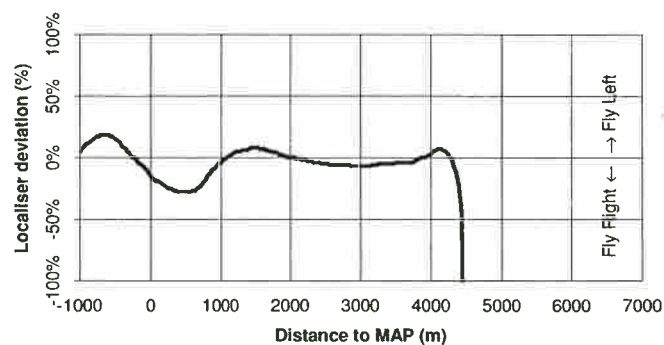
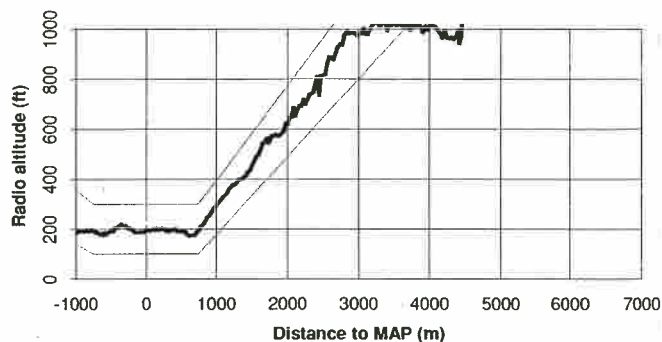
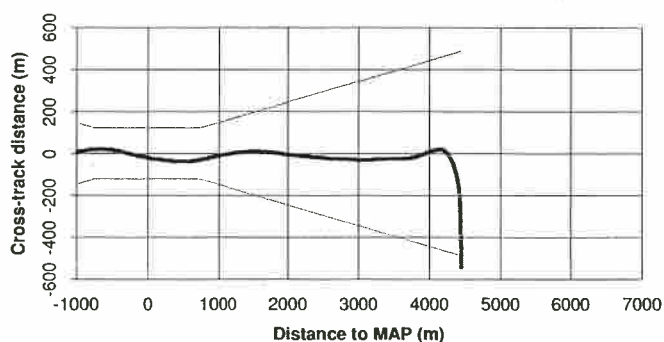
Flight number: 2	Approach number: 6	Location: Beatrice C	Wind: 020-040°M, 15kt
Approach track: QDM 040°M, 200m right offset		Approach angle: 6.0°	Overshoot angle: 3.5°
DGPS source: GD1 (MF-corrected Navstar)		Height source: radio altimeter	
Horizontal sensitivities:	4nm approach: ±850m	Level segment: ±120m	4nm overshoot: ±850m
Vertical sensitivities:	4nm approach: ±350ft	Level segment: ±100ft	4nm overshoot: ±350ft
Entry technique: aircraft flown directly to a point at around 4nm range to intercept the approach.			
Go-around technique: straight ahead from MAP, climbing as directed by DGPS guidance.			
Handling pilot: NT	Method: Raw data	Start Time: 14:05:03	End Time: 14:09:27
Other details: the pilot attempted to maintain the aircraft at the half-scale point on the localiser deviation indicator, to investigate the effect of being consistently off track. Into wind at 60kt IAS.			
Pilot comments: A 6° approach angle was perfectly manageable. The lateral flying task was quite difficult.			
Observations: Problems experienced with lateral guidance were attributed to the fact that the pilot was trying to maintain half-scale on the localiser indicator rather than maintaining the needle centred. The figure shows that the aircraft was close to the boundary of the linear region at one point, with the localiser indicator at full-scale deflection.			



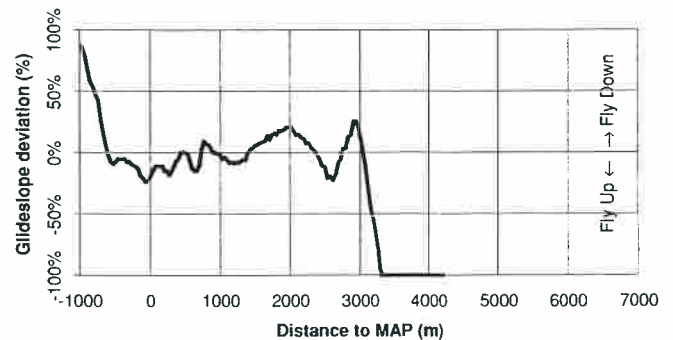
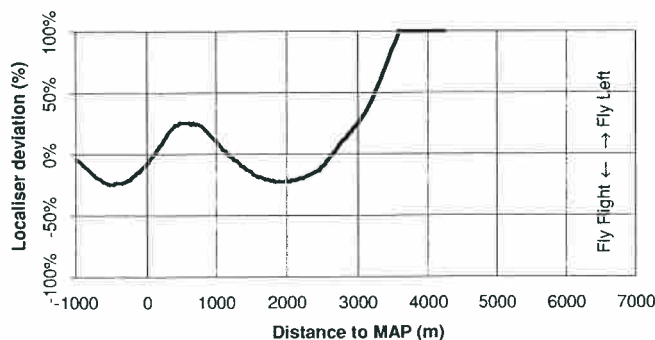
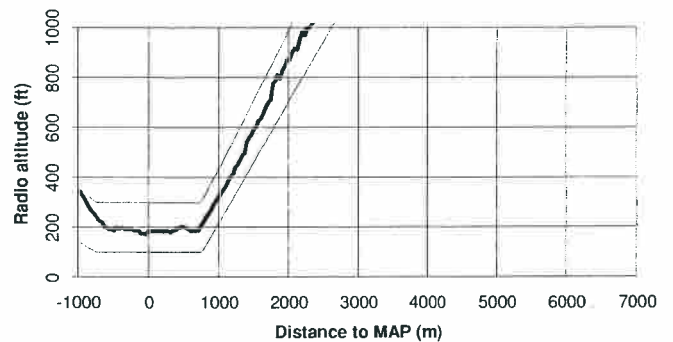
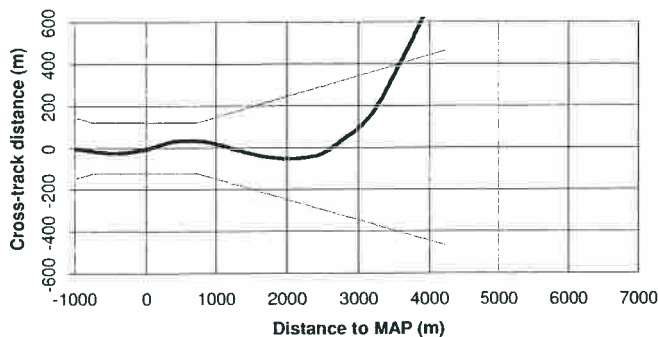
Flight number: 2	Approach number: 7	Location: Beatrice C	Wind: 020-040°M, 15kt
Approach track: QDM 220°M, 200m right offset		Approach angle: 6.0°	Overshoot angle: 3.5°
DGPS source: GD1 (MF-corrected Navstar)		Height source: radio altimeter	
Horizontal sensitivities:	4nm approach: ±850m	Level segment: ±120m	4nm overshoot: ±850m
Vertical sensitivities:	4nm approach: ±350ft	Level segment: ±100ft	4nm overshoot: ±350ft
Entry technique: aircraft flown directly to a point at around 4nm range to intercept the approach.			
Go-around technique: straight ahead from MAP, climbing as directed by DGPS guidance.			
Handling pilot: NM	Method: Raw data	Start Time: 14:11:35	End Time: 14:14:59
Other details: the radio altitude data filter bandwidth was reduced from 10Hz to 1Hz to investigate whether this had any noticeable effect on the vertical guidance, and the pilot attempted to maintain the aircraft at the half-scale point on the localiser deviation indicator, to investigate the effect of being consistently off track.			
Pilot comments: The rate of descent was high due to the 6° downwind approach.			
Observations: No comments (adverse or otherwise) were received regarding the effects of changing the radalt filter frequency.			



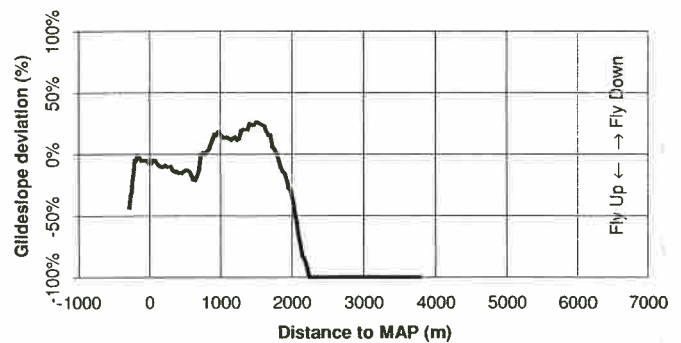
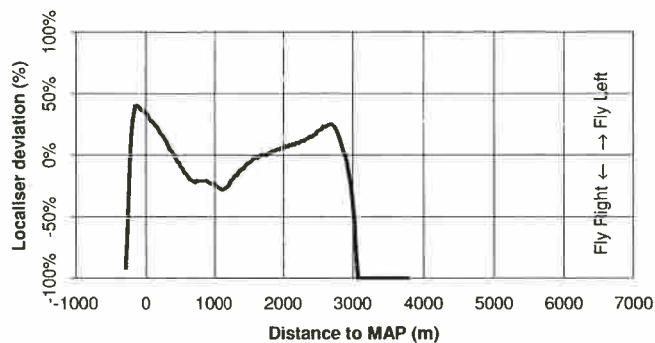
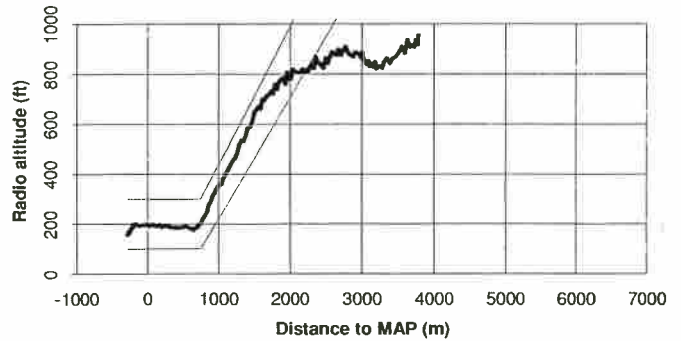
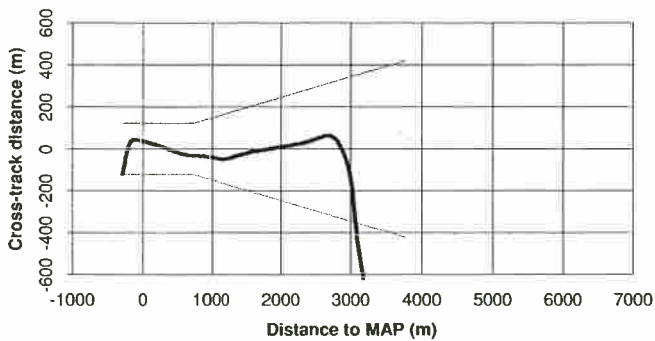
Flight number: 2	Approach number: 8	Location: Beatrice C	Wind: 020-040°M, 15kt
Approach track: QDM 040°M, 200m right offset		Approach angle: 6.0°	Overshoot angle: 3.5°
DGPS source: GD1 (MF-corrected Navstar)		Height source: radio altimeter	
Horizontal sensitivities:	4nm approach: ±850m	Level segment: ±120m	4nm overshoot: ±850m
Vertical sensitivities:	4nm approach: ±350ft	Level segment: ±100ft	4nm overshoot: ±350ft
Entry technique: aircraft flown directly to a point at around 4nm range to intercept the approach.			
Go-around technique: straight ahead from MAP, climbing as directed by DGPS guidance.			
Handling pilot: NT	Method: Raw data	Start Time: 14:16:47	End Time: 14:20:05
Other details: the radio altitude data filter bandwidth remained reduced to 1Hz.			
Pilot comments: The glideslope indication responded in a satisfactory manner to small variations in rate of descent during the approach segment.			
Observations: No comments were made regarding the change to the radalt filtering.			



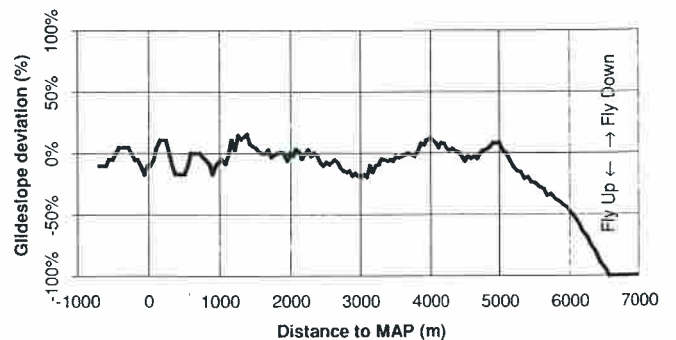
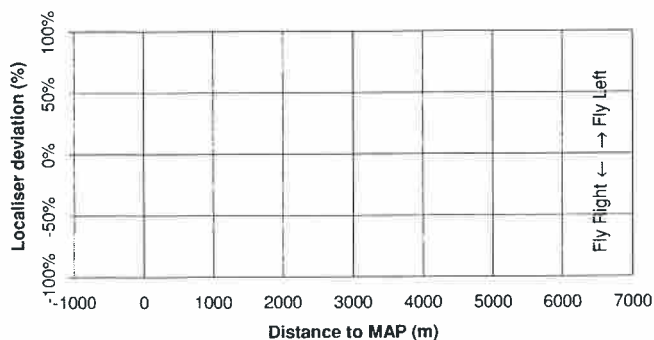
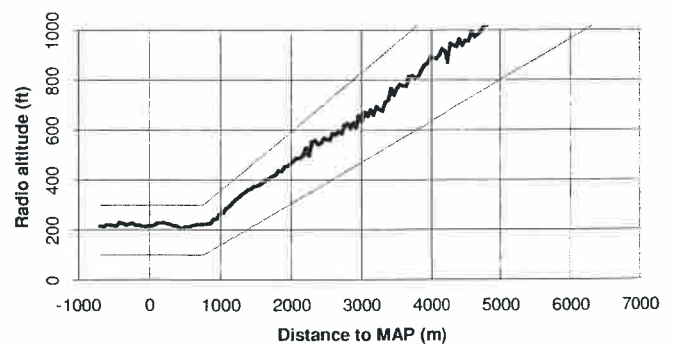
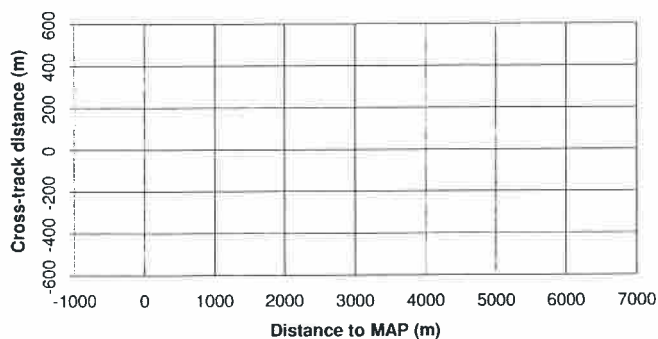
Flight number: 2	Approach number: 9	Location: Beatrice C	Wind: 020-040°M, 15kt
Approach track: QDM 220°M, 200m right offset		Approach angle: 9.0°	Overshoot angle: 3.5°
DGPS source: GD1 (MF-corrected Navstar)		Height source: radio altimeter	
Horizontal sensitivities:	4nm approach: ±850m	Level segment: ±120m	4nm overshoot: ±850m
Vertical sensitivities:	4nm approach: ±350ft	Level segment: ±100ft	4nm overshoot: ±350ft
Entry technique: aircraft flown directly to a point at around 4nm range to intercept the approach.			
Go-around technique: straight ahead from MAP, climbing as directed by DGPS guidance.			
Handling pilot: NT	Method: Raw data	Start Time: 14:22:20	End Time: 14:24:56
Other details: the radio altitude data filter bandwidth was returned to 10Hz. Flown downwind at 60kt.			
Pilot comments: It was a problem establishing on the 9° approach slope with the aircraft being close to autorotation (rate of descent around 1400 ft/min). This might not be a problem with an aircraft that exhibited greater drag. It was necessary to anticipate the transition to the level segment in advance to avoid descending significantly below MDH, due to the high rate of descent.			
Observations: n/a.			



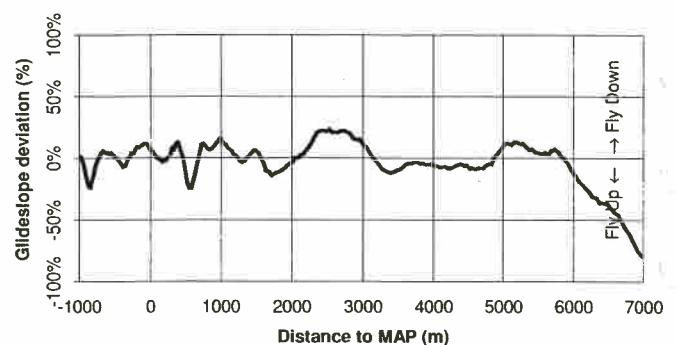
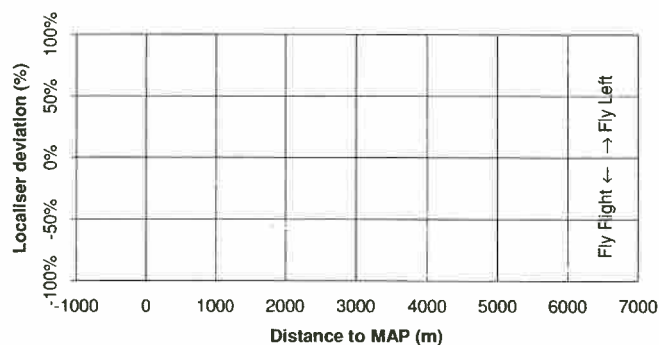
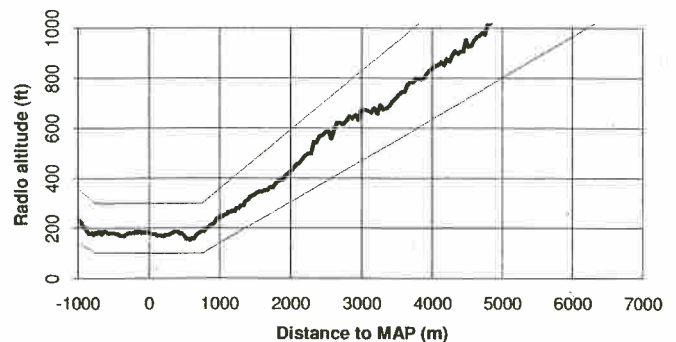
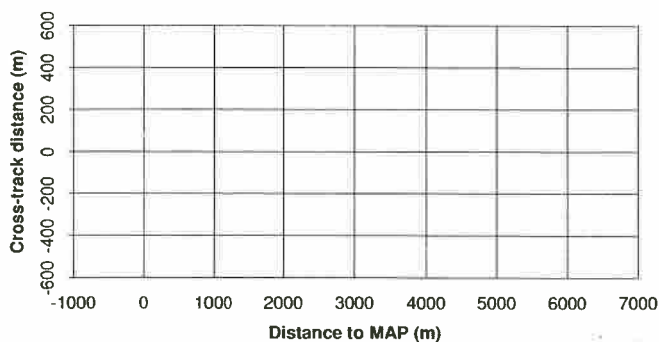
Flight number: 2	Approach number: 10	Location: Beatrice C	Wind: 020-040°M, 15kt
Approach track: QDM 040°M, 200m right offset		Approach angle: 9.0°	Overshoot angle: 3.5°
DGPS source: GD1 (MF-corrected Navstar)		Height source: radio altimeter	
Horizontal sensitivities:	4nm approach: ±850m	Level segment: ±120m	4nm overshoot: ±850m
Vertical sensitivities:	4nm approach: ±350ft	Level segment: ±100ft	4nm overshoot: ±350ft
Entry technique: aircraft flown directly to a point at around 4nm range to intercept the approach.			
Go-around technique: aircraft landed on the platform from the level segment.			
Handling pilot: NM	Method: Raw data	Start Time: 14:26:22	End Time: 14:28:57
Other details: flown into-wind at 90kt IAS.			
Pilot comments: Easier to fly this approach (possibly due to being into wind) than its predecessor. Anticipation of the transition to the level segment was still essential.			
Observations: n/a.			



Flight number: 2	Approach number: 11	Location: arbitrary	Wind: 020-040°M, 15kt
Approach track: n/a		Approach angle: 3.5°	Overshoot angle: 3.5°
DGPS source: GD1 (MF-corrected Navstar)		Height source: barometric altitude	
Horizontal sensitivities:	4nm approach: ±850m	Level segment: ±120m	4nm overshoot: ±850m
Vertical sensitivities:	4nm approach: ±350ft	Level segment: ±100ft	4nm overshoot: ±350ft
Entry technique: approach commenced during return transit to Aberdeen from Beatrice platform.			
Go-around technique: straight ahead from MAP, climbing as directed by DGPS guidance.			
Handling pilot: n/k	Method: Raw data	Start Time: 14:41:25	End Time: 14:44:10
Other details: Only the glideslope component of the approach guidance was followed, the localiser indications were ignored.			
Pilot comments: No problems were experienced following the vertical guidance.			
Observations: The aim of this approach was to investigate the effect of using barometric altitude in place of radio altitude as the source of height data for the synthetic approach guidance. The pressure altitude was corrected by means of a fixed offset, derived from knowledge of the local QFE, to provide an estimate of height above the sea. Examination of the plots suggests that satisfactory vertical guidance was provided to the pilot.			



Flight number: 2	Approach number: 12	Location: arbitrary	Wind: 020-040°M, 15kt
Approach track: n/a		Approach angle: 3.5°	Overshoot angle: 3.5°
DGPS source: GD1 (MF-corrected Navstar)		Height source: GPS altitude (GD1)	
Horizontal sensitivities:	4nm approach: ±850m	Level segment: ±120m	4nm overshoot: ±850m
Vertical sensitivities:	4nm approach: ±350ft	Level segment: ±100ft	4nm overshoot: ±350ft
Entry technique: approach commenced during return transit to Aberdeen from Beatrice platform.			
Go-around technique: straight ahead from MAP, climbing as directed by DGPS guidance.			
Handling pilot: n/k	Method: Raw data	Start Time: 14:47:04	End Time: 14:50:50
Other details: Only the glideslope component of the approach guidance was followed.			
Pilot comments: A slightly uncomfortable feeling due to the step change in vertical guidance at 200ft.			
Observations: The aim of this approach was to investigate the effect of using GPS altitude in place of radio altitude as the source of height data for the synthetic approach guidance. The GPS altitude was corrected by a fixed offset representing the best available estimate of the local difference between WGS84 geodetic and mean sea level heights. There is a single erroneous data point on the glideslope deviation plot (around 250m before the MAP) representing an instance where valid vertical guidance was not available. This is not believed to have been the explanation for the pilot's comment, however, and there is no readily identifiable feature that suggests an explanation.			



5.3 **Flight Trial 3**

The primary aim of the third test flight was to perform a series of special-purpose ground trials (the results of which are discussed in Volume 2) at Longside aerodrome.

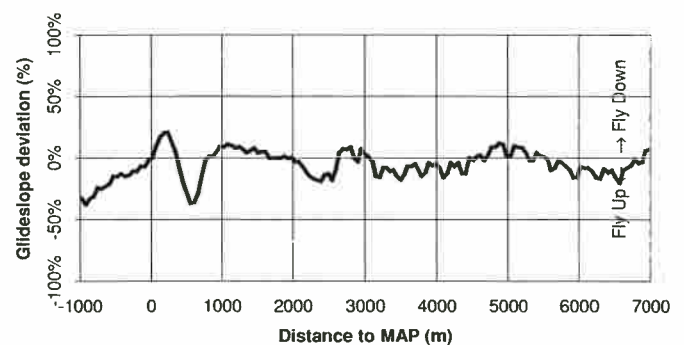
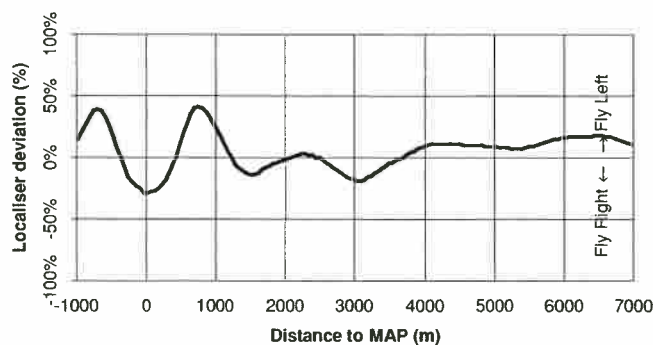
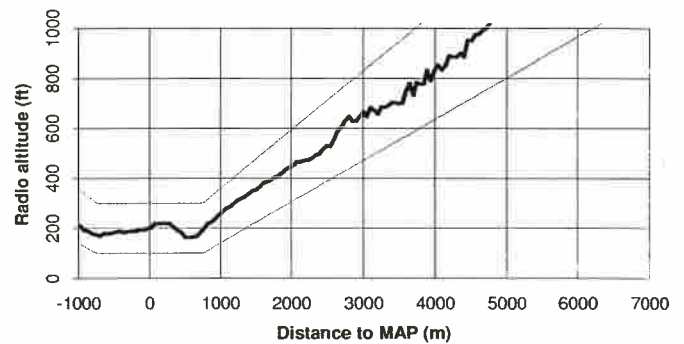
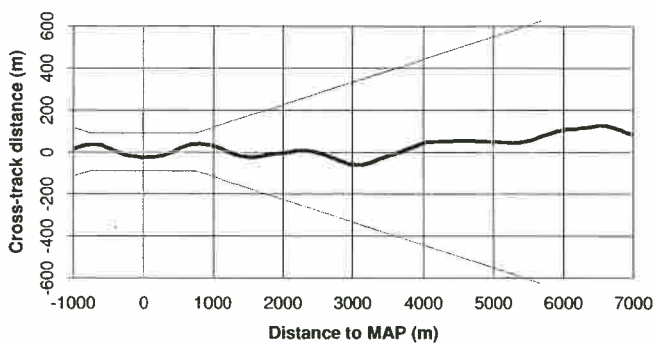
During the transit flights to and from Longside, a small number of test approaches were also performed at arbitrary locations. The objective was to investigate the effect of two forms of change to the approach guidance: increased horizontal sensitivity through the level segment, and the introduction of a faired vertical profile.

A change in the level segment horizontal sensitivity from $\pm 120\text{m}$ to $\pm 90\text{m}$ did not result in any adverse pilot comments and was deemed to be a useful improvement. A further change to $\pm 60\text{m}$ proved to be unsatisfactory, suggesting that the $\pm 90\text{m}$ value was close to being optimum.

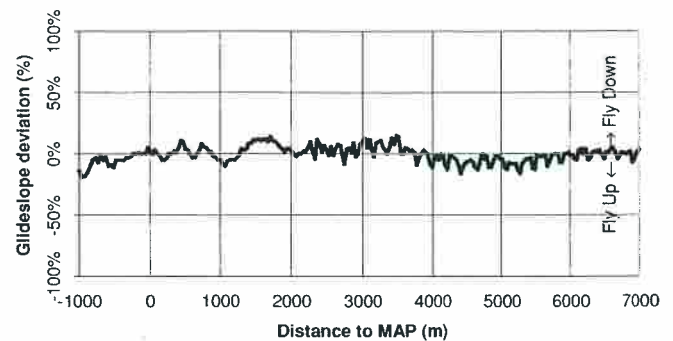
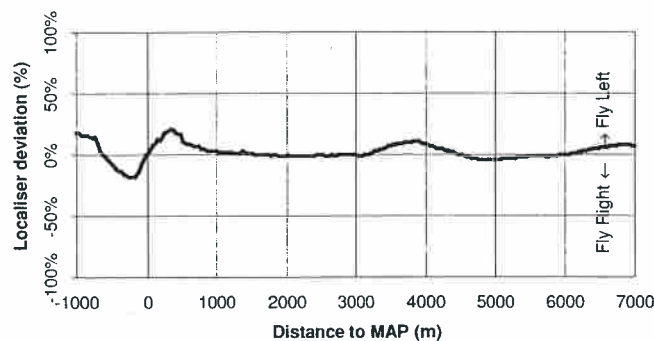
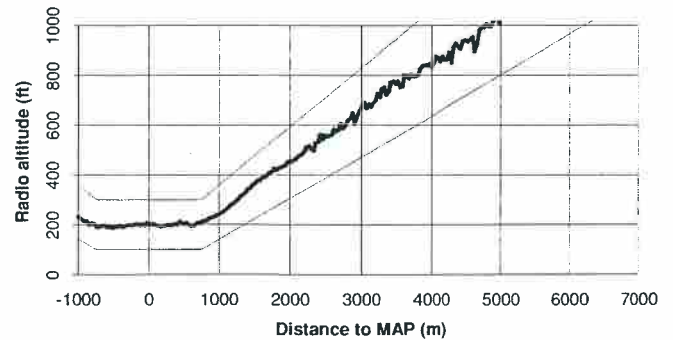
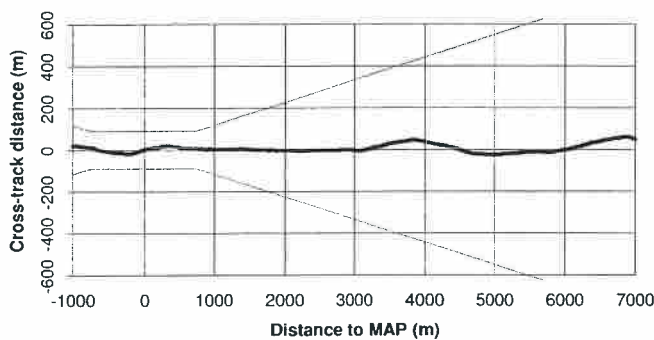
In an attempt to mitigate the effects of the transition between the approach and level segments, the guidance software was modified to incorporate a 'faired' vertical profile (section 4.5.1). Although only a single approach was performed with this feature correctly implemented, it appeared to offer a significant improvement to the transition between the approach and level segments. Fairing of the vertical profile between the level and overshoot segments was found to be inappropriate.

As a result of this trial, a decision was taken to retain the 50ft vertical fairing on subsequent flights.

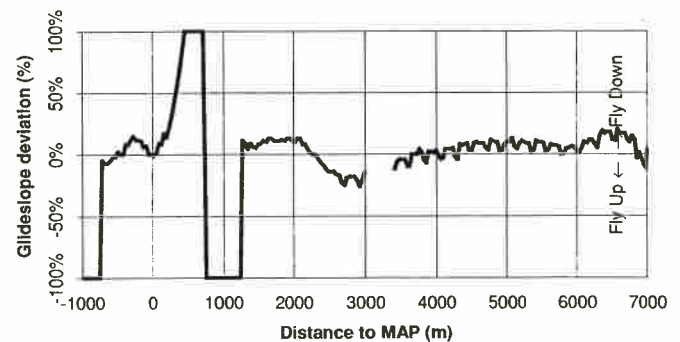
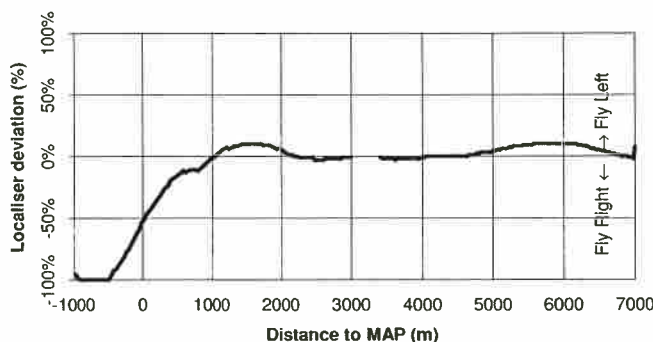
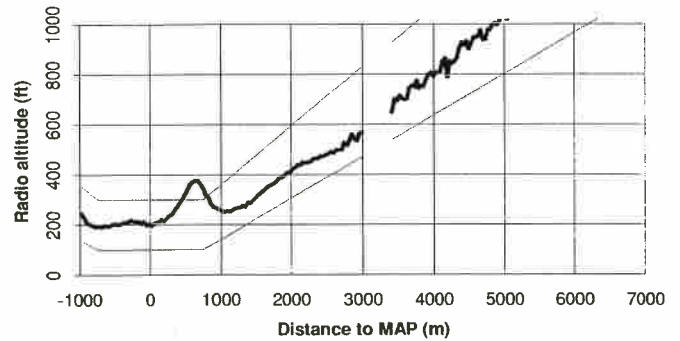
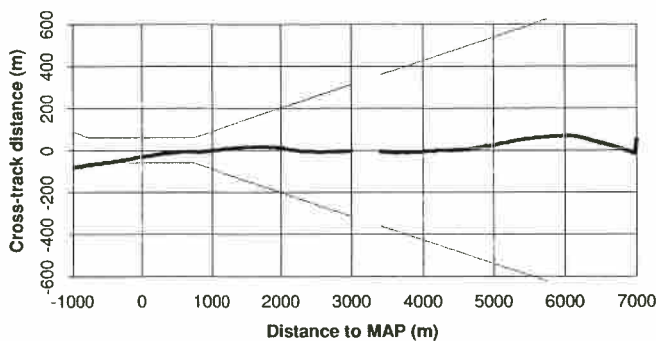
Flight number: 3	Approach number: 1	Location: arbitrary	Wind: 340-360°M, 20kt
Approach track: n/a		Approach angle: 3.5°	Overshoot angle: 3.5°
DGPS source: GD1 (MF-corrected Navstar)		Height source: radio altimeter	
Horizontal sensitivities:	4nm approach: ±850m	Level segment: ±90m	4nm overshoot: ±850m
Vertical sensitivities:	4nm approach: ±350ft	Level segment: ±100ft	4nm overshoot: ±350ft
Entry technique: approach commenced during transit from Aberdeen to Longside.			
Go-around technique: straight ahead from MAP, climbing as directed by DGPS guidance.			
Handling pilot: NM	Method: Raw data	Start Time: 09:46:44	End Time: 09:49:16
Other details: n/a.			
Pilot comments: The chosen speed of 120kt was felt to be too fast. A small amount of 'jitter' was present on the vertical deviation indication above 500ft. No adverse comments due to change in level segment lateral sensitivity.			
Observations: The 'jitter' in the vertical deviation indication was attributed to the change in radio altimeter scaling which occurs at 500ft with the radalt employed on the trials aircraft.			



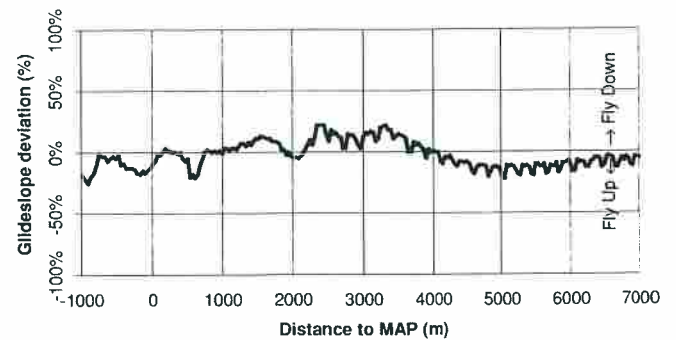
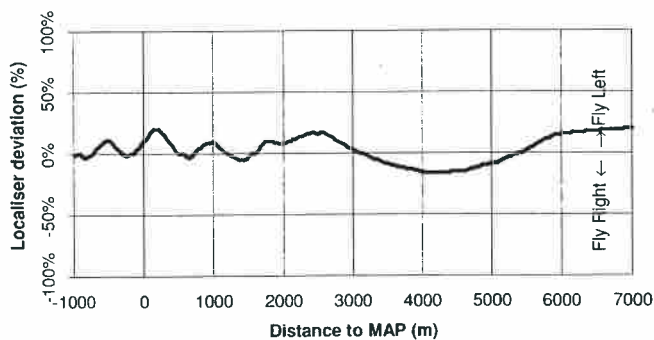
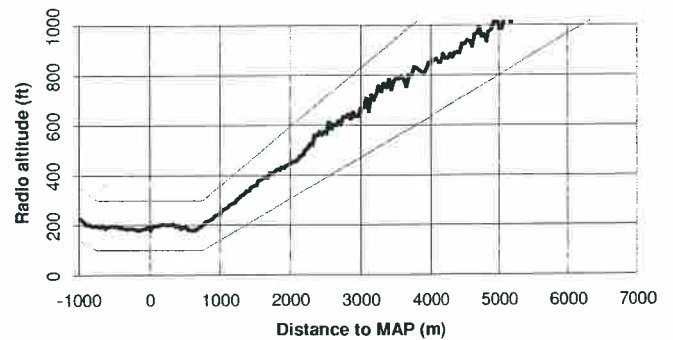
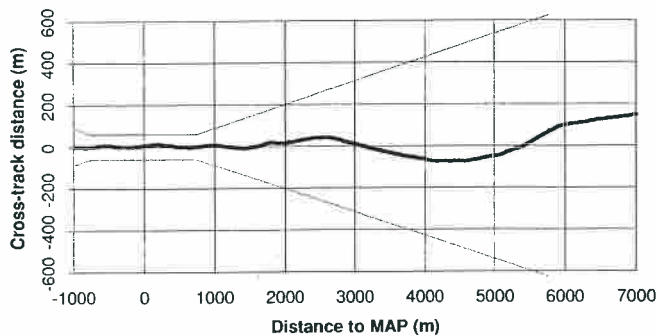
Flight number: 3	Approach number: 2	Location: arbitrary	Wind: 340-360°M, 20kt
Approach track: n/a		Approach angle: 3.5°	Overshoot angle: 3.5°
DGPS source: GD1 (MF-corrected Navstar)		Height source: radio altimeter	
Horizontal sensitivities:	4nm approach: ±850m	Level segment: ±90m	4nm overshoot: ±850m
Vertical sensitivities:	4nm approach: ±350ft	Level segment: ±100ft	4nm overshoot: ±350ft
Entry technique: approach commenced during transit from Aberdeen to Longside.			
Go-around technique: straight ahead from MAP, climbing as directed by DGPS guidance.			
Handling pilot: NM	Method: Raw data	Start Time: 09:51:56	End Time: 09:56:00
Other details: n/a.			
Pilot comments: The approach was just about manageable at 90kt. Jitter was still present above 500ft.			
Observations: n/a.			



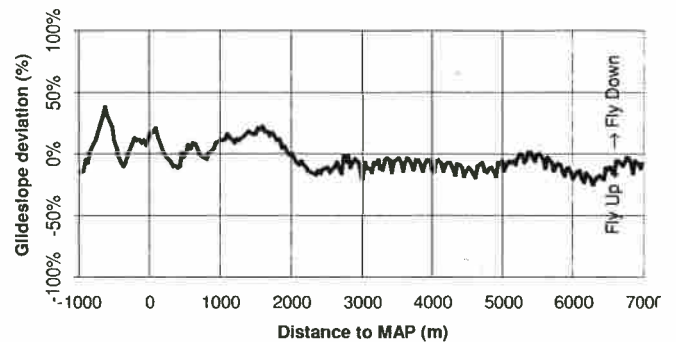
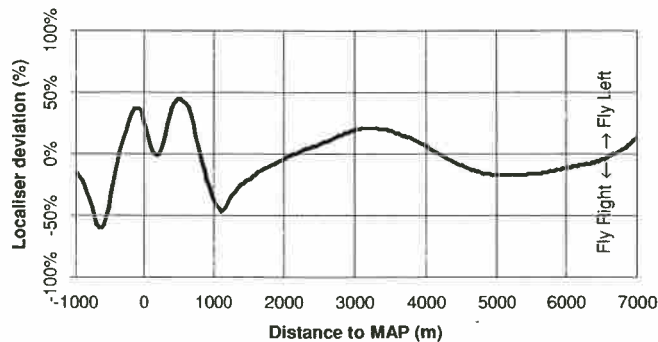
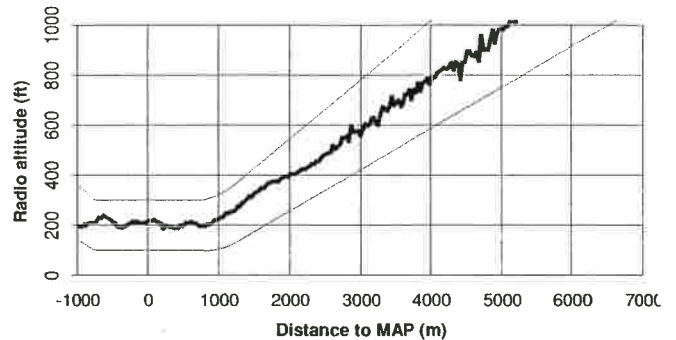
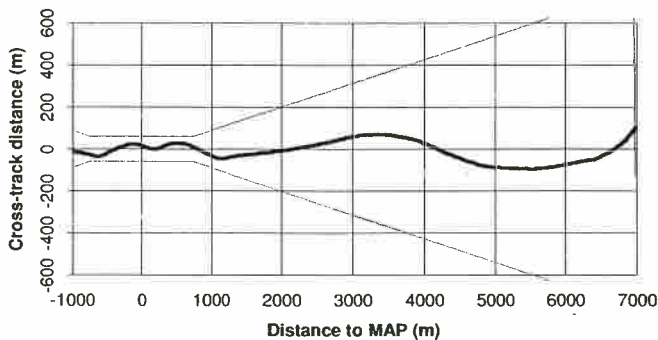
Flight number: 3	Approach number: 3	Location: arbitrary	Wind: 340-360°M, 20kt
Approach track: n/a		Approach angle: 3.5°	Overshoot angle: 3.5°
DGPS source: GD1 (MF-corrected Navstar)		Height source: radio altimeter	
Horizontal sensitivities:	4nm approach: ±850m	Level segment: ±60m	4nm overshoot: ±850m
Vertical sensitivities:	4nm approach: ±350ft	Level segment: ±100ft	4nm overshoot: ±350ft
Entry technique: approach commenced during transit from Aberdeen to Longside.			
Go-around technique: straight ahead from MAP, climbing as directed by DGPS guidance.			
Handling pilot: NM	Method: Raw data	Start Time: 09:58:48	End Time: 10:02:31
Other details: An attempt was made to introduce 50ft of fairing at the end of the approach segment, unfortunately an incorrect data entry by the FTE had the effect that guidance was lost totally for the duration of the faired section.			
Pilot comments: Erroneous vertical deviation indications were displayed at the end of the approach segment, the system then recovered.			
Observations: The plots show that the erroneous guidance data resulted in the pilot attempting to follow a fly up command, recovering to the correct height during the level segment. This problem precluded satisfactory evaluation of the change to ±60m sensitivity. The break in the recorded data at around 3500m was due to a temporary loss of the differentially corrected GD1 data.			



Flight number: 3	Approach number: 4	Location: arbitrary	Wind: 340-360°M, 20kt
Approach track: n/a		Approach angle: 3.5°	Overshoot angle: 3.5°
DGPS source: GD1 (MF-corrected Navstar)		Height source: radio altimeter	
Horizontal sensitivities:	4nm approach: ±850m	Level segment: ±60m	4nm overshoot: ±850m
Vertical sensitivities:	4nm approach: ±350ft	Level segment: ±100ft	4nm overshoot: ±350ft
Entry technique: approach commenced during transit from Aberdeen to Longside.			
Go-around technique: straight ahead from MAP, climbing as directed by DGPS guidance.			
Handling pilot: NM	Method: Raw data	Start Time: 10:08:00	End Time: 10:11:53
Other details: The FTE's attempt at a 50ft fairing selection was removed, to enable a full evaluation of the ±60m sensitivity change to be undertaken without distractions. Flown at 80kt IAS.			
Pilot comments: The localiser indications were 'dithery' during the level segment.			
Observations: The 'dithery' localiser indications were attributed to the horizontal sensitivity now being too high.			



Flight number: 3	Approach number: 5	Location: arbitrary	Wind: 340-360°M, 20kt
Approach track: n/a		Approach angle: 3.5°	Overshoot angle: 3.5°
DGPS source: GD1 (MF-corrected Navstar)		Height source: radio altimeter	
Horizontal sensitivities:	4nm approach: ±850m	Level segment: ±60m	4nm overshoot: ±850m
Vertical sensitivities:	4nm approach: ±350ft	Level segment: ±100ft	4nm overshoot: ±350ft
Entry technique: approach commenced during transit from Longside to Aberdeen.			
Go-around technique: straight ahead from MAP, climbing as directed by DGPS guidance.			
Handling pilot: NT	Method: Raw data	Start Time: 15:51:36	End Time: 15:55:45
Other details: A further attempt was made to introduce a 50ft fairing at the end of the approach segment, this time correctly. Fairing was also applied between the end of the level segment and commencement of the go-around.			
Pilot comments: Localiser gain was too high on the level segment. The fairing worked well but its inclusion at the 'far' end of the level segment was felt to be unnecessary: a more positive indication to go around would be better.			
Observations: n/a.			



5.4. **Flight Trial 4**

The fourth test flight was performed at the Piper B platform.

The first few approaches of this trial were performed using the 'standard' approach parameters (but incorporating the vertical profile fairing modification), by a pilot who had not been involved in the earlier development flying and who was therefore 'new' to the system. Favourable comments on the DGPS system were received.

The level segment horizontal sensitivity was, erroneously, changed back to $\pm 120\text{m}$ for this and the subsequent flight trial, despite the fact that the optimum sensitivity had been determined to be $\pm 90\text{m}$ on the previous flight.

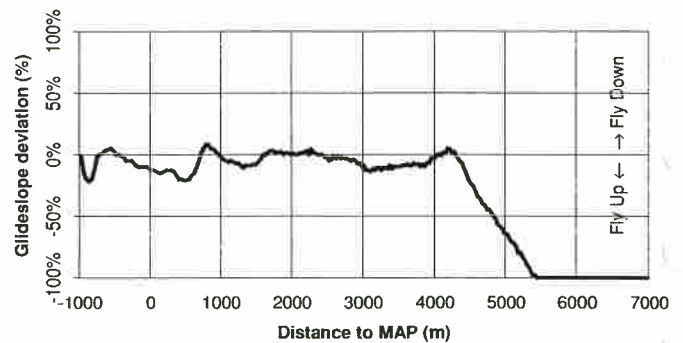
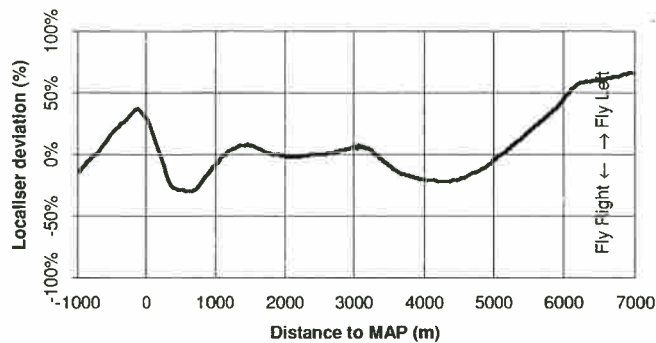
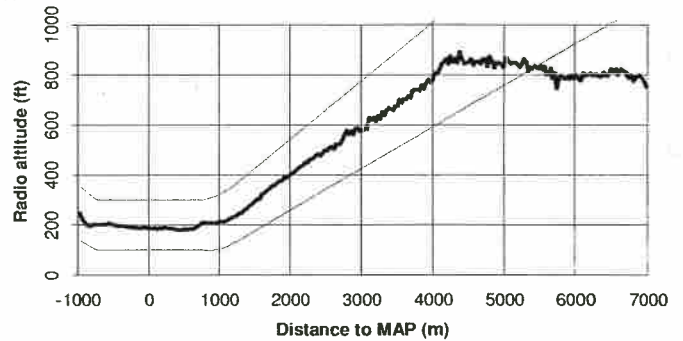
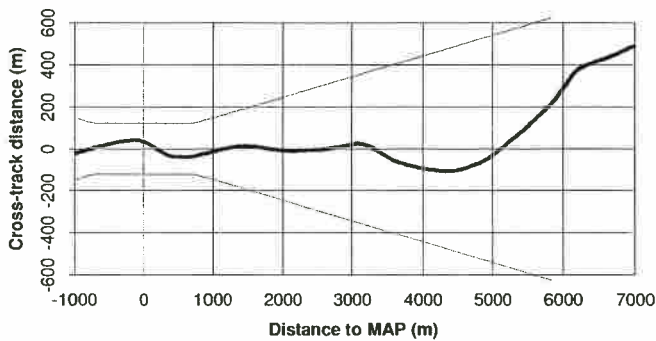
An autocoupled approach was attempted with the vertical fairing included. The 'undershoot' effect was still present and it was suggested that an increased amount of fairing might be necessary.

The effect of a change in overshoot angle, from 3.5° to 6° , was investigated. It was concluded that this provided a better rate of climb for the go-around and was retained for subsequent flights.

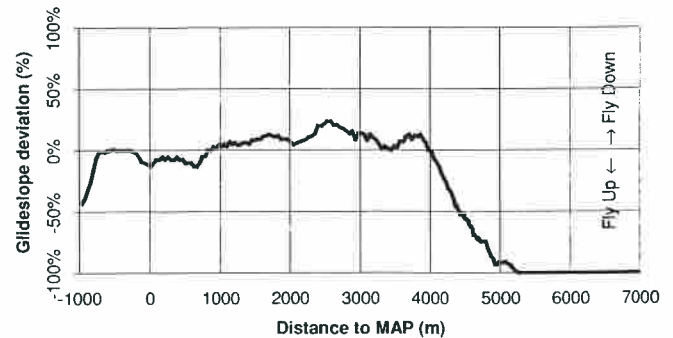
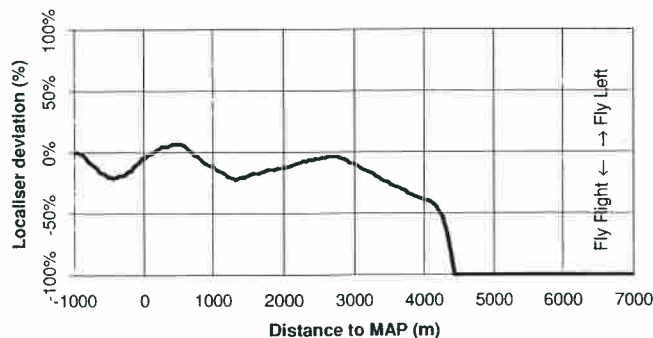
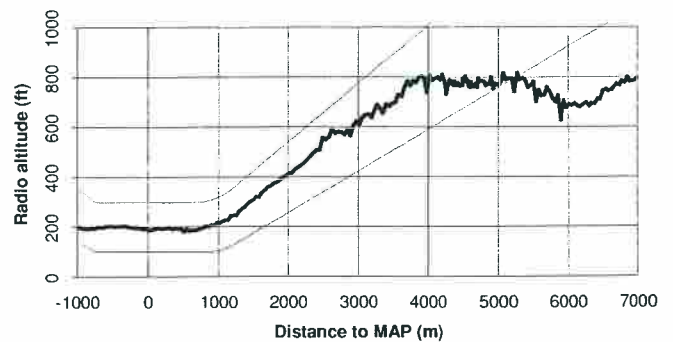
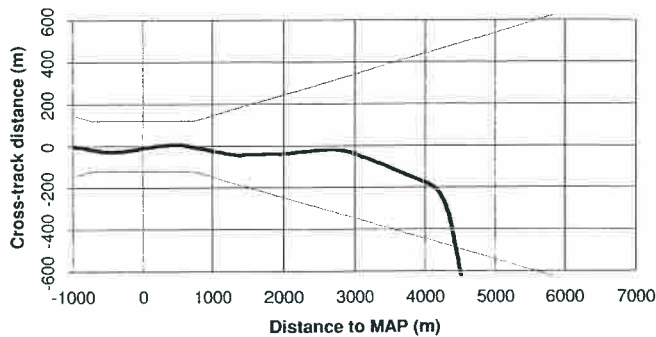
In response to previous comments regarding the remoteness of the central DME display for mode annunciation, the portable LED panel (section 4.5.2) was introduced midway through the flight. This proved to be an immediate improvement, although the sequencing of the indicator lights was not entirely correct.

One approach was flown which incorporated a horizontal track change at 4nm range: the purpose of this was to experiment with the curved/segment approach software facility (section 4.5.3). The lack of an automated HSI course carriage was identified as being a possible source of the problems experienced when using this facility.

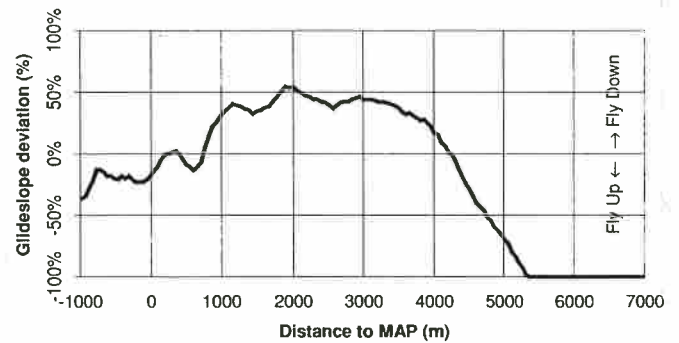
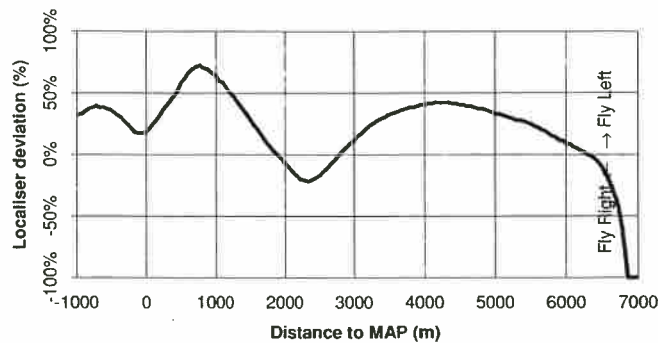
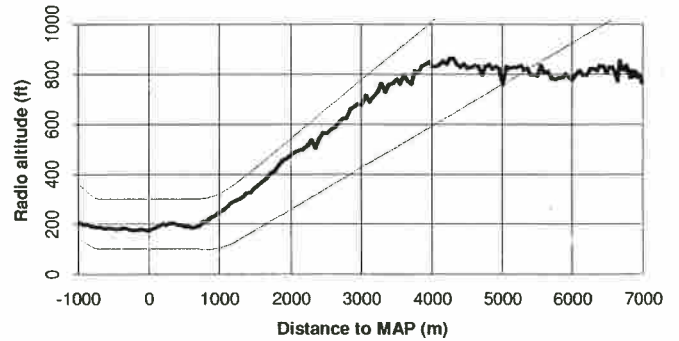
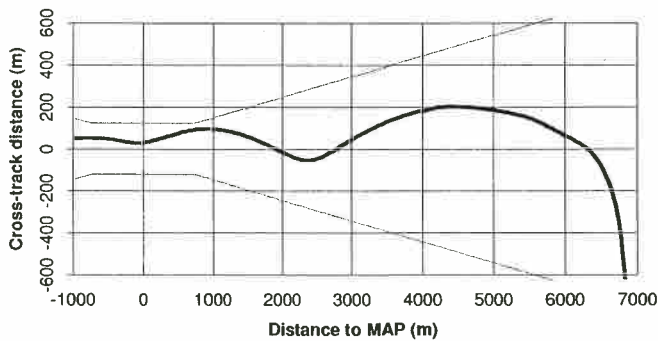
Flight number: 4	Approach number: 1	Location: Piper B	Wind 160-170°,10-25kt
Approach track: QDM 160°M, 250m left offset		Approach angle: 3.5°	Overshoot angle: 3.5°
DGPS source: GD1 (MF-corrected Navstar)		Height source: radio altimeter	
Horizontal sensitivities:	4nm approach: ±850m	Level segment: ±120m	4nm overshoot: ±850m
Vertical sensitivities:	4nm approach: ±350ft	Level segment: ±100ft	4nm overshoot: ±350ft
Entry technique: modified Aerad procedure commencing overhead the platform, with a left-hand outbound leg flown using RNAV-2 guidance and the turn commenced at 4nm range.			
Go-around technique: straight ahead from MAP, climbing as directed by DGPS guidance.			
Handling pilot: MW	Method: Raw data	Start Time: 13:17:50	End Time: 13:21:51
Other details: n/a.			
Pilot comments: The presence of the fairing allowed the aircraft to be levelled off in a satisfactory manner on entry to the level segment. The rate of climb demanded during the go-around was felt to be low.			
Observations: n/a.			



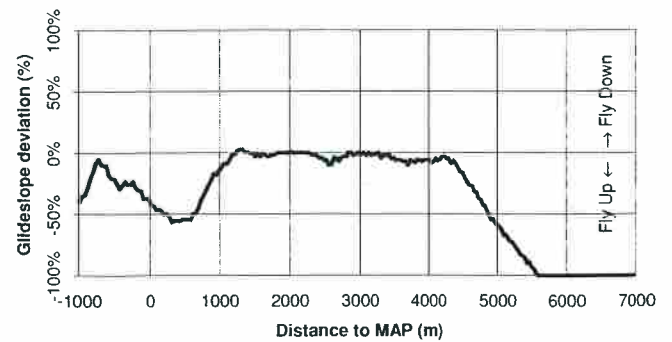
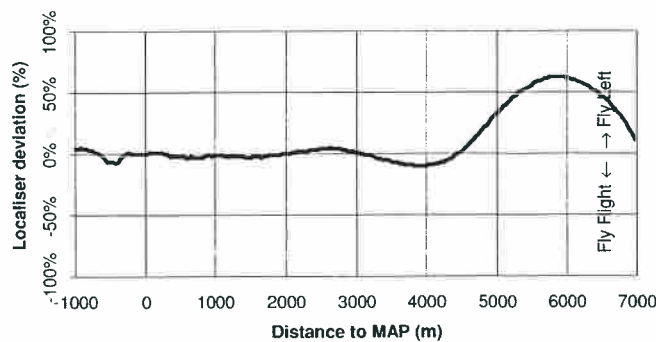
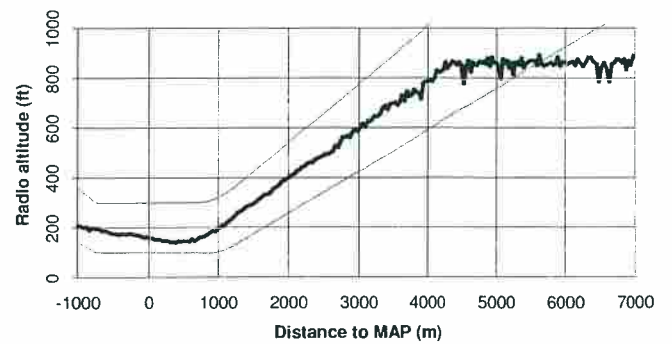
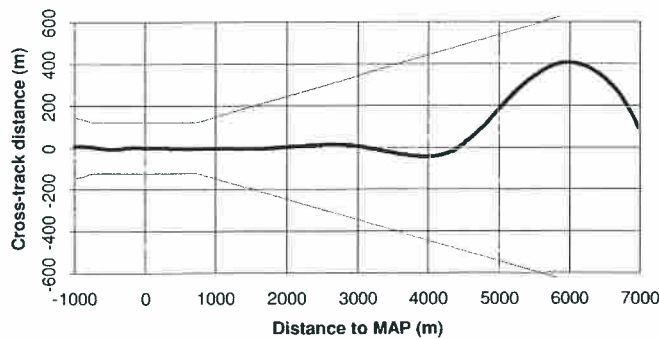
Flight number: 4	Approach number: 2	Location: Piper B	Wind 160-170°,10-25kt
Approach track: QDM 070°M, 250m right offset		Approach angle: 3.5°	Overshoot angle: 3.5°
DGPS source: GD1 (MF-corrected Navstar)		Height source: radio altimeter	
Horizontal sensitivities:	4nm approach: ±850m	Level segment: ±120m	4nm overshoot: ±850m
Vertical sensitivities:	4nm approach: ±350ft	Level segment: ±100ft	4nm overshoot: ±350ft
Entry technique: modified Aerad procedure commencing overhead the platform, with a left-hand outbound leg flown using RNAV-2 guidance and the turn commenced at 4nm range.			
Go-around technique: straight ahead from MAP, climbing as directed by DGPS guidance.			
Handling pilot: MW	Method: Raw data	Start Time: 13:34:11	End Time: 13:37:49
Other details: n/a.			
Pilot comments: The pilot attempted to descend from 800ft before the glideslope command was received (having attempted to follow normal practice rather than following the vertical guidance). The DGPS approach was 'quite gentle'.			
Observations: Examination of the plot reveals that the pilot had recovered back to 800ft by the time that the glideslope command to descend was received.			



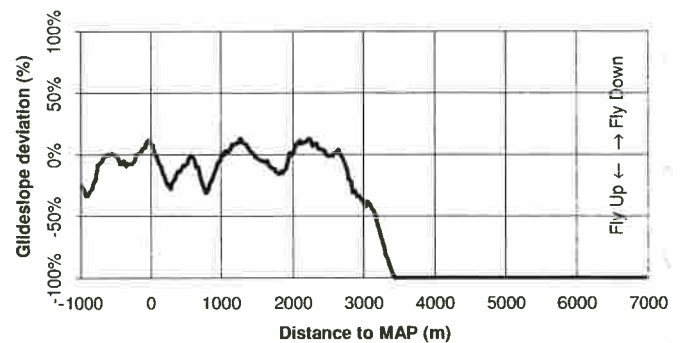
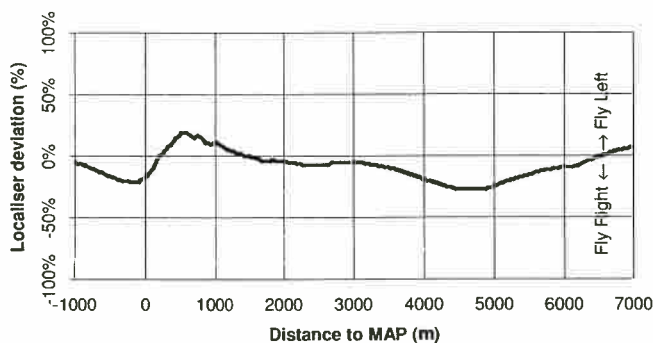
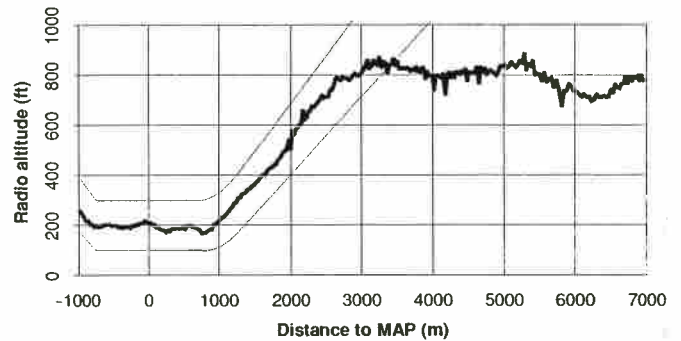
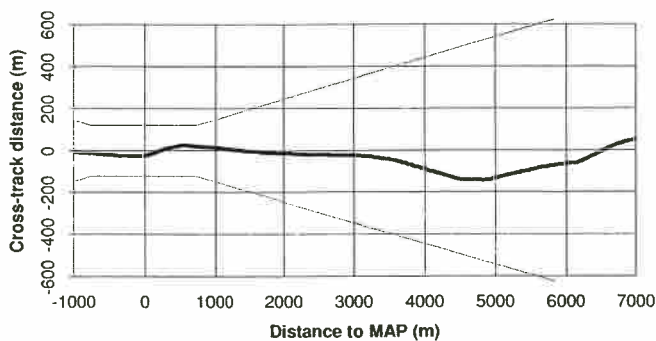
Flight number: 4	Approach number: 3	Location: Piper B	Wind 160-170°,10-25kt
Approach track: QDM 340°M, 250m left offset		Approach angle: 3.5°	Overshoot angle: 3.5°
DGPS source: GD1 (MF-corrected Navstar)		Height source: radio altimeter	
Horizontal sensitivities:	4nm approach: ±850m	Level segment: ±120m	4nm overshoot: ±850m
Vertical sensitivities:	4nm approach: ±350ft	Level segment: ±100ft	4nm overshoot: ±350ft
Entry technique: modified Aerad procedure commencing overhead the platform, with a left-hand outbound leg flown using RNAV-2 guidance and the turn commenced at 4nm range.			
Go-around technique: straight ahead from MAP, climbing as directed by DGPS guidance.			
Handling pilot: MW	Method: Raw data	Start Time: 13:51:20	End Time: 13:54:12
Other details: n/a.			
Pilot comments: The rate of descent at 80kt IAS was felt to be too high (this was a downwind approach). The pilot professed to be quite impressed with the DGPS system.			
Observations: n/a.			



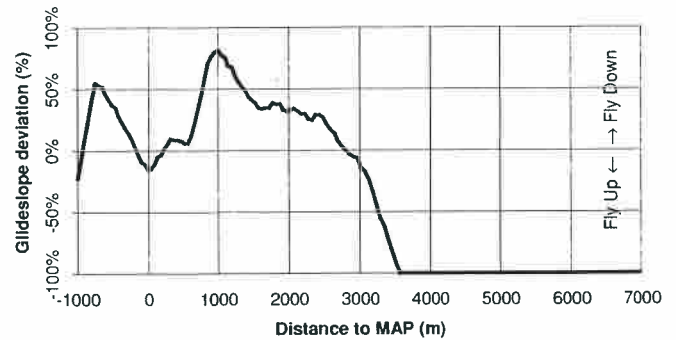
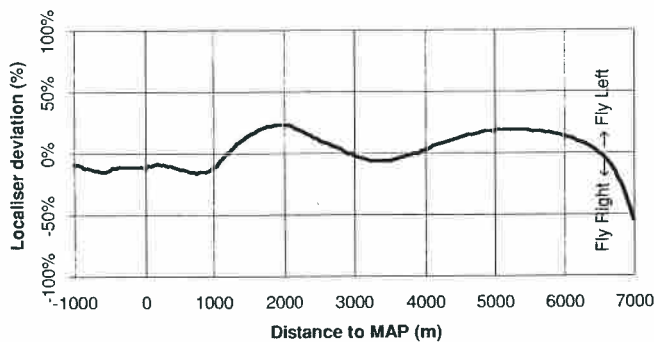
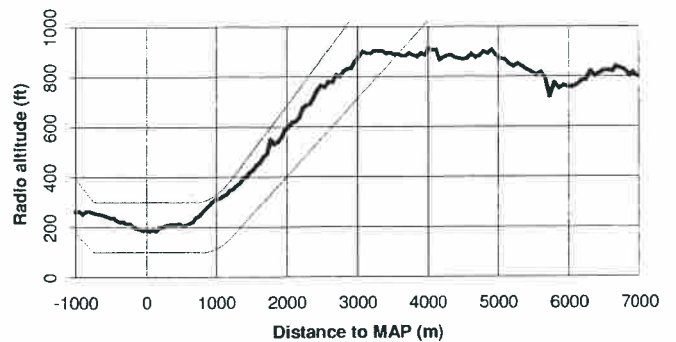
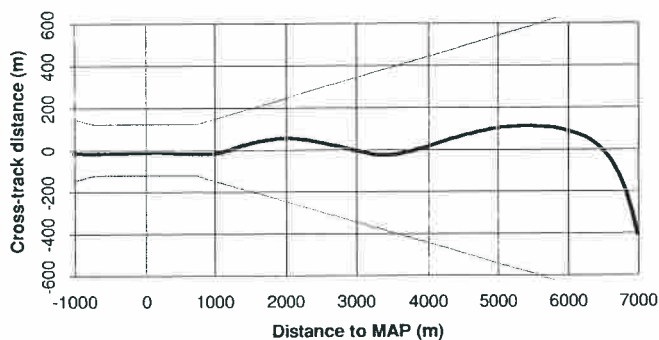
Flight number: 4	Approach number: 4	Location: Piper B	Wind 160-170°,10-25kt
Approach track: QDM 250°M, 250m right offset		Approach angle: 3.5°	Overshoot angle: 3.5°
DGPS source: GD1 (MF-corrected Navstar)		Height source: radio altimeter	
Horizontal sensitivities:	4nm approach: ±850m	Level segment: ±120m	4nm overshoot: ±850m
Vertical sensitivities:	4nm approach: ±350ft	Level segment: ±100ft	4nm overshoot: ±350ft
Entry technique: modified Aerad procedure commencing overhead the platform, with a left-hand outbound leg flown using RNAV-2 guidance and the turn commenced at 4nm range.			
Go-around technique: straight ahead from MAP, climbing as directed by DGPS guidance.			
Handling pilot: MW	Method: Autopilot	Start Time: 14:05:18	End Time: 14:09:04
Other details: n/a.			
Pilot comments: The entire autocoupled approach was observed to be very smooth.			
Observations: As for previous autocoupled approaches, the aircraft descended to around 150ft before recovering to MDH on the level segment. It was felt that this might be improved if the length of the fairing to the level segment were increased.			



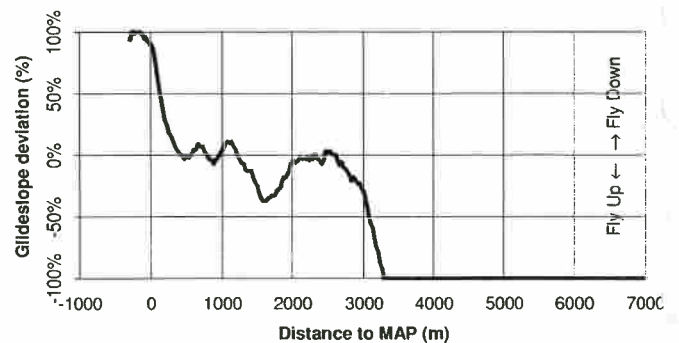
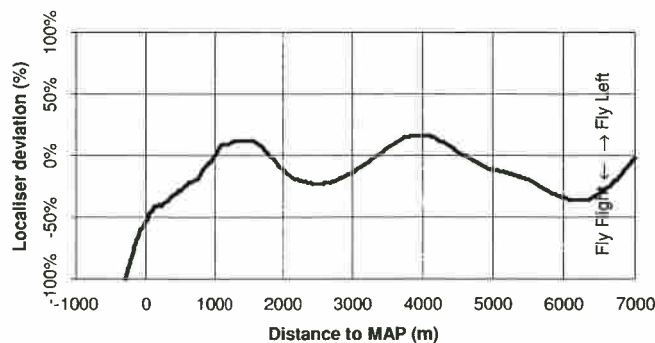
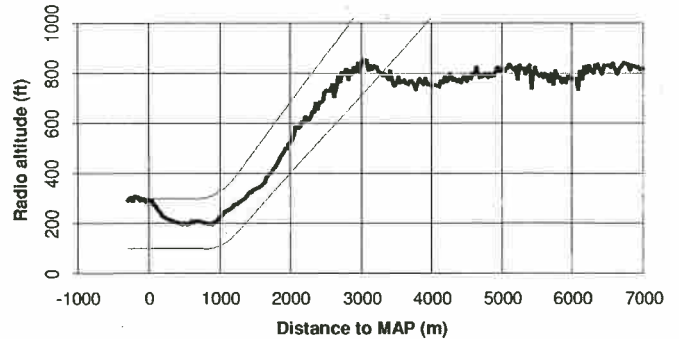
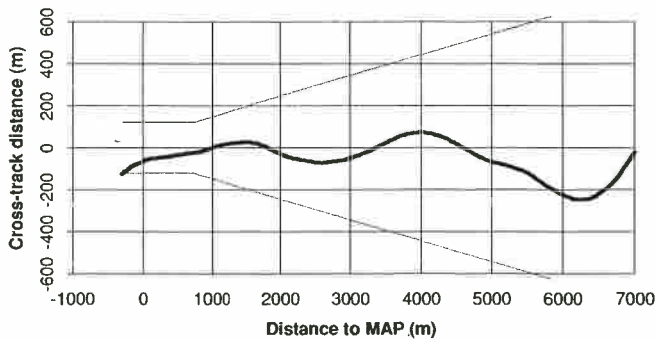
Flight number: 4	Approach number: 5	Location: Piper B	Wind 160-170°,10-25kt
Approach track: QDM 170°M, 250m right offset		Approach angle: 6.0°	Overshoot angle: 6.0°
DGPS source: GD1 (MF-corrected Navstar)		Height source: radio altimeter	
Horizontal sensitivities:	4nm approach: ±850m	Level segment: ±120m	4nm overshoot: ±850m
Vertical sensitivities:	4nm approach: ±350ft	Level segment: ±100ft	4nm overshoot: ±350ft
Entry technique: aircraft flown directly to a point at around 4nm range to intercept the approach.			
Go-around technique: straight ahead from MAP, climbing as directed by DGPS guidance.			
Handling pilot: NT	Method: Raw data	Start Time: 15:01:04	End Time: 15:05:46
Other details: the LED status panel was used for the first time.			
Pilot comments: The use of a 6° go-around angle was considered preferable due to the increased rate of climb, and the entire approach was considered to be smooth. It was observed that the 'LEVel' indication on the LED panel should appear at the start, rather than at the end, of the faired section.			
Observations: n/a.			



Flight number: 4	Approach number: 6	Location: Piper B	Wind 160-170°,10-25kt
Approach track: QDM 350°M, 250m right offset		Approach angle: 6.0°	Overshoot angle: 6.0°
DGPS source: GD1 (MF-corrected Navstar)		Height source: radio altimeter	
Horizontal sensitivities:	4nm approach: ±850m	Level segment: ±120m	4nm overshoot: ±850m
Vertical sensitivities:	4nm approach: ±350ft	Level segment: ±100ft	4nm overshoot: ±350ft
Entry technique: aircraft flown directly to a point at around 4nm range to intercept the approach.			
Go-around technique: straight ahead from MAP, climbing as directed by DGPS guidance.			
Handling pilot: NT	Method: Raw data	Start Time: 15:10:17	End Time: 15:12:48
Other details: the LED status panel was used.			
Pilot comments: The chosen speed of 80kt was felt to be too fast for a downwind 6° approach.			
Observations: n/a.			



Flight number: 4	Approach number: 7	Location: Piper B	Wind 160-170°,10-25kt
Approach track: QDM 170°M, 250m right offset		Approach angle: 6.0°	Overshoot angle: 6.0°
DGPS source: GD1 (MF-corrected Navstar)		Height source: radio altimeter	
Horizontal sensitivities:	4nm approach: ±850m	Level segment: ±120m	4nm overshoot: ±850m
Vertical sensitivities:	4nm approach: ±350ft	Level segment: ±100ft	4nm overshoot: ±350ft
Entry technique: see below.			
Go-around technique: aircraft landed on the platform from the level segment.			
Handling pilot: NT	Method: Raw data	Start Time: 15:19:24	End Time: 15:23:57
Other details: the LED status panel was used. As a first attempt at a segmented approach, a 20° right turn was introduced into the approach track at 4nm range (so that a track of 150°M was followed until the FAF).			
Pilot comments: Flying using raw data on the HSI meant that it was difficult to appreciate the effect of the track change at 4nm. Ideally the HSI course carriage should automatically have changed from 150° to 170° to indicate that a change in track had occurred, as would be the case with RNAV-2 guidance. The pilot levelled instinctively on reaching the level segment.			
Observations: n/a.			



5.5. **Flight Trial 5**

The fifth test flight was performed at the Tartan A platform.

Following a brief experiment during the preceding flight, the curved approach facility (section 4.5.3) was used to provide guidance throughout a standard 'Aerad' overhead leg. The main difficulty experienced was that the DGPS equipment did not automatically drive the HSI course carriage to display the desired track during the turn. With practice, this deficiency was partially overcome by the pilot manually rotating the HSI at the appropriate point.

In common with the previous trial, the level segment horizontal sensitivity had, erroneously, been changed back to $\pm 120\text{m}$, despite the fact that the optimum sensitivity had been determined to be $\pm 90\text{m}$ on Flight 3.

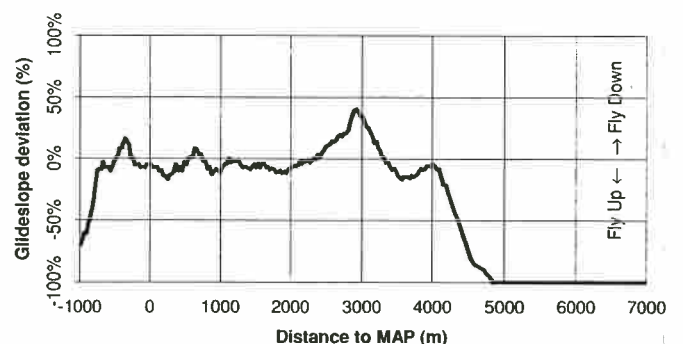
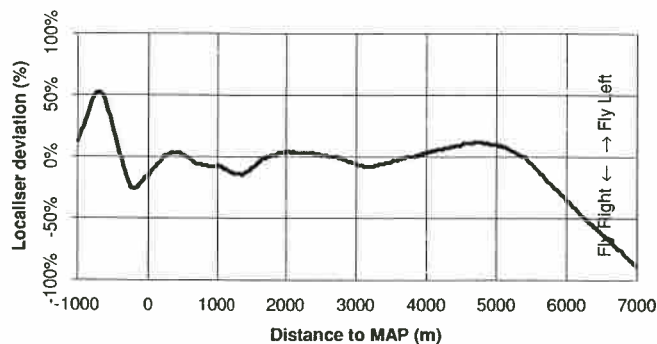
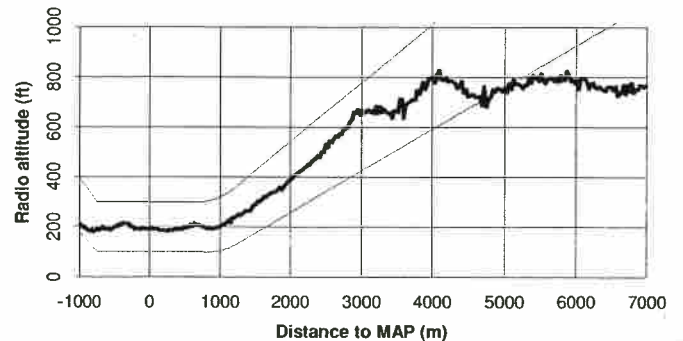
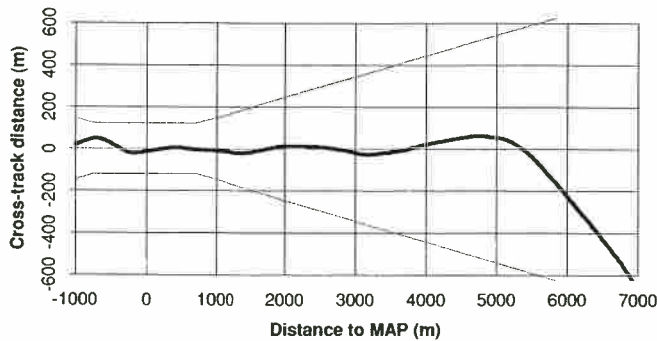
An increase in vertical guidance sensitivity for the level segment of $\pm 50\text{ft}$ was investigated, with mixed results. Comments were received that the new scaling was too sensitive, particularly at lower airspeeds. It was concluded that this change might be acceptable (providing 'tighter' altitude control) at higher speeds.

The autopilot go-around facility was employed for the first time as an alternative to the DGPS-guided overshoot segment.

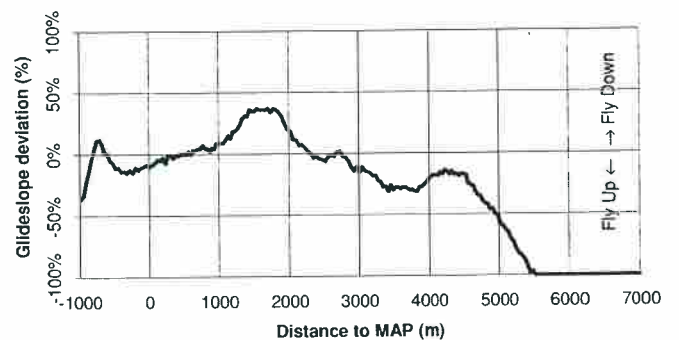
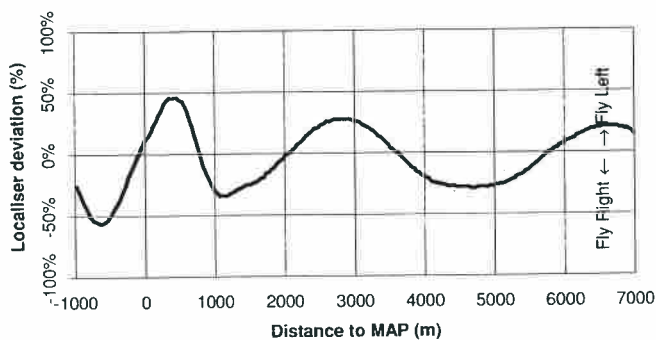
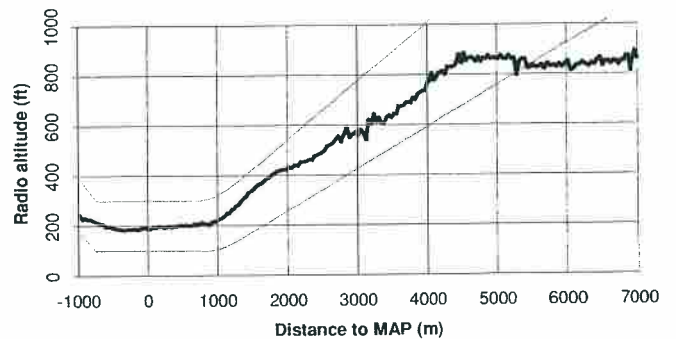
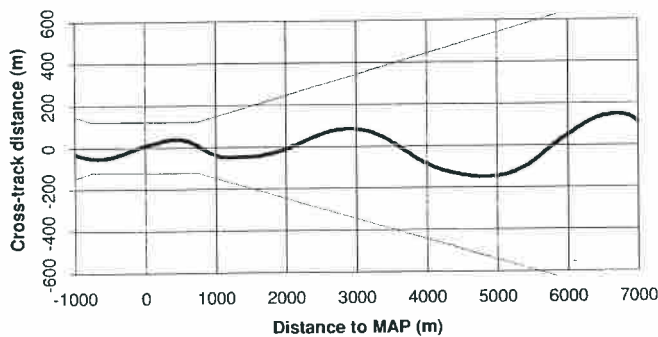
Further to the previous flight trial, an attempt was made to perform an autocoupled approach with the amount of vertical fairing doubled. This appeared to have little effect upon the altitude undershoot problem and it was concluded that there was a more fundamental problem with the matching of the autopilot gains to the DGPS profiles.

The LED indicators were retained and more comments were received regarding the optimum illumination sequence.

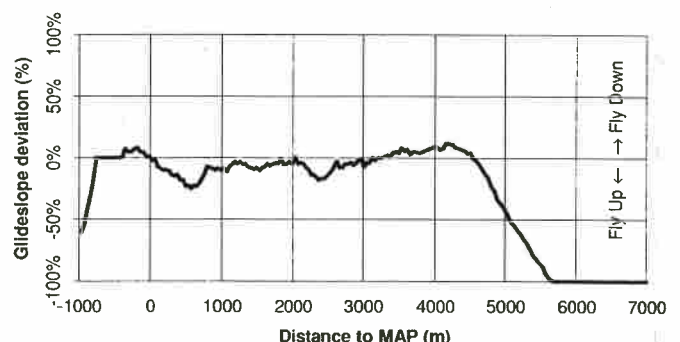
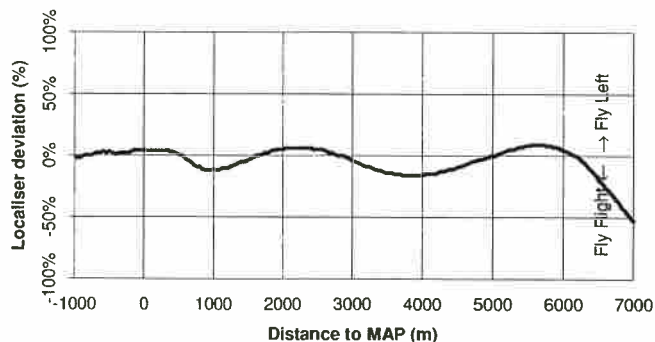
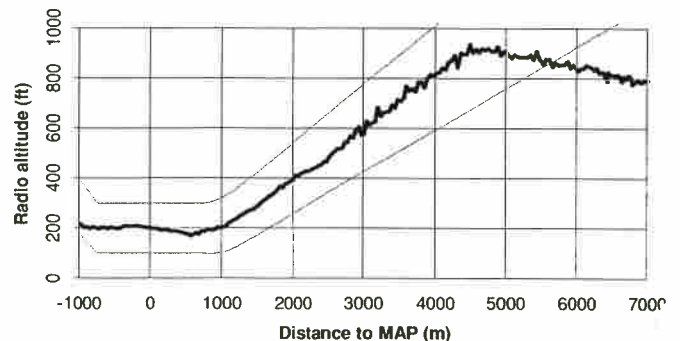
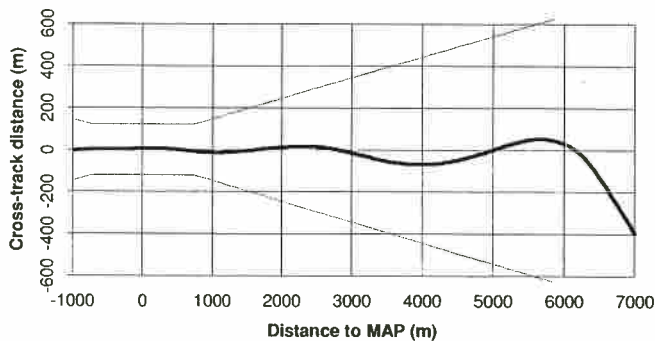
Flight number: 5	Approach number: 1	Location: Tartan A	Wind: 250-260°M, 30kt
Approach track: QDM 260°M, 250m right offset		Approach angle: 3.5°	Overshoot angle: 6.0°
DGPS source: GD1 (MF-corrected Navstar)		Height source: radio altimeter	
Horizontal sensitivities:	4nm approach: ±850m	Level segment: ±120m	4nm overshoot: ±850m
Vertical sensitivities:	4nm approach: ±350ft	Level segment: ±100ft	4nm overshoot: ±350ft
Entry technique: Aerad overhead procedure following guidance generated by the DGPS equipment throughout. A left turn onto the finals track was programmed to occur automatically at 4nm range.			
Go-around technique: straight ahead from MAP, climbing using autopilot go-around facility at end of level segment.			
Handling pilot: NT	Method: Raw data	Start Time: 10:28:11	End Time: 10:32:48
Other details: n/a.			
Pilot comments: It was difficult to perform the turn at 4nm range with only raw data guidance owing to lack of sufficient information to provide full situational awareness: in particular, the HSI course carriage was not driven automatically by the DGPS equipment.			
Observations: n/a.			



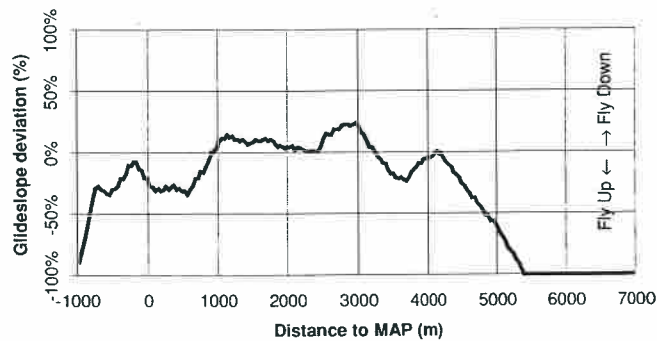
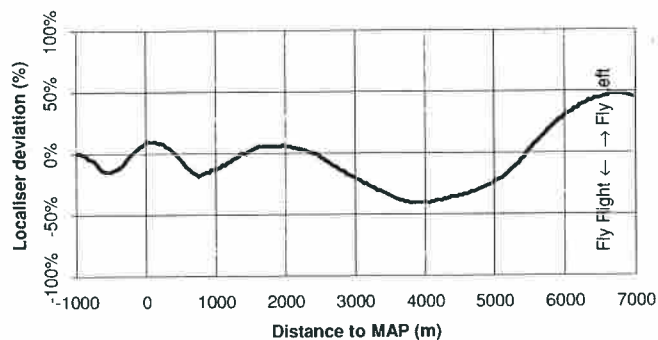
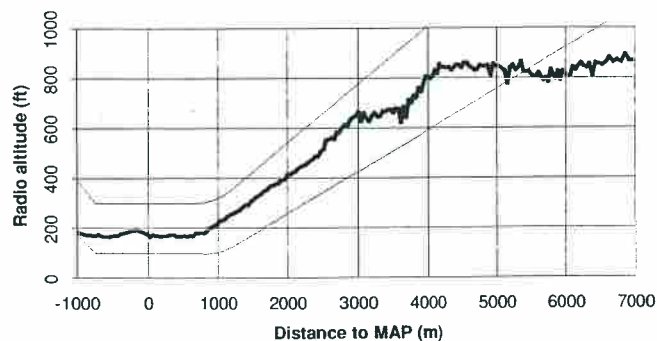
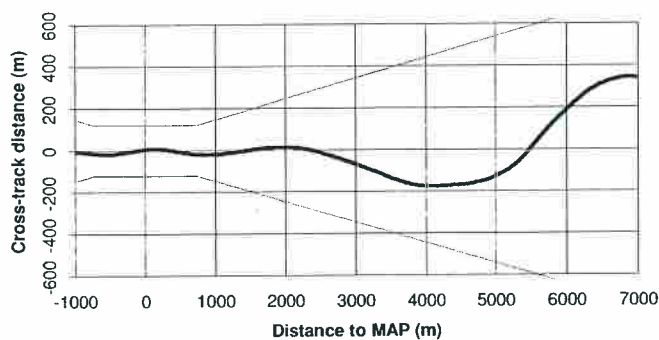
Flight number: 5	Approach number: 2	Location: Tartan A	Wind: 250-260°M, 30kt
Approach track: QDM 170°M, 250m right offset		Approach angle: 3.5°	Overshoot angle: 6.0°
DGPS source: GD1 (MF-corrected Navstar)		Height source: radio altimeter	
Horizontal sensitivities:	4nm approach: ±850m	Level segment: ±120m	4nm overshoot: ±850m
Vertical sensitivities:	4nm approach: ±350ft	Level segment: ±100ft	4nm overshoot: ±350ft
Entry technique: Aerad overhead procedure following guidance generated by the DGPS equipment throughout. A left turn onto the finals track was programmed to occur automatically at 4nm range.			
Go-around technique: straight ahead from MAP, climbing using autopilot go-around facility at end of level segment.			
Handling pilot: NT	Method: Flight director	Start Time: 10:42:29	End Time: 10:46:03
Other details: n/a.			
Pilot comments: The pilot found it difficult to follow the flight director guidance due to the fact that the instrument indications were being affected by vibration to such an extent that they appeared blurred. Partially as a result, the aircraft was not stabilised on the desired approach trajectory and a decision was taken to repeat this approach.			
Observations: The problems with the instrument indications appeared to be purely mechanical in nature and unrelated to the DGPS equipment: the beam-bar needles were resonating with airframe vibration.			



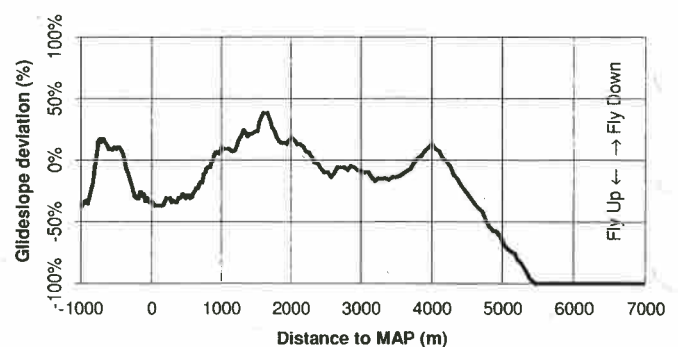
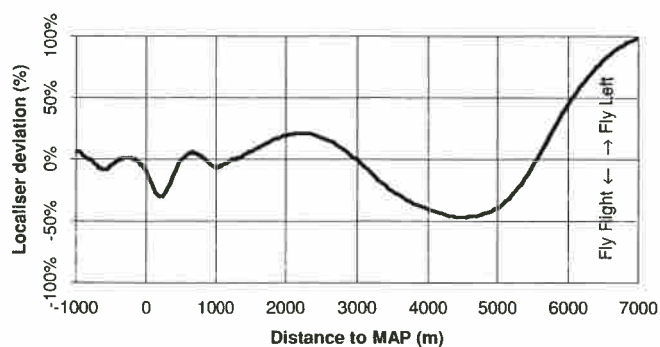
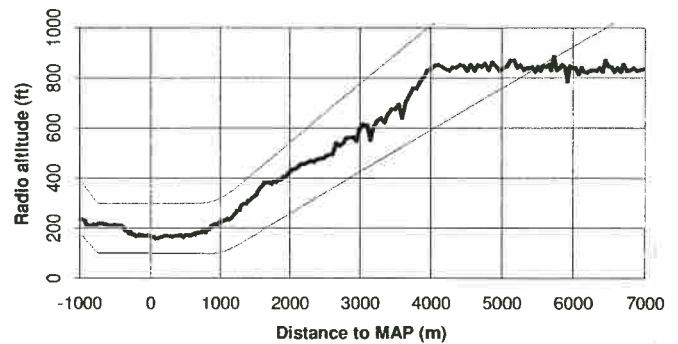
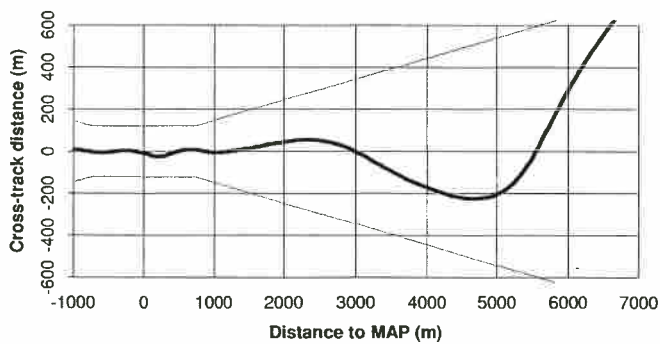
Flight number: 5	Approach number: 3	Location: Tartan A	Wind: 250-260°M, 30kt
Approach track: QDM 170°M, 250m left offset		Approach angle: 3.5°	Overshoot angle: 6.0°
DGPS source: GD1 (MF-corrected Navstar)		Height source: radio altimeter	
Horizontal sensitivities:	4nm approach: ±850m	Level segment: ±120m	4nm overshoot: ±850m
Vertical sensitivities:	4nm approach: ±350ft	Level segment: ±100ft	4nm overshoot: ±350ft
Entry technique: Aerad overhead procedure following guidance generated by the DGPS equipment throughout. A left turn onto the finals track was programmed to occur automatically at 4nm range.			
Go-around technique: straight ahead from MAP, climbing using autopilot go-around facility at end of level segment.			
Handling pilot: NM	Method: Flight director	Start Time: 10:54:34	End Time: 10:57:58
Other details: n/a.			
Pilot comments: The pilot was able to mentally overcome the indication problems and had no difficulty following the guidance on this approach. He stated that it was also possible to follow the DGPS guidance around the turn in a satisfactory manner.			
Observations: n/a.			



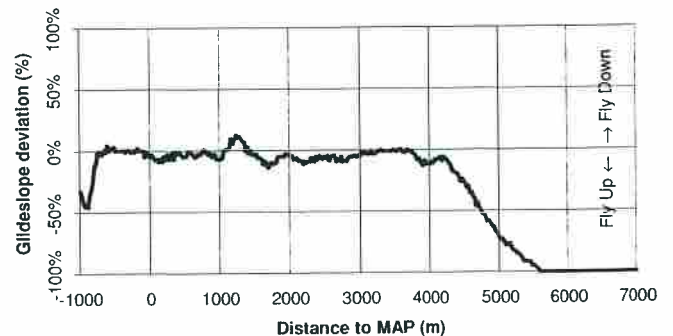
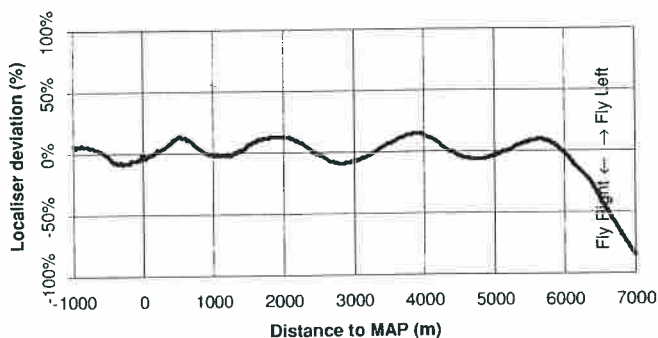
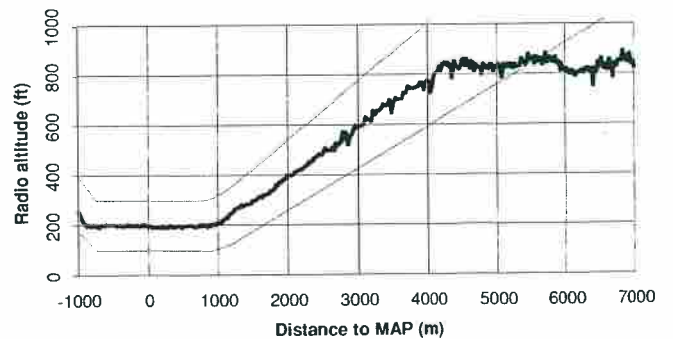
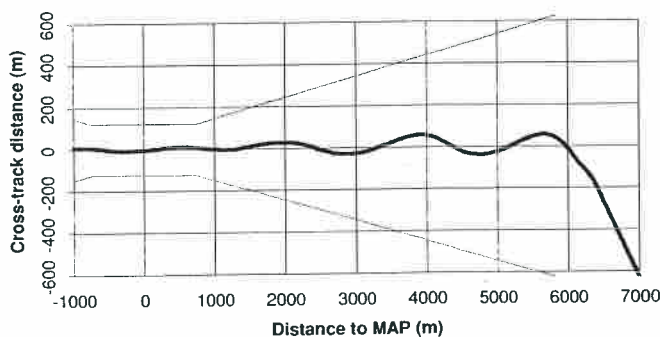
Flight number: 5	Approach number: 4	Location: Tartan A	Wind: 250-260°M, 30kt
Approach track: QDM 080°M, 250m left offset		Approach angle: 3.5°	Overshoot angle: 6.0°
DGPS source: GD1 (MF-corrected Navstar)		Height source: radio altimeter	
Horizontal sensitivities:	4nm approach: ±850m	Level segment: ±120m	4nm overshoot: ±850m
Vertical sensitivities:	4nm approach: ±350ft	Level segment: ±100ft	4nm overshoot: ±350ft
Entry technique: Aerad overhead procedure following guidance generated by the DGPS equipment throughout. A left turn onto the finals track was programmed to occur automatically at 4nm range.			
Go-around technique: straight ahead from MAP, climbing using autopilot go-around facility at end of level segment.			
Handling pilot: NM	Method: Flight director	Start Time: 11:07:04	End Time: 11:10:32
Other details: Downwind approach.			
Pilot comments: Performance around the turn was improved by anticipating the turn by manually rotating the HSI course selector. The approach was performed at 50kt and speed control was difficult as a result.			
Observations: n/a.			



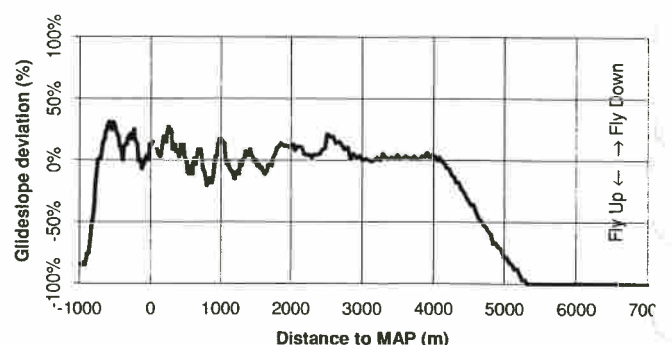
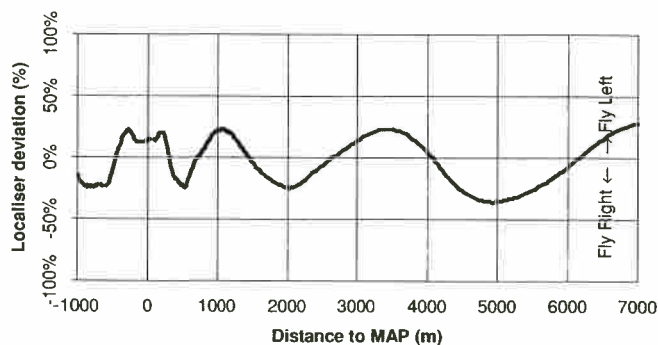
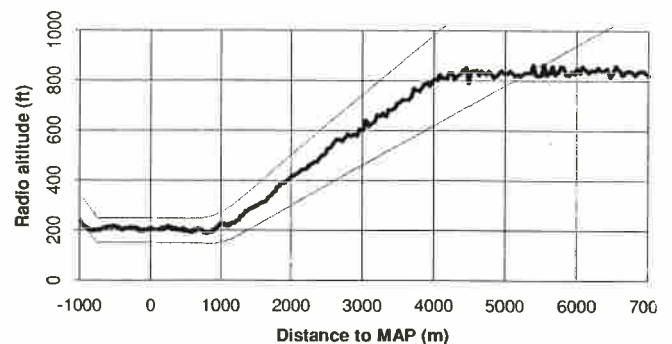
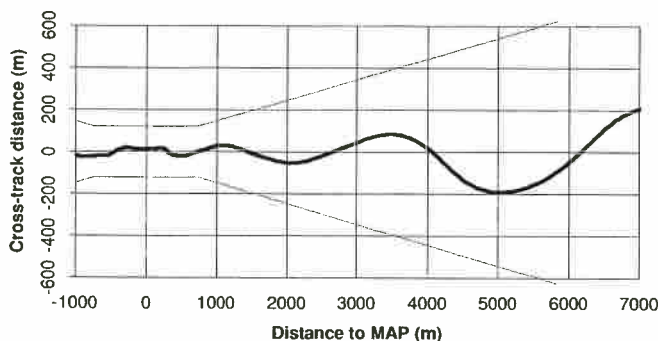
Flight number: 5	Approach number: 5	Location: Tartan A	Wind: 250-260°M, 30kt
Approach track: QDM 350°M, 250m left offset		Approach angle: 3.5°	Overshoot angle: 6.0°
DGPS source: GD1 (MF-corrected Navstar)		Height source: radio altimeter	
Horizontal sensitivities:	4nm approach: ±850m	Level segment: ±120m	4nm overshoot: ±850m
Vertical sensitivities:	4nm approach: ±350ft	Level segment: ±100ft	4nm overshoot: ±350ft
Entry technique: Aerad overhead procedure following guidance generated by the DGPS equipment throughout. A left turn onto the finals track was programmed to occur automatically at 4nm range.			
Go-around technique: straight ahead from MAP, climbing using autopilot go-around facility at end of level segment.			
Handling pilot: NM	Method: Flight director	Start Time: 11:20:08	End Time: 11:25:12
Other details: n/a.			
Pilot comments: Despite anticipating using the HSI course selector, the pilot overshoot during the turn and had to regain the finals track. Speed was reduced to 50kt midway through the approach and workload was increased as a result, due to speed control problems and the large (35°) drift angles introduced. It would be preferable for the 'APPROach' segment LED to only illuminate once the aircraft was established on finals.			
Observations: n/a.			



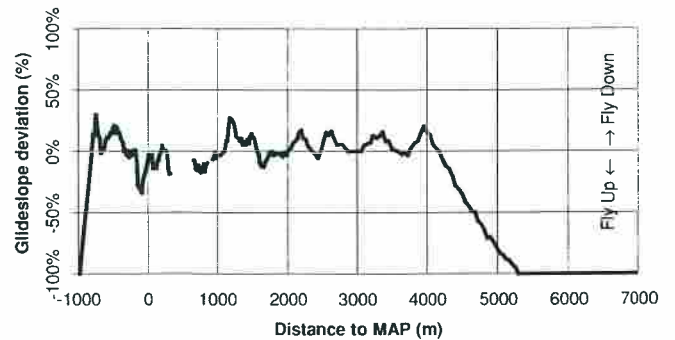
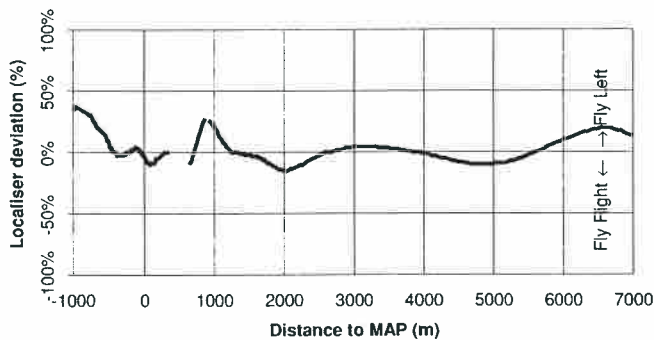
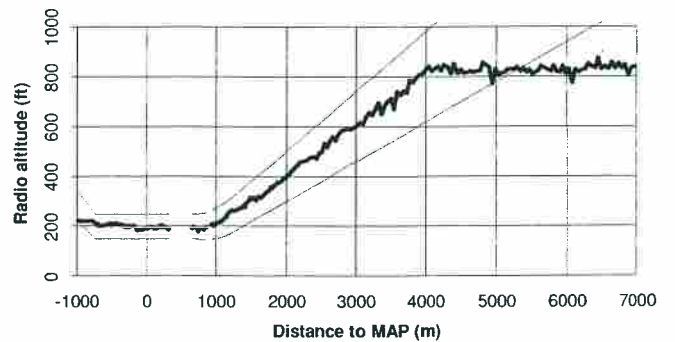
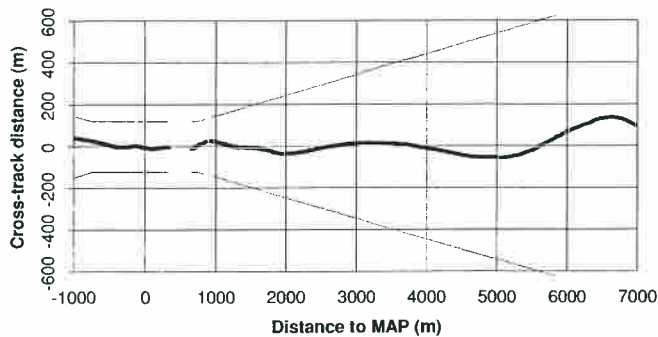
Flight number: 5	Approach number: 6	Location: Tartan A	Wind: 250-260°M, 30kt
Approach track: QDM 170°M, 250m right offset		Approach angle: 3.5°	Overshoot angle: 6.0°
DGPS source: GD1 (MF-corrected Navstar)		Height source: radio altimeter	
Horizontal sensitivities:	4nm approach: ±850m	Level segment: ±120m	4nm overshoot: ±850m
Vertical sensitivities:	4nm approach: ±350ft	Level segment: ±100ft	4nm overshoot: ±350ft
Entry technique: aircraft flown directly to a point at around 4nm range to intercept the approach.			
Go-around technique: straight ahead from MAP, climbing using autopilot go-around facility at end of level segment.			
Handling pilot: NT	Method: Flight director	Start Time: 12:28:36	End Time: 12:34:28
Other details: the approach was flown at 50kt.			
Pilot comments: This was a repeat of the approach on which the pilot had experienced handling problems (number 2), no difficulties were reported on this attempt. The more positive go-around provided by the autopilot was useful. It would be preferable for the 'APProach' segment LED to only illuminate once the aircraft was established on finals.			
Observations: n/a.			



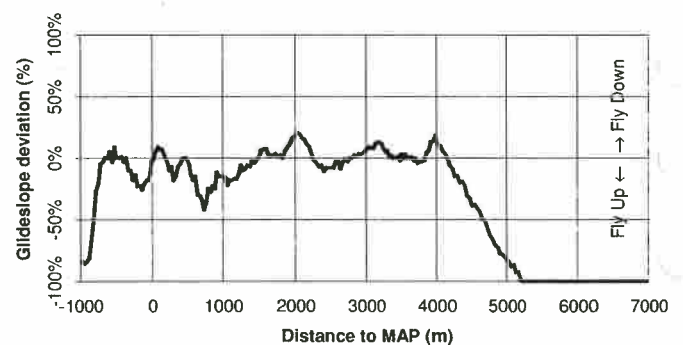
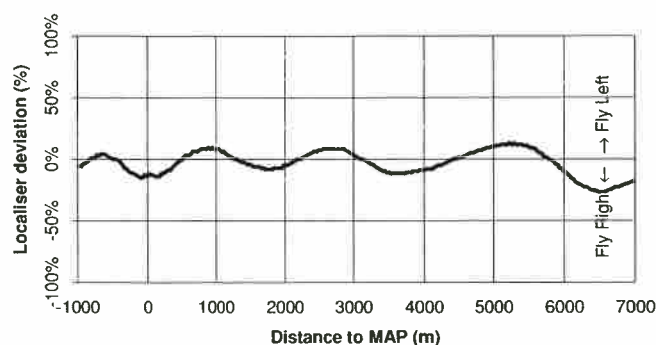
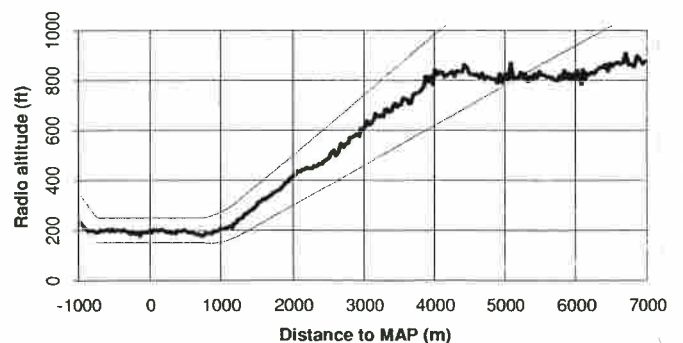
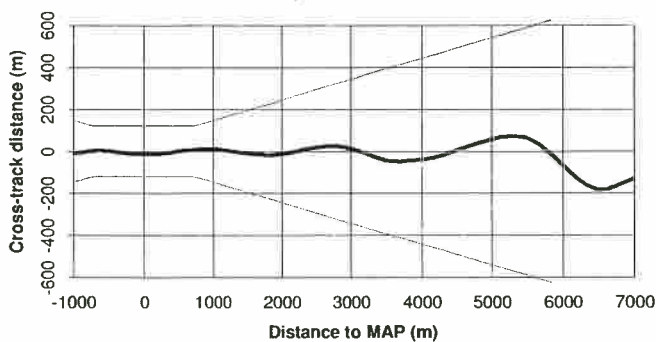
Flight number: 5	Approach number: 7	Location: Tartan A	Wind: 250-260°M, 30kt
Approach track: QDM 170°M, 250m right offset		Approach angle: 3.5°	Overshoot angle: 6.0°
DGPS source: GD1 (MF-corrected Navstar)		Height source: radio altimeter	
Horizontal sensitivities:	4nm approach: ±850m	Level segment: ±120m	4nm overshoot: ±850m
Vertical sensitivities:	4nm approach: ±350ft	Level segment: ±50ft	4nm overshoot: ±350ft
Entry technique: aircraft flown directly to a point at around 4nm range to intercept the approach.			
Go-around technique: straight ahead from MAP, climbing using autopilot go-around facility at end of level segment.			
Handling pilot: NT	Method: Flight director	Start Time: 12:43:27	End Time: 12:48:29
Other details: the approach was flown at 80kt reducing to 40kt midway.			
Pilot comments: A high workload resulted in the pilot failing to observe the 'MAP' LED indication. A 40kt approach speed was considered to be unacceptable owing to roll/yaw coupling problems. The change in vertical sensitivity to ±50ft meant that the vertical tracking task was now harder: the pilot assigned a Cooper-Harper rating of between 4 and 5.			
Observations: n/a.			



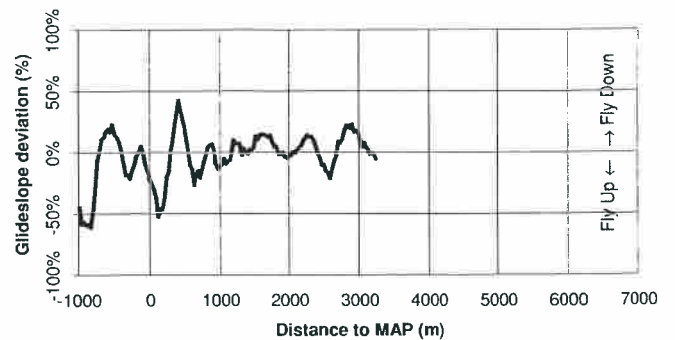
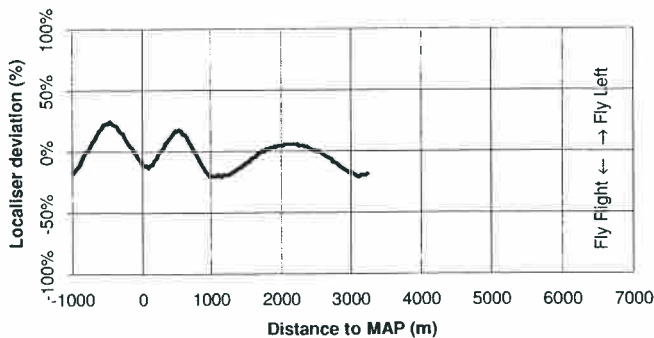
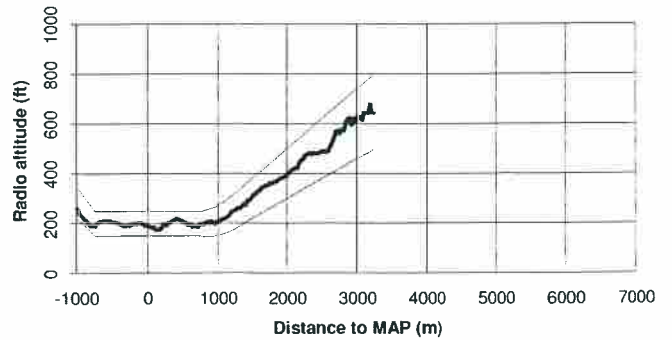
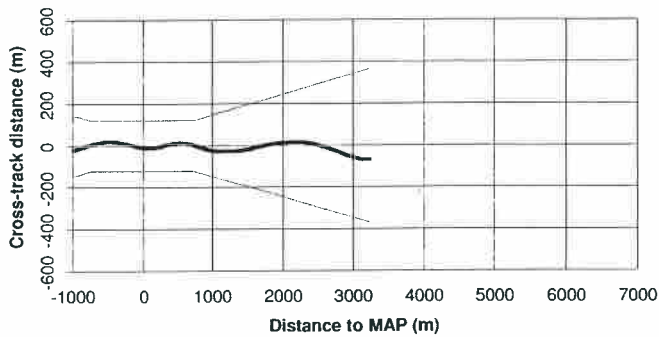
Flight number: 5	Approach number: 8	Location: Tartan A	Wind: 250-260°M, 30kt
Approach track: QDM 170°M, 250m left offset		Approach angle: 3.5°	Overshoot angle: 6.0°
DGPS source: GD1 (MF-corrected Navstar)		Height source: radio altimeter	
Horizontal sensitivities:	4nm approach: ±850m	Level segment: ±120m	4nm overshoot: ±850m
Vertical sensitivities:	4nm approach: ±350ft	Level segment: ±50ft	4nm overshoot: ±350ft
Entry technique: aircraft flown directly to a point at around 4nm range to intercept the approach.			
Go-around technique: straight ahead from MAP, climbing using autopilot go-around facility at end of level segment.			
Handling pilot: NM	Method: Flight director	Start Time: 12:57:07	End Time: 13:01:43
Other details: the approach was flown at 80kt reducing to 40kt midway.			
Pilot comments: The workload was high and possibly unacceptable: the drift angle at 40kt was 30°.			
Observations: The discontinuity in the traces at around 500m arises from a post-processing problem: continuous indications were, in fact, presented throughout the approach.			



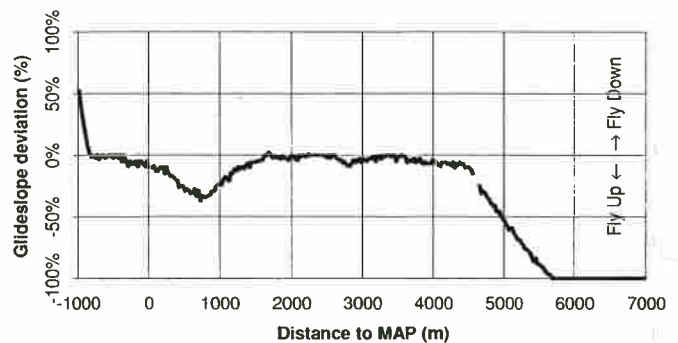
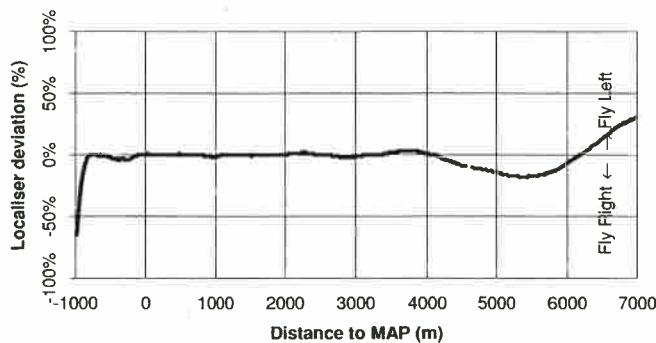
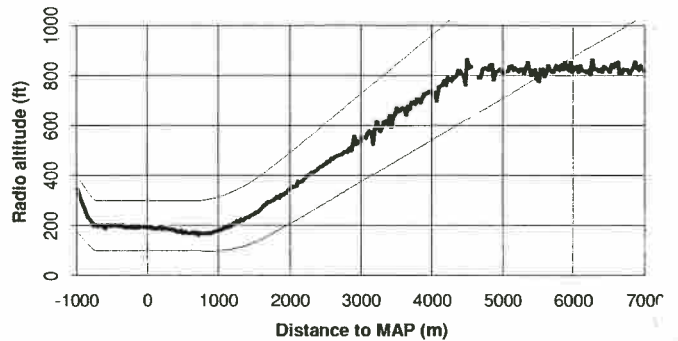
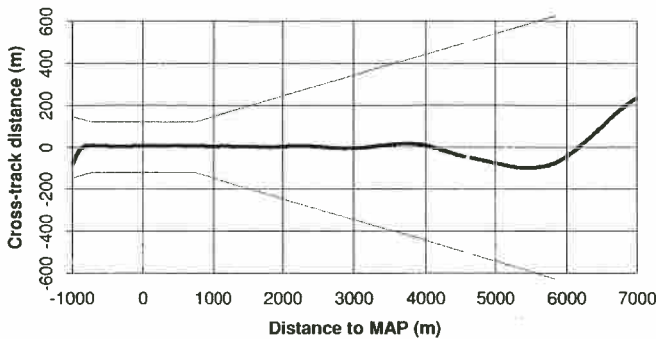
Flight number: 5	Approach number: 9	Location: Tartan A	Wind: 250-260°M, 30kt
Approach track: QDM 260°M, 250m left offset		Approach angle: 3.5°	Overshoot angle: 6.0°
DGPS source: GD1 (MF-corrected Navstar)		Height source: radio altimeter	
Horizontal sensitivities:	4nm approach: ±850m	Level segment: ±120m	4nm overshoot: ±850m
Vertical sensitivities:	4nm approach: ±350ft	Level segment: ±50ft	4nm overshoot: ±350ft
Entry technique: aircraft flown directly to a point at around 4nm range to intercept the approach.			
Go-around technique: straight ahead from MAP, climbing using autopilot go-around facility at end of level segment.			
Handling pilot: NM	Method: Flight director	Start Time: 13:07:39	End Time: 13:11:45
Other details: the approach was flown at 80kt into wind.			
Pilot comments: The increase in approach speed to 80kt improved the flying task considerably. The HSI glidepath indicator was considered to be too insensitive to cope with the ±50ft level segment; however there was no problem with the more sensitive ADI 'raw data' indications.			
Observations: n/a.			



Flight number: 5	Approach number: 10	Location: Tartan A	Wind: 250-260°M, 30kt
Approach track: QDM 260°M, 250m right offset		Approach angle: 3.5°	Overshoot angle: 6.0°
DGPS source: GD1 (MF-corrected Navstar)		Height source: radio altimeter	
Horizontal sensitivities:	4nm approach: ±850m	Level segment: ±120m	4nm overshoot: ±850m
Vertical sensitivities:	4nm approach: ±350ft	Level segment: ±50ft	4nm overshoot: ±350ft
Entry technique: aircraft flown directly to a point at around 4nm range to intercept the approach.			
Go-around technique: straight ahead from MAP, climbing using autopilot go-around facility at end of level segment.			
Handling pilot: NT	Method: Flight director	Start Time: 13:20:56	End Time: 13:23:20
Other details: the approach was flown at 80kt.			
Pilot comments: The pilot considered that the sensitivity was not excessive and allowed the height to be more tightly controlled.			
Observations: n/a.			



Flight number: 5	Approach number: 11	Location: Tartan A	Wind: 250-260°M, 30kt
Approach track: QDM 260°M, 250m right offset		Approach angle: 3.5°	Overshoot angle: 6.0°
DGPS source: GD1 (MF-corrected Navstar)		Height source: radio altimeter	
Horizontal sensitivities:	4nm approach: ±850m	Level segment: ±120m	4nm overshoot: ±850m
Vertical sensitivities:	4nm approach: ±350ft	Level segment: ±100ft	4nm overshoot: ±350ft
Entry technique: aircraft flown directly to a point at around 4nm range to intercept the approach.			
Go-around technique: straight ahead from MAP, climbing using autopilot go-around facility at end of level segment.			
Handling pilot: NT	Method: Autopilot	Start Time: 13:30:31	End Time: 13:35:34
Other details: the amount of fairing was doubled (to 1000m horizontal distance) to investigate whether this improved the autopilot's ability to handle the transition from the approach to the level segment.			
Pilot comments: Despite increasing the amount of fairing there was no significant improvement: the aircraft still descended to nearly 150ft.			
Observations: n/a.			



5.6. **Flight Trial 6**

The sixth test flight was performed at the Buchan A platform.

The approaches at the Buchan A were performed in weather conditions (low cloudbase, reduced visibility in rain, and winds in excess of 30kt) which were considerably more severe than had been experienced on previous test flights.

The availability of MF differential corrections was intermittent, causing reversion of the GD1 receiver solution to stand-alone mode for some of the early approaches. A decision was taken midway through the flight to change to the use of the GD2 (UHF-corrected) receiver for guidance.

The level segment sensitivities were reduced to $\pm 90\text{m}$ and $\pm 50\text{ft}$ in an attempt to perform further investigations with these scalings. Although good results had been achieved on a previous trial with the lesser value, a horizontal scale factor of $\pm 120\text{m}$ was preferred possibly due to the additional workload imposed by the weather and technical problems.

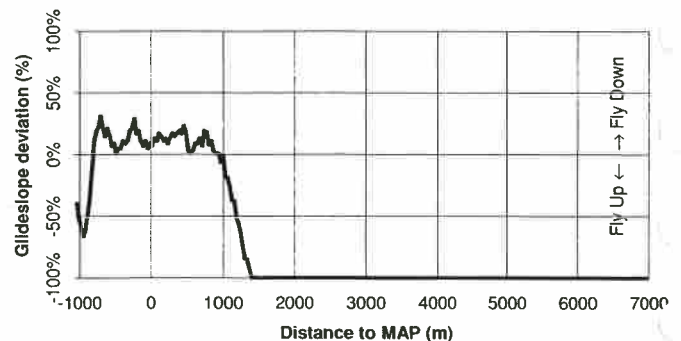
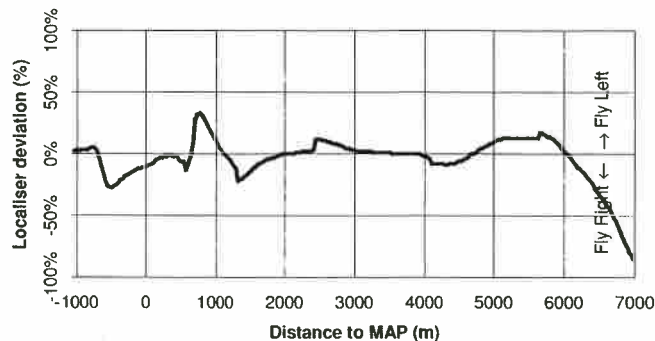
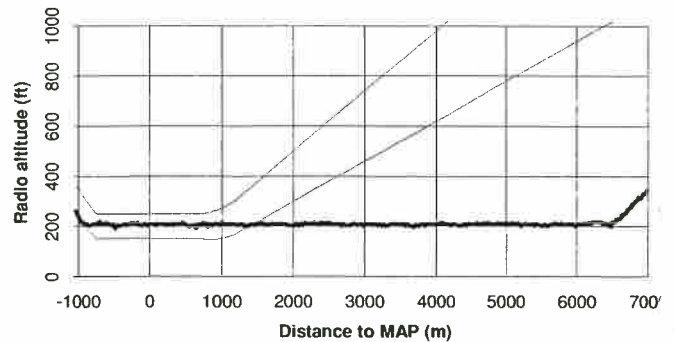
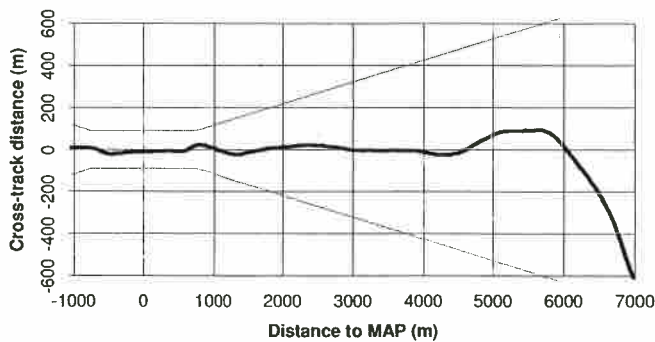
A further attempt was made to use the curved approach feature to provide an 'Aerad' overlay, but a combination of the known HSI course-carriage problem, and the additional workload, resulted in its abandonment and a reversion to the use of the more familiar RNAV-2.

A few approaches were performed with the go-around turnaway software modification (section 4.5.4) enabled, with generally satisfactory results.

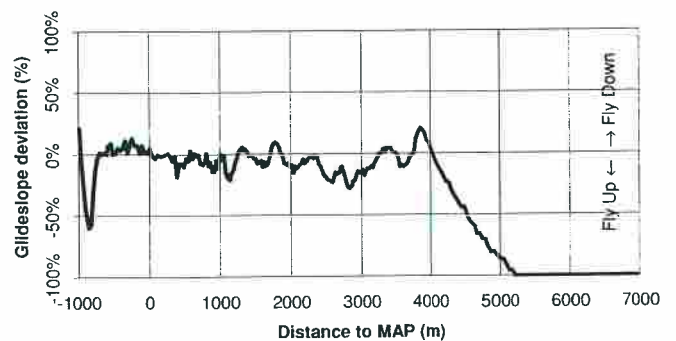
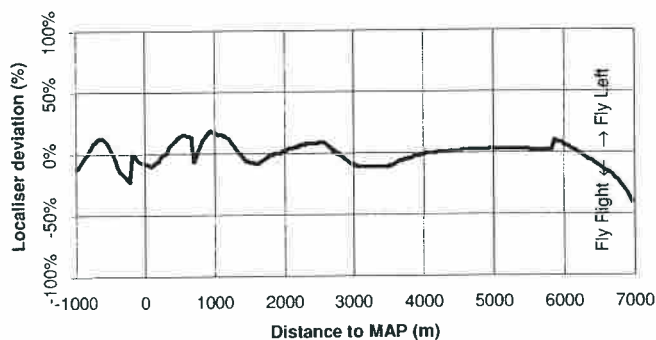
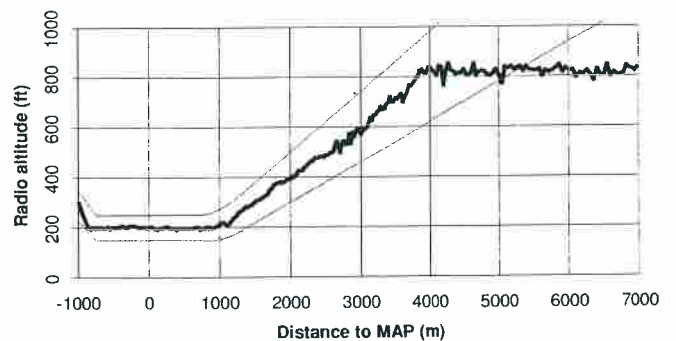
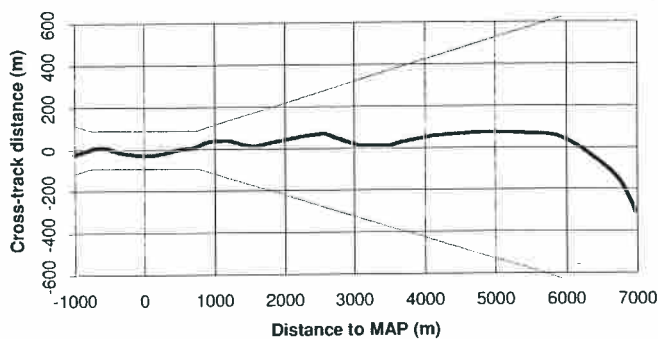
Approaches were also performed with the level segment removed, simulating a direct approach to a helideck, with some success.

More comments on the operation of the LED indicators were obtained.

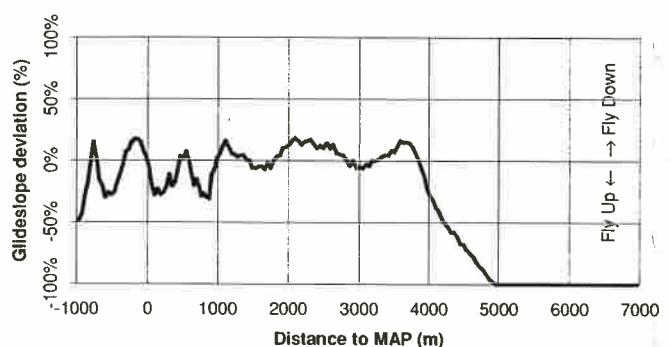
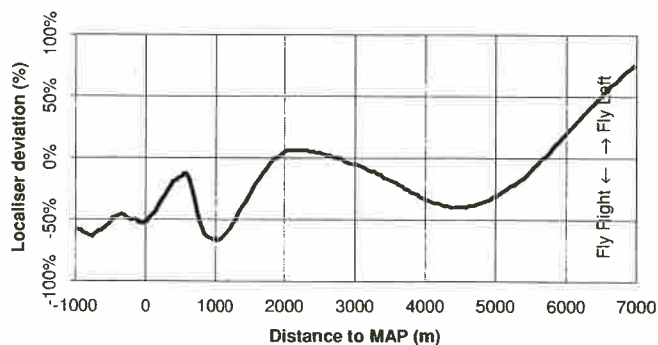
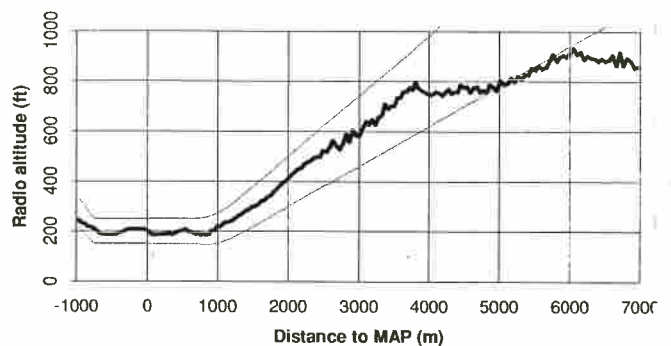
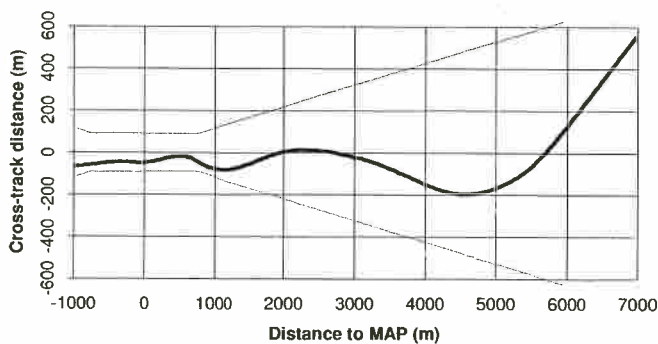
Flight number: 6	Approach number: 1	Location: Buchan A	Wind: 150°M, 30kt
Approach track: QDM 150°M, 200m right offset		Approach angle: 3.5°	Overshoot angle: 6.0°
DGPS source: GD1 (MF-corrected Navstar)		Height source: radio altimeter	
Horizontal sensitivities:	4nm approach: ±850m	Level segment: ±90m	4nm overshoot: ±850m
Vertical sensitivities:	4nm approach: ±350ft	Level segment: ±50ft	4nm overshoot: ±350ft
Entry technique: modified Aerad procedure commencing overhead the platform, with a left-hand outbound leg flown using RNAV-2 guidance and the turn commenced at 4nm range.			
Go-around technique: straight ahead from MAP, climbing as directed by DGPS guidance.			
Handling pilot: NM	Method: Raw data	Start Time: 11:59:33	End Time: 12:03:59
Other details: n/a.			
Pilot comments: A descent to 200ft was erroneously commenced by the pilot before intercepting the glideslope. Occasional short-duration transients were observed on the localiser deviation indicator, in particular at around 1nm range. The along-track distance display on the DME readout was confusing: true range to the platform would be preferable.			
Observations: The transients on the localiser deviation were attributed to the fact that the GD1 GPS receiver operated in non-differential mode for much of the approach due to loss of the MF corrections, giving rise to periodic step changes in the indications, particularly those shown on the expanded localiser needle associated with the ADI.			



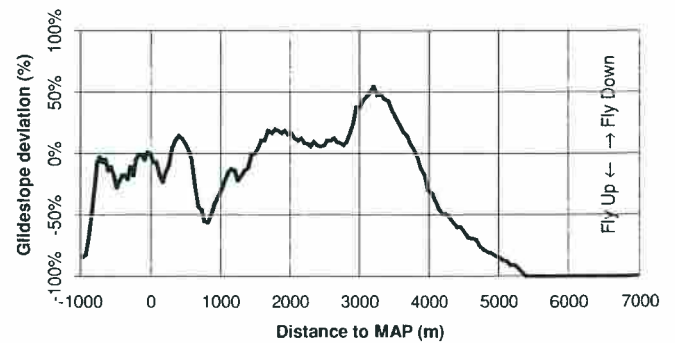
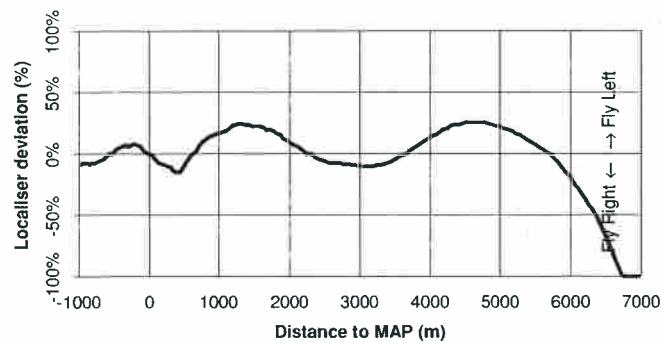
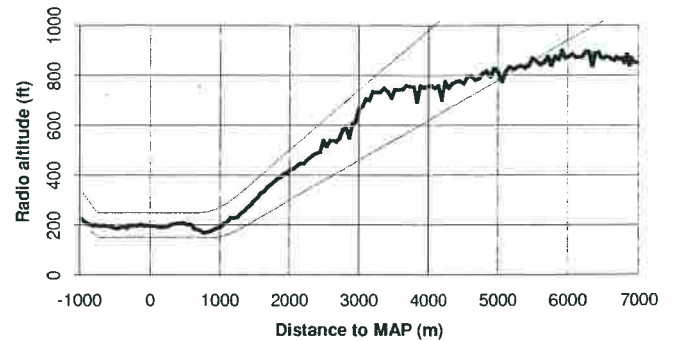
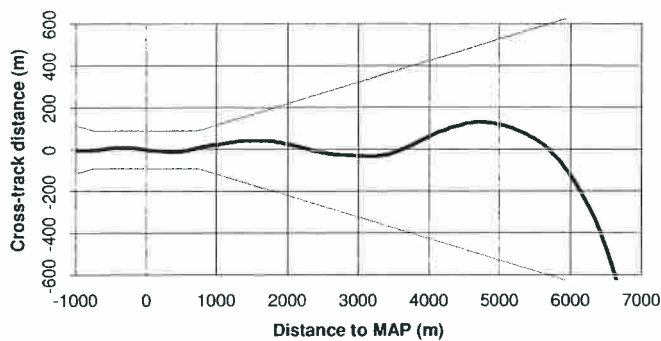
Flight number: 6	Approach number: 2	Location: Buchan A	Wind: 150°M, 30kt
Approach track: QDM 150°M, 200m right offset		Approach angle: 3.5°	Overshoot angle: 6.0°
DGPS source: GD1 (MF-corrected Navstar)		Height source: radio altimeter	
Horizontal sensitivities:	4nm approach: ±850m	Level segment: ±90m	4nm overshoot: ±850m
Vertical sensitivities:	4nm approach: ±350ft	Level segment: ±50ft	4nm overshoot: ±350ft
Entry technique: Aerad overhead procedure following guidance generated by the DGPS equipment throughout. A left turn onto the finals track was programmed to occur automatically at 4nm range.			
Go-around technique: straight ahead from MAP, climbing as directed by DGPS guidance.			
Handling pilot: NM	Method: Raw data	Start Time: 12:20:38	End Time: 12:24:49
Other details: n/a.			
Pilot comments: During the outbound leg a discrepancy of around 10° was observed between the NDB needle indication and the track demanded by the DGPS guidance (the reason for this was unclear). Significant difficulties were experienced in following the DGPS guidance around the turn, to such an extent that the pilot was only able to establish onto the final approach track at the second attempt. These problems were attributed to the lack of automated HSI course carriage indicator combined with the high workload situation resulting from the poor weather conditions.			
Observations: The GD1 GPS receiver again operated in non-differential mode for much of the approach.			



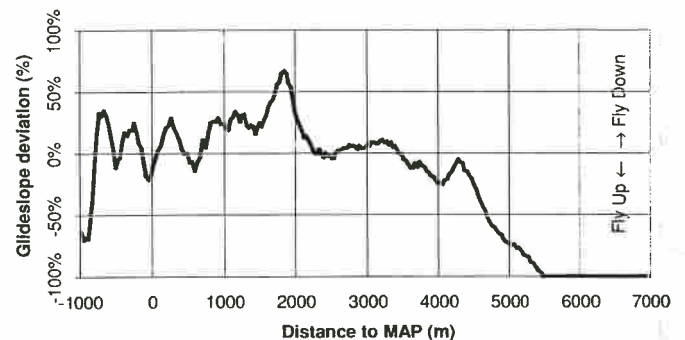
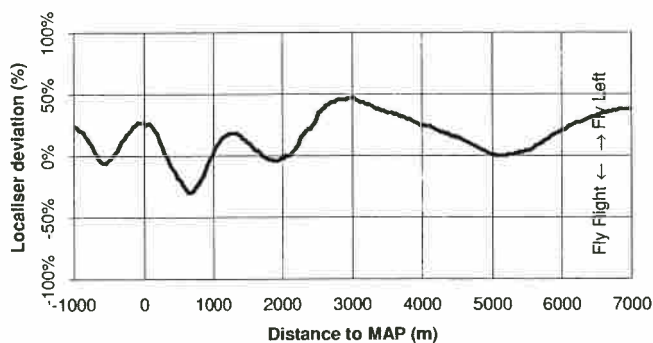
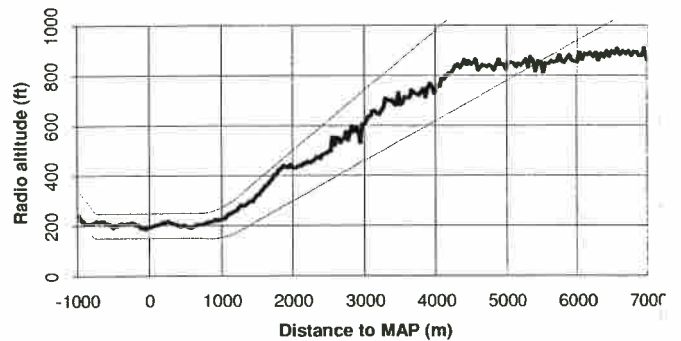
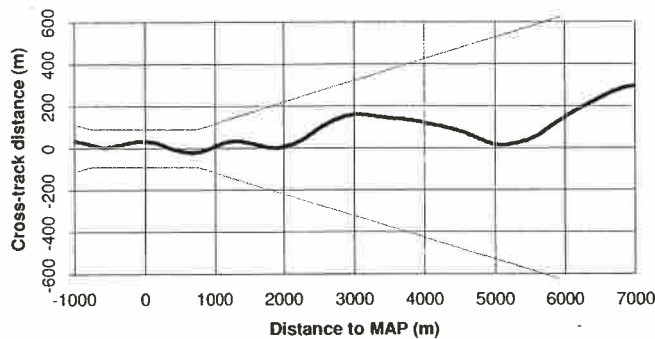
Flight number: 6	Approach number: 3	Location: Buchan A	Wind: 150°M, 30kt
Approach track: QDM 060°M, 200m right offset		Approach angle: 3.5°	Overshoot angle: 6.0°
DGPS source: GD2 (UHF-corrected Navstar)		Height source: radio altimeter	
Horizontal sensitivities:	4nm approach: ±850m	Level segment: ±90m	4nm overshoot: ±850m
Vertical sensitivities:	4nm approach: ±350ft	Level segment: ±50ft	4nm overshoot: ±350ft
Entry technique: modified Aerad procedure commencing overhead the platform, with a left-hand outbound leg flown using RNAV-2 guidance and the turn commenced at 4nm range.			
Go-around technique: straight ahead from MAP, climbing as directed by DGPS guidance.			
Handling pilot: NT	Method: Raw data	Start Time: 12:37:40	End Time: 12:40:39
Other details: n/a.			
Pilot comments: Performance of the turn manoeuvre was satisfactory using the RNAV-2 guidance. The localiser guidance was easy to follow (in spite of the large drift angle) except during the level segment, where short duration transients were again observed. The presence of a flashing LED indicating a go-around condition throughout the overshoot manoeuvre was distracting: it was only necessary for the LED to flash for a short time. A clearer annunciation of the MAP would also be helpful.			
Observations: The transients on the localiser indications could not be attributed to errors in the GPS solution and no other explanation could be identified. Changing to the GD2 receiver eliminated the drop-outs into non-differential mode.			



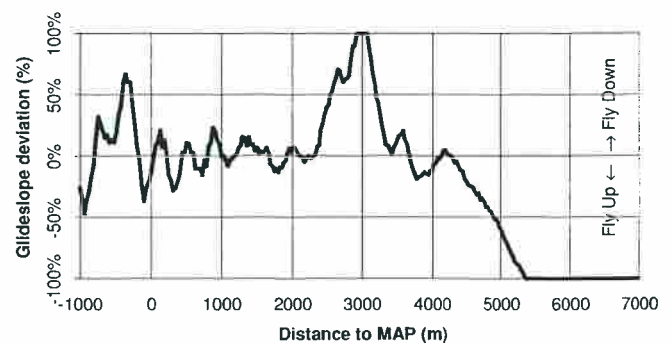
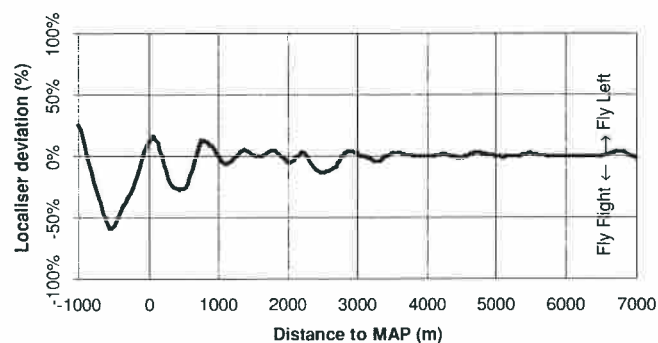
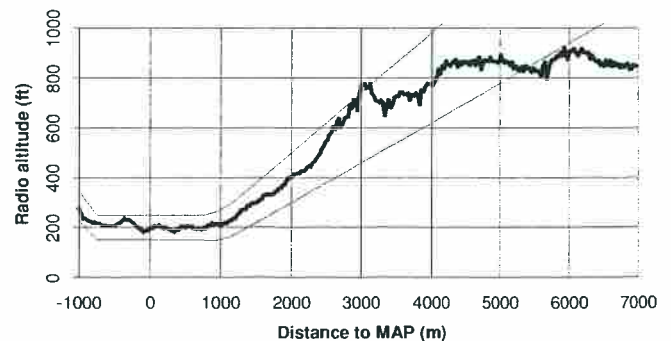
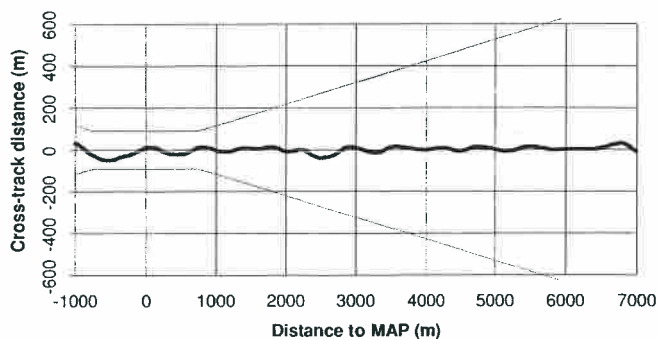
Flight number: 6	Approach number: 4	Location: Buchan A	Wind: 150°M, 30kt
Approach track: QDM 330°M, 200m right offset		Approach angle: 3.5°	Overshoot angle: 6.0°
DGPS source: GD2 (UHF-corrected Navstar)		Height source: radio altimeter	
Horizontal sensitivities:	4nm approach: ±850m	Level segment: ±90m	4nm overshoot: ±850m
Vertical sensitivities:	4nm approach: ±350ft	Level segment: ±50ft	4nm overshoot: ±350ft
Entry technique: modified Aerad procedure commencing overhead the platform, with a left-hand outbound leg flown using RNAV-2 guidance and the turn commenced at 4nm range.			
Go-around technique: straight ahead from MAP, climbing as directed by DGPS guidance.			
Handling pilot: NT	Method: Raw data	Start Time: 12:52:44	End Time: 12:55:33
Other details: downwind approach at 50-60kt IAS.			
Pilot comments: Due to the downwind approach (resulting in a groundspeed of around 120kt), a rapid rate of descent was required to maintain the aircraft on the glideslope. The sensitivity of the localiser deviation indicator was too high.			
Observations: n/a.			



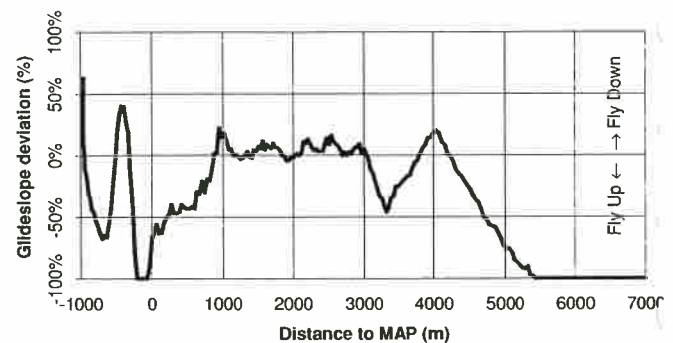
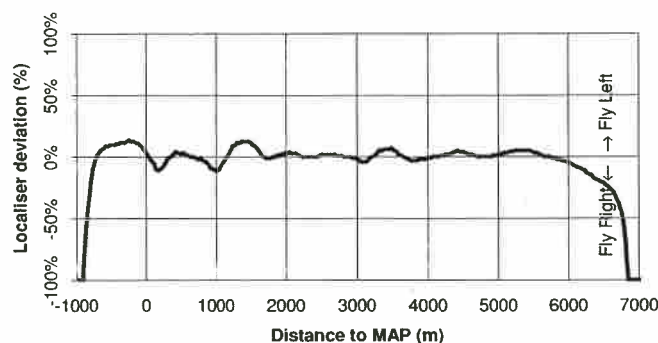
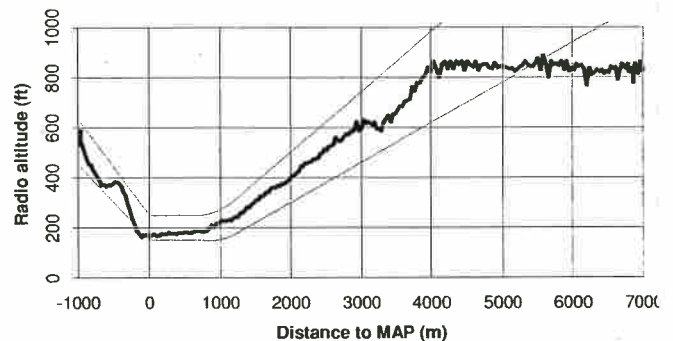
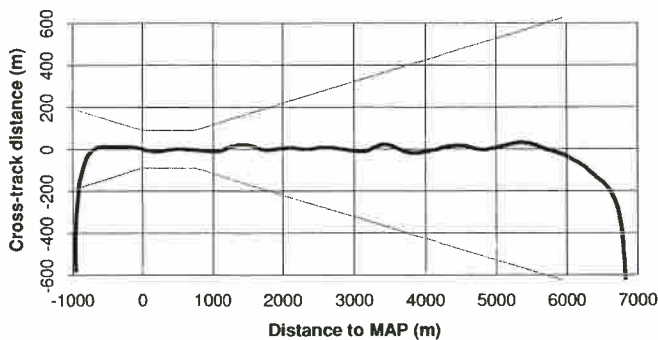
Flight number: 6	Approach number: 5	Location: Buchan A	Wind: 150°M, 30kt
Approach track: QDM 240°M, 200m right offset		Approach angle: 3.5°	Overshoot angle: 6.0°
DGPS source: GD2 (UHF-corrected Navstar)		Height source: radio altimeter	
Horizontal sensitivities:	4nm approach: ±850m	Level segment: ±90m	4nm overshoot: ±850m
Vertical sensitivities:	4nm approach: ±350ft	Level segment: ±50ft	4nm overshoot: ±350ft
Entry technique: modified Aerad procedure commencing overhead the platform, with a left-hand outbound leg flown using RNAV-2 guidance and the turn commenced at 4nm range.			
Go-around technique: straight ahead from MAP, climbing as directed by DGPS guidance.			
Handling pilot: NT	Method: Raw data	Start Time: 13:07:05	End Time: 13:11:07
Other details: n/a.			
Pilot comments: Difficulties were experienced in using the RNAV-2 to provide the necessary turn guidance. The localiser deviation indicator was too sensitive. A large drift angle was required due to the crosswind approach.			
Observations: n/a.			



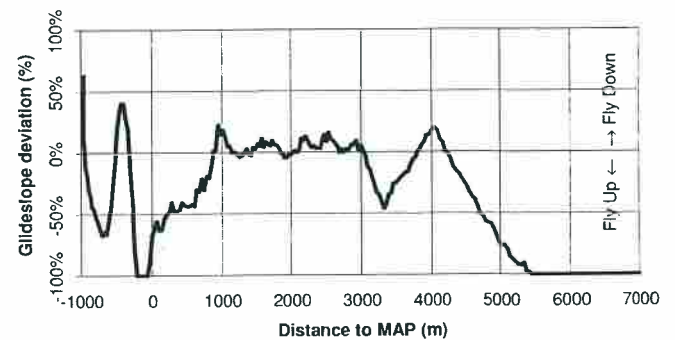
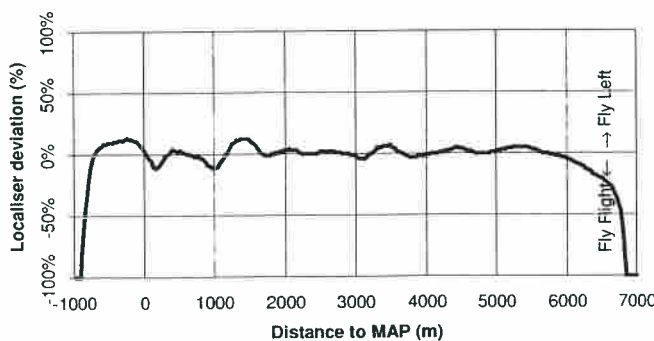
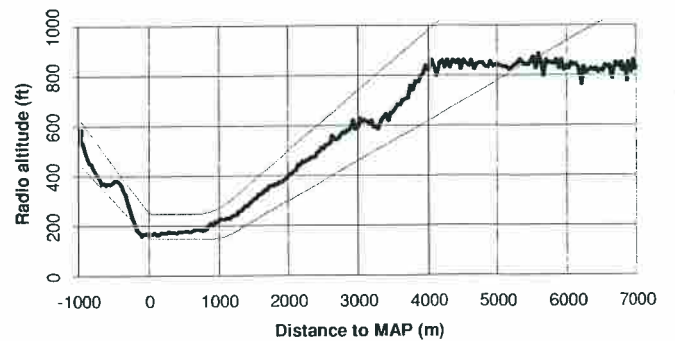
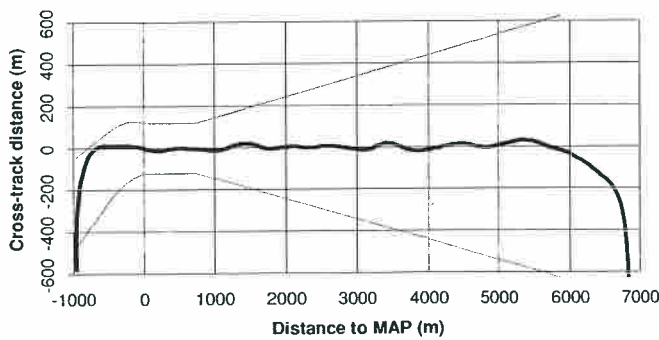
Flight number: 6	Approach number: 6	Location: Buchan A	Wind: 150°M, 30kt
Approach track: QDM 150°M, 200m right offset		Approach angle: 3.5°	Overshoot angle: 6.0°
DGPS source: GD2 (UHF-corrected Navstar)		Height source: radio altimeter	
Horizontal sensitivities:	4nm approach: ±850m	Level segment: ±90m	4nm overshoot: ±850m
Vertical sensitivities:	4nm approach: ±350ft	Level segment: ±50ft	4nm overshoot: ±350ft
Entry technique: modified Aerad procedure commencing overhead the platform, with a left-hand outbound leg flown using RNAV-2 guidance and the turn commenced at 4nm range.			
Go-around technique: straight ahead from MAP, climbing as directed by DGPS guidance.			
Handling pilot: NM	Method: Flight director	Start Time: 13:18:59	End Time: 13:23:39
Other details: n/a.			
Pilot comments: The LED panel should ideally be located next to the HSI, not the ADI. The 'raw data' localiser deviation indications were too sensitive, in particular those on the ADI (at one point these had almost reached full-scale deflection).			
Observations: No GPS solution errors were detected which could explain the large localiser deflections : the latter were instead attributed to physical deviations in the aircraft flight path.			



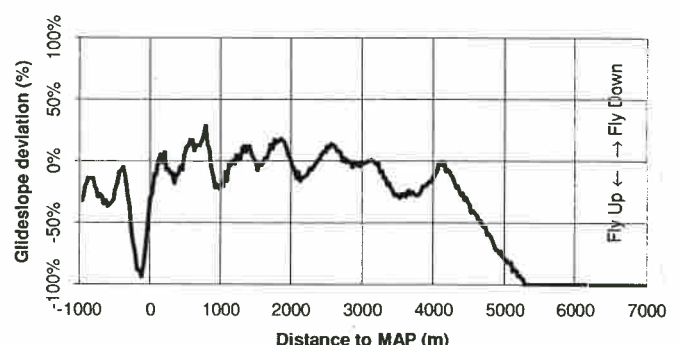
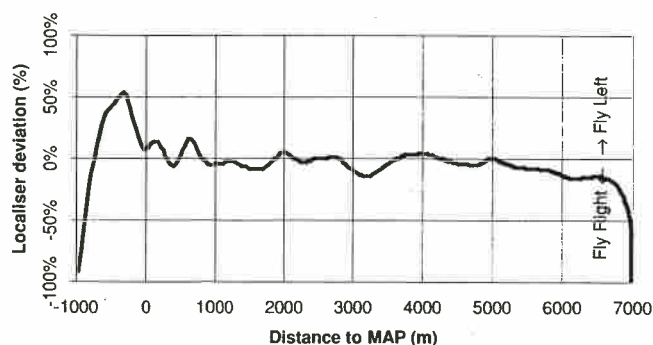
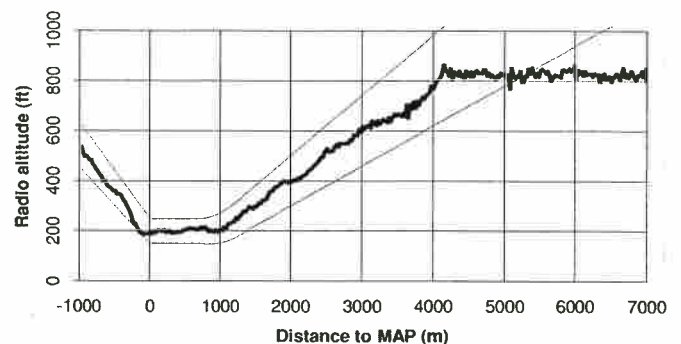
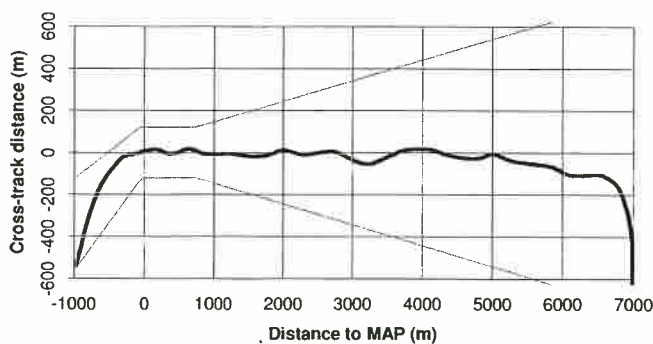
Flight number: 6	Approach number: 7	Location: Buchan A	Wind: 150°M, 30kt
Approach track: QDM 150°M, 200m left offset		Approach angle: 3.5°	Overshoot angle: 6.0°
DGPS source: GD2 (UHF-corrected Navstar)		Height source: radio altimeter	
Horizontal sensitivities:	4nm approach: ±850m	Level segment: ±90m	4nm overshoot: ±850m
Vertical sensitivities:	4nm approach: ±350ft	Level segment: ±50ft	4nm overshoot: ±350ft
Entry technique: aircraft flown directly to a point at around 4nm range to intercept the approach.			
Go-around technique: climbing left turn at MAP performed manually.			
Handling pilot: NM	Method: Raw data	Start Time: 14:31:23	End Time: 14:35:49
Other details: the length of the level segment was halved to 750m, with the overshoot segment commencing as soon as the MAP was reached.			
Pilot comments:			
Short duration transients were observed on the localiser deviation indications.			
There appeared to be an identifiable lag between the heading changes made by the pilot to maintain track, and the corresponding changes in the localiser indication.			
Observations:			
The second pilot comment is believed to arise from a latency effect, due to the fact that the guidance was based upon GPS data updates received at a relatively slow (1Hz) rate.			



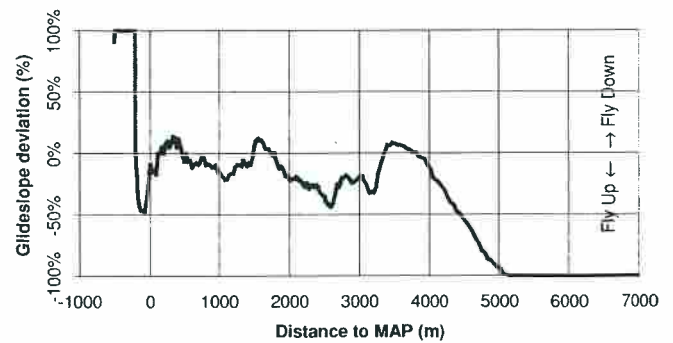
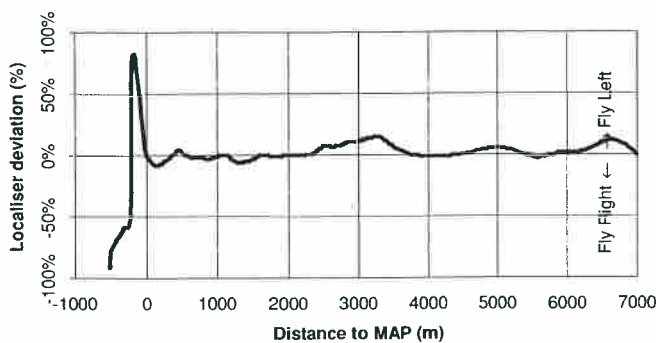
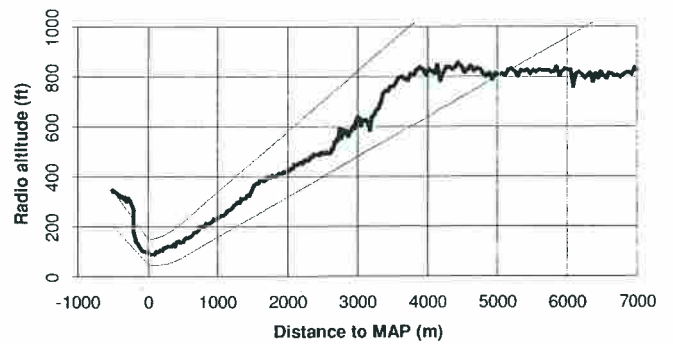
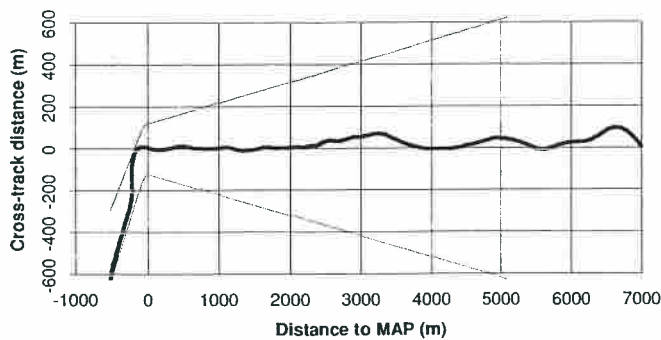
Flight number: 6	Approach number: 8	Location: Buchan A	Wind: 150°M, 30kt
Approach track: QDM 150°M, 200m left offset		Approach angle: 3.5°	Overshoot angle: 6.0°
DGPS source: GD2 (UHF-corrected Navstar)		Height source: radio altimeter	
Horizontal sensitivities:	4nm approach: ±850m	Level segment: ±120m	4nm overshoot: ±850m
Vertical sensitivities:	4nm approach: ±350ft	Level segment: ±50ft	4nm overshoot: ±350ft
Entry technique: aircraft flown directly to a point at around 4nm range to intercept the approach.			
Go-around technique: DGPS guidance arranged to command a 20° left turn at the MAP, to be introduced progressively over the following 500m.			
Handling pilot: NM	Method: Raw data	Start Time: 14:37:29	End Time: 14:41:50
Other details: the length of the level segment was retained at 750m, with the overshoot segment (including the 20° left turn) commencing as soon as the MAP was reached.			
Pilot comments: The change in level segment horizontal sensitivity to ±120m meant that the localiser deviation indications were much less sensitive, and more acceptable as a result. The track change demanded at the MAP was considered not to be sufficiently positive to indicate clearly that a heading change was required.			
Observations: n/a.			



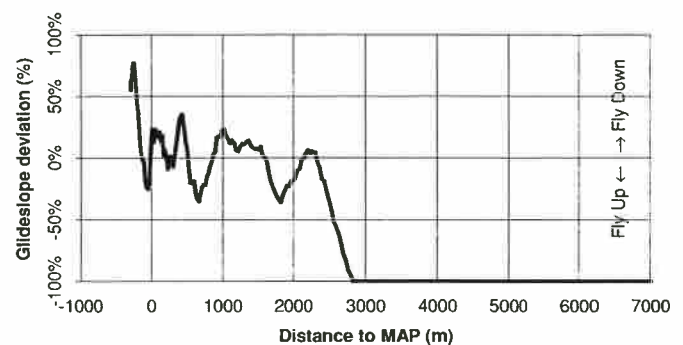
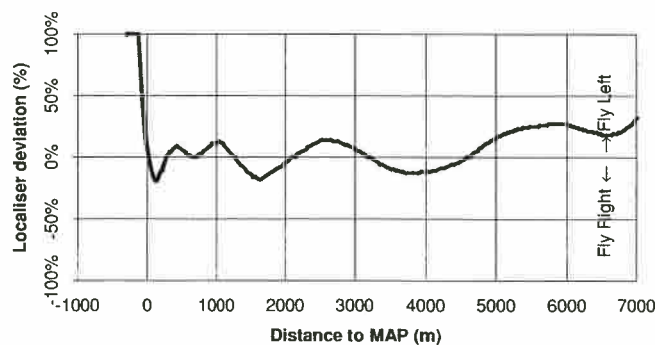
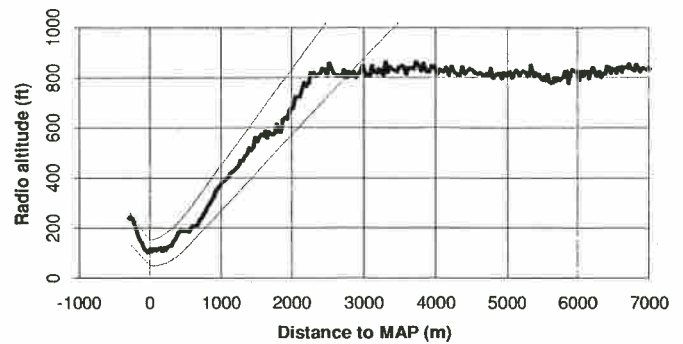
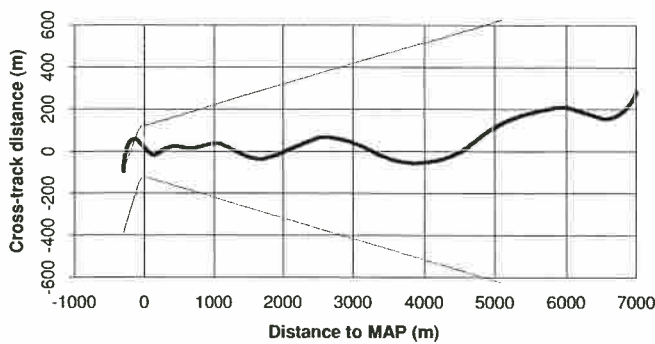
Flight number: 6	Approach number: 9	Location: Buchan A	Wind: 150°M, 30kt
Approach track: QDM 150°M, 200m left offset		Approach angle: 3.5°	Overshoot angle: 6.0°
DGPS source: GD2 (UHF-corrected Navstar)		Height source: radio altimeter	
Horizontal sensitivities:	4nm approach: ±850m	Level segment: ±120m	4nm overshoot: ±850m
Vertical sensitivities:	4nm approach: ±350ft	Level segment: ±50ft	4nm overshoot: ±350ft
Entry technique: aircraft flown directly to a point at around 4nm range to intercept the approach.			
Go-around technique: DGPS guidance arranged to command a 20° left turn at the MAP, to be introduced progressively over the following 100m, at the same time as the climb demand.			
Handling pilot: NM	Method: Raw data	Start Time: 14:45:20	End Time: 14:50:40
Other details: the length of the level segment retained at 750m, with the overshoot segment (including the 20° left turn) commencing as soon as the MAP was reached.			
Pilot comments: The reduction in the distance over which the 20° left turn was demanded was a significant improvement, and provided a good combination of go-around and turnaway commands. Ideally the HSI course carriage should rotate as well to indicate the required change in track (and heading). A sudden full scale fly left indication on the localiser was observed.			
Observations: No evidence for the full scale fly left indication was obtained from the recorded data and its source was not identified - there were no large errors in the GD2 solution.			



Flight number: 6	Approach number: 10	Location: Buchan A	Wind: 150°M, 30kt
Approach track: QDM 230°M, 60m left offset		Approach angle: 3.5°	Overshoot angle: 6.0°
DGPS source: GD2 (UHF-corrected Navstar)		Height source: radio altimeter	
Horizontal sensitivities:	4nm approach: ±850m	Level segment: ±120m	4nm overshoot: ±850m
Vertical sensitivities:	4nm approach: ±350ft	Level segment: ±50ft	4nm overshoot: ±350ft
Entry technique: aircraft flown directly to a point at around 4nm range to intercept the approach.			
Go-around technique: Commanded 45° left turn (introduced over the following 100m) at the MAP.			
Handling pilot: NM	Method: Raw data	Start Time: 14:54:11	End Time: 14:58:40
Other details: the level segment was removed completely, the MDH reduced to 100ft, and the MAP arranged to be at a point 60m abeam the platform centre (approximately 20m from the deck edge). The aim was to simulate a direct 3.5° descent to the helideck, although the track was offset laterally by 60m to avoid a direct overflight of the platform.			
Pilot comments: The original intention had been to reduce the aircraft speed to 10kt in the final stages of the approach: however the speed was allowed to remain at around 80kt, which would clearly have been unacceptable for a landing. The vertical fairing at the end of the approach segment served to reduce the rate of descent and level the aircraft as the MAP was reached.			
Observations: The fairing at the end of the approach was retained to provide a transition to level flight.			



Flight number: 6	Approach number: 11	Location: Buchan A	Wind: 150°M, 30kt
Approach track: QDM 230°M, 60m left offset		Approach angle: 6.0°	Overshoot angle: 6.0°
DGPS source: GD2 (UHF-corrected Navstar)		Height source: radio altimeter	
Horizontal sensitivities:	4nm approach: ±850m	Level segment: ±120m	4nm overshoot: ±850m
Vertical sensitivities:	4nm approach: ±350ft	Level segment: ±50ft	4nm overshoot: ±350ft
Entry technique: aircraft flown directly to a point at around 4nm range to intercept the approach.			
Go-around technique: aircraft landed on the platform from the level segment.			
Handling pilot: NT	Method: Raw data	Start Time: 15:03:11	End Time: 15:07:41
Other details: the level segment was removed completely, the MDH reduced to 100ft, and the MAP arranged to be at a point 60m abeam the platform. The aim was to simulate a direct 6.0° descent to the helideck (although the track was offset laterally by 60m to avoid a direct overflight of the platform).			
Pilot comments: Speed was maintained at 80kt which was unnecessarily fast for a satisfactory landing at the end of the approach. The vertical fairing at the end of the approach segment served to reduce the rate of descent and level the aircraft as the MAP was reached. Much more investigation of this form of profile would be required before it could be considered as a viable approach technique.			
Observations: The fairing at the end of the approach was retained to provide a transition to level flight.			



5.7. **Flight Trial 7**

The format of the seventh and last test flight was slightly different from the previous trials, involving two separate sorties during which approaches were performed at the Beatrice A and Beatrice C platforms.

The objective of the two sorties was to demonstrate the operation of the DGPS system to a number of industry representatives. A series of approaches was selected which highlighted a number of the system's capabilities: although the parameters for each approach were different, each of the constituent elements had been tested on previous flights.

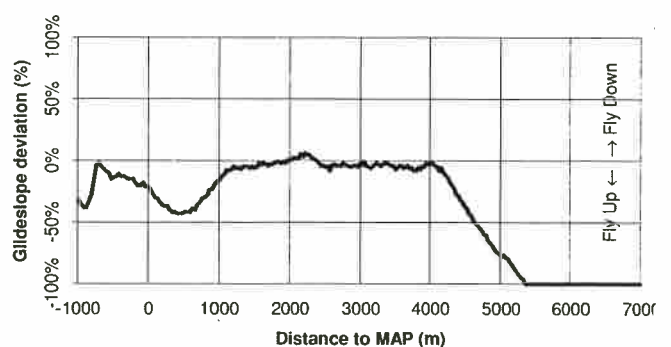
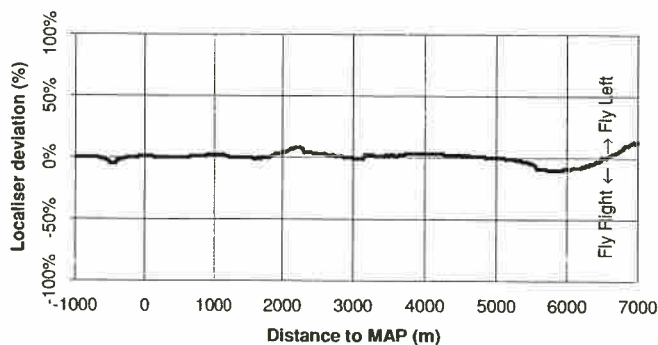
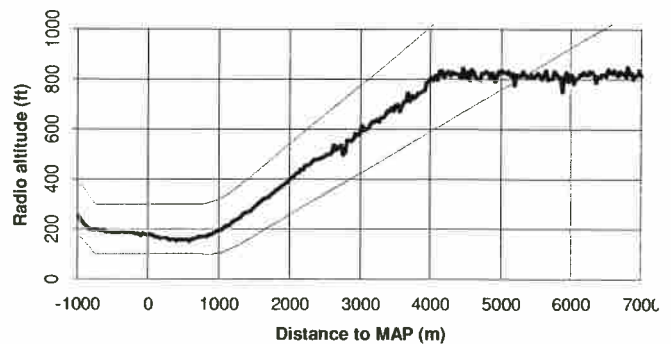
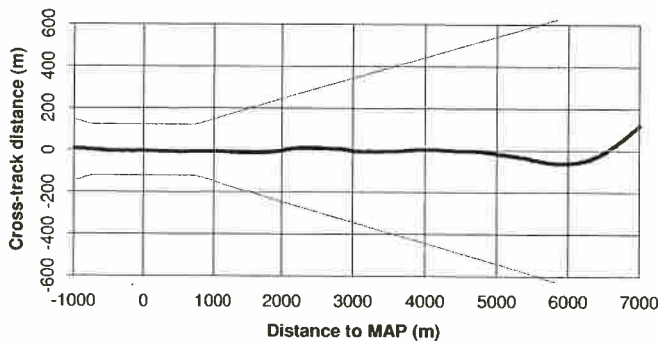
On each sortie the following sequence of approaches was performed:

- (1) A direct entry 3.5° approach to Beatrice A, with a 1500m level segment followed by a straight-ahead 6° overshoot.
- (2) A direct entry 6° approach to Beatrice A with the same level segment length, but executing a 6° go-around at the MAP incorporating a turn away from the platform.
- (3) Two 'modified Aerad' approaches at Beatrice C, with a 3.5° approach angle, 1500m level segment, and straight-ahead 6° overshoot.

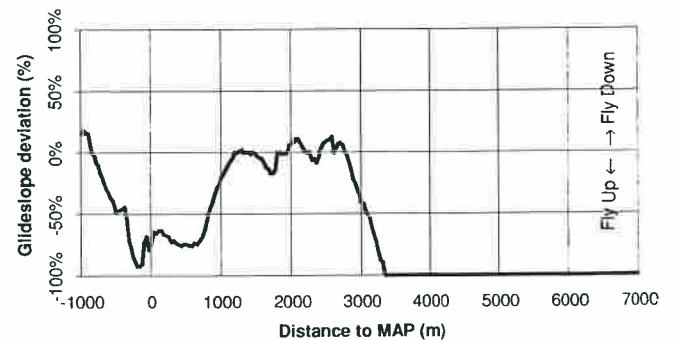
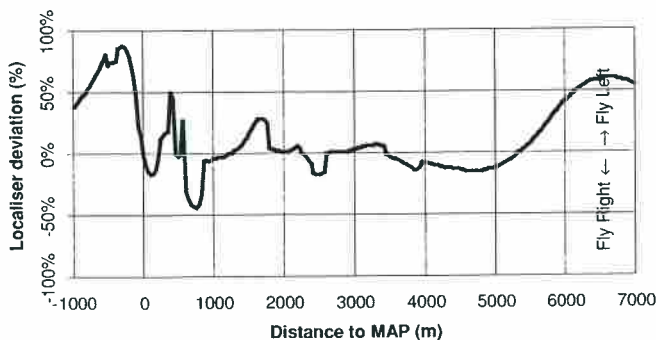
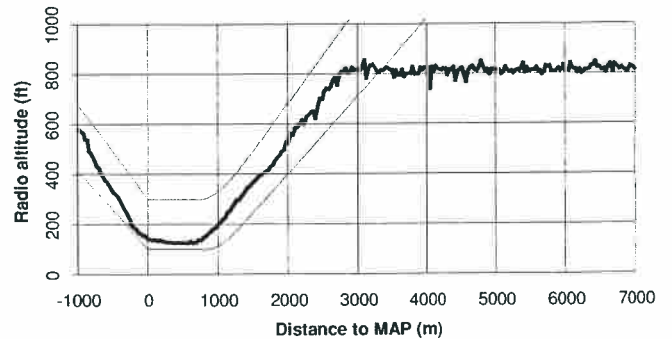
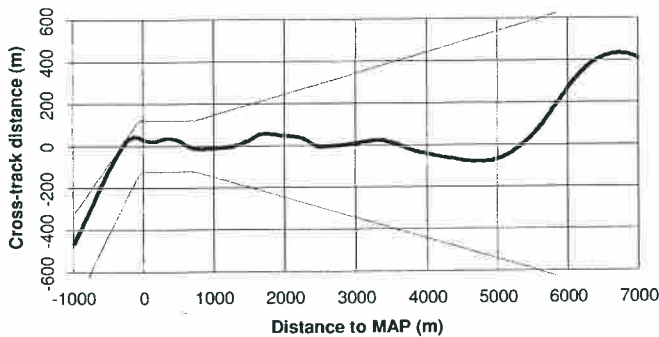
Two industry pilots were able to evaluate the system, one on each sortie. It was noted that, in each case, the pilot failed to correctly follow the transition to the level segment on his first approach.

The MF reception problems recurred, with the resulting reversion to stand-alone GD1 solutions causing instabilities on the displayed localiser indications.

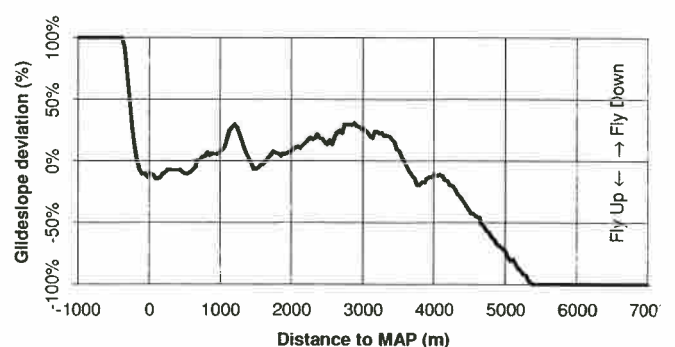
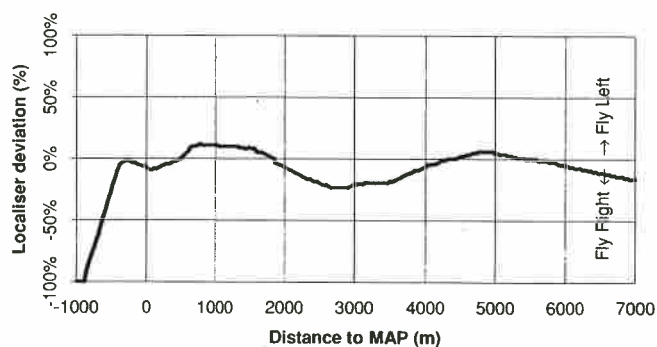
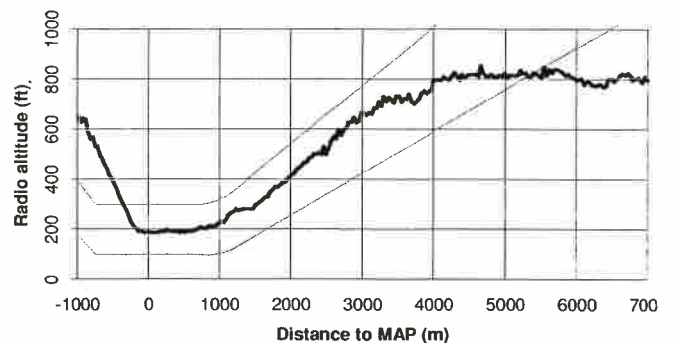
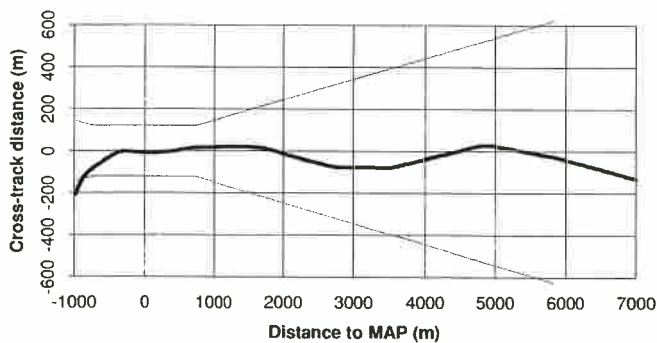
Flight number: 7	Approach number: 1	Location: Beatrice A	Wind: 170°M, 20kt
Approach track: QDM 240°M, 250m right offset		Approach angle: 3.5°	Overshoot angle: 6.0°
DGPS source: GD1 (MF-corrected Navstar)		Height source: radio altimeter	
Horizontal sensitivities:	4nm approach: ±850m	Level segment: ±120m	4nm overshoot: ±850m
Vertical sensitivities:	4nm approach: ±350ft	Level segment: ±100ft	4nm overshoot: ±350ft
Entry technique: aircraft flown directly to a point at around 4nm range to intercept the approach.			
Go-around technique: straight ahead from MAP, climbing using autopilot go-around function.			
Handling pilot: NM	Method: Autopilot	Start Time: 11:19:37	End Time: 11:23:53
Other details: n/a.			
Pilot comments: n/a.			
Observations: Loss of MF corrections caused the GD1 GPS receiver to revert to stand-alone mode for much of this approach. This did not appear to have a significant effect upon the approach guidance as the errors in the solution happened to remain relatively small (<15m), presumably due to low SA.			



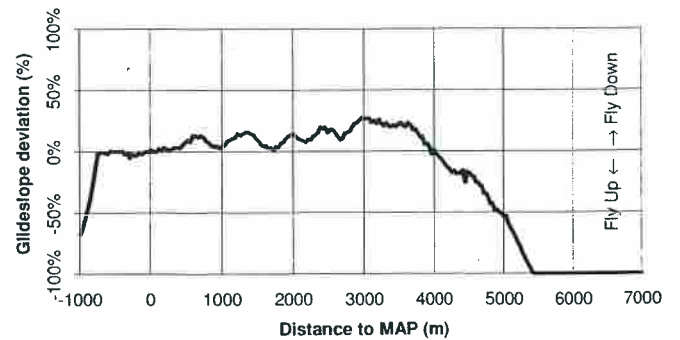
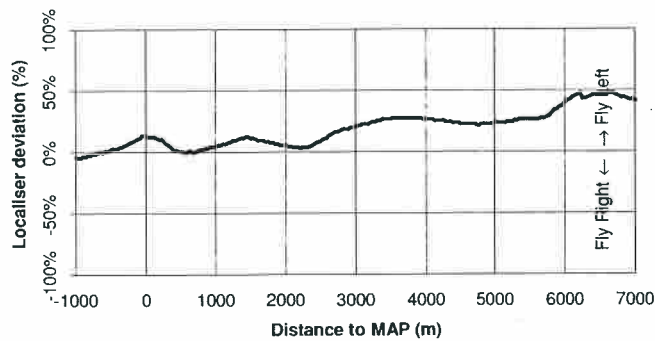
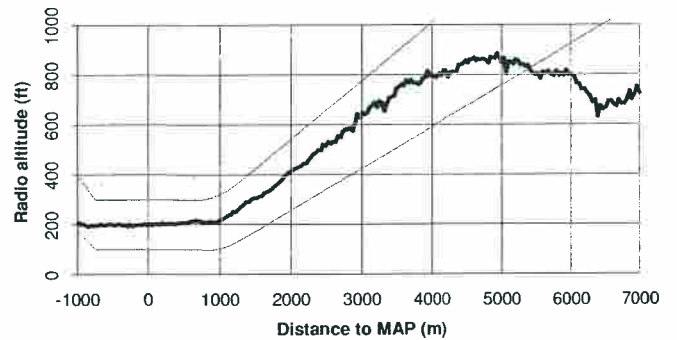
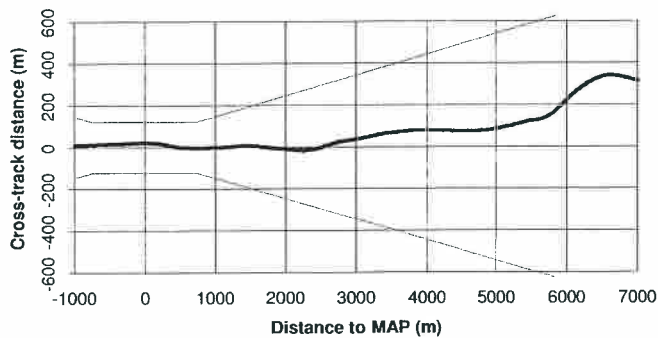
Flight number: 7	Approach number: 2	Location: Beatrice A	Wind: 170°M, 20kt
Approach track: QDM 240°M, 250m left offset		Approach angle: 6.0°	Overshoot angle: 6.0°
DGPS source: GD1 (MF-corrected Navstar)		Height source: radio altimeter	
Horizontal sensitivities:	4nm approach: ±850m	Level segment: ±120m	4nm overshoot: ±850m
Vertical sensitivities:	4nm approach: ±350ft	Level segment: ±100ft	4nm overshoot: ±350ft
Entry technique: aircraft flown directly to a point at around 4nm range to intercept the approach.			
Go-around technique: DGPS guidance arranged to command a 30° left turn at the MAP, to be introduced progressively over the following 100m.			
Handling pilot: NM	Method: Autopilot	Start Time: 11:29:08	End Time: 11:33:30
Other details: the length of the level segment was reduced to 750m, with the overshoot segment and 30° left turn commencing as soon as the MAP was reached. The approach angle was 6°.			
Pilot comments: Instabilities on the localiser deviations were observed, approaching full-scale deflection close to the platform.			
Observations: Loss of MF corrections caused the GD1 GPS receiver to revert to stand-alone mode for much of this approach. The large solution errors affected the localiser indications, in particular through the level segment where their sensitivity is greatest.			



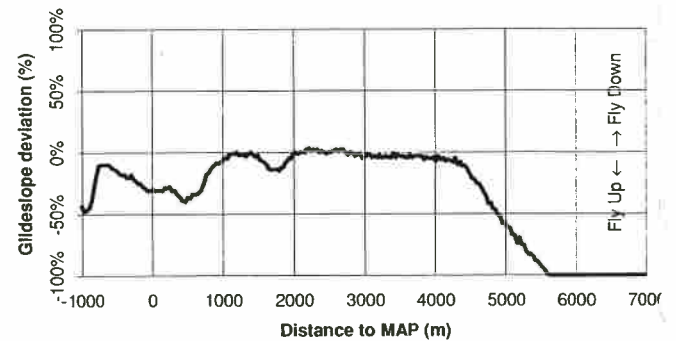
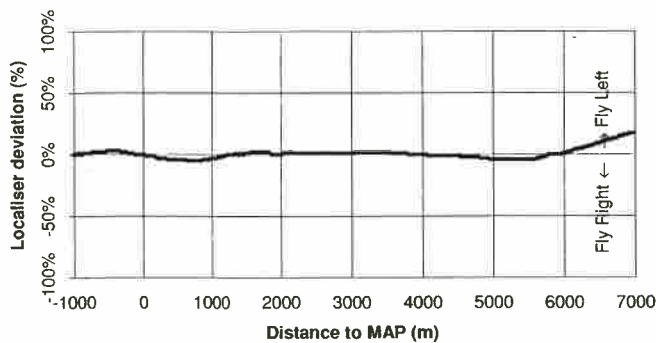
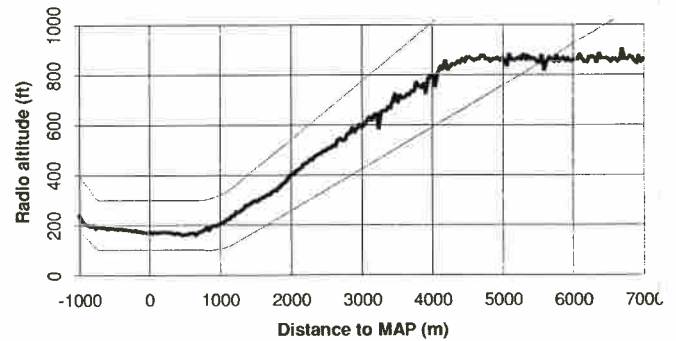
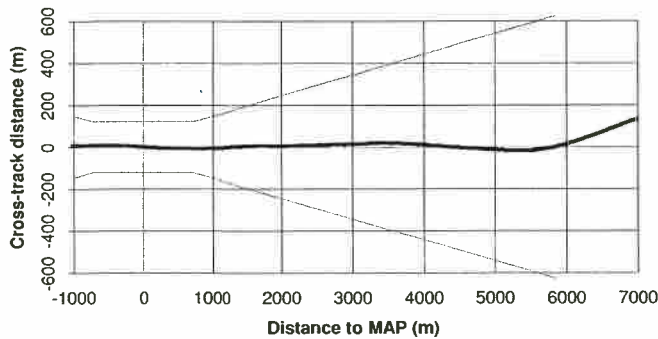
Flight number: 7	Approach number: 3	Location: Beatrice C	Wind: 170°M, 20kt
Approach track: QDM 170°M, 200m left offset		Approach angle: 3.5°	Overshoot angle: 6.0°
DGPS source: GD1 (MF-corrected Navstar)		Height source: radio altimeter	
Horizontal sensitivities:	4nm approach: ±850m	Level segment: ±120m	4nm overshoot: ±850m
Vertical sensitivities:	4nm approach: ±350ft	Level segment: ±100ft	4nm overshoot: ±350ft
Entry technique: modified Aerad procedure commencing overhead the platform, with a left-hand outbound leg flown using RNAV-2 guidance and the turn commenced at 4nm range.			
Go-around technique: straight ahead from MAP, climbing as directed by DGPS guidance.			
Handling pilot: GN	Method: Raw data	Start Time: 11:45:55	End Time: 11:49:40
Other details: n/a.			
Pilot comments: The approach guidance was easier to fly than ILS: there was less of a 'tunnelling' effect (understood to mean the increase in linear sensitivity as the aircraft approaches the threshold). The pilot erroneously turned away from the platform at the MAP rather than following the DGPS guidance.			
Observations: n/a.			



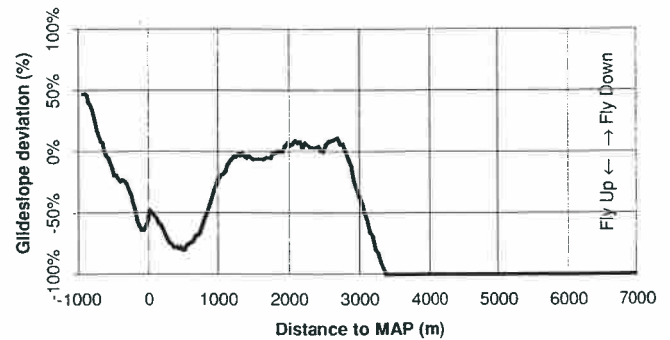
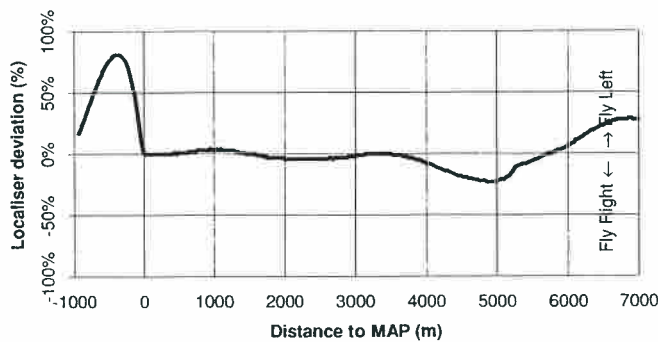
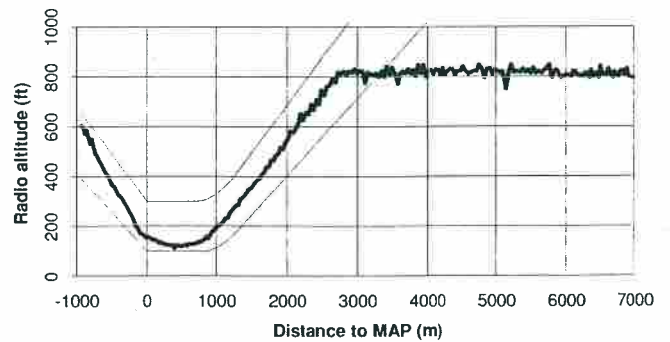
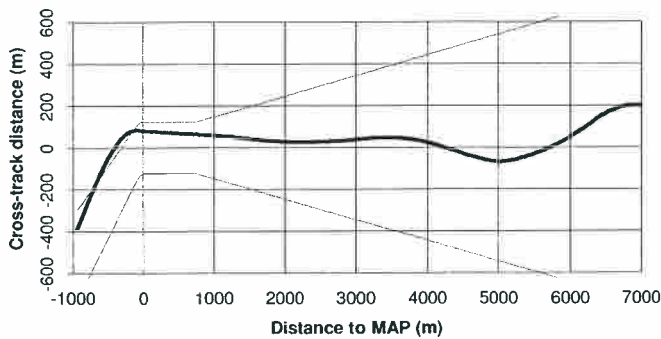
Flight number: 7	Approach number: 4	Location: Beatrice C	Wind: 170°M, 20kt
Approach track: QDM 260°M, 200m left offset		Approach angle: 3.5°	Overshoot angle: 6.0°
DGPS source: GD1 (MF-corrected Navstar)		Height source: radio altimeter	
Horizontal sensitivities:	4nm approach: ±850m	Level segment: ±120m	4nm overshoot: ±850m
Vertical sensitivities:	4nm approach: ±350ft	Level segment: ±100ft	4nm overshoot: ±350ft
Entry technique: modified Aerad procedure commencing overhead the platform, with a left-hand outbound leg flown using RNAV-2 guidance and the turn commenced at 4nm range.			
Go-around technique: straight ahead from MAP, climbing as directed by DGPS guidance.			
Handling pilot: GN	Method: Raw data	Start Time: 11:57:30	End Time: 12:01:18
Other details: n/a.			
Pilot comments: The indications were stable and easy to fly.			
Observations: n/a.			



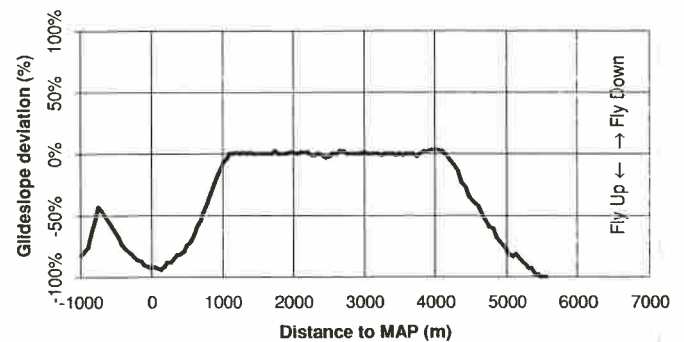
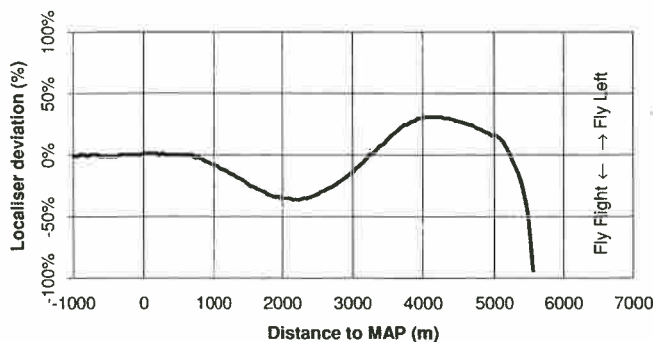
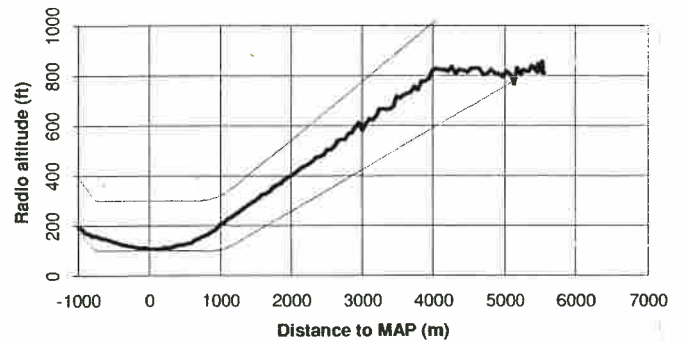
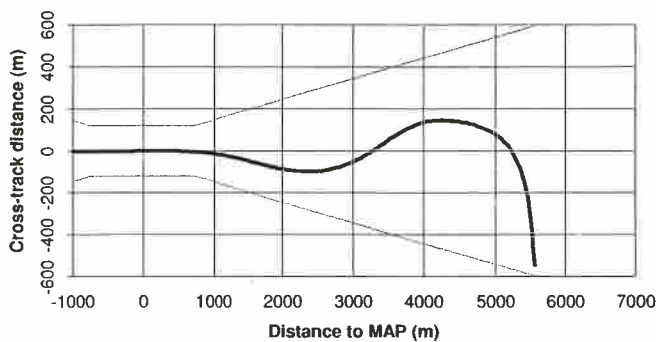
Flight number: 7	Approach number: 5	Location: Beatrice A	Wind: 220°M, 20kt
Approach track: QDM 240°M, 250m right offset		Approach angle: 3.5°	Overshoot angle: 6.0°
DGPS source: GD1 (MF-corrected Navstar)		Height source: radio altimeter	
Horizontal sensitivities:	4nm approach: ±850m	Level segment: ±120m	4nm overshoot: ±850m
Vertical sensitivities:	4nm approach: ±350ft	Level segment: ±100ft	4nm overshoot: ±350ft
Entry technique: aircraft flown directly to a point at around 4nm range to intercept the approach.			
Go-around technique: straight ahead from MAP, climbing using autopilot go-around function.			
Handling pilot: NM	Method: Autopilot	Start Time: 14:09:32	End Time: 14:13:32
Other details: n/a.			
Pilot comments: n/a.			
Observations: Loss of MF corrections caused the GD1 GPS receiver to revert to stand-alone mode for much of this approach. This did not appear to have a significant effect upon the approach guidance, despite errors of up to 25m in the GD1 solution.			



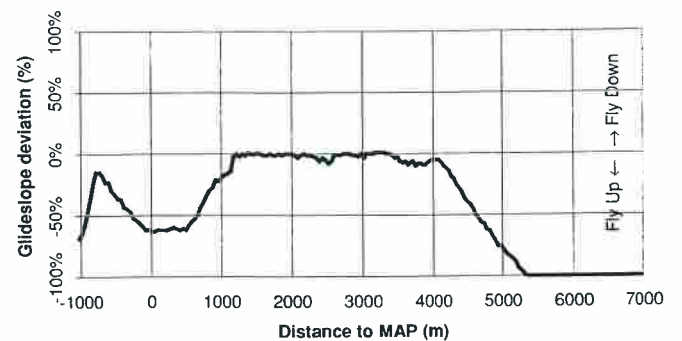
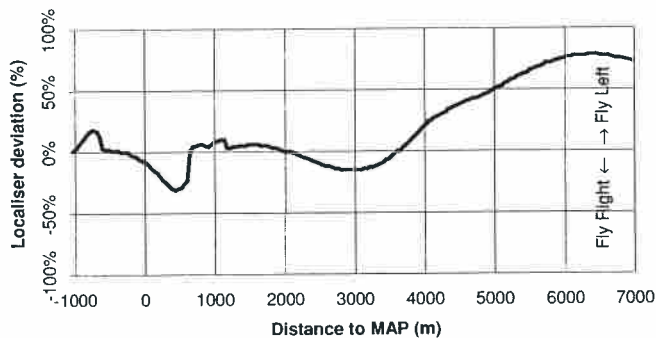
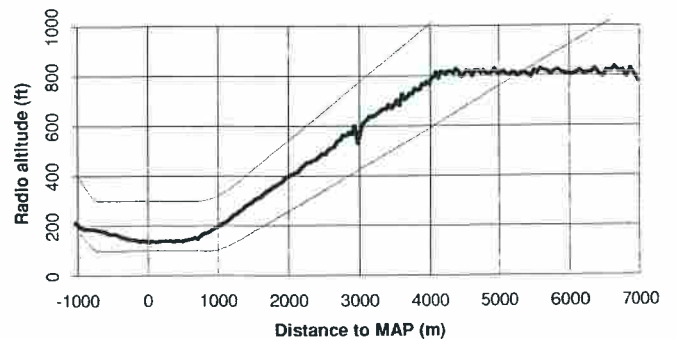
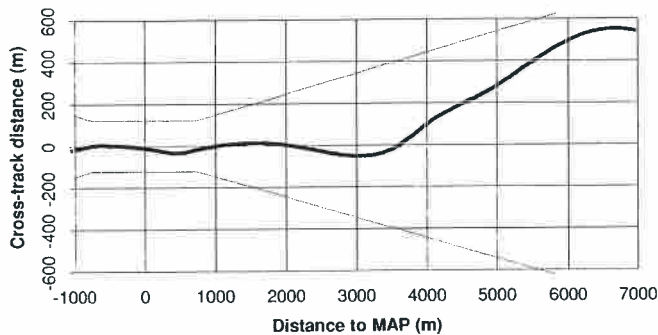
Flight number: 7	Approach number: 6	Location: Beatrice A	Wind: 220°M, 20kt
Approach track: QDM 240°M, 250m left offset		Approach angle: 6.0°	Overshoot angle: 6.0°
DGPS source: GD1 (MF-corrected Navstar)		Height source: radio altimeter	
Horizontal sensitivities:	4nm approach: ±850m	Level segment: ±120m	4nm overshoot: ±850m
Vertical sensitivities:	4nm approach: ±350ft	Level segment: ±100ft	4nm overshoot: ±350ft
Entry technique: aircraft flown directly to a point at around 4nm range to intercept the approach.			
Go-around technique: DGPS guidance arranged to command a 30° left turn at the MAP, to be introduced progressively over the following 100m.			
Handling pilot: NM	Method: Autopilot	Start Time: 14:18:59	End Time: 14:22:57
Other details: the length of the level segment was reduced to 750m, with the overshoot segment and 30° left turn commencing as soon as the MAP was reached. The approach angle was 6°.			
Pilot comments: Occasional instabilities on the localiser deviations were observed, in particular on the ADI.			
Observations: Loss of MF corrections caused the GD1 GPS receiver to revert to stand-alone mode for much of this approach.			



Flight number: 7	Approach number: 7	Location: Beatrice C	Wind: 220°M, 20kt
Approach track: QDM 080°M, 200m left offset		Approach angle: 3.5°	Overshoot angle: 6.0°
DGPS source: GD1 (MF-corrected Navstar)		Height source: radio altimeter	
Horizontal sensitivities:	4nm approach: ±850m	Level segment: ±120m	4nm overshoot: ±850m
Vertical sensitivities:	4nm approach: ±350ft	Level segment: ±100ft	4nm overshoot: ±350ft
Entry technique: modified Aerad procedure commencing overhead the platform, with a left-hand outbound leg flown using RNAV-2 guidance and the turn commenced at 4nm range.			
Go-around technique: straight ahead from MAP, climbing as directed by DGPS guidance.			
Handling pilot: SF	Method: Raw data	Start Time: 14:38:43	End Time: 14:41:04
Other details: n/a.			
Pilot comments: Occasional instabilities on the localiser indications.			
Observations: n/a.			



Flight number: 7	Approach number: 8	Location: Beatrice C	Wind: 220°M, 20kt
Approach track: QDM 350°M, 200m left offset		Approach angle: 3.5°	Overshoot angle: 6.0°
DGPS source: GD1 (MF-corrected Navstar)		Height source: radio altimeter	
Horizontal sensitivities:	4nm approach: ±850m	Level segment: ±120m	4nm overshoot: ±850m
Vertical sensitivities:	4nm approach: ±350ft	Level segment: ±100ft	4nm overshoot: ±350ft
Entry technique: modified Aerad procedure commencing overhead the platform, with a left-hand outbound leg flown using RNAV-2 guidance and the turn commenced at 4nm range.			
Go-around technique: straight ahead from MAP, climbing as directed by DGPS guidance.			
Handling pilot: SF	Method: Raw data	Start Time: 14:47:32	End Time: 14:50:38
Other details: n/a.			
Pilot comments: Large instabilities on the localiser indications during the level segment.			
Observations: Loss of MF corrections caused the GD1 GPS receiver to revert to stand-alone mode for much of this approach, which may explain the observed localiser instabilities.			



6 DISCUSSION OF RESULTS

6.1 Initial Pilot Reactions

The majority of the offshore approaches were undertaken by two pilots with recent offshore experience: a Senior Training Captain working for Bond Helicopters, and a CAA Senior Test Pilot. Three additional pilots (a CAA Flight Operations Inspector and two industry pilots) also had the opportunity to evaluate a small number of approaches.

The initial reaction of all of the pilots to the DGPS approach profile and the guidance presentation was generally favourable, and no adverse comments were received relating to the basic form of the approach profile.

The selection of an 'ILS look-alike' display format (in the sense that it was displayed using the same instruments and presentation as are employed for an ILS approach) was commented on favourably. In addition to the basic 'raw data' presentation, this also allowed flight director commands to be generated for display on the ADI, and the autopilot to be coupled to the DGPS system output.

6.2 Pilot Confusion

On two significant occasions (Flight 6 approach 1, Flight 7 approach 3) the handling pilot failed to follow the correct DGPS procedure: in each case the pilot's 'erroneous' action would have been correct for a standard weather radar approach and, as a result, safety was not compromised in either case. In the second of these instances, the problem manifested itself on the pilot's first ever attempt at a DGPS approach and was probably largely due to a failure to brief the pilot adequately before the flight.

The first instance, however, occurred with a DGPS-experienced pilot towards the end of the trials programme, and the fact that there was a problem was not immediately recognised by any of the other crew members. The following potential causal factors were identified:

- (1) The approach was the first to be carried out on the day in question, the previous DGPS trial in the series having taken place nearly two months previously.
- (2) Low in-flight visibility, and an ongoing attempt by the FTE to diagnose an equipment problem, were contributing to an increased cockpit workload.

It was concluded that similar problems could well occur in the future in the early stages of the use of a DGPS approach profile. This is an aspect which will require careful consideration in the training of pilots in the use of a new approach aid. A better estimate of the likely extent of the problem would be obtained from an extended operational trial with a wider pilot base.

6.3 **Transition to Level Segment**

The only significant problem that was directly attributable to the approach profile itself was the tendency for an altitude 'undershoot' (with a resulting deviation from the desired vertical path of up to 50ft) to occur at the transition from the approach segment to the level segment.

The pilots explained that this problem was due to a tendency to ignore the radio altimeter indications during the approach segment and to concentrate instead on the glideslope deviation, in order not to miss the sudden 'fly up' demand from the latter which occurred at the start of the level segment.

The introduction of a smoother transition (the so-called 'approach fairing'), over a horizontal distance of 500m between the approach segment and the level segment, eliminated this step change in vertical guidance. As a result, the undershoot effect was eliminated and the pilots' instrument scan was improved.

An approach was also attempted with fairing included at the transition between the level segment and the overshoot segment, but this gave a less positive go-around indication and was considered to be unnecessary and undesirable.

6.4 **Approach and Overshoot Angles**

An approach angle of 3.5° was initially selected, on the grounds that it was comparable with the flight path angle employed on a standard weather radar approach, and was almost identical to the standard ILS approach angle of 3° .

Experiments were subsequently performed with the use of steeper approach angles, which have the advantage of providing increased clearance from any obstacles in the area of the approach track.

A number of approaches were flown at 6° , at a variety of ground speeds (both into-wind and downwind) ranging between 45kt and 60kt. With a few exceptions (such as Flight 2 approach 7, and Flight 4 Approach 6) where the pilot commented upon the high rate of descent on a downwind approach, no significant difficulties were generally experienced.

A further increase in approach angle to 9° gave rise to problems, with a near autorotative state in the descent (1400ft/min at 60kt ground speed) and the necessity for the pilot to respond very quickly on transition to the level segment.

It was concluded that the figure of 6° was close to the optimum approach angle for the S76C for approaches performed into wind (a slightly shallower angle might prove necessary in the unlikely event that a downwind approach is required). Other helicopter types, exhibiting greater drag, might be able to support approach angles in excess of 6° .

The value initially selected for the overshoot angle was 3.5° : this was largely an arbitrary selection based upon commonality with the approach angle. In the event, it was found that this resulted in a rather slow rate of climb (of the order of 450ft/min). Increasing the overshoot angle to 6° provided a significant improvement, with the resulting rate of climb increasing to around 750ft/min.

6.5 Range Indications

The central DME display proved to be too remote from the pilots' instrument scan and was therefore not particularly useful, especially during the latter stages of an approach.

The ideal location for the range readout would be close to the HSI. Although the S76C HSI instruments incorporated a distance readout, this could not be used to display DGPS information on the trials aircraft owing to the absence of the necessary hardware interface.

The advantages of a range display with two decimal places (i.e. a display resolution of 0.01nm) were highlighted by the pilots as this provided useful information on range-rate, in addition to the range data itself. This was particularly useful close to the MAP.

Two alternative methods for the presentation of the range data on the DME display were employed: either the along-track distance to the MAP, or the true range to the platform centre.

The 'along-track from MAP' presentation was used on the early flights but it was found that it did not assist the pilots' situational awareness and could in certain circumstances be confusing, particularly at short ranges. The concept of displaying the range to an arbitrary point in space, rather than to a physical feature, is probably more appropriate to enroute navigation between waypoints than to the offshore approach case.

The alternative method of presentation (true range from platform) was favoured by the pilots, due to the fact that it always related to a true physical distance. The only disadvantage found with this method is the distance readout displayed upon reaching the MAP would be a particular numeric value (e.g. 0.22nm or 0.27nm) which was dependent upon the chosen decision range. This implied a requirement for some other form of unambiguous indication that the MAP had been reached.

6.6 Mode Annunciation

The positioning of the alphanumeric mode display on the central DME indicator was less than satisfactory owing to its remoteness from the pilots' instrument scan.

The introduction of the temporary LED panel (section 4.5.2), which the pilot could affix within his instrument scan, was an attempt to solve this problem. Since few aircraft are likely to possess suitable 'spare' indicator lights in this position, the implication is that additional mode annunciator lights would be required to be installed on an operational system.

Following the introduction of the LED panel, a number of minor software changes were implemented to improve the sequencing of the individual mode indications on the panel. In particular, flashing indications were employed to signify the transition from the fixed-angle approach to the level segment, and to provide a more compelling go-around indication.

With an indicator panel of this nature in close proximity to the instrument scan, the pilots were very conscious of the operation of the indicators. As a result it will be

important to ensure that the indications do not present an undue distraction, such as through the inappropriate use of flashing lights.

6.7 **Instrument Scalings**

With one exception, the '4nm range' scale factors (section 4.3.3) selected prior to the trials programme for the horizontal and vertical deviations proved to be appropriate. The exception was the 4nm horizontal sensitivity, which was found on the first trial flight to be too high and was giving rise to difficulties when establishing on the approach segment. Halving the sensitivity (by doubling the full-scale horizontal flight path deviation to $\pm 850\text{m}$) solved the problem.

Once this change had been made, efforts were concentrated on experimenting with the effect of modifying the instrument sensitivities for the level segment.

The level segment lateral sensitivity was initially set to $\pm 120\text{m}$, and was reduced to values of both $\pm 90\text{m}$ and $\pm 60\text{m}$ to investigate the effect of these changes upon the flyability of the approach. It was soon discovered (Flight 3 approach 4) that a change to $\pm 60\text{m}$ proved to be too sensitive, with an excessive pilot workload involved in attempting to satisfy the guidance demand. The results obtained with a sensitivity of $\pm 90\text{m}$ were generally favourable, for a range of ground speeds between 45kt and 105kt.

On some occasions, however (e.g. Flight 6) the indications were found to be slightly over-sensitive with $\pm 90\text{m}$ sensitivity - this appeared to be a particular problem where there were other factors (such as poor visibility) contributing to the pilots' workload.

Inevitably, the selection of a value for the horizontal sensitivity must be based upon a trade-off between pilot workload and path following accuracy. The latter, in turn, affects the safe distance by which the approach track can be offset from the platform, due to the need to maintain safe obstacle separation not only with the localiser needle centred, but also with, for example, a half-scale lateral deviation present. It is conceivable that, with low obstacle separation, some form of warning would need to be generated if the pilot deviates too far from the desired approach path; and this in turn will be increasingly likely as the lateral sensitivity is reduced.

In an attempt to investigate the effect of lateral sensitivity upon path following ability, a statistical analysis was performed, the results of which are presented in Table 3. For each approach, the cross-track distance statistics for the level segment were computed and are presented broken down by lateral sensitivity, pilot, and handling method. Approaches where the guidance was not followed for the entire duration of the level segment, due to equipment problems or other operational reasons, have been excluded from the analysis.

Lateral sensitivity	Pilot and handling method	Number of approaches	Samples	Mean	Std dev
±120m	Pilot 1, raw data	3	100	-1.9	8.7
	Pilot 1, flight director	5	257	-2.4	8.9
	Pilot 2, raw data	7	321	-1.4	21.5
	Pilot 2, flight director	3	206	1.5	12.0
	Pilot 3, raw data	3	107	11.4	32.3
	Pilot 4, raw data	1	43	13.0	8.1
	Pilot 5, raw data	2	67	-7.3	10.9
	Autopilot	7	292	1.2	8.1
	All pilots/methods	24	1101	0.3	17.9
±90m	Pilot 1, raw data	4	138	-2.7	14.5
	Pilot 1, flight director	1	47	-16.7	18.6
	All pilots/methods	5	185	-6.2	16.8
±60m	Pilot 2, raw data	2	88	4.6	14.4

Table 3 Cross-Track Statistics for Level Segment (metres)

From the results in the table it is difficult to determine whether any significant correlation exists between the lateral sensitivity and the path following accuracy, particularly since only a small number of approaches were performed using the reduced ($\pm 90\text{m}$ and $\pm 60\text{m}$) scalings, and the pilots in these two cases were different. The combined ('All pilots/methods') standard deviation figures for the three sensitivities are very similar and show no clear trend in either direction (the significantly lower mean for the $\pm 120\text{m}$ case, which would initially suggest a better accuracy, may simply be a result of the significantly greater sample size).

Comparison of the $\pm 120\text{m}$ figures for the different pilots reveals a number of interesting results: as might be expected, the autopilot provided the highest level of accuracy. Comparison of the figures for the two pilots (numbered 1 and 2) who performed the majority of the approaches suggests that those flown by the former, who was more familiar with the aircraft, were the more accurate.

Turning to the vertical sensitivity, the level segment value was initially set at $\pm 100\text{ft}$, and some experimentation was later performed to investigate the effect of reducing this value to $\pm 50\text{ft}$.

No significant problems were experienced with the use of the $\pm 100\text{ft}$ vertical sensitivity. Following the reduction to $\pm 50\text{ft}$, slight difficulties were reported at low

airspeeds around 40kt (Flight 5 approaches 7 and 8) but height control was judged to be 'tighter' at slightly higher speeds such as 80kt (Flight 5 approach 9).

It was observed that the horizontal and vertical sensitivities of a normal ILS installation, with a Category 1 decision height of 200ft, are approximately $\pm 90\text{m}$ and $\pm 50\text{ft}$ respectively at the decision height. In both cases, these also appeared to represent the lower bound of the acceptable range of sensitivity values for a DGPS-based approach.

6.8 **Crosswind and Reduced Speed Approaches**

Experiments were performed to investigate the effect of undertaking approaches at slower indicated airspeeds (50kt in place of 80kt) and in the presence of a significant crosswind at 40kt IAS.

Workload was found to increase at lower airspeeds, and the pilots appeared to experience more difficulty with the use of the more sensitive instrument scalings at these speeds. The comment was made that airspeed control was more difficult at lower speeds.

Significant difficulties were experienced when flying DGPS-guided approaches in a significant crosswind, due to the large drift angles which resulted. The presence of the latter were reported as the reason for difficulties in judging the heading corrections which were necessary to maintain the desired flight path.

It was also discovered that large drift angles could result in a potentially very disorientating visual effect being presented to the pilots. For example, during a right-hand offset approach flown in the presence of a significant crosswind from the left, the aircraft heading could be such that the nose would point to the left of the platform (i.e. the platform appeared to be on the 'wrong' side of the aircraft). The resulting false visual impression could present serious problems in the execution of a landing, or a go-around, manoeuvre if the platform was only sighted at a short decision range.

6.9 **Autocoupled Approaches**

A limited number of approaches were performed with the aircraft autopilot coupled to the output of the DGPS guidance system.

The main observation resulting from these approaches was that the autopilot was not able to supply the necessary flight control inputs to satisfy the transition from the approach segment to level flight: in each case the aircraft continued to descend down to approximately 150ft prior to regaining the demanded MDH of 200ft.

The explanation for this behaviour was assumed to be the fact that the autopilot design, and in particular the internal control law gains, had been optimised for a straight-line ILS approach and that the unit was not intended for use with approach profiles involving multiple segments in the vertical plane.

An attempt was made to reduce the 'undershoot' effect by doubling the length of the faired transition between the approach segment and the level segment to 1000m. This resulted in a small improvement but there was still a significant undershoot (the descent stopped at 165ft, rather than 150ft).

No further attempts were made to refine the autocoupled approach, since it was clear that a considerable amount of additional effort (beyond the scope of the trials programme) would be necessary to resolve these flight control problems.

6.10 **Loss of GPS and Go-Around Techniques**

If all DGPS data were to be lost at a critical phase of the approach, it would clearly not be possible for the pilot to continue to fly the aircraft along the level segment and into an overshoot under DGPS guidance. Instead, the most likely response would be to perform an immediate go-around, and it would be necessary for the approach profile to be designed such that obstacle clearance was maintained in the event of a go-around at any stage.

During the trials, total loss of GPS data was not experienced but there were several instances where the guidance solution reverted from differential to stand-alone mode, due either to loss of the correction signal or to a failure of the GPS receiver to accept the corrections provided. It is believed that this would be the more likely failure mode of an operational DGPS system.

For the purposes of the trials, loss of differential mode was generally not directly signalled to the pilot and guidance indications continued to be provided, based upon the reduced precision non-differential solution. In an operational situation, this might not be suitable for flight phases where the increased precision provided by DGPS was necessary to assure obstacle clearance.

MF differential corrections were lost on a significant number of occasions in the course of the trials programme. This level of unreliability is considered to be excessive but, since it is believed to have been largely the result of installation-dependent factors, does not in itself preclude the use of an MF correction source. Whatever the correction source employed, clear annunciation must be provided to the pilot of any failure affecting the ability to continue an approach, and consideration given to the type of missed approach manoeuvre to be performed if this occurs.

On most aircraft, a go-around following a missed approach would normally be required to be flown manually. However, the autopilot on the trials airframe incorporated a pre-programmed go-around facility which could be triggered by the pilot at any time. This facility maintained the current heading, and demanded a 700ft/min rate of climb with a minimum airspeed of 75kt.

Some experimentation was therefore performed to investigate the effect of triggering the automatic go-around on completion of the level segment (on receipt of the flashing 'G/A' indication on the LED panel). This operated satisfactorily and reduced pilot workload, but it was recognised that this was a feature which would not be available on the majority of the current offshore fleet.

Experiments were also performed (Flight 6) into the feasibility of performing a climbing turn, under DGPS control, away from the platform on initiation of the go-around. This proved to be satisfactory, provided that a sufficiently positive heading change was demanded (initially the turnaway manoeuvre was introduced gradually over the first 500m of the overshoot segment, but this failed to provide a sufficiently compelling turn cue and the turnaway distance was then reduced to 100m).

It was concluded that, whilst this type of manoeuvre was technically feasible, the possibility of loss of DGPS data (or reversion to stand-alone GPS) and obstacle clearance issues dictate that the approach profile should not be positioned such that the aircraft is required to perform a turn during the go-around to ensure obstacle separation.

6.11 **Seamless GPS Navigation**

On each test flight, enroute navigation capabilities were provided via the RNAV-2 computer, which used the DGPS system receiver (invariably the MF-corrected unit) as its data source in place of the Decca Navigator sensor normally used on the aircraft.

During the early test flights the RNAV-2 system was used to provide guidance for the overhead part of the modified Aerad-type approach, with the pilots switching over to the DGPS system shortly before establishing on the approach segment. Although DGPS was being used as a navigational sensor both before and after this switch selection, the mechanisms for selecting the desired flight path were very different for the RNAV-2 (which provides a waypoint-based enroute capability) compared to the experimental DGPS approach equipment.

In an attempt to avoid the necessity of performing this switch midway through an approach procedure, a number of approaches were performed where the experimental DGPS equipment provided continuous guidance through the overhead leg and inbound turn onto the approach segment using the curved guidance facility described in section 4.5.3. An immediate difficulty was that, unlike the RNAV-2 based system, no automatic indication of the desired course was provided (the RNAV-2 has the capability to drive the HSI course carriage to reflect the desired track).

This problem was partially overcome by the pilot manually changing the HSI course selection at the required point, but this was found to give rise to workload problems: if the selection was not made at the correct time, the displayed indications could become impossible to interpret.

Nevertheless, experimentation with this facility demonstrated the potential of using DGPS to provide 'seamless' guidance for the enroute and approach phases, provided that the necessary facilities (e.g. automated HSI carriage function) were made available to the guidance equipment.

6.12 **Removal of Level Segment**

In order to investigate the potential for undertaking approaches which offered maximum obstacle avoidance, two approaches (Flight 6 approaches 10 and 11) were flown which incorporated a descent directly to the MAP, with no intervening level segment. The MAP was arranged so as to be directly abeam the platform helideck.

The two approaches were performed with descent angles of 3.5° and 6°, and retained the vertical fairing for the final 500m prior to the MAP which assisted in arresting the descent. The pilots commented that it was essential to reduce speed significantly in the latter stages of the descent, particularly with the higher rate of descent required for the 6° approach.

It was concluded that, whilst approaches of this nature are probably technically feasible using DGPS guidance, a significant amount of further investigation would be required before they could be considered for operational use. This would need to cover such issues as the scheduling of the speed reduction, missed approaches, and the feasibility of performing the landing transition close to the helideck and platform structure.

6.13 **Entry of Approach Data**

For the flight trials programme, all of the parameters defining the approach profiles were set up by the FTE using the laptop PC located in the aircraft cabin. Whilst this provided the greatest degree of flexibility for the trials, it would clearly not be appropriate for use in a normal operational environment. An alternative method would need to be devised based upon either a dedicated control unit, or an integrated solution which employed an existing item of avionic equipment (such as the RNAV-2) for the entry of approach data.

The trials programme did not address the human factors and other technical issues related to the design of an operational data entry system. It is, however, possible to identify a number of key issues such as the advisability of minimising the amount of pilot interaction required to select an approach path. This might be achieved through the use of a database containing pre-programmed approach profiles for each destination, conceptually similar to the standard arrival routes and instrument approach patterns provided at onshore aerodromes, one of which would be selected by the pilot. This would need to be reconciled, however, with the advisability of ensuring that approaches are performed into wind wherever possible.

It would also be necessary to assure the integrity of the information contained in any database used for approach purposes. Many of the issues relating to database integrity, such as the consistency of co-ordinate datums (WGS84 is the current aeronautical standard, whereas ED50 is commonly used for North Sea offshore survey purposes), the possibility of transcription error, and the detection of corrupted data; are similar to those being addressed by the onshore community. However, very careful consideration would also need to be given to the treatment of the many mobile offshore structures.

6.14 **Applicability to Other Aircraft**

With the exception of the 'add-on' LED indicators, all of the display systems which were driven by the DGPS guidance system during the trials formed part of the basic aircraft avionics fit. The results of the trials should therefore be readily applicable to other offshore aircraft.

Whilst it is unlikely that the software implementation used for the trials would be directly suitable for use in an operational approach aid, there should be no fundamental bar to the incorporation of the guidance algorithms themselves into new equipment. The algorithms used for the trials are not complex (the ten principal steps involved are outlined in section 4.4) and it is believed that they, or variations thereof, could easily be incorporated into existing avionic equipment such as an area navigation system or a GPS receiver.

Similarly, although custom designed interface hardware was used on the DGPS trials pallet to generate drive signals for the basic aircraft instruments, the output circuitry

is similar to that which is found in other items of modern avionic equipment and could therefore be easily replicated.

6.15 **Applicability to Other Data Sources**

Although the flight trials programme was performed using DGPS as the primary source of navigational data, the majority of the trials results are probably equally applicable to other navigation sensor technologies offering a comparable level of accuracy, such as any of the GNSS systems which are currently being proposed as alternatives or complements to the GPS constellation.

The data processing algorithms, and the software which was used in the trials to generate the guidance information for display to the pilots, are largely independent of the specific GPS receivers used for the trials and they could readily be adapted to operate with alternative equipment.

Similarly, although the vast majority of the trial approaches used the radio altimeter as their sole source of vertical position, the operation of the system was also successfully demonstrated using alternative height sources (barometric and DGPS altitude) although only a very limited number of test approaches were performed using this data.

7 SUMMARY OF CONCLUSIONS

The Trials Installation

- (1) Approaches were successfully undertaken at five offshore structures using a combination of Differential Global Positioning System (DGPS) and radio altimeter data to provide horizontal and vertical guidance.
- (2) DGPS-guided autocoupled approaches were successfully undertaken, although the autopilot was not able to cope with an approach which included multiple segments in the vertical plane.

These facts demonstrate the suitability of the trials installation to provide the guidance facilities which the trials programme was intended to investigate.

Approach Profiles

- (3) The segmented vertical profile used for the flight trials was found to be practicable, provided that a sudden step change on transition to the level segment was avoided through the provision of appropriate anticipatory guidance.
- (4) For the S76C, the maximum acceptable approach angle was in the region of 6° (other aircraft types might support steeper approaches). A shallower approach angle might be required if the approach was not oriented into wind.
- (5) The Missed Approach Point (MAP) position employed for the flight trials appeared to be satisfactory, however the optimum MAP position for each individual offshore platform should be determined from a consideration of its layout and position relative to surrounding structures.
- (6) Lateral offsets in the range 200m to 250m were employed for the flight trials, however the minimum acceptable offset for each possible approach direction should be determined on a platform-by-platform basis, from a consideration of the obstacle environment and of the errors inherent in the GPS receiver outputs.
- (7) The approach profile must be arranged such that the aircraft is capable of executing a safe manual go-around manoeuvre, without loss of obstacle clearance, following the loss of DGPS guidance at any stage of the approach.
- (8) The optimum angle for a DGPS-guided overshoot manoeuvre was in the region of 6° for the S76C.
- (9) Approaches should ideally always be conducted into wind: the presence of a significant crosswind can give rise to undesirable visual effects particularly at low approach speeds, and these could potentially be dangerous in certain situations (such as low visibility).

Guidance Presentation

- (10) Instrument sensitivities similar to those used for ILS approaches appear to be appropriate for the DGPS approach, although more investigation is required to determine the optimum values.

- (11) Clear annunciation of the true range to the platform (preferably to a resolution of two decimal places) and of the current approach segment, well situated within the handling pilot's instrument scan, were found to be essential. Careful consideration needs to be given to the nature of the Decision Range (MAP) annunciation, which must be sufficiently compelling and may require a dedicated indicator. These indications must be implemented in a way which does not present an undue distraction to the pilot.
- (12) DGPS guidance is capable of offering a seamless transition between en-route and approach guidance, but unambiguous course and mode indications must be provided to the pilot.
- (13) Clear annunciation must be provided of any DGPS failures which significantly affect the accuracy of the guidance information.

Implications of the Results

- (14) Significant differences exist between aspects of the DGPS profile and the standard offshore and onshore procedures commonly employed by helicopter pilots. As a result, careful consideration will be required of the training requirements associated with the introduction of a new procedure.
- (15) The integrity of the data used to define the approach must be assured, and so consideration needs to be given to the human factors aspects of the method to be employed to enter data and select approach parameters in flight.
- (16) The results of the trials programme are believed to be generally applicable to aircraft types other than the S76C.
- (17) The results of the trials programme may be applicable to sources of guidance data other than DGPS, provided that due consideration is given to the effect of the expected error characteristics of any alternative technology. Since the accuracies of DGPS and uncorrected GPS are considerably different, it must not be assumed that all of the trials results will be equally applicable to a system based upon stand-alone GPS.

Future Work

The trials programme has identified a number of areas of uncertainty which could usefully be explored further by means of additional theoretical and practical studies.

These include the following:

- (18) The trials programme only involved a small number of pilots, flying a single aircraft type, and the range of operating conditions experienced was necessarily limited. As a result, additional flight trials (which would be most cost-effective if undertaken in revenue-earning service) are required to obtain a larger data set and to permit a more wide-ranging evaluation of DGPS guidance.
- (19) The trials airframe possessed some of the most up-to-date avionics and cockpit instrumentation currently in use on the North Sea. A study is required, involving the relevant operators and equipment manufacturers, into the implications of introducing a DGPS approach capability on a fleet-wide basis. Particular

attention will need to be paid to those aircraft with older technology installations.

- (20) Careful consideration must be given to how an operational approach procedure will be defined, and specified to the airborne equipment, in relation to the position of the destination platform. Again, this process will require input from the helicopter operators and equipment manufacturers.
- (21) Further investigation is required before direct approaches to a helideck, without a level segment, could be satisfactorily performed using DGPS guidance.
- (22) Careful analysis of the operation of the flight control system will be required in order to determine whether autocoupled approaches are operationally feasible.

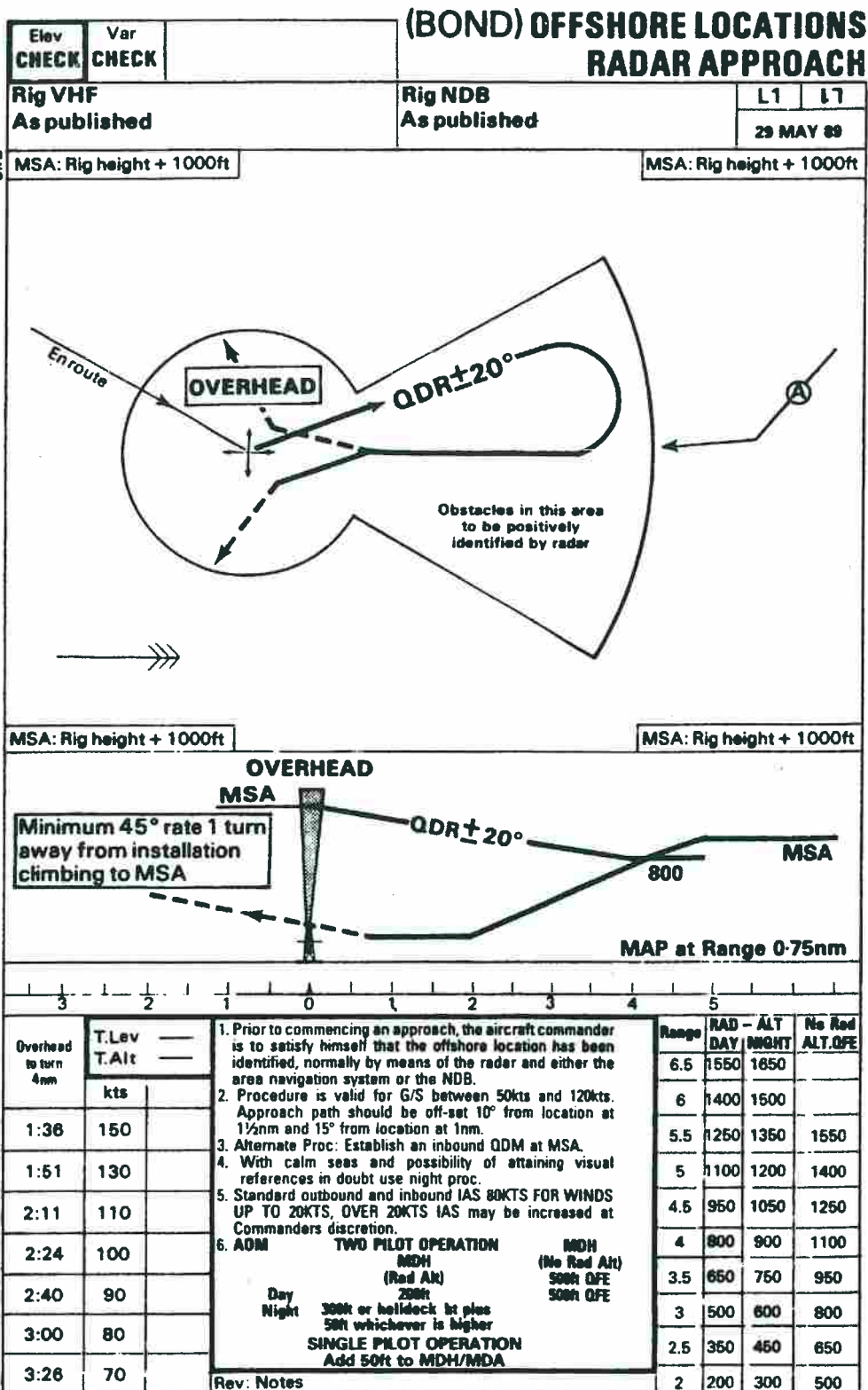


Figure 11 Bond Helicopters Offshore Weather Radar Approach Plate (reproduced by permission of British Airways AERAD)

(BOND/CRANFIELD/CAA) OFFSHORE LOCATIONS EXPERIMENTAL GPS APPROACH

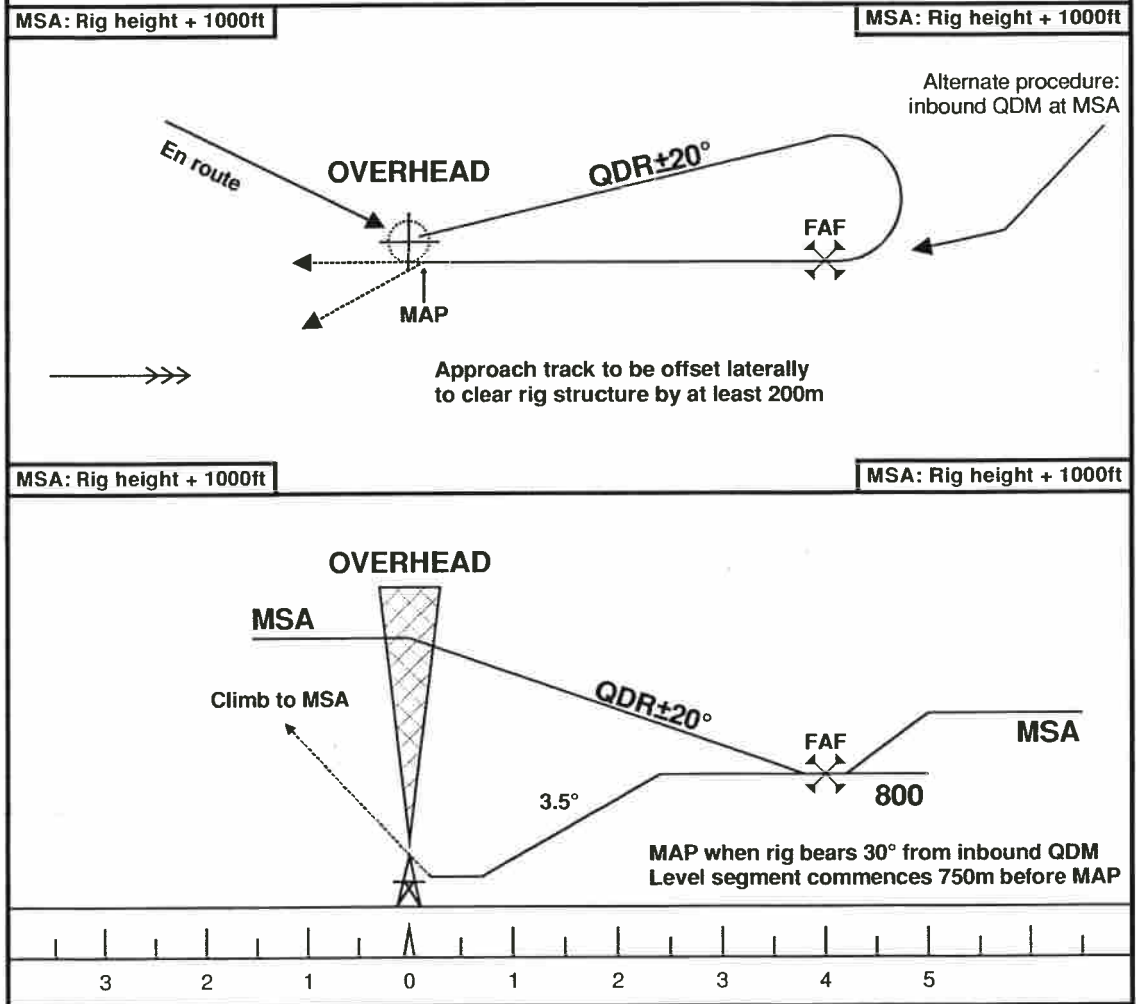


Figure 12 Experimental DGPS Approach Plate

the 1990s, the number of people with a mental health problem has increased in the UK, and the number of people with a mental health problem who are in contact with mental health services has also increased (Mental Health Act 1983, 1990, 1994, 1997, 2003).

There is a growing awareness of the need to improve the lives of people with a mental health problem, and to reduce the stigma and discrimination that they experience (Mental Health Act 1983, 1990, 1994, 1997, 2003).

One of the ways in which this can be achieved is by providing people with a mental health problem with the opportunity to participate in decisions about their care and treatment (Mental Health Act 1983, 1990, 1994, 1997, 2003).

One of the ways in which this can be achieved is by providing people with a mental health problem with the opportunity to participate in decisions about their care and treatment (Mental Health Act 1983, 1990, 1994, 1997, 2003).

One of the ways in which this can be achieved is by providing people with a mental health problem with the opportunity to participate in decisions about their care and treatment (Mental Health Act 1983, 1990, 1994, 1997, 2003).

One of the ways in which this can be achieved is by providing people with a mental health problem with the opportunity to participate in decisions about their care and treatment (Mental Health Act 1983, 1990, 1994, 1997, 2003).

One of the ways in which this can be achieved is by providing people with a mental health problem with the opportunity to participate in decisions about their care and treatment (Mental Health Act 1983, 1990, 1994, 1997, 2003).

One of the ways in which this can be achieved is by providing people with a mental health problem with the opportunity to participate in decisions about their care and treatment (Mental Health Act 1983, 1990, 1994, 1997, 2003).

One of the ways in which this can be achieved is by providing people with a mental health problem with the opportunity to participate in decisions about their care and treatment (Mental Health Act 1983, 1990, 1994, 1997, 2003).

One of the ways in which this can be achieved is by providing people with a mental health problem with the opportunity to participate in decisions about their care and treatment (Mental Health Act 1983, 1990, 1994, 1997, 2003).

One of the ways in which this can be achieved is by providing people with a mental health problem with the opportunity to participate in decisions about their care and treatment (Mental Health Act 1983, 1990, 1994, 1997, 2003).

One of the ways in which this can be achieved is by providing people with a mental health problem with the opportunity to participate in decisions about their care and treatment (Mental Health Act 1983, 1990, 1994, 1997, 2003).

One of the ways in which this can be achieved is by providing people with a mental health problem with the opportunity to participate in decisions about their care and treatment (Mental Health Act 1983, 1990, 1994, 1997, 2003).

One of the ways in which this can be achieved is by providing people with a mental health problem with the opportunity to participate in decisions about their care and treatment (Mental Health Act 1983, 1990, 1994, 1997, 2003).

One of the ways in which this can be achieved is by providing people with a mental health problem with the opportunity to participate in decisions about their care and treatment (Mental Health Act 1983, 1990, 1994, 1997, 2003).

One of the ways in which this can be achieved is by providing people with a mental health problem with the opportunity to participate in decisions about their care and treatment (Mental Health Act 1983, 1990, 1994, 1997, 2003).

One of the ways in which this can be achieved is by providing people with a mental health problem with the opportunity to participate in decisions about their care and treatment (Mental Health Act 1983, 1990, 1994, 1997, 2003).

One of the ways in which this can be achieved is by providing people with a mental health problem with the opportunity to participate in decisions about their care and treatment (Mental Health Act 1983, 1990, 1994, 1997, 2003).